CESDOC 2018

Civil Engineering for Sustainable Development-Opportunities and Challenges

18th-19th December 2018

Conference Proceeding

Department of Civil Engineering

Assam Engineering College,

Guwahati, Assam, India

Publication of Civil Engineering Department

Assam Engineering College, Guwahati-781013

Proceeding of the 2nd International Conference on

Civil Engineering for Sustainable Development-

Opportunities and Challenges (CESDOC)

Guwahati, Assam, India

18-19 December, 2018

Editors

- Dr. B. Talukdar
- Dr. J. Pathak
- Dr. D. Goswami

Communication Address

Civil Engineering Department

Assam Engineering College, Guwahati-781013, Assam, India

Website: www.cesdoc.aec.ac.in

ADVISORY COMMITTEE

PROF.(RETD.) NAYAN SARMA	(IIT Roorkee)
PROF. (RETD.) DK. PAUL	(IIT Roorkee)
PROF ARUP KUMAR SARMA	(IIT Guwahati)
DR. DOMINIK H. LANG	(NORSAR Norway)
DR. GUNAN PAUDYAL	(Nepal)
DR. S.K. DEB	(IIT Guwahati)
PROF G. SANKARA SUBRAMANIAN	(PSG College of Technology)
MR. BHARGAB MOHAN DAS	(Thai Global Energy Co. Ltd.)
DR. RAJIVALI	(Vancouver, USA)

ORGANISING COMMITTEE

President	: DR. ATUL BORA
Working President	: DR. PALASH JYOTI HAZARIKA
	: PROF. SUNIT KUMAR BHAGABATI
Organising Secretary	: DR. JAYANTA PATHAK
Jt. Org Secretaries	: DR. DIGANTA GOSWAMI
	: DR. BIPUL TALUKDAR
	: DR. MRINAL KUMAR BORA

TECHNICAL COMMITTEE

: DR. BINU SHARMA
: DR. MRINAL KR. BORA
: DR. BIBHASH SARMA
: DR. UTPAL KUMAR NATH
: DR. TRIPTIMONI BORAH
: DR. UTPAL KUMAR MISRA
: DR. MALAYA CHETIA
: MR. BIBHUTI B. BHARDWAJ
: MS. RUPALI SARMAH
: MS. JAYSHREE HAZARIKA

TREASURER

: DR. BIBHASH SARMA

TRAVEL ACCOMMODATION COMMITTEE

: DR. PANKAJ GOSWAMI

: MR. SASANKA BORAH

RECEPTION & VENUE COMMITTEE

: DR. TRIPTIMONI BORAH

: DR. BHARATI MEDHI

: MS. RUPJYOTI BORDOLOI

: MS. PUSHPANJALI SONOWAL

CULTURAL COMMITTEE

: DR. DIGANTA GOSWAMI

: DR. BIBHASH SARMA

LOGISTICS & FOOD COMMITTEE

: MR. BHASKAR JYOTI DAS

: DR. UTPAL KUMAR MISRA

PREFACE

The "2nd International Conference on Civil Engineering for Sustainable Development Opportunities and Challenges - CIDOC 2018" is being organized by the Civil Engineering Department, Assam Engineering College on 18th & 19th December, 2018. The 1st International conference CESDOC 2016 was organized in 2016 to commemorate 60 years of glorious existence of the Civil Engineering Department of the college, which received wide response from participants from India and abroad. The overwhelming response to the 1st conference encouraged the department to announce the 2nd conference on sustainability to be held on 2018.

The Assam Engineering College, the first engineering college of north-east India was established with Civil Engineering as its first department amidst the beauties of nature surrounded by lush green forests with majestic hills and Deepor Beel (Ramsar Site). AEC started as the Assam Civil Engineering College the year 1955 and was the first engineering college in the entire North East India to impart technical education for bachelor degree in Engineering. The Department, accredited by National Board of Accreditation (NBA) currently offers undergraduate postgraduate and doctoral programmes. The department has seven state-of-the-art laboratories and highly qualified faculty members to support the various educational programmes and also undertakes sponsored research and consultancy on behalf of government, PSU and private sector organisations of repute.

The vision of the department is to have complete synergy between teaching and learning for producing civil engineers, who are competent and socially responsible to contribute to the sustainable development of the state, the region and the nation, with global perspective. With depleting natural resources and increasing demand on energy and infrastructure, the paradigm within which engineers, architect and policy makers works has significant impact on progress toward sustainable development. The environmental, economic, social, technological development must be seen as interdependent and complement concepts, where economic competitiveness and ecological sustainability are important aspects of the common goal of improving the quality of life with appropriate engineering interventions.

The conference aims at congregation of policy makers, stakeholders, engineers, architects and planners to brainstorm on various issues to strengthen internationally mandated approach for sustainable development and discuss roles of the stake holders in various interdisciplinary core areas of sustainable development. The conference will provide a platform to champion the

effort to build capacity for sustainable development among technocrats and policy makers and influence a policy framework that demands more socially and environmentally responsible decision process for implementation of development projects.

The second version of the conference CESDOC 2018 has received wide response from stakeholders from India and abroad. The conference has accepted over 70 research papers for presentation and it is expected that more than 250 delegates will attend conference. There will be 9 (nine) technical sessions covering themes ranging from Sustainable Infrastructure, Sustainable Urban Development Sustainable Rural Development, Sustainable Energy Solutions, Sustainable Ecosystem Management. The conference will also see a confluence of eminent experts from various fields participating from institutions and industries from Australia, India, Nepal, Norway and USA.

I take this opportunity to congratulate the organising committee and the editorial committee members for being able to take out this proceeding. You will be happy to know that a topical volume of selected papers from this conference will be published by Springer Nature, The Netherlands. The mentoring and support from the conference Chair Dr. Atul Bora, Principal, AEC is sincerely acknowledged. The support received from Dr. P.J. Hazarika, Prof & Head of the department & Working President of the conference is gratefully acknowledged. The organising committee expresses gratitude to all participants, authors, speakers for their kind response and participation. We are grateful to the participating industries and Assam Science and Technology University for the support extended to the conference The support from each faculty member and the staff of the department has given the core strength to the organising committee and the committee remains profoundly grateful to each of them.

Dr. Jayanta Pathak
Organising Secretary, CESDOC 2018
Professor, Department of Civil Engineering
Assam Engineering College
Jalukbari, Guwahati, Assam
INDIA 781013

TABLE OF CONTENTS

Sustainable Infrastructure

Sustainable Infrastructure

Sustainable Construction Materials

Nano-modified asphalt binder: a sustainable construction material

Nazir, P.[1], Choudhary, R.[2], and Kumar, A.[3]

[1] PG Student, Department of Civil Engineering, IIT Guwahati, Assam 781039, India.
[2] Associate Professor, Department of Civil Engineering, IIT Guwahati, Assam 781039, India.
[3] Ph.D Research Scholar, Department of Civil Engineering, IIT Guwahati, Assam 781039, India.

ABSTRACT

For sustainable growth of road infrastructure, the optimal use and conservation of resources as well as reduction of energy consumption and emissions during roadway construction is of prime importance. The present study presents a review of the existing literature on nano-modified asphalt materials and their potential as a sustainable construction material. Different types of nanomaterials (nanoclay, nanosilica, carbon nano-tubes, *etc.*) have been incorporated in the field of asphalt modification owing to their novel properties and the potential to improve the properties of the base material. Extent of changes in the properties of nano-modified binders are dependent on modifier type, its content, its size, production process, and the base binder type. Nano-modification is reported to provide a 'bridge' effect between asphalt binder and the nano-particle that reduces the mitigation of micro-cracks, and thus improves the mix fatigue life and rut resistance. The addition of nanomaterials has also shown to enhance the resistance of asphalt mixtures towards distresses like moisture induced damages and aging, thereby contributing towards durable and efficient pavements. A special use of nanomaterials is in photo-catalytic pavements that have the ability to oxidize air pollutants and hence reduce air pollution caused due to automobiles. Overall, the paper highlights the need for continued research on nano-modified asphalt binder and its potential as a sustainable pavement construction material.

Keywords: nanotechnology, asphalt binder, sustainability

1. INTRODUCTION

Ever increasing traffic loads and extreme fluctuations in pavement temperatures have rendered the traditional asphalt binders unable to meet the demand for an acceptable pavement performance. In response, various kinds of materials are being introduced in the asphalt binder with the objective to enhance one or several performance aspects with regard to resistance towards permanent deformation, aging, moisture-induced damage, and cracking. The materials that are used as asphalt modifiers include polymers, natural asphalt, tyre rubber, and a more recently introduced class of modifiers, the nano-materials.

Nanotechnology is an emerging technology with size of the material (at least one dimension) in the nano-size range (10^{-9} m). The novel behaviour of material at nano-range facilitates the improvement of construction materials, including pavement materials. Although major nano-technological developments have taken place in the field of electronics, physics and chemistry, the field has taken a recent stride towards construction engineering (Steyn, 2009). The nano-materials can enhance the properties of asphalt binders and mixtures, and thus may open the door for use as high performance pavement materials.

This paper documents a review of some common nano-materials that have been employed in the field of pavement technology followed by summary of various studies conducted to evaluate properties of nano-modified asphalt binders and asphalt mixtures. The different test methods used to characterise nano-modified asphalt materials is also presented. Further, the environmental and economic aspects of nano-modified asphalt materials is highlighted.

2. NANO-MATERIALS USED IN ASPHALT

2.1 Carbon nano tubes (CNT)

Carbon nano tubes (CNTs) are allotropes of carbon with diameter in the nano-scale range. The carbon atoms in CNTs are sp^2 hybridised. CNTs can be imagined as sheets of graphene rolled into a cylindrical structure (Fig. 1). They may be single walled, double walled or multi walled. They are manufactured by three common techniques: arc discharge, laser ablation, and chemical vapour deposition (Aqel *et al*., 2012). They possess a very high aspect ratio (ratio of length to diameter) approaching 1000000:1, high tensile strength and high Young's modulus (Amirkhanian *et al*., 2010). The excellent mechanical and thermal properties of CNT may lead to improved performance in the asphalt binders as well.

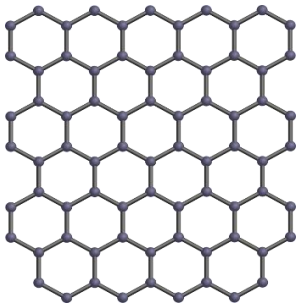

Fig. 1a Hexagonal lattice of graphene sheet

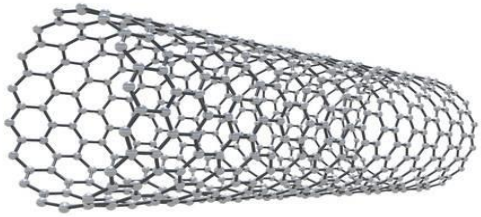

Fig. 1b Carbon nano-tube

2.2 Nano-silica

Silica is abundantly found in nature since it is a major constituent of sand. Nano-silica is a white, powdery inorganic material, and has applications in medicine for drug delivery. It is widely used in engineering due to its beneficial properties such as huge surface area, strong adsorption, good dispersion ability, high chemical purity, and excellent stability (Yao *et al*., 2013). Sol-gel method is a popular method to synthesize silica nano-particles from silica. Other methods include reverse micro emulsion and flame synthesis (Rahman *et al*., 2012). It has been reported that morphology and nano-dimension of the nano-silica provides a much higher surface area for interaction with asphalt binders in comparison to a conventional filler material. Further, nano-silica has higher polarity and a chemically active surface, which altogether may have a positive effect when used as an asphalt modifier (Fini *et al*., 2016).

2.3 Nano-clays

Layered silicates (nanoclays) are used in the modification of polymer matrices for improvement in mechanical, thermal, and barrier properties (You *et al*., 2011). Depending on chemical composition and morphology, nano-clays are classified as montmorillonite, kaolinite, halloysite, *etc*. Nano clays exhibit good potential towards improvement of the asphalt binder based on intercalation and exfoliation mechanisms (Fig. 2). Intercalation is the reversible inclusion or insertion of a molecule or ion into material with layered structure. An extreme case of intercalation is the complete separation of the layers of material, which is known as exfoliation. Past studies have shown that the structure of nanoclays can transform from intercalated to exfoliated at higher nanoclay dosages, which can provide an enhanced rutting resistance properties to the binders (Ashish *et al*., 2016). It has been the most employed nano-material for modifying the asphalt binder due to its low cost of production and wide abundance in nature.

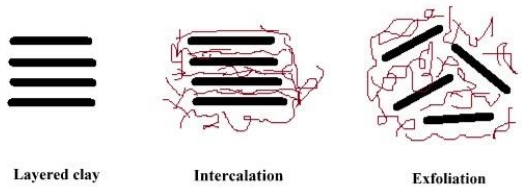

Fig. 2 Intercalation and exfoliation in clay mineral layers

3. VARIOUS TESTS TO EVALUATE NANO-MODIFIED ASPHALT MATERIALS

3.1 Advanced techniques

3.1.1 X-Ray diffraction (XRD)

X-ray diffraction (XRD) is a tool to identify and characterise compounds based on their diffraction patterns. You *et al*. (2011) performed XRD test to examine the morphology of nanoclay modified asphalt binder. Nanoclays may adhere each other due to their internal electrostatic charge, therefore it is important to verify the extent of dispersion after blending process. XRD is a useful technique as it provides a quantitative assessment of dispersion of the nano-material in asphalt binder.

3.1.2 Scanning electron microscopy (SEM)

Electron microscopy is used to produce morphological images of a sample by scanning the surface with a focused beam of electrons. The electrons are reflected or radiated out of the sample, and are then analysed to collect information about the sample's surface morphology. SEM can be used to study the morphology of original binder, nanomaterials, or nano-modified binders.

3.1.3 Atomic force microscopy (AFM)

Atomic force microscopy is a scanning probe microscopy with very high resolution. AFM is employed to examine nano-scale forces for asphalt binders. The technique can be used to assess forces of adhesion between aggregate and asphalt, or to evaluate the uniformity of dispersion of nanomaterials in the asphalt binder.

3.1.4 Fourier transform infrared spectroscopy (FTIR)

In this technique, infrared spectra is analysed to identify interatomic bonds in chemical compounds while measuring absorbed light at each wavelength (Fini *et al*., 2015). The frequencies at which there are absorptions of

IR radiation referred to as peaks can be correlated directly to chemical groups within the material's chemical structure. FTIR can be used to analyse chemical functional groups present in nano-modified asphalt binders before and after nano-modification.

3.2 Test methods to evaluate properties of asphalt binder

Conventional tests to characterize the asphalt binders include specific gravity, penetration, softening point, ductility, apparent and kinematic viscosity, *etc*. Advanced rheological characterisation can be carried out using the dynamic shear rheometer (DSR) and bending beam rheometer (BBR) to measure viscoelastic properties of asphalt at high, intermediate and low service temperatures. Complex shear modulus (G*) measures the total resistance against deformation of an asphalt binder when subjected to a sinusoidal shear stress, whereas phase angle (δ) represents the time lag between applied stress and resultant strain (Kumar *et al.*, 2018; Julaganti *et al*., 2017). Superpave parameter G*/sin δ is used to evaluate the rutting performance and G*sin δ is used to evaluate the fatigue performance of asphalt binders. Higher G*/sin δ values are desirable for better rutting resistance, whereas a lower G*sin δ indicates better fatigue performance of an asphalt binder. The creep stiffness of asphalt binders versus loading time is determined by the BBR (Yao *et al*., 2013).

3.3 Test methods to evaluate properties of asphalt mixture

3.3.1 Marshall flow and stability test

These tests provide performance prediction for Marshall mix design method. Stability measures the maximum load supported by test specimen when loaded diametrically at the rate of 50 mm/min at a temperature of 60 °C. Flow is the deformation undergone by the specimen at the peak load. It provides an indication of the ductility of asphalt mixture and its ability to adjust to gradual settlements and movements without cracking (Taherkhani *et al*., 2017).

3.3.2 Test for rutting

Rutting is one of the most serious forms of pavement distress that occurs due to permanent deformation of the asphalt surface that generally accumulates along the wheel paths. Commonly used devices to simulate and evaluate mixture rutting potential include asphalt mixture performance tester (AMPT), creep tests (dynamic or static), Hamburg wheel tracking device (HWTD), and asphalt pavement analyzer (APA).

3.3.3 Test for fatigue

Fatigue is a one of the most critical asphalt pavement distresses and occurs due to excessive traffic load repetition or a weak pavement structure. Fatigue performance of asphalt mixtures can be evaluated by tests such as indirect tensile fatigue test, 4-point beam fatigue test, semi-circular bend test, and cyclic direct tension test.

3.3.4 Test for moisture induced damage

Moisture damage indicates the failure of adhesion between aggregate and binder, or the failure of cohesion in the binder itself. Moisture damage has adverse effect on the serviceability and durability of asphalt pavements. Modified Lottman test is a widely used test to evaluate the effect of moisture on HMA. This test basically compares the indirect tensile strength results of a dry sample and a sample subjected to moisture conditioning procedure that includes a freeze and thaw cycle. Several other test methods such as resilient modulus test (before and after moisture conditioning) and wet Hamburg test are also conducted for moisture performance evaluation.

4 PERFORMANCE OF ASPHALT BINDERS WITH NANO-MATERIALS

Several studies have been conducted to evaluate the performance of asphalt binder incorporated with different nano-materials as modifiers. Fini *et al*. (2016) evaluated a 60/70 base binder blended with 2, 4, and 6% nano-silica by weight of the binder. SEM micrographs of nano-silica modified binders confirmed uniform dispersion of the modifier. Rheological characterisation results showed that nano-modified binders were less susceptible to oxidative aging, which was further confirmed by a reduced carbonyl area seen in the FTIR results. Modified binders showed better permanent deformation resistance in terms of G*/sin δ. The improvement in the rutting resistance was further confirmed by the MSCR test.

In another study, You *et al*. (2011) used nanoclay as the nano-modifier to a neat PG 64-28 base binder in two dosages: 2 and 4% by weight of binder. The extent of dispersion of nanoclay was investigated using the XRD technique. Results showed that XRD peak for nanoclay (at 5° and 1900 intensity) was not prominent in the XRD spectrum of nano-modified binder, which suggested a uniform dispersion of nanoclay. Increase in the nanoclay content resulted in increased viscosity and increased complex shear modulus (G*) of the asphalt binders (Fig. 3). Low temperature cracking resistance properties evaluated by the direct tension tester showed that the performance of the original binder was better than nano-modified binders. Addition of nanoclay was found to enhance the toughness properties of the asphalt binder.

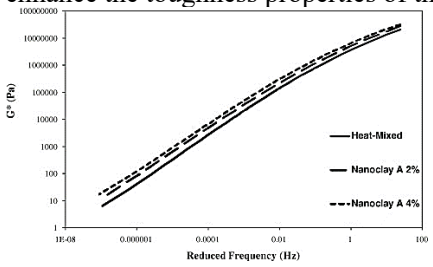

Fig. 3 G* master curve for nanoclay modified binders

(You *et al.*, 2011)

Ashish and Singh (2018) utilised carbon nanotubes (CNT) for asphalt binder modification in dosages of 0.4, 0.75, 1.5 and 2.25% by weight of control binder. Superpave rutting parameter G*/sin δ increased up to 1.5% CNT content and showed a decrease at 2.25% CNT content (Fig. 4). However, significant improvement was observed in the recovery value from MSCR tests at all CNT dosages. The authors emphasised that based on the recovery properties, the improvement in rutting resistance of CNT-modified binder can be expected at higher CNT dosages. Results showed that addition of CNT content up to 2.25% did not have any storage stability issues. It was further demonstrated that the aging resistance of CNT-modified binders was better than the control binder.

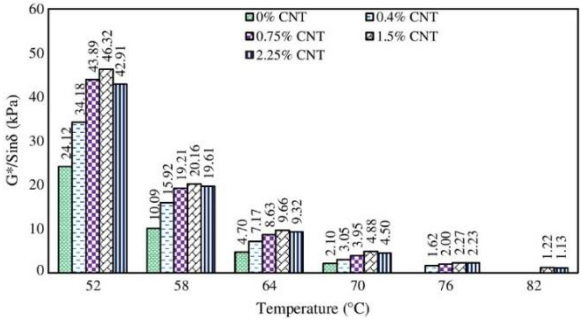

Fig. 4 Results of G*/sin δ for CNT-modified binders (Ashish and Singh, 2018)

Santagata *et al*. (2015) investigated the fatigue properties of asphalt binders reinforced with CNTs. A standard PG 58-22 penetration grade base binder was modified by two dosages of CNTs: 0.5% and 1% by weight of the binder. Fatigue resistance of the binders was evaluated by subjecting them to sinusoidal oscillatory shear loading at 10 Hz frequency and 10 and 20 °C temperatures. Strain sweep test showed that CNT-modified binders exhibited higher linear viscoelastic (LVE) limits, indicating a widening of the LVE region. Fatigue results showed that CNTs can significantly improve fatigue resistance of the asphalt binders provided that their dispersion in the binder is uniform and adequate.

Jahromi and Khodaii (2009) studied the effect of two types of nano clay: nanofil-15 and cloisite-15A, on physical and rheological properties of a 60/70 pen grade asphalt binder. The nanoclays were used in dosages of 0, 2, 4, and 7%. Conventional test results showed a decrease in penetration and ductility value, while increase in softening point was observed for nanoclay modified binder. DSR was used to plot master curves for G* and δ. Results indicated that the addition of nanoclay increased the stiffness and aging resistance, and reduced the phase angle of the modified binders. The temperature susceptibility of the modified binders was found to be lower compared to the control binders. The authors emphasised the need to ensure a homogeneous dispersion of nanoclay in the binder to realise the benefits of nano-modification.

Yao *et al*. (2013) investigated the rheological properties of asphalt binder blended with 4% and 6% nano silica. A PG 58-34 binder was used as the base and control binder in the study. SEM images were analysed to observe the microstructural changes as well as to ensure the homogeneous dispersion of nanosilica particles in the asphalt binder. From FTIR spectroscopy, it was proved that modification with nano-silica was not only a physical phenomenon, but also it altered the chemical bonding of the neat binder. Addition of nanosilica slightly reduced the viscosity of asphalt binders. Superpave rheological tests showed that nanosilica modified binders had better rutting and fatigue performance compared to the control binders in addition to improved recovery ability. Low temperature rheological testing on BBR indicated that low temperature grade of modified binder was the same as the control binder. FTIR results also indicated an improved anti-aging resistance of nano-modified binders.

5 PERFORMANCE OF ASPHALT MIXES WITH NANO-MATERIALS

Arabani and Faramarzi (2015) evaluated the performance properties of asphalt mixtures containing 0, 0.1, 0.5 and 1% multi-walled CNT. Resilient modulus, dynamic creep and fatigue life of the mixtures were determined. Highest resilient moduli of the mixes were observed at 1% CNT content at three test temperatures (5, 25 and 40 °C), indicating a better resistance to permanent deformation (Fig. 5). Results of dynamic creep showed that the mixtures with 1% CNT had the lowest final strain at the three stress levels of 100, 200 and 300 kPa used in the test. The strain values decreased with increase in the CNT content. Further, asphalt mixtures containing CNT showed noticeably improved fatigue life compared to the control mixtures without CNT. The improvement in rutting resistance and fatigue life was attributed to higher tensile strength of CNTs, which enables them to act as a reinforcement in the asphalt mixtures and reduce the propagation of micro cracks.

Performance properties of asphalt mixtures with nano-silica were investigated in the study by Enieb and Diab (2017). Nano-silica contents used in the study were 0, 2, 4, and 6% by weight of the binder. Mixtures were characterised based on resilient modulus, indirect tensile strength, fracture energy, moisture susceptibility and fatigue life. The addition of nano-silica had a positive effect on the resilient modulus values measured at 25 °C. The authors reported that increased resilient modulus indicated increased elasticity and therefore better resistance to permanent deformation than the control mixtures. Nano-silica modified asphalt mixtures showed higher ITS values (measured at 25 °C) than the control mixture with the highest ITS observed at 4% nano-silica

content. Nano-silica modified mixtures also showed higher strains to failure than the control mixtures, indicating an improved cracking resistance. The TSR values also increased with increase in nano-silica content, indicating better resistance of the nano-modified asphalt mixtures to the effect of moisture (Fig. 6). Addition of nano-silica also improved the fatigue life of mixtures. However, the results at 4% and 6% nano-silica content were similar to each other.

Omar *et al*. (2018) studied moisture performance of asphalt mixtures containing 2 and 4% nanoclay. The mixtures were tested through boiling water test, Vialit adhesion test, surface free energy (SFE) test, and ITS tests. Boiling water and Vialit adhesion tests showed that addition of nanoclay improved adhesion between aggregates and the binder compared to the control mix. Addition of nanoclay improved the SFE of binders and therefore resulted in better resistance to water damage. This improvement was attributed to the presence of both positive and negative charges on nanoclay, which improved the polarity of the modified binder.

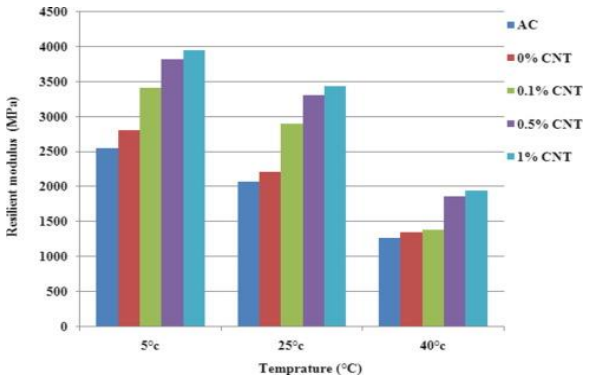

Fig. 5 Resilient modulus results at 5, 25 and 40 °C (Arabani and Faramarzi, 2015)

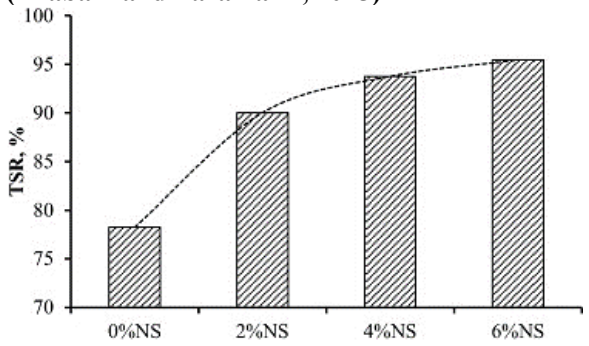

Fig. 6 TSR results of nanosilica-modified asphalt mixtures (Enieb and Diab, 2017)

Latifi and Hayati (2018) evaluated HMA mixtures containing CNT in the dosages of 0, 0.5, 1 and 2% by weight of the binder. A PG 64-22 binder was used as the control binder. Two mixing methods were used to disperse CNT in the asphalt binder: simple high shear mixing; and wet process using kerosene as dispersing agent. Based on SEM images, wet mixing technique found to be more efficient in dispersion of CNT in the asphalt binder. Performance of mixtures was evaluated through ITS, resilient modulus test and indirect tensile fatigue test. ITS results showed that the addition of 1% CNT increased the ITS by 17% compared to the control mix. Higher ITS values indicate more resistance towards cracking. The reason for the improvement in ITS with CNT addition was attributed to reinforcement of asphalt with CNT and development of resisting tensile force at the moment of crack formation. The authors also observed increase in resilient modulus and the increment was more prominent at the low test temperature (5 °C). High Young's modulus of CNT was considered as the reason for improvement in resilient modulus of the asphalt mixtures. Results of indirect tensile fatigue test showed that CNT modification resulted in fatigue life of nano-modified mixtures that were almost twice that of the control mixture. Fatigue life increased with increment in the CNT dosage.

Yao *et al*. (2013) characterized the performance of asphalt mixtures containing nano silica (4% and 6% by wt. of neat binder) with the help of dynamic modulus, flow number, and APA rutting tests. The mixtures containing nano-silica exhibited almost 30% higher dynamic modulus than the control mixture (without nanosilica). This indicated improved resistance of nano-modified asphalt mixtures towards permanent deformation relative to the control mixture. The improvement was attributed to strengthened bonding connections between aggregates and the nano-modified asphalt binders, as determined from micro-structural observations. Results of APA rutting test showed that nanosilica modified asphalt mixture had lower rut depths after 8000 cycles than the control mixture, and rut depth of the mixture with 6% nanosilica was lower than the mixture with 4% nanosilica.

Taherkhani *et al*. (2017) investigated the effects of two nano-material namely nanosilica (1, 3, and 5%) and zyco-soil (0.1, 0.3, and 0.5%) on engineering properties of asphalt mixtures. The performance of nano-modified mixtures was analysed based on ITS test, resilient modulus test, and dynamic creep test. ITS values of dry and moisture conditioned specimens were higher for nano-modified mixtures compared to the control mix. The values increased with increase in nanosilica and zyco-soil content. TSR results showed that the nano-modified mixtures had higher resistance to the effect of moisture, with a better performance by zyco-soil than nanosilica. Resilient modulus results showed that nanosilica was more effective than zyco-soil in improving the stiffness of asphalt mixtures. It was reported that the high specific surface area of nanosilica particles resulted in a high interaction with the asphalt binder leading to higher stiffness. In the dynamic creep test, accumulated vertical strain of the mixtures decreased with increase in nanosilica content, indicating an improved rutting performance. Increase in nanosilica content also increased the primary creep region and the flow number.

6 ENVIRONMENTAL BENEFITS WITH THE USE OF NANO-MATERIALS

6.1 Photocatalytic pavement

Photocatalytic pavement is a remarkable technology towards a sustainable and environment-friendly road construction. The main ingredient for the technology is nano-titanium dioxide (TiO_2). Titanium dioxide is an N-type intrinsic semi-conductor. It has the ability to oxidize harmful air pollutants like oxides of nitrogen (NO and NO_2), sulphur dioxide and volatile organic compounds (VOC) in presence of sunlight. Nano TiO_2 can be incorporated into pavement by spraying its solution over the pavement surface or by modifying asphalt with nano TiO_2. Hassan *et al*. (2012) showed that using surface spray coating, TiO_2 was effective in removing NO_x pollutants from air stream with an efficiency of 31–55%. The maximum NO_x removal efficiency was achieved at an application rate of 0.05 L/m^2. The SO_2 reduction efficiency was 19.8% with the coverage rate of 0.05 L/m^2. Osborn and co-workers (2013) investigated the durability of surface coating of nano TiO_2 on concrete and asphalt pavements. After extensive studies, it was suggested that the durability of TiO_2 in concrete pavements is between 6 and 11 months and is between 10 and 16 months in asphalt pavements. Nano ZnO can also be applied as a photocatalytic material as it has nearly similar properties and semiconductor band-gap as that of nano-TiO_2 (Segundo *et al.*, 2018).

6.2 Overcoming the drawbacks of Warm Mix Asphalt (WMA)

In comparison to HMA, WMA mixtures can reduce energy consumption and emissions by significant amounts due to production of asphalt mixes at lower temperatures. But lower mixing and compaction temperatures may also result in incomplete drying of aggregates making the mixes prone to moisture-induced damages, localized bleeding and formation of potholes. Abdullah *et al*. (2016) showed that use of nano-additives like nano-clay can effectively improve the moisture damage resistance of WMA mixes and hence facilitate environment friendly pavement construction through WMA. It was also attempted to measure gaseous pollutants produced during the manufacture of the WMA mixtures modified with nano-clay and a chemical WMA additive. As compared to chemical additives, nano-clay (4%) showed much more potential to reduce the gaseous pollutants like CO_2, SO_2, *etc*. Nano-hydrated lime is another widely used additive for enhancement of performance WMA mixes against different distresses.

7 COST ASPECTS OF THE USE OF NANO-MATERIALS

The cost of nano-materials depend upon their abundance, process of manufacturing and stability over the time. Naturally abundant materials that can be easily produced at nano scale have relatively low cost. The stability factor also influences the price of nano-material. The nano-materials generally have a tendency to agglomerate, therefore a more stable material costs less compared to a relatively unstable material. This is because unstable materials require further processing to improve the stability, which may increase their cost. Based on Indian market analysis, the cost of nano-silica is Rs. 250-1000/kg, the cost of nano zinc oxide is Rs. 3000-4000/kg. Different nano-clays have a price range of Rs 1000-5000/kg. Other nano-materials such as carbon nano-tubes have comparatively much higher price as the technology utilized for their synthesis is highly intensive. Carbon nano-tubes have enormous applications in other fields such as manufacturing of bulletproof jackets, antennas for radio and other electromagnetic devices, *etc*. Multiwall carbon nano-tube cost around Rs. 450/gm, while the price of single walled carbon nano-tube goes up to Rs. 1500/gm.

8 SUMMARY AND CONCLUSIONS

Application of nano-materials in modification of asphalt binders and mixes has been recently introduced and is rapidly gaining momentum. Various nano-materials having different physio-chemical characteristics have been employed for asphalt binder modification to achieve improved performance properties. This paper presents a review of research efforts made towards performance of asphalt binders and mixes incorporated with several nano-materials. Major nano-materials covered in the review are carbon nano-tubes, nano-clays, and nano-silica. The following are the major findings from the study:

- Addition of nano-materials to asphalt binders increases the viscosity and also helps to improve the rutting characteristics.
- The positive effect of nano-material addition generally remains up to a certain dosage beyond which it may reduce.
- Nano-materials enhance aging resistance and resistance to moisture-induced damages of the asphalt mixes.
- Ensuring a uniform and homogeneous dispersion of the nano-modifier in asphalt binder is of paramount importance to realise the benefits of nano-modification. More research is needed to arrive at a simple, cheap, industry relevant, and rapid technique for nano-material dispersion in the asphalt binder.
- Use of nano-materials are also associated with several environmental advantages. Some nano-materials such as nano-TiO2 have photocatalytic properties by virtue of which they can trap and decompose air pollutants when added to asphalt binders. Addition of some nano-material can

exceptionally improve moisture damage resistance of warm asphalt mixes, and therefore it allows realisation of environmental benefits through the use of warm mix asphalt without compromising the moisture resistance of mixes on being produced at lower temperatures. The practical application of nano-material is still limited in the paving industry, especially in India. Recently, MoRTH also recommended the use of nano material zycotherm as an anti-stripping agent for bituminous mixes. Still, there is a long way to go forward in the direction of nano-modified asphalt materials.

REFERENCES

1) Abdullah, M. E., Hainin, M. R., Yusoff, N. I. M., Zamhari, K. A., and Hassan, N. (2016). Laboratory evaluation on the characteristics and pollutant emissions of nanoclay and chemical warm mix asphalt modified binders. Construction and Building Materials, 113, 488-497.
2) Amirkhanian, A. N., Xiao, F., and Amirkhanian, S. N. (2010). Evaluation of high temperature rheological characteristics of asphalt binder with carbon nano particles. Journal of Testing and Evaluation, 39(4), 583-591.
3) Aqel, A., El-Nour, K. M. A., Ammar, R. A., and Al-Warthan, A. (2012). Carbon nanotubes, science and technology part (I) structure, synthesis and characterisation. Arabian Journal of Chemistry, 5(1), 1-23.
4) Arabani, M., and Faramarzi, M. (2015). Characterization of CNTs-modified HMA's mechanical properties. Construction and Building Materials, 83, 207-215.
5) Ashish, P. K., and Singh, D. (2018). High-and Intermediate-Temperature Performance of Asphalt Binder Containing Carbon Nanotube Using Different Rheological Approaches. Journal of Materials in Civil Engineering, 30(1), 04017254.
6) Ashish, P. K., Singh, D., and Bohm, S. (2016). Evaluation of rutting, fatigue and moisture damage performance of nanoclay modified asphalt binder. Construction and Building Materials, 113, 341-350.
7) Enieb, M., and Diab, A. (2017). Characteristics of asphalt binder and mixture containing nanosilica. International Journal of Pavement Research and Technology, 10(2), 148-157.
8) Fini, E. H., Hajikarimi, P., Rahi, M., and Moghadas Nejad, F. (2015). Physiochemical, rheological, and oxidative aging characteristics of asphalt binder in the presence of mesoporous silica nanoparticles. Journal of Materials in Civil Engineering, 28(2), 04015133.
9) Hassan, M., Mohammad, L. N., Asadi, S., Dylla, H., and Cooper III, S. (2012). Sustainable photocatalytic asphalt pavements for mitigation of nitrogen oxide and sulfur dioxide vehicle emissions. Journal of Materials in Civil Engineering, 25(3), 365-371.
10) Jahromi, S. G., and Khodaii, A. (2009). Effects of nanoclay on rheological properties of bitumen binder. Construction and Building Materials, 23(8), 2894-2904.
11) Julaganti, A., Choudhary, R., and Kumar, A. (2017). Rheology of modified binders under varying doses of WMA additive–Sasobit. Petroleum Science and Technology, 35(10), 975-982.
12) Kumar, A., Choudhary, R., Kandhal, P.S., Julaganti, A., Behera, O.P., Singh, A., and Kumar, R. (2018). Fatigue characterisation of modified asphalt binders containing warm mix asphalt additives, Road Materials and Pavement Design, Published Online, DOI: 10.1080/14680629.2018.1507921
13) Latifi, H., and Hayati, P. (2018). Evaluating the effects of the wet and simple processes for including carbon Nanotube modifier in hot mix asphalt. Construction and Building Materials, 164, 326-336.
14) Omar, H. A., Yusoff, N. I. M., Ceylan, H., Rahman, I. A., Sajuri, Z., Jakarni, F. M., and Ismail, A. (2018). Determining the water damage resistance of nano-clay modified bitumens using the indirect tensile strength and surface free energy methods. Construction and Building Materials, 167, 391-402.
15) Osborn, D., Hassan, M., Asadi, S., and White, J. R. (2013). Durability quantification of TiO 2 surface coating on concrete and asphalt pavements. Journal of Materials in Civil Engineering, 26(2), 331-337.
16) Rahman, I. A., and Padavettan, V. (2012). Synthesis of silica nanoparticles by sol-gel: size-dependent properties, surface modification, and applications in silica-polymer nanocomposites—a review. Journal of Nanomaterials, 2012, 1-15.
17) Rocha Segundo, I. G. D., Dias, E. A. L., Fernandes, F. D. P., Freitas, E. F. D., Costa, M. F., and Carneiro, J. O. (2018). Photocatalytic asphalt pavement: the physicochemical and rheological impact of TiO2 nano/microparticles and ZnO microparticles onto the bitumen. Road Materials and Pavement Design, 1-16.
18) Santagata, E., Baglieri, O., Tsantilis, L., and Chiappinelli, G. (2015). Fatigue properties of bituminous binders reinforced with carbon nanotubes. International Journal of Pavement Engineering, 16(1), 80-90.
19) Steyn, W. J. (2009). Potential applications of nanotechnology in pavement engineering. Journal of Transportation Engineering, ASCE, 135(10), 764-772.
20) Taherkhani, H., Afroozi, S., and Javanmard, S. (2017). Comparative Study of the Effects of Nanosilica and Zyco-Soil Nanomaterials on the Properties of Asphalt Concrete. Journal of Materials in Civil Engineering, 29(8), 04017054.
21) Yao, H., You, Z., Li, L., Lee, C. H., Wingard, D., Yap, Y. K. and Goh, S. W. (2013). Rheological properties and chemical bonding of asphalt modified with nanosilica. Journal of Materials in Civil Engineering, 25(11), 1619-1630.
22) You, Z., Mills-Beale, J., Foley, J. M., Roy, S., Odegard, G. M., Dai, Q., and Goh, S. W. (2011). Nanoclay-modified asphalt materials: Preparation and characterization. Construction and Building Materials, 25(2), 1072-1078.

Growth of calcium carbonate crystals due to accelerated carbonation in cement matrix

Barbhuiya, S.A. [1] and Jennings, K.[2]

[1] Lecturer, School of Civil Engineering, University of Leeds, Leeds LS2 9JT, United Kingdom.
[2] Graduate Structural Engineer, ACOR MCE Consultants Pty Ltd, Perth, Australia

ABSTRACT

In this research cement paste samples were exposed to accelerated carbonation in carbonation chamber where CO_2 level was controlled at 5(±1)% and relative humidity was maintained at 67(±3)% for a period of up to 8 weeks. The growth of calcium carbonate crystals in cement matrix due to accelerated carbonation was studied using Scanning Electron Microscopy (SEM). The effects of these crystals on the nanomechanical properties of cement past were also studied using nanoindentation. Spherical crystals of vaterite were found in samples after 4 weeks of accelerated carbonation. After 8 weeks, calcite crystals characterised by blocky, rhombic structure were observed. Results of nanoindentation testing showed an increase in the frequency of elastic modulus values between 30-45GPa and hardness values between 0.3-2.4GPa.

Keywords: carbonation, nanoindentation, elastic modulus, hardness, calcite, vaterite, aragonite

1. INTRODUCTION

Carbonation is a widely studied phenomenon, often linked with the corrosion of steel reinforcement and macroscopic changes in concrete volume. There is no single reaction associated with carbonation; instead there are multiple reactions occurring at various rates depending on diffusivity, concentration of CO_2 and relative humidity. Calcium hydroxide (mineral name Portlandite) is the most chemically reactive mineral involved in the carbonation process and has been widely studied [1, 2]. The carbonation of C-S-H is quite a different process in comparison to the carbonation of calcium hydroxide. As C-S-H is an amorphous material, there is no defined crystal structure for calcium carbonate to precipitate onto and prevent from further carbonation; this means that C-S-H reaches a much higher degree of carbonation than calcium hydroxide [3]. Typically this reaction occurs once the sources of more reactive calcium hydroxide have been exhausted and leads to the formation of not only calcium carbonate but also silica gel [4]. The primary product of carbonation is calcium carbonate, which exists in three naturally occurring anhydrous polymorphs (vaterite, aragonite and calcite). Generally vaterite has a spherical shape, while aragonite has a needle like shape and calcite a blocky, cubic or rhombohedral shape.

Lilkov et al. (2016) [5] studied the carbonation of cement paste with the additions of clinoptilolite and silica fume during the early hydration (24 hours). It was found that the crystallization of calcite on the surface proceeds due to the reaction of calcium ions from the pore solution and CO_2 from air without the formation of portlandite and ettringite. It was reported that the compressive strength of carbonated concrete was more than the un-carbonated concrete [6]. The increase in density, strength, modulus of elasticity and shrinkage due to carbonation has also been reported by other researchers [7, 8].

The nanomechanical properties of hydrated cement paste are a relatively new topic of research, with very few studies pre-dating the year 2000. The reactions occurring at the nanoscale and the resulting material properties of the involved constituents can provide the information to understand how the cement gains its macroscopic strength. Nanomechanical testing can also serve to identify small weaknesses in the cement microstructure, which can be altered or substituted in order to improve the overall strength of the material. Constantinides and Ulm (2007) [9] characterised the nanomechanical properties of the various phases of cement paste and also identified four phases: low stiffness phase, low density C-S-H phase, high density C-S-H phase and portlandite phase. A study performed by Zugner et al., (2006) [10] on the nanomechanical properties of other crystals such as calcite, sodium chloride, crystalline lactose and sodium ascorbate displayed similarly high results for both hardness and Young's modulus. Calcite is, however, an intrinsically anisotropic mineral, which means its nanomechanical properties could vary depending on the direction of load application [11]. Other studies [12] used nanoindentation and found that calcite approximately exhibits a Young's modulus of 76.6 GPa and a hardness of 1.9 GPa.

Much of the literature on the nanomechanical

properties of calcite involves testing of large singular crystals with high purities. The calcite, which forms during the carbonation process, involves many smaller crystals, even nanocrystals, of calcite arranged in a far less organised structure. It is likely that these much smaller crystals will result in far lower mechanical properties than those recorded for pure crystals. The smaller, less organised crystals will more easily move past one another under the application of loading, moving into a more organised form and in turn resulting in lower nanomechanical properties. Aragonite and vaterite also have quite high nanomechanical properties. Katti et al., (2006) [13] reported the Young's modulus of aragonite to be between 60-80 GPa for large crystals found in Nacre, an important constituent of seashells. Just as with calcite, both aragonite and vaterite are likely to be affected by their small crystal presence within the carbonated cement.

An attempt has been made in this research to study the effects of carbonation on the growth of calcium carbonate crystals in cement matrix and their effects on nanomechanical properties of cement paste. The growth of crystals was studied using Scanning Electron Microscopy (SEM). The nanomechanical properties of hydrated cement paste before and after accelerated carbonation were studied using nanoindentation.

2 EXPERIMENTAL METHODS

2.1 Materials

Commercial Swan General Purpose Portland cement (Type GP) with normal consistency of 28.5% and specific surface area of 352 m^2/kg (blain fineness) was used. The chemical composition and physical properties of cement used in this study are reported in Table 1. The X-ray diffraction (XRD) analysis showed that cement had typical peaks of minerals alite, belite and ferrite.

Table 1. Chemical composition and physical properties of cement

Chemical composition	
Oxides	(%)
SiO_2	21.1
AI_2O_3	4.7
Fe_2O_3	2.8
CaO	63.8
MgO	2.0
Physical properties	
Particle size	25-40%≤ 7μm
Specific gravity	2.7-3.2
Surface area (m^2/kg)	352
Loss of Ignition (%)	2.4

2.2 Sample preparation

50mm cement paste cube samples were prepared using ordinary Portland cement (OPC) with a water-cement ratio of 0.4. The samples were cured for 16 hours before de-moulding. After remoulding the samples were placed in limewater with a 3g/L concentration of calcium hydroxide and allowed to cure for 28 days. The limewater serves the purpose of preventing the calcium hydroxide in the cement paste from leaching out during curing, which would otherwise alter the microstructure of the samples. After 28 days of curing, the samples were exposed to accelerated carbonation in a carbonation chamber. The CO_2 level was controlled at 5(±1)%. Relative humidity was maintained at 67(±3)% with a saturated solution of sodium nitrite. Four samples were removed and prepared for testing at two week intervals, following an initial exposure time of four weeks, resulting in samples being prepared for testing after 4, 6 and 8 weeks of exposure. Of the four samples; three were broken to measure the depth of carbonation; one was sectioned and prepared for SEM and nanoindentation.

Small cube samples of size 10 mm were cut from 50 mm cubes using Precision saw for nanoindentation testing. The samples were cast in Epoxy resin in plastic moulds. This was done in order to provide stability to the samples for grinding, polishing and nanoindentation. After 24 hours the samples embedded in hardened resin were removed from the moulds and ground using diamond carbide papers (52.2 μm, 35.0μm, 21.8μm and 15.3μm). The grinding was done in order to expose the surface of the samples, which were covered by resin. Once the surface was exposed impregnation was carried out to fill the voids and pores in the samples. This was done with a thin coat of Epoxy using vcauum chamber. After this, the samples were again ground using the diamond carbide papers. Finally, the polishing was done using decreasing sizes of Polycrystalline diamond suspensions (9μm, 6μm, 3μm and 1μm). The samples used for SEM were small broken pieces collected after 4, 6 and 8 weeks of accelerated carbonation.

2.2 Test methods

In order to measure the depth of carbonation, samples were broken into half using a mortar chisel and

mallet. Phenolphthalein indicator was sprayed on the broken face of the samples and the depth of carbonation was measured using Vernier callipers at the central point along each edge (Figure 1). As non-carbonated cement has a pH of around 13, phenolphthalein indicator shows up as a bright purple colour when applied to the surface. Tescan Mira3 (Brno, *Czech Republic)* Field Emission Scanning Electron Microscope (SEM) was used to microstructural changes in hydrated cement paste.

Nanoindentation was carried out using *Agilent Nano Indenter G200* (Keysight Technologies, Inc. Santa Rosa, USA). Controlled loads (0.5 mN and 1.0 mN) were applied in two cycles on the surface of the samples to induce localised deformation. A typical load-displacement curve is shown in Figure 2. The loads were kept constant for a period of 30 seconds at 0.5 mN and 1.0 mN before unloading. The unloading curve (displacements: 400-450 nm) was used to determine the reduced modulus and hardness values using equations based on the principles of elastic contact theory [14]. Altogether 8 grids with each grid having 40 indents were made with an indent spacing of 20 μm. This resulted 320 indents made on each sample. The elastic modulus and hardness were then statistically analysed to produce a frequency histogram.

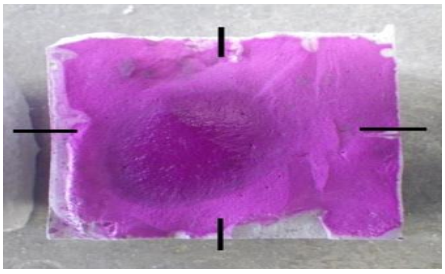

Figure 1. Typical measurement points for depth of carbonation.

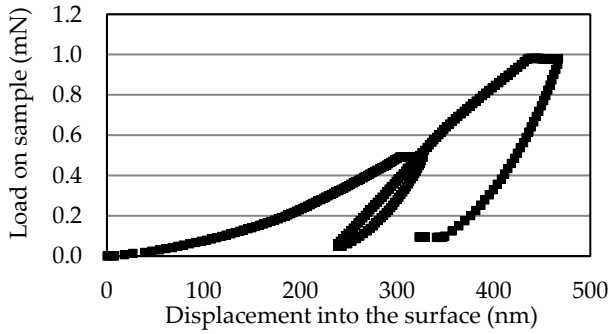

Figure 2. Typical load- displacement curve

3 RESULTS AND DISCUSSION

3.1 Growth of calcium carbonate crystals in cement matrix

The SEM images of the samples after 4 weeks of accelerated carbonation are shown in Figures 3 and 4. The crystals of portlandite are prevalent in the samples exposed for 4 weeks in accelerated carbonation (Figure 3). These crystals have been reported to become the growing platform for carbonation products such as calcite and aragonite due to their relatively large surface area and the high reactivity of calcium hydroxide [17]. The crystals of ettringite and C-S-H gel were also observed in the samples exposed for 4 weeks as can be seen in Figure 4. Figures 5 and 6 show the SEM images of the samples after 6 weeks exposure to accelerated carbonation. The crystals of ettringite can still be seen beneath the crystals of calcite, which are formed as a result of the carbonation process (Figure 5). Small amounts of spherical crystals of vaterite were present in the samples as well (Figure 6). Vaterite is a metastable polymorph and readily transforms into more stable calcium carbonate polymorphs (aragonite and calcite).

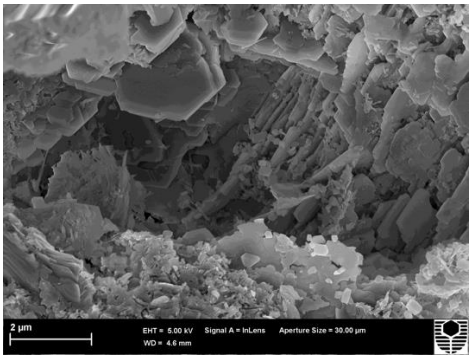

Figure 3. SEM showing crystals of portalndite (exposure period 4 weeks)

The SEM images of the samples after 8 weeks of accelerated carbonation are shown in Figures 7 and 8. The large crystals of calcite with small amounts of aragonite were present in the samples (Figure 7). Aragonite is another polymorph of calcium carbonate and is characterised by a needle like structure. Although aragonite is more stable than vaterite, it is still a metastable polymorph and readily transforms to the more stable polymorph calcite. The most commonly observed form of calcium carbonate is the stable polymorph calcite crystal as can be seen in Figure 8. Calcite is characterised by its blocky, rhombic structure, which was observed having a large size variation from approximately 0.25 μm to around 1 μm. The size variation of the observed calcite crystals may be due to the higher concentration of carbon dioxide used to accelerate carbonation forcing calcium carbonate to precipitate faster and therefore not allowing the

surrounding crystals time to grow.

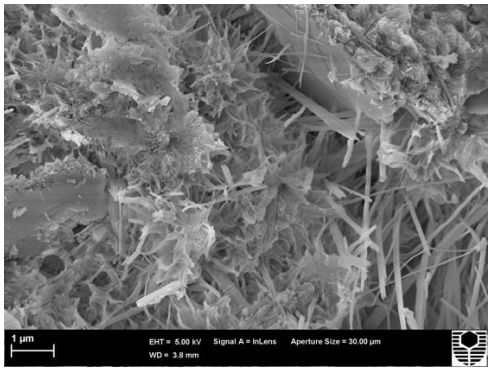

Figure 4. SEM showing crystals of ettringite and C-S-H gel (exposure period 4 weeks)

Figure 5. SEM showing ettringite beneath the crystals of calcite (exposure period 6 weeks)

Figure 6. SEM showing spherical crystals of vaterite (exposure period 6 weeks)

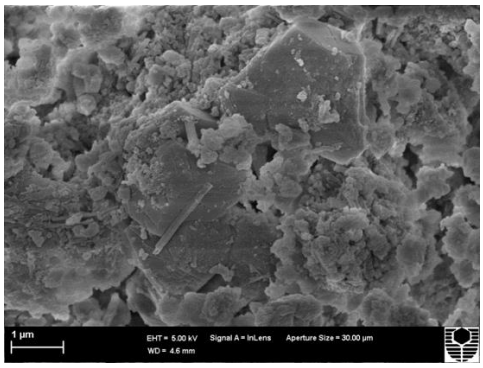

Figure 7. SEM showing crystals of calcite with small amounts of aragonite (exposure period 8 weeks)

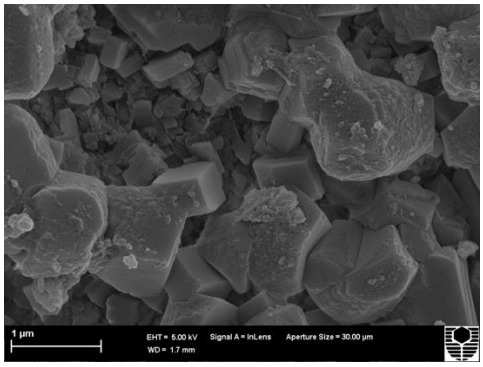

Figure 8. SEM showing crystals of calcite (exposure period 8 weeks)

3.2 Nanomechanical properties

The nanomechanical properties of samples before and after carbonation were extracted by statistically analysing the experimental data. The frequency plots (indentation moduli plotted against their probability of occurrences) of elastic modulus for samples before and after accelerated carbonation for a period of 8 weeks are shown in Figures 9 and 10, receptively. One particular observation, which was especially apparent in the samples exposed to accelerated carbonation, was the development of a small group of results with a elastic modulus value of between 30-45GPa. This group of results possibly signifies the precipitation of calcium carbonate polymorphs mainly calcite and aragonite. It has to be mentioned here that it was not the intention of this study to determine the elastic modulus of these individual crystals. The intention was to find out the difference in the modulus values of other phases due to the growth of these crystals in cement matrix as a result of carbonation.

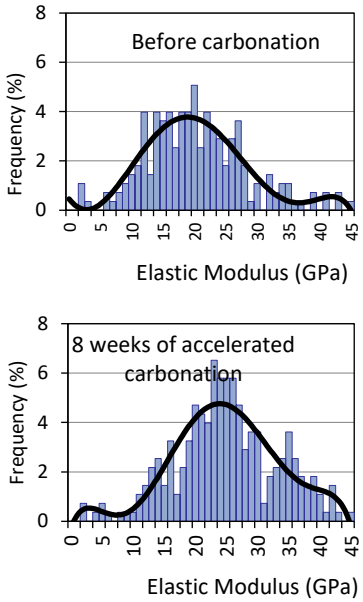

Figure 9. Frequency plot of elastic modulus

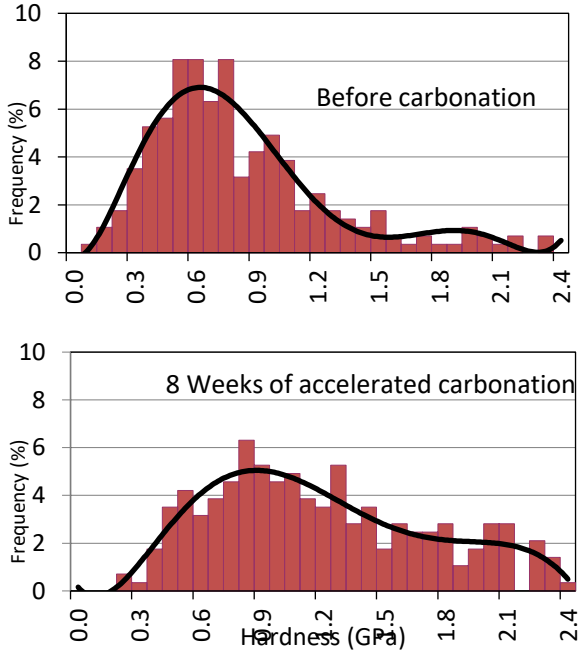

Figure 10. Frequency plot of hardness

A comparison of the data from nanoindentation with the microstructural observations from SEM discussed in the previous section suggests that calcite, the most abundant polymorph of calcium carbonate, precipitated within the pore structure of the cement paste, reducing the porosity of C-S-H gel and therefore increasing the average nanomechanical properties. This is supported by the colloidal model of C-S-H presented earlier; as the strength variation between the high and low density phases is dependent on the inter-particle contact points between the C-S-H nanoparticles.

4 CONCLUSIONS

The growth of calcium carbonate crystals in cement matrix due to accelerated carbonation was studied in this research using SEM. It was found that small amounts of spherical crystals of vaterite were present in the samples after 4 weeks of accelerated carbonation. After 8 weeks of accelerated carbonation, calcite crystal, the stable polymorph form carbonates, was observed. This was characterised by blocky, rhombic structure, with a large in size variation from approximately 0.25 µm to around 1 µm. Nanoindentation analysis showed an increase in the frequency of elastic modulus values between 30-45GPa and hardness values between 0.3-2.4GPa. This is due to the formation of calcium carbonates crystals within cement matrix, which strengthens the structure of C-S-H gel by increasing the inter-particle contact points. Further investigation into the implications of the observed variation in calcium carbonate crystal size on the nanomechanical properties of cement paste should be undertaken.

REFERENCES

1) Montes-Hernandez G.; Renard F.; Geoffroy N.; Charlet L.; Pironon J. Calcite precipitation from CO_2–H_2O–$Ca(OH)_2$ slurry under high pressure of CO_2. J. Cryst. Growth. 2007. *308(1)*: 228-236.
2) Regnault O.; Lagneau V.; Schneider H.; Experimental measurement of portlandite carbonation kinetics with supercritical CO_2. Chem. Geol. 2009. *265(1)*: 113-121
3) Thiery M.; Faure P.; Morandeau A.; Platret G.; Patrick Dangla J.F.; Baroghel-Bouny V. Effect of carbonation on the microstructure and moisture properties of cement-based materials" XII DBMC (12th International Conference on Building Materials and Components, 2001
4) Black L.; Garbev K.; Gee I. Surface carbonation of synthetic CSH samples: a comparison between fresh and aged CSH using X-Ray photoelectron spectroscopy. Cem. Conc. Res. 2008. *38(6)*: 745-750
5) Lilkov V.; Petrov O.; Kovacheva D.; Rostovsky I.; Tzvetanova Y.; Petkova V.; Petrova N. Carbonation process in cement with mineral additions of natural zeolite and silica fume – Early hydration period (minutes) up to 24 hours. *Const. Build. Mater.* 2006, *124*, 838–845
6) Xiao J.; Li J.; Zhu B.; Fan Z. Experimental study on strength and ductility of carbonated concrete elements. *Const. Build. Mater.* 2002, *16(3)*, 187-192.
7) Jerga J. Physico-mechanical properties of carbonated concrete. Const. Build. Mater. 2004, 18(9) 645-652.
8) *Chang, C.F.; Chen J.W.* Strength and Elastic Modulus of Carbonated Concrete, *ACI. Mater. J.* 2005, 102(5), 315-321.
9) Constantinides G.; Ulm F.J. The nanogranular nature of C–S–H. J. Mech. Phys. Solids. 2007. *55(1)*: 64-90.
10) Zügner S.; Marquardt K.; Zimmermann I. Influence of nanomechanical crystal properties on the commination process of particulate solids in spiral Jet Mills. Eur. J. Pharm Biopharm. 2006. *62(2)*: 194-201

11) Anderson P.M.; Hsieh S.; Wu M.K.; Chuang T.J. Nanomechanics of materials and structures: Springer. 2006.
12) Presser V.; Gerlach K.; Vohrer A.; Nickel K.G.; Dreher W.F. Determination of the elastic modulus of highly porous samples by Nanoindentation: a case study on Sea Urchin spines." J. Mater. Sci. 2010. *45(9)*: 2408-2418.
13) Katti K.S.; Mohanty B.; Katti D.R. Nanomechanical properties of Nacre. J. Mater. Res. 2006. *21(05)*: 1237-1242.
14) Fischer-Cripps, A.C. Critical review of analysis and interpretation of nanoindentation test data. *Surf. Coat. Technol*. 2006, *200(14–15*), 4153-4165.
15) Morandeau A.; Thiery M.; Dangla P. Investigation of the carbonation mechanism of CH and CSH in terms of kinetics, microstructure changes and moisture properties. Cem. Conc. Res. 2014. *56*: 153-170
16) Hyvert N.; Sellier A.; Duprat F.; Rougeau P.; Francisco P. Dependency of C–S–H carbonation rate on CO_2 pressure to explain transition from accelerated tests to natural carbonation." Cem. Conc. Res. 2010. *40(11)*: 1582-1589
17) Yang T.; Keller B.; Magyari E.; Hametner K.; Günther D. Direct observation of the carbonation process on the surface of calcium hydroxide crystals in hardened cement paste using an Atomic Force Microscope. J. Mater. Sci. 2003. *38(9)*: 1909-1916.

Mix design of self compacting concrete

Sonowal, D.B. [1], Banerjee, S. [2], Sarkar, G. [2], Bhushan, A. C. [2] and Tetarwal, R.[2]

[1] Assistant Professor, Department of Civil Engineering, Tezpur University, Napam, Tezpur 784028, India.
[2] Student, Department of Civil Engineering, Tezpur University, Napam, Tezpur 784028, India.

ABSTRACT

Self-compacting concrete (SCC), a new kind of high performance concrete (HPC) with excellent deformability and segregation resistance, was first developed in Japan in 1986. It is a special kind concrete that can flow through and fill the gaps of reinforcement and corners of the different structural members without any need for vibration and compaction during the placing process. But, the design of SCC is always a challenging task and since it is affected by the characteristics of materials and the mix proportions; it becomes necessary to evolve an effective procedure for mix design of SCC. The work presented here is an experimental study to set up a new and easy procedure for the design mix of self-compacting concrete using IS: 10262:1982 and IS: 10262:2009 both and to setup a detailed calculation of the amount of materials required along with the paste of binders to fill into the voids of aggregates to ensure that the SCC thus obtained has the flow ability, self-compacting ability and other desired SCC properties. The amount of aggregates, binders and mixing water, as well as type and dosage of superplasticizer (SP) to be used are the major factors that influencing the properties of SCC. However utilization of high reactive silica fume as a mineral admixtures which causes great improvement in the pore structure. The test results for acceptance characteristics of self-compacting concrete such as slump flow; V-funnel and L-Box are presented here. Further, compressive strength at the ages of 7, 28, and 56 days was also determined and results are discussed here.

Keywords: self-compacting, compressive strengths, superplasticizer, silica fumes, slump flow, V-funnel, L-box

1. INTRODUCTION

Self-compacting concrete (SCC), a new kind of high-performance concrete (HPC) with excellent deformability and segregation resistance, was first developed in Japan in 1986. It is a special kind concrete that can flow through and fill the gaps of reinforcement and corners of molds without any need for vibration and compaction during the placing process. Though showing good performance, SCC is different from the HPC, which emphasizes on high strength and durability of concrete. In terms of workability, HPC merely improves fluidity of concrete to facilitate placing; however, it cannot flow freely by itself to pack every corner of molds and all gaps among reinforcement. In other words, HPC still requires vibration and compaction in the construction process. Comparatively, SCC has more favorable characteristics such as high fluidity, good segregation resistance and the distinctive self-compacting ability without any need for vibration during the placing process.

In 1993, Okamura proposed a mix design method for SCC. His main idea was to conduct first the test on paste and mortar in order to examine the properties and compatibility of superplasticizer (SP), cement, fine aggregates and Pozzolanic materials, then followed by the trial mix of SCC. The major advantage of this method is that it avoids having to repeat the same kind of quality control test on concrete, which consumes both time and labor. However, the drawbacks of Okamura's method are that it requires quality control of paste and mortar prior to SCC mixing, while many ready-mixed concrete producers do not have the necessary facilities for conducting such tests and the mix design method and procedures are too complicated for practical implementation.

Then china started to develop the SCC. The principal consideration of the Chinese Method is that the voids of the aggregate are filled with paste (cement, powder, water). The voids need to be filled with paste so that a workable fresh concrete is attained. The Chinese Method starts with the content of aggregate, which greatly influences the workability. Subsequently, the amount of cement is assessed.

As said, the main consideration of the Chinese Method is that voids present in loose aggregate are filled with paste, and that the packing of the aggregates is minimized. But all the methods and procedures are only use for specified types of materials not for general case and that's why we follow the mix design procedure of IS: 10262:1982 and 2009 to implement it easily as much as possible.

1.1 Mix Proportions

A total of 12 concrete mixtures were designed and tabulated in table no. 1 at water cement ratio of 0.36, 0.4 and 0.45 with total cementitious materials content range may be vary based on the replacement of silica fumes at different levels. The replacement ratios of silica fumes are 20%, 25% and 30%

1.2 Selection of mix proportions

The following data are required for mix proportioning of a particular grade of concrete-

i. Maximum nominal size of aggregate.
ii. Minimum cement content.
iii. Maximum water-cement ratio.
iv. Slump flow value.
v. Exposure conditions as per Table 4 and Table 5 of IS 456 (2000).
vi. Maximum temperature of concrete at the time of placing.
vii. Method of transporting and placing.
viii. Early age strength requirements, if required.
ix. Type of aggregate.
x. Maximum cement content.
xi. Whether an admixture shall or shall not be used and the type of admixture and the condition of use.

1.3 Research Implication

A simplified and easy method of design for SCC has been developed on the basis of IS 10262:2009.

1.4 Outline of the paper

This paper includes the selection of mix proportions for SCC from the relevant literature, the experimental study, material properties, evaluation of SCC mix design and conclusions.

2 EXPERIMENTAL STUDY

2.1 Experimental program

In this study, trials have been carried to design a SCC mix having 30%, 25% & 20% replacement of cement with Silica fumes and 0.36, 0.4, 0.45 water/cement ratio (by weight). Crushed granite stones of size 20mm and 10mm are used with the blending 60:40 by percentage weight of total coarse aggregate.

2. 2 Material properties

This section contains the chemical and physical properties of the ingredients. Bureau of Indian Standards (IS) procedures were followed for determining the properties of the ingredients in this study.

2.2.1 Cement

Ordinary Portland Cement 43 grade was used corresponding to IS-8112(1989).The specific gravity of cement is 3.08.

2.2.2 Coarse Aggregate

Crushed stones of size 20mm and 10mm are used as coarse aggregate. As per IS: 2386 (Part III)-1963 [8], the bulk specific gravity in oven dry condition and water absorption of the coarse aggregate are 2.65 and 0.3% respectively. The coarse aggregate blending is 60:40 (20mm and 10mm) as per IS: 2386 (Part III)1963 [8].

2.2.2 Fine Aggregate

Natural river sand is used as fine aggregate. As per IS: 2386 (Part III)-1963 [8], the bulk specific gravity in oven dry condition of the sand is 2.63.

2.2.3 Chemical Admixtures

MasterEase 3603 is used as high performance super plasticizer having specific gravity of 1.15

2.2.4 Mineral Admixture

Silica fume of specific gravity 2.23 is used as mineral admixture.

2.2.5 Water

Ordinary treatment plant supply water.

3. DESIGN OF SSC

3.1 Detailed steps for SCC mix design

Procedure for concrete mix design requires following step by step process:

i. Data for Mix Proportioning.
ii. Selection of water-cement ratio.
iii. Selection of water content.
iv. Calculation of cementitious material content.
v. Estimation of coarse aggregate proportion.
vi. Estimation of fine aggregate proportion.
vii. Trial mixes for testing concrete mix design strength.

3.2 Data for mix proportioning

The following data are required for mix proportioning of a particular grade of concrete-

i. Maximum nominal size of aggregate.
ii. Minimum cement content.
iii. Maximum water-cement ratio.
iv. Slump flow value.
v. Exposure conditions as per Table 4 and Table 5 of IS 456 (2000).
vi. Maximum temperature of concrete at the time of placing.
vii. Method of transporting and placing.
viii. Early age strength requirements, if required.

ix. Type of aggregate.
x. Maximum cement content.
xi. Whether an admixture shall or shall not be used and the type of admixture and the condition of use.

4. CALCULATIONS OF MIX PROPORTIONS

The detailed steps for calculation of mix proportions are presented below with an example.

4.1 Stipulation for proportions

Type of cement=OPC 43
Nominal maximum size of aggregate=10 mm
Exposure condition=Moderate
Degree of supervision=Good
Type of aggregate=Crushed angular aggregate
Chemical admixture used=Plasticizer of specific gravity 1.15

4.2 Test data for materials

Cement OPC 43
Specific gravity of Cement 3.15
Chemical admixture 1.15
Specific gravity
i. Coarse aggregate2.65
ii. Fine aggregate2.63
Water absorption
i. Coarse aggregate= Nil
ii. Fine aggregate= Nil
Free surface moisture
i. Coarse aggregate=Nil
ii. Fine aggregate=Nil

4.3 Gradation

Zone III (Table 4 of IS 383-1970)

4.4 Selection of Water Cement ratio

Max. w/c ratio=0.45
Selected w/c ratio=0.36

4.5 Selection of water content

From Table 2, IS456-2000
Maximum water content for 10 mm =208 L (for 25-50 mm slump)
For 200mm slump, water content=244 L
Plasticizers can reduce water upto 22%
So, Water content arrived=244×0.78L =190 L

4.6 Calculation for cement content

w/c ratio =0.36
Cement content =529 kg/m^3
.

4.7 Proportion of volume of coarse and fine aggregates

For w/c-0.5 and Zone III, Volume of coarse aggregate (±0.01 for every ±0.05 change in w/c ratio)=0.48
Therefore, for w/c-0.45
Volume of coarse aggregate=0.505×0.9=0.46
Volume of fine aggregate=0.54

4.8 Mix Calculations

a) Volume of concrete = 1m^3
b) Volume of cement = 0.1678 m^3
c) Volume of water = 0.190 m^3
d) Volume of Plasticizer(@2% by mass of cementitious material) = 0.009 m^3
e) Volume of all in aggregate =0.633 m^3
f) Mass of coarse aggregate = e ×Vol. of coarse aggregate×G_s ×1000 =766 kg
g) Mass of fine aggregate = e ×Vol. of fine aggregate×G_s ×1000 = 903 kg

4.9 Final Mixing Proportions

Cement	= 396.75 kg/m^3
Silica fume	= 132.25 kg/m^3
Water	= 190 kg/m^3
Super plasticizer	= 10.57 kg/m^3
Coarse Aggregate	= 766 kg/m^3
Fine aggregate	= 903 kg/m^3
w/c ratio	= 0.36

4.10 Test Result

The following mix design was performed and the following values of the tests were obtained-

Slump Flow	820 mm
L-box	H_1=84 mm , H_2=100 mm
V-funnel	9.1 secs

4.11 Mix design proportioning of different combinations

Table 1. Trials for Mix Design.

Trial	Cement kg/m^3	Silica kg/m^3	C.A. kg/m^3	F.A kg/m^3	Water kg/m^3	Admix. kg/m^3	w/c
1	444	---	740	930	210	8.88	0.45
2	355.2	88.8	740	930	210	8.88	0.45
3	333	111	740	930	210	8.88	0.45
4	310.8	133.2	740	930	210	8.88	0.45
5	525	--	733	888.9	200	10.4	0.40
6	420	105	733	888.9	200	10.4	0.40
7	393.75	131.25	733	888.9	200	10.4	0.40
8	367.5	157.5	733	888.9	200	10.4	0.40
9	529	--	766	903	200	10.57	0.36
10	423.2	105.8	766	903	190	8.88	0.36
11	396.75	132.25	766	903	190	10.57	0.36
12	370.3	158.7	766	903	190	10.57	0.36

Table 2. Compressive strength of SCC w/c=0.45

Trail No	Percentage Silica	7 days strength (MPa)	28 days strength (MPa)	56 days strength (MPa)
1	0	7.56	14.22	22.22
2	20	8.44	15.11	24.89
3	25	8.89	15.56	25.77
4	30	9.33	16	26.22

Table 3. Compressive strength of SCC w/c=0.40

Trail No	Percentage Silica	7 days strength (MPa)	28 days strength (MPa)	56 days strength (MPa)
5	0	10.67	17.78	28.89
6	20	11.56	18.67	30.67
7	25	12	19.11	32
8	30	12.44	19.56	32.89

Table 4. Compressive strength of SCC w/c=0.36

Trail No	Percentage Silica	7 days strength (MPa)	28 days strength (MPa)	56 days strength (MPa)
9	0	12.89	22.22	38.22
10	20	13.78	23.56	40.44
11	25	14.67	25.33	42.67
12	30	15.11	25.78	47.11

5. CONCLUSIONS

Errors in the past will dictate the design of the future. Until now, there is no standard procedure to design self-compacting concrete that will yield a high compressive strength and reasonable workability. Therefore, continuous research is being carried out by researchers throughout the globe to develop a range of new results that will yield a functional design.

Mix design of SCC provided additional information regarding selection of appropriate water cement contents, size of aggregates. The purpose of our research work is to design and perform tests on self-compacting concrete

Initially all the materials are tested and the specific gravity of cement, admixture, fine and coarse aggregates, grain size distribution curve, zoning of fine aggregates, fineness modulus of coarse aggregates are determined. The compatibility study of the chemical admixtures with cement is then analyzed. Efficiency of admixtures is then calculated.
Then mix design of self-compacting concrete is done without mineral admixtures and by replacing cementitious materials with mineral admixtures i.e. silica fumes. After the SCC is prepared the L-box, V-funnel and Slump flow tests are performed for the quality check of self-compacting concrete.
Finally the interrelationship between w/c ratios, percentage of mineral admixture replaced with cement, curing and compressive strength is studied.

- From this study we can say that self-compacting concrete can also designed by modifying the Indian Standard Codes for Concrete Mix Proportioning.
- Chemical admixtures play a vital role in self-compacting concrete. The fluidity of the mix is actually created by the chemical admixtures.
- The L-box test for SCC cannot be passed with greater size of aggregates, generally 12.5mm and 10mm aggregates are preferred.

- To attain higher slump flow values of SCC i.e. to increase the filling ability the water content should be increased.
- From the results obtained, we can say that by addition of mineral admixtures like silica fumes we can increase the compressive strength of SCC to a significant amount.
- For self-compacting concrete rather than conventional concrete, the curing period required is more. As we can see that even after 28 days of curing, the compressive strength increases by significant amount.

REFERENCES

1) Nagamoto N., Ozawa K., Mixture properties of Self-Compacting in Concrete Technology, SP-172, V. M. Malhotra, American Concrete Institute, Farmington Hills, Mich. 1997, p. 623-637.
2) Okamura, H. (1997). Self-Compacting High-Performance Concrete, Concrete International, pp.50-54.7.
3) EFNARC, (2002). Specifications and Guidelines for Self-Compacting Concrete, EFNARC, UK (www.efnarc.org), pp. 1-32.
4) Japanese Society of Civil Engineering, Guide to Construction of High Flowing Concrete, Gihoudou Pub., Tokyo, 1998 (in Japanese).
5) IS: 3812-2003, Specifications for Pulverized fuel ash, Bureau of Indian Standards, New Delhi, India.
6) IS 10262:2009 Concrete Mix Proportioning – Guideline, Bureau of Indian Standard, Delhi, pp 1-11
7) Indian standard Part III, Method of test for soil, Bureau of Indian Standard, Delhi, IS 2720: 1980 Part III
8) Indian standard part III, Method of test of aggregate for concrete, Bureau of Indian Standard, Delhi, IS 2386:1963 Part III
9) IS:383-1970, Specification for coarse and fine aggregates from natural sources for concrete, Bureau of Indian Standard, Delhi, pp 6-11
10) IS 9103:1999, Concrete Admixtures: Specification, Bureau of Indian Standard, Delhi, pp. 1-14.
11) IS 456 : 2000- Plain And Reinforced Concrete – Code Of Practice (Fourth Edition), Bureau of Indian Standard, Delhi, pp 5-91

Study of better acoustic system for smart classroom by using some sound absorbing material

Rahman, M.[1], Patwari, N. N.[2]

[1] PG Student, Department of Civil Engineering, Assam Don Bosco University, Azara, Guwahati, Assam, India.
[2] Professor, Department of Civil Engineering, Assam Don Bosco University, Azara, Guwahati, Assam, India.

ABSTRACT

This paper deals with the acoustics of sound absorbing materials for reducing background noise and absorb the reflection of sound, generated inside the acoustic room. As such an open cell melamine based foam of 25mm thickness and cardboard paper box material as a construction material tried. For measurement of airborne sound insulation in buildings and of interior building elements have been standardized as per IS: 11050 (Part I)/ ISO 717/1. The sound reduction system for building has been used as precultivated sample system. The measurement and calculation have been regulated by ISO 140/3 by separation element between two different rooms, such as doors, glass window blocks. These tests are being analyzed in the transmission room. The source room has been sealed off with the sample made with cardboard paper box and open cell melamine based foam. The test is being done by generating sound signal frequency of 125 Hz to 3150 Hz in the source room and the sound levels in both the rooms (in one third octave bands) are measured using standardized sound meter application as per ISO 717/1. The technical calculation of weighted sound reduction index R_W has been found to be 18.76 dB as according to the formula given by ISO 140/3 standards.

Keywords: sound absorbing materials, airborne sound insulation, interior building elements, weighted sound reduction Index

1. INTRODUCTION

Development of sustainable urbanization to improve the quality of life for society with smartly planned and well executed with the ecological balance for urban environments, becomes an essential event. The development which takes place in the society needs to get right education and knowledge for the better use and inhibit in one's daily lifestyle and for upliftment of the society. The education and knowledge comes from an educational institute; so a proper smart green school is the basic requirement. The maximum time is invested in school from the

Lowest level till the highest degree of education; but the fact is that people are happy to invest in poorly designed places. The poor classroom acoustics can create a jumbled learning environment for many students, but the real fact is that children need to get good, clear signals, low background noise and less reverberant surface for getting better understanding in the education process. It is therefore important for the institute to have classroom with comfortable acoustics for all children in schools.

1.1 REQUIREMENTS OF SMART GREEN SCHOOL/ INSTITUTE

For a smart school the requirements which are to be fulfilled as per the guidelines given by IGBC are

a) Site Selection & Planning (such as Local Building Bye Laws, Top Soil Preservation, Eco-Friendly Commuting practices, parking capacity, greenery in campus, minimizing heat exposure to sun for both roof and non-roof),
b) Sustainable Water Practices (such as Rainwater Harvesting, water efficient plumbing fixtures, waste water treatment, water use monitoring),
c) Conserving & Harvesting Energy (such as energy efficient lighting, appliances and equipment, energy sub-metering, On site renewable energy, solar panel both for energy and water heater),
d) Eco- friendly school material (such as Waste Segregation, Green policy, Salvaged materials, Local materials),
e) Indoor Environmental Quality (such as Tobacco Smoke control, Minimum Day lighting, Fresh Air ventilation, Classroom Acoustics, Toxin free dust free environment, exhaust systems),
f) Health and Hygiene (such as Toilet Facilities, Drinking water facility, Minimum Sports Amenities, Dedicated Playground),
g) Green Education (such as Green School Committee, Green Extra-curricular Activities).

For this research paper we are concentrating on **Indoor Environmental Quality for Classroom Acoustics**.

Inclusion of sound acoustic absorbing materials as for better audible to every students present in the classroom, without any reflection of sound and the lessons taken by the teachers will be much clearer, loud and audible to every students from the first row till the last and every corner of the room.

1.2 Importance of classroom acoustics

a) Classroom acoustics are an important, but often neglected under design aspect of the learning environment. Mostly 60% of classroom activities which involve speech or lectures between teachers and students or between students, indicating the importance of environments that support clear communication. However, classrooms that have been constructed with poorly designed places for better engage students in activities or discussions that have often resulted in active, noisy environments.

b) Higher levels of background noise, more reverberation time which inhibit problems in reading and pronunciation ability, behavior, attention, concentration, and academic performance, children who develop language skills in poor acoustic environments may develop long term speech comprehension problems. Thus good classroom acoustics are a basic classroom need.

c) Using of sound-absorbing materials for classrooms has led to concerns about indoor air quality. However, good acoustical design and indoor air quality can be achieved when proper materials that are specified and maintained over time.

1.3 Objective

The objective of this paper is to focus on the use of sound absorbing materials and measurements of airborne acoustic insulation as per standard measuring instruments and following the ISO 717/1 , IS:11050(Part 1), IS:2526-1963 codes for acoustic system design of a smart classroom. The type of absorbing materials which will be used, are environment friendly, low cost and easily available in the market. The sample material which will be proposed to install at the acoustic room, will be evaluated by producing sound frequency of 125Hz to 3150 Hz and the sound reduction will be measured using a sound meter.

2 METHODOLOGY

For the evaluation of acoustic sound absorbing materials the measurement of airborne sound insulation in buildings and of interior building elements (such as a smart classroom) have been standardized as per is: 11050(part1)/ISO 717/1. The passive insulation of acoustic system for building was used as existing precultivated system. The system is based on waste material as cardboard which are being used for packing any items as a box and open cell melamine-based foam which is mainly found by the old sofas, or any other old and unused furniture which are generally being dumped, this material possess to be a good sound absorbing material as per IS: 2526-1963.

Hang, et al. (2011) established that by adjusting the size of absorbing particles and arranging their routes acoustic absorption properties of the room can be improved. In their research it was obtained that even if small air gap is present the open cell alloy foams with well graded pore size may exhibit better acoustic absorption properties.

Abdullah, et al. (2013) made a comparison of different thickness of foam materials and revealed that the thicker foam material produces better sound absorption from the lower to higher frequency.

2.1 MEASUREMENT OF AIRBORNE SOUND INSULATION

The measurement and calculation of the sound insulation properties of building elements is being regulated by ISO 140/3 standards. The separation elements is between two different rooms, such as doors, glass window blocks. These tests are being carried out in transmission rooms, depending on the analysis. The acoustic room has been sealed off with cardboard paper box and foam where the background noise has been reduced. During the test, a sound signal is generated in the acoustic room, and the sound levels in both of the rooms (one-third octave bands) are measured, as per ISO 717/1.

According to Azkorra,et al. (2015) the sound isolation and sound level difference curve for the tested partition is being obtained and is technically named as the Sound Reduction Index (R) of the analyzed building element, which depends on the frequency. The sample that was used consisted of modular precultivated units, representing an area of 4250mm wide by 1900mm high and 25mm thickness. The foam and cardboard box sample was inserted in a frame of glass and aluminum with air space of 20mm and sealed with sealing tape to fulfill the test requirement.

The Sound Reduction Index (R) for each one-third octave has been calculated which is defined in ISO 140/3. The expression for R is as follows:

$$\mathbf{R = L_1 - L_2 + 10 \log \left(\frac{S}{A} \right)} \qquad (1)$$

Where,

a) L_1 is average sound pressure in the source room

b) L_2 is the average sound pressure level in the receiving room,

c) S is the area of the sample, and

d) A is the equivalent sound absorption area in the receiving room

The average sound pressure levels L_1 and L_2 was measured by generating frequency noise (between 125 Hz and 3150 Hz) as per ISO 717/1

3. EXPERIMENTAL RESULTS AND DISCUSSIONS

The appropriate single number quantity shall be given with reference to the code ISO 717/1 The Sound Reduction Index (R) characterizes the sound insulating properties of a material or construction element in a stated frequency band test measurement, R is calculated according to ISO 140/3 by using Calibrated Sound Meter Application. The test were carried out at the 2nd floor of the building.

The condition under which the test was carried out were as follows:

a) Volume of the receiving room was 55.678 m^3

b) Volume of the source room was 41.438 m^3

c) Specimen sample area was 14.18 m^2.

The Weighted Sound Reduction Index (R_w) is a single number quantity that characterizes the airborne sound insulation of a material or constructive element over a range of frequencies. The R_w is calculated from R values according to ISO 717/1 standard and the calculation is being substituted in equation 1

Where

$L1$ = Average sound pressure level in the source room = 50 dB

L_2 = Average sound pressure level in the receiving room = 29.84 dB

S = the area of the sample = 14.385 m^2

A= Equivalent sound absorption area in the receiving room = 19.885 m^2

$$R= (50 – 29.84) + 10 \log \left(\frac{14.385}{19.885}\right)$$

R = 18.76 dB

Therefore it can be stated that the sound absorbing material which was being used for acoustics of the room, the calculated weighted sound reduction index **R_w = 18.76 dB**

The Sound Reduction Index (R) values from the test measurement are summarized in Table 1 , Fig.1 and Fig.2

TABLE 1. SOUND MEASUREMENTS

FREQUENCY	REFERENCE CURVE (L_1)	REDUCTION R CURVE (L_2)
125	36	20
250	45	20
500	52	30
1000	55	39
2000	56	35
3150	56	35

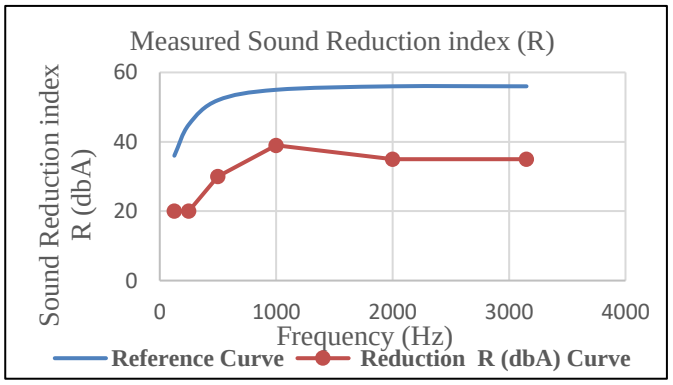

Fig. 1. Graphical Representation of Measured Sound Reduction Index (R).

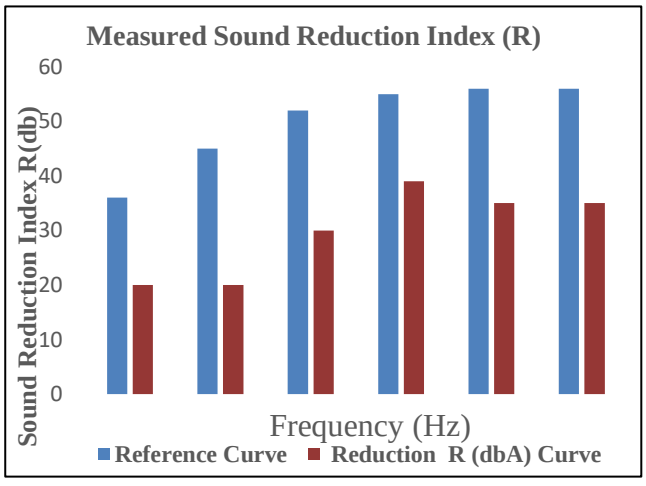

Fig. 2. Histogram representation of Measured Sound Reduction.

4. CONCLUSIONS

A smart green school gives proper education and knowledge, which plays an important role in

incorporating with the green education which implies with the development of the better green environment. The green school consists of classroom where the knowledge is being delivered, so a properly design places of classroom acoustics is one of the important factor for the better quality of education.

In this study, the use of environment friendly construction material is being used as a sound absorbing materials which is used as a passive acoustic insulation system for interior buildings was being evaluated as per the rules and guidelines given by the code ISO 717/1. The foam material which we have used are freely available materials from various households, as they are very new construction material system, it is necessary to obtain some datas which is about their acoustic properties, like sound absorbing coefficient which is being given in the code IS: 2526-1963, for the proper real time project there will be some costing for the purchasing of the materials depending upon the quantity of the material required for the project work.

Concentrating on the primary interest of the study we can conclude by stating that for a smart green school the classroom acoustic system can be achieved by using open cell melamine based foam as a construction sound absorbing material, even for the treatment of the existing classrooms acoustic can be improved by using the material.

REFERENCES

1) Huang, K., Donghri, Y., Siyuan, H., Deping, H. (2011) "Acoustic absorption properties of open cell Al-alloy foams with graded pore size", Journal of Applied Physics, Vol No- 44, pp.36-44.
2) Abdullah,M., Jamaluddin,L., Abdullah,A., Razak,R., Hussin,K. (2013) "Influence of Multilayer Textile Biopolymer Foam doped with Titanium Dioxide for Sound Absorption Materials", Key Engineering Materials, Vol No- 594, pp. 750-754.
3) Rahman, M., Patwari, N., Singh, N. (2018) "An Approach for a smart classroom with reference to comfortable Acoustic System", M-Tech Thesis, Assam Don Bosco University, pp. 1-43.
4) IGBC: Indian Green Building Council IGBC Green Schools Rating System, Reference Guide, Pilot Version.
5) IS: 11050 (Part 1) / ISO 717/1 : Rating of Sound Insulation in Buildings and of Building Elements for Airborne Sound Insulation of Interior Buildings Elements.
6) IS: 2526-1963 (Reaffirmed 2010) : Indian Standard Code of Practice for Acoustical Design of Auditoriums and Conference Halls.
7) Azkorra,Z., Perez,G., Coma,L., Bures,S., Alvaro,J., Erkoreka,A., Urrestarazu,M. (2015) "Evaluation of Green Walls as a passive acoustic insulation system", Elsevier, Journal of Applied Acoustics, Vol No- 89, pp.46-56.

An experimental study on the effects of river sand and rock quarry dust on quality of concrete

Kakoty, A. [1], Nath, U.K. [2] and Deka, G.[3]

[1] Assistant Professor, Department of Civil Engineering, Assam Kaziranga University, Jorhat-6, Assam, India.
[2] Associate Professor, Department of Civil Engineering, Assam Engineering College, Guwahati-13, Assam, India.
[3] Associate Professor (Retd.), Department of Geology, Assam Engineering College, Guwahati-13, Assam, India.

ABSTRACT

Modern construction industry is a massive industry growing at a very fast rate. So, the materials are also being used at a faster rate which takes a great toll on the natural resources. River sand is a prime material used for the preparation of concrete. But due to the extensive use of river sand, these deposits are exhausting very rapidly. This reduction in the sources of natural sand and the requirement for reduction in the cost of concrete production has resulted in the increased need to find new alternative materials to replace river sand so that excess river erosion is prevented and high strength concrete is obtained at a lower cost. One such alternative is Quarry dust, which is a by-product obtained during quarrying process. Due to the similarity in mineral composition and inertness in coarse grained structure, quarry dust can be used in various applications in place of river sand. The advantage of replacement of river sand by quarry dust is that the quarry dust generated is consumed, the requirement of land fill area is reduced and also the problem of natural sand scarcity is solved.

In this paper, an attempt has been made to examine the suitability of quarry dust as an alternative of river borne fine aggregate in concrete. The river sand samples and quarry dust samples are collected from Jorhat district of Assam. At first, the geological and engineering properties of both river sand and quarry dust are determined in the laboratory. Then concrete is prepared using quarry dust as a partial and total replacement of river borne aggregates to observe the effects of these aggregates on concrete. It is expected that the present study will benefit the quality of construction in this region. Although there are a good number of rivers in North-Eastern part of India, the aggregates of only some of the rivers are usable. The use of quarry dust in place of river sand would result not only in conservation of these natural resources but also help in maintaining good environmental conditions.

Keywords: river sand, concrete, quarry dust, replacement, suitability

1. INTRODUCTION

Concrete is the most important construction material in the world and one of the most significant constituents of concrete which plays a major role in improving its strength is fine aggregate. River sand is the main natural and cheapest resource of fine aggregate. But the growing use of river sand as a raw material in production of concrete and other industrial applications means that depletion of deposits of natural sand is inevitable.

In Jorhat district, various construction activities are going on at a very fast rate and river Bhogdoi is the only source of sand for construction purpose. Heavy collection of sand, particularly from the upper reach of its plain course has been taking place at an ever-increasing rate since the eighties. This has caused lowering of the river bed to a significant extent and steepening of the gradient of the river bed. Moreover it is important to note that the sand of river Bhogdoi is fine to medium and so the sand of only the upper reach of the river is used for light construction works and that of the lower reach is used for filling purposes. Hence for making high strength concrete, the river sand from Bhogdoi is not suitable. So the sand is collected from Kanaighat area of river Kaliani which is located in Golaghat district of Assam. This increases the transportation charges which are becoming costly day by day. Thus it has become necessary to locate an alternative source of locally available fine aggregate. The use of quarry dust which is a by-product of rock quarrying is a suitable option to substitute river borne fine aggregates. Large volumes of quarry dust are produced by rock quarrying industries which cause environmental problems. Only a little fraction of the quarry dust is used as filler in wearing courses of asphalt pavements. Using quarry dust as an alternative to river sand in concrete can provide solutions to problems of waste management, environmental degradation and depletion of natural resources.

In the present study, investigations have been conducted on utilisation of quarry dust as total or partial replacement of river sand in concrete. The compressive strength of quarry dust concrete with river sand concrete is compared using the same mix ratio, water/cement ratio, same quantity and type of cement, water and coarse aggregate.

2 REVIEW OF LITERATURE

Significant research was carried out on the use of quarry dust as a replacement of river sand and a few published works are reviewed in this section.

Opara et al. (2018) compared the physical and mechanical properties of river sand concrete with quarry dust concrete in terms of slump, density and compressive strength and concluded that both river sand concrete and quarry dust concrete can be applied in non-structural members and lightly-loaded members where high strength is not a prerequisite.

Jyothi et al. (2018) has done a comparative study on the use of Partial Replacement of Cement with Bagasse Ash and Fine Aggregate by Quarry Dust. They concluded that full replacement of quarry dust can slightly decrease the compressive strength compared to river sand. They also observed that Partial replacement of cement by Bagasse ash and full replacement of fine aggregate by quarry dust increases workability of fresh concrete; therefore use of super plasticizers is not substantial.

Geeta et al. (2018) in Kerala, carried out an investigation on the effect of saw dust and quarry dust on the quality of concrete and observed that the compressive strength has been increased for 50% replacement of quarry dust alone for a 28 days strength compared to the conventional mix. Hence by replacement of river sand by quarry dust and saw dust, the cost of construction will be minimized by effective utilization of waste product and also reduce the environmental effect.

Janardhanan et al. (2018) conducted an experimental study on cement concrete with PVC powder and quarry dust as partial replacement to fine aggregate. The analysis of experimental data showed that the addition of quarry dust improved the strength properties of concrete which was on par with that of conventional concrete. But when the quarry dust has high fineness, its usage in the normal concrete is limited because it increases the water demand

Agrawal et al. (2017) carried out some work on the utilization of Quarry Dust as Fine Aggregates in Concrete. They found that sand obtained from the river beds and the quarry dust obtained from the quarries has almost equal specific gravity but have a large variation in the water absorption. The water absorption of quarry dust was very high due to which the concrete mix prepared with higher proportion of quarry dust has very low workability.

Reddy et al. (2017) investigated the durability properties of concrete with partial replacement of sand by quarry dust and cement by fly ash. The results on strength and durability studies give a clear conclusion that Quarry Dust can be used as a good substitute for natural river sand and Fly Ash can be used as replacement for Cement with higher strength at 20% replacement, saving in cost of concrete and reducing the demand for sand.

Shyam Prakash et al. (2016) found that the replacement of natural fine aggregate by quarry dust could improve the utilization of generated quarry dust, thus reducing the requirement of land fill area and conserving the scarcely available natural sand sustainable development.

Priya et al. (2016) carried out an experimental investigation on partial replacement of fine aggregate by quarry dust in concrete with steel powder and found that under certain conditions, replacement of fine aggregate by quarry dust and addition of steel powder appeared to increase the strength of concrete. They found that the compressive strength is increased up to 40% replacement of quarry dust with 1% of steel powder. With 40 % replacement of quarry dust the value is increased over the conventional concrete, but decreased when increasing the percentage of replacement of quarry dust with steel powder.

However, no detailed and systematic engineering study has been carried out in Jorhat region with reference to the comparison of river sand and quarry dust on the quality of concrete. Under these circumstances, the present study is of utmost importance for future general purposes in this region.

3 OBJECTIVES OF STUDY

The main purposes of the project are as follows:

(i) To carry out a comparison between the geological and engineering properties of river borne fine aggregates and quarry dust.

(ii) To interpret the results to find their suitability as construction material.

(iii) To observe the effects of river sand and rock quarry dust on the quality of concrete.

4 MATERIALS AND METHOD

The river sand used in this work is collected from Kanaighat (Kaliani River) of Golaghat District, Assam. The quarry dust is collected from a quarry located in Mariani, Jorhat, Assam, India. The collected samples are brought to the laboratory and microscopic observation is performed to identify the various minerals present in the fine aggregate samples. Grading of aggregates is performed by the IS sieves as per requirements of the various tests. The laboratory tests performed on each of the samples for determining the engineering properties are as follows:

i. Moisture content
ii. Presence of organic impurities

iii. Specific gravity
iv. Water absorption
v. Bulking of sand
vi. Direct shear test
vii. Permeability
viii. Compaction.

Cement concrete is prepared using quarry dust as a replacement of river sand using M20. The combinations used for this study are:

i. Concrete with 100 % river sand
ii. Concrete with 100 % quarry dust
iii. Concrete with 50 % river sand and 50 % quarry dust

4 TEST RESULTS

4.1 Geological properties

The microscopic view of the river sand is shown in figure-1.

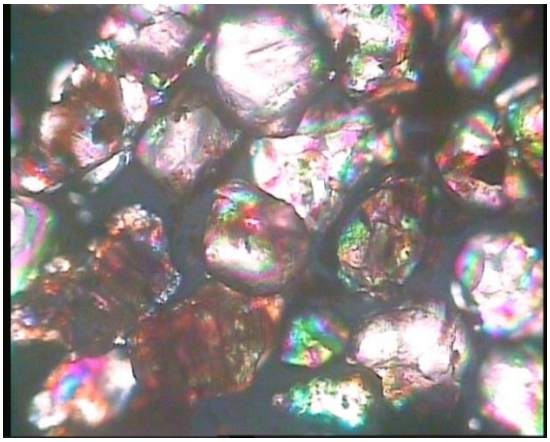

Fig. 1. Micro-photograph showing petrographic characteristics of river sand sample (x 25)

The microscopic view of the quarry dust is shown in figure-2.

Fig. 2. Micro-photograph showing petrographic characteristics of quarry dust (x 25)

The details of the minerals present in these aggregate samples are given in the table-1.

Table 1. Geological Properties of river sand and quarry dust

Sl. No.	Mineral constituent	Shape, Texture and colour	River sand	Quarry dust
1	Quartz	Rounded to sub rounded, Even to uneven, wavy extinction	94 %	70 %
2	Muscovite	Flaky, Irregular boundary, Dirty white	2%	4 %
3	Biotite	Flaky, Irregular boundary, Light brown	2%	3 %
4	Feldspar	Elongated, 1-2 sets of cleavage, Dirty white	1%	15 %
5	Iron Oxide	Rounded to sub rounded, Irregular, black	0.5%	1%
6	Rock fragments	No particular shape, Irregular, Multi-coloured	0.5%	7 %

4.2 Engineering properties

The test results for fine aggregates of river sand as well as quarry dust are given in table-2.

Table 2. Engineering Properties of river sand and quarry dust

Sl. No.	Property	River sand	Quarry dust
1	Moisture content	5.8 %	2.5 %
2	Fineness modulus	2.8	2.66
3	Specific Gravity	2.585	2.425
4	Water absorption	1.41 %	1.81 %
5	Organic impurities	absent	Absent
6	Bulking	2.69 %	3.34 %
7	Cohesion	0.05	0
8	Angle of internal friction	36°	39°
9	Permeability	0.0437cm/s	0.039cm/s
10	Optimum moisture content	8.46 %	10.2 %
11	Dry density	1.55 g/cc	1.75g/cc

4.3 Compressive strength of concrete

Cement concrete is prepared using quarry dust as a partial and total replacement of river sand using the same mix ratio (M20), water/cement ratio of 0.45, same quantity and type of cement, water and coarse aggregate. The results of compressive strength of concrete are given in table-3.

Table 3. Experimental observation of compressive strength of concrete

Type of aggregate	Days	Strength (N/mm^2)			Average strength (N/mm^2)
		Trial 1	Trial 2	Trial 3	
100 % river sand	7 days	20.78	20.89	21	20.89
	28 days	31.77	32.87	31.85	32.16
50% river sand + 50% quarry dust	7 days	26.92	27	27.78	27.23
	28 days	38.11	37.33	38	37.81
100 % quarry dust	7 days	23.44	23	24.67	23.70
	28 days	33.89	34.52	34.31	34.24

5 DISCUSSION OF TEST RESULTS

1. From geological point of view, it can be seen that both river sand and quarry dust contains mainly Quartz (table 1). Quartz is a very hard mineral. Its hardness is 7. Quartz is weather-proof and resists the action of acids. From this point of view, both river sand and quarry sand are usable. But the percentage of Quartz in river sand is more than that in quarry sand.

2. From sl. No. 2 and 3 of table 1, it is seen that the amount of mica i.e. Biotite and Muscovite present in the river sand is only 4 %, which is not objectionable. But its amount in quarry dust is slightly higher i.e. 7%. So from this point of view we can say that the quarry aggregate is inferior because the presence of mica has been found to considerably reduce the compressive strength of concrete.

3. From sl. No. 4 of table-1, it is seen that the amount of Feldspar in quarry dust is considerably higher than that of river sand. We know that Feldspar mineral can be easily weathered when comes into contact with water and air. So we can conclude that the aggregate from this quarry should not be used for under-water concreting methods.

4. From table-2, it is seen that the various engineering properties like moisture content, specific gravity, water absorption, bulking, angle of internal friction, permeability, compaction lies within the specified limits for both river sand and quarry dust. Also there is very little variation in engineering properties of both river sand and quarry dust. Hence all the aggregates are usable as construction material so far as engineering properties are concerned.

5. From table 3, it can be observed that the compressive strength of concrete increases with the use of quarry dust as a replacement of river sand. This could be because of the fact that the shape of quarry dust is mostly angular, due to which it exhibits better interlocking effect in concrete and makes it superior in concrete used for roads and pavements.

6. The maximum compressive strength is achieved with 50 % replacement of river sand with quarry dust.

6 CONCLUSION

The present study "An experimental study on the effects of river sand and rock quarry dust on quality of concrete" can be concluded as follows:

- The shape of river sand is rounded to sub-rounded whereas that for quarry dust is mostly angular to sub-angular. We know that angular aggregates are preferred to rounded aggregates because angular aggregates exhibit a better interlocking effect in concrete, which makes it superior in concrete used for roads and pavements. Thus quarry dust is preferred to river sand with regards to its shape.

- From the study of geological properties, it has been observed that the amount of quartz in quarry dust is less than that in river sand. Again the amount of mica and feldspar is more in case of quarry sand ass compared to river sand. Hence from geological point of view we can conclude that river sand is preferred to quarry dust.

- From engineering point of view, there is very little variation between the properties of river sand and quarry dust. This means that quarry dust has all the desired properties of fine aggregates to be used in place of river sand.

- With the use of quarry dust as a replacement to river sand, the compressive strength of concrete increases and 50 % replacement level gave the maximum value.

Although Assam is said to be a land of rivers, but the fine aggregates of only some of the rivers are usable as construction material. Major part of the rivers contains fine sand or silt which could be used only for plastering or filling purposes. But to make concrete of high strength and durability, we need medium to coarse sand. Owing to the large number of constructions going on all around the region in such a fast pace, the consumption of concrete is increasing every year and eventually a time will come when the natural resources may get depleted. Thus, it is becoming inevitable to use alternative materials for aggregates in concrete and the use of quarry dust in place of river sand is one such alternative. The use of such materials not only results in conservation of natural resources but also helps in maintaining good environmental conditions.

REFERENCES

1) Agrawal, V., Shah, P., Gupta, A. and Shah, R. (2017): The Utilization of Quarry Dust as Fine Aggregates in Concrete, *International Conference on Research and Innovations in Science, Engineering & Technology*.
2) Geeta, H. K., Prabhu, L., Shrivatsa, J., Sowmya, D., Ganesha, S. R. (2018): *International Research Journal of Engineering and Technology,* e-ISSN: 2395-0056
3) Hamid, N.J., Kadir, A.A., Kamil, N.A., Hassan, M.I., (2018): Overview on the Utilization of Quarry Dust as a Replacement Material in Construction Industry, *International Journal of Integrated Engineering,* Vol. 10 No. 2 (2018) p. 112-117
4) Ilangovana, R., Mahendrana, N. and Nagamanib, K. (2008): Strength and durability properties of concrete containing quarry rock dustas fine aggregate, *ARPN Journal of Engineering and Applied Sciences*
5) IS: 2386 (part I)-1963, "Methods of test for aggregates for concrete (Particle size and shape)"
6) IS: 2386 (part I)-1963 – Methods of test for aggregates for concrete (Estimation of deleterious materials and organic impurities)
7) IS: 2386 (part III)-1963 – Methods of test for aggregates for concrete (Specific gravity, density, voids, absorption and bulking)
8) IS: 2386 (part IV)-1963 – Methods of test for aggregates for concrete (Mechanical properties)
9) IS: 2720 (part 17)-1986 – Methods of test for soil (Permeability)
10) IS: 2720 (part IIV)-1980 – Methods of test for soil (Compaction test)
11) Janardhanan , K. N., Priya, E.M. (2018): Experimental study on cement concrete with PVC powder and Quarry dust as partial replacement to fine aggregate, *International Research Journal of Engineering and Technology,* e-ISSN: 2395-0056
12) Jyothi, D. N., Mandeep, G. (2018): An Experimental Study on Concrete by Partial Replacement of Cement with Bagasse Ash and Fine Aggregate by Quarry Dust, *International Research Journal of Engineering and Technology,* e-ISSN: 2395-0056, Volume: 05 Issue: 02 | Feb-2018
13) Opara, H. E., Eziefula, U. G., Eziefula, B. I. (2018): Comparison of physical and mechanical properties of river sand concrete with quarry dust concrete, *SSP - Journal of civil engineering,* Special Issue, March 2018
14) Prakash, K.S., Rao, C.H. (2016): Study on Compressive Strength of Quarry Dust as Fine Aggregate in Concrete, *Advances in Civil Engineering,* Hindawi Publishing Corporation, Volume 2016, Article ID 1742769
15) Priya, R.R., Athithan, A.K.K. and Ramya, E.(2016): Experimental investigation of partial replacement of fine aggregate by quarry dust in concrete with steel powder, *International Journal of Advances in Engineering Research*, Vol. No. 11, Issue No. IV
16) Reddy, K.C., Omkar, S.M. (2017): Investigation on durability properties of concrete with partial replacement of sand by quarry dust & cement by fly ash, *International Journal of Research in Engineering and Applied Sciences,* ISSN: 2249-3905

Effect of marble-dust on the sub-grade characteristics of soil

Baishya, P. [1], Choudhury, S. [2] and Borah, S.[3]

[1] Graduate Engineer, Assam Public Works Department, Mangaldai Rural Road Division, Darrang- 784125, India.
[2]Assistant Manager Civil, Assam Power Generation Corporation Limited, Guwahati-781026, India.
[3] Assistant Professor, Civil Engineering Department, Assam Engineering College, Guwahati-781013, India.

ABSTRACT

The performance of a pavement is very responsive to the characteristics of sub-grade soil which provides the base for the whole pavement structure. For this reason of utmost significance, the performance of the sub-grade soil has been investigated with the addition of marble-dust. Marble is one of the most preferred stone in the construction industry and marble-dust is produced during the cutting and grinding processes of the marble pieces. The disposal of this generated marble-dust is a serious environmental issue across the world. Moreover, it has been identified to cause lung disease. Thus, it shows that there is an urgent need for exploring the alternative of disposal of this material. Hence an attempt has been made to utilize the marble dust as a sub-grade material for the improvement of pavement. This paper presents the details and results of laboratory tests which were carried out to determine the various properties of soil and marble-dust composite like Atterberg limit, particle size distributions, maximum dry density, optimum moisture content, CBR values and coefficient of permeability. The soil sample was collected from Assam Engineering College Guwahati -13, while the marble-dust was obtained from the local market in Guwahati. The marble-dust in proportions of 5, 10, 15, 20 and 25% by weight were added to the soil. The test results showed remarkable improvements in the physical properties of the soil with the addition of marble-dust, which can be used in practice as a potential stabilizer to strengthen the sub-grade characteristics of soils.

Keywords: marble-dust, sub-grade soil, CBR value

1. INTRODUCTION

Economic development of any country is controlled to a great extent by highway, railway and airway networks. Therefore, the development and use of methods to strengthen the pavements is very necessary. For this work, it is essential to know the condition of the subgrade soil before designing the type and the thickness of pavement. The subgrade is the lowest layer of the pavement layer system which ultimately supports all other pavement component layers. It is essential that at no time, the soil subgrade is over-stressed. If the subgrade settles down or yields due to inadequate compaction or any other cause, different types of failures start developing in the pavement. Existing subgrade strength governs the design and life of pavements.

Generally road construction requires large quantities of soil having sufficient strength. If locally available soil is used as fill materials for subgrade, it would be economically helpful for the project rather than imported materials. In Assam most of the entire land is covered by alluvial soils which are not suitable for construction either as fill or as subgrade due to poor engineering properties. These soils are formed when streams and rivers slow their velocity. Other one alluvial soil are highly fertile and a good crop soil. These soils possess poor shear strength, low bearing capacity and penetration resistance and exhibit higher deformations. When these types of soils come in the contact of water then they causes swelling and when water content decreases shrinkage occurs in the soil.

So there need some improvements of behaviors of soil, which is known as Soil Stabilization. It is done by various methods and one of them is mixing the Stabilizing Additives. Marble-dust can be used as effective pavement material and improves strength of soft clayey soil and provides good workability in the field.

2. MOTIVATION AND OBJECTIVE OF THE STUDY

Industrial activities are essential for the socio-economic progress of a country but it also produces a huge quantity of solid and liquid waste. Marble-dust is one of the major industrial wastes, which is produced by marble processing industries. In India, around 7 million tons of wastes mainly in the form of marble powder are produced during sawing and polishing processes of marble pieces. These generated wastes are dumped indiscriminately on to the soil, leading to dust pollution and it also contaminates the surface and underground water reservoirs.

Hence, in this paper, an attempt has been made to study how marble-dust may be effectively utilized in combination with locally available soil to get an improved quality of composite material which may be used as subgrade material.

3. A BRIEF HISTORY OF PREVIOUS WORKS

There are numbers of researches that have been done in the direction of utilizing the marble-dust into the soil stabilization technique in the last decade.

Sabat and Nanda (2011) had studied the effect of marble-dust on strength and durability of rice husk ash stabilized expansive soil and found that addition of marble-dust increased the strength, decreased the swelling pressure and made the soil –rice husk ash mixes durable. The optimum proportion of soil: rice husk ash: marble-dust found to be 70:10:20.

Sharma et al (2015) studied the effect of marble dust on the consistency limit and compaction parameters of soil. They concluded in their study that the addition of marble-dust to the soil reduces the clay content and make the soil coarser in nature. It also reduces the liquid limit, raises the shrinkage limit and decreases the plasticity of the soil. The rate of swell and swelling percentage decreases for the stabilized soil.

Muthu Kumar and Tamilarasan (2015) studied the behaviour of expansive soil using marble powder. They added the marble powder with clay 0-25% at the interval of 5%. It was observed that the expansive soil was modified into low plasticity. Also the unconfined compressive strength of stabilized clay is increased by 15% to that of the soil.

Minhas and Devi (2016) investigated the effect of marble powder as a stabilizer to strengthen the weak natural sandy soil. It was observed that with addition of marble powder content the maximum dry density of the soil decreases whereas no significant change was observed in the optimum moisture content. Besides there was improvement in the CBR properties of soil with addition of marble powder.

4. MATERIALS AND METHODOLOGY

4.1 Materials

The soil sample used in this study was taken from the campus of Assam Engineering College, Guwahati. The sample had been air-dried, pulverized and sieved through IS 4.75 sieve. The moisture content of the soil sample was found to be 7.1% during sampling. The soil sample was identified as CH soil as per the Indian Standard Soil Classification System (ISSCS).

Fig. 1. Soil sample

The marble-dust was collected from local marble cutting industry in Guwahati. The physical properties of marble-dust have been tabulated below.

Table 1.Physical Properties of marble-dust

Properties	Test Results
Specific Gravity	2.61
Particle size	<300μ
Colour	White
Odour	Odourless
Moisture Content (%)	0.59
Bulk density(without compaction)gm/cm^3	1.438
Bulk density (with compaction)gm/cm^3	1.870

Fig. 2. Marble-dust

4.2 Methodology

In order to study the effect of Marble-dust on the properties of the soil, the soil sample was mixed with 5%, 10%, 15%, 20% and 25% marble-dust (on the basis of its dry weight) and the

Atterberg limit test, Standard Proctor test, CBR test and permeability test were done.

5. LABORATORY TESTS

As mentioned above, the samples prepared by mixing with 5%, 10%, 15%, 20% and 25% marble-dust has been subjected to various tests as per the procedures mentioned in their relevant IS codes.

5.1 Particle Size Distribution

In this test, the soil has been sieved through a series of IS sieves as per IS 2720 (Part IV) 1985.

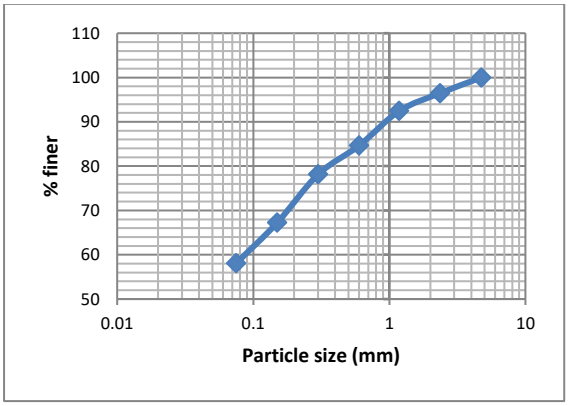

Fig. 3. Particle size distribution curve of soil sample

From the result it can be interpreted that 58.09% of the soil sample has passed through 75µ sieve. Hence, the soil may be classified as fined grained soil. It may contain silt or clay. For more details the tests for determining Atterberg Limits have been done.

5.2 Atterberg Limit Test

The soil samples mixed with the above mentioned percentage of marble-dust, have been subjected to Liquid Limit (LL) and Plastic Limit (PL) tests and from the test results it can be observed that the LL, PL and Plasticity Indices (PI) of the soil decreases with increase in the percentage of marble-dust. The variation in LL, PL and PI of soil sample has been presented in Fig-4. This variation in LL, PL and PI is due to the coarser size of Marble-dust particle. The size of marble-dust is larger than clay soil particle; for which the specific surface area of the mixture has decreased. Hence it requires less water to reach its required boundary limits.

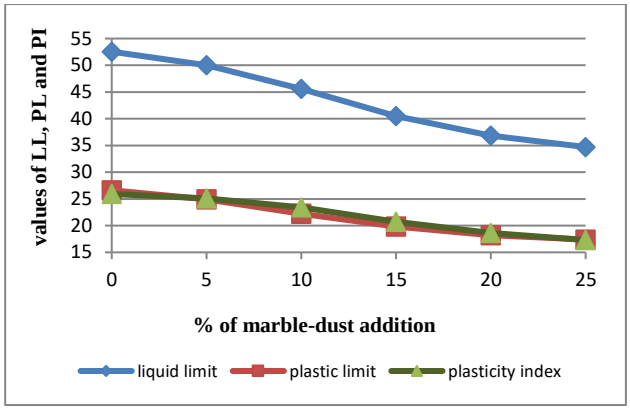

Fig. 4. Variation of plasticity characteristics of soil with increase in marble-dust content

5.3 Compaction test

The Standard Proctor test is performed to establish a relationship between dry density and moisture content and also to determine the Optimum Moisture Content (OMC) corresponding to Maximum Dry Density (MDD). In this study, the compaction test was performed as per the procedure mentioned in IS 2720 (Part VII) – 1980.

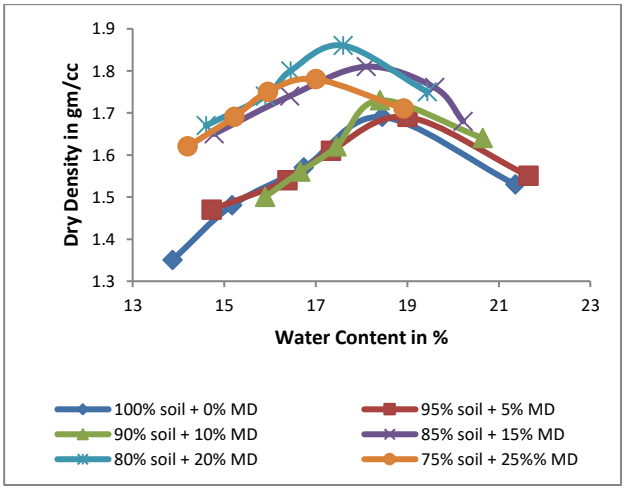

Fig. 5. Standard Proctor test results at various percentages of marble-dust content

It can be observed that with increase in percentage of marble-dust the Maximum Dry Density (MDD) increases up to 20% marble-dust addition. This is because the clay particles fill up the voids between the marble-dust. After that it goes on decreasing with the further addition of marble-dust. While the Optimum Moisture Content (OMC) of the soil sample decreases. This behavior of the soil may be attributed to the non-plastic behavior of the marble-dust added in the highly plastic clay soil, facilitating the compaction at lower OMC.

5.4 CBR Test

The California Bearing Ratio (CBR) test

was conducted on the soil sample with varying percentages of marble-dust to determine most appropriate percentage of soil and marble-dust composite required to obtained a good CBR value. The test is performed as per IS 2720 (Part XVI)-1980.

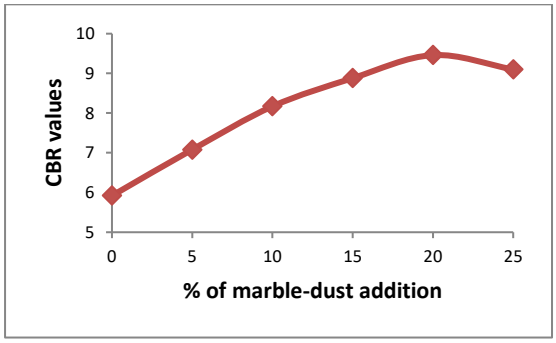

Fig. 6. CBR values at various percentages of marble-dust content

From above figure, it is observed that the CBR value of the soil sample has been increasing up to 20% of marble-dust addition. The maximum value of CBR was obtained as 9.46. The formation of a cation exchange reaction and pozzolanic reaction were responsible for the increase in CBR value. The reduction in the CBR value when the marble-dust exceeds the optimum percentage indicates that excess marble-dust is not used up in the marble-dust-soil reaction.

5.5 Permeability test

This test has been done to determine the co-efficient of permeability of the given soil sample. The test is done according to IS:2720 (Part-17) - 1986 (Reaffirmed- 2002). In this experiment falling head test has been used.

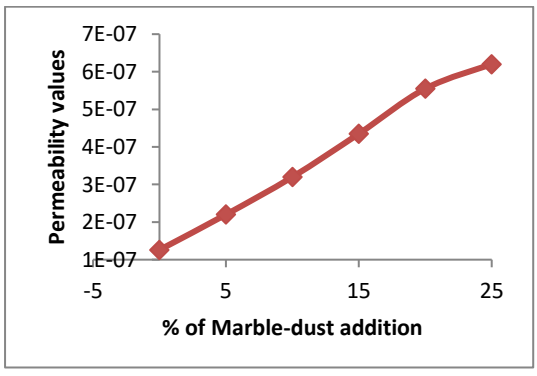

Fig. 7. Permeability values at various percentages of marble-dust content

From above figure, it can be seen that the Permeability of the soil samples have increased as the percentage marble dust increased. The Coefficient of Permeability at 0% addition of marble-dust is found to be 1.26×10^{-7} cm/sec. As the percentage of marble dust addition has increased the Coefficient of Permeability gradually increases. Hence at 25 percent addition of marble dust the value of Coefficient of Permeability is 6.20×10^{-7} cm/sec. Permeability value increases in the Soil and marble dust mixture due to increased in marble-dust, which is a coarser material.

6. TEST RESULTS AND INTERPRETATIONS

Addition of few percentage of marble-dust in soil can improve the engineering properties of the mixture significantly. Addition of marble-dust increases the value of CBR and hence thickness of subgrade layer decreases and in turn overall thickness of the pavement decreases which help in economy in the project. Based on the experimental study of the soil and marble-dust, the following conclusions can be drawn:-

1. Gradation of the soil sample is done through sieve analysis which indicates that more than 58.09% of soil sample had passed through 75μ sieve. Hence, the soil may be classified as fined grained soil. It may contain silt or clay.
2. From the Atterberg Limit test the soil sample can be classified as CH soil.
3. The liquid limit, plastic limit and plasticity index of soil sample are found to be decreasing with the addition of the Marble-dust.
4. The maximum dry density values are increasing up to 20% addition of marble-dust and then it decreases.
5. Optimum moisture content of soil sample taken for laboratory investigation is found to be decreasing.
6. The CBR values of the soil sample have been increasing up to 20% addition of marble dust and then decrease.
7. The Coefficient of Permeability has increased from 1.26×10^{-7} cm/sec at 0% to 6.20×10^{-7} cm/sec at 25% addition.

7. CONCLUSION

From the experiment it can be concluded that, marble-dust can be used as a soil stabilizer and can be contribute greatly to the field of construction. The utilization of this waste is not only cost effective but is also helpful from the

environmental point of view, as it's usage will reduce its deposition and future harmful consequences resulting from such deposits. However further studies are required to arrive at an effective conclusive statement to be made in this regard.

ACKNOWLEDGEMENTS

We express our deepest gratitude and sincere thanks to all the faculty members, laboratory staff and bearers of the department of Civil Engineering, Assam Engineering College, Guwahati-13. We also like to thank Mr. D.K. Baishya (EE, PWRD Mangaldai) and Mr. B.J. Saharia (AEE, PWRD Sipajhar Sub-division) for their encouragement and valuable advice.

REFERENCES

1) Agrawal, V. and Gupta, M. (2011) Expansive Soil Stabilization Using Marble Dust, *International Journal of Earth Sciences and Engineering ISSN 0974-5904, Volume 04, No 06 SPL, October 2011, pp 59-62.*
2) Ali, R., Khan, H., and Shah, A.A. (2004) Expansive Soil Stabilization Using Marble Dust and Bagasse Ash, *International Journal of Science and Research (IJSR) Volume 3 Issue 6, June 2004.*
3) Baser, O. (2009) Stabilization of expansive soils using waste marble dust, Master of Science thesis submitted to Civil Engineering Department, Middle East, Technical University.
4) Gandhia, K.S. (2013) Stabilization of Expansive Soil of Surat Region using Rice Husk Ash & Marble Dust, International Journal of Current Engineering and Technology ISSN 2277 – 4106. Vol.3, No.4 Oct. 13.
5) Gupta, C. and Sharma R. K. (2014) Influence of Marble Dust, Fly Ash and Beas Sand on Sub Grade Characteristics of Expansive Soil, *IOSR Journal of Mechanical and Civil Engineering (IOSR-JMCE) e-ISSN: 2278-1684.*
6) IS 2720 (Part IV) (1985), *Method of test for soils: Grain Size Analysis*, Bureau of Indian Standards, New Delhi, India.
7) IS 2720 (Part V) (1985), *Method of test for soils: Determination of Liquid and Plastic Limit*, Bureau of Indian Standards, New Delhi, India.
8) IS 2720 (Part VII) (1980, Reaffirmed 2011) – *Determination of Water Content-Dry Density relation, using Light Compaction*. Bureau of Indian Standards, New Delhi, India.
9) IS 2720 (Part XVI) (1987), *Laboratory Determination of CBR*, Bureau of Indian Standards, New Delhi, India.
10) Minhas, A. and Devi, U.V. (2016) Soil stabilization of alluvial soil by using marble dust, *International Journal of Civil Engineering and Technology (IJCIET) Volume 7, Issue 5, September-October 2016.*
11) MuthuKumar., M. and Tamilarasan., V.S.(2015), Experimental Study on Expansive Soil with Marble Powder, *International Journal of Engineering Trends and Technology (IJETT) – Volume 22 Number 11 - April 2015.*
12) Rajasekharan, G. and NarasimhaRao, S. (2002) Compressibility behaviour of lime-treated marine clay, *J. in Ocean Engineering, 29(5), pp. 545-559, ISSN: 0029-8018.*
13) Sabat, A. K. and Nanda, R. P. (2011) Effect of marble dust on strength and durability of Rice husk ash stabilised expansive soil, *ISSN 0976 – 4399, Volume 1, No 4, 2011.*
14) Singh et al. (2008) Effect of Lime on properties of soil, 12th *Int. Conference of Int. Association of Computer Method and Advances in Geomechanics (IACMAG), Goa, India.*

Study of unconventional concrete using different admixtures

Zaman, S,[1], Chetia, N.[2], Kalita, K.[2]

[1] PG Student, Department of Civil Engineering, Jorhat Engineering College, Jorhat – 785007, India.
[2] Assistant Professor, Department of Civil Engineering, Jorhat Engineering College, Jorhat – 785007, India.

ABSTRACT

Taking sustainable development in view, in this study an attempt has been made to partially replace OPC cement by various admixtures like Bamboo fibre, Bamboo powder, Fly-ash Micro silica etc in different percentages in order to optimize the strength, sustainability and economic criteria in conventional concrete. The specimen of concrete cubes are prepared with different proportion of Fly ash, Micro silica, Fly ash-Bamboo fibre, Micro silica- Bamboo fibre etc for the investigation. The Mix design has been performed as per IS 10262:2009 for M25 grade of concrete. Slump test, compaction factor test, bulk density, compression test and split tensile test are carried out to check the quality and strength of the specimen. Compression tests were performed for 7days, 28 days and 56 days of curing and split tensile tests were carried out for 28 days of curing. After analysing the various test results, it was observed that replacement of cement by Bamboo fiber at 4%, Bamboo powder at 3%, Fly ash at 20% and Micro silica at 15% by weight showed the maximum improvement factor and also the combination of these admixtures shows satisfactory results. Regression analysis namely SPSS tool has been used for regression analysis as well as modelling. Cost analysis for various mixes has been also presented herewith.

Keywords: compressive strength, split tensile strength, improvement factors, regression analysis.

1. INTRODUCTION AND LITERATURE REVIEWS

In the light of progress nature has been ignored and destroyed in the form of using conventional materials in constructional work. The cost of the construction increases with increase in population and urban development. Efforts are being made in the field of concrete technology to develop concretes with special characteristics which can considerably minimize the use of cements and reduce the cost of construction**.** In this paper some admixtures have been used as partial replacement OPC cement for making concrete which are sustainable as well as economic. Ahmad et al (2014) replaced volume of concrete by 1% bamboo fibre in the concrete cube and found that the strength of concrete cubes with fibres doesn't show much improvement up to 28 days but surprisingly strength become double in 50 days. Kazmi1 et al. (2015) investigated the possibility of utilizing micro silica as partial replacement of cement in the production of concrete and concluded that replacement of silica fumes between 5% to 10% would render the concrete stronger and more durable. Kiran et al. (2014) & Mohod et al. (2016) showed that concrete with replacement of cement with fly ash shows good compressive strength and split tensile strength for 28 days strength and the cubes containing fly ash is the better acid resistance than the conventional concrete. The results shown that Concrete with 15% replacement of cement with fly ash shows good compressive strength and split tensile strength for 28 days of curing.

2. METHODOLOGY

The materials use in the project work are OPC – 43 grade of cement (Dalmia), coarse sand from Kanaighat (Kalioni River), coarse aggregates (Bihubor). Locally available Rich husk ash, wood ash and wood powder are collected. CCB treated Bamboo fibres and Bamboo powder collected from Rain Forest Research Institute, Jorhat (ICFRE) and another admixture Fly ash is taken from Rajasthan NTPC with the help of TOPCEM INDIA Plant's Quality Control Department. Admixtures are collected from market. The Mix design has been performed as per IS 10262:2009. The codes used for physical properties of cement, FA, CA and admixtures are IS 383-1970, IS 8112: 2013, IS 4031:1996 (P-1), IS 269-2015, IS 5513-1959, IS 2720 (P-3), IS 1199-1959, IS 516-1959, IS 456:2000 and IS 5816-1999.

2.1 Physical properties of materials and concrete

The various physical properties of Fine aggregates and Coarse aggregates are given in Table 1

Table -1: Physical properties of FA and CA

Sample	Avg. Water absorption	Avg. Specific gravity	Size in mm
FA	1.181	2.77	4.75 down
CA	0.523	2.525	20 down

The various physical properties of cement are given in Table 2

Table - 2: Physical properties of Cement

Reference: IS 8112:1989

Tests	Value
Consistency of cement	31.50%
Initial Setting Time	2.05 hours
Final Setting Time	9.10 hours
Fineness	92%
Avg. Specific gravity	3.14
Colour	Grey

The various physical properties of Admixtures are given in Table 3 and 4

Table-3: Physical properties of various Admixtures

Sample	Fineness	Avg. Specific gravity	Colour
Fly Ash	85%	2.24	Light Grey
Micro silica	94%	2.270	Dark Grey
Bamboo powder	2.62%	0.635	Light yellow
Bamboo fibre	3mm Square in size with 1.5 inch long	0.534	Light brown

Table - 4: Slump and Compaction factor

Sample	Slump	Compaction factor
NC	48	0.931
BA2	40	0.823
BP1	46	0.911
F1	65	0.963
M2	43	0.910
BAF1	47	0.939
BAM1	41	0.849
FM2	57	0.948

3. RESULT AND DISCUSSION

The cubes with various proportion and w/c of 0.45 with different amounts admixtures are tested for Compressive strength at 7, 28, 56 days of curing are given in the Table 5, 6, 7, 8, 9, 10 and 11.

Table - 5: Compressive strength of specimen with Fly ash (F) as an admixture

% of Admixture used		Average Compressive strength in N/mm²			Improvement factor at 28 days
		7 days	28 days	56 days	
NC	0%	28.29	39.26	42.92	1.0
F1	20%	26.15	40.45	43.92	1.030
F2	25%	22.88	35.56	42.00	0.906
F3	30%	13.33	28.67	35.00	0.730
F4	35%	13.00	26.33	33.89	0.671
F5	40%	11.11	25.33	25.33	0.645

Table - 6: Compressive strength of specimen with Bamboo fibre (BA) as an admixture

% of Admixture used		Average Compressive strength in N/mm²			Improvement factor at 28 days
		7 days	28 days	56 days	
NC	0%	28.29	39.26	42.92	1.0
BA1	2%	25.67	39.0	44.44	0.993
BA2	4%	23.77	39.89	44.44	1.016
BA3	6%	19.22	35.44	39.34	0.903

Table - 7: Compressive strength of specimen with Bamboo Powder (BP) as an admixture

% of Admixture used		Average Compressive strength in N/mm²			Improvement factor at 28 days
		7 days	28 days	56 days	
NC	0%	28.29	39.26	42.92	1.000
BP1	3%	25.11	35.67	42.55	0.909
BP2	6%	17.22	33.11	35.00	0.843
BP3	9%	13.44	23.89	29.55	0.609

Table – 8: Compressive strength of specimen with Micro Silica (M)as an admixture

% of Admixture used		Average Compressive strength in N/mm²			Improvement factor at 28 days
		7 days	28 days	56 days	
NC	0%	28.29	39.26	42.92	1.0
M1	10%	22.00	31.11	34.22	0.792
M2	15%	22.44	31.56	35.11	0.804
M3	20%	18.22	22.67	28.66	0.577
M4	25%	15.77	18.44	24.67	0.470
M5	30%	12.67	15.44	22.44	0.393
M6	35%	10.44	14.67	19.33	0.374

Table - 9: Compressive strength of specimen with Bamboo fibre + Fly ash (BAF) as an admixture

% of Admixture used	Average Compressive strength in N/mm²			Improvement factor at 28 days
	7 days	28 days	56 days	
NC	28.29	39.26	42.92	1.0
BAF1	26.11	36.78	39.33	0.937
BAF2	22.42	33.44	35.78	0.852

Table - 10: Compressive strength of specimen with Bamboo fibre + Micro Silica (BAM) as an admixture

% of Admixture used	Average Compressive strength in N/mm²			Improvement factor at 28 days
	7 days	28 days	56 days	
NC	28.29	39.26	42.92	1.0
BAM1	19.78	27.11	32.67	0.691
BAM2	21.11	32.89	34.22	0.838

Table - 11: Compressive strength of specimen with Fly ash + Micro Silica (FM) as an admixture

% of Admixture used	Average Compressive strength in N/mm²			Improvement factor at 28 days
	7 days	28 days	56 days	
NC	28.29	39.26	42.92	1.0
FM1	19.33	33.33	35.77	0.849
FM2	22.67	30.22	32.89	0.770
FM3	21.11	28.22	31.11	0.719

The comparison on compressive Strength at 7days, 28 days and 56 days of curing of different admixtures in various proportions with 0% admixture are given in the fig. 1, 2, 3, 4, 5, 6 and 7

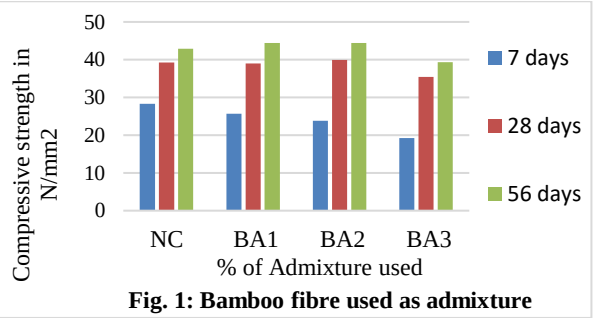

Fig. 1: Bamboo fibre used as admixture

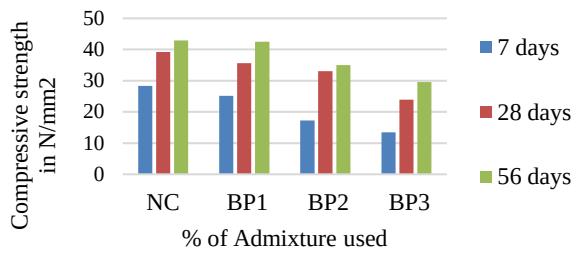

Fig. 2: Bamboo Powder used as a admixture

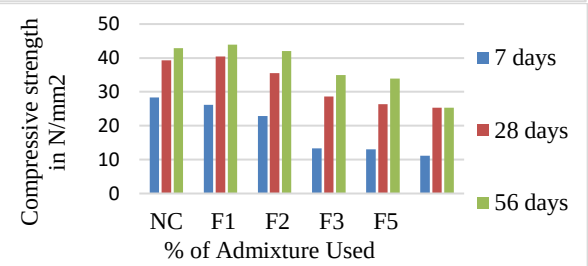

Fig. 3 : Fly ash used as a admixture

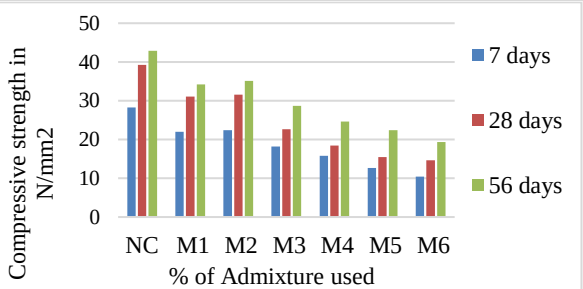

Fig . 4: Micro Silica used as admixture

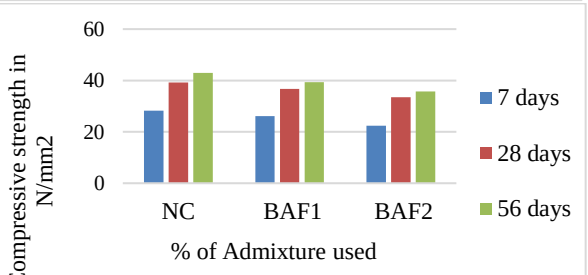

Fig. 5: Bamboo fibre and Fly as used as admixture

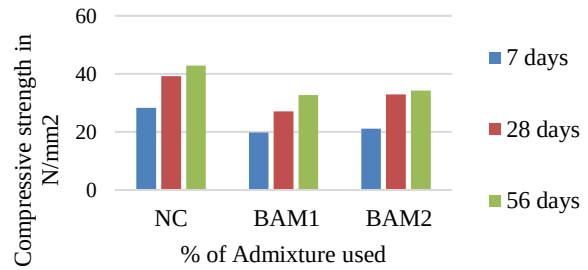

Fig. 6: Bamboo fibre and Micro silica used as Admixture

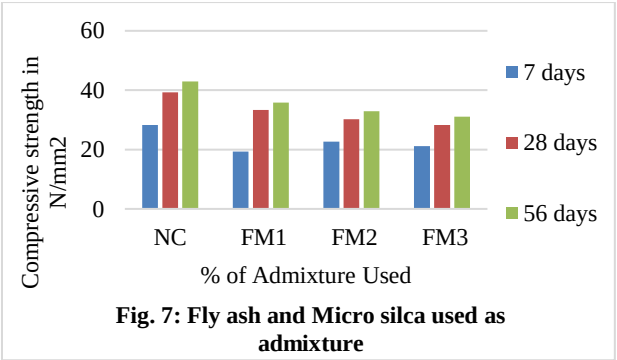

Fig. 7: Fly ash and Micro silca used as admixture

The Split Tensile Strength and Bulk density of various admixtures with 0% admixture are given in the Table 12

Table -12: Split tensile strength and Bulk density

Admixture used	Split tensile strength at 28 days	Improvement Factor	Avg. Bulk Density
NC	2.900	1.000	2320.000
BA2	3.254	1.122	2232.000
BP1	2.759	0.951	2218.667
F1	2.688	0.927	2306.667
M2	2.334	0.805	2154.667
BAF1	2.829	0.976	2208.000
BAM1	2.546	0.878	2186.667
FM2	2.546	0.878	2106.667

Comparison on Split Tensile Strength at 28 days of curing of different admixtures in various proportions with 0% admixture are given in the fig.8

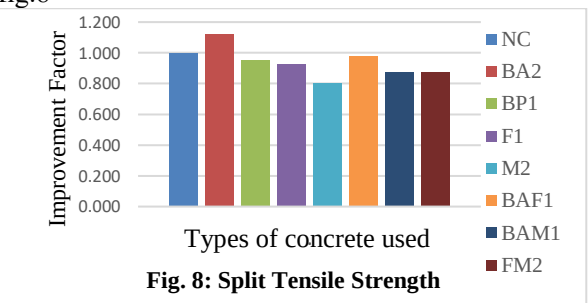

Fig. 8: Split Tensile Strength

4. REGRESSION ANALYSIS

The regression analysis is done with help of SPSS software. It means "**S**tatistical Package for the **S**ocial **S**ciences" and was first launched in 1968. Since SPSS was acquired by IBM in 2009, it's officially known as IBM SPSS Statistics but most users still just refer to it as "SPSS". The focus is on the relationship between a dependent variable and one or more independent variables. The Table13provides the *R*, R^2, adjusted R^2, and the standard error of the estimate, which can be used to determine how well a regression model fits the data:

Table - 13: Model Summary

Model	R	R Square	Adjusted R Square	Std. Error of the Estimate

1	0.954	0.910	0.845	2.875

4.1 Fixing Dependent variable and predictors

a. Dependent Variable: Average Compressive strength in N/mm^{2}at 28 days of curing

b. Predictors: (Constant), BA, BP, F, M, BAF11, BAF22, BAM11, BAM22, FM11, FM22

The Table 14 shows that the independent variables statistically significantly predict the dependent variable

Table -14: ANOVA Table

Model		Sum of Squares	df	Mean Square	F	Sig.
1	Regression	1165.29	10	116.53	14.1	0.0
	Residual	115.75	14	8.27		
	Total	1281.04	24			

From the regression co-efficient obtained from SPSS, the predict compressive strength at 28 days expressed in general form of the equation i.e

Predicted compressive strength at 28 days = 44.26 − 0.228 × BA − 0.451 × BP − 0.090 × F − 0.206 × M + 0.440 × BAF11 − 0.189 × BAF22 − 2.000 × BAM11 + 0.286 × BAM22 − 0.073 × FM11 − 0.168 × FM22 ……Eq.(a)

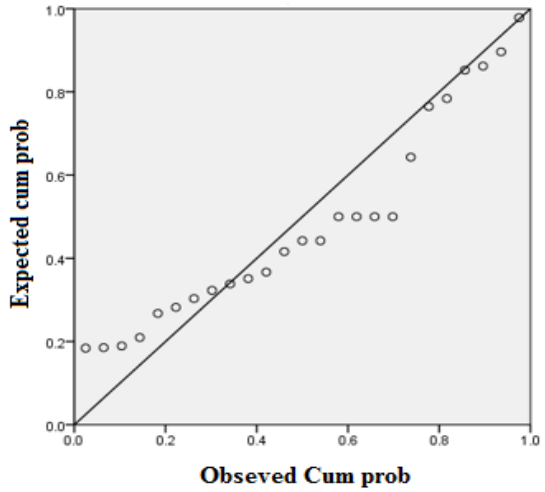

Fig. 9: Measured and Predicted Compressive strength at 28 days (Normal P-P Plot of regression standardized residual)

5. COST ANLYSIS

The rate of different materials, labours are taken as per the market price and cost analysis of concrete work are carried out and given in Table 15

Table - 15: Cost Analysis of per cu.m of concrete work as per Market price

Mixed Proportion	Total	Rate per cu.m	% of decreased in cost per cum
NC	77813	7781.34	0.00
BA2	76112	7611.18	2.19
BP1	77381	7738.10	0.56
F1	69813	6981.25	10.28
M2	117618	11761.77	- 51.15
BAF1	71304	7130.40	8.37
BAM1	95783	9578.33	-23.09
FM2	82815	8281.49	-6.43

6. CONCLUSION

From the experimental results observed so far, the various admixtures exhibit different of improvement in compressive strength while used in different proportion. The partial replacement of cement was carried out for M25 grade of concrete.

- At 4% partial replacement of cement by Bamboo fibre, observed improvement factor 1.016 and reduce 2.19% cost per cu.m of concrete work.At 3% partial replacement of cement by Bamboo Powder, observed improvement factor 0.909 and reduce 0.56% cost per cu.m of concrete work.
- At 20% partial replacement of cement by Fly ash, observed improvement factor 1.030 and reduce 10.28 % cost per cu.m of concrete work.
- At 15% partial replacement of cement by Micro silica, observed improvement factor 0.804 and increased 51.15% cost per cu.m of concrete work.
- Another admixture Bamboo fibre + Fly ash is considered at a proportion of 4% of Bamboo fibre + 15% of Fly Ash observed improvement factor 0.937 and reduce 8.378% cost per cu.m of concrete work.
- When the partial replacement of Bamboo fibre + Micro silica is considered at a proportion of 4% of Bamboo fibre + 20% of Micro silica observed improvement factor 0.838 and it increased 23.09% cost per cu.m of concrete work.
- When the partial replacement of Fly ash + Micro silica is considered at a proportion of 10% of Fly ash + 10% of Micro silica observed improvement factor 0.849 and it increased 6.43% cost per cu.m of concrete work.

This work immensely highlights the proper use of waste materials in an engineered and eco-friendly way. A sustainable concrete meet performance requirement of owner, designer, contractor, producer plus minimize the energy and CO_2 footprint, minimize potable water use, minimize waste, increase use of recycled cement etc. This study is an effort of the same direction and the results ensure an eco-friendly environment and

also reduce the cost of construction.

ACKNOWLEDGEMENTS

I would like to express my special thanks of gratitude to Dr. (Mrs) Nayanmoni Chetia, Assistant Professor, Civil Engineering Department, Jorhat Engineering College, Jorhat, for her excellent guidance and encouragement and support during the course of my work. Special thanks for Mr. Koushik Kalita, Faculty of Jorhat Engineering College for his valuable support. I am very thankful to all the Scientists and staff of RFRI, Jorhat for their help in providing treated bamboo products and valuable information... I would also like to thank TOPCEM INDIA Plant's Quality Control Department for helping in the collection of samples.

REFERENCE

1) Ahmad, S et al (2014) "Mechanical Properties of Bamboo Fibre Reinforced Concrete", *Second International Conference on Research in Science, Engineering and Technology.*
2) Kazmi1, Md Athar et al. (2015) "Investigations on Micro Silica (Silica Fume) as Partial Replacement of Cement in Concrete" *International Journal of Science and Research (IJSR) ISSN (Online): 2319-7064, Vol – 6*
3) Kiran1, T.G.S; Ratnam2, M.K.M.V (Dec. 2014) "Fly Ash as a Partial Replacement of Cement in Concrete and Durability Study of Fly Ash in Acidic (H_2SO_4) Environment" *International Journal of Engineering Research and Development, e-ISSN: 2278-067X, Vol - 10, Issue 12, PP.01-131*
4) Mohod, M.V; Samrit, Swapnil; Shrikhande , Piyush (2016) "Use of Fly Ash as Partial Replacement of Cement in Concrete Pavements" *International Conference on Science and Technology for Sustainable Development (ICSTSD) ISSN: 2348 – 8352,Page60*

Notations

CCB	Copper Chrome Boron	FM3	Fly ash 10% + Micro silica 15%
NC	Normal concrete	BAF11	Bamboo fibre 4% + Fly ash 0%
BAF1	Bamboo fibre 4% + Fly ash 15%	BAF22	Bamboo fibre 0% + Fly ash 15%
BAF2	Bamboo fibre 4% + Fly ash 15%	BAM11	Bamboo fibre 4% + Micro silica 0%
BAM1	Bamboo fibre 4% + Micro Silica 10%	BAM22	Bamboo fibre 0% + Micro silica 10%
BAM2	Bamboo fibre 4% + Micro Silica 15%	FM11	Fly ash 15% + Micro silica 0%
FM1	Fly ash 10% + Micro silica 10%	FM22	Fly ash 0% + Micro silica 15%
FM2	Fly ash 15% + Micro silica 10%		

Comparative study on concrete cubes using different waste materials

Victory, W.[1], Sachidananda, K.[1] and Leimapokpam, D.[2]

[1] Lecturer, Department of Civil Engineering, NIT Manipur, Langol – 795004, India.
[2]UG Student, Department of Civil Engineering, NIT Manipur Langol – 795004, India.

ABSTRACT

The study aims at the utilization of crushed bricks, broken marbles and tiles waste as a substitution of the coarse aggregates in concrete. The strength and performance of conventional concrete and waste substituted concretes are studied and compared. A concrete mix designed of 1:1:2 (cement-sand-aggregate) are maintained. The samples are prepared along with a mixture of cement-sand-crushed bricks, cement-sand-broken marbles and cement-sand-broken tiles by replacing the coarse aggregate. A total of 12 concrete cubes are casted with and without waste materials for 7, 14 and 28 days. These concretes are tested under compression for the mentioned respective days. Test results indicate that broken marble waste gives the highest compressive strength of concrete upon the other materials. From the study, it thus revealed that the strength and the properties of concrete can be enhanced by using the waste materials which is economically viable and environment-friendly.

Keywords: aggregates, broken tiles, broken marbles, mix design

1. INTRODUCTION

In concrete mix design, aggregate plays a vital role and constitutes over 70% of the total volume of the concrete [1]. Therefore, aggregate is the main challenging issue nowadays. It depends on the availability and the cost at the site. Due to this reason, recycled aggregates from construction, demolition and excavation wastewere used as partial or full replacements of natural aggregates. Moreover, the rapid growth of construction activity reduces the available sources of natural aggregates. The only way is to search an alternative material which can fully or partially replaced naturally available material in construction.

Husain et al. studied crushed bricks as the replacement of the coarse aggregate and observed that the compressive strengths of crushed brick concrete were 75-80% more than that of normal concrete at 28 days. Besides, the splitting tensile strength increases and modulus of elasticity decreases for the modified concrete mix [2].Cachim studied the crushed burnt bricks as partial substitute for gravel as coarse aggregate and observedthat the mechanical properties of concrete were almost similar up to 15% replacement of aggregates with burnt bricks [3].Khaloo investigated the properties of brick aggregates and compares the properties of concrete with brick aggregates and stone aggregates. Further, observed that the replacement does not reduced the strength of concrete for up-to 20% [4].Khalaf and DeVenny investigated the thermal properties of brick aggregates and concluded that the brick aggregates performed better than gravel at elevated temperatures [5]. Sadek *et a*l. investigated the waste generated from the marble processing units and used as a partial replacement of conventional coarse aggregate and fine aggregate in different volume (0%- 100%) by weight in solid concrete bricks and observed that the compressive strength increased as the percentage of replacement increased [6]. Hebhoub *et al.* studied the conventional coarse aggregate by replacing marble waste aggregate with constant water-cement ratio of 0.5. The results showed that, workability decreased as replacement level increased. Further, the compressive and tensile strength of all concrete mixes containing marble aggregate increased up to 75% by weight [7].Fengli *et al*. concluded that recycled ceramic tiles aggregate under 9.5 mm as partial replacement of natural aggregate in concrete are feasible to reuse. The apparent density of ordinary concrete is higher than that of Recycled Ceramic Concrete (RCC) and it helps to reduce the self- weight of constructions. However, under similar workability condition, when the replacement rate is lower than 20%, the splitting tensile strength of RCC is poor because the ultra-fine sand has high mud content. Moreover, when the replacement rate is greater than 40%, the compressive strength and splitting tensile strength are higher than those of the reference concrete. The use of 100% recycled ceramic as fine aggregate increases both splitting tensile strength and compressive strength significantly [8].Torgal *et al*. investigated the ceramic powder and was

used in concrete mixes as partial substitution of cement, while fine and coarse ceramic tiles aggregates were used as 100% substitution of fine and coarse natural aggregates and foundthat compressive strengthincreases by incorporating ceramic tiles waste in concrete [9]. In another study, Al Bakri *et al*. useddifferent types of recycled ceramic tiles waste as partial replacement of coarse aggregateinconcrete mixes with different w/c ratio; 0.4, 0.5, and 0.7. It was observed that all concrete mixes incorporating ceramic aggregates have compressive strength higher than that of conventional concrete [10].

In this study, an attempt has been made to study the feasibility of using demolished crushed bricks, broken marbles and tiles obtained from flooring worksand to observe the compressive strength of the concrete grade with these materials for assessing the feasibility of saving natural resources.The experimental studies were conducted at Universal Testing Machine (UTM) to determine the compressive strength of concrete mix on replacement of coarse aggregates by these waste materials.

2. MATERIALS AND METHODOLOGY

The materials used in the study are demolished waste materials such as broken tiles, marbles and bricks from the construction site near NIT Manipur, Langol as a replacement of coarse aggregates along with cement and sand. The primary test such as fineness of cement [14], normal consistency test [15], initial and final setting time of cement[16], fineness modulus of aggregates [11], specific gravity of sand[12], bulking of sand [12], water absorption test [12], Aggregate Impact Value (AIV) test [13], flakiness and elongation index for aggregates [11] were also conducted and found that the value lies within the permissible limit. The M-25 mix design has been adopted in the study with different waste materials. Further, the workability test or slump test of concrete [17] and compressive strength of concrete cubes in UTM were conducted.

Fig. 1. Broken tiles

Fig. 2. Broken marbles

Fig. 3. Broken bricks

Fig. 4. Mannually crushing process

Fig. 5. Crushed bricks

Fig. 6. Crushed marbles

Fig. 7. Crushed tiles

3. RESULTS AND DISCUSSION

The compressive strength of concrete is given in terms of the characteristic compressive strength of 150 mm size cubes tested at 28 days (f_{ck}). The characteristic strength is defined as the strength of the concrete below which not more than 5% of the test results are expected to fall.The strength of concrete increases with age. Table 1 shows the strength of concrete at different ages of the samples.

Fig. 8. Sample 1 placed in UTM

Fig. 9. Sample 2 placed in UTM

Fig. 10. Sample 3 placed in UTM

Fig. 11. Sample 4 placed in UTM

Table1. Compressive Strength of Different Samples

Sl. no	Sample	Compressive strength (N/mm^2)		
		7days	14days	28days
1.	Cement + sand + coarse aggregate,S_1	18.07	21.3	32.62
2.	Cement + sand + broken bricks,S_2	22.25	22.67	29.95
3.	Cement + sand + broken marble,S_3	24.04	26.31	33.76
4.	Cement + sand + broken tiles,S_4	21.90	24.67	31.35

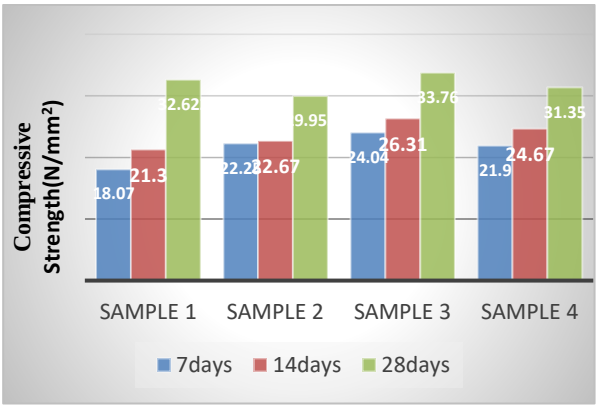

Fig 12: Compression of Compressive Strength of Concrete Cubes

4. CONCLUSION

The study reveals the effect of brick, marble and tile aggregates on the properties of concrete. Concrete mixes containing brick, marble and tile aggregate shows marginal increase in compressive strength as compared with normal grade concrete for 7 days and 14 days. It has been observed that for 7 days, 14 days and 28 days, the compressive strength of normal grade concrete are 18.07 N/mm^2, 21.30 N/mm^2 and 32.62 N/mm^2 respectively while the strength of concrete grade with different demolished waste materials have been increased as compared with the normal grade concrete except for the brick concrete and broken tiles concrete in 28 days. Further, it has been investigated that the concrete with broken marble have the highest compressive strength among all the concrete grades using different waste materials. The compressive strength of the broken marble concrete are found to be 24.04 N/mm^2, 26.31 N/mm^2 and 33.76 N/mm^2 for the respective 7 days, 14 days and 28 days. Furthermore, observed that the natural aggregates can be replaced by demolished waste materials in concrete mixes. In future, the strength and properties of the concrete can be studied by using

various materials like coconut shell, rice husk ash and jute fibers that are readily available and regarded as waste materials. Besides, it will reduce the cost and environmental hazard.

REFRENCES

1) Agbede, I.O., and Joel, M., (2008): Use of Cement sand Admixture in Laterite brick production for low cost housing ISSN 1583-1078, *Leonardo Electronic Journal of Practices and Technologies*, 12, 163-174
2) Husain M. Husain, Al Hamed Abdul-hafidh M.S. and Mustafa KH. Kasim, (1995): The Use of Crushed Brick Pretreated with Cement Syrup as Aggregate for Concrete, S.J. Tikrit Univ. Engg. Sci., 2(2).
3) Cachim, P. B., (2009): Mechanical Properties of Brick Aggregate Concrete, *Construction and Building Materials***,** 23, 1292-1297.
4) Khaloo, A. R., (1994): Properties of Concrete Using Crushed Clinker Brick as Coarse Aggregate, *ACI Materials Journal*, 91(2), 401-407.
5) Khalaf, F. M., and De Venny A. S., (2004): Performance of Brick Aggregate Concrete at High Temperatures , *Journal of Materials in Civil Engineering, ASCE*, 16(6), 556-565.
6) Sadek, D.M., EL-Sayed, W.S., Heniegal, A. M. A., and Mohamed, A.S., (2013): Utilization of Solid Wastes in Cement Bricks for an Environmental Beneficial, *International Journal of Engineering*, 188(3), *ISSN 1584 – 2673.*
7) Hebhoub, H., Aoun, H., Belachia, M., Houari, H., and Ghorbel, E., (2011): Use of Waste Marble Aggregates in Concrete, *Construction and Building Materials*, 25, 1167-1171.
8) Fengli, LIU, Junhua LIU, Baoguo,M.A, Jian, HUANG, Hainan, LI, (2015): Basic Properties of Concrete Incorporating Recycled Ceramic Tiles Aggregate and Ultra-fine Sand, *Journal of Wuhan University of Technology*, 30 (2).
9) Torgal, F. Pacheco, Jalali, S., (2010): Reusing ceramic tiles wastes in concrete, *Construction and Building Materials*, 24, 832-838.
10) Al Bakri A. M. M., Norazin M.N, Kamarudin H., CheMohdRuzaidi G.,(2008): The Potential of Recycled Ceramic Tiles Waste as Coarse Aggregates for Concrete, *Proceedings ofMalaysian Universities Conferences on Engineering and Technology, MUCET held at March 8th -10th, 2008 in PutraBrasmana,Perlis,Malaysia.*
11) IS Code: 2386 part-1-1963 – Sieve analysis and fineness modulus of aggregate, flakiness and elongation index of coarse aggregate
12) IS Code: 2386 part-3-1963 – Bulking of sand, specific gravity and water absorption test
13) IS Code: 2386 part-4-1963 – Aggregate Impact Value (AIV) Test
14) IS Code: 4031-part-1-1996 – Fineness of cement by sieve analysis
15) IS Code: 4031-part-4-1988 – Normal consistency of cement
16) IS Code: 4031-part-5-1988 – Initial and final setting time of cement
17) IS Code: 1199-1959 – Slump test of concrete.

Rheological study of bitumen using low density polyethylene

Victory, W.[1], Sachidananda, K.[1] and Devi, N.R.[2]

[1] Lecturer, Department of Civil Engineering, NIT Manipur, Langol – 795004, India.
[2]UG Student, Department of Civil Engineering, NIT Manipur, Langol – 795004, India.

ABSTRACT

In this paper an attempt is made to utilize the plastic waste derived from Low Density Polyethylene (LDPE) used in packaging of bakery products and other sweets as an additive to upgrade the physical properties of VG-10 grade bitumen used in flexible pavement. The basic rheological parameter test like viscosity, penetration and ductility are conducted both for VG-10 grade bitumen and bitumen mixed with LDPE in different proportions at the rate of 5%, 6%, 7% and 8% by weight of bitumen. It has been observed that the plastic waste modified bitumen mix shows better rheological properties than the normal grade bitumen. The study will not only increased the properties of the bitumen but also helps in improving the environment and handling non-biodegradable plastic waste easily thereby minimizing the cost of road construction.

Keywords: Low Density Polyethylene, bitumen, viscosity, ductility, penetration.

1. INTRODUCTION

Bhardwaj *et al*. studied the variation of the properties of bitumen on addition of waste plastic at different percentages and observed that the properties of bitumen enhances with addition of the waste plastic [1]. Prasad and Sowmya observed that the bitumen which is conventional material used in road construction can be partially replaced by the waste plastic and rubber. Further, reveals that the addition of rubber and plastic in different percentages in bitumen were found out the optimum content to be 6% and the used of plastic in 6% by weight of bitumen improves the pavement stability [2].Barad investigated the properties of modified bitumen and compared to normal bitumen. It was also observed that the aggregate coated with plastic shows the improved binding properties as due to increase area of contact between bitumen and polymer [3]. Sasane *et al*. investigated the use of plastic in bitumen as an innovative technology and reveals that the strength and life of the pavement increases by using the plastic [4]. Rajasekaran *et al*. investigated that aggregate coated with the polymer has many advantages and helps in improving the flexible pavement quality as well as the aggregate quality. It helps in the disposal of waste plastic obtained from the domestic and industrial packing materials. The dry process is more valuable as it disposed the 80% of waste polymer in eco-friendly way. And use of polymer reduces the equivalent bitumen quantity and therefore reducing the construction cost of road [5]. Ahmed studied the concept of utilization of plastic waste in construction of flexible road pavement in India. Further, observed that the quality of modified bitumen using the polymer had more advantageous other than the normal bitumen. It has better resistance towards temperature, water and other extreme change in climate and it was regarded as the most important construction material for flexible road pavement [6]. Tiwari and Rao studied the use of waste plastic in the construction of roads to reduce the environmental pollution created by plastic in economic way by using the plastic waste in the construction of road [7].

In this study, the VG-10 grade bitumen with different percentages of Low density polyethylene (5%, 6%, 7% and 8% by weight of bitumen) as additive has been used. Further, the rheological properties of bitumen have been investigated by conducting penetration, ductility and viscosity test.

2. TEST MATERIAL

2.1. Bitumen

VG-10 grade bitumen has been used in the study and the properties are described in table 1.

Table 1: Properties of VG-10 grade bitumen

Property	Value
Penetration (mm)	80-100
Viscosity at 60 (p)	800
Viscosity at 135 (cst)	250
Ductility at 25 (cm)	75

1.2. Low Density Polyethylene (LDPE)

Low Density Polyethylene (LDPE) is a thermoplastic made from the monomer ethylene. LDPE contains element carbon and hydrogen. It is defined by a density range from 0.910 gm/cm^3 to 0.940 gm/cm^3& is not reactive at room temperature, except by strong oxidising

agent. LDPE can withstand temperatures of 80℃ continuously and 95℃ for short time & is quite flexible, and tough but breakable. It has more branching, so its intermolecular forces are weaker, its tensile strength is lower & its resilience value is higher LDPE is widely used for manufacturing various containers, dispensing bottles, wash bottles, tubing, plastic bags for computer components, and various moulded laboratory equipment. Its most common use is in plastic bags[11].

Fig. 1: Low Density Polyethylene(LDPE)

Fig. 2: Shredded LDPE

2. METHODOLOGY

The LDPE shredding is done by drying the polyethylene packets and cut into tiny pieces of 2 mm size as the polyethylene is to be added with bitumen, it is to be ensured that the mixing will be proper. The smaller the size of the polyethylene, the more is the chance of good mixing. Further, the samples were prepared by heating the bitumen with the percentages of LDPE at more than 135 ℃ until the fluidity flows.

3. TEST CONDUCTED

3.1. Penetration Test

The consistency of bituminous materials varies depending upon several factors such as constituents, temperatures etc. Penetration test determines the consistency of bitumen. In this test, the penetration is measured by needle in a bitumen sample maintained at 25°C during 5s.[10].

Fig. 3: Penetrometer with needle

3.2. Viscosity Test

Viscosity is measured by determining the time taken by 50ml of the binder in fluid state to flow through a specified orifice under standard temperature and conditions [8].

3.3. Ductility Test

Ductility test is carried out on bitumen test adhesive property of bitumen and its ability to stretch [9].

Fig.4. Ductility Testing Machine

Fig. 5. Briquette Mould Filled with Bitumen

Table 2: Results of the Test Conducted

LDPE %	Viscosity (cst) at 135℃	Ductility (cm)	Penetration (mm)
0	250	75	80
5	265	64.5	73
6	279.2	54.7	67
7	291.5	45.7	61.5
8	307.5	38.3	57.3

4. RESULT AND DISCUSSION

The viscosity and penetration increased as the LDPE % increased while the penetration decreased as the LDPE % increased. The result is shown in table 2. This means the rheological properties were enhanced as the LDPE content increased.

5. CONCLUSION

From the study, itis observed that the viscosity increase with increasein LDPE while ductility and penetration decrease with increase in LDPE. The properties of VG-10 grade bitumen enhances by adding LDPE as additives. The properties are improved in modified bitumen with LDPE than the normal conventional bitumen. Besides, it can provide better strength and longer life period with low maintenance cost. The study will help to reduce the volume of plastic waste to be disposed off by incineration and land filling thereby developing an eco-friendly environment.Further studies should be done to investigate the characteristic properties of modified bitumen using different test such as Fourier Transform Infra-RedTest (FTIR) or Fourier Transform Infra-Red Spectroscopy with higher bitumen grade like VG-20, 30 and 40. Certain additives can also implement like Crumb Rubber, HDPE& other tire rubber that enhances the properties of the bitumen.

REFERENCES

1) Bhardwaj, A., Kesav, B. K. and Singh, A. D., (2017): Application of Waste Plastic in Modifying Bitumen Properties, *International Journal of Engineering and Research Application*,7(4), 79-81.
2) Prasad, A.R., Sowmya N. J., (2015): Bituminous Modification with Waste Plastic and Crumb Rubber, *IOSR Journal of Mechanical and Civil Engineering*, 12 (3), 108-115
3) Barad Mahesh M., (2014): Use of Plastic in Bituminous Road Construction, *Journal of Information, Knowledge and Research in Civil Engineering*, 3(2), 208-212.
4) SasaneNeha, B., Harish, G., Patil, J.R., Khandekar, S.D., (2015): Application of Waste Plastic as an Effective Construction Material in Flexible Pavement, *International Research Journal of Engineering and Technology*, 2 (3), 1943-1948.
5) Rajasekaran, S., Vasudevan, R. andPaulraj, S., (2013): Reuse of Waste Plastics Coated Aggregates- Bitumen Mix Composite for Road Application, *Green Method American Journal of Engineering Research*, 2(1), 01-13.
6) Ahmed, M.A.,(2014): Low Density Polyethylene Modified Dense Graded Bituminous Macadam, *International Journal of Engineering Trends and Technology*, 16(8).
7) Tiwari, A. V. and Rao, Y. R. M., (2017): Study of Plastic Waste Mixed Bituminous Concrete Using Dry Process for Road Construction, *The Asian Review of Civil Engineering Journal of Engineering Research and Studies*, 6(2),1-6.
8) Indian Standards (IS), 1206 (1978): Methods for determining viscosity, *IS 1206 Bureau of Indian Standards, New Delhi, India*.
9) Indian Standards (IS), 208 (1978): Methods for determining ductility, *IS 208 Bureau of Indian Standards, New Delhi, India*.
10) Indian Standards (IS), 1203 (1978): Methods for determining penetration, *IS 1203 Bureau of Indian Standards, New Delhi, India*.
11) Singh., R.I., (2016): Use of Waste Plastics in Road Construction, Central Institute of Plastics Engineering and Technology.

Marshall stability test by replacing aggregates with over burnt bricks and marble stones

Paul, S.R.[1] and Mazumdar, N.[2]

[1] UG Student, Department of Civil Engineering, Royal Global University, Guwahati – 781035, India.
[2] Assistant Professor, Department of Civil Engineering, Royal Global University, Guwahati - 781035, India.

ABSTRACT

In the present research work, an attempt has been made to determine the increase or decrease in strength of bitumen mix with sustainable materials used for road constructions. The bitumen mixed has been replaced by over burnt bricks and Bhutan mosaic marble stones by three different proportion 100% coarse mix, 80% coarse + 20% fine mix, 60% coarse + 40% fine mix in the present study. The sieve size for coarse and fine mix is 12.5mm passing and 9.5mm, 6mm, 4.75mm, 2mm retained. The bitumen grade used in this research is A25 and it is divided into three parts 3%, 5% & 7% for better determination of strength by performing Marshall Stability Test.

This report is not a plea to implement over burnt bricks and marble stones as replacement of aggregates unconditionally. The Ministry of Road Transport and Highway has suggested that minimum value of Marshall Stability should be 900kg. In the present study 7 samples have stability more than other 27 samples. The minimum Marshall stability should be 900kg which is accepted as per IS 1202 (1978). Over burnt bricks can be used as replacement of aggregates in plane areas where presence of aggregates might be less. Marble stones can be used as aggregate replacement because of its high stability and marble refuse is cheap in cost and is used where presence of aggregate is minimal or transportation cost of aggregate is high.

Keywords: bitumen, over burnt bricks, Bhutan mosaic marble stones, aggregates, marshall stability

1. INTRODUCTION

Roads are used by various types of road vehicles like passenger cars, buses, trucks, two and three wheeled automobiles, pedal cycles and animal drawn vehicles and also the pedestrians. Road transport infrastructure requires the lowest initial investment in comparison to that for the infrastructure of other transportation modes. The cost of any class of road vehicle is much lower than that of other carriers like the railways, ships and aircrafts. The initial cost of construction and the cost for maintenance of roads is also lesser than those for railway tracks, harbours and airports.

2. METHODOLOGY OF STUDY

In the present study, the outcome is the strength of the aggregate mix by performing Marshall Stability Test & replacing the aggregates with over burnt bricks & Bhutan mosaic marble stones for road construction. At the beginning of this experiment some tests are performed to determine the softening point and grade of bitumen. Then the aggregates are crushed into sieve size 12.5mm (passing) and 9.5mm, 6mm, 4.75mm, 2mm (retained). Out of which 9.5mm and 6mm is coarse aggregate and rest are fine aggregate. Similarly this procedure is followed for over burnt bricks & marble stones too. Here A-25 grade bitumen is used and classified into three parts 3%, 5% and 7% respectively. The required amount of bitumen is calculated for each of the percentage from the total aggregate sample used i.e. 1200gms. Lastly Marshall Stability Test is performed to obtain the strength of the three samples, comparing their stability and determining economic and future prospects.

3. OBSERVATION, RESULTS AND GRAPHS

3.1 Softening point of a bitumen.

Table no.1

Temperature	46° C	47° C
Average	46.5° C	
Softening point of bitumen	46.5° C	

The softening point of bitumen is at 46.5° C.

3.2 Penetration value of bitumen.

Table no. 2

Penetrometer reading		Penetration
Initial Reading	Final Reading	(mm)
0	225	22.5

The penetration value of given sample of bitumen is 22.5mm and the bitumen grade is A25.

3.3 Stripping value of road aggregate.

The stripping value of road aggregate is 2%.

3.4 Ductility test.

Table no. 3

Reading (cm)	Briquette No.		Mean value (cm)
	50mm/min	20mm/min	
Initial reading	0	0	0
Final reading	8	8.2	8.1
Ductility	8	8.2	8.1

The ductility of bitumen is 8.1cm. The minimum ductility value of A25 bitumen is 5-9cm. "A" stands for Assam petroleum.

3.5 Marshall stability test of bituminous mixture.

3.5.1 Aggregates

Table no. 4

Sample 1.	Aggregate	Bitumen %	Division	Load (kg)
Aggregates	100% CA	3%	15	49.35
		5%	55	180.95
		7%	155	509.95
	80% CA + 20% FA	3%	15	49.35
		5%	125	411.25
		7%	300	987
	60% CA + 40% FA	3%	120	394.8
		5%	155	509.95
		7%	355	1167.95

Graph no. 1

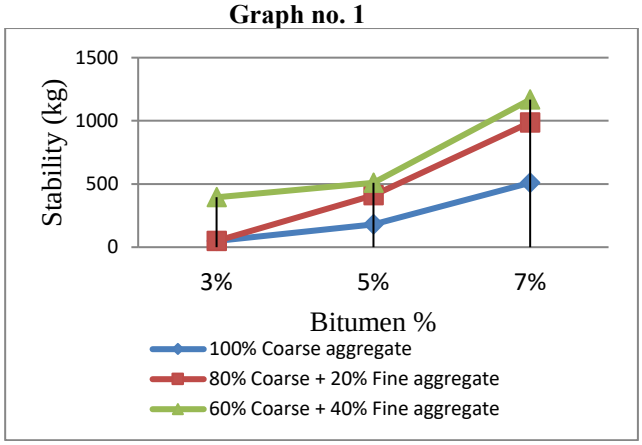

In 100% coarse mix the maximum stability is at 7% bitumen.

In 80% coarse + 20% fine mix the maximum stability is at 7% bitumen.

In 60% coarse + 40% fine mix the maximum stability is at 7% bitumen

3.5.2 Over burnt bricks

Table no. 5

Sample 2.	Over burnt bricks	Bitumen %	Division	Load (kg)
Over burnt bricks	100% Coarse	3%	105	345.45
		5%	120	394.8
		7%	25	82.25
	80% Coarse + 20% Fine	3%	0	0
		5%	0	0
		7%	0	0
	60% Coarse + 40% Fine	3%	170	559.3
		5%	325	1069.25
		7%	330	1085.7

Graph no. 2

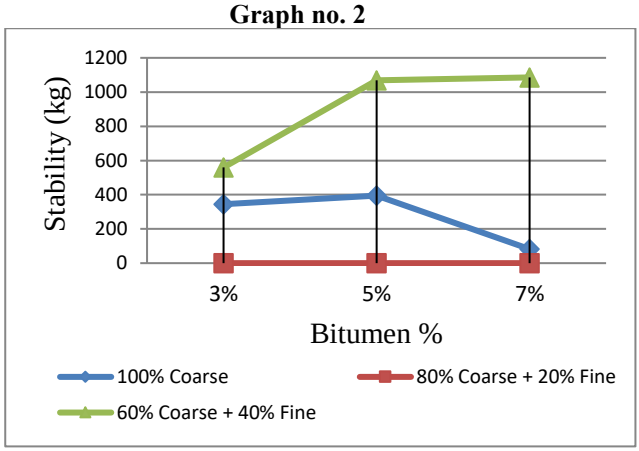

In 100% coarse mix the maximum stability is at 5% bitumen.

In 80% coarse + 20% fine mix there is no stability.

In 60% coarse + 40% fine mix the maximum stability is at 7% bitumen.

3.5.3 Marble stones

Table no. 6

Sample 3.	Marble stones	Bitumen%	Division	Load (kg)
Marble stones	100% Coarse	3%	50	164.5
		5%	190	625.1
		7%	255	838.95
	80% Coarse+ 20% Fine	3%	140	460.6
		5%	150	493.5
		7%	315	1036.35

	60% Coarse + 40% Fine	3%	255	838.95
		5%	660	2171.4
		7%	650	2138.5

Graph no. 3

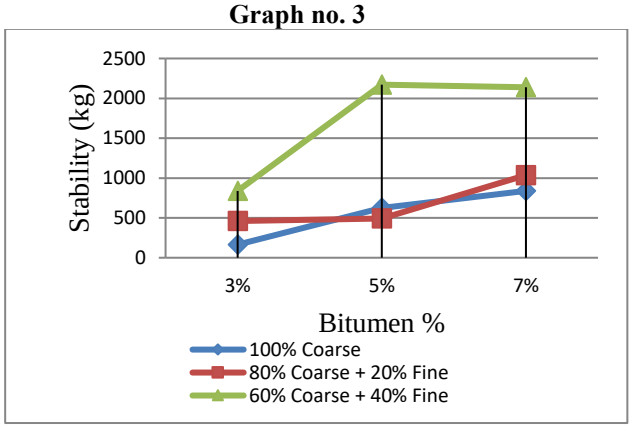

In 100% coarse mix the maximum stability is at 7% bitumen.

In 80% coarse + 20% fine mix the maximum stability is at 7% bitumen.

In 60% coarse + 40% fine mix the maximum stability is at 5% bitumen.

3.5.4 Comparing the graphs which has high amount of stability

Table no. 7 100% Coarse

Samples	Mix	Bitumen%	Division	Load (kg)
Aggregate	100% Coarse	3%	15	49.35
		5%	55	180.95
		7%	155	509.95
Over burnt bricks	100% Coarse	3%	105	345.45
		5%	120	394.8
		7%	25	82.25
Marble stones	100% Coarse	3%	50	164.5
		5%	190	625.1
		7%	255	838.95

Graph no. 4 100% Coarse

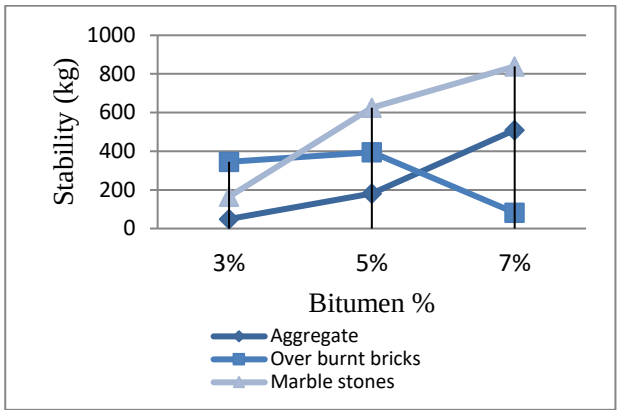

Marbles stones have the maximum stability at 7% bitumen content but it will not be used in road construction because it doesn't satisfy The Ministry of Road Transport and Highway proposed criteria i.e. minimum stability value should be 900kg.

Table no. 8 80% coarse + 20% fine

Samples	Mix	Bitumen%	Division	Load (kg)
Aggregate	80% Coarse + 20% Fine	3%	15	49.35
		5%	125	411.25
		7%	300	**987**
Over burnt bricks	80% Coarse + 20% Fine	3%	0	0
		5%	0	0
		7%	0	0
Marble stones	80% Coarse + 20% Fine	3%	140	460.6
		5%	150	493.5
		7%	315	**1036.35**

Graph no. 5 80% coarse + 20% fine

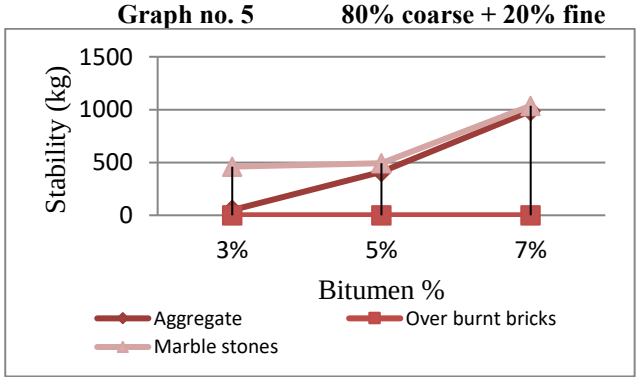

Marbles stones & over burnt bricks have the maximum stability at 7% bitumen content and it will be used in road construction because it satisfy The Ministry of Road Transport and Highway proposed criteria i.e. minimum stability value should be 900kg.

Table no. 9 60% coarse + 40% fine

Samples	Mix	Bitumen%	Division	Load (kg)
Aggregate	60% Coarse + 40% Fine	3%	120	394.8
		5%	155	509.95
		7%	355	**1167.95**
Over burnt bricks	60% Coarse + 40% Fine	3%	170	559.3
		5%	325	**1069.25**
		7%	330	**1085.7**
Marble stones	60% Coarse + 40% Fine	3%	255	838.95
		5%	660	**2171.4**
		7%	650	**2138.5**

Graph no. 6 60% coarse + 40% fine

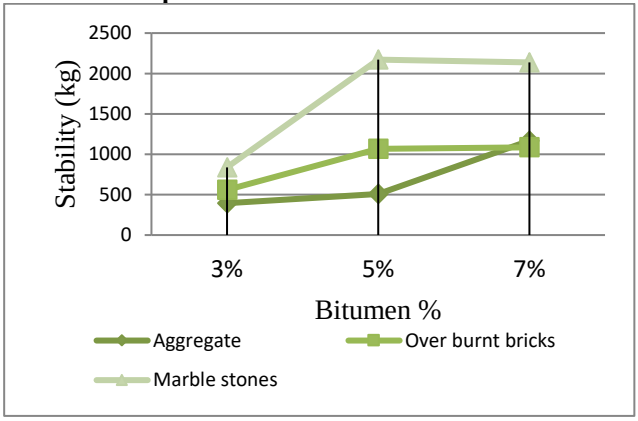

Marbles stones have the maximum stability at 5% & 7% bitumen content; over burnt bricks have the maximum stability at 5% & 7% bitumen content and the aggregates have the maximum stability at 7% bitumen content. But it will be used in road construction because it satisfies The Ministry of Road Transport and Highway proposed criteria i.e. minimum stability value should be 900kg.

4. CONCLUSIONS

From the present research work it can be concluded that the strength of bitumen mix when mixed with sustainable materials increases its strength up to the acceptable limit as per IS 1202 (1978). Further, The Ministry of Road Transport and Highway has suggested that minimum value of Marshall Stability should be 900kg.

In the present research work 7 samples fulfills the above mentioned criteria and are as follows:-

- (80%coarse + 20% fine) aggregate mix at 7% bitumen is 987kg.
- (60%coarse + 40% fine) aggregate mix at 7% bitumen is 1167.95kg.
- (60%coarse + 40% fine) over burnt brick mix at 5% bitumen is 1069.25kg.
- (60%coarse + 40% fine) over burnt brick mix at 7% bitumen is 1085.7kg.
- (80%coarse + 20% fine) marble stone mix at 7% bitumen is 1036.35kg.
- (80%coarse + 20% fine) marble stone mix at 5% bitumen is 2171.4kg.
- (60%coarse + 40% fine) marble stone mix at 7% bitumen is 2138.5kg.

5. ACKNOWLEDGEMENTS

The satisfaction of completing a project successfully would remain incomplete without the mention of people whose constant encouragement and guidance has been a great source of inspiration throughout the course of this project.

We would like to take this opportunity to express our sincere and heartfelt gratitude to our H.O.D Sir Dr. Arnab Sarma for giving us the opportunity to do the project work. We would also like to thank our project guide Nitisha Mazumdar, Assistant Professor, Department of Civil Engineering, Royal School of Engineering and Technology, for supporting and guiding us through the completion of the project work. We would also like to thank our civil engineering laboratory assistants and staff for providing us the required instruments which were required in our project work and helping us throughout the duration of the project.

I would like to thank my fellow friends Swagat Kumar Medhi, Sivanga Pratim Sarma and Zeshan Zakaria as without their support and help it is impossible to complete this project.

Finally, we would like to extend our gratitude to beloved parents for supporting and helping us in the completion of this project work.

6. REFERENCES

1) Mohammed A. Ali (2004) INTERNATIONAL JOURNAL OF PAVEMENT ENGINEERING approach towards Effect of Mineral Fillers types on Marshal Stability and retained strength.
2) Adewale O., Abah, U. Raymond (2015) INTERNATIONAL JOURNAL OF CIVIL ENGENEEERING approaches towards experimental evaluation of the effects of partial replacement of aggregate with Graded Palm Kernel Shell *ISSN 0976-4399*.
3) Roshan K., Tamrakar, G. (2018) INTERNATIONAL JOURNAL OF TRANSPORTATION ENGINEERING comparative study of using paving materials.

Soil based blocks stabilised with cement and sugarcane bagasse ash

Das, J.K. [1]

[1] Assistant Professor, Department of Civil Engineering, Assam downtown University, Panikhaiti, Guwahati 781026, India.

ABSTRACT

Aim of this paper is to check the effect of sugarcane bagasse ash (SBA) in cement stabilised soil blocks. In addition, it also contributes in waste management by utilising sugarcane bagasse. The locally available soil was stabilised with 10% and 15% OPC and SBA were mixed as admixture with 1%, 2%, 3%, 4% and 5% by weight of dry soil. The soil based blocks were manufactured using wooden mould of size 19 cm × 9cm × 9cm. Casting were done at one target density and water content and then curing for a period of 28 days. All blocks were then tested in the laboratory to check their compressive strength and water absorption as per Bureau of Indian Standards (BIS) specifications. The test results indicates that cement stabilisation of soil at 10% and 15% cement content meet the specification of Class 20 and Class 30 blocks as per IS: 1725-1982. Also, addition of SBA to cement stabilised soil block results in an increased compressive strength and there was slight increase in water absorption but was still comfortably within the norms stipulated by BIS.

Keywords: SBA, soil stabilisation, compressive strength

1. INTRODUCTION

Fired bricks have been the primary building material for construction for a long time. However, in the recent years there has been a shift away from the utilization of fired bricks towards eco-friendly building materials. Utilization of waste based construction materials like flyash bricks has become one of the popular choices. However, in developing countries like India, where there is a need for low cost building materials for housing, earth block is one of the best alternatives. The advantages of compressed earth block construction include easy availability of material, economy, ease of use, fire resistance, beneficial climatic performance, and low energy consumption.

1.1 Sugarcane bagasse ash (SBA)

India is one of the largest growers of sugarcane. The major solid wastes generated from the sugar manufacturing process include sugarcane trash, bagasse, press mud, bagasse fly ash, and spent wash. Bagasse is the fibrous remains of the cane after extraction of sugarcane juice. In many industries, bagasse is used as fuel resulting in the generation of ash called SBA. SBA is one of the wastes of economic importance generated from the sugar industry, as it has lots of potential uses. SBA has been used in the manufacture of low cost adsorbents, ceramics, biomass ash filters, concrete, soil stabilization and recently in stabilized earth blocks.. stabilised with 10% and 15% OPC and SBA were mixed as admixture with 1%, 2%, 3%, 4% and 5% by weight of dry

1.2 Ordinary portland cement (OPC)

Ordinary Portland Cement (OPC) is one of the most common stabilizers used for soil stabilization. However, it is well-known fact that manufacture of OPC contributes to a lot of CO_2 emissions which cannot augur well for a low cost green material. Earlier research in the manufacture of stabilized soil blocks have mostly concentrated on cement and lime stabilization of blocks The primary objective of this study is to analyse the performance of cement stabilized earth blocks admixed with SBA in terms of compressive strength and water absorption.

2. LITERATURE STUDY

Following are some of the investigations have been done earlier by different research worker around the world:

J. Jijo, P. Kasinatha et.al studied the agricultural waste as a soil stabilizer. In their study, agricultural waste such as sugarcane bagasse ash along with cement was used as a stabilizer in the manufacturing of compressed stabilized earth block. From the result they observed that the addition of SBA increased the compressive strength of the blocks and slightly increased the water absorption but still met the standard requirement of BIS code. It is concluded that addition of SBA to OPC in stabilized block manufacture was capable of producing stabilized blocks at reduced OPC content that met the minimum required standards.

B.N patowary, N.Nath et.al studied the compressed stabilized block using cement and lime as a stabilizer. The fly ash was also used as cement admixture. From their study, it was found that the maximum strength was obtained for CSEB with stabilizer than CSEB without stabilizer. They concluded that the strength of the blocks (unburnt one) will increase eventually, but un-burnt bricks are more economic than the standard fired one as the production of CSEBs require less labour and does not require coal.

Millogo.Y et.al studied the Characteristics of soil-cement blocks when admixed with cow dung for the reason that cow dung is abundantly available and is a green building material. The various conclusions drawn from this study is that the compressive strength obtained after the addition was found to be greater than the block without stabilizer. Also there is significant improvement in the water resistance property.

H.B. Nagaraja, M.V. Sravan researched on the role of lime with cement in long-term strength of compressed stabilized earth blocks. In their study, the stabilizer content was maintained at 8%. Water absorption initially remained around 14%, which is slightly less than the pre- scribed value of 15% for good quality bricks but later with time, blocks have shown a continuous reduction in the water absorption. However, the combination of cement and lime has been found to be mutually very beneficial in imparting strength to the blocks in a much better way.

3. METHODOLOGY

Present study mainly focused on the utilization of sugarcane bagasse ash in compressed soil block construction. A number of test sample of soil block have been prepared mixing cement and SBA in various combination and characteristics like compressive strength and water absorption are determined for different combinations of SBA and cement. Various compositions of test samples are shown in table 1. The soil blocks were cast to its maximum dry density and at optimum moisture content.

Table 1 Material composition in %

Test ID	Soil	Cement	SBA
Case 1	89	10	1
Case 2	88	10	2
Case 3	87	10	3
Case 4	86	10	4
Case 5	85	10	5
Case 6	84	15	1
Case 7	83	15	2
Case 8	82	15	3
Case 9	81	15	4
Case 10	80	15	5

The methodology of this study is shown as flow diagram in fig. 1.

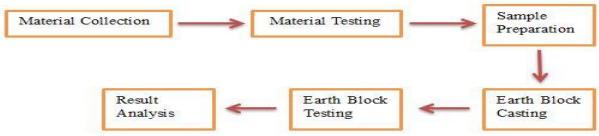

Fig. 1 Flow Diagram of Investigation.

4. EXPERIMENTAL WORKS

The materials adopted in the manufacture of the compressed stabilized earth blocks include the locally available soil, cement, and SBA. The soil adopted in the study was collected from near the Workshop Lab, within Assam Downtown University campus, Guwahati, India. Various soil properties were determined in the laboratory in accordance with the Bureau of Indian Standards (BIS) codes. The soil properties are listed in table 2.

The cement adopted in the stabilization of the soil for the manufacture of compressed stabilized block is Ordinary Portland Cement (OPC 53).

SBA adopted in the study was obtained from street sugarcane juice vendor and burnt in open space to obtain SBA.

Table 2 Soil properties

Soil Property	Value
Liquid limit	26%
Plastic limit	15%
Plasticity index	11%
Natural water content	18%
Field bulk density	1.47 g/cm^3
Maximum dry density	1.56 g/cm^3
Optimum moisture content	23%
BIS classification	Well graded soil

4.1 Selection of block size and mould fabrication

BIS code suggests three sizes for cement stabilized soil blocks with dimensions 19 × 9 × 9, 19 × 9 × 4, and 29 × 19 × 9, all dimensions being in cm. The block dimension adopted in this study was 19 cm × 9 cm × 9 cm. Based on the selected block size, two identical wooden moulds were fabricated and used for moulding of the blocks. Fig.2. shows the fabricated moulds adopted in the study.

Fig. 2 Mould adopted for moulding of stabilized block

4.2 Casting and curing of blocks

The soil blocks were cast to a fixed density of 1.56 g/cm^3 and a moisture content of 23%.The weights of soil, cement, and SBA were carefully measured and mixed in dry conditions thoroughly. The required content of water was measured, added to the mixture, and thoroughly mixed to get an even wet mix. The wet mix was then placed in the mould, and a rammer was used to compact the soil achieving more or less uniform density of blocks for testing. After the formation of the block, the mould was opened and the block was removed and was moisture-cured for a period of 28 days by sprinkling of water and covering with plastic gunny bags to prevent loss of moisture.

4.3 Compressive strength of stabilised block

The compression test on the stabilized soil blocks was done in accordance with BIS code specifications (fig.3). Fig.4. and fig.5.shows the compressive strength of 10 % cement stabilized blocks admixed with SBA. According to BIS specification, for cement stabilized blocks, there are two classes of blocks, class 20 and class 30 with minimum permissible standard strength of 1.96 MPa (20 kgf/cm²) and 2.94 MPa (30 kgf/cm²), respectively. The figure includes the compressive strengths of the two classes of blocks as well for comparison.

Fig. 3 Compression test on test block

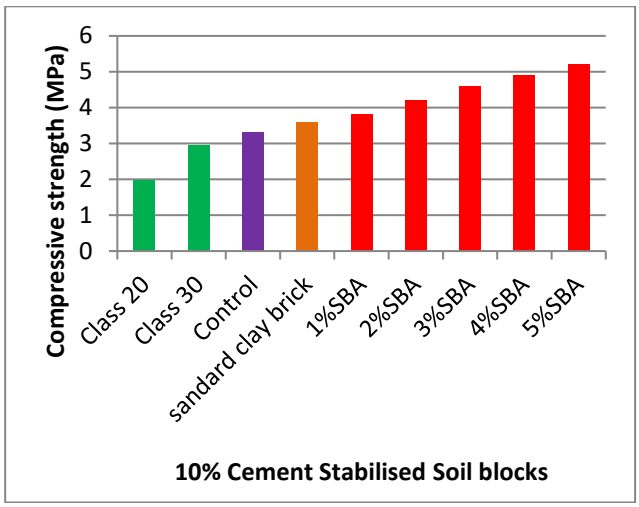

Fig. 4 Comparison of compressive strength of soil block mixed with 10% cement and varying percentage of SBA

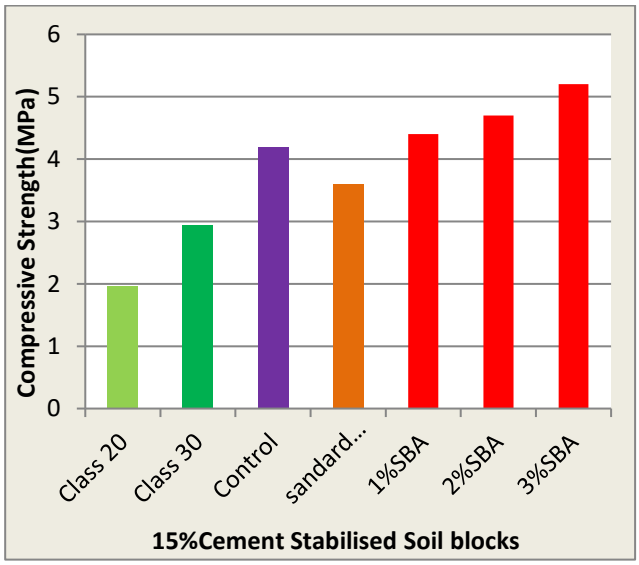

Fig. 5 Comparison of compressive strength of soil block mixed with 15% cement and varying percentage of SBA

4.4 Water absorption capacity of soil block

Water absorption test was also done in accordance with BIS specification. Fig.6. and fig.7.shows the water absorption of 10% cement stabilized soil blocks. The permissible limit for water absorption according to BIS specification of cement stabilized blocks is 15% which has also been included in the figure for comparison.

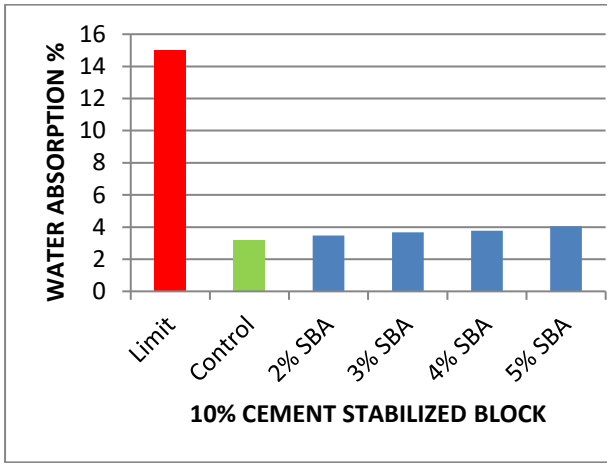

Fig. 6 Comparison of water absorption capacity of soil block mixed with 10% cement and varying percentage of SBA

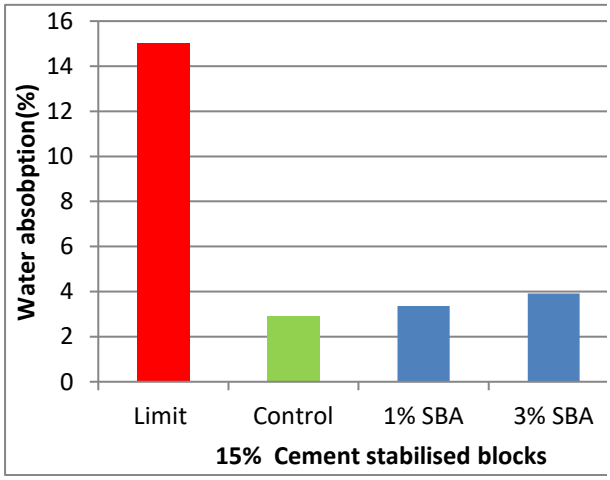

Fig. 7 Comparison of water absorption capacity of soil block mixed with 15% cement and varying percentage of SBA

5. RESULTS AND DISCUSSION

From compression test result of all the test blocks, it was observed that the compressive strength of 10% cement stabilized block steadily increases from 3.8 MPa to 5.1 MPa with addition of SBA. But for 15% cement stabilized block, compressive strength increases from 4.1 MPa to 5.4 MPa.

From water absorption test of test blocks, it is evident that there is no big difference in the water absorption of the 10% cement stabilized blocks upon addition of SBA. The water absorption of the control specimen increases marginally from 2.53% to 3.61% on addition of 5% SBA, which is only a mere 1.08% increase in water absorption. Another important observation is that all the combinations are well within the permissible limit suggested by BIS code. However, in case of 15% cement stabilized block, it increases from 2.82% for the control specimen to 3.92 % for 3% SBA addition, which is an increase by more than 1%.

6. CONCLUSION

Based on the experimental investigation carried, the following points can be concluded:

a) Cement stabilization of locally available soil can be used in the manufacture of stabilized soil blocks to meet the compressive strength and water absorption norms of BIS specifications. Cement stabilization of soil at 10% & 15 % cement content meets the specifications of class 20 blocks & class 30 blocks as per IS1725-1982 and also of locally available burnt brick (IS1077:1992).

b) Addition of SBA to cement in stabilization results in an increased compressive strength of the blocks. However, SBA addition is more effective at higher cement content of 15% producing higher strength gains when compared to lower cement content of 10%.

c) Addition of SBA to cement in stabilization results in an increase in the water absorption of the blocks but is still comfortably within the norms stipulated by BIS. However, the addition of SBA produces more water absorption at higher cement content of 15% than lower cement content of 10% for similar SBA contents, again reinforcing the inference that SBA addition is more effective at lower cement content.

d) Addition of 5% SBA to 10% cement content increases its compressive strength to meet the strength requirements of class 30 blocks from the original category of class 20 blocks. Thus it can be seen that addition of 5% SBA can result in utilization of just 10% cement for achieving class30 block specifications. This leads to saving of 5% cement in comparison with the other combination adopted in this study.

REFERENCES

1) H.B. Nagaraja, M.V.Sravan (2014), The Role of limeWith cement in long-term strength of Compressed Stabilized Earth Blocks, International Journal of Sustainable Built Environment Volume 3, Issue 1, June 2014, Pages 54-61
2) IS1077 (1992), Common burnt bricks specification, Bureau of Indian standards.
3) IS 1725 (1982), Soil based blocks used in general building construction, Bureau of Indian standards.

4) IS 1498(1970), Classification and identification of soils for general engineering purposes, Bureau of Indian standards.
5) IS 2720(1985), Methods of test for soils, part 5, determination of liquid limit and plastic limit, Bureau of Indian standards.
6) Jijo.J, Pandian.P.K, et.al. (2015), Cement stabilized soil block admixed with sugarcane bagasse, Journal of Engineering, Volume 2016, Article ID 7940239, 9 pages.
7) Patowary B.N. et. al. (2015), Study of compressed Stabilised Earth Block, International Journal of Scientific and Research Publications, Volume 5, Issue 6, June 2015 1 ISSN 2250-3153.
8) P.J.Walker (1995), Strength, durability and shrinkage characteristics of cement stabilized soil blocks, Cement and Concrete Composites, vol.17, no.4, pp.301–310.
9) Millogo.Y, Aubert J.E, Sere.A.D (2016), Earth block stabilized by cow dung, Materials and Structures, Springer, November, Volume 49, Issue 11, pp 4583–4594.

Effect of production temperature on permanent deformation characteristics of WMA mixes

Bhardwaj, B. B. [1], Choudhary, R. [2] and Julaganti, A. [3]

[1] Assistant Professor, Dept. of Civil Engineering, Assam Engineering College, Guwahati, Assam-781013, India.
[2]Associate Professor, Dept. of Civil Engineering, IIT Guwahati, Assam-781039, India.
[3] Assistant Professor, Dept. of Civil Engineering, Bapatla Engineering College, Andhra Pradesh- 522102, India.

ABSTRACT

Rutting or permanent deformation is one of the most common distresses in bituminous pavements due to increased traffic loads and tyre pressures, usually appearing as longitudinal depressions along the wheel path. The occurrence of permanent deformation in the bituminous layers depends on various factors including binder stiffness, binder type and contents etc. There is an increasing concern among highway engineers to enhance sustainability in asphalt production and construction by lowering fuel and energy consumption without impoverishing the level of mechanical performance of mixes. Warm Mix Asphalt (WMA) is a new technology that reduces the production temperatures by approximately 20-50°C resulting in less stiff binder. In spite of many advantages, the resistance of WMA mixes against permanent deformation remains skeptical. This paper is aimed to address the permanent deformation characteristics of WMA mixes solely as a function of production temperatures.

Keywords: Warm Mix Asphalt (WMA), permanent deformation, rutting, Sasobit®, modified binder, PMB, CRMB, static creep

1. INTRODUCTION

Road transportation in India has amplified over the years with the improvement in connectivity between cities, towns and villages in the country. Still, this evolution of the highway infrastructure, especially in major metropolitan areas is unable to meet up the mounting traffic demand. The inequity in supply and demand is causing an unprecedented level of safety challenges. Considering the statistics of the recent years' escalation in motorization, infrastructure development and snowballing mobility of people in Indian cities, the same inclination is expected to endure in the coming years. Although, the road network is expanding in an exponential rate, noteworthy qualitative improvement of the roads have not been observed over the years. **Singh et al. (2011)** stated that road accidents now leads the list of accidental deaths in India much more than any other such as by drowning, fire, rail or air mishaps etc. A share of these accidents is due to poor quality of the pavement surfaces. In developing countries like India, flexible pavements dominate rigid pavements for various benefits associated with them. However, lack of proper design and maintenance of flexible pavements results into premature failures or distresses of the same. Due to inadequate design, construction and maintenance, flexible pavements generally suffer from several categories and subcategories of distresses which eventually lead to progressive decline of ride condition, structural strength and motorist/pedestrian safety.

Warm Mix Asphalt (WMA) is a new technology that helps in reducing the production temperatures by approximately 20-50°C, either by reducing the viscosity of binder through foaming or by using organic or chemical additives. The lower production temperatures help in reducing the energy consumption which in turn reduces the emission of greenhouse gases during the production process. Additional advantages of WMA technologies include longer hauling distances, quicker turnover to traffic, cold weather paving, low plant wear and tear, improved workability, better working environment for the paving crew, reduced binder aging etc.

As the WMA mixes are produced at lower temperatures, it comes at a cost of reduced evaporative hardening of the binder; since volatiles present in the bitumen are not lost unlike in HMA. The binder in WMA doesn't become stiff enough as compared to that of HMA.

Hence the permanent deformation characteristics of WMA mixes associated with binder stiffness of the mix need to be evaluated. Rutting occurs due to progressive accumulation of unrecoverable strains appearing as longitudinal depressions along the wheel path of vehicles.

Xiao et al. (2013) showed that the rut depths of all mixtures (dry and wet conditioned) slightly

increased with a reduction in compaction temperature regardless of aggregate moisture content, foaming WC, and aggregate source using Asphalt Pavement Analyzer (APA) and also concluded that a compaction temperature below 102°C generally has no noticeable aging effects on the mixture and does not significantly increase the rutting resistance of WMA mixes Some authors also tried to establish relationship between air void content and production temperature. **Yongjoo et al. (2012)** found that that the air voids of the WMA-LEADCAP (130°C) and the control HMA pavements (160°C) were not significantly different. **Alvarez et al. (2011)** used an X-ray CT equipment on both WMA and control-HMA and found that Sasobit®-WMA and Evotherm®-WMA specimens showed no connectivity in the central portion of the specimen unlike the control HMA samples. **Kumar et al. (2014)** tested warm mix asphalt mixtures with additives (Sasobit®) for dense bituminous macadam (DBM) Grade-2 and reported that the lowering of compaction temperature has increased the percent of air void content significantly.

The objective of the study is to evaluate the effect of binder stiffness or production temperature reduction on rutting properties of WMA mixes.

2. MATERIALS AND METHODS

2.1 Mixture Designs and Specimen Properties

This paper is aimed to address the permanent deformation characteristics of WMA mixes solely as a function of production temperatures. Sasobit® belonging to organic family of WMA additives, was used in the study for the preparation of WMA mixes. Sasobit® forms a homogeneous solution with the base binder at temperature around 120°C. It works on the principle of reducing viscosity of the binder and thereby reducing the production temperatures of bituminous mixes at temperatures above its melting point. It also imparts additional strength to the binder/mix at temperatures below its melting point.

The experimental design for this study includes two types of modified binders (PMB-40 and CRMB-60), one aggregate source and four production temperatures. Bituminous Concrete Grade-2 (BC-2) used as wearing course in India is selected for the study. 2% of Sasobit® by weight of binder is used for the preparation of WMA mixes throughout the study. Marshall method of mix design, currently followed in India, is employed for the preparation of WMA mixes at 0°C, 20°C, 30°C, and 40°C reduction in mixing and compaction temperature. WMA mixes are prepared at 4% air void content at all production temperatures by varying the compaction effort through trial and error process. To keep air void constant at different production temperatures for both the binders, trial samples are prepared by varying the no. of Marshall blows. The compaction energy hence necessary to produce the mixes with required amount of air void content was estimated and the same is applied to yield the specimens with required air void content with a tolerance limit of 0.02.

The permanent deformation characteristics of the bituminous mixes are evaluated using Static Creep Test in a Universal Testing Machine. The average results from three replicates are only presented.

2.2 Aggregates

Aggregates used in this study were procured from a crusher located in Deodhar village near IIT- Guwahati. The requirements of various physical properties as per MoRTH-fifth revision, 2013 along with the results obtained are listed below in Table 1 also in Table 2.

Table 1. Physical requirements and results for coarse aggregate for bituminous concrete

Property	Test	Standard	Requirement	Result
Particle Shape	Combined Flakiness and Elongation Index	IS 2386 Part I	Max. 35%	20.22%
Cleanliness	Sieve Analysis	IS 2386 Part I	Max. 5% passing 75µ sieve	1.61%
Strength	Los Angeles Abrasion Value	IS 2386 Part IV	Max. 30%	27%
	Aggregate Impact Value	IS 2386 Part IV	Max. 24%	21%
Water Absorption	Water Absorption	IS 2386 Part III	Max. 2%	Less than 2%
Stripping	Stripping Test	IS 6241	Min. retained coating 95%	More than 95%

The aggregate gradation of Bituminous Concrete Grade-2 selected in this study is as per MoRTH-fifth revision, 2013 and the same has been presented here

Table 2 Aggregate Gradation of Bituminous Concrete Grade-2 as per MoRTH (2013)

Sieve (mm)	Percentage passing		
	Upper Limit	Lower limit	Mid-Point
19	100	100	100
13.2	100	90	95
9.5	88	70	79
4.75	71	53	62
2.36	58	42	50
1.18	48	34	41
0.6	38	26	32
0.3	28	18	23
0.15	20	12	16
0.075	10	4	7

2.3 Binder

In India during the last decade, traffic loads and tyre pressures have been amplified which has increased the use of modified binders to achieve enhanced mixes which have higher ability to resist rutting, fatigue and thermal cracking more efficiently. Two modified binders have been selected for the study viz. PMB-40 and CRMB-60 as per criteria given in Table 3.

Table 3 Selection Criteria for Grade of Modified Bitumen [IRC: 111-2009]

Lowest Daily Mean Air Temperature, °C	Highest Daily Mean Air Temperature, °C		
	Less than 20 °C	20 °C to 30 °C	More than 30 °C
	Grade of Modified Bitumen		
More than -10 °C	PMB/NRMB 120 CRMB 50	PMB/NRMB 70 CRMB 55	PMB/NRMB 40 CRMB 60
-10 °C and lower	PMB/NRMB 120 CRMB 50	PMB/NRMB 120 CRMB 50	PMB/NRMB 70 CRMB 55

PMB = Polymer Modified Bitumen, NRMB = Natural Rubber Modified Bitumen, CRMB = Crumb Rubber Modified Bitumen

The mixing temperatures for CRMB-60 binder is 175 °C and that for PMB-40 is 170 °C. The compaction temperature is 10^0 C lower than the mixing temperature. The loose mixes are then conditioned for 2 hours at the compaction temperature before compaction to simulate the delay faced in site in between mixing and compaction of the mixes. Properties of the two binders *viz.* PMB-40 and CRMB-60 selected for the study are presented in Table 4 as found out in the laboratory.

Table 4 Test Results on Modified Bitumen and Requirements as per IS 15462-2004

Sl. No	Test	PMB-40		CRMB-60	
		Require-ment	Result	Require-ment	Result
1	Penetration at 25°C. 0.1 mm, 100g, 5 Sec	30 to 50	39	30 to 50	35
2	Softening Point, (R & B),°C	Min.60	64.5	Min.60	64.5
4	Flash point, COC, °C	Min.220	300	Min.220	320
5	Elastic Recovery of half thread in ductilometer at 15°C, %	Min. 60	76.5	Min. 60	68
6	Complex Modulus as ($G^*/\sin\delta$) as Min 1.0 kPa at 10 rad/sec at a temperature, °C, Min.	76	77.5	76	82
7	Separation Difference in Softening Point, R & B, °C	Max. 3	1.9	Max. 3	2.9
Thin Film Oven Test (TFOT) on Residue (IS 9382: 1992)					
8	Loss in Weight, % Maximum	Max. 1.0	0.62	Max. 1.0	0.56
9	Increase in Softening Point, °C, Maximum	Max. 5	4.1	Max. 5	3.5
10	Penetration at 25°C, 0.1 mm, 100g, 5 Sec, % of Original	NA	NA	Min. 60	68.57
11	Elastic Recovery of Half Thread in Ductilometer at 25°C. % Maximum	Min.50	58	Min. 35	48

2.4 Methods for preparation of the mixes

The BC-2 samples were prepared at different production temperatures and at constant air void content of 4%. The mixing and compaction temperature can be controlled as per requirement, but the air void content of a sample depends on various properties of the mixes such as compaction energy, viscosity of the binder, aggregate type etc. For that, trial mixes are prepared by varying the compaction energy so that even at different production temperatures, 4% of air void can be obtained. The bulk specific gravity of all the samples are measured

using water displacement method. The air void contents of the samples are then found out using the following Equation 1-

$$\text{Air void content (\%)} = \frac{G_{mm}-G_{mb}}{G_{mm}} \times 100 \quad \textbf{(1)}$$

where,

G_{mm} = maximum specific gravity of the bituminous mixture

G_{mb} = bulk specific gravity of the specimens

G_{mm} of the loose mixes are measured using CoreLock. The optimum binder content of the BC-2 mixes are found to be 6.6% and 6.2% for binder CRMB-60 and PMB-40 respectively. After achieving air void content of 4%, the specimens are then tested to evaluate the rutting properties of the mixes. The rutting property is evaluated using Static Creep Test.

2.5 Static Creep Test

BS 598 (Part 111)-1995 "Method for determination of resistance to permanent deformation of bituminous mixtures subject to unconfined uniaxial loading" is followed as test protocol in this study for performing the static creep tests. **Van der Loo (1989)** analyzed the correlation between rutting in the field and creep (static and dynamic) testing in the laboratory. After analyzing the use of results from laboratory-prepared specimens to predict rutting behavior, Van der Loo concluded that the main purpose of laboratory creep test methods should be limited to the ranking of materials rather than the prediction of rut depth. Test specimens were placed in a temperature-controlled chamber maintained at 40 °C for 4 hours prior to the start of the test to bring the specimens to the specified test temperature. After 4 hours, the specimen is then mounted inside the universal testing machine (UTM) as shown in Figure 1.

Fig. 1 The specimen is mounted in UTM for static creep test

These tests are performed at 40°C in the universal testing machine. A conditioning load of 10 kPa was applied on a Marshall specimen for 600 seconds followed by a 100 kPa load for 3600 seconds. A rest period of 900 seconds was selected after the loading period by removing the vertical load from the specimens. Total strain and unrecoverable strain are the two parameters which are measured. Vertical deformation is measured using two linear variable displacement transducers (LVDT) placed diametrically opposite during the test. The average deformation of a specimen under the static load is calculated by averaging the two LVDT readings. Total strain corresponds to the deformation that the specimen attains per unit height of the specimen at the end of the loading period. Unrecoverable strain corresponds to the permanent deformation per unit thickness of the specimen at the end of the recovery period.

3. TEST RESULTS

The effect production temperature on total strain at 4% air void contents are shown in Figure 2 and 3. It is seen that there is an effect of production temperature at all air void contents, which is to make the mixes more susceptible to deformation with lowering of production temperature. As the production temperature decreases, stiffness of the binder reduces compared to the one in case of higher mixing temperatures.

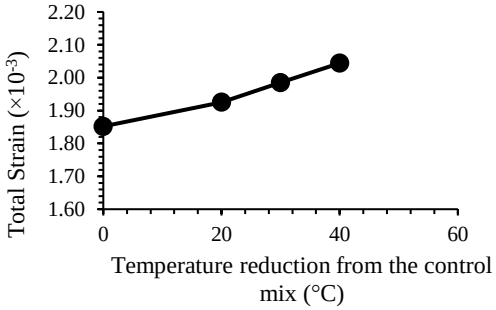

Fig. 2 Effect of production temperature reduction on total strain of BC-2 samples (CRMB-60 as binder)

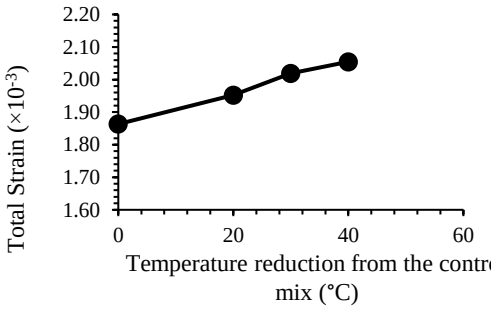

Fig. 3 Effect of production temperature reduction on total strain of BC-2 samples (PMB-40 as binder)

This effect is due to absence of evaporative hardening of volatile constituents of the binder at lower production temperature makes the mixes lesser resistant to deformation. The average rates of changes in total strain values with respect to production temperature have no differences for both the binders.

Similarly, the unrecoverable strain values are plotted against different production temperature reduction in Figure 4 and Figure 5 for binder CRMB-60 and PMB-40 respectively.

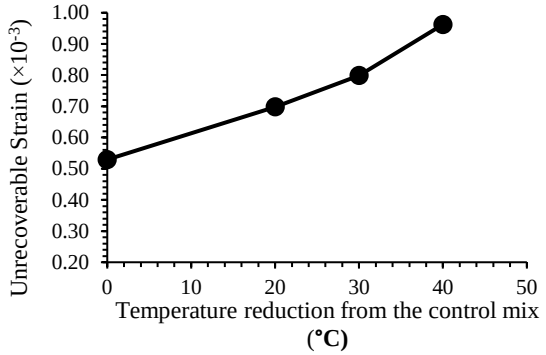

Fig. 4 Effect of production temperature reduction on unrecoverable strain of BC-2 samples (CRMB-60 as binder)

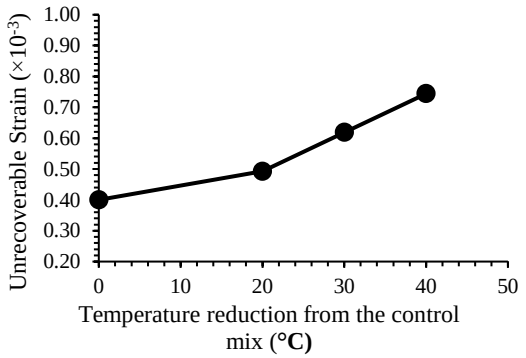

Fig.5 Effect of production temperature reduction on unrecoverable strain of BC-2 samples (PMB-60 as binder)

It is observed that with decrease in production temperature, due to absence of evaporative hardening of the binder, unrecoverable strain also gets increased. Regardless to binder type, mixes prepared with PMB-40 binder are showing better resistance towards permanent or unrecoverable strain than that of mixes with binder CRMB-60. This might be due to elastomeric polymer modified binder used in the study that helps in recovering the total strain more compared to the CRMB-60 mixes.

4. CONCLUSION

Conclusions are drawn on the basis of the results of static creep test.

- Total strain and unrecoverable strain of WMA mixes were also found to increase with reduction in production temperature regardless of the binder type.
- Bituminous Mixes prepared with PMB-40 binder showed better resistance towards permanent deformation that that of the mixes with PMB-40 binder.

5. RECOMMENDATIONS

In this study only two parameters were considered viz. binder type and production temperature to see their effects on rutting properties of WMA mixes. The WMA additive (Sasobit) and its dosage (2% by weight of binder) were also kept constant. Future studies can be carried out using other WMA additives and by varying the dosage amount. By keeping in mind the increasing popularity of modified binders, two types of modified binders have been used in the study, but in many ongoing projects the use of neat bitumen is still prominent. So, the same study can be carried out using neat binder also.

6. ACKNOWLEDGEMENT

The study described in this paper was supported by the Technology Systems Development (TSD) Programme of the Department of Science and Technology (DST), India.

7. REFERENCES

1) Alvarez, A. E., Macias, N. and Fuentes, L. G. (2011): Analysis of connected air voids in warm mix asphalt, *Dyna-79*, NRO- 172, 29-37.
2) Kumar, D. and Varadraj, N.K. (2014): Density and compaction characteristics of WMA using additives, *International Journal of Research in Engineering and Technology*, 3(6), 603-607.
3) Singh, A. P., Agarwal, P. K. and Sharma, A. (2011): Road safety improvement: A challenging issue on Indian roads, *International Journal of Advanced Engineering Technology*. 2(2), 363-369.
4) Van der Loo, P. J. (1974): Creep Testing: A Simple Tool to Judge Asphalt Mix Stability, *Proceedings of the Association of Asphalt Paving Technologists*. Vol. 43.
5) Xiao, F., Zhao, W. and Amirkhanian, S. N. (2010): Aging influence on fatigue characteristics of RAC mixtures containing warm asphalt additives, *Advances in Civil Engineering*, Vol. 2010 and Article ID 329084.
6) Yongjoo, K., Lee, J., Baek, C., Yang, S., Kwon, S. and Suh, Y. (2012): Performance evaluation of warm and hot mix asphalt mixtures based on laboratory and accelerated pavement tests, *Advances in Materials Science and Engineering*, Vol. 2012 and Article ID 901658.

Study on compressive strength of concrete using foundry sand as fine aggregate

Nath, P.[1], Lunawat, R.[1], Saleh, R.N.[1], Devi, P[1], Dey, Y.[2]

[1]Student, Department of Civil Engineering, Royal School of Engineering & Technology, Guwahati-781035, India.
[2]Assistant Professor, Department of Civil Engineering, Royal School of Engineering & Technology, Guwahati-781035, India.

ABSTRACT

Concrete has become most extensively used material in the world because of its high strength and ability to be moulded to different shapes. All the major structures like bridges, buildings, dams, etc. needs high durability and serviceability. Thus, in modern days scenario, structures cannot be conceptualized without concrete because of its high durability and serviceability, cement being prime component. The ingredients of concrete mix i.e. cement, fine aggregate and coarse aggregate are nowadays becoming costlier. The fine aggregate, collected from river basins has now been imposed banned in the extraction by Government in several places. On the other hand, foundry sands used is metal casting industries are dumped into a dumping ground after casting is completed. These Waste Foundry Sand(WFS) are used in the study to observe the effect in M20 Grade Concrete by testing the compressive strength.
This study gives a brief insight into the replacement of traditional sand i.e. fine aggregate by waste foundry sand. Standard cubes of 150mm x 150mm x 150mm were cast using the prime ingredients of concrete – cement, fine aggregate and coarse aggregate along with foundry sand in different trials where traditional sand was substituted with WFS in percentage by weight. The concrete cubes were then tested under compressive load in Compression Testing Machine on 7th day, 14th day and 28th day of casting and a comparative result is drawn on the behaviour shown by the test samples on the respective days of tests with variation in percentage of Waste Foundry Sand.

Keywords:, concrete, compressive strength, cubes, fine aggregate, sand replacement, waste foundry sand.

1. INTRODUCTION

Concrete has become indispensable in construction of modern buildings, bridges, nuclear structures, off shore structure and in many other applications. It is the second largest material consumed by human civilization nowadays just after water. Over the recent years, there is a huge increase in the use of concrete throughout the world. Concrete is neither strong nor tough as steel but yet used widely primarily due to the fact that concrete possesses excellent resistance to water. Unlike wood and steel, the ability of concrete to withstand the action of water without serious deterioration makes it an ideal material for building structures to control, store and transport water. Another reason of concrete being used widely is because of the ease with which structural concrete elements can be made into a variety of shapes and sizes as freshly prepared concrete is of a plastic consistency which permits the material to flow into prefabricated formwork.
Due to rise in inflation, cost of materials has become a prime factor nowadays that needs to be taken care of. Without compromising the quality of concrete, the preparation at cheapest is desired. Alternatives to be used as replacement of raw materials for concrete work is being adopted worldwide to reduce the cost of concrete. Such materials which not only reduces the cost but can also increase the compressive strength of concrete is desired.

Industries are growing exponentially in developing countries like India. The wastes of the industries are dumped in dumping zones which are not used anywhere purposefully. Foundry sand is also one such industrial waste which is generated by metal casting industries as Waste Foundry Sand and dumped into landfills or dumping zones without its proper utilization. In this work, an attempt is made to use waste foundry sand as an alternative for sand (fine aggregate) in concrete so as to reduce the cost of concrete and increase its compressive strength.

2. WASTE FOUNDRY SAND

Foundry sand consists primarily of clean, uniformly sized, high-quality silica sand or lake sand that is bonded to form moulds for ferrous (iron and steel) and nonferrous (copper, aluminium, brass) metal castings. Although these sands are clean prior to use, after casting they may contain Ferrous (iron and steel). Industries account for approximately 95 percent of foundry sand used for castings. The automotive industry and its parts suppliers are the major generators of foundry sand. The metal casting industry generates waste or used foundry sands. Foundries purchase new, virgin sand to make casting moulds, and the sand is reused numerous times within the foundry. This reuse eventually renders the sand unsuitable for use in casting moulds, and a portion of the sand is continuously removed and replaced with virgin sand. The used foundry sand is either recycled in non-

foundry applications or landfills.

Fig 1: Waste Foundry Sand at Industry

Concrete is a composite construction material, made by mixing of cement, coarse aggregates, fine aggregate (sand), water and admixtures (if required). The property of concrete is affected by proportionate quantity of each material. It is the most extensively used construction material in the world, second to water. Increasing rate of urbanization and industrialization has led to over exploitation of natural resources such as river sand and gravels, which is giving rise to sustainability issues. Furthermore, the subsistence of construction industry has been severely affected due to the restrictions in the extraction of sand from the river resulting in rise of the price of sand. Thus, it has now become imperative to look for alternatives of constituent materials of concrete. Waste foundry sand, a by-product of ferrous and non-ferrous metal casting industries is one such promising material which can be used as an alternative to natural sand in concrete.

Various researchers have conducted their experimental investigation on using waste foundry sand as a replacement of traditional sand as fine aggregate in concrete and the results of which clearly indicates that waste foundry sand can be effectively used as a replacement for traditional sand. It was also found in results of some cases that use of WFS not only will help reduce the cost of traditional sand but also increases the strength of concrete to some extent.

Thus, the present study aims at evaluating the strength of concrete containing discarded foundry sand as a replacement of fine aggregates and finding out if a low-cost and eco-friendly concrete can be made and the results concluded have been further explained through experimental investigations in the subsequent chapters.

Table 1: Composition

TRIAL	SAND IN %	FOUNDRY IN %
Standard	100	0
1	20	80
2	30	70
3	40	60
4	50	50
5	60	40

3. METHODS AND METHODOLOGY

The following steps were involved to perform the work

- Preliminary Tests of Aggregates
- Design Mix Calculation as per IS 10262-2009
- Casting of Cubes of 150mm x 150mm x 150mm
- Curing Process
- Testing for Compressive Strength

a. Preliminary Tests

A) Sieve analysis of the fine aggregate is conducted and the results are compared to check if the sample conforms to the IS 383-1970 specifications and found to be of ZONE III. Also, the waste foundry sand upon sieve analysis is found to conform to ZONE III grading.

B) Sieve analysis of the coarse aggregate of 20mm and 12.5mm nominal size shows that the do not conform to IS 383-1970 requirements. Thus, a blend of aggregate with nominal size 20mm is taken with 80% 12.5mm and 20% 20mm aggregates. The blended aggregate conforms to the IS 383-1970 specification.

C) The specific gravity and water absorption of the coarse aggregate is found to be 2.665 kg/cm^3 and 0.62 % respectively.

b. Design Mix Calculation as per IS 10262-2009

The process of selecting suitable ingredients of concrete and determining their relative amounts with the objective of producing a concrete of the required strength, durability and workability as economical as possible is termed as concrete mix design.

MIX DATA:

a) Characteristics strength (fck) : 20 MPa
b) Target mean strength : 26.6 N/mm^2
c) Standard Deviation (s) : 4
d) Probability Factor (k) : 55
e) Workability (Slump) : 100mm
f) Exposure Condition : Moderate
g) Cement use : OPC – 43 Grade
h) Water-cement ratio adopted : 0.50
i) Cement content : 394.32 kg

Table 3: Mix Proportion

w/c Ratio		Cement	Water	CA	FA

0.5	Quantity of materials (in kg)	394.32	197.16	1156.4	645.6
	Ratio of materials	1	0.5	2.93	1.637
	Materials per bag of cement	50 kg	25 kg	147 kg	82 kg

Ratio of mix proportion – 1: 1.64: 2.93

c. Casting of Cubes of 150mm X 150mm X 150mm

A) Preparation of Concrete:

The concrete is mixed by hand following the steps below:

i. Mix the cement and fine aggregate on a water tight none-absorbent platform until the mixture is thoroughly blended and is of uniform colour.
ii. Add the coarse aggregate and mix with cement and fine aggregate until the coarse aggregate is uniformly distributed throughout the batch.
iii. Add water and mix it until the concrete appears to be homogeneous and of the desired consistency.

B) Slump Test for Measurement of Workability:

Slump test is the most commonly used method of measuring consistency of concrete which can be employed either in laboratory or site of work. It does not measure all factors contributing to workability, nor is always representative of the placability of concrete. However, it is used conveniently as a control test and gives an indication of the uniformity of concrete from batch to batch.

The apparatus for conducting the slump test essentially consists of a metallic mould in the form of a frustum of a cone having the internal dimensions as under:

Bottom diameter : 20 cm
Top diameter : 10 cm
Height : 30 cm

The concrete mix that is prepared for the tests are tested in batches of trials for their workability using the Slump cone.

Table 4: Slump Height

TRIAL	SLUMP in mm
Standard	90
1	29
2	45
3	54
4	63
5	70

The slump obtained for each of the trial batch meets the requirement of IS 10262 – 2009 and thus the concrete batch can be used further.

C) Curing:

The Indian Standard IS 456 – 2000 recommends that curing duration of concrete must be at least 7 days in case of ordinary Portland Cement, at least 10 days for concrete with mineral admixtures or blended cements are used. It also recommends that the curing duration should not be less than 10 days for concrete exposed to dry and hot weather conditions and 14 days for concrete with mineral admixtures or blended cement in hot and dry weather. Cubes must be cured before they are tested. Unless required for test at 24 hours, the cube should be placed immediately after demoulding in the curing tank or mist room.

D) Test for Compressive strength:

The concrete cube is loading with uniform loading gradually without shock and continuously at the rate of 140 kg/cm^2/minute till the specimen fails. The maximum load gives the ultimate strength of the concrete cube.

Fig 2: M20 Concrete Cube after failure

4. RESULTS

Table 5: Compressive Strength of M20 concrete

Trial	7 Day Strength (N/mm^2)	14 Day Strength (N/mm^2)	28 Day Strength (N/mm^2)	Mean Strength (N/mm^2)
Standard	12.44	18.67	28.00	29.11
			30.22	
1 (20:80)	15.56	21.33	31.11	30.00
			28.89	
2 (30:70)	16.44	24.44	31.56	32.44

			33.33	
3 (40:60)	18.67	31.11	37.33	36.67
			36.00	
4 (50:50)	18.22	25.33	34.67	34.00
			33.33	
5 (60:40)	17.33	25.33	32.00	31.56
			31.11	

5. OBSERVATIONS

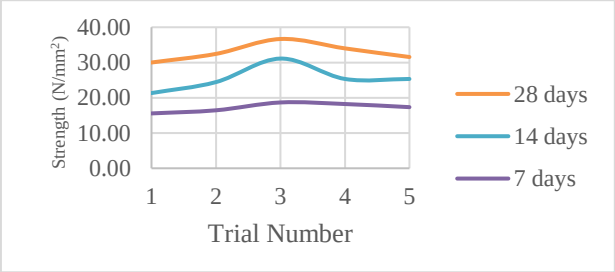

Fig 3: Comparison of 7 day, 14 day and 28 day Compressive Strength

6. CONCLUSION

From the plot above, it is observed that all the Trial composition of M20 grade concrete using Waste Foundry Sand shows a significantly higher strength than the strength of standard M20 concrete. The peak values of strength are of Trial Batch 3 which consists of 60% Waste Foundry Sand and 40% Zone III Sand as fine aggregate in the concrete mix. The maximum strength in case of 7 day, 14 day and 28 day is obtained from the batch of Trial-3. Also, the Slump obtained as per Table 4 is 54mm which conforms the guidelines of IS 10262 – 2009. Thus, the composition of Trial 3 may be taken as the optimum composition in terms of percentage replacement of traditional sand by Waste Foundry Sand.

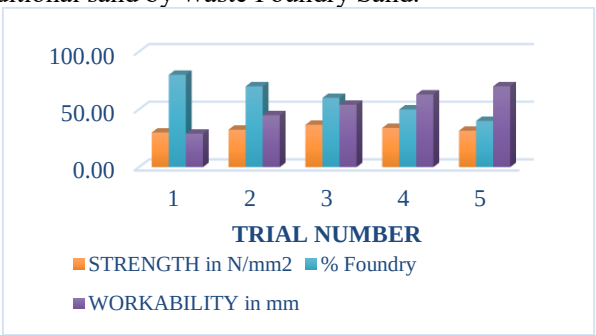

Fig 4: Comparison of Strength, Percentage WFS Replaced and Workability

The prime objective of the present study was directed towards using waste foundry sand as an alternative for sand (fine aggregate) in concrete so as to reduce the cost of concrete and increase its compressive strength.

In the results obtained, it was seen that the use of foundry sand in the concrete decreased the workability of the fresh concrete to some extent. Though the workability decreased with the increase of replacement level of waste foundry sand, the strength parameters has shown very promising results. Compressive strength increased on increase in percentage of waste foundry sand when compared to traditional concrete. Use of waste foundry sand in concrete also reduced the production of waste through metal industries i.e. it is an eco-friendly building material.

From the experiment, the parameters undertaken for study are compressive strength, workability and economy. Analysing the data, it can be concluded that the compressive strength of concrete gradually increases with the increase in percentage of foundry sand from 40 to 60 percent replacement and then the strength decreases with further increase in foundry sand upto 80 percent. The maximum compressive strength is obtained at 60% replacement of fine aggregate by waste foundry sand for 7 day, 14 day and 28 day strength. But as far as economy is concerned, we get the desired strength in trial 1 as well where the replacement by waste foundry sand is maximum. Hence, it can be found that considering both economy and strength trial 1 is the best trial. Considering only strength as priority, trial number 3 is the best proportion.

REFERENCES

1) Siddique, R.; deSchutter, G. and Noumowe, A. *"Effect of used-foundry sand on the mechanical properties of concrete"*, Construction and Building Materials Vol. 23, Issue 2, February 2009 (976-980)
2) Siddique, R.; Aggarwal, Y.; Aggarwal, P.; Kadri, E.L. and Bennacer, R. *"Strength, durability, and micro-structural properties of concrete made with used-foundry sand (UFS)"*, Construction and Building Materials Vol. 25, Issue 4, April 2011 (1916-1925)
3) Siddique, R. and Singh, G. *"Utilization of waste foundry sand (WFS) in concrete manufacturing"*, Resources, Conservation and Recycling Vol. 55, Issue 11, September 2011 (885-892)
4) Siddique, R. and Singh, G. *"Abrasion resistance and strength properties of concrete containing waste foundry sand (WFS)"*, Construction and Building Materials Vol. 28, Issue 1, March 2012 (421-426)
5) Prabhu, G.G.; Hyun, J.H. and Kim, Y.Y. *"Effects of foundry sand as a fine aggregate in concrete production"*, Construction and Building Materials Vol. 70, 15 November 2014 (514-521)
6) Siddique, R.; Singh, G.; Belarbi, R.; Mokhtar, K.A. and Kunal *"Comparative investigation on the influence of spent foundry sand as partial replacement of fine aggregates on the properties of two grades of concrete"*, Construction and Building Materials Vol. 83, 15 May 2015 (216-222)

7) Gurumoorthy, N. and Arunachala, K. *"Micro and mechanical behaviour of Treated Used Foundry Sand concrete"*, Construction and Building Materials Vol. 123, 1 October 2016 (184-190)
8) Bhardwaj, B. and Kumar, P. *"Waste foundry sand in concrete: A review"*, Construction and Building Materials Vol. 156, 15 December 2017 (661-674)
9) Manoharan, T.; Laksmanan, D.; Mylsamy, K.; Sivakumar, P. and Sircar, A. *"Engineering properties of concrete with partial utilization of used foundry sand"*, Waste Management Vol. 71, January 2018 (454-460)
10) Rangawala, "*Engineering Materials*", Charotar Publishing House Pvt. Ltd.
11) Shetty, M.S., *"Concrete Technology"*, S. Chand & Company Pvt. Ltd.
12) Laskar, Dr. A.I., *"Concrete Technology"*, University Science Press

Mechanical and durability properties of bagasse ash blended high performance concrete

Praveenkumar S.[1], Sankarasubramanian G.[2]

[1] Assistant Professor, Department of Civil Engineering, PSG College of Technology, Tamil Nadu-641014, India.
[2] Professor & Head, Department of Civil Engineering, PSG College of Technology, Tamil Nadu-641014, India.

ABSTRACT

The use of supplementary cementitious materials has become an integral part of high strength and high performance concrete mix design, which may be natural by-products or industrial wastes. Some of the frequently used supplementary cementitious materials (SCMs) are fly ash, silica fume (SF), Ground Granulated Blast Furnace Slag (GGBS), Rice Hush Ash (RHA) and Bagasse Ash (BA). Bagasse ash (sugarcane industry waste product) is considered to be an active pozzolan because of its large surface area with significant amount of amorphous SiO_2 . The Mix Design for high performance concrete is done as per the method proposed by P.C.Aitcin. This method is simple and follows the same approach as ACI 211-1 standard practice for selecting proportion of normal, heavy and mass concreting. Ordinary Portland cement (OPC) was replaced at different levels of 0%, 5%, 10%, 15% and 20% by bagasse ash. This investigation presents results on the strength & durability properties of high performance concrete with and without Bagasse Ash, which includes cube compressive strength, splitting tensile strength, flexural strength, saturated water absorption, sorptivity, porosity, impact test, alkalinity measurement. The test results indicate that the incorporation of BA up to 10% provides improved properties of hardened concrete.

Keywords: Bagasse ash, High performance concrete, mechanical properties, durability propertie

1. INTRODUCTION

In both cement and concrete, ordinary portland cement is major element of infrastructure and also a durable construction material [1]. Production of cement emits 2.5% waste worldwide, which causes environmental issues [2]. Utilization of supplementary cementitious materials as a partial replacement of cement mortar and concrete is the most effective way of reducing the environmental impact, which also minimizes energy, cost and waste emission [3,4]. The waste from various industries such as Silica fume, fly ash and blast furnance slag were used as mineral admixtures. Bagasse ash, rice husk ash and wheat straw ash were also being used as pozzolanic materials in various forms [5,6]. Mineral admixtures as partial replacements of cement improve the mechanical and durability properties of concrete [7].

In India sugarcane production was about 300 million tons per year [8] and plenty of bagasse is available in sugar industry. As a fuel, bagasse is partly used in sugar industry and the remaining was dumped as waste material in ground. Silica content present in the pozzolan reacts with the free lime during hydration and forms Calcium silicate hydrate (CSH) [9]. Formation of CSH gel during hydration process of mineral admixtures and cement in concrete, improves mechanical properties of hardened concrete. However, Hydration time is inversely proportional to the porosity, which also increases pore structure and permeability of mortar and concrete. The waste from agro industry was burnt in incinerating temperature of below 700°C for 1 hour which converts the silica content of the ash into amorphous phase [10]. In order to achieve the required size, ash was grinded in laboratory ball milling. The grinded ash mixed with ordinary Portland cement produces blended cement. The characteristics of agricultural industry waste ash purely depend on the following process such as burning, maintaining constant temperature, drying and grinding.

The objective of the present study is to assess the performance of bagasse ash as supplementary cementitious material in mechanical and durability properties of high performance concrete, as well as to make out the optimal level of replacement.

2. MATERIALS

2.1 Cement & Bagasse ash

OPC 53 grade was used for making high performance concrete specimens. The bagasse ash used in the test was obtained from Gobichettipalayam, TN, India. Bagasse ash varied up to 20% by weight of cement. The used cement and bagasse ash have specific gravity of 3.15 and 2.18. Initial and final setting time of ordinary Portland cement is found to be 80 min and 150 min with 29.5 % standard consistency. BA has almost 5 times better

silica content than that of OPC and consists of rational quantity of CaO and Al_2O_3. In addition, BA showed an LOI value of 5.4%.

2.2 Aggregate

Coarse aggregate in surface dry condition of size confirming to 20mm was used. River sand was used as fine aggregate in saturated surface dry condition. Coarse aggregate and fine aggregate specific gravity is found to be 2.85 and 2.66. Water absorption of coarse aggregate and fine aggregate was 0.85% and 3.09% respectively. All the aggregates were conforming to IS 383: 2016 [11] specifications.

2.3 Super plasticizers

The properties of super plasticizer were given as Polycarboxlic ether based super plasticizer, Colour – Light brown, Specific Gravity – 1.08 ± 0.01 at 25°C, pH ≥ 6. The dosage of super plasticiser is adopted is 10 lit/m^3 of concrete. It was primarily developed for application in High Performance Concrete for reducing water content.

3. EXPERIMENTAL WORK

3.1 Mix Proportion and Casting of HPC specimens

M60 grade mix design was done as per the method proposed by P.C.Aitcin [12], a simple approach that follows ACI 211-1 standard practice. Cement content is 510 kg/m^3 for the control specimen and 5%, 10%, 15%, 20% of cement is replaced by bagasse ash for the remaining mixes. The weight of fine aggregate and coarse aggregate are 809 kg/m^3 and 1125 kg/m^3 respectively. The water content of the mix and W/B ratio are 130 kg/m^3 and 0.28. The dosage of the super plasticizer was adopted as 10 lit/m^3 of concrete. The mixes were designated as HPC-BA0 for control specimen and HPC-BA1 – HPC-BA4 for bagasse ash blended high performance concrete.

Ordinary Portland cement was replaced with bagasse ash of proportions 5, 10, 15, 20% by weight of cement. Five different concrete mixtures including control mixtures were prepared with a water binder ratio of 0.29. Concrete was mixed for about five minutes in laboratory drum mixer. The details of the number of concrete specimens cast for the present study are as follows: 30 Nos. of cube specimens of size 150 mm, 30 Nos. of cylindrical specimens of size 150 mm diameter and 300 mm height, 30 Nos. of prism specimens of size 100 mm x 100 mm x 500 mm, 63 Nos. of cube specimens of size of 100 mm and 21 Nos. of disc specimens of size of 152 mm diameter and 62.5 mm thickness. After twenty four hours of casting, the test specimens were demoulded and immersed in water for curing, till the age of test.

3.2 Mechanical Properties

The cube compressive strength was calculated as per IS 518-2004[13] for bagasse ash blended high performance concrete. Splitting tensile strength was carried out on bagasse ash blended high performance concrete cylinders as per IS 5816-2004 [14] .Prism specimens were cast to determine the flexural strength of bagasse ash blended High performance concrete. The test was carried out at the age of 7 and 28 days curing.

3.3 Durability Properties

Saturated water absorption (SWA) tests were carried out on bagasse ash blended high performance concrete cube specimens as per ASTM C642 [15] at the age of 7 and 28 days curing. percentage of water absorption of HPC is a measure of the volume of pores (porosity) in hardened concrete, in which water is occupied under saturated condition. Sorptivity measures the rate of infiltration of water into pores available in concrete. The sorptivity values of bagasse ash blended high performance concrete specimens after 28 and 90 days were calculated using the formula $I = S \times T^{0.5}$, Where I is absorption per unit area (mm), S is Sorptivity (mm/$hr^{0.5}$) and t is the time elapsed. The impact strength tests were carried out on bagasse ash blended high performance concrete specimens at the age of 28 days curing using drop weight testing device as per ACI Committee 544. 2R-89. By using hammer, tested bagasse ash blended high performance concrete cube specimens were broken into small pieces. Further the small pieces were powered using laboratory ball milling and pulversier. For all the mixes, processed powder sample was tested for alkalinity.

4. RESULTS AND DISCUSSIONS

4.1 Compressive strength

The compressive strength of HPC mixes containing bagasse ash decreases at 7 days curing compared to that of conventional concrete. HPC mixes with bagasse ash HPC-BA1 and HPC-BA2 shows improvement in the compressive strength at 28 days curing, which was up to 6% compared to the mix without bagasse ash (HPC-BA0). HPC-BA3 and HPC-BA4 specimens show decrease in the compressive strength of 10.5% respectively. Thus from the results, it has been observed that the maximum compressive strengths were obtained for mixes HPC-BA2 (10%). Increase in the compressive strength may be due to reaction of bagasse ash with calcium hydroxide and forms CSH gel [16]. The calcium silicate hydrate is the component which gains strength due to binding effect. Up to 10% replacement of cement with bagasse ash shows increased in compressive strength, Addition of bagasse ash beyond 10% has no significant reaction with calcium hydroxide. Excess bagasse ash does not react or act as binder in HPC; hence it reduces strength at 28 days curing. The variations of compressive strength of HPC mixes containing 5 to 20 % of replacement of cement by bagasse ash at different 7 and 28 days are shown in the Fig.1.

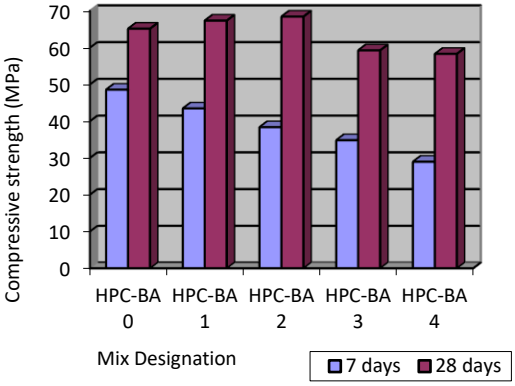

Fig.1.Variation of Compressive strength

4.2 Splitting Tensile strength

Splitting tensile strength values of bagasse ash blended high performance (HPC-BA) at different ages are presented in Fig.2. It can be observed from the results that up to 10% (HPC-BA2 & HPC-BA3) of bagasse ash, the splitting tensile strength increases [16] . The percentage increase in splitting tensile strength at the age of 7 and 28 days are 18.98 and 25.17, compared to the conventional concrete.

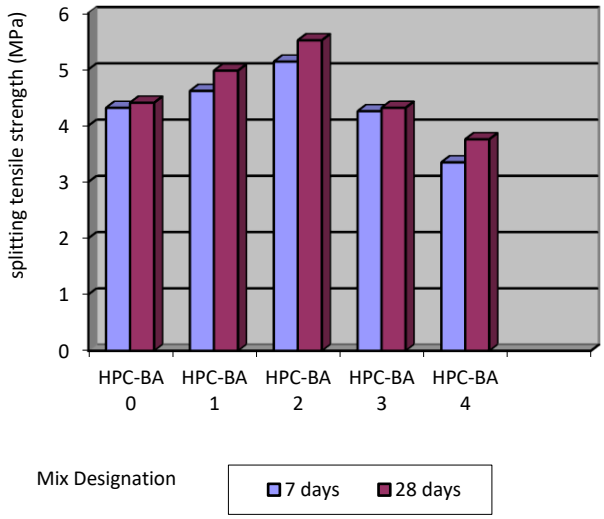

Fig.2.Variation of Splitting Tensile strength

4.3 Flexural strength

Flexural strength results of bagasse ash blended high performance (HPC-BA) at different ages are shown in Fig.3. High performance concrete without bagasse ash (HPC-BA0) attains a flexural strength of 7.65 N/mm^{2,} whereas flexural strength increases up to 6.14 % for the specimens of HPC-BA1 and HPC-BA2 compared to HPC mix without bagasse ash. Specimens HPC-BA3 and HPC-BA4 attains lower flexural strength compared to the mix without bagasse ash.

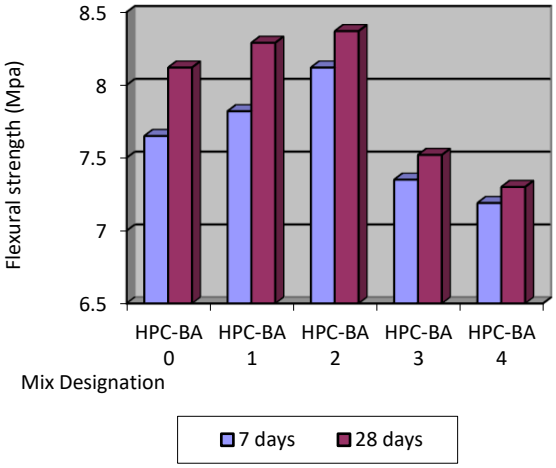

Fig.3. Variation of Flexural strength

4.4 Saturated water absorption

The saturated water absorption tests for various High performance concrete blended with bagasse ash (HPC-BA) mixes at the age of 28 days curing was 1.75, 1.51,1.21,1.10 and1.15 % and at the age of 90 days, the water absorption values was around 1.57, 1.30, 1.15, 1.08 and 1.27 % respectively. The addition of bagasse ash with high performance concrete mixes on the water absorption and the variation of saturated water absorption with various proportions of bagasse ash are shown in Fig. 4. The optimum percentage of replacement of cement by bagasse ash was 15% for achieving the lowest values of SWA. It is also seen from the figure.4 that the bagasse ash blended high performance concrete mixes at the age of 28 days varies from 13 to 38 % decrease in water absorption compared to with that of HPC without bagasse ash. The reduction in percentage of water absorbed is due to the filler effects of small pores in concrete and pozzolanic reaction between the blended materials which strengthened the surface morphology of concrete, bringing about fine and intermittent pore structure.

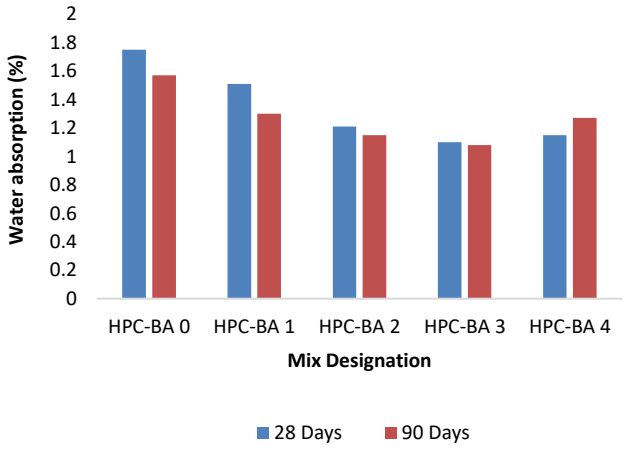

Fig.4. Variation of water absorption

4.5 Sorptivity

From the Fig.5, it is experiential that the sorptivity of the HPC mixes containing bagasse ash was lesser when compared with that of HPC mixes free from

bagasse ash. The reduction in sorptivity varies from 14.81 to 9.25 % for different bagasse ash blended high performance concrete. It was observed that due to fineness of bagasse ash, water level rises, due to which capillary action decreases in HPC [17].

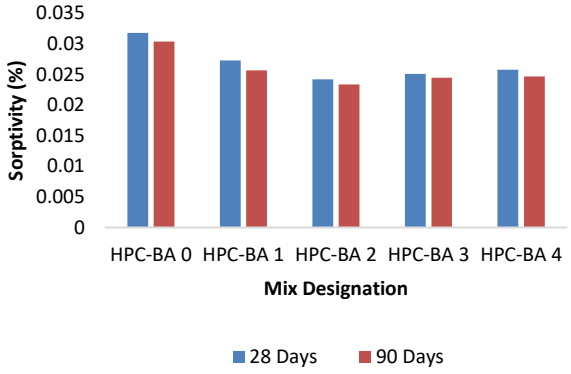

Fig.5. Variation of Sorptivity

4.6 Porosity

The porosities of concrete containing 15% and 20% of bagasse ash (HPC-BA3 and HPC-BA4) were higher than conventional concrete at the same period. It was observed that more the bagasse ash content, more the porosities of HPC. On the other hand, for the 10% of BA replacement (HPC-BA2), the fine particle size of pozzolan modified the pore structure and reduced the porosity of concrete. The variation in porosity of bagasse ash blended high performance concrete is shown in Fig.6.

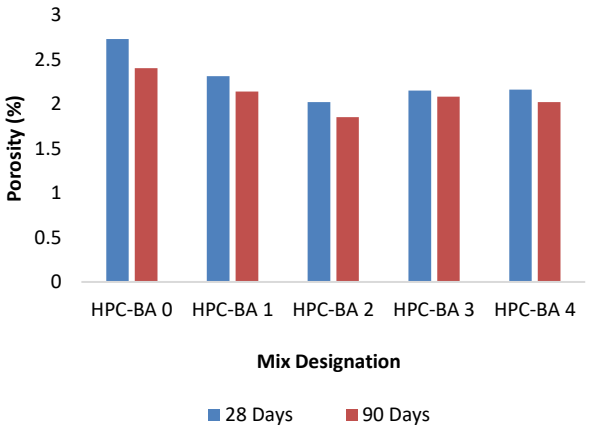

Fig.6. Variation of Porosity

4.7 Impact test

From the Fig.7, it is noted that the impact resistance of High performance concrete mixes containing bagasse ash was more than that of HPC mixes without bagasse ash. Increase in the percentage of bagasse ash enhanced the impact resistance of HPC. This is because of the formation of certain quantity of constant C-S-H in high performance concrete with bagasse ash.

4.8 Alkalinity measurement

The pH values of the aqueous solution prepared from HPC powder samples at 28 days curing are shown in Fig.8. The HPC mixes containing bagasse ash showed lower value of pH compared to HPC mixes without bagasse ash. The concrete mixes containing bagasse ash showed lesser value of pH as compared to concrete mix without bagasse ash. The lower value of pH is due to lime consumption in pozzolanic reaction, the free lime in concrete required to keep high pH in cement concrete is very low. Hence, there is no significant loss of alkalinity due to pozzolanic reaction between silica of bagasse ash and free calcium hydroxide of cement paste.

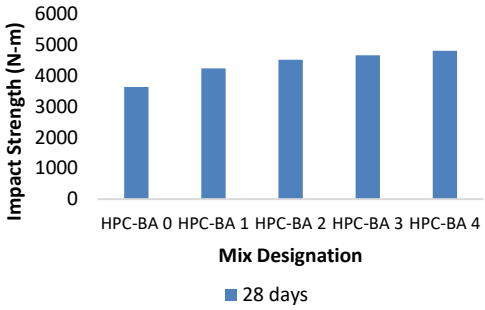

Fig.7. Variation of Impact Test

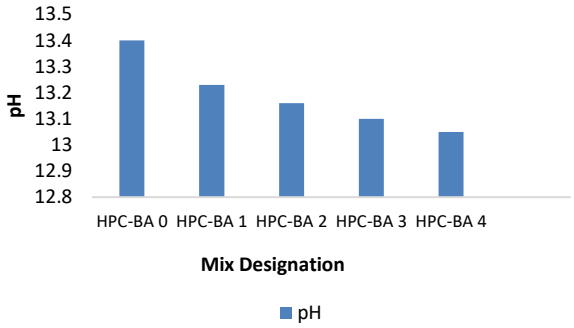

Fig.8.Variation of pH values

5. CONCLUSIONS

From the experimental work carried out, the following conclusions can be obtained.

1. Addition of bagasse ash improves strength properties of concrete up to 10%. BA acts as micro filler and improves the density of cement paste. Therefore, the bond between the cement paste and the aggregate particles is enhanced and improves the concrete strength.
2. Durability properties of HPC mixes blended with bagasse ash shows significant improvement between 10% and 15% of replacement of cement.
1. Impact resistance of bagasse ash blended HPC mixes showed higher values compared to that of mixes without bagasse ash
2. pH values of powder sample blended with bagasse ash showed lower value compared to sample without bagasse ash, where there is no loss of alkalinity significantly.

ACKNOWLEDGEMENT

The authors wish to thank UGC, NewDelhi , for their financial support under minor research project (MRP-6458/16(SERO/UGC) and Dr. R. Rudramoorthy, Principal, PSG College of Technology, Coimbatore for the facilities and support provided in carrying out this research work at Advanced Concrete Research Laboratory.

REFERENCES

1) Bentur, A (2002): Cementituous materials-nine millennia and a new century: past, present and future. ASCE Journal of Materials in Civil Engineering; 14(1):1-22.
2) Caldarone, M.A., Gruber, K.A., and Burg, R.G.,(1994): High reactivity metakaloin: A new generation mineral admixture. Concrete International; 16(11):37-40.
3) Ismat, A.,(2004): Biomass: An ideal fuel for sugar mills for steam/power generation. Fuel Research centre, PCSIR, 197: 12-20.
4) Wild,S.,Khatib,J.M., and Jones, A.,(1996): Relative strength pozzolanic activity and cement hydration in superplasticised metakolin concrete. Cement and concrete research, 26:1537-1544.
5) Mehta,PK.,(1977):Properties of blended cement made from rice husk ash. ACI Materials journal; 74(9):440-442.
6) Biricik,H.,Akoz,F., Berktay, I., Tulgar, AN.,(1999):Study of pozzolanic properties of wheat straw ash. Cement and concrete research; 29: 637-643.
7) Boateng,A.A., and Skeete,D.A.,(1990): Incineration of rice hull for use as a cementitious materials: the guyana experience. Cement and concrete research; 20(5):795-802.
8) Balasubramanian,S,V., Ratnavelu, K. N.,(2001): Budget performance of sugar industry. Proceeding of South India sugar mills association.
9) Hernandez, J. M., Rodriguez, B.S., and Middendorf, B.,(2001):Pozzolanic properties of residues of sugar industries (second part). Materials and Construction; 51(261): 67-72.
10) Amin, N., Shah, M.T., and Ali,K.,(2009): Raw mix designing and clinkerization high strength Portland cement from the raw material of Darkhula Nizampur. Magazine of Concrete Research; 61(10):779-785.
11) IS 383, Coarse and the Fine Aggregate for concrete-Specification. Bureau of Indian Standards 2016. India.
12) Aitcin P.C.,(1998): “High performance concrete”, CRC press.IS 516, Method of Tests for Strength of Concrete, Bureau of Indian standards 2004. India. IS 5816, Splitting Tensile Strength of Concrete- Method of Test, Bureau of Indian standards 2004. India.
13) ASTM C 642, Standard Test method for specific grvaity, absoprtion, and voids in Hardened concrete. American society for Testing Materials standard 1990.
14) Ganesan,K.,Rajagopal, K., and Thangavel, K.,(2007): Evaluation of bagasse ash as supplementary Cementitious material. Cement and Concrete Research, 2007; 29: 515-524.
15) Cordeiro, G.C., Tavares, L.M., Toledo Filho, R.D.,(2016): Improved Pozzolanic activity of sugarcane baggase ash by selective grinding and classification. Cement and Concrete Research;89: 269-275.

Sustainable Infrastructure

Sustainable Geotechnical Solutions

Influence of compacted water content on unconfined compressive strength of bentonite and sand mixes

Das, D. [1] and Chetia, M. [2]

[1] PG Student, Department of Civil Engineering, Assam Engineering College, Guwahati- 781013, India.
[2] Assistant Professor, Department of Civil Engineering, Assam Engineering College, Guwahati- 781013, India.

ABSTRACT

Sand is a pervious material in nature and bentonite has a high swelling and shrinkage properties. Compacted layers of bentonite and sand mixes have been proposed and used in a variety of geotechnical structures. The objective of this study is to investigate the effect of compacted water content on unconfined compressive strength of compacted bentonite and sand mixes. For this, bentonite of different proportion is mixed with 90%, 80%, 70% and 60% sand and unconfined strength is determined by adding different water content to these mixes. Water contents that are added to the mix are taken from the compaction curve of the respective mixes and they are- (i) dry side of optimum moisture content (OMC) (ii) at OMC and (iii) wet side of OMC. Results indicated that for all the bentonite and sand mixes the compressive strength increased in dry side of optimum and decreased in wet side of optimum.

Keywords: bentonite, sand, mix, unconfined compressive strength, water content, influence

1. INTRODUCTION

Waste disposal has always created a great challenge to mankind. With increased environment pollution and its realization has led to the need of planned and engineered waste management facilities. Compacted layers of bentonite and sand mixes are being used in many of the geotechnical structure and engineered liners. To work the liner system properly and safely, the structural stability is one of the major factors to be ensured. The unconfined compressive strength (UCS) is used for this purpose. The UCS test is performed for quick determination of shear strength for both undisturbed and remoulded soils. In this study an effort is made to study the effect of compacted water content on bentonite-sand mixes.

Khan et al. (2014) in his study on compressive behaviour of compacted clay-sand mixes with high plastic clay found that a brittle behaviour was observed in dry side of optimum and ductile on the wet side of optimum. Prakash and Chadrasekaran (2005) has carried consolidation and static and cyclic triaxial tests on Indian marine soils as mixtures of sand and clay with various proportions. They concluded that the inclusion of sand grains in a clay matrix leads to an increase in pore pressure, which resulted as a decrease in undrained shear strength. Tang et al. (2002) in his paper presented strength and section characteristics for dense, unsaturated sand-bentonite mixture under various conditions. Results indicates that the shear strength increases with decreasing water content. Wiebe et al. (1998), performed triaxial tests on undrained sand-bentonite buffer at elevated temperature and pressures. Results indicate that undrained strength increases with decreasing degree of saturation and increasing confining pressure.

From the literature, it was seen that when the test is performed by means of UCS, there is a significant change with the variation of water content. However, a few literatures are available on the effect of water content on bentonite and sand mixes. In this study, an attempt was made to investigate the effect of compacted water content on UCS of bentonite and sand mixes and variation in UCS with bentonite content variation in these mixes. UCS test was performed on unconfined compressive testing equipment on remoulded bentonite-sand mixes with water content at OMC-3%, OMC and OMC+3%.

2. MATERIAL AND METHOD

The sand used in this study is collected from Kulsi riverbank, in district- Kamrup, Assam, India. The bentonite used in this study is commercially available sodium bentonite. The basic test of sand and bentonite such as specific gravity, grain size distribution and Atterberg limits are performed according to Indian standard (IS) guidelines. The mineralogical composition of the sand and bentonite is determined by microscopic photograph with the help of

electroscope (25x) and X-ray diffraction respectively which are shown in Fig. 1 and Fig. 2. Mineralogy of sand showed that it has 95% of quartz in it. Table 1 and Table 2 represent the physical characteristics of sand and bentonite respectively.

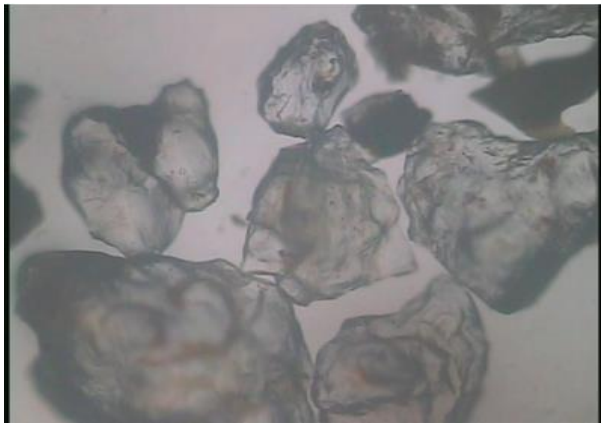

Fig. 1. Microscopic photoghaph of sand

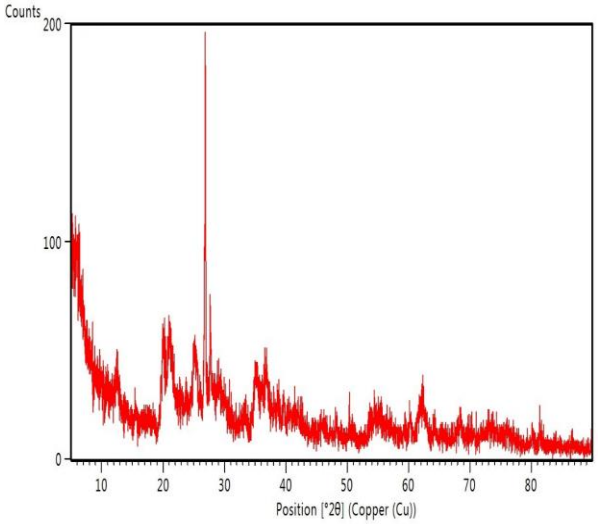

Fig. 2. Microscopic photoghaph of sand

Table 1. Properties of used sand

Properties	
Specific gravity	2.76
[1]D_{10} (mm)	0.22
[2]D_{30} (mm)	0.39
[3]D_{60} (mm)	0.64
Coefficient of uniformity	2.90
Coefficient of curvature	1.08
Classification as per IS: 1498-1970	SP (Poorly graded)
Quartz (%)	95

[1]Diameter of the particle at 10 % finer on the grain size distribution curve

[2]Diameter of the particle at 30 % finer on the grain size distribution curve

[2]Diameter of the particle at 60 % finer on the grain size distribution curve

Table 2. Properties of used bentonite

Properties	
Liquid limit (%)	207.00
Plastic limit (%)	55.50
Plasticity index (%)	151.50

The plastic bentonite was mixed thoroughly and uniformly with non-plastic sand in four different proportions as listed in Table 3. Table 4 represents the OMC and MDD values of the mixes.

Table 3. Mix designation of bentonite and sand

Mix	Sand (%)	Bentonite (%)
90:10	90	10
80:20	80	20
70:30	70	30
60:40	60	40

The process of preparing specimen is as follows. Firstly, distilled water was added by dry weight of these mixes and kept it for 24 hours in sealed plastic bags, so that the water can distribute uniformly. Then the soil was poured cylindrical mold and compacted to the desired dry density. Finally, the moisture content and dry densities were calculated and plotted in graph to get the optimum dry density (OMC) and maximum dry density (MDD) of the respective mixtures as shown in Fig. 3.

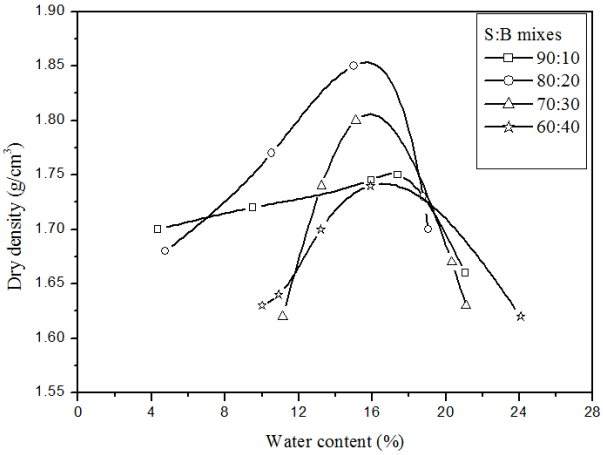

Fig. 3. Compaction curves for four different mixes

Table 4. MDD and OMC of different mixes

Mix	MDD (g/cm^3)	OMC (%)
90:10	1.75	17.39
80:20	1.85	15.00

70:30	1.81	15.10
60:40	1.74	15.90

3 RESULTS AND DISCUCUSSIONS

Three points (OMC and OMC±3%) were picked from the compaction curve of the bentonite and sand mixes and samples are prepared. For different proportion of mixes, water content equal to OMC and OMC±3% is added to the dry weight of the particular mix proportion and kept it in sealed plastic bags and inside a desiccator for 24 hours for the uniform distribution of water. After 24 hours, calculated amount of mix is placed inside the UCS sampler to get a sample of size 76 mm x 38 mm. The UCS test is conducted as per is 2710 (part 10) : 1991.

Fig. 4 to 7 shows the typical stress strain curves of all the four different mixes. The test results indicated that with the increased in water content, the UCS values decreased. In all the bentonite and sand mixes, OMC-3% showed the highest UCS values. But as the water content increased to OMC and OMC+3%, the values decreased gradually. The UCS values with respect to compaction water content for all the mixes are listed in Table 5.

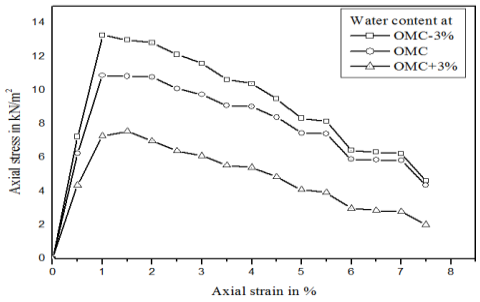

Fig. 4. Stress-strain curve for four 90:10 mix

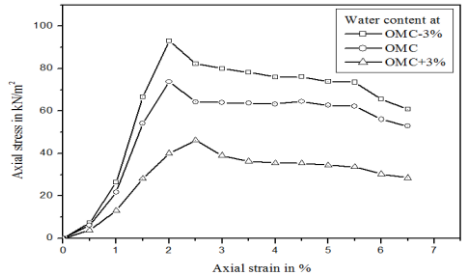

Fig. 5. Stress-strain curve for four 80:20 mix

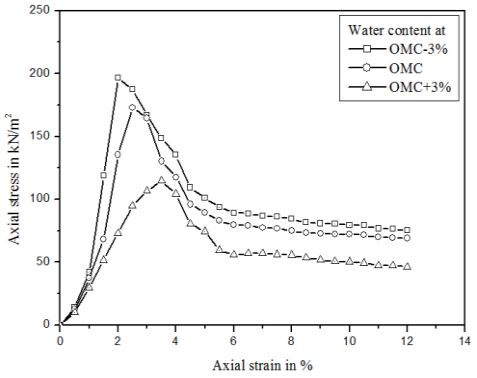

Figure 6. Stress-strain curve for four 70:30 mix

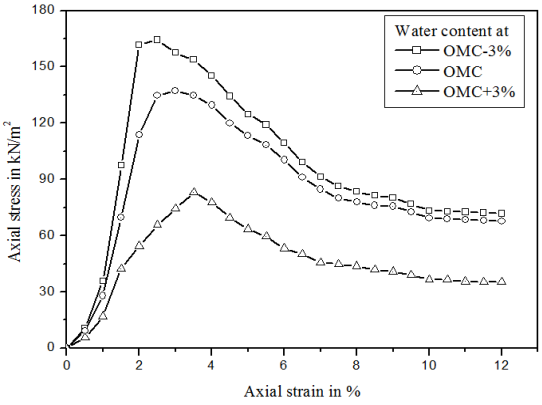

Fig. 7. Stress-strain curve for four 60:40 mix

Table 5. UCS values for different deformation rates

Mixes	Water content (%)	UCS (kPa)
90:10	OMC-3 = 14.40	13.27
	OMC = 17.40	10.88
	OMC+3 = 20.40	7.58
80:20	OMC-3 = 12.00	93.06
	OMC = 15.00	73.86
	OMC+3 = 18.00	46.29
70:30	OMC-3 = 11.80	196.48
	OMC = 14.80	172.99
	OMC+3 = 17.80	114.71
60:40	OMC-3 = 12.90	164.35
	OMC = 15.90	137.07
	OMC+3 = 18.90	83.18

The UCS value increased by 13% to 26%, when water content varied from OMC to OMC-3%. When the water content varied from OMC to OMC+3%, the UCS values decreased by 30% to 40% for all the tested bentonite and sand mixes. It was also observed that as the bentonite content increased from 10% to 40 % in bentonite and sand mixes, the variation of UCS values increased too. The maximum variation of UCS value due to water content variation was found in 60:40 mix. The variation of UCS with different water content of theses mixes are shown in Fig. 8.

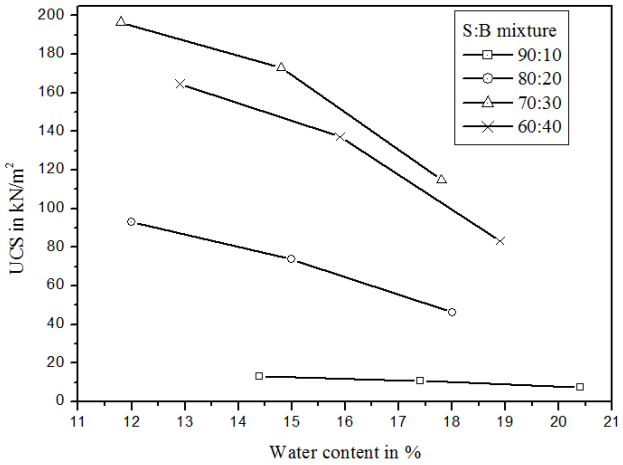

Fig. 8. Variation of UCS with water content

4 CONCLUSIONS

The following conclusions have been drawn from the results of the investigation:

- With increase in water content, the UCS value decreases in the bentonite and sand mixes.
- As the bentonite content increases, the variation of UCS value due to difference in water content also increases. In this study, bentonite and sand mix having 40% bentonite shows maximum variation of UCS value.

5 REFERENCES

1) Tang, G.X., Graham, J. Blatz and Rajapase, R.K.N.D. (2002): Suctions, stresses and strengths in unsaturated sand-bentonite, *Engineering Geology*, 64(2), 147-156

2) Wiebe B., Graham, J., Tang, G.X. and Dixon, D. (1998): Influence of pressure, saturation and temperature on the behavior of unsaturated sand-bentonite, *Canadian Geotechnical Journal*, 35(2), 194-205.

3) Khan, F.S., Azam, S., Raghunandan, M.E. and Clark, r. (2014): Compressive strength of compacted clay-sand mixes, *Advances in material science and engineering*, 2014, 1-6.

4) Prakasha K.S. Praasha and Chandrasekaran, V.S. (2005): Behavior of marine sand-clay mixtures under static and cyclic triaxial shear, *Journal of Geotechnical and Geoenvironmental Engineering*, 131(2), 213-222.

Bio-mediated soil improvement

Baruah, P. [1] and Khaund. P. K. [2]

[1] PG Student, Department of Civil Engineering, Jorhat Engineering College, Jorhat-7, Assam, India.
[2] Professor, Department of Civil Engineering, Jorhat Engineering College, Jorhat-7, Assam, India.

ABSTRACT

Bio-mediated soil improvement has recently emerged as a new sustainable technique of ground improvement. The technique takes advantages of a biological process, technically known as microbial induced calcite precipitation (MICP) to produce calcite in soil matrix. The calcite generated is responsible for cementing and clogging the soils, and hence improve the engineering properties of the soils. It is a new, exciting opportunity for utilizing biological processes to modify the engineering properties of the subsurface (e.g. strength, stiffness, permeability). MICP is enabled by interdisciplinary research at the confluence of microbiology, geochemistry and civil engineering. This new field has the potential to meet society's ever-expanding needs for innovative treatment process that improve soil supporting new and existing infrastructure. This paper presents a review on the soil microorganisms responsible for this process and factors that affect their metabolic activities and geometric compatibility with the soil particle sizes.

Keywords: MICP, biological process, microbiology, geochemistry, civil engineering

1. INTRODUCTION

Nowadays, new construction on weak has become necessary because of the growing worldwide scarcity of land. The weak soil deposits are commonly characterised by low strength and high compressibility. Soil improvement technique require evaluation in order to ensure efficient improvement, and at the same time possess sustainable and environment friendly characteristics. Microbial-induced calcite precipitation (MICP) is a relatively new and innovative soil improvement technique based on biochemical treatment. In terms of geotechnical engineering, soil improvement, refers to existing engineering properties of soil to accommodate the needs of construction. Current construction trend has put great emphasis on sustainable development and construction with minimal pollution. Soil improvement through MICP can provide an alternative to "green construction" as the treatment process exerts minimal distribution to soil, human health and environment. The aim of this study is to get the basic idea of MICP and how it can be used to improve the soil properties by studying various research papers. The effectiveness of MICP treatment is assessed by comparing the engineering properties of the residual soil before and after treatment.

MICP is a process that exists in nature, urease-producing microorganism can be found in natural soil and groundwater. For the purpose of soil improvement, the MICP process is intensified by increasing the concentration of urease-producing microorganisms and cementation reagent in soil. However, it should be noted that the MICP process is not perfectly environmental friendly. The process generates by-product of ammonium and its oxidized by-product nitrate, which can be toxic for soil organism, particularly at high concentration (Van Paassen , 2011).

DeJong et al. (2006) treated loose and collapsible sand specimens and found that MICP improved the soil strength by enhancing shear stiffness and shear capacity.

Several researchers attempted to formulate appropriate procedure to distribute and fix urease-producing bacteria homogeneously in soil to promote effective MICP. Researchers found that two-phase injection procedure could contribute to homogeneous distribution of *S.pasteurii* in sand column. The two-phase injection was first, injection of *S.pasteurii* suspensions and second, injection of a fixation fluid (high salt content).

Ivanov and Chu (2008) presented a detailed review on the applications of MICP for soil improvement. At present, promising MICP applications only focus on bio-cementation and bio-clogging. Bio-cementation improves soil strength by formation of cementation materials through microbial means.

Most studies of MICP treatment have been performed on a laboratory scale (Ivanov and Chu 2008; Dejong et al., 2010; Mitchell and Santamarina 2005). Van Passen (2011) provided an overview of research development in Netherlands, using scale-up laboratory tests and field-scale experiments. The MICP technique has been applied successfully in field to strengthen the wall of

borehole from soil collapsing during drilling process.

Ivanov and Chu performed an approximate cost comparison between the raw materials for microbial grouting and the conventional chemical grouting. They suggested that the cost for microbial grouting (Rs 31.92/- to Rs 574.56/- per m^3 of soil) is significantly cheaper than that of chemical grouting (Rs 127.68/- to 4596.48/- per m^3 of soil).

2. OVERVIEW OF BIO-MEDIATED SOIL IMPROVEMENT SYSTEMS

According to Jason T. DeJong et al. (2010), a bio-mediated soil improvement system broadly refers to a chemical reaction that is managed and controlled within soil through biological activity and whose by-products alter the engineering properties of soil.

2.2.1 Underlying chemical reaction networks

Central to these systems is a network of chemical reactions whose by-products have the potential to alter the engineering properties of soil. The by-products generated can be generally categorised into: inorganic precipitation, organic precipitation and gas generation.

2.2.2 Role of biological process

Biological activity provides an ability to control and manage the timing, rate and spatial distribution of the chemical network reaction and hence the by-product which improve soil properties.

When bio-mediated, the chemical processes of inorganic precipitation, organic precipitation and gas generation can be considered as bio-mineralization, biofilm formation and bio-gas generation respectively.

In bio-mediated soil improvement, the bio-mediated chemical reaction network is regulated to control the timing of the reaction. This is enabled by the amendment of chemicals into the surface. The microbial population in-situ is typically either stimulated (bio-stimulation) through the injection of nutrients or augmented (bio-augmentation) by the injection of additional microbes. In either case, the goal is to increase activity levels and/or concentrations of the microbial population to the level required to initiate and sustain a chemical reaction.

Microbial activity gradually alters the environmental conditions-often in the form of increasing the pH-until the environmental conditions required to initiate the chemical reaction are reached.

Once the chemical reaction is triggered, the desired rate of by-product production (e.g. calcite precipitation) is governed by the rate of microbial metabolic processes and/or the available chemicals.

2.2.3 Biological reaction of MICP

According to a report given by Ng Wei Soon, Calcite precipitation can be induced in several MICP processes. Some researchers have conducted an extensive review on potential carbonate precipitation process include photosynthesis, sulphate reduction, nitrogen cycle and other unspecified pathway.

A nitrogen cycle involves ammonification, nitrate reduction or urea hydrolysis. These three mechanisms are all capable of producing calcium carbonate (Fujita et al., 2000).

The potential of urea hydrolysis, aerobic oxidation, de-nitrification and sulphate reduction for MICP were studied and compared by Paassen et al. (2010). They concluded that urease production possesses a greater calcite conversion rate compared to other processes. Urea hydrolysis is the most common MICP process for soil improvement. This is supported by the fact that most of the studies pertaining to the topic of MICP have adopted the urea hydrolysis process for calcite precipitation.

Urease enzyme decomposes ($CO(NH_2)_2$) in soil through a chemical reaction known as urea hydrolysis. The enzyme can be either supplied externally into soil (Nemati and Voordouw, 2003) or produced in-situ by urease-producing microorganism (Whiffin et al., 2007;; DeJong et al., 2006). Quantitavely, 1 mole of urea is hydrolysed to 2 moles of ammonium, in the presence of urease enzyme:

$$CO(NH_2)_2 + 2H_2O \xrightarrow{\text{urease}} 2NH_4^+ + CO_3^{2-} \quad \dots (1)$$

The ammonium (NH_4^+) released from the urea hydrolysis results in a local pH rise that begins the precipitation of calcium carbonate (calcite). Calcite is precipitated through the reaction between carbonate ions (CO_3^{2-}) from the urea hydrolysis and calcium ions (Ca^{2+}) from the supplied calcium chloride:

$$Ca^{2+} + CO_3^{2-} \Rightarrow CaCO_3 \quad \dots (2)$$

The calcite ($CaCO_3$) formed is responsible for improving the engineering properties of soil.

The process of calcite precipitation by microbes can be described in sequences by Figures 1(A)-2(D) (De Muynck et al., 2010). At Figure 1(A), calcium ions in the solution are attracted by negative charges to the cell wall of microbes. Addition of urea leads to the release of dissolved inorganic carbon (DIC) and ammonium in the

microenvironment of the microbes. At Figure 1 (B), the existence of calcium ions cause local super-saturation and thus heterogeneous calcite precipitation on microbial cell wall. At Figure 1 (C), after certain period of time, the microbes become encapsulated by calcite, resulting in limited or no nutrient transfer and eventually destroy the microbes. Figure 1 (D) shows the imprint of microbial cells that take part in calcite precipitation.

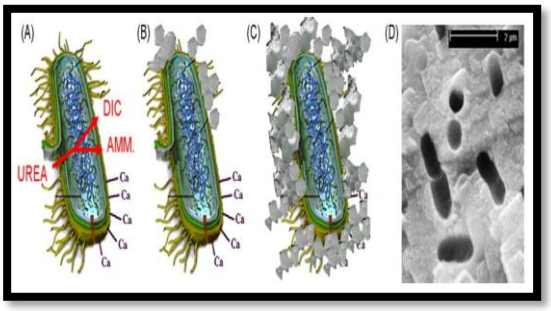

Fig.1.Simplified representation of the events occurring during the ureolytic induced carbonate precipitation (A) calcium ion attracted to cell wall; (B) calcite precipitated near cell wall; (C) calcite increased in quantity and encapsulated cell; (D) imprint of cell that take part in calcite precipitation (De Muyck et al., 2010)

3. MECHANISMS OF SOIL IMPROVEMENT THROUGH MICP

Microbial Geotechnology is an emerging technology, which derived from geotechnical engineering and biology. DeJong et al. (2006) stated that this innovative soil improvement that consists of combination of microorganism, nutrients, biological processes application that naturally present in soil subsurface could effectively improve the engineering properties of soil. There are diverse kinds of potential application of microorganisms in soil improvement; so far are only bio-clogging and bio-cementation resulting in more reliable and effective results.

The main purpose of bio-cementation in soil matrix is to enhance the strength and stiffness of the soil through the microbially-induced products, while bio-clogging reduces the soil porosity and hydraulic conductivity. According to Ivanov and Chu (2008), bio-cementation can be utilized to prevent the soil avalanching, minimize the risk of liquefaction of soil, mitigate the swelling potential of clayey soil and densify the soil of reclaimed land sites. Bio-clogging has the potential to reduce the hydraulic conductivity of dam, forming barrier to confine soil pollution sites, prevent soil erosion etc.

4. FACTORS AFFECTING MICP

According to Firas Jawad Kadhim, Jun-Jie Zhenh (2016) and a report given by Ng Wei Soon (2013), since MICP is a process that rely on the chemical and biological reactions there will be numerous factors influence it. MICP process us regulated mainly by four key factors:

1. Concentrations of calcium ion
2. Availability of nucleation sites
3. Concentration of dissolved inorganic carbon
4. pH

4.1 Bacteria

Since bacteria is the only living organism found in the MICP system, so it is considered as one of the most influential factors in the precipitation process.

A) Bacteria types

The bacteria types that are suitable for MICP application should be able to catalyst urea hydrolysis, and they are usually urease positive bacteria. The typical urease positive bacteria are genera *Bacillus, Sporosarcina, Spoloactobacilus, Clostridium* and *Desulfotolaculum* (Kucharski et al., 2008).

B) Bacteria Cell Concentration

A high bacterial cell concentration to the soil sample would certainly increase the amount of calcite precipitated from MICP process (Okwadha and Li 2010). A high concentration of bacteria produces more urease per unit volume to commence the urea hydrolysis.

C) Geometric Compatibility of bacteria

The size of the microbes are mostly ranging from 0.5 to 3.0 μm (Mitchell and Santamarina, 2005). The geometric compatibility of urease-producing bacteria is critical whenever the transportation of bacteria within the soil is required for soil treatment. Small pore throat size would limit their free passage, depends on the size of microbes and soil composition.

4.2 Nutrients

Nutrients are the energy source for bacteria, and hence it is essential to provide proper and sufficient nutrients for urease-producing bacteria. Nutrients are supplied to bacteria during culture stage and soil treatment stage. Common nutrients for bacteria include CO2, N, P, Mg, K, Ca, Fe etc. (Mitchell and Santamarina, 2005).

4.3 Chemical solutions

To induce urea hydrolysis and calcium carbonate precipitation in the soil in addition to bacteria, chemical solutions are needed to be injected to the location where improvement is required. The chemical solutions and additives used in the experiments included calcium sulphate,

calcium chloride, sodium carbonate, sodium chloride, ammonia, alcohol and sodium acetate.

4.4 pH

Like all other enzymes, urease enzyme only activate at certain range of pH. The urease activity of bacteria, such as S. pasteurii has an optimum pH value of 8 (Stocks-Fischer et al., 1999)

4.5 Temperature

Temperature has a significant influence on the urease activity, and hence on the rate of MICP. At temperatures below 5°C, the urease activity is negligible (Van Passen, 2011).

4.6 Injection methods

Most researches on MICP were performed by injection method which is similar to the grouting of artificial material for soil improvement. On the other hand, continuous injection method promotes abundant calcite precipitation near the injection point.

5. CONCLUSION

Microbial-induced calcite precipitation (MICP) can be considered as a practicable technique that improves soil-supporting new and existing structures and can be used in many geotechnical engineering applications, such as slope stabilization and subgrade reinforcement. The process has shown greater potential in many engineering applications, but much work has to be done to bring this convenient technology to field applications. Comparative studies need to be conducted to assess the feasibility of MICP with that of traditional grouting.

Successful field implementation requires up-scaling of biological, chemical and geotechnical (soil) systems that is not empirical, but instead based on fundamental principles. This effort will need analytical work, numerical modelling and experimentation. The field of bio-mediated soil improvement is rapidly emerging, the range of opportunities continues to expand, and challenges lie ahead.

6. REFERENCES

1) DeJong et al. (2006), Microbially induced cementation to control sand response to undrained shear, *ASCE Journal of Geotechnical and Geoenvironmental Engineering.*
2) De Muynck W. et al. (2010), Microbial carbonate precipitation in construction materials: A review, *Ecological Engineering*, Vol. 36, pp. 118-136
3) Firas Jawad Kadhim and Jun-Jie Zheng. (2016). Review of the Factors That Influence on the Microbial Induced Calcite Precipitation. *Civil and Environmental Research.* ISSN 2224-5790 (Paper) ISSN 2225-0514 (Online), Vol.8, No.10
4) Ivanov V, Chu Jian (2008), Applications of microorganisms to geotechnical engineering for bioclogging and biocementation of soil in situ, *Environmental Sci. Biotechnol*, DOI 10.1007/s11157-007-9126-3
5) Jason T. DeJonga, Brina M. Mortensenb, Brian C. Martinezb, and Douglas C. Nelsonc. (2010) Bio-mediated soil improvement. *Ecological Engineering*, Vol. 36, No. 2, pp. 197-210.
6) Kucharski et al. (2008), Microbial Biocementation, *U.S. Patent Documents.*
7) K T P Chiet, K A Kassim, K B Chen, U Martula, C S Yah and A Arefnia. (2015). Effect of Reagents Concentration on Biocementation of Tropical Residual Soil. *Soft Soil Engineering International Conference 2015 (SEIC2015)*
8) Lee M.L., Ng W.S., Tan C.K., and Hii S.L. (2012). Bio-mediated soil improvement under various concentrations of cementation reagent. *Applied Mechanics and Materials*, Trans Tech Publications. 204-208, pp. 326-329.
9) Li et al. (2015), Bio-grout based on microbially induced sand solidification by means of asparaginase activity.
10) Mitchell K. J. and Santamrina C.J. (2005), Biological Considerations in Geotechnical Engineering, *ASCE Journal of Geotechnical and Geoenvironmental Engineering,* pp. 1222-1233
11) Murtala Umar, Khairul Anuar Kassim and Kenny Tiong Ping Chiet.(2016). Biological process of soil improvement in civil engineering: A review. *Journal of Rock Mechanics and Geotechnical Engineering*. Vol. 8, pp. 767-774
12) Ng W. S., Lee M. L.., Hii S.L. (2012). An Overview of the Factors Affecting Microbial-Induced Calcite Precipitation and its Potential Application in Soil Improvement. *International Journal of Civil and Environmental Engineering*, Vol.6, No.2, pp. 188-194.
13) Ng Wei Soon. (2013). Improvements in Engineering Properties of Tropical Residual Soil by Microbially-Induced Calcite Precipitation. *A dissertation submitted to the Department of Civil Engineering, Faculty of Engineering Science, Universiti Tunku Abdul Rahman, Malaysia.*
14) Ng W. S., Lee M.L., Tan C.K., and Hii S.L. (2014). Factors affecting improvement in engineering properties of residual soil through microbial induced calcite precipitation. *ASCE Journal of Geotechnical and Geoenvironmental Engineering.*
15) Ng W.S., Lee M.L., Tan C.K., and Hii S.L.(2013) Improvements in engineering properties of soils through microbial-induced calcite precipitation.,*KSCE Journal of Civil Engineering*, Vol.17, No. 4, pp.718-728.
16) Nemati M., Voordouw G. (2003), Modification of porous media permeability, using calcium carbonate produced enzymatically in situ, *Enzyme and Microbial Technology*, Vol. 33, pp. 635-642.
17) Okwadha D.O. George, Li Jin (2010), Optimum conditions for microbial carbonate precipitation, *Chemosphere*, Vol. 81, pp. 1143-1148
18) Paasse L.A. Van (2011) Bio-mediated ground improvement: From laboratory experiments to pilot applications. *Geo-Frontiers Congress*, DOI: 10.1061/41165(397)419
19) Stocks-Fischer et al. (1999), Microbiological precipitation of $CaCO_3$, *Soil Biology and Biochemistry*, Vol. 31, pp. 1563-1571
20) W. de Muynck, K. Verbeken, N. de Belie, W. Verstraete (2010), Influence of urea and calcium dosage on the

effectiveness of bacterially induced carbonate precipitation on limestone, *Ecological Engineering*, Vol.36, pp. 99-111

21) Whiffin et al. (2007), Microbial Carbonate Precipitation as a Soil Improvement Technique, Geomicrobiology Journal, Vol.24, pp. 417-423.

Numerical analysis of the performance of skirted raft foundation on medium dense sand using Plaxis 2D®

Hussain, R. [1], Sarma, K. [1] and Chetia, N.[2]

[1] Student, Department of Civil Engineering, Jorhat Engineering College, Jorhat, Assam, India.
[2] Assistant Professor, Department of Civil Engineering, Jorhat Engineering College, Jorhat, Assam, India.

ABSTRACT

Skirted foundation is one in which vertical or inclined wall surrounds one or more sides of the soil mass beneath the footing slab. An alternative approach used for improving the bearing capacity of raft foundation of settlement sensitive structure is by using structural skirts fixed to the edges of the raft foundation. So, a raft laid at ground level with skirt walls at edges to confine the soil beneath will have a load carrying capacity approximately equal to that of a raft founded at a depth equal to the depth of confinement provided. On this basis, numerical study with Plaxis 2D® is carried out to study the behaviour of raft foundation with vertical skirt and compared with the behaviour of raft foundation without any skirt on medium dense sand. The geometry of the finite element soil model adopted for the analysis is 200m×100m with varying raft size B = 6m with thickness of raft is 0.5m and for skirted raft, different skirt depth ratio (D_p/B) of 0, 0.5, 1, 1.5 and 2 are taken. The thickness of the skirt is 4mm. The soil properties are taken from experimental results. In this analysis plane strain model is used with 15 noded element. The maximum applied pressure is 1000 kN/m^2 and for this pressure, first settlement is measured and at settlement 100 mm which is permissible settlement for raft foundation according to IS:1904-1986, the corresponding safe bearing capacity is noted. After numerical analysis it is seen that as the depth of the skirts increases bearing capacity also increases. Here maximum improvement factor obtained from calculation is 2.10 for a skirt depth equal to twice the size of foundations. The study shows that the installation of skirts with sufficient anchorage length is a good method of improving bearing capacity of subgrade.

Keywords: skirted foundation, skirt depth ratios (S-D_p), improvement factor

1. INTRODUCTION

A mat or raft is a combined footing that covers the entire area beneath a structure and supports all the walls and columns. In case the allowable soil pressure is low or the building loads are very heavy, the use of spread footings would cover more than one half of the area and it may prove more economical to use mat or raft foundation. They are also used where the soil mass contains compressible lenses or the soil is sufficiently erratic so that the differential settlement would be difficult to control. Raft foundations are also used in supporting structures for weak soil conditions or heavy columns loads. They may require more area to transfer heavy load or need to place at greater depth to keep stress level within permissible bearing capacity. By providing skirt wall, the load from the superstructure is transferred safely to the strata below. It may also be noted that this type of confinement will control the tilt and hence increase the load bearing capacity of footing resting on non-uniform soil condition in which some portion of the soil is weak compared to other. Therefore, it is an alternative approach for improving the bearing capacity of raft foundation. This approach is based on the use of "structural skirts" fixed to the edges of the foundation. This method of improvement does not need excavation of the soil and hence it cannot be restricted by the presence of a high water table. On this basis numerical study is carried out to study the behaviour of raft foundation with vertical skirt and compared with the behaviour of raft foundation without any skirt in different site conditions. Different skirt-depth ratios are adopted for this study.

2 NUMERICAL MODELLING

The geometry of the finite element soil model adopted for the analysis is 200m×100m with varying raft size B = 6m with thickness of raft is 0.5m and for skirted raft, different skirt depth ratio (D_p/B) of 0, 0.5, 1, 1.5 and 2 are taken. The thickness of the skirt is 4mm. Here the ground water condition is neglected. Only the raft foundation is modeled. Superstructure is

replaced by an equivalent amount of loading and that equivalent amount of vertical pressure is applied on the raft. The soil property used for this study is given in Table 1. The soil properties are taken from experimental results for medium dense sand and the plate properties are taken from a literature of Azzam (2011) having raft and skirt size same as above. Axial Stiffness for steel skirt, EA is taken 63000 kN/m. In this analysis plane strain model is used with 15 noded element. Material properties of sand are listed in Table1.

Table 1. Material Properties.

Properties	Value
Type of material	Sand
Soil model	Hardening soil model
Stiffness modulus, E_{50} (kN/m^2)	40000
Unsaturated unit weight, (kN/m^2)	16.0
Angle of internal friction, ϕ°	33.3
Interface reduction factor, R_{inter}	.67

Analysis is carried out in Plaxis 2D® for raft foundation without skirt and with skirt using above modeling and soil properties. The maximum applied pressure is 1000 kN/m^2 and for this pressure, first settlement is measured. Also at settlement 100 mm which is permissible settlement for raft foundation according to IS:1904-1986, the corresponding safe bearing capacity is noted. The load application procedure is taken from literature by Pusadkar and Bhatkar (2013) for this analysis and the results obtained from analysis is verified by this literature. The geometries obtained in the analysis for a raft foundation without skirt are shown below.

3 NUMERICAL ANALYSIS

3.1 Raft foundation without skirt

Following geometries are obtained when maximum pressure of 1000 kN/m^2 is applied to the raft foundation during analysis. Fig. 1 and Fig. 2 show the total displacement contour and stress zone of the soil bin for raft size of 6 m respectively.

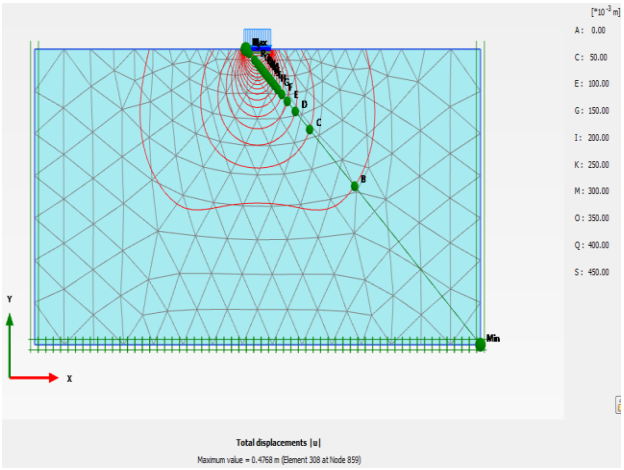

Fig. 1. Total Displacement Contour

Total displacement and total stress are maximum just below the raft foundation and spreads laterally. The stress contour and the displacement contour follow the same trend as given in the literature of Pusadkar and Bhatkar (2013).

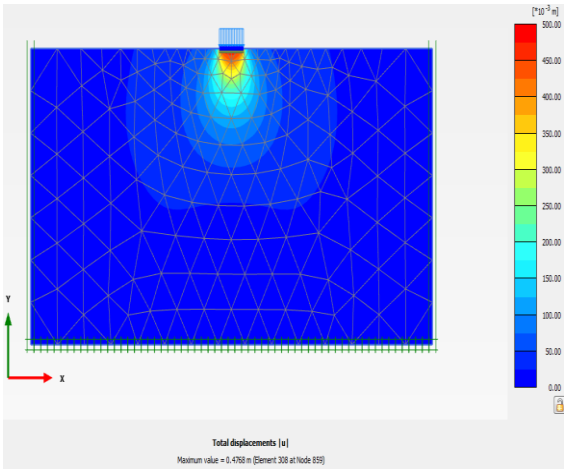

Fig. 2. Stress Zone

Fig.3 shows the load-displacement behaviour of the foundation without skirt under the vertical pressure. From this curve, pressure against 100mm settlement is measured and is taken as ultimate bearing capacity.

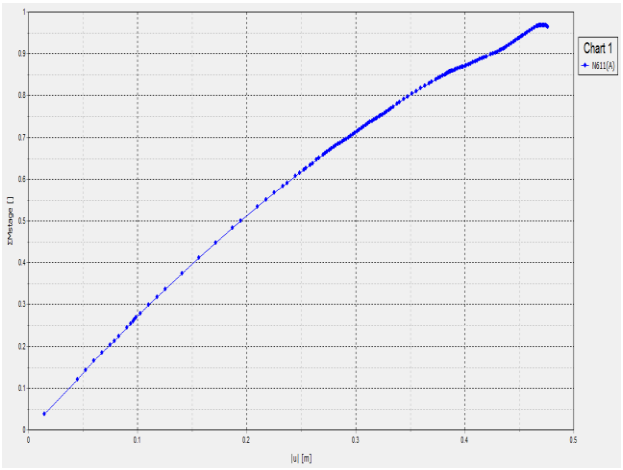

Fig. 3. Load –Displacement Curve of 6m Size Raft Foundation

3.2 Raft foundation with skirt

Following geometries are obtained when maximum pressure of 1000 kN/m^2 is applied to the raft foundation with skirt during analysis. Fig. 4. and Fig. 5. show the total displacement contour and stress zone of the soil bin for a 6m raft size and for skirt depth of 0.5B i.e. 3m. The skirt prevents the stress from lateral spreading and confines the maximum stress inside the confined zone since it acts as a single

unit. The above contour also follows the trend of decreasing lateral spreading due to skirt as described in the literature of Pusadkar and Bhatkar (2013).The analysis was repeated for all the skirt depth ratios and the similar kind of profile was obtained for each case. A representatitive presentation for skirt depth ratio 0.5 has been presented in Fig 4 and Fig 5.

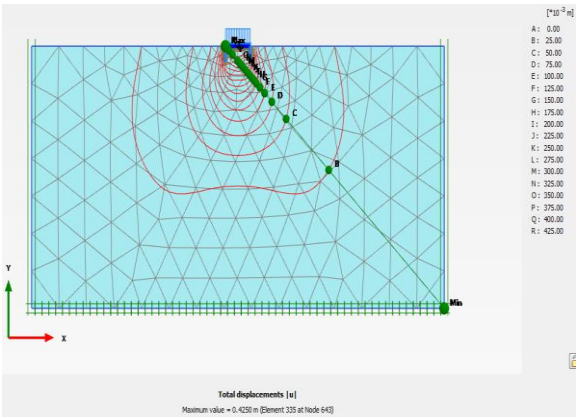

Fig. 4. Total Displacement Contour for Skirt Depth Ratio 0.5

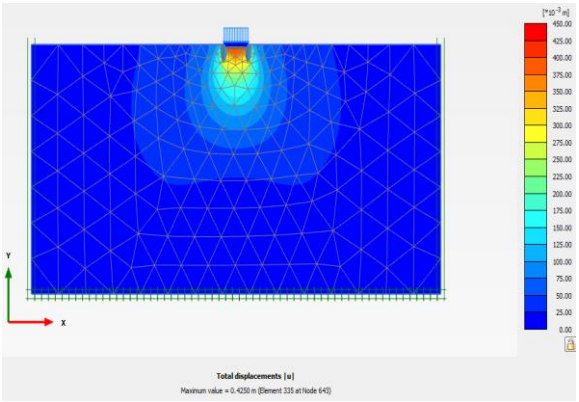

Fig. 5. Stress Zone for Skirt Depth Ratio 0.5

Fig. 6 shows the load-displacement behaviour of the skirted raft foundation.

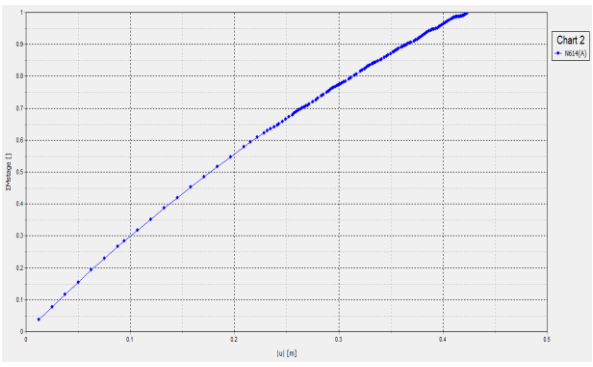

Fig. 6. Load –Displacement Curve of 6m Size Raft Foundation for Skirt Depth Ratio 0.5

Since the permissible settlement of raft foundation is 100 mm according to IS:1904-1986, pressure against 100 mm settlement is calculated from load-displacement graph and the improvements due to installation of skirts are given below.

4 RESULTS

Results from the load displacement curves for different raft sizes and skirt depths are given in Table 2.

Table 2. Results Obtained From Analysis

Raft size(m)	Skirt size (m)	Skirt-depth ratio	Bearing capacity for 100 mm settlement(kN/m^2)	Improvement factor
6	6	0	270	-
6	6	0.5	300	1.11
6	6	1	353	1.3
6	6	1.5	472	1.74
6	6	2	567	2.10

5 CONCLUSION

From Table 2 it is seen that the bearing capacity of the horizontal cohesionless ground where raft foundation is rested can be increased by installation of skirts. As the depth of the skirts increases bearing capacity also increases. It is denoted by Improvement factor. Here maximum improvement factor obtained from calculation is 2.10 for a skirt depth equal to twice the size of foundations. It can be concluded from this analysis that the installation of skirts with sufficient anchorage length may be suggested for improving bearing capacity of subgrade. For such kind of settlement sensitive structure, soil confinement using skirts of different depths helps in increasing bearing capacity at the same allowable settlement.

REFERENCES

1) Azzam, W. R. (2011): Numerical Modeling of Skirted Foundation Subjected to Earthquake Loading, *Proceedings of the 15th African Regional Conference on Soil Mechanics and Geotechnical Engineering*.
2) IS: 1904-1986. Code of Practice for Design and Construction of Foundations in Soils: General Requirements.
3) Pusadkar, S. S., and Bhatkar, T. (2013): Behaviour of Raft Foundation with Vertical Skirt Using Plaxis 2d. *International Journal of Engineering Research and Development*, Volume 7, Issue 6, 20-24.

Comparative study on the performance of circular skirted foundation on both cohesionless soil and cohesive soil

Chetia, N.[1], Sarma, K. [2] and Hussain, R. [2]

[1]Assistant Professor, Department of Civil Engineering, Jorhat Engineering College, Jorhat, Assam, India.
[2] Student, Department of Civil Engineering, Jorhat Engineering College, Jorhat, Assam, India.

ABSTRACT

Improvement of bearing capacity and reduction in settlement of shallow foundation is a matter of utmost concern on weak soil conditions. Structural skirt to a conventional shallow foundation may prove to be beneficial in this context. Generally structural skirts consist of a slab and a shell and may have any shape depending upon the shape of the shallow foundation. Structural skirt restrains the soil beneath laterally and behaves as a single unit with the confinement to transfer the load from superstructure to soil. **It generally increases the effective depth of the foundation.** The aim of this study is to compare the improvement in Bearing Capacity (BC) in cohesionless soil (loosely packed sand) using circular skirt. Both experiments and model analysis with PLAXIS 2D® is performed and parametric variations have been done for different Skirt Depth ratios (S-D_p) and Skirt Diameter ratios (S-D_a). The improvements are estimated by a non-dimensional term Improvement Factor (IF). Improvement factor is the ratio of value of bearing capacity of skirted foundation to the value of bearing capacity of foundation without skirt taken from the experiments done in loose sand. The results obtained from experiment and model analysis are in close proximity. Hence the process of analysis PLAXIS 2D® is extended for clayey soil. Improvement factor is found to be increased upto 4 for different S-D_p ratios and S-D_a ratios in loose sand. Similarly from analysis done by PLAXIS 2D® in clayey soil, improvement factor is found to be increased upto 2.5 for the same S-D_p ratios and S-D_a ratios. It is seen from the result that use of circular structural skirt is more beneficial in cohesionless soil than cohesive soil.

Keywords: skirted foundation, skirt depth ratios (S-D_p), skirt diameter ratios (S-D_a), improvement factor

1. INTRODUCTION

It has become necessary to utilize all types of land of strong and weak condition to raise different structures. Since the availability of good construction ground are in a declining trend, improvement of bearing capacity and reduction in settlement of shallow foundation is a matter of utmost concern on weak soil conditions. Nowadays numbers of **soil improvement techniques have been used to increase the performance of the ground.** The aim of this study is to estimate the improvement in bearing capacity by using circular skirts. Parametric variations have been done for different skirt-depth ratios, s-d_p and skirt-diameter ratios, s-d_a in loose sand and clay. The improvement will be estimated by a non-dimensional term improvement factor i.e. The ratio of bearing capacity of skirted foundation to the bearing capacity of foundation without skirt.

2 LITERATURE REVIEW

Horizontal and vertical reinforcements are used in shallow foundation to improve the bearing capacity and (Mahmoud and ABDRABBO, 1989; Das, 1999). Confined cylinders such as structural skirts are used to improve the resistance of soil to all types of bearing failure (Al-aghbari and Mohamedzein, 2004). Structural skirts are rigid plates penetrating a sufficient depth into the soil. It restrains the soil beneath laterally and behaves as a single unit with the confinement to transfer the load from superstructure to soil

3 METHODOLOGY

The test set up consists of a loading frame and steel plates loaded with cement concrete cubes, a mechanically operated hydraulic jack of capacity 20 kN. The test tank of size 0.95m × 0.95m × 0.95m constructed with steel plates. The width of the test pit is not less than 5 times the size of the test plate, so that the

failure zones are freely developed without any interference from sides (Basheeruddin and Narayan, 2016). Pre-calibrated pressure gauge of capacity 20 kN is clamped to the pumping unit to measure the magnitude of the applied load. Two deflection dial gauges of accuracy 0.01mm are placed on the centre line of the plates with the help of the horizontal datum bars to measure the settlements of the plates. Fig. 1 shows the prepared test set up for this study.

Fig. 1. Test set up

4 MATERIAL USED

4.1 Model footing and model structural skirts

Model footing for the tests is made up of mild steel plate having diameter (B) 0.15m and thickness 0.006m. Model skirted footings are also made up of mild steel sheets having diameters 0.15m, 0.225m and 0.30m and depths 0.075m and 0.15m.

4.2 Sand

The material used for this study is coarse sand from Kanaighat (Kalioni River) of Golaghat District, Assam. The properties of sand i.e. angle of internal friction (ϕ), uniformity coefficient (C_u), co-efficient of curvature (C_c) and grading characteristics D_{10}, D_{30}, D_{60} etc. are determined and shown in Table 1.

Table 1. Properties of collected kanaighat sand

Material	$\varphi(^0)$	D_{60} (mm)	D_{30} (mm)	D_{10} (mm)	C_u	C_c
sand	29	0.55	0.34	0.19	3.0	0.87

The maximum and minimum dry unit weights are 21.18 kN/m^3 and 12.77 kN/m^3. The model tests are performed on sand beds prepared with average unit weight of 14.68 kN/m^3 and corresponding relative density 32.76% representing loose density.

4.3 Clay

Table 2 shows the clay properties used in the study**.**

Table 2. Properties of clay

Type of material	Clay
Stiffness modulus E50 (kN/mm^2)	4×10^{-4}
Bulk density(kN/mm^3)	1.87×10^{-8}
Cohesion, c (kN/mm^2)	5.1×10^{-6}
Friction angle(ϕ)	0
Axial stiffness for steel skirts EA,(kN/mm)	495

5 FOR SAND

5.1 Methodology for test

Load test is performed on the model test tank and test procedure is taken same as for plate load test as per is 1888:1982. After the preparation of sand bed model footing is placed centrally, under the spindle of jack so that the plate, reaction girder and the spindle are coaxial. The dial gauges are arranged and settlement is measured. Load is applied in cumulative equal increments of 10 kg. Dial gauges observations are recorded for each load increments after the time interval mentioned in is: 1888-1982. Next higher load is applied and the process is repeated. Test is continued till a very high settlement is obtained. For the testing of skirted model footing the skirt is inserted centrally into the sand bed and then the model footing is placed above it and same test procedure is also followed

5.2 Interpretation of results

First the average settlements are calculated taking the average of the dial gauge readings. Then the cumulative settlement corresponding to load intensity is calculated. Load intensity and corresponding cumulative settlement are plotted on log-log scale. According to IS: 1888-1982 settlements are plotted as abscissa against corresponding load intensities as ordinate, both to logarithmic scale, which give two straight lines, the intersection of which is considered as yield value of soil. The load intensity at yield point is determined as the ultimate bearing capacity. Also the ultimate bearing capacity for 15 cm diameter of model footing is calculated from the ultimate bearing capacity equations given by Terzaghi (T_r). Bearing capacities of model footings are found experimentally and the experimental values (E_x) of bearing capacity is extracted from respective load-displacement graph and is compared to the analytically found values from Terzaghi equation and have been presented in Table 3.

Table 3. Bearing capacity in kN/m^2

B of MF(m)	E_x	T_r
0.15	22.63	23.56
0.30	45.27	43.85

Close proximity has been observed between the ultimate bearing capacity values obtained from

Terzaghi's equations and the experimental set up. Convinced with the reliability of the test set up, now the effect of skirt-depth ratio is studied for model skirted footing of diameter 0.15 m. For different S-D_p ratios load-settlement curves for 0.15 m diameter obtained from experiments are shown in Fig. 2 and it is seen that as the skirt-depth ratio increases load taken by the model footing also increases and settlement decreases.

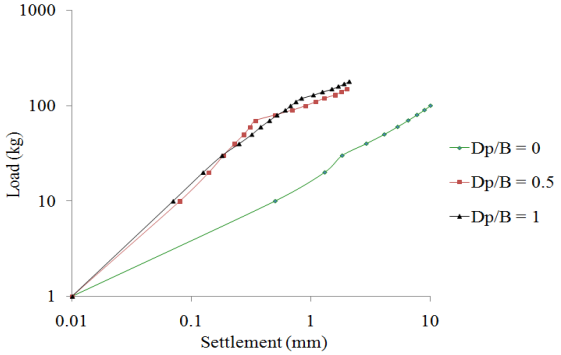

Fig. 2 . Load–settlement curve for different S-D_p ratio on loose sand

In Fig. 3. the effects of different skirt-diameter ratio for Model footing of diameter 0.15 m and depth 0.075 m maintaining skirt-depth ratio 0.5 are shown.

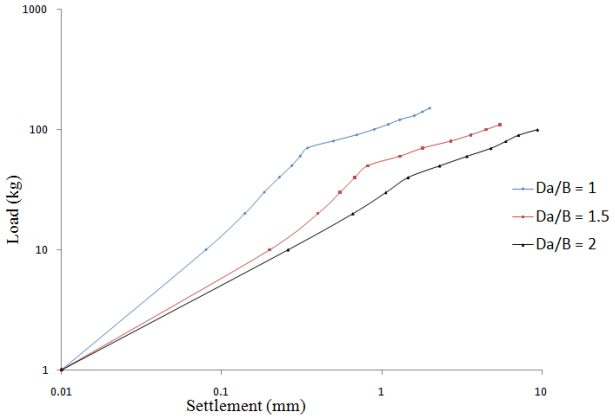

Fig. 3. Load –settlement curve for different S-D_a ratio

The test has been performed on footing diameter 0.15 m and skirt diameter 0.15 m, 0.225 m and 0.30 m with skirt depth of 0.075 m for each of the skirts. Increase in skirt-diameter ratio corresponding to the dimension of model footing results in lateral spreading of soil inside the skirt, thus resulting lesser value of bearing capacity. To validate the experimental results finite element analysis (FEA) is done in PLAXIS 2D®. It is as finite element program developed specially for the analysis of deformation geotechnical engineering projects. To model the footing and the skirted footing 15 nodded axisymmetric model with plate material is used. For modelling the soil bin where the shallow foundation rests, Hardening soil model is used and to analyze results the experimentally found shear parameters are used.

5.3 Important outcomes

The performance of a model skirted foundation can be quantified by improvement factor. In this study the diameter under consideration is 0.15 m. The effect of skirt depth ratio both by experimental and PLAXIS 2D® (FEA) is presented in Table 4.

Table 4. Improvement factor (IF) for different S-D_p ratio

B (m)	D_a (m)	D_p (m)	S-D_P	BC (kN/m^2)		IF
				E_x	FEA	(E_x)
0.15	0	0	0	16.97	23.61	-
0.15	0.15	0.075	0.50	45.27	53.79	2.67
0.15	0.15	0.15	1.0	67.90	98.46	4.00

The calculated IF for S-D_a ratios are shown in Table 5.

Table 5. Improvement factor (IF) for different S-D_a ratio

B (m)	D_a (m)	S-D_a	D_p (m)	BC (kN/m^2)		IF
				E_x	FEA	(E_x)
0.15	0	-	0	16.97	23.61	-
0.15	0.15	1.0	0.075	45.27	53.79	2.67
0.15	0.225	1.5	0.075	28.29	50.91	1.67
0.15	0.30	2.0	0.075	22.64	56.75	1.33

From Table 4 and Table 5 most of the values found from experimental and FEA shows proximity. Improvement factors are calculated corresponding to the experimental results. This validates the accuracy of the test results.

6 FOR CLAY

Using the clay properties of Table 2 analysis was done in Plaxis 2D for circular footing of diameter D=15cm, without skirt and with vertical skirt at two sides. The analysis is done on six skirt depths viz; D_S = 0.5B, 1B, 1.5B, 2B, 2.5B, 3B for 15cm dia. footing The modelling and results obtained from PLAXIS 2D for one typical case of 15cm diameter without skirt and with 0.5B skirt depths is presented in Fig 4 and Fig 5.

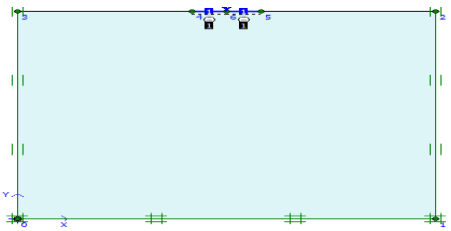

Fig.4. Geometry model in plaxis 2D® for 15cm circular footing without skirt.

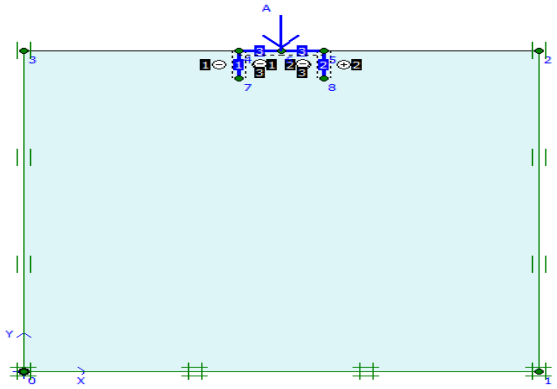

Fig.5. Geometry model in plaxis 2D® for 15cm circular footing with skirt.

6.1 Model skirted footing with D_1=15cm

Fig. 6. shows typical pressure-displacement responses of footing of diameter, D_1=15cm without skirt and with skirt for six skirt depths (i.e; D_S = 0.5B, 1B, 1.5B, 2B, 2.5B and 3B) on log-log plot respectively. As per IS 1888:1982 when well defined yield point is not observed, for such cases, plotting the settlements along abscissa and corresponding load intensities as ordinates in log-log plot, the points are joined together and two straight lines are obtained. The intersection of the two lines is considered as yield value. Thus, the ultimate bearing capacity values obtained from the log-log plot are tabulated in Table 6.

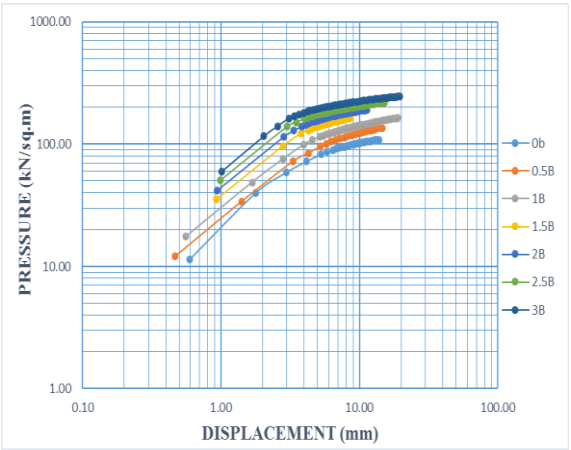

Fig.6. Log-Log plot for pressure-displacement curve of 15cm dia circular footing without skirt and with six different skirt depths

6.2 Important outcome

Table 6 shows the ultimate bearing capacity and improvement factors from graph.

Table 6. Ultimate bearing capacities and improvement factors (IF) from graph

Serial no.	Footing diameter (m)	D_S/B	Bearing capacity (kN/sq.m)	IF
1	0.15	0	39.75	1
2	0.15	0.5	72.56	1.83
3	0.15	1	99.12	2.5
4	0.15	1.5	121.97	3.1
5	0.15	2	128.91	3.24
6	0.15	2.5	139.60	3.51
7	0.15	3	162.52	4.1

7 CONCLUSION

This paper investigates the influence of lateral confinement with skirts on the bearing capacity of circular footing on locally available Kanaighat sand (loose sand) and clay. Based on the experimental study and numerical study the following conclusions may be drawn.

1) A structural skirt increases the bearing capacity of soil. For skirt-depth ratio consideration, maximum bearing capacity improvement factor obtained is 4.00 for skirt-depth ratio of 1. For skirt-depth ratio of 0.5, bearing capacity improvement factor is 2.67.
2) For skirt-diameter ratio consideration, maximum bearing capacity improvement factor obtained is 2.67 for skirt-diameter ratio of 1, 1.67 for skirt-diameter ratio of 1.5 and 1.33 for skirt-diameter of 1.67.
3) Bearing capacity is found to be maximum for a skirt-depth ratio of 1 and skirt-diameter ratio of 1.
4) For the same skirt-depth ratio i.e. 1, the ultimate bearing capacity of clay is observed 2.5. this means structural skirts shows best results on cohesionless soil.

REFERENCES

1) Al-Aghbari, M.Y. and Mohamedzein (2006) Y.E.A., Improving the Performance of Circular Foundations, *Ground Improvement*, 10(3), 125-132.
2) Basheeruddin, M. and Narayan, A. (2016) Detail Study on the Load Carrying Capacity of Shallow Foundation Resting over Geogrid Reinforced Sand, *IJASTEMS-ISSN: 2454-356X*, Volume.2,Issue.11.
3) Mahmoud, M.A. and Abdrabbo, F.M. (1989) Bearing Capacity Tests on Strip Footing Resting on Reinforced Sand Subgrades, *Canadian Geotechnical Journal*, 26(1), 154-159.
4) IS: 1888-1982, Method of Load test on Soil, *Bureau of Indian Standards*, New Delhi, India.

Effect of surcharge on multi-tier reinforced soil retaining walls

Kumari, S. [1], Bhattacharjee, A.[2]

[1] PG Student, Department of Civil Engineering, Jorhat Engineering College, Jorhat – 785007, India.
[2] Professor, Department of Civil Engineering, Jorhat Engineering College, Jorhat – 785007, India.

ABSTRACT

Geosynthetics are used as reinforcement in earth retaining structures which are commonly known as reinforced soil retaining walls. Reinforced soil retaining walls are both economically and technically very advantageous over their conventional counterparts, especially under poor soil conditions and when there are property line limitations. With the development of economy and expansion of cities in India, land resources for construction are becoming scare. When the height of reinforced soil retaining wall is increased, these types of walls are built in multi-tier configuration for variety of reasons such as aesthetic, stability etc. This paper presents the results of investigation on the behaviour of reinforced soil retaining walls in tired configurations using the finite element method of analysis. 2D finite element analyses are performed on tired walls with three offset distance. Cases with equivalent surcharge as suggested by the NCMA design guideline are additionally analyzed in an attempt to confirm the appropriateness of the equivalent surcharge model adopted by NCMA. Deformations and stress characteristics of a tiered wall with small offset distance suggest that interaction between the upper and lower walls significantly affects the performance of lower as well as upper walls, suggesting that the upper walls should be designed with due consideration of interaction.

Keywords: geosynthetics, reinforced soil, multi-tier retaining walls, finite element analysis

1. INTRODUCTION

Geosynthetic-reinforced soil walls in a tiered configuration are acceptable alternatives to conventional retaining wall systems because of several benefits such as cost, stability and construction constraints, and aesthetics. A tiered wall is a transitional structure between a single wall and slope (Fig.1) that can reduce construction costs and increase system stability compared with a single wall. Because of its configuration, the tiers interact and mutually affect each other. The upper and lower tiers interact through the equivalent surcharge from the upper tier acting on the lower tier, and the vertical and lateral deformation of the lower tier influences the behavior of the upper tier. Surcharge loads acting on retaining wall are additional vertical loads above the top of the wall. It can be either dead loads for example sloping backfill above the wall height or live load which could result from highway or parking lot, paving or adjacent footing. As per NCMA design approach upper tier is designed as if it were a single wall without taking into consideration of the possible interaction between the upper and the lower tiers. But in actual practice deformations and stress characteristics of a tiered wall with small offset distance suggest that interaction between the upper and lower walls significantly affects the performance of lower as well as upper walls, suggesting that the upper walls should be designed with due consideration of interaction.

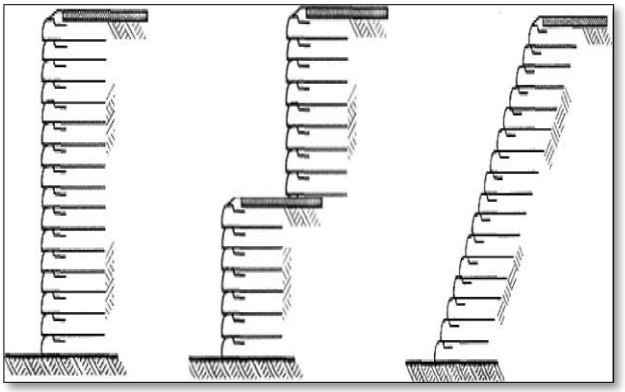

Fig. 1 GRS structures with various configurations.

2. DESIGN APPROACHS

2.1 NCMA design approach

The NCMA design approach (Collin 1997) basically replaces the upper tier with an equivalent surcharge of which its magnitude is determined according to the offset distance D (Fig. 2). External and internal stability calculations for the lower tier are performed assuming the lower tier being a single wall under the equivalent surcharge. The upper tier is designed as if it were a single wall without taking into consideration of the possible interaction between the upper and the lower tiers. As for a single wall, the local stability calculations

for the connection failure, local overturning, and internal sliding are required to be checked for both tiers. Details of the design procedure are available elsewhere (Collin 1997).

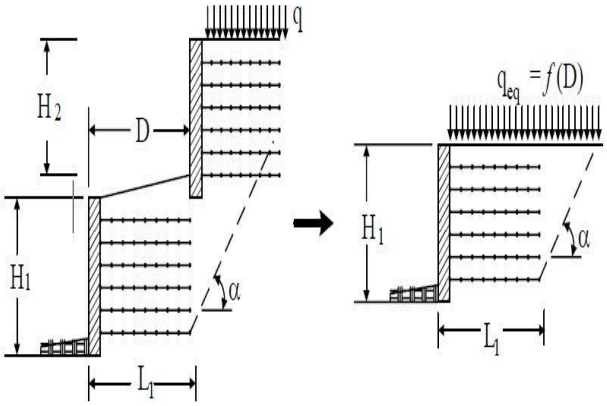

Fig. 2 Equivalent surcharge model (NCMA)

2.2 FHWA design approach

The FHWA design guideline requires determining the lower and the upper reinforcement length L_1 and L_2, respectively, that satisfy external stability requirements based on the offset distance D together with the lower and upper tier height, H_1 and H_2 , respectively, as follows (Fig. 3):

- D⟩H_1 tan (90 −φ) ⇒ No interaction. Each tier is independently designed.
- D ≤ 1/20 (H_1 + H_2) ⇒ Design for a single wall with a height of H = H_1+H_2.
- D⟩ 1/20 (H_1 + H_2) ⇒ For lower tier: $L_1 \geq 0.6H_1$, For upper tier: $L_2 \geq 0.7H_2$

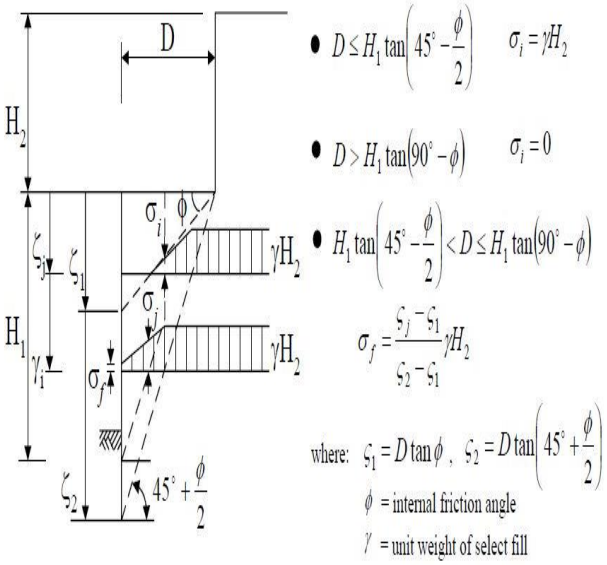

Fig.3 Calculation model for vertical stress increase due to upper tier (FHWA)

3. NUMERICAL APPROACH

In recent years, numerical simulation has been a great development with the costs reduction and speed increases of the computational systems. With these improvements, the mathematical algorithms are able to work properly with more realistic problems. A two-dimensional finite element program PLAXIS 2D is used to perform the numerical modeling and analysis of geo-synthetic-reinforced soil retaining wall. To compare the effect of surcharge with tiered walls we replaced the 1st tier from two tiered wall with equivalent surcharge load of 1st tier. Geometry of tired wall and surcharged wall are shown in (Fig. 4).

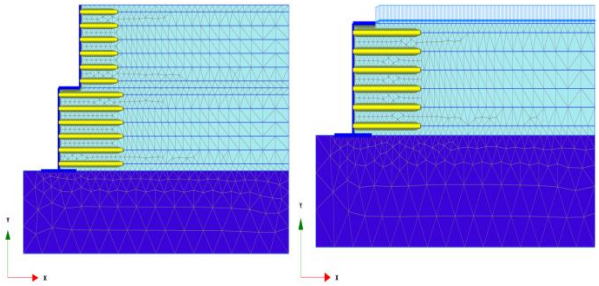

Fig. 4 Geometry of two-tiered wall and equivalent surcharge of upper tier

The foundation soil has the same properties as the backfill soil. Mohr–Coulomb model is used to represent the soil. The foundation and concrete facing panels are modeled as linear elastic material. The geogrid reinforcements are modeled as linear elastic material. Reinforcements are models as geogrid elements with its axial stiffness (EA).The interface can be described with an elasto-plastic mode to simulate the interaction. The transfer of stress is decided by the strength of the interface, which equals to the strength of surrounding soil multiplied by the friction coefficient R_{inter} between soil and the interface element.

Table1. Material properties of the FE model

Properties	Backfill	EPS board	Facing wall	Geogrid
Material model	Mohr-Coulomb	Linear elastic	Linear elastic	Linear elastic
Elastic Modulus (kN/m^2)	2E5	2E6	2E6	
Mass-density (kN/m^3)	14.3	1	23	
Poisson's ratio (v)	0.33	0.2	0.2	
Angle of friction (°)	38			
EA [kN/m]				680

4. RESULTS AND DISCUSSIONS

4.1 Wall deformation

The effect of offset distances on the performance of lower and upper tiers is examined using the wall deformations of tiered walls and walls with equivalent surcharge loads. Fig. 5 shows the comparison of horizontal displacement of facing wall for different tier offset. The displacement is very high for surcharged wall at the top of wall compared to tiered walls for different offsets. The wall displacement in tiered configuration at the top is found to be 11.46 mm and 11.14 mm for 1.2 m offset, and 2.4 m offset wall respectively but in equivalent surcharge walls the displacement was quite high i.e. 106.26 mm, and 74.08 mm for 1.2 m offset, and 2.4 m offset respectively.

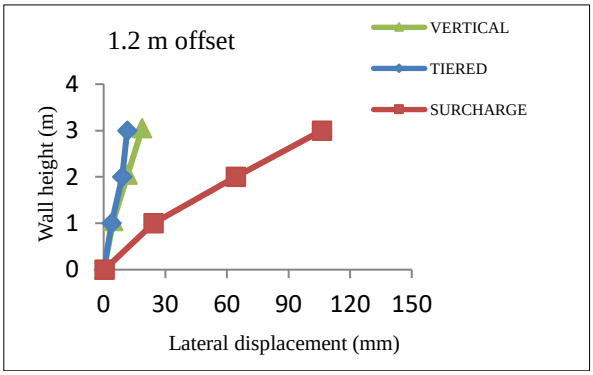

Fig. 5 Horizontal displacements of tiered walls and surcharge walls for 1.2 m offsets.

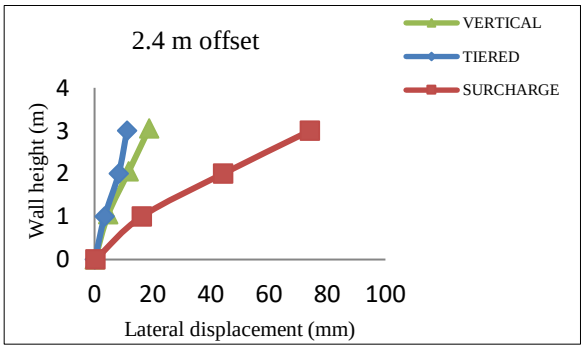

Fig. 5 Horizontal displacements of tiered walls and surcharge walls for 1.2 m offsets.

4.2 Lateral pressure

The lateral pressure distribution shows a typical earth pressure distribution on retaining walls. (Fig. 6) shows the comparison of lateral soil pressure distribution exerted by the soil at the face of the wall for different tier offset. The maximum pressure is near the base of the wall and reduces with the increasing height, become minimum at the top of the wall. The surcharge walls shows maximum lateral stresses compared to tired wall and vertical wall. This indicates that in tired walls there is an interaction between the tiers which reduces the lateral stress compared to vertical wall and surcharge walls.

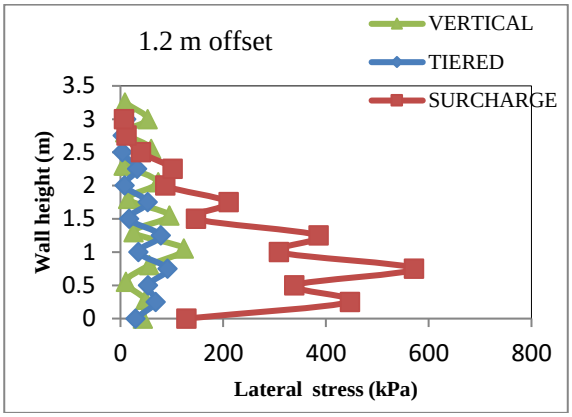

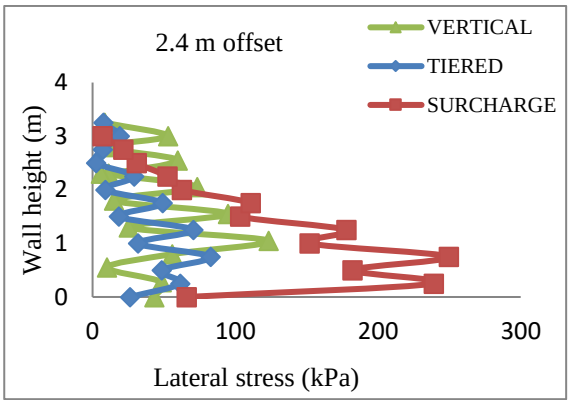

Fig. 6 Comparison of lateral soil pressure on the face of the wall for different tier offset.

The walls are studied for surcharge effect of upper tier. It is found that, the upper wall does not act as a surcharge on the lower tier, which increases the deformation near the mid height of the wall. With increasing number of tiers, the lateral displacement decreases which indicated that there is a mutual interaction between the two tiers. The deformations of bottom tier of multi tiered wall are less than the deformations of wall of same height with equivalent surcharge (i.e surcharge equal to the weight of upper tier). The upper tiers are not acting as surcharge on bottom tier.

5. CONCLUSIONS

The effect of offset distances on the performance of lower and upper tiers is examined using the wall deformations of tiered walls and walls with equivalent surcharge loads. The displacement is very high for surcharged wall at the top of wall compared to tiered walls for different offsets. The maximum pressure is near the base of the wall and reduces with the increasing height, become minimum at the top of the wall. The surcharge walls shows maximum lateral

stresses compared to tired wall and vertical wall. This indicates that in tired walls there is an interaction between the tiers which reduces the lateral stress compared to vertical wall and surcharge walls. Deformations and stress characteristics of a tiered wall with small offset distance suggest that interaction between the upper and lower walls significantly affects the performance of lower as well as upper walls, suggesting that the upper walls should be designed with due consideration of interaction.

6. REFERENCES

1) AASHTO (1998). Standard specifications for highway bridges, American Association of State Highway and Transportation Officials, Washington, DC.

2) Bathurst, R.J. and Hatami, K. (2006). Parametric analysis of reinforced soil walls with different height and reinforcement stiffness. *Geosynthetics*, ISBN 9059660447, pp. 1343- 1346.

3) Bergado, D.T. and Teerawattanasuk, C. (2007). 2D and 3D numerical simulations of reinforced embankments on soft ground. *Geotextiles and Geomembranes*, 26 (2008) 39– 55, pp. 39-55.

4) FHWA (2001). *Mechanically Stabilized Earth Walls and Reinforced Soil Slopes Design and Construction Guidelines*. Publication No. FHWA-NHI-00-043, US Department of Federal Highway Administration (FHWA).

5) FHWA (2010). *Mechanically Stabilized Earth Walls and Reinforced Soil Slopes Design and Construction Guidelines*, Vol. I & II. Publication No. FHWA-NHI-10-024, US Department of Federal Highway Administration (FHWA).

6) NCMA (1997). Design Manual for Segmental Retaining Walls. National Concrete Masonry Association, Collin, J., Editor, Second Edition, Herndon, Virginia, USA.

7) NCMA (1998). Segmental Retaining Walls Seismic Design Manual. National Concrete Masonry Association, Bathurst, R.J., Editor, First Edition, Herndon, Virginia, USA.

Study of piled raft foundation on layered soil

Nath, U.K. [1], Patowary, B.N. [2]

[1] Associate Professor, Department of Civil Engineering, Assam Engineering College, Jalukbari, Guwahati-781013, India.
[2] Ph.D Student, Department of Civil Engineering, Guwahati University, Jalukbari, Guwahati-781013, Assam, India.

ABSTRACT

In recent years, there have been an increasing number of structures using piled-raft foundation to reduce the overall and differential settlement. The concept of piled raft foundation leads to economical design. In this paper a numerical model was developed using the software PLAXIS 3D to analyze piled-raft foundations. This model account for the effect of interaction factors among pile, raft and soil by employing very accurate element, namely, 15-node triangular element. The performance of piled raft foundation on layered soil with varied stiffness is studied. Performance on swampy areas that are recently filled are also included and compared with the same loading after soil replacement. Also, the effect of lateral load on piled raft foundation is also studied.

Keywords: piled raft, stiffness, layered soil

1. INTRODUCTION

Piled-raft foundations, known also as piled rafts, are a combination of a shallow foundation (raft) and a deep foundation (pile group). In this type of foundations, the role of the raft is to provide the required bearing capacity and the piles are used mainly as settlement reducers but can also contribute to the bearing capacity. In general, the raft alone can provide the required bearing capacity but it cannot control the settlement. Therefore, the piles are crucial to reduce the settlement of the raft. Due to combining raft and piles in one system, piled-raft foundations are regarded as very complex systems. The complexity of this type of foundations is caused by the presence of many interaction factors involved in the system such as pile-to-soil, pile-to-pile, raft-to-soil and raft-to-pile interactions.

2. PARAMETRIC STUDY

In this study a 16 m x 16 m raft with massive circular piles of varied diameter were analyzed using a software finite element package for soil and foundation. a plane strain finite element model was used to model the piled raft foundation. the raft and piles were assumed to be linearly elastic. the mohr-coulomb yield criterion was used to represent the soil type as elastic-perfectly plastic material. a single layer homogenous isotropic soil with water table at a varied depth ground level was assumed for the study. here a drained condition was assumed and total vertical displacement was calculated using plastic calculations. The soil was discretized as 15 noded triangular elements. The piles and raft were modeled using a plate element. The side skin friction in piles was taken into account by applying interface reduction factor R_{inter}.

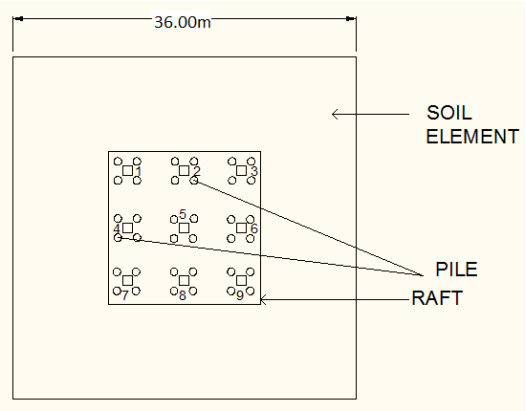

Fig. 1 Plan of Piled Raft Foundation

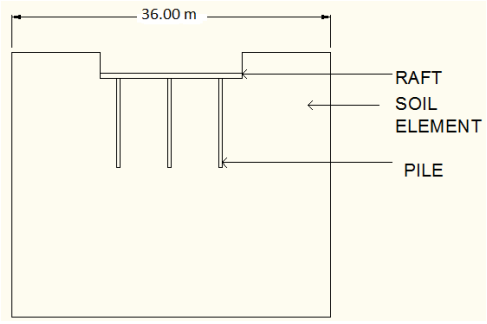

Fig. 2 Cross-section of Piled Raft Foundation

Sub-soil thickness is considered up-to a depth of 30m from ground surface for both the soil types. A non-uniform vertical loading in the form of concentrated column loads has been imposed on the piled raft.

The table 1 below shows the cohesion and angle of internal friction of layered soil that is used in the study.

Table 1: C and ϕ values of layered soil

Depth (m)	Cohesion(C) (kg/cm^2)	Angle of Internal Friction 'ϕ' (Degrees)
3.5	0.24	10
5.5	0.41	8
8.0	0.32	10
10.0	0.29	12
12.5	0.23	14

The table 2 below describes the type and properties of materials being used in the study.

Table 2: Soil Properties used in the study

Material	Bored Pile	Raft (Floor)
Material model	Linear elastic	Linear isotropic
Material type	Non-porous	Non-porous
Stiffness (E_{ref})	2.920E+07 kN/m^2	1.000E+07 kN/m^2
Poisson's ratio (υ)	0.30	0.20
Unit weight (Υ_{sat})	24 kN/m^3	24 kN/m^3
Permeability	0 m/day	0 m/day

The table 3 below describes the properties of soil-pile interface and soil-raft interface.

Table 3: Properties of the soil-pile and soil-raft interface

Soil type	Sand
R_{inter}	0.7
Angle of friction (ϕ_i)	25.6^0
Cohesion (C_i)	1.0 kN/m^2

The table 4 below describes the dimensions of the materials being used in the study.

Table 4: Dimensions used in the study

Material	Pile	Raft
Diameter, D	0.4m	-
Thickness, d	-	0.4m
Length, L	10m	-
Number, N	0, 36	-
Spacing, S	3D	-
S/D ratio	10	

The table 5 below describes the type and properties of soil available from site.

Table 5: Soil Properties used in the study

Depth (m)	Sp. Gravity (G)	In-Situ Water Content w(%)	Bulk Density (Υ) (gm/cm^3)	Dry Density (Υ_d) (gm/cm^3)	Liquid Limit (w_L) %	Plastic Limit (w_P) %
3.5	2.62	30.82	1.96	1.5	38.5	25.79
5.5	2.63	29.41	2.03	1.57	36.5	23.86
8	2.63	29.3	2.02	1.56	35.9	23.35
10	2.63	28.71	2.04	1.58	NP	NP
12.5	2.63	28.59	2.07	1.61	NP	NP

3. INFLUENCE OF PILED RAFT

The images of different models of piled raft foundation with varied parameters along with their generated mesh are shown below. Various numbers of models are created to check the effect of raft and piled raft on settlement criteria.

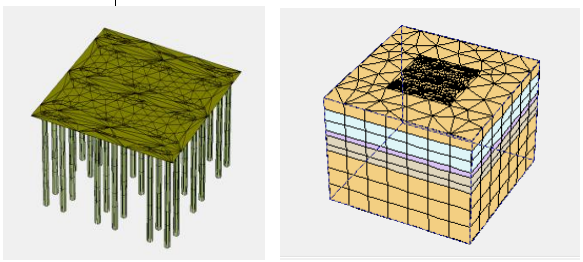

Fig. 3. Model of piled raft with generated 3D mesh (N_P=36, L_P= 10m, D_P= 400 mm, T_r = 400 mm, W.T= 4.5m)

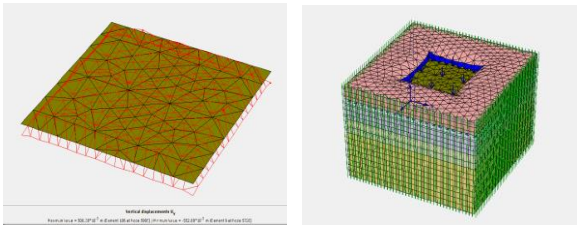

Fig. 4. Model of raft with generated 3D mesh (T_r = 400 mm, W.T= 4.5m)

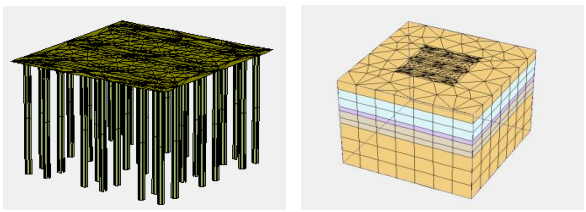

Fig.5. Model of Piled Raft with Generated 3D mesh (Lateral Load) (N_p=36, L_P= 10m, D_P= 400 mm, T_r = 400 mm, W.T= 4.5m)

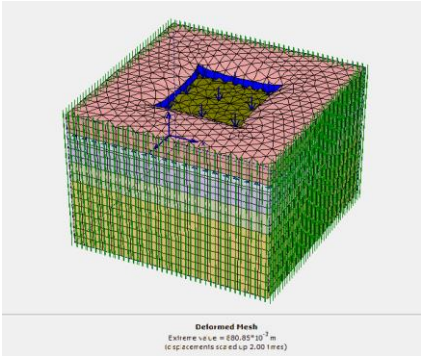

Fig.6. 3D Mesh of Soil and Piled Raft Subjected to Lateral Load

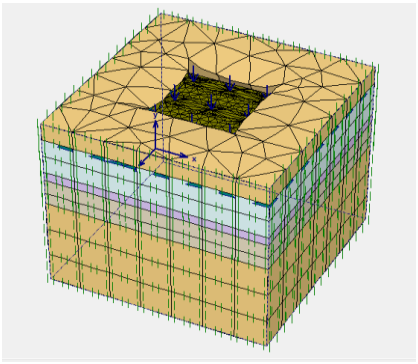

Fig.7. 3D Mesh of Soil and Piled Raft after Soil Replacement of Top Layer

3.1 Effect of Piled Raft on Total Settlement

The total vertical load is 4500kN which is equally distributed on nine equally spaced columns with 500kN vertical load each. Figure 8 shows the variation of total settlement of the superstructure as well as foundation before introduction of pile (i.e. only raft) and after introduction of pile (i.e. Piled Raft) on layered soil.

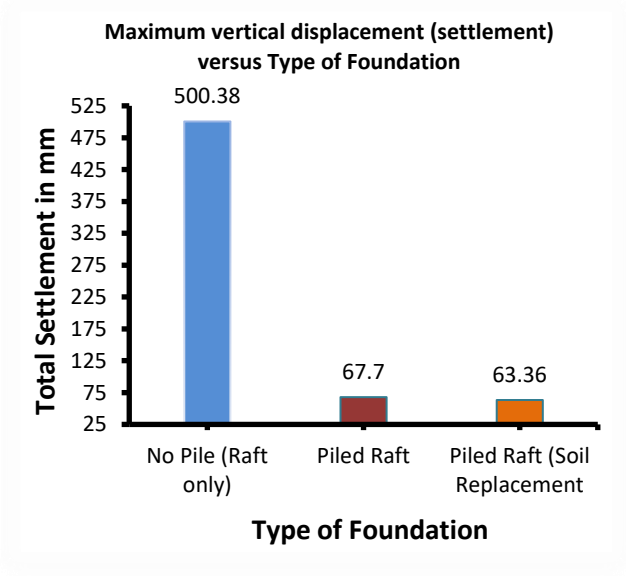

Fig. 8. Variation of Total Settlement with Foundation Type

The maximum settlement (total vertical settlement) of the foundation decreases with the introduction of piled raft. Introduction of piled raft foundation in place of simple raft shows a decrease in total settlement up-to 86.6%.

3.2 Effect of Piled Raft subjected to lateral load on Total Settlement

A lateral load of 5kN per column in both X and Y-direction is introduced, along with the total vertical load of 4500kN. Figure 9 shows the variation of total settlement of the superstructure as well as foundation subjected to lateral load, before introduction of pile (i.e. only raft) and after introduction of pile (i.e. Piled Raft) on layered soil.

The maximum settlement (total vertical settlement) of the foundation decreases with the introduction of piled raft in case of foundation subjected to lateral load also. Introduction of piled raft foundation in place of simple raft shows a decrease in total settlement up-to 82.75%.

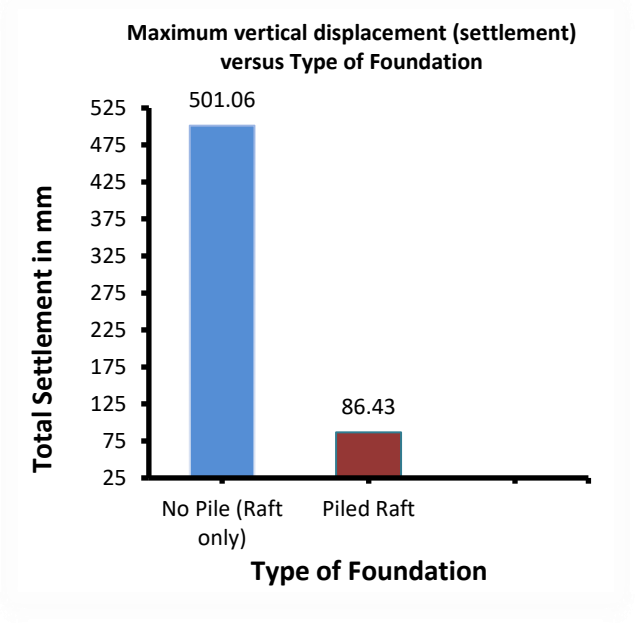

Fig. 9. Variation of total settlement with Foundation type Subjected to Lateral Load

Figure 10 shows the variation of total horizontal displacement of the superstructure as well as foundation subjected to lateral load, before introduction of pile (i.e. only raft) and after introduction of pile (i.e. Piled Raft) on layered soil.

The maximum horizontal displacement of the foundation decreases with the introduction of piled raft in case of foundation subjected to lateral load. Also, introduction of piled raft foundation in place of simple raft shows a decrease in total settlement up-to 73.66%.

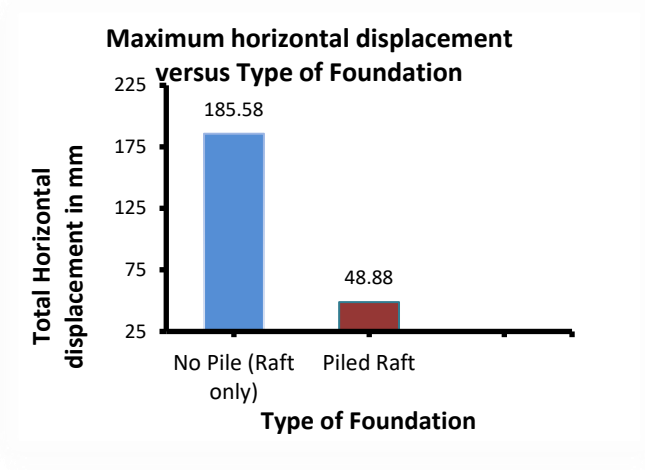

Fig. 10. Variation of Total Settlement with Foundation Type

Figure 11 shows the variation of total horizontal displacement of the superstructure as well as foundation subjected to lateral load, before introduction of pile (i.e. only raft) and after introduction of pile (i.e. Piled Raft) on layered soil.

The maximum settlement (total vertical settlement) of the foundation decreases with the replacement of top layer of newly filled up soil with soil of good bearing capacity, but the outcome is not satisfactory in terms of economy. Replacement of soil by soil replacement method shows a decrease in total settlement up-to 6.41%. Since the raft level is at 3m below the ground surface and the newly filled loose soil of top layer is up-to a depth of 4m below the ground surface, it is possible that soil replacement will have less effect on the settlement. Also, soil replacement below the foundation will be un-economical,as piled-raft foundation may be termed as the alternate provision of soil replacement.

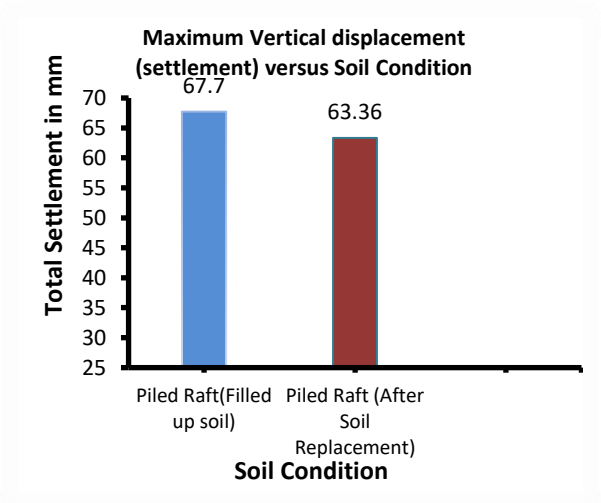

Fig. 11. Variation of Total Settlement with Soil Condition

4. CONCLUSIONS

1) Introduction of piles to raft (i.e. piled raft of 36 piles) in layered soil with varied soil properties can reduce the total settlement in case of vertical loading.
2) In case of vertical as well as lateral load, piled-raft (36 piles) in layered soil with varied soil properties can reduce the total settlement up-to eighty percent.
3) For foundations subjected to lateral load, piled raft reduces the horizontal deflection up-to seventy percent.
4) Replacement of soil up to raft bottom does not affect much on the settlement criteria.

REFERENCES

1) Burland, J.B. (1995), Piles as Settlement Reducers, *Keynote Address, 18th Italian Congress on Soil Mechanics*, Pavia, Italy.
2) Comodromos, E. M., Papadopoullou, M. C. and Rentzeperis, I. K. (2009), Pile Foundation Analysis and Design using Experimental Data and 3-D Numerical Analysis, *Computers and Geotechnics.* Vol. 36. pp. 819-836.
3) Desai, C. S. (1974), Numerical Design Analysis for Piles in Sands, *Jl. Geot. Engg. Div*., ASCE, Vol. 100, No.G26, pp. 613-635.
4) El-Mossallamy, Y. (2002), Innovative Application of Piled Raft Foundation in stiff and soft subsoil, *Deep Foundations* 2002, ASCE, pp. 426-440.
5) El-Mossallamy, Y., Lutz, B. and Duerrwang, R. (2009), Special Aspects Related to the Behavior of Piled Raft Foundation, *17th the International Conference on Soil mechanics & Geotechnical Engineering ICSMGE*, Alexandria, Egypt. pp. 1366-1369.
6) Fioravante, V., Giretti, D. and Jamiolkowski, M. (2008), Physical Modeling of Raft on Settlement Reducing Piles, *From Research to Practice in Geotechnical Engineering Congress* 2008. ASCE, pp. 206-229.
7) Katzenbach, R., Schmitt, A. and Turek, J. (2005), Assessing Settlement of High-Rise Structures by 3D Simulations, *Computer-Aided Civil and Infrastructure Engineering.* Vol. 20. pp. 221-229.
8) Kuwabara, F. (1989), An Elastic Analysis for Piled Raft Foundations in a Homogeneous Soil, *Soil and Foundations*. Japanese Society of Soil Mechanics and Foundation Engineering. Vol. 29. No. 1. pp. 82-92.
9) Mendonca, A.V. and Paiva, J.B. (2003), An Elasto-static FEM/BEM Analysis of Vertically Loaded Raft and Piled Raft Foundations, *Engineering Analysis with Boundary Elements*. Vol.27. pp. 919-933.
10) Ottaviani, M. (1975), Three-dimensional Finite Element Analysis of Vertically Loaded Pile Groups, *Geotechnique*, Vol. 25, No. 2, pp. 159-174
11) Patowary, B.N. and Nath, U. K., (2015), "Parametric Study of Piled Raft Foundation" *Indian Geotechnical Conference (50th IGC 2015)*, Pune.

Improvement of Brahmaputra bed silt using bentonite and cement

Jessia, M.[1], and Bhattacharjee, A.[2]

[1] PG Student, Department of Civil Engineering, Jorhat Engineering College, Jorhat-785007, India.
[2] Associate Professor, Department of Civil Engineering, Jorhat Engineering College, Jorhat-785007, India.

ABSTRACT

Siltation is a major cause of flood problems in the river Brahmaputra every year. Dredging of this bed silt from the river bed and utilizing it in various constructional activities can tackle this heavy flood problems. The present study is intended to study the feasibility of this bed silt to be used as a constructional material for road embankment. But due to lack of stability and high permeable properties, it cannot be used alone for embankment construction. However, use of a suitable admixture to improve its engineering properties is found to be the possible solution for embankment construction. Use of bentonite alone as an admixture causes swelling problems in the soil as its content is increased (Jessia, M. and Bhattacharjee, A. 2018). Hence, the original soil is mixed with 10%,15% and 20% bentonite with further addition of 2% cement with each of the bentonite added samples. The permeability reduced appreciably after addition of this combined mix of bentonite+cement. From all the detailed study, 10%bentonite+2%cement mix is found to be the economic mix as this content satisfies all the stability criteria for embankment construction.

Keywords: Brahmaputra bed silt, Bentonite, cement, Shear Parameter, Permeability, Swell Index

1. INTRODUCTION

Assam with its mighty river Brahmaputra is known for its heavy silting problem causing rise in its river bed level from time to time. This considerably reduced the water carrying capacity of the channel and causes devastating floods and erosion on both the banks of the river in the monsoon period every year. In a fight against this, the government of Assam has proposed to dredge out the bed silt of the river Brahmaputra and use it as constructional alternative for different projects. This material is cheap and naturally available which makes it attractive towards use for different useful purposes such as for construction of embankment, filling material etc. Use of this material can solve the problem of flooding and erosion to some extent. As its demand will increase for use as a constructional material, more and more bed silt will be dredged out of the river bed thus increasing the water carrying capacity of the channel. However, due to the poor geotechnical properties of the soil, it cannot be used directly for embankment construction (Medhi and Deka 2017). The Brahmaputra silt collected is found to be highly permeable and unstable to be used as embankment construction. This high permeability can lead to the formation of raincuts and breaches during the rainy season, leading to its failure. Hence, use of a suitable admixture is the possible solution to stabilise the soil for embankment construction. The use of combined mix of bentonite and cement is found to be suitable for improving its properties. Mixing of bentonite alone as an admixture causes excess swelling problems in the soil as its content is increased (Jessia, M. and Bhattacharjee, A. 2018). Hence, small amount of cement is used to prevent the swelling condition.

The main objective of the present work is to study the suitability of the Brahmaputra bed material to be used for embankment construction.

2 MATERIALS AND METHODOLOGY

The materials used for the present investigation work is Brahmaputra bed silt, bentonite and cement. The Brahmaputra bed silt used is collected from the Nimati ghat location of Jorhat district. The soil is classified as SM(Silty sand) according to Indian Standard Soil Classification System. Various laboratory tests were conducted such as Atterberg limits, Proctor compaction, Direct shear, Falling head permeability, Free swelling index and CBR test. Table 1 shows the geotechnical properties of the bed silt.

Bentonite is a clay material with high amounts of montmorillionite with some illite, quartz and feldspar. It is known for its high swelling and shrinkage potential. Bentonite has high water retention capacity because of their small grain size with large surface contact area. Moreover, its use as

an admixture with sand appears to be a good option as its swelling property seals the voids of the sand thus lowering the hydraulic conductivity. Basically, two types of bentonite are available- swelling type (sodium bentonite) and non swelling type (calcium bentonite). The bentonite used for the study is sodium bentonite and is obtained from the local market in powdered form.

Cement is a fine powder material that has excellent binding capacity. It mainly consists of silica content like C_2S and C_3S. Ordinary Portland cement is used here for the study which is also obtained from the local market. Cement is used as an additive to increase the strength of the sand bentonite mixture, and also reduce the hydraulic conductivity and possibility of crack formation. It further stabilizes the soil by reducing the swelling effect caused by bentonite.

Table 1. Geotechnical properties of the bed silt

Properties	Values
Classification of soil	SM
Plastic limit	NP
Liquid limit	27%
Plasticity Index	NP
Optimum Moisture content(OMC)	16%
Maximum Dry Density (MDD), g/cc	1.57g/cc
Direct shear cohesion, kPa	2
Direct shear of Internal Friction	22º
Coefficient of Permeability, cm/s	3.49×10^{-4} cm/s
California Bearing Ratio,%	3.41%
Free Swelling Index,%	0%

3 METHODOLOGY

In the present study, 10%, 15% and 20% bentonite is mixed with the Brahmaputra bed silt with further addition of 2% cement with each of the bentonite added samples. Proctor Compaction test for optimum moisture content,OMC and maximum dry density, MDD, Direct shear test for shear parameters, Falling head permeability test for permeability, CBR test for strength and Free swelling index tests were conducted to evaluate the engineering properties of the admixed soil. The detailed test programme is presented in table 2.

4 RESULTS AND DISCUSSIONS

4.1 Effect on Compaction characteristics

Proctor compaction tests were conducted to evaluate the optimum moisture content and maximum dry density as per IS: 2720 (Part 8) – 1983. After 10%bentonite+2%cement, 15%bentonite+2%cement and 20%bentonite+2%cement is mixed with the original soil, both OMC and MDD increased. The evaluated values of OMC and MDD is shown in table 3. The OMC of the original soil was found to be 16% which increased to 19% at 20%bentonite+2%cement addition as shown in figure 1. This increase in OMC is attributed to the fine nature of the admixtures which require more water to achieve MDD.

The Maximum dry density of the original soil was found to be 1.57g/cc which increased upto 1.722g/cc at 15%bentonite+2%cement addition after which it showed a decreasing trend as shown in the figure 2. The increase in MDD is because of the higher specific gravity of cement and fine nature of the bentonite particles filling in the voids of the sand.

Table 2. Detail Tests Programmes

TESTS	MIX
Compaction test California Bearing Ratio	Soil + 10% Bentonite + 2% cement
Direct shear Falling head permeability	Soil + 15% Bentonite + 2% Cement
Free Swelling Index	Soil + 20% Bentonite + 2% Cement

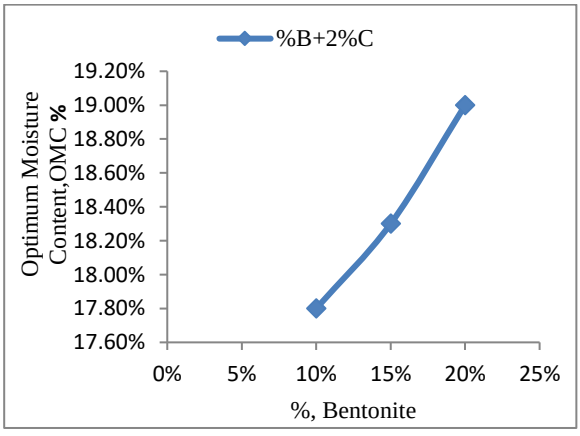

Fig 1: Variation of OMC with admixture content

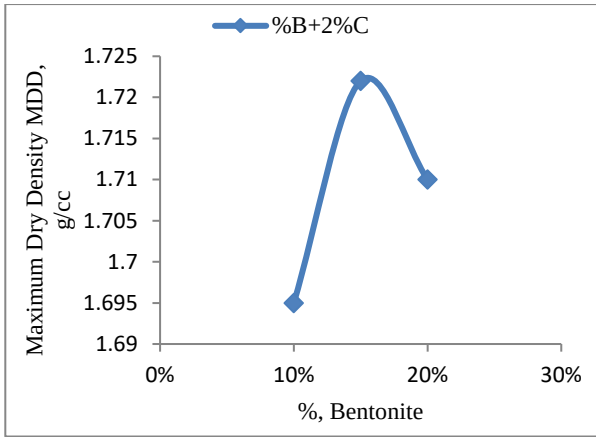

Fig 2: Variation of MDD with admixture content

Table 3: OMC and MDD values with admixture content

Mix	OMC,%	MDD,g/cc
Untreated soil	16%	1.57
S+10%B+2%C	17.8%	1.695
S+15%B+2%C	18.3%	1.722
S+20%B+2%C	19%	1.71

4.2 Effect on shear parameters

Direct shear test is conducted on all the admixed samples to evaluate the shear parameters as per IS:2720(Part 13)-1986. The samples are prepared at the OMC and MDD of their respective soil+bentonite+2%cement mixtures. The cohesion of the original soil was found to be 2kPa which increases to 19kPa, 26kPa and 30kPa for 10%bentonite+2%cement, 15%bentonite+2%cement and 20%bentonite+2%cement as shown in the figure 3.

The angle of internal friction showed a decreasing trend after addition of combined bentonite+cement mix as shown in the figure 4.

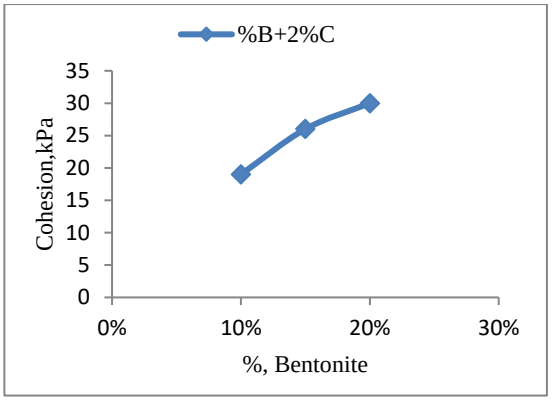

Fig 3: Variation of Cohesion with admixture content

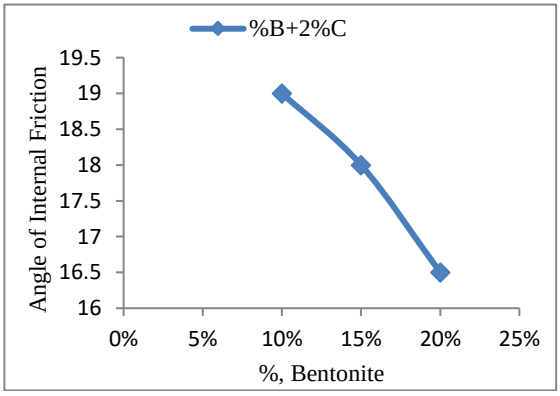

Fig 4: Variation of Angle of Internal Friction with Admixture content.

4.3 Effect on permeability characteristics

The coefficient of permeability was determined by conducting Falling head permeability test as per IS: 2720(Part15)-1986. The coefficient of the original soil was found to be 3.49×10^{-4} cm/s which means the soil is highly permeable which reduced appreciably after addition of bentonite+cement mix with the original soil as shown in figure 5. The variation of the permeability values of the three mixes are shown in table 4. This low permeability is mainly due to the high swelling potential and fineness of bentonite. Also addition of the 2% cement formed strong bonds between the soil particles, reducing the voids and reducing permeability.

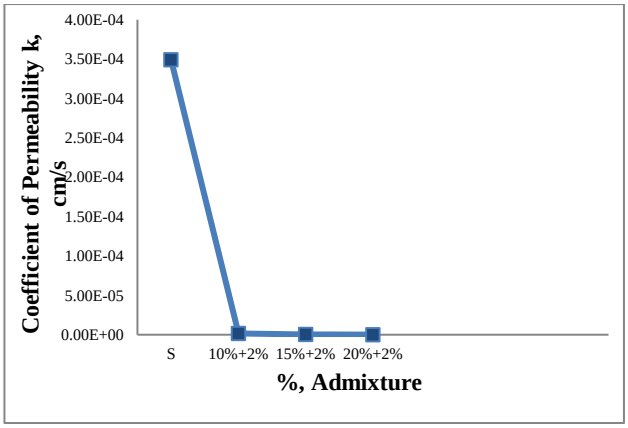

Fig 5: Variation of coefficient of Permeability with admixture content.

Table 4: Coefficient of permeability values for different admixture content.

% Admixture	Coefficient of permeability, cm/s
10%B+2%C	1.46×10^{-6}
15%B+2%C	1.5×10^{-7}
20%B+2%C	1.24×10^{-7}

4.4 Effect on California Bearing Ratio, CBR

California Bearing Ratio (Unsoaked) test is conducted on the bentonite+cement mixed samples as per IS:2720(Part16)-1987. All the samples were compacted at their respective OMC and MDD before carrying out the penetration test. The CBR is calculated for 2.5mm and 5mm penetrations. However, 5mm penetration CBR value is found to be greater than that of 2.5mm penetration. Hence, bearing ratio corresponding to 5mm penetration is taken as the design value. The CBR(unsoaked) of the untreated soil was found to be 3.41% which increased after being treated with bentonite+2%cement as shown in the figure6.The CBR increased to 4.90% at 20%bentonite+2%cement addition. This is because of the densification of the mix after addition of bentonite and cement. Also, this increase is because of the gradual formations of the cementitious compounds with the addition of cement with the soil samples. The evaluated CBR values are shown in table 5.

4.5 Effect on Free Swelling Index

Free swelling index was conducted according to IS: 2720 (Part 40) – 1970. 10%Bentonite+2%cement, 15%Bentonite+2%cement and 20%Bentonite+2%cement is mixed with the original swell and the admixed samples were kept for determination of free swell for 24 hours or more. The evaluated swell values is presented in table 6. The excess swelling effect caused due to bentonite addition is prevented with the addition of 2% cement. The free swell index of all the admixed samples were found to be under permissible value of 50% (NRRDA,2007) and is shown in figure 7. Addition of cement leads to a strong bonding between the soil particles, thus preventing swelling.

Table 5: CBR values with admixture content

Mix	CBR,%
Untreated soil	3.41
S+10%B+2%C	4.80
S+15%B+2%C	4.85
S+20%B+2%C	4.90

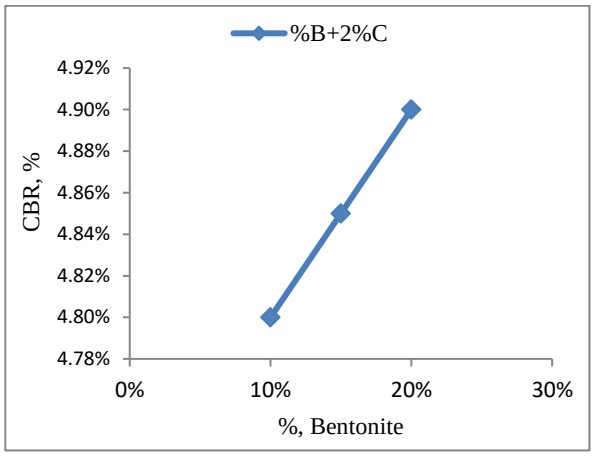

Fig 6: Variation of CBR with admixture content

Table 6: Free swell Index values with admixture content

Mix	Free Swelling Index,%
S+10%B+2%C	6%
S+15%B+2%C	15%
S+20%B+2%C	22%

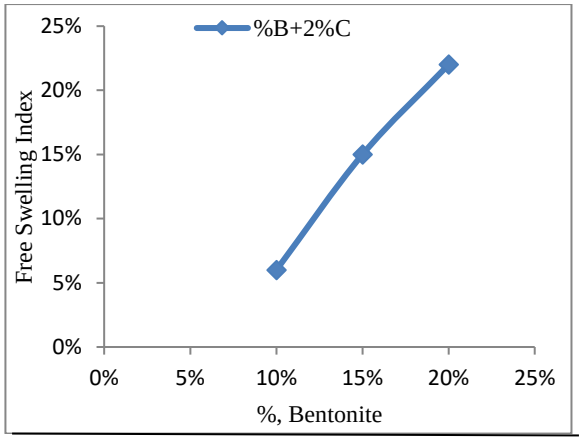

Fig 7: Variation of free swelling index with admixture content.

5 COST ANALYSIS

The embankment is considered as 2.66 m high; 15m wide at bottom and 5.5m wide at top (Deka K, 2017). The embankment consist of different material such as natural Brahmaputra bed material and Brahmaputra bed material treated with 10%bentonite+2%cement, 15%bentonite+2%cement and 20%bentonite+2%cement by weight. The basic rate of silt is considered as per APWD SOR (Building) 2013-2014; basic rate of cement is considered as per APWD SOR (Road) 2016-2017 and for bentonite market price is considered in the analysis. The cost analysis is performed per meter length of the embankment. The analysis is presented in figure 8. From the data calculated, 10%bentonite+2%cement is found to be the most economical mix to be used as admixture with Brahmaputra silt.

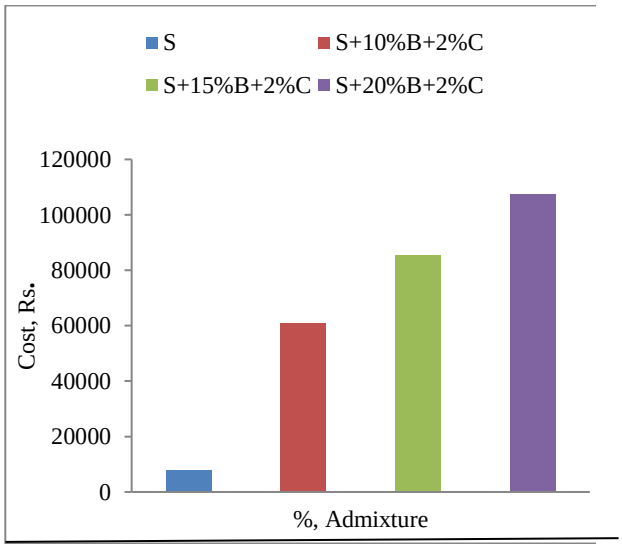

Fig 8: Cost Analysis of the materials used.

6 CONCLUSION

The suitability of the Brahmaputra bed silt mixed with the combined bentonite+cement mix is studied here. After conducting all the laboratory experiments, the following results are drawn.

a) OMC increased with the increased percentage of bentonite+2%cement mix. MDD also showed an increasing trend upto 15%bentonite+2%cement mix after which it decreased.
b) Cohesion increased and angle of internal friction decreased with the increased percentage of bentonite+2%cement mix.
c) Coefficient of permeability decreased appreciably with increasing content of admixture content.
d) The CBR value also increased with increasing content of bentonite+2%cement mix.
e) The free swelling index of all the bentonite+2%cement mixed samples attained a permissible value due to the presence of 2% cement.

From all the detailed study it is seen that although the maximum MDD is found at 15%B+2%C admixture content but the most ideal content to be mixed with Brahmaputra bed silt is 10%bentonite+2%cement. This 10%bentonite+2%cement content satisfies all the stability criteria's for embankment construction and is also economic as obtained from cost analysis. Hence, 10%bentonite+2%cement mix is recommended to be suitable for embankment construction.

7 REFERENCES

1) Deka, K. (2017). Improvement of Brahmaputra silt for Embankment construction.
2) IS: 2720 (Part 4)-1985, *Method of Test for Soil:* Grain size analysis, Bureau of Indian Standard, New Delhi.
3) IS: 2720 (Part 5)-1985, *Method of Test for Soil:* Determination of Liquid Limit and Plastic Limit, Bureau of Indian Standard, New Delhi.
4) IS: 2270 (Part 13)-1986, *Method of Test for Soil:* Direct Shear test, Bureau of Indian Standard, New Delhi.
5) IS: 2720 (Part 8)-1983, *Method of Test for Soil:* Determination of water content-dry density relation using heavy compaction, Bureau of Indian Standard, New Delhi.
6) IS: 2720 (Part 17)-1966, *Method of Test for Soils:* Laboratory determination of permeability, Bureau of Indian Standards, New Delhi.

7) IS 2720 (Part 40) – 1970, *Method of Test for Soils:* Determination of Free Swelling Index, Bureau of Indian Standards, New Delhi.

8) IS: 2720 (Part 16)-1987, *Method of Test for Soils*: Laboratory Determination of CBR, Bureau of Indian Standards, New Delhi

9) Medhi, A and Deka, N. 2017. Characterization of River Brahmaputra Bed Materials. *Proceedings of ACN International Conference*, Goa, India, ISBN: 978-93-86291-639.

10) NRRDA (2007), Quality Assurance Handbook for Rural Roads, Vol II, Ministry of Rural Development, Govt. of India.

Stability analysis of earthen dam with improvised soil

Baruah, P. [1] and Khaund, P. K. [2]

[1] PG Student, Department of Civil Engineering, Jorhat Engineering College, Jorhat-785007, India.
[2] Professor, Department of Civil Engineering, Jorhat Engineering College, Jorhat-785007, India.

ABSTRACT

Stability is a major concern for construction of earthen dam as well as embankments. In Brahmaputra valley and nearby its adjoining areas in the North-East India the surface soil is predominantly silty in nature and thereby it is very essential to increase the cohesive properties of silty soil for construction of earthen dam. An experimental investigation has been carried out with mixing different percentages of bentonite to improve the cohesive properties of silty soil. The change in maximum dry density, optimum moisture content, plasticity index, shear parameters, permeability etc. are evaluated using different laboratory tests for various soil bentonite mixes. After finding different improved geotechnical properties, stability analysis of a homogeneous earthen dam with different upstream and downstream slopes has been carried out using Swedish Slip Circle Method and effect of improvised soil on factor of safety are analysed.

Keywords: silty soil, earthen dam, bentonite, Swedish slip circle method

1. INTRODUCTION

Dam is a hydraulic structure constructed as a barrier across a river or a stream to increase the head of water at its upstream side. Earthen dams are the most ancient type of embankments, as they can be built with natural materials with minimum equipment and require less skilled labour and is almost stable against earthquake. In these days earthen dams are constructed with a fair degree of theoretical accuracy, provided the properties of the soil used in the construction of the dam are properly controlled. Earthen dams can be constructed on earth foundations, but it is more susceptible to failure as it is less rigid compared to gravity dams. Correct analytical approach to determine the various soil types for a homogeneous earthen dam or embankment is very important. This approach include selecting the soil to be used, laboratory testing to ensure the selected materials are suitable and interpretation of the results of these tests to permit the appropriate materials to be used. If the locally available soil is not appropriate for construction of an earthen dam or embankment, the soil must be improved and stabilized to get the desired properties of soil.

2. METHODOLOGY

In this present study the soil sample is collected from a few kilometres away from the Brahmaputra dike and the various geotechnical properties are evaluated by different laboratory tests. To improve the geotechnical properties of the collected natural soil sample, bentonite as an admixture is used in 3% to 20% by weight to the natural soil sample. For each sample geotechnical properties are evaluated and the properties are used in analysis of an earthen dam with three different upstream and downstream slopes using Swedish Slip Circle method.

3. RESULTS AND DISCUSSION

3.1 Effect on atterberg's limit

Liquid limit was determined by static cone penetration method. With the addition of bentonite content, the Liquid limit of the natural soil sample is increased to 37%. This is due to the reason of bentonite having higher liquid limit. From Fig.1 it can be observed that, Plastic limit and Plasticity index increased with addition of Bentonite to the natural soil sample.

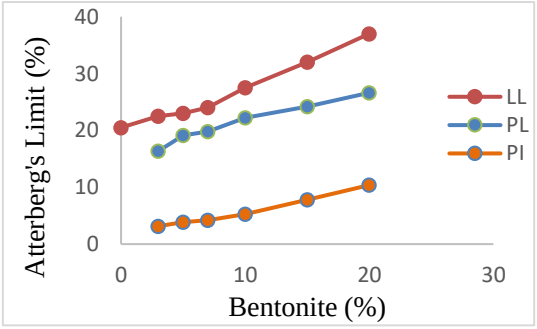

Fig. 1. Variation of atterberg's limit with addition of Bentonite.

3.2 Effect on compaction characteristics

Standard proctor tests were conducted to obtain optimum moisture content (OMC) and maximum dry density of natural soil and soil treated with bentonite. From Fig.2 it can be observed that as the percentage of bentonite increased OMC increased and MDD decreased. OMC is increased due to the reason of bentonite having finer particles than the collected natural soil sample. Because of more surface area, higher amount of water is required for well lubrication. The decrease in MDD may be attributed to the decrease in specific gravity.

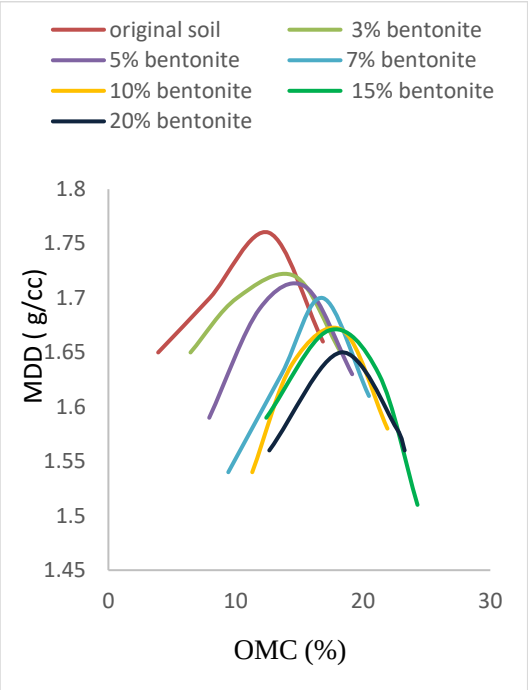

Fig. 2. Variation of OMC and MDD with addition of Bentonite.

3.3 Effect on shear parameters

To evaluate shear parameters Direct Shear test was conducted as per IS: 20270 (Part 13)-1986. Fig. 3 shows that, as the percentages of bentonite increased, Cohesion (c) increased, due to the presence of strong inter-particular attractive forces between the particles of bentonite the mixture gradually develops cohesion with an increase in bentonite content. Angle of Internal Friction (φ) decreased with addition of bentonite this is due to the reduction of intra-granular friction between soil particles.

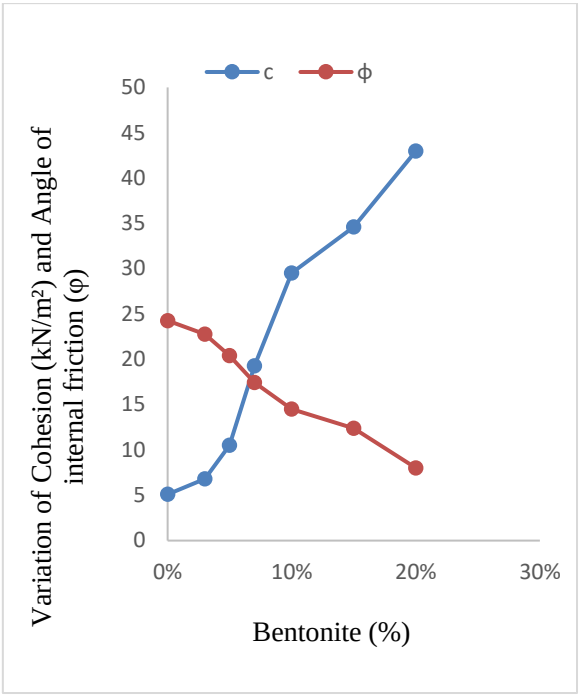

Fig. 3. Variation of c and φ with addition of Bentonite.

3.3 Effect on permeability

From falling head permeability test as per IS: 2720 (Part 17)-1986 the coefficient of permeability was determined. From Fig. 4 it can be observed that, natural soil sample was highly permeable but, after addition of bentonite, the coefficient of permeability (K) reduced significantly.

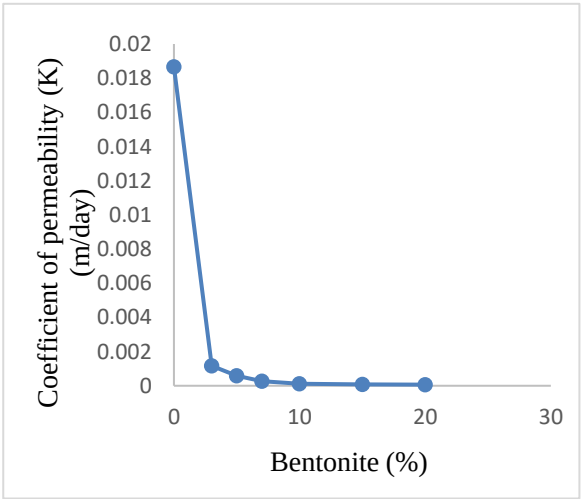

Fig. 4. Variation of K with addition of Bentonite

3.4 Analysis with swedish slip circle method

For the study using Swedish Slip Circle method a representative earthen dam is considered with three different upstream and downstream slopes as shown in table 1. The height of the earthen dam is considered as 30 m for all three cases. The

crest width is taken as 5 m. Water level is considered at 25 m.

Table 1. Upstream and Downstream slope for Analysis.

Sl No.	Upstream slope	Downstream slope
Case 1	2:1	2.5:1
Case 2	2.5:1	3:1
Case 3	3:1	3:1

For the analysis parameters of 5%, 7%, 10%, 15% and 20% bentonite mixed with soil are considered.

Case 1

Stability of downstream slope during steady seepage (design with 5% to 20% bentonite + soil)

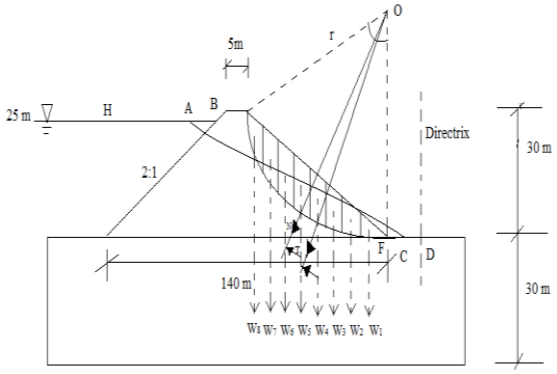

Fig. 5. Stability of D/S slope for Case 1

The various Factor of safety (FOS) obtained for case 1 are listed below.

Table 2. List of FOS for case 1 with different percentages of Bentonite.

% of Bentonite	FOS
5%	1.12
7%	1.17
10%	1.27
15%	1.29
20%	1.30

Case 2

Stability of downstream slope during steady seepage (design with 5% to 20% bentonite + soil)

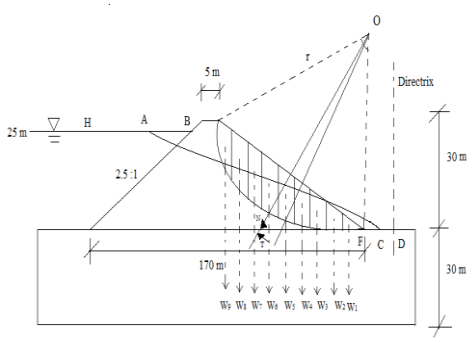

Fig. 6. Stability of D/S slope for Case 2

Table 3. List of FOS for case 2 with different percentages of Bentonite.

% of Bentonite	FOS
5%	1.33
7%	1.39
10%	1.50
15%	1.53
20%	1.54

Case 3

Stability of downstream slope during steady seepage (design with 5% to 20% bentonite + soil)

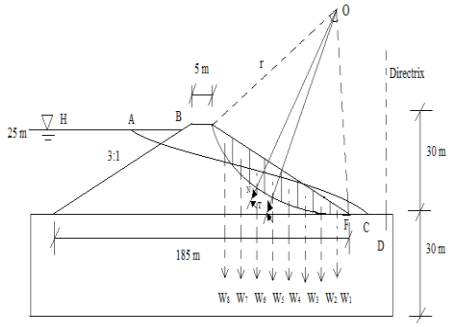

Fig. 7. Stability of D/S slope for Case 3

Table 4. List of FOS for case 3 with different percentages of Bentonite.

% of Bentonite	FOS
5%	1.374
7%	1.54
10%	1.75
15%	1.80
20%	1.89

4. CONCLUSIONS

The conclusions drawn from this research study are:

1. Addition of Bentonite effects the Atterberg's limit.

2. OMC increased and MDD decreased with addition of Bentonite.

3. As the percentages of bentonite increased, Cohesion increases and Angle of internal friction decreases.

4. Coefficient of permeability of the natural soil sample reduced significantly.

5. From the analysis using Swedish Slip Circle method, it was observed that for all three different cases, FOS increased with increase in bentonite content.

ACKNOWLEDGEMENTS

I would like to thank HOD, Department of Civil Engineering, JEC, Jorhat, Assam to allow avail the facility of civil engineering dept. laboratory. I am thankful to all the faculties of Dept. of Civil Engineering, JEC for their support. The co-operation of the technical staff is thankfully acknowledged.

REFERENCES

1) Ahmed, Akbar A. And Choudhury, S. (2014). A Parametric Study on Slope Stability of Earthen Dam. *International Conference on Multidisciplinary Research & Practice*, Volume I Issue VIII, PP: 569-573, ISSN 2321-2705.
2) Daud Khalida A., "Cohesionless Soil Properties Improvement Using Bentonite", *ARPN Journal of Engineering and Applied Sciences*, VOL. 13, NO. 1, JANUARY 2018, PP 271-275, ISSN 1819-6608 (2018)
3) IS: 2720 (Part 5)-1985, *Method of Test for Soil:* Determination of Liquid Limit and Plastic Limit, Bureau of Indian Standard, New Delhi.
4) IS: 2720 (Part 4)-1985, *Method of Test for Soil:* Grain size analysis, Bureau of Indian Standard, New Delhi.
5) IS: 20270 (Part 13)-1986, *Method of Test for Soil:* Direct Shear test, Bureau of Indian Standard, New Delhi.
6) IS: 2720 (Part 8)-1983, *Method of Test for Soil:* Determination of water content-dry density relation using heavy compaction, Bureau of Indian Standard, New Delhi.
7) IS: 2720 (Part 17)-1966, *Method of Test for Soils:* Laboratory determination of permeability, Bureau of Indian Standards, New Delhi.
8) IS: 7894-1975, *Code of Practice for Stability Analysis of Earth Dams*, Bureau of Indian Standards, New Delhi.
9) Proia et. al (2016). Experimental Investigation of Compacted Sand Bentonite Mixtures, *VI Italian Conference of Researchers in Geotechnical Engineering, CNRIG2016*, PP: 51-56.

Parametric study of hill-slopes vulnerable to landslides in Guwahati city of Assam

Kalita, M.[1], Nath, U. K.[2] and Bhuyan, A.[3]

[1] Assistant Professor, Department of Civil Engineering, Assam Don Bosco University, Guwahati, 781017, India.
[2] Associate Professor, Department of Civil Engineering, Assam Engineering College, Guwahati, 781013, India.
[3] PG Student, Department of Civil Engineering, Assam Don Bosco University, Guwahati, 781017, India.

ABSTRACT

This study attempts to validate the landslide vulnerability data obtained from district disaster management authority (DDMA) of Assam for determination of slope stability on the basis of limit equilibrium methods of slices. Stability computations have been carried out by Geo-Studio 2012 on two highly vulnerable slopes of Guwahati's hillock having latitude $26^0$11'52.3" N and longitude $91^0$47'39.8" E using Bishop's Simplified method, Janbu's Simplified method, Spencer method and Morgenstern-Price method. The slope geometry is defined based on the field data obtained and all the analyses are done assuming a homogeneous slope. The material model for soil is represented by Mohr-Coulomb model and the soil parameters such as cohesion, angle of internal friction and unit weight of soil are determined from laboratory tests of each soil sample collected from the field. The slip surfaces have been defined using two methods i.e. entry exit method and grid and radius method. Both the methods provide nearly same results regarding variation in factor of safety. The main observations from the study is that the Factor of Safety (FoS) values computed using Bishop's Simplified method and Morgenstern-Price method are sensitive to the assumed locations of slip surfaces. The critical slip surface in the form of semi-circular arc describes the failure plane of the slope along which local shear failure may occur. The activating moments along the critical slip surfaces are found to be significantly high as compared to the resisting moments. The slopes are further analysed under the application of surcharge loads which results in increase of negative pore water pressure and decreased value of factor of safety. The study also provides recommendations on some planning and measures that can be used to stabilise the existing slopes with high vulnerability of failure under any triggering factors.

Keywords: landslide, slope-stability, Geo-Studio, slip surfaces, factor of safety

1. INTRODUCTION

Landslide in Guwahati city of Assam usually occurs during the rainy seasons. But the fact that various anthropogenic factors such as rise in water table of unsaturated slopes, increase in surcharge loading per running metre, and toe cutting also lead to catastrophic damage of vulnerable slopes in various hillocks of Guwahati city cannot be denied. Previous studies have suggested that rainfall infiltration has a significant effect on the factor of safety (FOS) of slopes. The instability induced in the slope due to saturation of the soil is further intensified when coupled with various anthropogenic landslide triggering factors. This research focuses on the effect of rise in water table on the FOS of unsaturated slope with different heights of water table viz. 2m, 4m and 6m. Three different analyses were conducted to understand the variation in FOS values with change in water table depths. The effect of hydraulic conductivity of soil on the factor of safety of the slopes were also observed. The analysis were done using SLOPE/W for investigating the slope stability.

Fig. 1. Well depth in Anandanagar hill slope, Guwahati

1.1 Stability analysis of slope

A 14 m high slope overlying a rigid bedrock foundation located in Anandanagar (26.19733°N,

91.796028°E) of Sunsali hillock was taken into consideration and analysed against instability due to a single boundary condition i.e. instability due to hydraulic condition (change in depth of water table).

Fig. 2. Anandanagar slope in Sunsali hillock

2. METHODOLOGY

Field verification of the slope was carried out to understand its geometry in addition to measuring the height, width and collecting the soil sample for determination of total strength parameters of the underlying soil. The soil slope was considered homogeneous as collection of soil samples from various points of the slope revealed the same type of soil along with its uniform textural properties.

The height of the slope as gauged by the measuring tape was found to be 14 m and the base width of the slope was around 35 metres. Since the slope was a finite slope and was continuous throughout the Sunsali hillock, the exposed surface vulnerable to slope failure was only taken into consideration. Presence of trees, shrubs, grasses and other form of vegetation was found at the top of the slope. The well data was collected based on the measurement of well depths in the surrounding locality.

2.1 Identification of Geotechnical Properties

Soil samples from slope of the hillock were collected using a shovel. Around fifteen kilograms of soil sample were collected. The remoulded soil samples were further analysed for their textural properties. The index properties of soil such as Atterberg limits were not verified as these properties are not required in this analysis. The unit weight of soil and the total strength parameters such as soil cohesion (C) and angle of internal friction (φ) were determined with the help of standard laboratory tests. To determine the cohesion value and angle of internal friction direct shear test was conducted on the soil sample. The angle of internal friction was determined using the Mohr-Column theory. The permeability test was conducted to understand the hydraulic conductivity of the soil samples. The 'k' (constant of permeability) value of the soil was obtained through summation analysis using the falling head Permeameter. Standard Proctor test was conducted to establish the dry density versus moisture content relationship from where the optimum moisture content (OMC) of the soil was obtained. Specific gravity of the soil was obtained through a series of Pycnometer tests. Moreover, the tests were standardized and calibrated using standard laboratory equipment certified by Indian Standard Soil lab equipment.

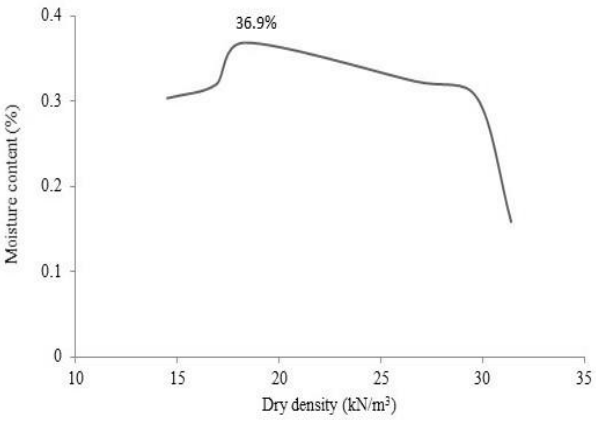

Fig 3. Dry density versus moisture content graph

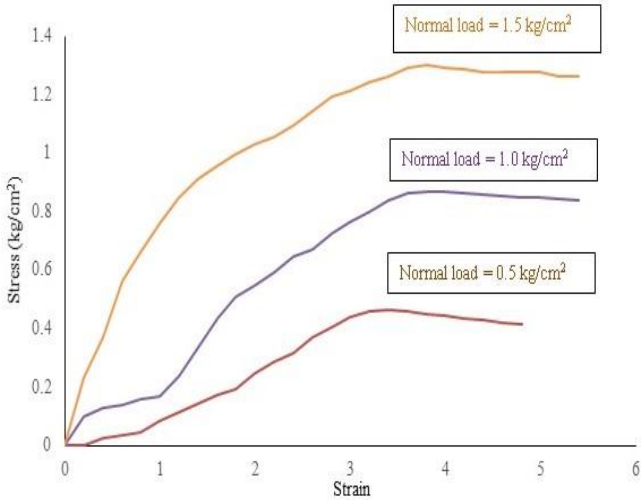

Fig. 4. Stress versus strain graph of direct shear test

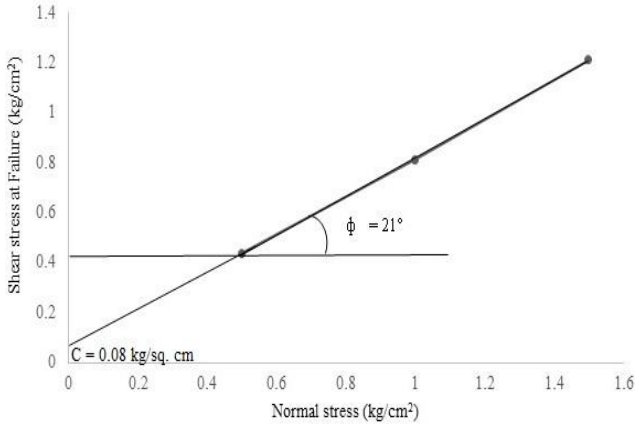

Fig. 5. Normal stress versus shear stress at failure

The average coefficient of permeability of the soil was found to be 0.0034 cm/sec.

In order to check the stability of the slope under rising water table, the pore water pressure in the slope model was increased by adjusting the height of the phreatic line from its native position. A rough estimate of the original depth of water table of the analysed slope was made with the help of well data recorded by measuring the depth of the deep well in the local slope area.

It is not practically possible to measure the actual pore water pressure in any slope as it is an independent variable and does not rely on the total stresses acting on the soil and is merely controlled by the flow pattern of the ground water table, induced seepage forces or variation in the water table. Hence a virtual simulation of varying pore water pressures on the existing field conditions was generated through the model to understand the behaviour of the slope under increased height of the water table.

The depth of the well was found roughly to be around 6.04 m from the ground surface. The PWP conditions for this study was defined with the help of phreatic line. The phreatic line was so adjusted based on this data by specifying the entry height in left side of the slope and gradually falling towards the right slope plane. The effect of application of the phreatic line in the slope was applied to both the materials comprising the upper red soil layer and the underlying bedrock.

The slope with Mohr Coulomb material model was analysed keeping other parameters constant and changing the height of the phreatic line so as to describe the change in depth of the water table. The analysis was done in three stages; in the first stage of analysis the phreatic line was set as per field conditions and later it was increased by a height of approximately two metres in the subsequent stages.

Table 2 shows the schematic representation of the slope model taken into account for analysis. As per field conditions the PWP line was fixed at a depth of approximately 6m from the ground surface which had a gradually decrease in its height towards the toe of the dam. For the current analysis, the maximum allowable suction of the slope was set to the default values as there was no relevant data available to determine the suction capacity of the soil sample from the slope. The cap suction command was disabled in order to ensure the development of negative pore water pressure within the slope to give more realistic results.

Table 1. Slope models for rise in water table due to high intensity short duration rainfall

Material Model	Slope Geometry	Boundary Conditions	F.O.S
Mohr Coulomb C =8.4 kPa Φ =21° γ = 23 kN/m³	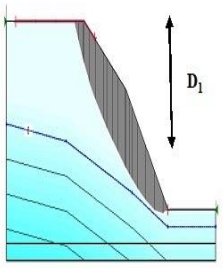	Depth of Water Table (D_1) = 6m	0.991
Mohr Coulomb C =8.4 kPa Φ =21° γ = 23 kN/m³	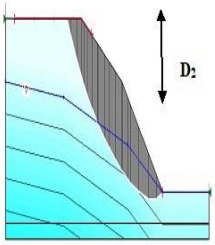	Depth of Water Table (D_2) = 4m	0.858
Mohr Coulomb C =8.4 kPa Φ =21° γ = 23 kN/m³	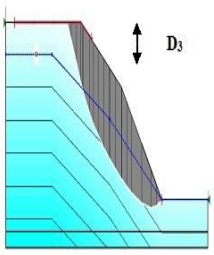	Depth of Water Table (D_3) = 2m	0.795

3. RESULTS

The factor of safety values obtained from the analyses were 0.991, 0.858 and 0.795 for depth of water table at 6m, 4m and 2m respectively with a critical slip surface highlighted in white arc. The critical slip surface along with the corresponding factor of safety generates the PWP contour map. The pore water pressure contour map in the slope model depicts the presence of positive and negative pore pressures below and above the phreatic line respectively.

3.1 Results of pore water pressure over slices

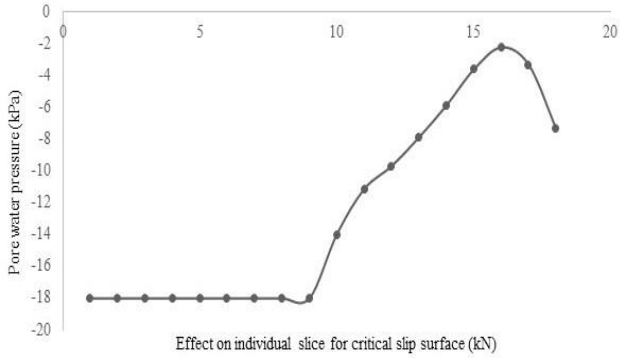

Fig. 6. PWP versus effect on slice for critical slip surface (water table depth = 6 m)

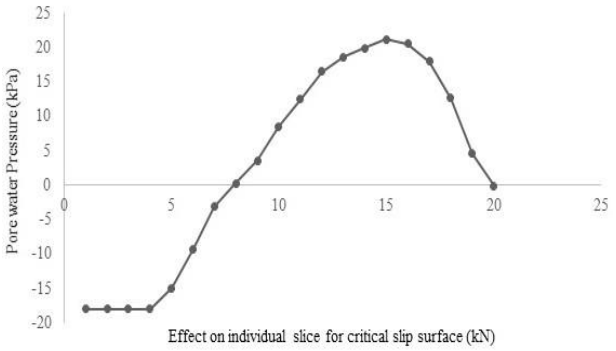

Fig. 7. PWP versus effect on slice for critical slip surface (water table depth = 4 m)

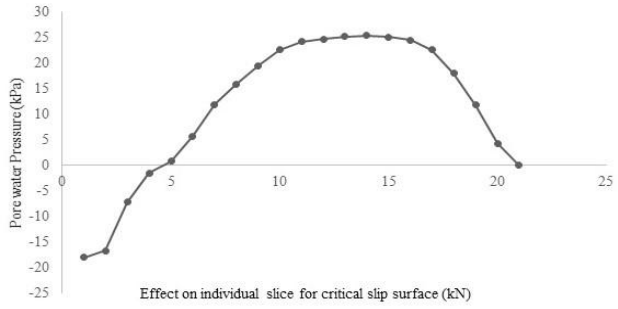

Fig. 8. PWP versus effect on slice for critical slip surface (water table depth = 2 m)

Figures 6, 7 and 8 depict the change in pore water pressure corresponding to the individual analysis performed. It has been observed in Fig. 6 that the pore water pressure curve does not attain any positive values throughout the curve when the numerical analysis was done on its native field values. On the other hand, the pore water pressures in Fig. 7 and Fig. 8 attain positive values at specific points when the depth of the phreatic line was reduced from the ground surface level indicating loss of matric suction. It is due to the fact that the slope considered is a partially saturated slope in which the negative pore water pressure tends to decline aggressively and destabilize the slope. The positive values in the graph indicate that the magnitude of seepage force taking place in the slope is rising with the rise in water table.

It can be seen that the negative pore water pressure adds to the stability of the slope. Slopes having low cohesion values as in this case may become saturated due to the apparent rise in the water table but it does not signify any substantial effect on the slope stability as it may withdraw it effect with the passage of time.

It is also observed that the reduction of negative pore water pressure takes place at certain specific points on the curve and does not remain constant thereafter indicating that pore water pressure alone cannot make significant destabilization of slope under normal circumstances. The variation in factor of safety is not as high as compared to other analysis. However, the apparent rise in the positive pore water pressure may destabilize the slope under the influence of other triggering factors.

3.2 Graphical interpretation of rising water table

The rise in positive pore water values may induce uplift forces at the slope face which may increase the hydrostatic forces to maximum value and decrease the total stresses to minimum value, and may thereby destabilize the slope. Due to factors like rainfall infiltration, the value of negative pore pressure may become zero and even positive. Therefore, pore-water pressure distribution in soil attaining positive values accompanied by loss of matric suction may have significant influence on slope stability as it reduces the frictional forces between the sliding masses considering the influence of other external conditions with time.

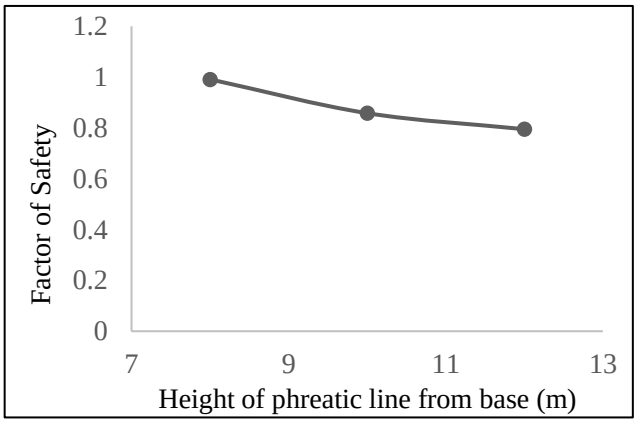

Fig. 9. Factor of safety versus depth of water table

4. CONCLUSION

The plot between computed factors of safety for the individual analysis relative to rise in the water table depicts that there is a marginal reduction in factor of safety which may or may not pose threat to the stability of the slope. Pore water pressure being a completely independent parameter may either form due to the

physical location of the soil or presence of any external pressure. If the permeability result obtained through falling head Permeameter test for the soil sample of Anandanagar, Guwahati i.e. k = 0.0034 cm/sec is considered against the results of the PWP analysis, it can be assumed that this permeability of the soil will not allow a significant rise of water table through rainfall or any other external conditions. However, it does increase the probability of shear strength reduction due to decrease in negative pore water pressure which may be induced for a very short duration of time and may subside with change in other environmental conditions, indicating no immediate substantial impact on the stability of slope.

REFERENCES

1) Anderson, M. G., and Howes, S. (1985): Development and application of a combined soil water-slope stability model, *Quarterly Journal of Engineering Geology and Hydrogeology*, pg. 225-236
2) Atkinson, J. H., and Farrar, D. M. (1985): Stress path tests to measure soil strength parameters for shallow landslips, *Proceedings of 11th International Conference on Soil Mechanics and Foundation Engineering*, Vol 2. San Francisco. Pg. 983–986
3) Bishop, A. W. (1955): The use of the slip circle in the stability analysis of earth slopes, *Geotechnique*, pg. 7–17
4) Brand, E. W. (1981): Some thoughts on rain-induced slope failures, *Proceeding of the 10th International Conference on Soil Mechanics and Foundation Engineering*, pg. 372-376
5) Brenner, R. P., Tam, H. K., and Brand, E. W. (1985): Field Stress Path Simulation of Rain Induced Slope Failure, *Proceedings of 11th International Conference on Soil Mechanics and Foundation Engineering*, pg. 991-996.
6) Cai, F., and Ugai, K. (2004): Numerical analysis of rainfall effects on slope stability, *International Journal of Geomechanics*, pg. 69-78
7) Duncan, J. M. (1996): Soil Slope Stability Analysis in Landslides: Investigation and Mitigation, *Transportation Research Board*, Washington, DC. pg. 337-371

Assessment of CBR values of coarse grained soil using geotechnical properties and evaluating the CBR values at different compaction energy input

Saikia, B.D.[1], Gogoi, B.[2]

[1] Professor, Department. of Civil Engineering., Royal Global University, Guwahati-781035, India.
[2]Assistant Professor, Department of Civil Engineering., Royal Global University, Guwahati-781035, India.

ABSTRACT

The most common method of determining subgrade strength of flexible pavements is with the help of California Bearing Ratio (CBR) value for design purposes. The entire process of evaluating soaked and unsoaked CBR values by the CBR tests is very time consuming and tedious. Therefore, attempts have been made in the present study to assess the soaked and unsoaked CBR values of cohesionless soils using other geotechnical properties of the soil. Again it is noticed that the requirement of the subgrade strength may vary from site to site; which necessitated the evaluation of CBR values corresponding to different level of compaction energy input. In the present study three coarse grained soil samples of SP classification (ISSCS) have been selected and particle size distribution curves are determined so as to find the C_u and C_C values. The maximum dry density (MDD) and optimum moisture content (OMC) values for each soil are obtained by conducting Modified Proctor compaction test to have field condition. Series of CBR tests are carried out with different compaction energy input by different number of blows (10, 25 and 56) for all the three samples under soaked and unsoaked conditions. Finally, attempts have been made to establish some correlation between CBR values (corresponding to 56 no of blows) with MDD and OMC values respectively and another correlation between CBR values and compaction energy input in terms of number of blows.

Keywords: soaked CBR value, unsoaked CBR value, correlation, geotechnical properties, compaction energy

1. INTRODUCTION

California Bearing Ratio (CBR) test is most commonly employed in determining the sub-grade strength of a flexible pavement. The CBR test has been extensively used in civil engineering from decades. But the entire process of determining CBR value (soaked and unsoaked) is very tedious and time consuming. Again, it is noticed that the requirement of the sub-grade strength may vary from site to site; which necessitated the evaluation of CBR values corresponding to different level of compaction energy input.

In the present study it is attempted to assess the soaked and unsoaked CBR values of cohesionless soils using geotechnical properties, such as, MDD and OMC of the soil. This study is further extended towards evaluation of the CBR values (both soaked and unsoaked) at different compaction energy input.

2. LITERATURE REVIEW

Some of the available literatures relating to this domain are briefly discussed below. Patel and Desai (2010) found a correlation between CBR and Plasticity Index (PI), MDD, OMC for alluvial soil. Agarwal and Ghanekar (1970) proposed an equation that correlates soaked CBR with OMC and Liquid Limit (LL) of fine grained soil. Other research workers like Venkatasubramanian and Dhinakaran (2011); Naveen *et al.* (2014); Deepak *et al*. (2014); Roy *et al*. (2009); correlated CBR values of soil with the LL, Plastic Limit (PL), PI, Shrinkage limit, fine content, OMC, MDD and Unconfined Compressive Strength values of soil.

3. TEST PROGRAMME AND TEST RESULTS

All together three coarse grained soil samples are collected from different location and sieve analysis is done as per IS: 2720 (Part IV) to determine the gradation of the soils. Sample 1 is collected from the bank of the river Brahmaputra at Uzan Bazar, Guwahati. Sample 2 is collected from market which is mostly used as a material in the construction of buildings. Sample 3 is collected from the deposits at Juripar, Six Mile, Guwahati, caused by the rain water from the hills of Meghalaya. The results of sieve analysis are given in Table-1, which shows that all the soil samples are of SP class as per Indian Standard Soil Classification System (ISSCS).

Table 1. Sieve Analysis test Results

Sample No	% of sand	Cu	Cc	IS classification
1	97.2	1.08	1.00	SP
2	99.6	2.24	1.24	SP

3	99.4	2.23	1.20	SP

The Modified Proctor test is done on the three soil sample as per IS: 2720 (part VIII) to determine the maximum dry density (MDD) and optimum moisture content (OMC) of the soil samples. Then on the three soil samples California bearing ratio (CBR) tests were conducted to evaluate the CBR values (both at soaked and unsoaked condition) as per IS: 2720 (part 16). Apart from providing standardized 56 numbers of blows to the soil sample; CBR tests were performed at two more compaction energy input i.e. 10 & 25 numbers of blows so as to determine a correlation between CBR values and compaction energy in terms of numbers of blows. Here in this test programme, for all the CBR tests soil sample are prepared by providing modified Proctor compaction effort and keeping the moisture content at OMC. The Modified Proctor test results and the CBR test results (corresponding to 56 numbers of blows) are given in Table-2 and all the CBR test results at different compaction energy input are given in Table-3.

It is observed from the CBR test results that the soaked CBR values for all the three coarse grained soil samples are greater than that of unsoaked CBR value, which contrast to the conventional CBR test result shown by fine grained soils. But, literature [Ranjan and Rao (2000)] already reports that, for gaining maximum density state of coarse grained soils, it must be compacted either in dry state or in saturated state by flooding with water. So, the test results are very relevant in this context.

Table 2.Modified Proctor and CBR Test Result

Sample No	MDD (g/cc)	OMC (%)	Unsoaked CBR (%)	Soaked CBR (%)
1	1.65	16	17.52	17.62
2	1.68	15.5	24.33	28.22
3	1.64	16.2	14.11	16.52

Table 3. CBR values at different compaction energy input

Sample No	UnsoakedCBR (%) no of blow			Soaked CBR (%) no of blow		
	10	25	56	10	25	56
1	6.08	12.4	17.52	6.47	13.63	17.62
2	5.6	10.46	24.33	6.08	11.43	28.22
3	6.42	12.16	14.11	6.57	14.59	16.54

4. ANALYSIS OF TEST RESULTS

First it is attempted to establish a correlation between the CBR (%) values and MDD values for the tested soil sample (Fig.1) using test results from Table-2, the relationship between CBR and MDD obtained from regression equation are given in Eq.(1) and Eq.(2).

$(CBR)_{Unsoaked}$ = 248.9 (MDD) – 393.7; R^2 = 0.991 (1)

$(CBR)_{Soaked}$ = 306.5 (MDD) – 487.0; R^2 = 0.975 (2)

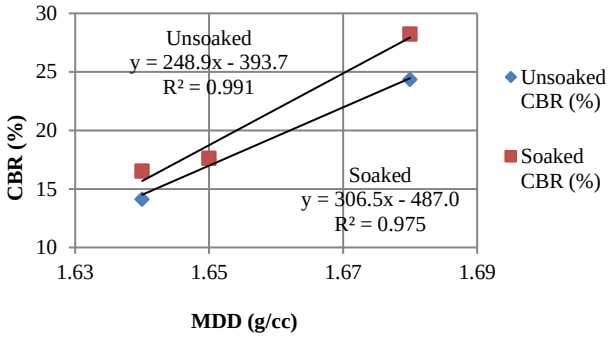

Fig.1.Corelation between CBR(%) and MDD(g/cc)

Next, a correlation is found between the CBR (%) values and OMC values for the selected soil samples as shown in Fig.2. These correlation equations are expressed in Eq.(3) and Eq.(4).

$(CBR)_{Unsoaked}$ = -14.41 (OMC) +247.80; R^2 = 0.997 (3)

$(CBR)_{Soaked}$ = -17.57 (OMC) + 300.20; R^2 = 0.962 (4)

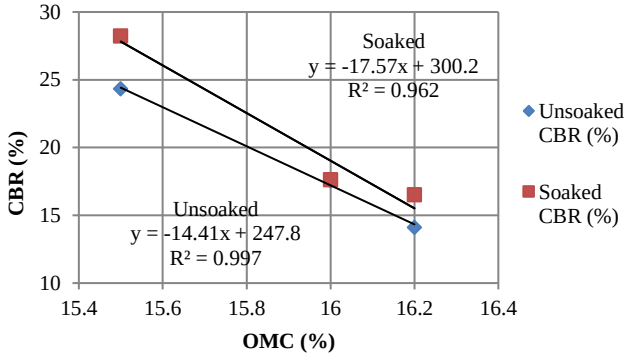

Fig.2.Corelation between CBR(%) and OMC(%)

Finally a correlation is obtained between CBR (%) values and number of blows for all the soil samples for both soaked and unsoaked conditions. These correlations for each of the three samples are shown in Fig.3, Fig.4 and Fig.5.

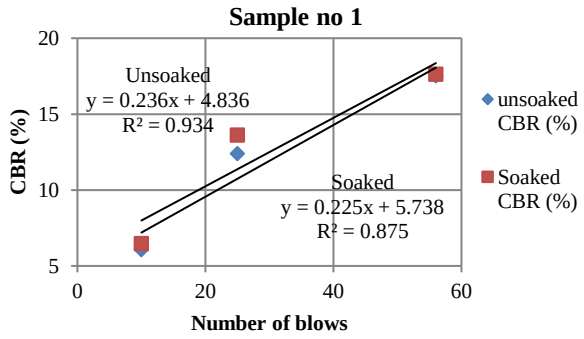

Fig.3.Corelation between CBR(%) and number of blows for sample 1

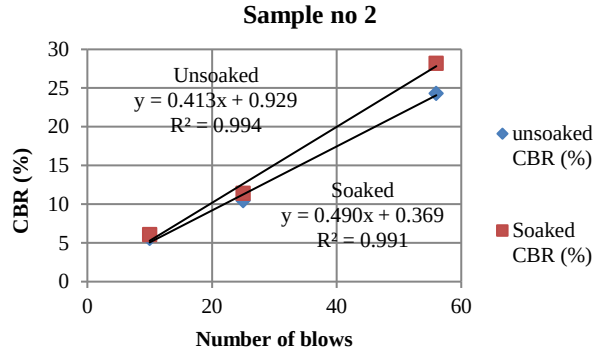

Fig.4.Corelation between CBR(%) and number of blows for sample 2

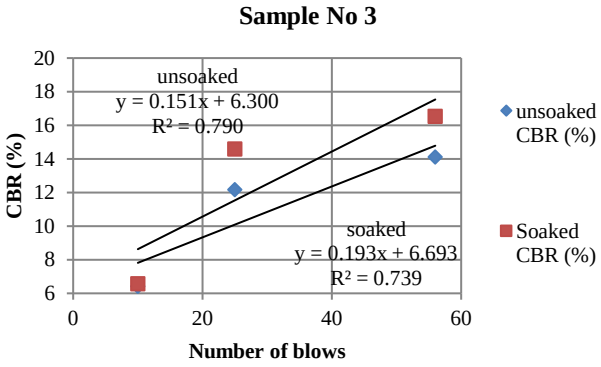

Fig.5. Corelation between CBR(%) and number of blows for sample 3

Combining results of all the three soil samples, the final correlation between CBR (%) values and number of blows is shown in Fig.6. The correlation equations are given in Eq.(5) and Eq.(6). The regression coefficients for these correlations are not very good still they are in acceptable limit. So, for a given CBR value an approximate amount of compaction energy required can be predicted using these equations.

$(CBR)_{Unsoaked}$ = 0.267 (No. of blows) + 4.022; R^2 = 0.793 (5)

$(CBR)_{Soaked}$ = 0.303 (No. of blows) + 4.267; R^2 = 0.756 (6)

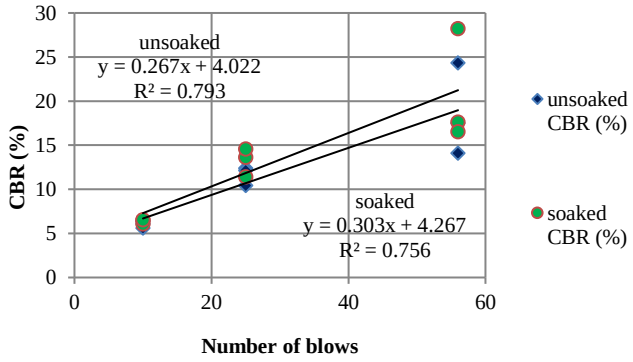

Fig.6. Corelation between CBR(%) and number of blows for all the soil samples

5. CONCLUSIONS

The present study determined the correlations between CBR (%) values both in soaked and unsoaked conditions with geotechnical properties such as MDD and OMC and with compaction energy input in terms of numbers of blows.

The correlation equations between CBR (%) values and geotechnical properties like MDD and OMC (Eq.(1) to Eq.(4)) show very good regression coefficients. Therefore these equations may be used to evaluate CBR value for given values of MDD and OMC for a particular cohesionless soil.

Though the regression coefficients for the correlation equations between CBR (%) values both in soaked and unsoaked conditions with compaction energy input in terms of numbers of blows are not very good still they are in acceptable limit. So, for a given CBR value approximate amount of compaction energy required to attain that resistance can be predicted using Eq.(5) and Eq.(6).

It is to be noted that more number of soil samples need to be incorporated in the further study to have better a correlation equation, since this work is conducted with only three soil samples' data. Further, the investigation can be extended towards fine grained cohesionless soil using vibration compaction technique.

REFERENCES

1) Agarwal, K.B. and Ghanekar, K.D. (1970):*Prediction of CBR from Plasticity Characteristics of Soil*, Proceedings of 2nd South-East Asian Conference on Soil Engineering, Bangkok, Singapore, 571-576.
2) Bureau of Indian Standards (1983): Methods of test for

soils: Determination of water content-dry density relation using Heavy Compaction, IS 2720-8, New Delhi, India.

3) Bureau of Indian Standards (1980): Methods of test for soils: Grain size analysis. IS 2720-4, New Delhi, India.
4) Bureau of Indian Standards (1987): Methods of test for soils: Laboratory Determination of CBR, IS 2720-16, New Delhi, India.
5) Deepak, Y., Jain, P.K. and Rakesh, K. (2014):*Prediction Of Soaked CBR Of Fine Grained Soils From Classification And Compaction Parameters*, International Journal of Advanced Engineering Research and Studies, III(IV): 119-121.
6) Naveen, B., Shirurand Santosh Hiremath, G. (2014): *Establishing Relationship between CBR Value and Physical Properties of Soil*, IOSR-JMCE, 11(5): 26-30.
7) Patel, R. S. and Desai, M.D. (2010):*CBR Predicted by Index Properties of Soil for Alluvial Soils of South Gujarat* , Proceedings of Indian Geotechnical Conference, IIT Bombay, Vol. I, 79-82.
8) Ranjan, G. and Rao, A.S.R. (2000):*Basic and applied soil mechanics*, New age international publication, New Delhi, PP.-112.
9) Roy, T. K.., Chattopadhyay, B.C. and Roy, S.K. (2009): *Prediction of CBR from Compaction Characteristics of Cohesive Soil*, Highway Research Journal, July-Dec., 77-88.
10) Venkatasubramanian, C. and Dhinakaran, G. (2011):*ANN model for predicting CBR from index properties of soils*, International Journal of Civil and Structural Engineering, 2(2): 605-611.

Liquefaction potential evaluation of Guwahati city

Saikia, J. [1], Pathak, J. [2] and Goswami, D.[3]

[1] Ph.D Student, Department of Civil Engineering, Assam Engineering College, Guwahati-781013, India.
[2] Professor, Department of Civil Engineering, Assam Engineering College, Guwahati-781013, India.
[3] Associate Professor, Department of Civil Engineering, Assam Engineering College, Guwahati-781013, India.

ABSTRACT

Liquefaction is a catastrophic natural phenomenon in which the strength and stiffness of a soil is reduced by earthquake shaking or other rapid loading. Soil liquefaction is one of the critical problems and is of major concern after the onset of a seismic activity. Liquefaction causes soil failures and therefore causes severe damages to structures supported on such grounds leading to significant economic losses. This paper attempts to find out the liquefaction potential in and around Guwahati city as it falls into a zone that is highly prone to seismic activity (Zone V). Moreover the city has seen a lot of unplanned growth with various high rise buildings. Hence, it is of utmost necessity to analyze and review the soil of various areas to assess the level of seismic hazard in terms of liquefaction. The study involves SPT N Values for the calculation of Cyclic Stress Ratio (CSR) and Cyclic Resistance Ratio (CRR) and finally, evaluation of liquefaction potential by calculating Factor of Safety based on the Summary report 1996 and 1998 NCEER/NSF workshops on evaluation of liquefaction resistance of soils and Idriss and Boulanger methods. In this paper 336 boreholes are considered from various locations of the city and the liquefaction potential of Guwahati is evaluated.

Keywords: earthquake, liquefaction potential evaluation, Guwahati, SPT N Value

1. INTRODUCTION

Soil liquefaction occurs when a saturated or partially saturated soil substantially loses strength and stiffness in response to an applied stress such as shaking during an earthquake or other sudden change in stress condition, in which material that is ordinarily a solid behaves like a liquid. The phenomenon is most often observed in saturated, loose (low density or un compacted), sandy soils. This is because loose sand has a tendency to compress when a load is applied. Dense sands by contrast tend to expand in volume or 'dilate'. If the soil is saturated by water, a condition that often exists when the soil is below the water table or sea level, then water fills the gaps between soil grains ('pore spaces'). In response to soil compressing, the water pressure increases and the water attempts to flow out from the soil to zones of low pressure (usually upward towards the ground surface). However, if the loading is rapidly applied and large enough, or is repeated many times (e.g. earthquake shaking, storm wave loading) such that the water does not flow out before the next cycle of load is applied, the water pressures may build to the extent that it exceeds the force (contact stresses) between the grains of soil that keep them in contact. These contacts between grains are the means by which the weight from buildings and overlying soil layers is transferred from the ground surface to layers of soil or rock at greater depths. This loss of soil structure causes it to lose its strength (the ability to transfer shear stress), and it may be observed to flow like a liquid (hence 'liquefaction'). The simplified methods for liquefaction potential evaluation that follow Seed and Idriss (1971) were all developed from field performance case histories at level ground sites that had been characterized with in situ tests (such as standard penetration test, SPT). These simplified methods are generally expressed as a deterministic model. In a deterministic approach, liquefaction of a soil is predicted to occur if the factor of safety (F_S), defined as the ratio of cyclic resistance ratio (CRR) over cyclic stress ratio (CSR), is less than or equal to 1; on the other hand, no soil liquefaction is said to occur if F_S>1. Alternatively, and perhaps more rationally, probabilistic assessment of liquefaction potential may be performed to account for all the uncertainties that exist in the adopted model and the input data. The probabilistic assessment of liquefaction potential yields the probability of liquefaction (P_L) for a future case. It is interesting to note that the 15% probability is also adopted by Cetin et al. (2004) as the basis for establishing a deterministic boundary curve (i.e. limit state) based on their probabilistic model. To determine the liquefaction probability of a soil in a future case, reliability methods that allow for explicit consideration of model and parameter uncertainties should be a method of choice, if these uncertainties can be characterized statistically (e.g. Haldar and Tang 1979); Juang et. al.(2006) etc. In the absence of the complete knowledge of model and/or parameter uncertainties, simplified probabilistic models may be used to estimate the probability of liquefaction. The simplified models are generally derived from a given database of case histories. Like many investigators Christian and Swiger (1975); Liao, Veneziano, and

Whitman (1988); Youd and Noble (1997); Toprak et al. 1999) etc.

2 STUDY AREA

2.1 Topography of the Area

The Guwahati city is situated on an undulating plain, on the banks of River Brahmaputra, comprising of a bowl-shaped valley that consist several hills and Beels interspersed along its landscape. To the North, there is the Nilachal Hill & mighty Brahmaputra river beyond which connectivity to the capital is very less as compared to the main city. The southern and eastern sides of the city are surrounded by hillocks namely, Sarania Hill, Nabagraha Hill, Chunchali Hill & the hills of Meghalaya and water bodies like, Dighalipukhuri and Silsako Beel. In the west, there is the Deepor Beel. In addition, the city is covered by swamps, marshes, etc. The relatively steep-sided granite hillocks do not provide adequate conditions for building development. Hence, for the overall assessment of the liquefaction potential of the city 336 numbers of boreholes are considered in the study.

2.2. Source of Data

Source: Department of Civil Engineering, Assam Engineering College, Guwahati.
Study Area: Guwahati City and its adjoining areas.
Sample Size: 336 Boreholes.

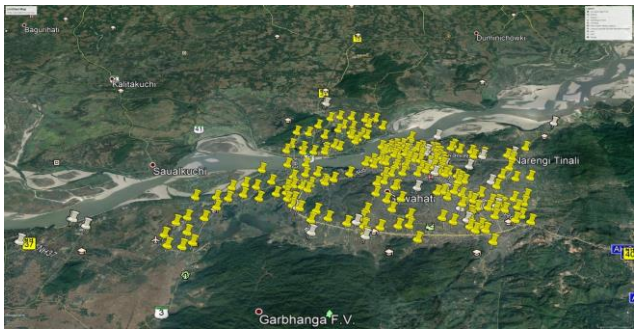

Fig 1. Map of Guwahati City showing all the boreholes analyzed (Courtesy: Google Earth)

3 PREOCEDURES FOR LIQUEFACTION POTENTIAL EVALUATION

In the study for the evaluation of liquefaction potential various methods are implemented. They are as follows:-

1. Seed and Idriss Method (NCEER Workshop Methodologies) using SPT N-Value.
2. Chinese Criteria by Seed and Idriss (1982), specify that liquefaction can only occur if all three of the following conditions are met:
   i. The clay content (particles smaller than 5 m) is <15% by weight.
   ii. The liquid limit is <35%.
   iii. The natural moisture content is >0.9 times the liquid limit.
3. NCEER Workshop criteria using Shear Wave Velocity (Correlations used).

Table 1. Correlations for calculation of Shear Wave Velocity used in the Analysis

Sl. No.	Correlation given by	Correlation
1.	Bablu Kirar, B. K. Maheshwari and Pradeep Muley	$Vs = 99.5N^{0.345}$
2.	S. Ohba and I. Tourumi	$Vs = 84N^{0.31}$
3.	T Imai	$Vs = 91N^{0.34}$
4.	MK Jafari, A Shafiee and A Razmkhah	$Vs = 121N^{0.27}$
5.	GA Athanasopolous	$Vs = 107.6N^{0.36}$
6.	C Hanumantharao and GV Ramana	$Vs = 82.6N^{0.43}$

Where V_s is the Shear Wave Velocity in m/sec and N is the Standard Penetration Resistance obtained from SPT Test.

4. According to the Analysis given by IM Idriss and RW Boulanger in 2010.

4. ANALYSIS AND RESULTS

Analysis of liquefaction potential

Sample analysis shown for borehole no.1
Location: - Behind Building Center (Assam Engineering College)

Table 2. Analysis of Liquefaction potential using SPT N Value using NCEER Workshop.

Depth	N Value	N 1 (60) values	CRR Values for 7.5 Mw Earthquake	CSR Values	Factor of Safety
1.5	20	19	0.2048	0.446	0.459
3	17	17	0.1845	0.442	0.418
4.5	20	18	0.1971	0.437	0.451
6	10	9	0.1039	0.432	0.241
7.5	12	10	0.1111	0.433	0.257
9	15	11	0.1247	0.429	0.2

					91
10.5	32	24	0.2675	0.419	0.639
12				0.402	
13.5				0.375	
15				0.349	
16.5				0.323	
18				0.301	
19.5				0.282	
21				0.267	
22.5				0.254	
24				0.244	
25.5				0.236	
27				0.229	
28.5				0.223	
30				0.218	

Where N is the Standard Penetration Resistance obtained from SPT Test, $(N_1)_{60}$ is the corrected N Value, CRR is Cyclic Resistance Ratio and CSR is the Cyclic Stress Ratio.

Table 3. Analysis of Liquefaction potential using Chinese Criteria

Depth of the Soil Layers	Criteria 1, The clay content is <15% by weight	Criteria 2, The Liquid limit is less than 35%	Criteria 3,The Natural Moisture Content is >0.9 the liquid limit
1.5	NO	NO	NO
3	NO	NO	NO
4.5	NO	NO	NO
6	YES	NO	NO
7.5	YES	NO	NO
9	YES	NO	NO
10.5	YES	NO	NO
12	YES	NO	NO
13.5	YES	NO	NO
15	YES	NO	NO
16.5	NO	NO	NO
18	NO	NO	NO
19.5	NO	NO	NO
21	NO	NO	NO
22.5	NO	NO	YES
24	NO	NO	YES
25.5	NO	NO	YES
27	NO	NO	YES
28.5	NO	NO	YES
30	NO	NO	YES

Where "YES" implies that liquefaction will occur and "NO" implies that liquefaction will not occur.

Table 4. Factor of Safety for Liquefaction Potential

Depth	Hanumantharao and Ramana	Ohba and Tourumi	Imai	Jafari et al.	Athanasopolous	Kirar, Maheshwari and Pradeep Mulay
1.5	1.176	0.534	0.805	0.951	1.321	1.014
3	0.691	0.254	0.462	0.580	0.805	0.605
4.5	0.648	0.185	0.407	0.505	0.737	0.546
6	0.143	0.643	-0.22	0.165	0.292	0.125
7.5	0.194	0.712	-0.13	0.169	0.316	0.154
9	0.275	1.148	0.014	0.203	0.3713	0.214
10.5	0.692	0.110	0.382	0.437	0.7288	0.525

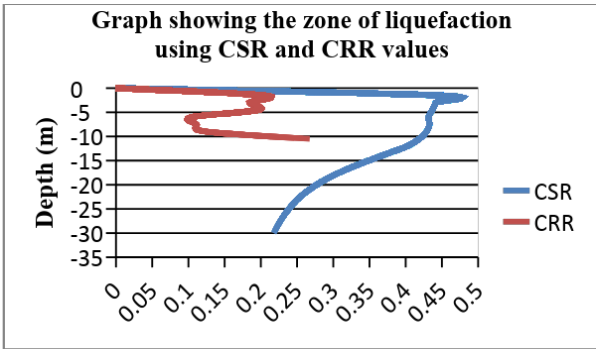

Table 5. Comparison of the Factor of safety for NCEER Workshop method, Shear wave velocity method and Boulanger method

Depth (m)	NCEER Workshop Criteria	Shear Wave Velocity, Hanumantharao and Ramana	Shear Wave Velocity, Ohba and Tourumi	Shear Wave Velocity, Imai	Shear Wave Velocity, Jafari et al.	Shear Wave Velocity, Athanasopolous	Shear Wave Velocity, Bablu Kirar, Maheshwari and Pradeep Mulay
1.5	0.46	1.18	0.53	0.80	0.95	1.32	1.01

3	0.42	0.69	0.25	0.46	0.58	0.81	0.61
4.5	0.45	0.65	0.19	0.41	0.51	0.74	0.55
6	0.24	0.14	0.64	-	0.17	0.29	0.13
7.5	0.26	0.19	0.71	-	0.17	0.32	0.15
9	0.29	0.28	1.15	0.01	0.20	0.37	0.21
10.5	0.64	0.69	0.11	0.38	0.44	0.73	0.53

5. DISCUSSIONS AND INTERPRETATIONS

In the study 336 bore holes are taken into consideration for finding out the liquefaction potential analysis. For finding out the liquefaction potential of the city four procedures are employed. Using procedure 1, which is the NCEER Workshop procedure based on the simplified procedure, the analysis is carried out as shown in Table 2. The moment magnitude of the input earthquake is taken as M_w=7.5, a_{max}=0.36 and the magnitude scaling factor is calculated accordingly. The SPT N value is corrected to calculate $(N_1)_{60}$ using all the correction parameters. Assuming and calculating all the necessary parameters the factor of safety is calculated for at various locations. It can be seen that for the given earthquake magnitude the factor of safety obtained is less than 1 at all depths (Table 2). Hence from the analysis for Borehole 1 it can be said that there is a potential of liquefaction occurring at Borehole 1 according to the NCEER Workshop criteria. The graph for zone of liquefaction for Borehole 1 is shown below:

Fig 2. Graph showing the zone of liquefaction using CSR and CRR values

The second procedure used in the study is based on the Chinese Criteria. According to the Criteria Liquefaction will occur if and only if the three conditions viz. The clay content (particles smaller than 5 m) is <15% by weight, the liquid limit is <35% and the natural moisture content is >0.9 times the liquid limit. In the study it can be seen that for borehole 1, from depth 6m to 13.5m the clay content is less than 15% but the other two criteria is not fulfilled for liquefaction to occur (Table 3). So it can be interpreted that there is no liquefaction potential according to the Chinese Criteria at Borehole No. 1.

The third procedure used in the study for based on the liquefaction potential is based on the Shear Wave velocity. NCEER Workshop proceedings gave idea about the use Shear Wave Velocity in Liquefaction Potential Analysis. The Shear Wave velocity of the soil is obtained by using correlations for SPT N Values. Six correlations are used given various research workers and the details are shown in Table No. 1. The results obtained for the Factor of Safety against Liquefaction for various depths for Borehole 1 are shown in Table No. 4. It can be observed that at particular depths some of the Factor of safety values are very low and as such liquefaction could occur in those depths for Borehole No. 1. The moment magnitude of the input earthquake is taken as M_w=7.5, a_{max}=0.36 and the magnitude scaling factor is calculated accordingly.

The fourth procedure used in the study for evaluation of liquefaction potential is based on the procedure given by IM Idriss and RW Boulanger in 2010. The procedure also uses SPT N Values for calculation of the liquefaction potential of a particular area. The CSR is calculated for M_w=7.5. The analysis for Borehole No. 1 is shown below. The CSR (M_w=7.5) verses $(N_1)_{60cs}$ are plotted as shown below.

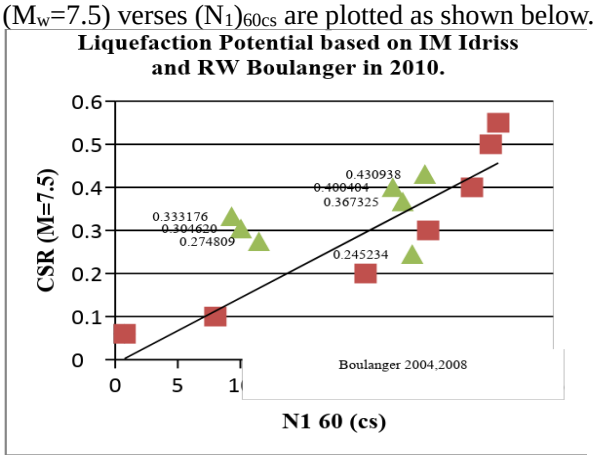

Fig 3. Graph showing the evaluation of liquefaction using IM Idriss and RW Boulanger method 2010.

It can be seen from the curve that most of the points lay above the Boulanger (2004, 2008) Curve. So it can be interpreted that Borehole No. 1 is free from liquefaction with respect to the I.M. Idriss and R.W. Boulanger in 2010 criteria.

6. CONCLUSIONS

In the study, for carrying out the liquefaction potential evaluation, 336 Boreholes from different locations across the Guwahati City were considered. A sample analysis is shown for Borehole No. 1. In the same way the liquefaction potential was analyzed for all the other locations as shown in Figure 1. In most of the cases it is observed that at shallow depths the factor of safety calculated is less than 1 at shallow depths. As the depth increases the Factor of safety also increases. This is due to the fact that the SPT N value increases at greater depths in most of the cases. Moreover it is seen that in some cases loose sand deposits exists and as such in those locations there is a susceptibility of liquefaction.

ACKNOWLEDGEMENTS

We are grateful to the Department of Civil Engineering, Assam Engineering College for

providing the necessary data for carrying out the study.

REFERENCES

1) Andrus, R. D., and Stokoe, K. H., II (1997). ‘‘Liquefaction resistance based on shear wave velocity.’’ Proc., NCEER Workshop on Evaluation of Liquefaction Resistance of Soils, Nat. Ctr. for Earthquake Engg. Res., State Univ. of New York at Buffalo, 89–128.
2) Andrus, R. D., and Stokoe, K. H., II (2000). ‘‘Liquefaction resistance of soils from shear-wave velocity.’’ J. Geotech. and Geoenvir. Engg., ASCE, 126(11), 1015–1025.
3) Arango, I. (1996). ‘‘Magnitude scaling factors for soil liquefaction evaluations.’’ J. Geotech. Engg., ASCE, 122(11), 929–936. ASTM. (2000). ‘‘Annual book of ASTM standards.’’ 04.08, D 1586-99, West Conshohocken, Pa.
4) Athanasopoulos GA (1995) Empirical correlations Vso-NSPT for soils of Greece: a comparative study of reliability. Proceedings of the 7th International Conference on Soil Dynamics and Earthquake Engineering Computation Mechanics Publications. Southampton, Boston, pp 19–25
5) Boulanger R.W. and Idriss I.M., Liquefaction susceptibility criteria for silts and clays. Journal of Geotechnical and Geo environmental Engineering, ASCE, 132(11), 2006, 1413-426.
6) Cetin, K.O., and Seed, R.B. [2004], “Nonlinear Shear Mass Participation Factor (rd) for Cyclic Shear Stress Ratio Evaluation”, J. Soil Dynamics and Earthquake Engg., Vol. 24, pp. 103-113.
7) Christian, J.T. and Swiger, W.F. (1975), "Statistics of Liquefaction and SPT Results." Journal of the Geotechnical Engineering Division, ASCE, Vol. 101, GTll, pp. 1135-1150.
8) Finn W.D.L., Byrne P.M., and Martin, G.R. (1976), Seismic Response and Liquefaction of Sands, Journal of Geotechnical and Geo Environmental Engineering, Volume: 102, Issue Number: GT8, Publisher: American Society of Civil Engineers, ISSN: 1090-0241, p. 841-856.
9) I.M. Idriss, and R. W. Boulanger, Semi-Empirical Procedures for Evaluating Liquefaction Potential during Earthquake. Soil Dynamics and Earthquake Engineering 26, 2006, 115–130.
10) Idriss, I. M. (1990). ‘‘Response of soft soil sites during earthquakes’’ Proc., H. Bolton Seed Memorial Symp., Vol. 2, BiTech Publishers, Ltd., Vancouver, 273–290.
11) Imai T, Tonouchi K., Correlation of N-value with S-wave velocity and shear modulus. Proceedings of the 2nd European Symposium of Penetration Testing, Amsterdam (1982): 57–72
12) Jafari M.K., Asghari A, Rahmani I., Empirical correlation between shear wave velocity (Vs) and SPT-N value for south of Tehran soils. Proceedings of 4th International Conference on Civil Engineering, Tehran, Iran (in Persian), (1997).
13) Kramer S. L. (1996). Geotechnical earthquake engineering, Prentice- Hall, Englewood Cliffs, N.J., 653.
14) Kumar S.S. and Dey A. (2015), 1D Ground Response Analysis to Identify Liquefiable Substrata: Case Study from Guwahati City, UKIERI Workshop on Seismic Requalification of Pile Supported Structures (SRPSS), 7-9 January 2015, Guwahati.
15) Liao, S. S. C., and Whitman, R. V. (1986b). ‘‘Catalogue of liquefaction and non-liquefaction occurrences during earthquakes.’’ Res. Rep., Dept. of Civ. Engg., Massachusetts Institute of Technology, Cambridge, Mass.
16) Liao, S. S. C., Veneziano, D., and Whitman, R. V. (1988). ‘‘Regression models for evaluating liquefaction probability.’’ J. Geotech. Engg., ASCE, 114(4), 389–411.
17) Ohba S, Toriumi I., Dynamic response characteristics of Osaka Plain. Proceedings of the Annual Meeting, A. I. J (in Japanese), (1970).
18) Olsen, R. S. (1984). ‘‘Liquefaction analysis using the cone penetrometer test (CPT).’’ Proc., 8th World Conf. on Earthquake Engg., Vol. 3, 247–254.
19) Olsen, R. S. (1997). ‘‘Cyclic liquefaction based on the cone penetration test.’’ Proc., NCEER Workshop on Evaluation of Liquefaction Resistance of Soils, Nat. Ctr. for Earthquake Engg. Res., State Univ. of New York at Buffalo, 225–276.
20) Seed, H. B. (1979). ‘‘Soil liquefaction and cyclic mobility evaluation for level ground during earthquakes.’’ J. Geotech. Engg. Div., ASCE, 105(2), 201–255.
21) Seed, H. B., and Idriss, I. M. (1971). ‘‘Simplified procedure for evaluating soil liquefaction potential.’’ J. Geotech. Engg. Div., ASCE, 97(9), 1249–1273.
22) Seed, H. B., and Idriss, I. M. (1982). ‘‘Ground motions and soil liquefaction during earthquakes.’’ Earthquake Engineering Research Institute Monograph, Oakland, Calif.
23) Seed, H. B., Tokimatsu, K., Harder, L. F., and Chung, R. M. (1985). ‘‘The influence of SPT procedures in soil liquefaction resistance evaluations.’’ J. Geotech. Engg., ASCE, 111(12), 1425–1445.
24) Toprak, S., Holzer, T. L., Bennett, M. J., and Tinsley, J. C. I.1999.“CPT- and SPT-based probabilistic assessment of liquefaction.”Proc.,7th U.S.–Japan Workshop on Earthquake Resistant Design of Lifeline Facilities and Countermeasures against Liquefaction, MCEER, Seattle, 69–86.
25) Youd T.L., Idriss I.M., Andrus R.D., Arango I., G. Castro, J.T. Christian, R. Dobry, W.D.L. Finn, L.F. Harder, M.E. Hynes, K. Ishihara, J.P. Koester, S.S.C. Liao, W.F, Marcuson, G.R. Martin, J.K. Mitchell, Y. Moriwaki, R.B. Seed, and K.H. Stokoe, Liquefaction Resistance of Soil: Summary report from The 1996 NCEER and 1998 NCEER / NSF Workshops on Evaluation of Liquefaction Resistance of Soils”, Journal of Geotechnical and Geo environment Engineering, 127(10), 2001,817 – 833

26) Youd, T. L., and Noble, S. K. (1997a). ‘‘Magnitude scaling factors.’’ Proc., NCEER Workshop on Evaluation of Liquefaction Resistance of Soils, Nat. Ctr. for Earthquake Engg. Res., State Univ. of New York at Buffalo, 149–165.
27) Youd, T. L., and Noble, S. K. (1997b). ‘‘Liquefaction criteria based on statistical and probabilistic analyses.’’ Proc., NCEER Workshop on Evaluation of Liquefaction Resistance of Soils, Nat. Ctr. for Earthquake Engg. Res., State Univ. of New York at Buffalo, 201–215.

Assessment of hill cut slopes using C-programming

Bhardwaj, B.B.[1], Sapkota, G.[2]

[1]Assistant Professor, Dept. of Civil Engineering, Assam Engineering College, Guwahati-781013, India.
[2]Lecturer, Dept. of Civil Engineering, Sibasagar Polytechnic, Sobasagar-785662, India.

ABSTRACT

Landslide is a geological phenomenon which occurs when the hill slope becomes unstable. The change in stability of a slope can be an outcome of various factors, acting together or alone. Rainfall acts as one of the primary factors of landslide all wide, which is often triggered and assisted by the steepness of the slope and the type of soil present. In India, although the national highways are being widened to cope up with the augmentation of traffic, the hill slopes adjacent to many of those highways are cut and left un-engineered. The angle of cut is not evaluated beforehand and hence the steep cuts result in a no. of landslides preceded by rainfall. A quantitative knowledge of the effect of steepness of the slopes for different types of soils and stratification present at the site always helps the concerned authority to have an idea on the safe slopes to be maintained at that place. Most of the times the authority doesn't feel the need to carry out stability analysis as the softwares used for the same are not available for free. Looking at the problems, the authors felt an urgent need of an indigenous tool that can be used for such slope stability assessment. The works in this paper deal with development of a program written in C-language which uses the field data of the nearby hills of NH-37 at Jorabat, near Guwahati. The shear parameters of the soils have been evaluated with tri-axial test and the results are incorporated in the program. The program provides the freedom to go for both stratified and homogeneous soil, and also to set different stratification heights. The validation of the tool has been done and some test results is added in the full-length paper.

Keywords: landslide, slope, stability, programming, hill-cut

1. INTRODUCTION

In our country, traffic is a huge problem. Some people say that it is inevitable due to growing number of population but there are various remedies to resolve this issue. Road widening is one of the several ways to diminish traffic congestion. It increases the flow of traffic because more vehicles can be accommodated particularly buses and trucks which require additional space that sometimes makes the road narrower.

Hills lying near roads or highways are often cut and severed to provide extra space for road driving surface. The part of road cross-section at Jorabat in Guwahati has been widened to make way for a 4-lane highway due to which the hill slopes near the road has been cleared and excavated. Even though the exposed cut slopes look unwavering at first sight but it might not be the case during intense rainfall conditions.

Moreover, the hills in study have a history of being affected by landslides. The area records many landslide activities during the rainy seasons leading to loss of lives and damage to property.

2. BACKGROUND

Vanden Berge and Daniel (2013) in their publication stated that the strength envelopes for many soils, including those for fully softened strength, are curved. the application of curved envelopes in practice has often lagged in favor of "equivalent linear" or piece-wise linear envelopes. Linear envelopes with no effective cohesion coincide with our understanding of normally consolidated clay behavior but tend to underestimate strength for shallow slides. When an effective stress cohesion intercept is used, linear envelopes usually over-predict strength at low normal stresses. Curved failure envelopes are more appropriate than linear envelopes for representing fully softened strengths. Sengupta during his research found that some of the common factors responsible for the frequent failures and closure of roadways in the hilly terrains are earthquake, steep slopes, toe erosion by rivers, heavy rainfall, melting of snow at high altitude, loss of vegetation, mining and unplanned urbanization. Some of the major factors found to be responsible for the landslides within the study area are regional geology or rock type, structure of the bedrocks (like, orientation of the rock foliations and faults), excessive rainfall and human interference (like, mining of stones and fines, and diversion of streams). Janbu (1980) showed a comparison of factors of safety for simple slopes composed of soils with both cohesive and frictional components of strength. His conclusion was definite and stated as follows: "The difference are so small that the procedures compared are numerically equal for all practical purpose". Fredlund (1981) stated that the shape of the unknown slip surface is generally assumed while the location is determined by trial and error procedure. If the shape of the slip circle is assumed to

be circular, a grid of centers can be selected and the radius varied at each center providing coverage of all possible conditions.

The problem of landslide can be eradicated if someone knows the safe slope of the hill beforehand and hence can put restrictions maintaining the safe slope in the hill-cuts. The softwares used for analyzing the safe slope of the hills come with very high prices. The authority sometimes doesn't feel the need of undergoing slope stability analysis using those softwares and simply goes with some thumb rules. The authors hence felt an urgent need of a simple yet reliable tool to analyze the stability of slopes keeping the regional conditions in mind. This resulted in writing of a 526 line long C-Program to find out the factor of safety of the given slopes for various conditions.

3. ANALYSIS

The failure of a mass of soil located beneath a slope is called a slide. It involves a downward and outward movement of entire mass of soil that participates in the failure. The action of gravitational forces and seepage forces within the soil are two main causes of landslide. The slopes under study fail suddenly without any prior warning.

Every mass of soil which is bounded by a sloping surface is subjected to shearing stresses on nearly all its internal surfaces because of the gravitational forces which tend to pull the upper portions of the mass downward towards a flatter surface.

The stability of a finite slope can be investigated by a number of methods, however the authors have used the Swedish Slip Circle Method to analyze the slopes. The method developed by Swedish engineers assumes that the surface of sliding is an arc of a circle.

Two cases are considered in this study-

- Analysis of purely cohesive soil (ϕ=0 analysis). Fig. 1 shows the relevant diagram to the analysis.

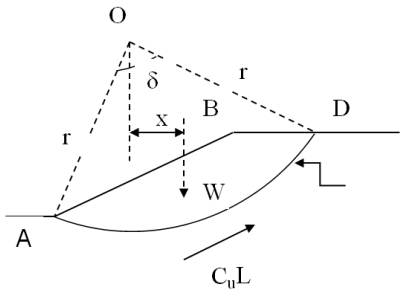

Fig 1 ϕ=0 analysis

The factor of safety, F.S. is then given by -

$$F.S.= \frac{M_R}{M_D} = \frac{r.C_u\hat{L}.}{W\bar{x}}.$$

- Analysis of soil possessing both cohesion and friction (c-ϕ analysis).

  For the entire slip surface AB, we have
  Driving moment, $M_D = r\sum T$;
  Resisting moment, $M_R = r[c\sum \Delta L + \tan\phi \sum N]$
  Where $\sum T$ = algebraic sum of all the tangential components
  $\sum N$ = sum of all the normal components
  $\sum \Delta L = \hat{L} = \frac{2\pi r\delta}{360^\circ}$ = length AB of slip circle

Hence factor of safety, F against sliding is given by-

$$F.S. = \frac{M_R}{M_D} = \frac{c\hat{L}+\tan\phi\sum N}{\sum T}$$

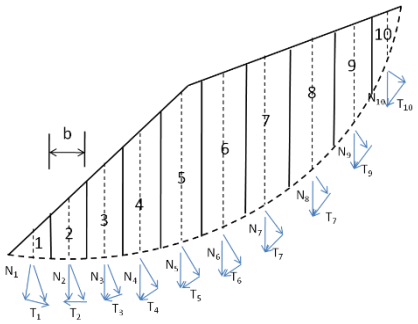

Fig 2 c-ϕ analysis

A number of trial slip circles are chosen and factor of safety of each is computed. The circle giving the minimum factor of safety is the critical slip circle. Fig.2 shows the relevant diagram to the analysis.

In order to reduce the number of trials to find the center of critical slip circle, Felinious method of locating the locus has been used.

4. HILL GEOMETRY

A survey was conducted at the site of Jorabat to have an idea of the different input to be provided. It is found that most of the hill sections have a complex slope containing two different angles (i_1 and $i_2$in Fig. 3) and the soil stratification is also not homogeneous in nature. Two distinct layers could be seen at many sections, the top layer comprising of red soil and the bottom one comprising of a white soil in color. The shear and other properties of these two soils were analyzed and incorporated inside the program.

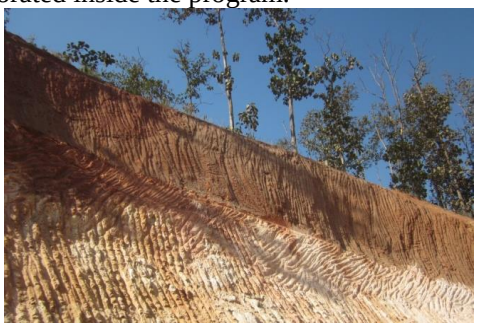

Fig. 3 Hill section near Jorabat, Assam

5. DEVELOPMENT OF PROGRAM

To begin with writing the algorithm of the program, a complex slope (allowing the user to give input of two slopes at a time, here i_1 and i_2) and a height (at two stages) are taken and the equations are manually solved to develop a vague idea about the program. The solutions of the equations holding the variables are used inside the program. The cross section of the soil profile is shown in Fig. 4 describing the slope angles and the lines.

Using Fellinious' method, a locus on which the probable centre may lie i.e. the centre of the slip circle may lie is assumed on the line PQ in which the point Q has its coordinates H downwards from toe and 4.5H horizontally away, as shown in the figure. The other point P is located with the help of directional angle α and β.

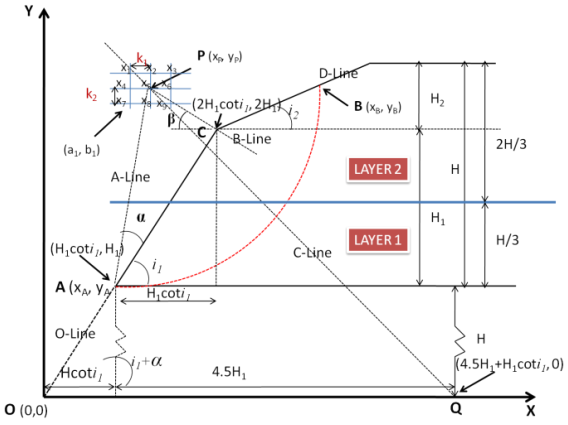

Fig. 4 Figure describing slope angles and lines

When the line PQ is obtained, trial centers are obtained around it and factor of safety corresponding to each centre is calculated using Swedish slip circle method.

Suppose, with P as centre, a trial slip circle is drawn. Next the slip circle area so obtained is divided into convenient number of vertical slices as shown in Fig. 2. The forces between the slices are neglected, and each slice is assumed to act independently as a column of soil of unit thickness and of unit width b. The weight W of each slice is assumed to act at its centre. This weight of each slice is resolved into normal (N) and tangential (T) components. The tangential components cause a driving moment. Moreover, we get the resisting moment from the Coloumb's equation. So, the factor of safety, which is the ratio of the resisting moment and the driving moment, is calculated.

The sequences of occurrence of different calculations inside the program are presented in the form of flow chart in Fig. 5.

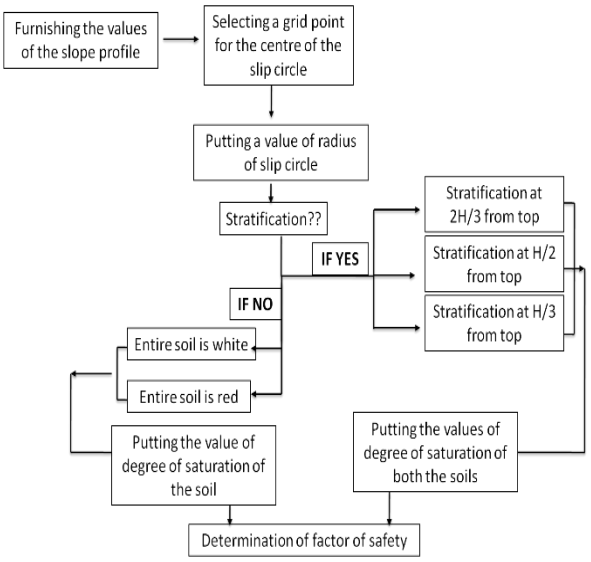

Fig. 5 Flow-chart of the algorithm

The program is user friendly and during its run it keeps on asking different parameter from the user and the user has to feed in all the data one by one. The steps involved in feeding of the data and processing of the same is discussed here-

STEP I

It will ask the angles of the hill slopes viz. i_1 and i_2

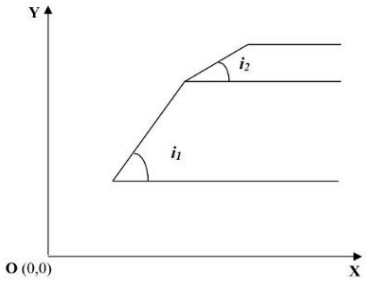

STEP II

It will ask the heights of the hill slopes viz. H_1 and H_2

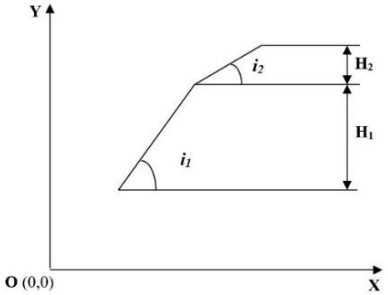

STEP III

It will give the co-ordinates of the reference point P and will ask to put the values of k_1 and k_2.

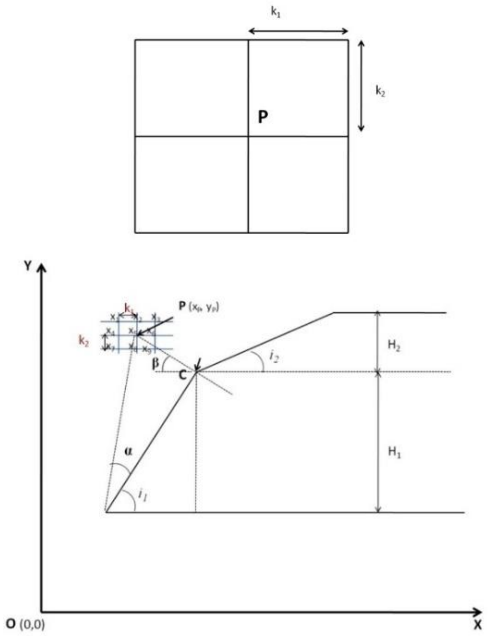

STEP IV

It will give the value of r_{max} and r_{min}; then will ask to put a value falling in this range.

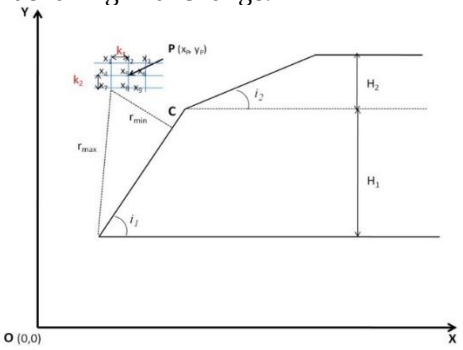

STEP V

It will ask thereafter if the hill is stratified or homogeneous. If homogeneous then it will ask for the name of the soil and if stratified then the depth at which the stratification interface is present.

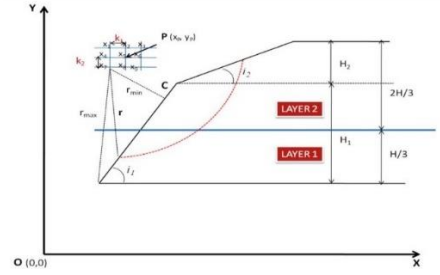

STEP VI

It will then ask to put the value of degree of saturation of the soil/soils.

STEP VII

After all the calculations it will finally give the value of Factor of safety for the given data.

The output results of the program have been compared with the manual calculation results and the necessary angles, lines, arcs etc. are measured by drawing the same in AutoCAD 2010.

The following table shows the comparison of the results of both the program and manual calculations. At the end, the results are found to satisfactory.

The factors of safety obtained from both the sources are same upto two decimals. Figure 6 shows the screenshot of the program used and Figure 7 shows the screenshot of the AutoCAD diagram used for validation of the results. Table 1 shows the comparison of the results of both the program and manual calculations

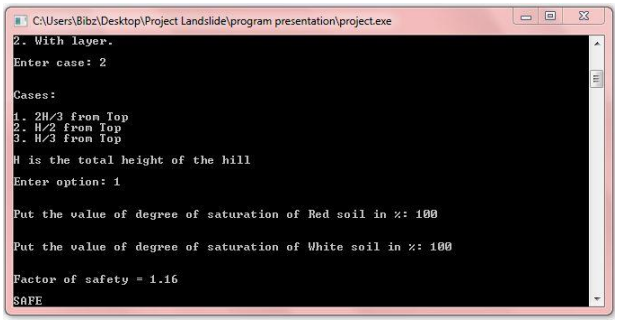

Fig. 6 Program run by the given inputs

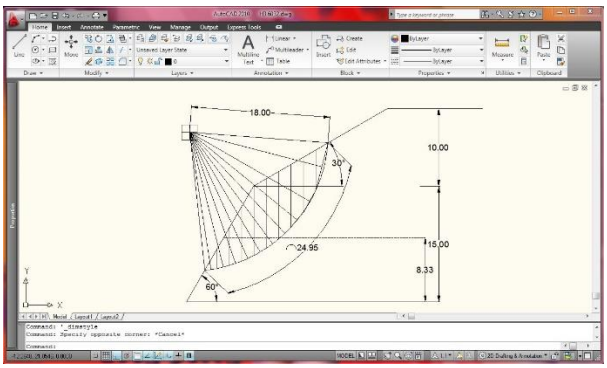

Fig. 7 Screenshot of the AutoCAD diagram used for validation of the results.

Table 1 Comparison of the results of both the program and manual calculations

Input	Program output	Manual output
$i_1=60^0$, $i_2=30^0$ H_1= 15 m, H_2= 10 m	$\alpha = 29^0$, $\beta = 40^0$	$\alpha = 29^0$, $\beta = 40^0$
$k_1 = 0$, $k_2 = 0$	R_max = 21.95 m R_min = 10.64m	R_max = 21.95 m R_min = 10.64 m
	The angle subtended by the slip circle = 79.42^0	The angle subtended by the slip circle = 79.42^0
	Arc Length = 24.95 m	Arc Length = 24.95 m
	Width of a slice =	Width of a slice =

Input	Program output	Manual output
r =18 m	1.60 m	1.60 m
	The area of the slices are- A_1= 2.02 m^2 A_2= 5.93 m^2 A_3= 9.59 m^2 A_4= 12.91 m^2 A_5= 14.44 m^2 A_6= 14.21 m^2 A_7= 13.52 m^2 A_8= 12.21 m^2 A_9= 9.88 m^2 A_{10}= 4.19 m^2 A_{total}= 98.90 m^2	The area of the slices are- A_1= 2.02 m^2 A_2= 5.93 m^2 A_3= 9.59 m^2 A_4= 12.97 m^2 A_5= 14.44 m^2 A_6= 14.21 m^2 A_7= 13.52 m^2 A_8= 12.21 m^2 A_9= 9.88 m^2 A_{10}= 5.07 m^2 A_{total}= 99.84 m^2
	The angles of the tangents are- θ_1= 8.82^0 θ_2= 14.02^0 θ_3= 19.34^0 θ_4= 24.84^0 θ_5= 30.61^0 θ_6= 36.74^0 θ_7= 43.43^0 θ_8= 50.98^0 θ_9= 60.15^0 θ_{10}= 75.47^0	The angles of the tangents are- θ_1= 8.82^0 θ_2= 14.02^0 θ_3= 19.34^0 θ_4= 24.84^0 θ_5= 30.61^0 θ_6= 36.74^0 θ_7= 43.43^0 θ_8= 50.98^0 θ_9= 60.15^0 θ_{10}= 75.47^0
	The reaction components for each slice R_1= 1.99 R_2= 5.75 R_3= 9.05 R_4= 11.71 R_5= 12.43 R_6= 11.38 R_7= 9.82 R_8= 7.69 R_9= 4.92 R_{10}= 1.05	The reaction components for each slice R_1= 1.99 R_2= 5.75 R_3= 9.05 R_4= 11.77 R_5= 12.43 R_6= 11.38 R_7= 9.82 R_8= 7.69 R_9= 4.92 R_{10}= 1.27
	The tangential components for each slice T_1= 0.31 T_2= 1.44 T_3= 3.18 T_4= 5.42 T_5= 7.35 T_6= 8.50 T_7= 9.29 T_8= 9.49 T_9= 8.57 T_{10}= 4.06	The tangential components for each slice T_1= 0.31 T_2= 1.44 T_3= 3.18 T_4= 5.45 T_5= 7.35 T_6= 8.50 T_7= 9.29 T_8= 9.49 T_9= 8.57 T_{10}= 4.91
Case 2: With layers Case 1: 2H/3 from top	Height upto Layer interface H_3= 23.33 m	Height upto Layer interface H_3= 23.33 m
Degree of saturation of Red Soil = 100% Degree of saturation of White Soil = 100% Cohesion for red soil= 22.53 kPa Cohesion for white soil= 0.87 kPa ϕ for Red soil= 30.69^0 ϕ for White Soil = 33.54^0	g_{tot} (Red soil) =18.07 kN/m^3 g_{tot}(White soil) =18.52 kN/m^3 Nos. of slices possessing cohesion of Red soil =4 Nos. of slices possessing cohesion of White soil =6 Arc length in Layer1 L_1= 10.88 m Arc length in Layer2 L_2= 14.07 m Total Reaction force in Layer1 R_sum1 = 52.31 Total Reaction force in Layer2 R_sum2 = 23.48 Total Tangential force in Layer1 T_sum1 = 26.20 Total Tangential force in Layer2 T_sum2 = 31.41	g_{tot} (Red soil) =18.07 kN/m^3 g_{tot}(White soil)=18.52 kN/m^3 Nos. of slices possessing cohesion of Red soil =4 Nos. of slices possessing cohesion of White soil =6 Arc length in Layer1 L1= 10.88 m Arc length in Layer2 L2= 14.08 m Total Reaction force in Layer1 R_sum1 = 52.37 Total Reaction force in Layer2 R_sum2 = 23.70 Total Tangential force in Layer1 T_sum1 = 26.23 Total Tangential force in Layer2 T_sum2 = 32.26
	M_disturbing = 18946.53	M_disturbing = 18950.45
	M_resisting = 21968.25	M_resisting = 22028.41
	Factor of Safety = **1.16**	Factor of Safety = **1.16**

6. CONCLUSION

The authors were able to come up with the tool to analyze the stability of slopes of different hilly sections with different geometry and stratifications. The tool can be used with some simple guidelines and doesn't require any separate installation in the computer. However, visual interpretation of the geometry of sections may become difficult for the users, but with the help of a pictorial manual the problem can be solved easily. The tool has been successfully used by the authors to further find out the critical slopes of the hill sections at different conditions and the results will be published soon.

7. ACKNOWLEDGEMET

The authors would like to express sincere thanks to the Department of Civil Engineering, Tezpur University for providing the opportunity to conduct the laboratory experiments.

8. REFERENCES

1) Huat, A. & Rajoo (2006): Stability Analysis and Stability Chart for Unsaturated Residual Soil Slope, *American Journal of Environmental Sciences* **2**, 154-160.
2) Janbu, N. (1980): Critical Evaluation of the Approaches to stability analysis of landslides and other mass movements, *International symposium on landslides*, Vol. 2, Delhi ,109-128.
3) Sengupta, A., Gupta,S. & Anbarasu,K. (2010): Landslides - Investigations And Mitigation In Eastern Himalayan Region, *Journal of the Indian Roads Congress* **560**, 135-136.
4) Vanden, B., Daniel R., Duncan ,J. Michael & Brandon ,Thomas, L. (2013): Fully Softened Strength of Natural and Compacted Clays for Slope Stability, *Geo-Congress*, San Diego, California, 1-7.

Effect of slenderness ratio of pile foundation on soil-pile interaction

Sharma, N. [1], Goswami, D. [2] and Pathak, J.[3]

[1] Ph.D Student, Department of Civil Engineering, Assam Engineering College, Guwahati 13, India.
[2] Associate Professor, Department of Civil Engineering, Assam Engineering College, Guwahati, Assam, India.
[3] Professor, Department of Civil Engineering, Assam Engineering College, Guwahati, Assam, India.

ABSTRACT

Pile foundations have been providing ample scope of research since several decades. Usually, pile offers a good agreeable performance in complex soil conditions like loose and soft soils with less bearing capacity. However, the study of behaviour of pile foundation and its sustainability during earthquakes is of paramount importance in earthquake-prone areas such as, the Guwahati city. An understanding from the major earthquakes in the past clearly indicates that ground motions were responsible for the failure of foundations, leading to damage to the structures, resulting in loss of property and lives. Therefore, in this paper, numerical analysis of a single pile subjected to the 1940 El Centro earthquake ground motion was carried out to understand the soil-pile interaction for different slenderness ratio of piles. The numerical model was developed using Finite Element Program "OpenseesPL". Through analysis of an idealized single pile, the results generated provide an overview of the effect of slenderness ratio of pile foundation on soil-pile interaction.

Keywords: soil-pile, slenderness ratio

1. INTRODUCTION

Pile foundation is one of the most widely used deep foundations to support structures like high rise and mid-rise buildings. Buildings with more than 6 storeys is called a high-rise building, with less than 3 storeys is a low-rise building, and having storeys between 4 and 6, are called mid-rise buildings (Pathak & Lang, 2013). These buildings are subjected to static loads coming from the superstructure as well as dynamic loads mainly in the form of earthquake. During vibration, the pile interacts with surrounding soil and develops stiffness and damping of the soil-pile system (Bhowmick et al., 2013). Soil-Pile interaction refers to the complex phenomena in which the response of the soil influences the response of the pile foundation and the response of the pile influences the soil movement. It is necessary to predict the response of a structure considering soil-pile interaction for its performance based design. However, during earthquake, this process becomes very complicated and is not always taken into account in seismic design of a structure.

A lot of research has been done on the background and development of soil-pile interaction. Over the last few decades, various methods have been developed for the analysis of soil-pile interaction under dynamic load. These methods are broadly grouped under three categories – Numerical method, Experimental studies and Analytical Method. Kavitha et al (2016) reviewed the SSI analysis of laterally loaded piles and concluded that the soil–pile system behavior is predominantly nonlinear and depends on factors like soil properties, pile material, pile diameter, loading type and bed slope of ground. Soil-Foundation interaction was also studied by Banerjee (2018) using Abaqus and concluded that the response of clay and piles subjected to seismic loading is affected by various factors such as pile modulus, soil modulus, slenderness ratio, natural frequencies of clay layer and pile-raft, superstructure mass, density of the soil and peak ground acceleration.

To have an accurate estimation of soil-pile interaction, both static and dynamic loadings need to be considered. For a better judgment on the structural performance of buildings, the analysis of the effects of dynamic soil-structure interaction on seismic behaviour and lateral structural response of moment resisting building frames is essential (Tabatabaiefar et al., 2013). The present study involves numerical analysis of a single pile subjected to the 1940 El Centro earthquake ground motion carried out to understand the soil-pile interaction for different slenderness ratio of piles.

2. NUMERICAL SIMULATION

The Finite Element Method (FEM) is a very efficient tool for numerical analysis of nonlinear dynamic response of soil-pile system (Bhowmick et al., 2013). This method is a numerical approach based on elastic continuum theory that can be used to model soil-pile interaction by considering the soil as a three-dimensional, quasi-elastic continuum (Pulikanti & Ramancharla, 2013). The numerical analysis is carried out in a computational platform OpenSeesPL developed by PEER, Berkeley18. It is a graphical user interface (GUI) for three dimensional (3D) ground and ground structure response. This interface allows conducting

pushover pile analyses as well as seismic simulations. The model is simulated using Von Mises theory. The pile and soil is modeled with linear beam element. The interface between pile and soil is simulated with zero-length elements.

OpenSeesPL includes a pre-processor for definition of the pile geometry (circular or square pile) and material properties (linear or nonlinear), 3D spatial soil domain, boundary conditions and input excitation or push-over analysis parameters, and selection of soil materials from an available menu of cohesionless and cohesive soil materials. The user interface also allows convenient pre-processing and graphical visualization of the analysis results including a deformed mesh, ground response time histories and pile response profiles. This user interface helps geotechnical and structural engineers to rapidly build a model, run the FE analysis, and evaluate performance of the pile-ground system (Lu et al., 2006).

3. SOIL PROFILE AND PILE PARAMETERS

Numerical analysis is carried out for circular concrete pile, modelled with a semi-infinite cohesive medium soil. The elastic soil medium considered is of size 40m x 40m x 20m having elasticity 5 x 10^4 kPa. Elasticity of the pile material is 3 x 10^7 kPa and an axial load of 1000 kN is applied on the pile. The pile is considered to be fixed at the bottom and pinned at the top to find its response against the given dynamic load.

Table 1 shows the various pile dimensions taken for the static and dynamic analyses on a single pile.

Table 1. Pile Dimensions adopted

Sl. No.	Pile length (m)	Radius of pile (m)	Slenderness ratio
1.	7	0.35	20
2.	9	0.3	30
3.	8	0.2	40
4.	10	0.2	50
5.	12	0.2	60

4. STATIC ANALYSIS

After carrying out static analysis for an axial load of 1000 kN on a single pile of various slenderness ratios, in OpenseesPL, values of lateral displacement along the pile length, bending moment and shear force of the pile are obtained.

4.1 Lateral Displacement of pile

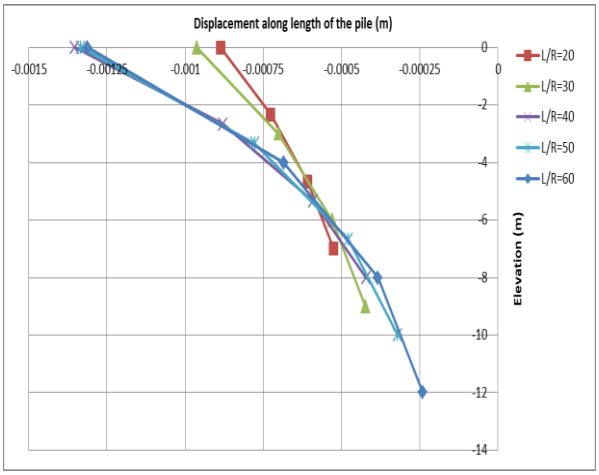

Fig. 1. Lateral Displacement of piles along its length under static load

Fig 1 shows the comparison of lateral displacement of piles along its length for different slenderness ratios.

4.2. Maximum Bending Moment of the pile

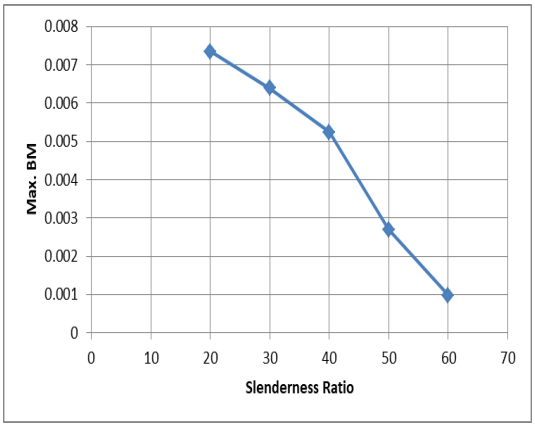

Fig. 2. Maximum BM for piles for different slenderness ratios under static load

In Fig 2, a comparison is made between the maximum bending moments obtained for piles with various slenderness ratios.

4.3. Maximum Shear Force of the pile

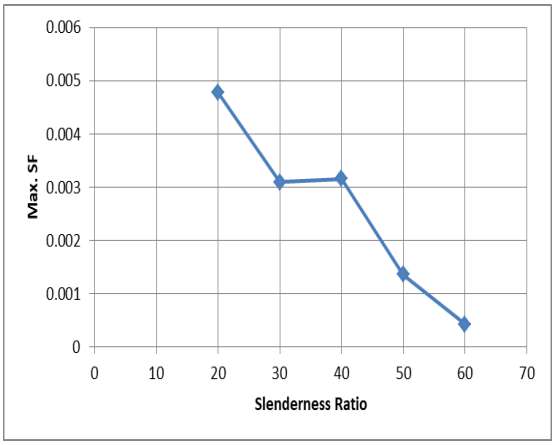

Fig. 3. Maximum SF for piles for different slenderness ratios under static load

Fig 3 shows the trend of the maximum shear forces for piles with different slenderness ratios.

5. DYNAMIC ANALYSIS

Dynamic analysis is carried out for an axial load of 1000 kN and a dynamic load in the form of El Centro ground motion of magnitude 6.9 and peak ground acceleration 0.3g, which is applied at the rigid end of the pile to perform a single motion analysis.

5.1. Lateral Displacement Of Pile

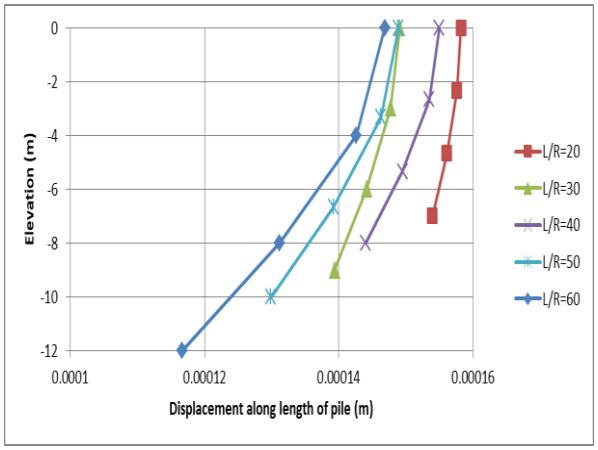

Fig 4: Lateral displacement of piles along its length under dynamic load

In Fig 4, the lateral displacement of a pile along its length for varying slenderness ratios are shown.

5.2. Maximum Bending Moment Of The Pile

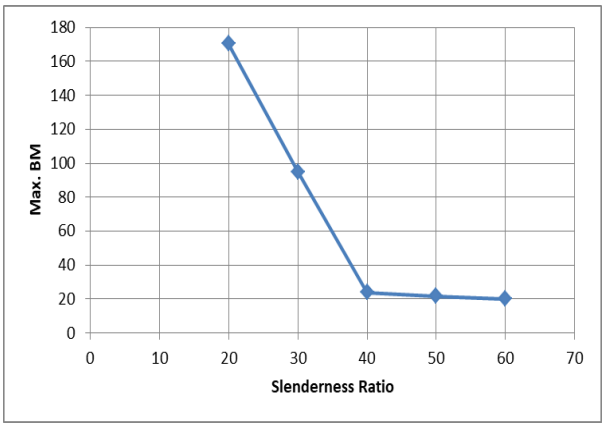

Fig. 5. Maximum BM for piles for different slenderness ratios under dynamic load

Fig 5 shows the comparison of maximum bending moment of piles with different slenderness ratios.

5.3. Maximum Shear Force Of The Pile

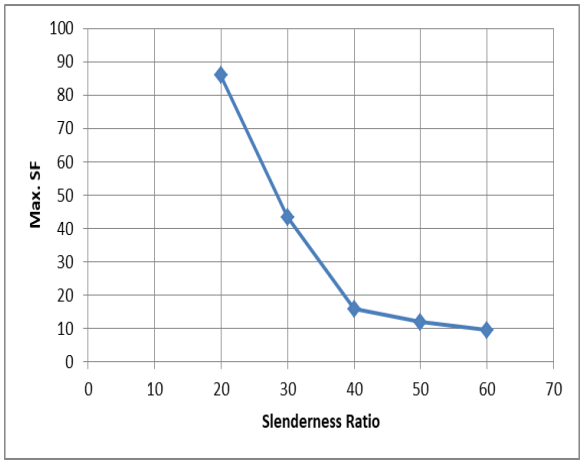

Fig. 6. Maximum SF for piles for different slenderness ratios under dynamic load

In Fig 6, the maximum shear forces of piles, with various slenderness ratios are shown.

6. OBSERVATIONS

In this study, static analysis is carried out on a single pile under an axial load of 1000 kN and dynamic analysis is carried out for the same pile under same axial load but for an additional load in the form of El Centro seismic ground motion. After performing static and dynamic analysis on the pile of different slenderness ratios on a finite element computational platform, following observations are made:

- From Fig. 1, it is observed that the lateral displacement of a pile along its length increases as its slenderness ratio increases.
- From Fig 2, it can be seen that the maximum bending moment of a pile under a given axial load, decreases with increasing slenderness ratio of the pile.
- As observed in Fig 3, the maximum shear force of a pile under a given axial load, decreases with increasing slenderness ratio of the pile.
- From Fig 4, it is observed that the lateral displacement of a pile along its length decreases as its slenderness ratio increases.
- From Fig 5, it can be seen that the maximum bending moment of a pile, decreases with increasing slenderness ratio of the pile.
- As observed in Fig 6, the maximum shear force of a pile, decreases with increasing slenderness ratio of the pile.

7. CONCLUSIONS

To carry out a comparative study on soil-pile interaction for different slenderness ratios, for the soil subjected to earthquake load, a finite element analysis is done on a computer program OpenseesPL. Following interpretations are drawn from the present study :

- While under static load, lateral displacement of the pile along its length increases with the increasing slenderness ratio, but under dynamic load, displacement decreases as slenderness ratio increases.
- Both under static and dynamic load, the maximum bending moment of a pile, decreases with increasing slenderness ratio of the pile.
- The maximum shear force of a pile under static and dynamic load, decreases with increasing slenderness ratio of the pile.

From the present study, the finite element tool is proved to be highly efficient and user friendly interface for modeling of pile in a soil medium and performing its analysis for a static as well as seismic load.

REFERENCES

1) Banerjee S. (2018) Modeling Soil–Foundation Interaction and Beyond, Geotechnics for Natural and Engineered Sustainable Technologies, Developments in Geotechnical Engineering, Springer, Singapore.
2) Bhowmik, D., Baidya, D.K., Dasgupta, S.P. (2013), Numerical Analysis Of Soil-Pile System Subjected To Vertical Dynamic Loading, Proceedings of Indian Geotechnical Conference, December 22-24, 2013, Roorkee.
3) Codoori, P., Kummari, J. M. (2017), Seismic Analysis of Soil-pile Interaction under Various Soil Conditions, International Journal of Applied Engineering Research ISSN 0973-4562 Volume 12, Number 18 (2017) pp. 7566-7571.
4) Elgamal, A. (2007), Nonlinear Modeling of Large Scale Ground-Foundation-Structure Seismic Response, ISET Journal of Earthquake Technology, Paper No. 488, Vol. 44, No. 2, June 2007, pp. 325–339.
5) Elgamal, A., Lu, J., Yang, Z., Shantz, T. (2010), A 3D Soil-Structure Interaction Computational Framework, Proceedings of the Joint Conference, 7th International Conference on Urban Earthquake Engineering (7CUEE) & 5th International Conference on Earthquake Engineering (5ICEE), March 3-5, 2010, Tokyo Institute of Technology, Tokyo, Japan.
6) Kavitha P.E, Beena K.S, Narayanan K.P (2016), A review on soil–structure interaction analysis of laterally loaded piles. Innovative Infrastructure Solutions 1 (1).
7) Lu, J., Yang, Z., and Elgamal, A. (2006), OpenSeesPL three-dimensional lateral pile-ground interaction version 1.00 user's manual, Report No. SSRP-06/03, Department of Structural Engineering, University of California, San Diego.
8) Mazzoni, S., McKenna, F., and Fenves, G. L. (2006), Open system for earthquake engineering simulation user manual, Pacific Earthquake Engineering Research Center, University of California, Berkeley.
9) McKenna, F. T., and Fenves, G. L. (2001), The OpenSees Command Language Manual, Version 1.2, Pacific Earthquake Engineering Research Center, University of California, Berkeley.
10) Mukhopadhyay, M., Choudhury, D., Phanikanth, V.S., Reddy, G.R. (2008), Pushover Analysis Of Piles In Stratified Soil, The 14th World Conference on Earthquake Engineering, October 12-17, 2008, Beijing, China.
11) Pathak,J., Lang, D.H., Building Classification Scheme for the City of Guwahati, Assam, 2013.
12) Pulikanti, S., Ramancharla, P.K. (2013), SSI Analysis of Framed Structures Supported on Pile Foundations: A Review, Frontier in Geotechnical Engineering, Volume 2, Issue 2, pp. 28-38.
13) Ravishankar, P., Satyam, N. (2014), Dynamic Analysis to Study Soil-Pile Interaction Effects, International Journal of

Earth Sciences and Engineering ISSN 0974-5904, Vol. 07, No. 04, August, 2014, pp. 655-658.

14) Sharma, N., Pathak, J. and Goswami, D. (2016): Soil-Pile Interaction Under Dynamic Load: State-of-the-art, Proceedings of the 1st International Conference on Civil Engineering for Sustainable Development – Opportunities and Challenges, held from 19th to 21st December 2016 in Guwahati, Assam, 79-83.
15) Tabatabaiefar, S.H.R., Fatahi, B., Samali, B. (2013), Lateral seismic response of building frames considering dynamic soil-structure interaction effects, Structural Engineering and Mechanics, Vol. 45, No.3, pp. 311-321.
16) Teymur, B., and Şekerer, Z. (2013), Behaviour of Laterally Loaded Piles, Proceedings of International Conference on Case Histories in Geotechnical Engineering, April, 29 – May, 12, 2013, Missouri University of Science and Technology, Chicago, Paper No. 8.12 a.
17) Yang, Z., Lu, J., and Elgamal, A. (2004), A web-based platform for computer simulation of seismic ground response, Advances in Engineering Software, 35(5), 249-259.

Soil quality assessment and its impact on agriculture demand

Kalita, P.

Junior Engineer, Department of Irrigation, Guwahati West Division, Guwahati -08, India.

ABSTRACT

Soil is a complex, dynamic and heterogeneous body of material. The purpose of studying any soil sample is to gather as much as information as possible about a particular soil. Soil properties vary spatially both on the surface and among the horizons of a given profile. In irrigation, agriculture is facing new challenges that require refine management and innovative design. Meeting these challenges require improved prediction of irrigation water required. Irrigation water requirements can be defined as the quantity or depth of irrigation water in addition to precipitation regarding to produce to desired crop yield and quality and to maintain an acceptable salt balance in the root zone. This quantity of water must be determined for such uses as irrigation scheduling for a specific fields and seasonal water needs for planning, management and development of irrigation projects. Depending on the available water storage capacity of soils and the crop rooting depth, irrigation may be needed for short periods during the growing season in this area. The objective of the research is to determine the nutrients present in the soil as per the water requirements for the purpose of the irrigation.

Keywords: soil water mechanism, permanent wilting point, field capacity, irrigation requirement, CROPWAT 8

1. INTRODUCTION

A soil quality is the ability of a soil to perform functions that are essential to people and environmental soil analysis involves steps of collection of sample in the field, subdivision in the laboratory and analyse it .It is important to consider the field water balance to determine the irrigation water requirements .Plant roots require moisture and oxygen to live where either is out of balance root function are slowed and crop yield reduced. All crops have critical growth periods when even small moisture stress can significantly impact crop yield and quality, critical roots used periods vary crop by crop. To mitigate this problem, and to obtain optimum yields of crops in agriculture, quality of agricultural soil has been analysed. In this study soil has been collected from three locations in agricultural field at three depths and various tests have been performed to assess the soil quality in terms of agricultural requirements .On the basis of soil water characteristics obtained from test results, the Irrigation demand of a particular crop has been evaluated with the help of CROPWAT8 model.

2. STUDY AREA

2.1 Sample collection

To study the problem, two locations have been selected in agricultural field. First location is near an irrigation Canal present in Maloibari area. Second location is at a distance of about 3m from the irrigation canal (location external mentioned).Third one is at the agricultural field of Assam Agriculture University ,Jorhat .

Fig 1 Agriculture field of Sonapur and Assam Agriculture University ,jorhat

From each location, samples have been collected at three depths viz. (0-30) cm, (30-60) cm and (60-90) cm respectively during the period of Februaryto March period.

2.2 Data collection

To study the soil sample and to quantify the water and nutrients requirements, required data like Rainfall, Sunshine, temperature, humidity and wind which are used as input data in CROPWAT 8 model has been collected from R.M.S(Regional Meteorological Station), Guwahati.

3. QUALITY ANALYSIS

3.1 Chemical and Physical parameters

Field capacity ,Permanent wilting point , available moisture content and maximum water holding capacity are important physical parameters to analyze soil water

characteristics.On the basis of first part of the study, soil is classified and the results of experimental data shown in Table 1.0 and Table 2.0

Table 1.0 Results of soil quality analysis (Soil chemical and Soil fertility analysis)

Sample	Depth	Types of soil	OC in (%)	Rating	N in kg/ha	Rating	P in kg/ha	Rating	K in kg/ha	Rating	pH	Rating
Sample 1(SonapurMaloibari)	0-30	Sandy Loam	0.96	High	315	medium	54	medium	145	medium	5.57	Acidic
	30-60		0.24	Very low	109	Very low	74	High	98	low	6.14	Acidic
	60-90		0.09	Very low	66	Very low	46	medium	93	low	6.34	Acidic
Sample 2(SonapurMaloibari)	0-30	Sandy Loam	0.75	High	84	Very low	28	medium	66	low	6.6	Acidic
	30-60		0.21	Very low	101	Very low	33	medium	82	low	6.51	Acidic
	60-90		0.27	Very low	118	Very low	31	medium	87	low	6.47	Acidic
Sample 3(Jorhat)	0-30	Sandy Loam	2.0	very high	612.01	High	50	medium	36	low	6.12	Acidic
	30-60		1.9	very high	583.44	High	40	medium	46	low	6.85	Acidic
	60-90		1.7	very high	526.3	High	127	medium	36	low	5.86	Acidic

Maximum Water holding Capacity (MHC), Field Capacity (FC), Permanent Wilting point (PWP) and Available Moisture Content (AMC) are determined with the help of Keen Box (K Box) test and Pressure Plate Apparatus and it is shown in Table 2.0.

Table -2.0 Results of soil quality analysis (Soil Physical analysis)

Sample	Depth (cm)	MHC (%)	F.C (%)	PWP (%)	AMC (%)
Sample 1	0-30	54.19	45.18	15.55	29.63
	30-60	51.04	36.73	12.26	24.47
	60-90	56.93	35.16	12.22	22.94
Sample 2	0-30	53.14	38.46	12.90	25.56
	30-60	60.26	38.32	11.01	27.31
	60-90	53.60	42.86	13.88	28.98
Sample 3	0-30	41.63	22.86	4.41	18.45
	30-60	40.97	22.46	5.41	17.05
	60-90	41.28	22.97	5.00	17.97

3.2 Irrigation requirement

For raising a field crop effectively, it is essential to supply water through artificial irrigation supplementing the rain falling over the plot of land and raising the soil moisture .Crops require water mainly to meet evapotranspiration demands. In many instances, waste of water means that fewer acres of land can be irrigated. Irrigation efficiencies may be improved through the use of better irrigation methods, practices, and better system designs considering the soil moisture condition of agriculture field. CROPWAT is a water balance- based computer program to calculate crop water requirements and irrigation water requirements from climate and crop data. The results which are shown in Table 1.0 and Table 2.0 are used in CROPWAT 8 model to quantify Irrigation requirement and results obtained from the modeling has been tabulated in Table 3.0.

Table3.0 Results of water analysis (CROPWAT 8 Model)

Sample	Depth (cm)	Drainable porosity (%)	Irrigation Required (mm/dec)
Sample 1	0-30	9.01	122.9
	30-60	14.31	134.5
	60-90	21.77	158.7
Sample 2	0-30	14.68	161.0
	30-60	21.94	135.0
	60-90	10.74	144.3
Sample 3	0-30	18.77	204.2
	30-60	18.51	205.8
	60-90	18.31	204.1

4. COMPARISIONAND DISCUSSION

4.1 *Bulk Density and Maximum Water Holding Capacity*

Bulk density is the mass per unit volume of an oven dry soil.Soils with a high bulk density due to compaction have

limited water holding capacity and often restricted drainage and Soils with a low bulk density have a large total pore volume however their drainage or moisture holding properties is influenced by the size of the pores which is largely a function of soil texture.

Table4.0 Comparision between Bulk Density and Maximum Water Holding Capacity

Sample	Depth (cm)	Bulk Density Gram/cc	maximum water holding capacity (%)
Sample 1	0-30	1.62	54.19
	30-60	1.72	51.04
	60-90	1.62	56.93
Sample 2	0-30	1.76	53.14
	30-60	1.53	60.26
	60-90	1.59	53.60
Sample 3	0-30	1.34	41.63
	30-60	1.3	40.97
	60-90	1.34	41.28

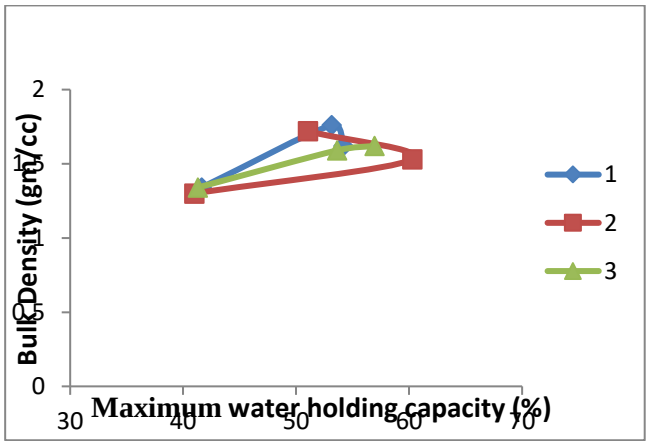

Fig3.0 Maximum water holding capacity versus Bulk Density plot

4.2 Organic carbon and Maximum Water holding capacity relationship

Soil water holding capacity is influenced by the organic matter level in the soil. Soils with a high level of organic matter will hold more plant available water than lower organic matter soils. But soil organic carbon is only carbon component of organic compounds. From the study, results are graphically represented forthree samples at three different depths .It is found that the lower value of organic carbon content shows higher value of maximum water holding capacity. The relationship between them is shown in figure 4.0.

Table5.0 Comparision between Organic carbon and Maximum Water Holding Capacity

1. Sample	2. (0-30) cm		3. (30-60)cm		4. (60-90)cm	
	5. Organic carbon in kg/ha	6. Maximum water holding capacity (%)	7. Organic carbon in kg/ha	8. Maximum water holding capacity (%)	9. Organic carbon in kg/ha	10. Maximum water holding capacity (%)
11. Sample 1	0.96	54.19	0.24	51.04	0.09	56.93
12. Sample 2	0.75	53.14	0.21	60.26	0.27	53.6
13. Sample 3	2	41.63	1.9	40.97	1.7	41.28

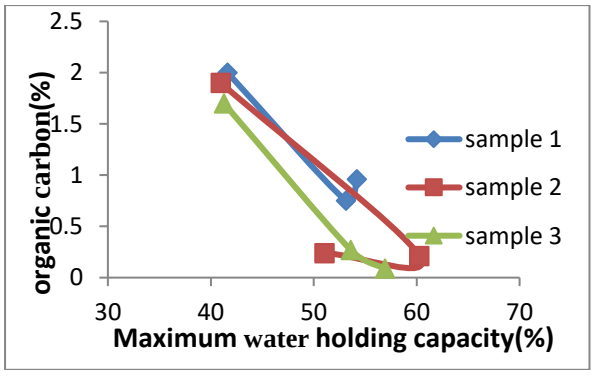

Fig4.0 Maximum water holding capacity versus Organic Carbon plot

4.3 Field Capacity and Irrigation Requirement relationship

The field capacity has been calculated using pressure plate apparatus and irrigation requirements from CROPWAT8 model. The relationship between field capacity and irrigation requirements of three samples at three depths

has been shown in figure 5.0.

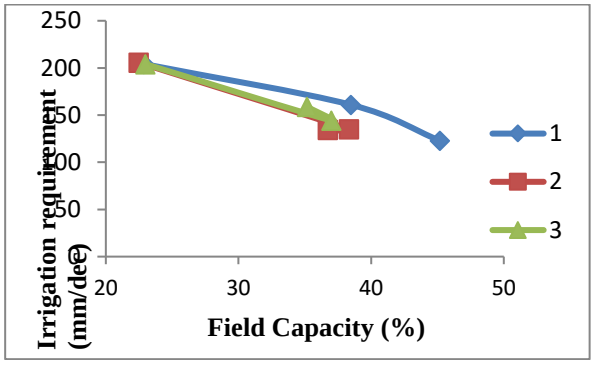

Fig5.0 Field capacity versus Irrigation requirement plot

5 CONCLUSIONS

In many instances waste of water means that fewer acres of land can be irrigated. Frequently water losses through percolation, together with canal losses, may raise the water table high enough to require the installation of an expensive drainage system and/or cause a reduction in crop yield. It is responsible, occasionally, for developing a serious alkali problem. Irrigation efficiencies may be improved through the use of better irrigation methods, practices, and better system designs, though it is assumed that the amount of irrigation water required depends upon how much is available from other sources. The following points may be noted from the study –

1. From quality analysis through three samples at three depths 0-30 cm , 30-60 cm and 60- 90 cm it is seen that all soil samples are sandy loam soil with acidic in nature**.**

2. Nitrogen content in Sonapur soil sample is lower than Jorhat AAU campus soil sample .

3. Maximum water holding capacity of first soil sample decreases and in second sample it increases with depth.

4.Lower organic carbon content of soil particular Sample signify higher value of maximum water holding capacity and lower maximum water holding capacity of soil in that Sample among the depths carry higher bulk density .Only in sample three the maximum water holding capacity is higher with higher value of organic carbon .

5. From CROPWAT 8 model analysis it is seen that for the sample of a particular location for higher value of field capacity, irrigation requirement is lower.

From this soil quality analysis it is recommended the rating of soil sample in different depths in different location and from this rating amount of required nutrients which to be applied to crop with minimum pollution of underground water , water logging and soil salinity problem .Secondly data collected from soil quality analysis is used as input in CROPWAT 8 model and irrigation water required is estimated under effect of climate to protect the irrigation system from ill aeration of soil and from colder and damper climate .Using both nutrients contents and water requirements data to crop for a particular crop ,farmers may be benefited and health of soil can be improved for better achievement in agriculture .

REFERENCES

1) Almeida Monteiro ,J.EBoffino de, CostaAzevedo,Leticiada , Assad, E. D., and Sentelhas, P. C., (2013) ,Rice yield estimation based on weather conditions and on technological level of production systems in Brazil , Pesq.
2) Muhhamamad, A. and Majeed, A.(2006) , Water requirements of major crops for different agro –climatic zones of Balochistan , IUCN , ISBN: 969-8141-85-5.
3) Banik ,P. ,Tiwari N.K. and Ranjan,S.(2014),Comparative Crop Water Assessment Using CROPWAT, IJSMPE , Volume 1 ,ISSN 2374 –1651
4) Allen R.G ,Pereira L.S , Raes, D. and Smith, M.(1998), Crop evapotranspiration :Guidelines for computing crop water requirement .Irrigation and drainage paper 56 ,FAO ,Rome
5) Gogoi, N., Barua, J.P., and Nath,D.C.,(2015), Analytical procedures and FertiliserRecomendations for Soil Health Card of Assam ,horticulture Research
6) Anderson SH and Cassel DK 1986 . Statistical and autoregressive analysis of soil physical properties of Portsmouth sandy loam .Soil Science society of American Journal50 :1096-1104
7) Hillel d 1982 : Introduction to soil physics :Academic Press .San Diego California
8) Doorenbos .J and Pruitt W.O 1975 Guidelines for predicting crop water requirements .irrigation and drainage paper 24 , FAO ,Rome.
9) Hanks RJ and Hill RW 1980 .Modelling crop responses to irrigation ,Intl Irrig info Ctr , Bet Dagan, Israel

Reengineering of geotechnical investigation with continuous energy logging for sustainable design and construction of structures

Sarma, D.[1]

[1]Dean International Affairs and Professor, Assam down town University, Guwahati-781026, India.

ABSTRACT

Essential requirement for sustainable design and construction of structure is obviously comprehensive subsurface characterisation which is difficult to achieve through the common practices of sounding and sampling conducted at the selected locations of the exploration boreholes. Further, reliability of investigation largely depends on the driller and any missing information on penetration tests and on loose or soft materials may negate the advantages of geostatistical approaches for subsurface characterisation and their modelling. Although validation is debatable, a meaningful application of probabilistic modelling of profiles and spatial variability of parameters can only be achieved through comprehensive characterisation of subsurface in the exploration boreholes. Developing an integrated exploration technique an innovative 'Continuous Energy Logging' (CEL) was practised for general and forensic investigation, risk and reliability analysis, and performance based design and analysis by recording disparity in encountered subsurface and modelling continuous characteristics. 'CEL' was found to be economical, advantageous in operation, and reliable over conventional shell and auger, percussion, and wash-boring techniques due to its unique integrated facilities. This paper outlines the reengineering of geotechnical investigation with 'CEL'.

Keywords: reengineering, geotechnical investigation, continuous energy logging, reliability of investigation, forensic investigation, geostatistical method, characteristic interpretation.

1. INTRODUCTION

The last few decades have witnessed considerable developments in structural analysis and design of structures for sustainability against heavy-static and earthquake forces. Based on the model tests new theories have been developed and being applied for design of skyscrapers, heavy civil engineering offshore, onshore and underground structures, and long-span bridges. All such structural designs are based on the consideration that the foundation soil/rock would safely withstand the forces without perceptible deformations. With similar comparable developments in soil and rock mechanics too, prediction of bearing capacities of foundation soil/rock within permissible vertical and differential settlement is now possible for different static and dynamic conditions. However, there are several case-histories where collapse of structures is due to the failure of foundation soil/rock rather than structural elements. One of the reasons attributable to such type of failure is the inadequate characterisation of subsurface due to incomprehensive subsurface investigations and deceptive extrapolation of subsurface properties from the information of exploration boreholes.

The essential requirement of comprehensive investigation of subsurface was particularly appreciated upon noticing failure of almost all the initial test piles for the foundation of 100m high super heavyweight telecommunication tower in northwest Assam, Republic of India. The design of foundation was based on subsoil investigations following standard specifications and hence failure investigation was undertaken by the Department of Telecom. Inspired from the necessity, the technique of 'Continuous Energy Logging' (CEL) was developed by the author (Sarma 2008) for facilitating comprehensive investigation of subsurface in the exploration-holes and eventually applied in practice, starting with the forensic investigation of the failure of initial test piles in 1990. The application of 'CEL' for the forensic investigation of the failure of piles revealed encounter of a soft alluvial stratum of 500 to 900 mm thick within the active zone of the pile base, existence of which was not recorded in the subsurface investigation report, possibly due to the oversight of the driller. Subsequently 'CEL' technique was adopted for subsoil investigations of a number of important projects in northeast India. Such subsoil investigations were focused for the risk and reliability analysis and for the performance based design and analysis of structures. The outcome of 'CEL' in terms of continuous-characterisation- modelling of the design parameters in exploration-holes is

particularly found useful for the Performance Based Design and Analysis of Foundation. In this paper critical aspects of the practices of prevailing investigation techniques, scope and limitations of the practices of geostatistical methods, development and practising experience with CEL technique and its characteristic interpretations are discussed with an approach to characteristic modelling for reengineering of geotechnical investigation. Moreover, practising potential in various countries, its other applications, and continuing further developments are also indicated

2 PREVAILING INVESTIGATION TECHNIQUES

Where information on 'existing local knowledge' is not adequate, the Indian Standard (IS 1982:1979) has specified geophysical investigations for site reconnaissance in order to acquire useful information on stratifications. Among the common geophysical methods, both electrical resistivity and seismic wave methods have been recommended in order to distinguish reasonable changes in relevant properties of subsurface, namely, electric conductivity and elastic properties, measuring which subsurface formation is investigated.

In exploratory investigation programme, depending upon the nature of structure(s) proposed the disposition and spacing of trial pits and exploration-holes are recommended such as to reveal any major changes in the stratifications. In such investigations besides in-situ tests, representative samples are also collected for confirmation through laboratory investigations. Further, besides exploratory drilling, locations of continuous sounding, as for example, static and/or dynamic cone penetration tests (SCPT/DCPT) is also recommended in grids for penetration record. More advanced methods of logging of exploration-holes by radioactive methods are also suggested in the detailed investigations.

With such widely covered specifications it is in-deed possible to get comprehensive characteristics of subsurface through careful combination of different techniques, however, at considerable cost and time. In recommending exploratory investigations various feasible techniques are suggested, out of which, shell and auger, percussion, wash-boring, and rotary drilling are mostly used. Based on the principle of operation both wash and rotary drilling are comparable; the difference is in their tools only. The exploration technique, adopted to practice 'CEL', was based on an integrated approach wherein most of the activities were similar to wash-boring and found to be economical and rapid, fulfilling the requirements of Indian Standard. Wash-boring has also been widely used in North America and occasionally in Britain (BS 5930: 1999). In conjunction with Standard Penetration Tests (SPT) wash-boring may be carried out more satisfactorily in South Africa (CSRA 1993). Wash boring with SPT and sampling at selected spacing in soil and continuous coring in rock is a recommended practise in Australia. It is practised to log soil variations from the settling tank. Generally water is recommended as the drilling fluid, and if stability becomes an issue bentonite and polymer additives are recommended to aid the drilling. By logging the soil variations the preliminary subsurface profile model is either confirmed or adjusted appropriately (AS 1726). Therefore, within the scope of the requirements of North American, British, South African and Australian specifications the practice of 'CEL' is possible.

3 CRITICAL ASPECT OF PREVAILING PRACTICES

In the prevailing electrical resistivity methods (IS 1982: 1979), variation of mean resistivity among different types of clay, silt and sand are generally insignificant as resistivity depends primarily on constituent minerals. Further, it is common in electrical and electromagnetic geophysical methods to define the electrical characteristics of a thin layer by its conductance, i.e., the ratio of its thickness and conductivity, because it is difficult to separately determine the thickness and resistivity of thin layers (Lahti et al 1991). Therefore, unless costly equipment of high-resolution is used, the specified geophysical methods may not distinguish thin soft/loose materials for their characterisation during exploratory investigations. It is also possible that these geophysical investigations may give dubious results in the case of grounds having high water table, high moisture regime, or frosts. According to British Standard (BS 5930: 1999), interpretation of resistivity soundings may not necessarily provide a definite solution, because the theoretical models assume unrealistic horizontal strata. Further, inherent problem of ambiguity, as number of models fit the resistivity data, compels interpretation of a model that is consistent with the geotechnical information derived from borehole investigation. In concluding the seismic wave methods, it is recommended (BS 5930: 1999) to calibrate seismic velocity data by laboratory tests on borehole cores.

In recommending exploratory investigations, limitations of prevailing boring/drilling techniques are also mentioned in the referred code of practices.

In describing mode of operations of shell and auger, and percussion drilling, their drawback due to rapid pulverisation of encountered materials is considered as major limitation by the referred code of practices for monitoring changes of stratifications. Similarly, in describing the mode of operation for wash-boring, it stipulates the changes of stratifications through 'good guess' from the rate of progress and colour of wash water (drilling mud). However, it is possible that such 'good guess' from the rate of progress may be subjective depending upon the experience of the driller and may vary considerably with individuals. Further, as the colour of circulating wash water is dominated by the colour of drilling mud (usually bentonite slurry), only a highly experienced driller can identify the changes of stratifications from the slight changes of the colour of circulated drilling mud. Therefore, critical observations, choice of sampling, and sounding at the depths other than specified largely remains with the driller. In context to collection of samples the referred code of practices have specified that the extruded materials out of wash-boring are not representative and therefore samplings for all types of tests need to be carried out separately. Further, possibility of undisputable logging and proper record of thin loose/soft stratifications following wash-boring method is debatable from the practical aspects.

It is worth mentioning that during specifying in-situ tests and undisturbed sampling in the item of works of detailed subsoil investigation, a spacing not exceeding 1.5 m within a continuous stratum is generally specified including additional sampling and in-situ tests at every change in strata. For determination of stratum properties, using equipment normally available for sampling and testing, it is specified (BS 5930: 1999) Standard Penetration Tests (SPT) at the top of each new stratum of sand and gravel and thereafter at one metre intervals. Disturbed sampling of such material is specified at the top of each new stratum and thereafter at 1.5 m intervals. Similarly, for cohesive soil, collection of 100 mm diameter samples is recommended at the top of each new stratum and thereafter at 1.5 m intervals. In case of inadequate recovery, SPT is recommended to follow immediately. In practice, it has been observed during advancement of boring that by the time an encounter with soft/loose soil is perceived, necessity of sampling or sounding sometimes becomes redundant, particularly when thickness of such stratum is thin. Therefore, influence of human factor and its negative impacts in exploratory investigations cannot be ruled out. Despite identification during preliminary investigation, such situation may reoccur even in detailed investigation, as the depth of such a stratum may vary considerably between normally spaced boreholes unless additional boreholes are investigated by the side of previous boreholes. Unless pre-planned, this is not generally done provided additional funds are available and when delayed decision is not expected. Case studies revealed that even with thin unnoticed soft/loose stratum an overlaying structure may experience excessive vertical / differential settlements. On the other hand critically sustaining structures may suffer catastrophic settlement during an earthquake.

Among the common techniques of exploratory investigations, it is possibly the rotary-core-drilling which is generally the preferred choice for investigation of rocks for civil engineering purposes without much alternative(s), despite this being an undesirable choice for sandy and/or clayey deposits. Unless core samples are obtained, identification of subsurface materials during the progress of drilling is equally problematic like wash-boring and percussion drilling. However, with the advancements in the technique of instrumented rotary drilling that enables record of mud pressure, down thrust, rotation, and time component, continuous characteristic response of encountered rock is possible for civil engineering purposes (Gui et al 2002). Unfortunately, mobilisation of rotary drill is relatively costly and generally not feasible for all types of projects unless impenetrable stratum is expected within the general extent of exploration.

In all the prevailing and commercially feasible exploratory investigation techniques the process of withdrawing boring and drilling tools, for sampling and in-situ testing, and subsequent reinsertion for further advancements is a serious disadvantage in terms of time consumption particularly with increasing depth.

4 APPLICATION OF GEOSTATISTICAL METHODS

Uncertainties in subsurface investigation which imparts statistical trends and/or random variation can be analysed by statistical methods. Standard univariate or multivariate analytical techniques cannot deal with the spatial variable data as applicable to subsurface half-space. Such spatial variable data may be analysed by geostatistical methods.

Various geostatistical methods have been developed for prediction of missing information among which semivariogram analysis and kriging estimation can be used for analysis of variable subsurface properties and their characteristics at any missing or desired locations. Application of these methods to linear and two dimensional fields have already been practised in geotechnical

engineering and satisfactory levels of correlations were reported based on analysis of field data of 27 boreholes for linear and 23 boreholes for two-dimensional fields (Aitch et al 1999). Based on the above analysis, predictions were made for 2 and 12 numbers of locations for linear and two-dimensional fields respectively. Results indicated that these potential methods can be used efficiently for improving quality of detailed investigations or for planning further investigations based on preliminary information.

The result of geostatistical analysis (Aitch et al 1999) revealed that the estimated values were deviated from field value to a maximum extent of 16.7% and 13.51% for linear and two dimensional fields respectively. The average deviations are, however, 5.7 and 3.8 % for linear and two dimensional fields respectively indicating fair reliability in prediction. For reliable prediction at least eight samples were expected in the influencing zone (Issacs et al 1989). Therefore, reliability of such prediction would obviously suffer in case of missing information, as for example, unnoticed thin layers of soft/loose materials during exploratory investigations.

5 DEVELOPMENT OF 'CEL' TECHNIQUE

The integrated exploration technique which was adopted to practice 'Continuous Energy Logging' (CEL) is a development taking all the advantageous principles of wash-boring and light percussion drilling whilst overcoming most of their demerits. The three phases of the drilling operations, namely, disintegration of subsurface materials, disposition of disintegrated materials, and stabilisation of exploration-hole, are carried out by an integral process. Therefore, unlike prevailing exploratory investigation techniques the process of withdrawing boring and drilling tools, for sampling and in-situ testing, and subsequent reinsertion for further advancements is not necessary. This enables considerable saving of time vis-à-vis cost.

The operation principles pertaining to the three phases of the drilling operations for 'CEL' were well documented (Sarma 2008). It was also described the outlines of various tools needed and how they function. Further, it was also detailed how continuous energy logging was derived from the penetration record and energy input in K-Joules. Furthermore, it was also described how from such 'CEL' profile extent of disparity of encountered subsoil was monitored, mitigating human factor and its negative impacts in exploratory investigations. Detailed elaboration of drill-bit and head-assembly are restricted owing to author's intellectual right pending status.

6 PRACTISING EXPERIENCE WITH 'CEL' TECHNIQUE

The integrated exploration technique, which was adapted to practice 'CEL' technique, was developed by the author to overcome the general demerits associated with wash-boring and percussion drilling as outlined above. Since the year 1990, the 'CEL' technique had been practised advantageously in a number of important projects in northeast India, the most earthquake prone region of the country. In this exploration technique, a simple derrick was used for hoisting and drilling operations. Depending upon the height of the derrick, segments of drill pipes of length 2.5 m and of nominal bore up to a maximum of 100 mm were used with both ends threaded to attach with the assembly as boring progressed.

In all the investigation sites it was noticed that soils, having at least some cohesion, move up in the form of cores for collection at the ground surface. Such core samples were considered representative for classification tests and no separate samplings were found necessary. Moreover, crumbling the cores of those representative samples continuous visual identification was possible as drilling progressed.

Unlike cohesive soils, collection of representative samples of pure granular materials requires a little extra care despite simple identification process. Depending upon the depth of boring, viscosity and velocity of the drilling mud, size and shape of particles, the disintegrated materials drift up to the ground surface at different times. It is obvious that due to buoyancy and thrust of viscous drilling mud all the materials up to particle size of around 75 mm generally drift up to ground level as noticed during geotechnical investigation for construction of Tezpur Central University in India. However, it was noticed that smaller size particles drift up quicker than larger particles, which gradually accumulate at the bottom of the borehole building-up higher velocity of the drilling mud due to gradual reduction of inter-particle void at the bottom of drill pipe and eventually drift-up once the critical velocity is attained. The only considerable fact is that the particles do not drift up simultaneously and therefore relatively larger volume of granular materials is needed for relevant tests. Unlike wash-boring this process does not have any scope for contamination with upper borehole materials as particles drift up through the inner hollow-core of the assembly. Moreover, intermittent stages of sampling and in-situ testing are simple and rapid. The head assembly can be removed and reinstalled within 2 to 3 minutes making sampling and in-situ testing much simpler to perform.

In the project sites, bedrock was seldom encountered within 50 m extent of the exploratory investigation making this technique a self-reliant without support of any rotary drilling. However, similar to wash-boring and percussion drilling, this technique also requires additional support when impenetrable stratum encounters. Such deposits of cobble, encountered boulders, and bedrocks can be penetrated supported by a rotary drill. 'CEL' technique can be continued in such rock explorations logging continuous energy from the information on down thrust and rate of penetration/drilling.

The rotary drill can be mobilised without withdrawal of the drill-pipe-assembly, which acts like a casing during the operation of rotary drill and/or chisel bit. Lowering of rotary drill-bit is possible simply by replacing topmost standard segment of the drill-pipe-assembly with head by appropriate one, whenever necessary.

7 CHARACTERISTIC INTERPRETATIONS

A typical plot of 'Continuous Energy Logging' (CEL) of two boreholes 10 m apart at the site of Export Promotion Industrial Park, North Guwahati (India) is shown in Fig. 1 along with SPT ('N' values) and undrained cohesion (C_u) in KPa at comparable sampling depths of borehole 2 and 3. The idealised subsoil profiles were designated based on visual features and index properties, where CH and CI denotes cohesive soils of highly and intermediate plasticity respectively in conformity to Indian Standard. It is apparent from the figure that within any designated stratum, considerable amount of disparity possesses and linearly varied or uniformly extrapolated laboratory test results can contradict actual ground situations whether with or without application of appropriate 'factor of safety'. Unlike common practices of drawing characteristic profiles connecting individual SPT values and selected subsoil properties, it is the considered opinion of the author that such profiling may be ambiguous as the test results testify properties only at specific locations. Such ambiguity can be overcome drawing characteristic profiles based on 'CEL' response for various risks scenarios.

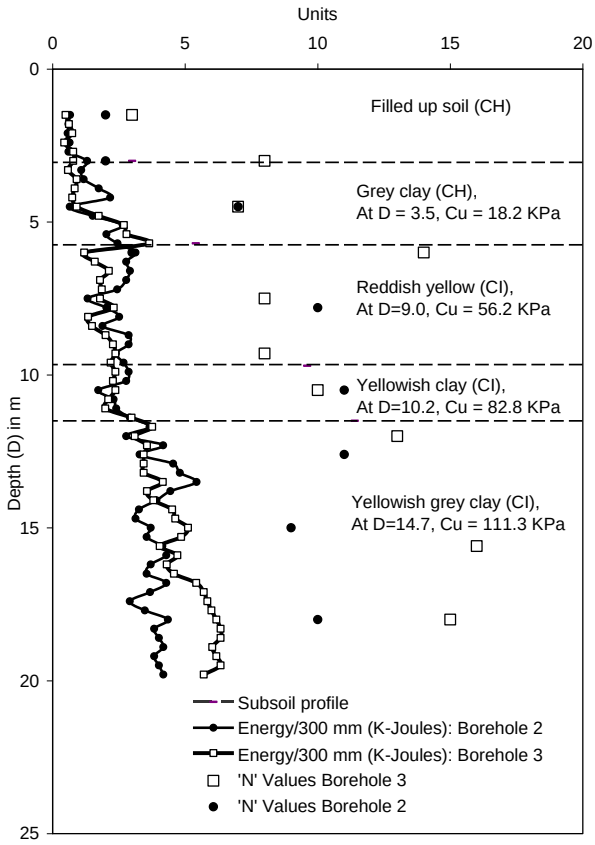

Figure-1. 'CEL' profile, SPT values, and subsoil characteristics for Borehole 2 & 3 at the site of Export Promotion Industrial Park, North Guwahati, India.

In this developing technique, characteristic profiles of shear strengths and densities of soil are modelled simulating field scenarios based on available laboratory test results, in-situ testing, and the 'CEL' response. Such approach to modelling of characteristic profile is adopted expressing the recorded response of 'CEL' as:

$$D = f(x) \qquad (1)$$

where, 'D' and 'x' are the depth and the corresponding unit of 'CEL' respectively. Based on equation (1), the characteristic function of a dependent parameter at a depth 'D' and at a horizontal distance 'Δ' from 'CEL' response can be expressed as:

$$D_{i,j} = f(x) + \Delta_{i,j} \qquad (2)$$

wherein $D_{i,j}$ and $\Delta_{i,j}$, 'i' denotes type of parameter and 'j' the relative value of specific parameter. The above equation can be expressed for two limiting scenarios as 'conservative' and 'generous' by equations (3) and (4) respectively:

$$D_{i,j_{\min}} = f(x) + \Delta_{i,j_{\min}} \qquad (3)$$

$$D_{i,j_{\max}} = f(x) + \Delta_{i,j_{\max}} \qquad (4)$$

For number of specific parameter 'n' the 'moderate' scenario of equation (2) can be expressed as:

$$D_{ij_{av}} = f(x) + \frac{\sum_{i,j=1}^{i,j=n} \Delta_{i,j}}{n_{i,j}} \quad (5)$$

Based on the above equations, characteristic spectra of design parameters are derived for the entire depth of exploration for three scenarios, choice of which depend on the importance factor, and used for forensic investigation, risk and reliability analysis, and performance based design and analysis of foundations (Sarma 2008). Characteristic shear strengths of rock may be plotted simulating field scenarios based on down thrust and rate of penetration of drilling tool, Rock Quality Designation, and point load strengths (Gui et al. 2002).

With the emerging practice of geostatistical approaches a meaningful application of probabilistic modelling of subsurface profile and practices of modelling spatial variability of soil parameters is now possible for comprehensive subsurface characterisation with greater level of confidence and accuracy based on 'CEL' information.

Through the application of 'CEL' the uncertainties in the geotechnical parameters can be reduced significantly nullifying the use of arbitrary safety factors so that the actual performance of the structure can be modelled by the foundation engineer. Thus the best estimate of geotechnical performance can be achieved through characteristic interpretation of the geotechnical parameters. Further, reduced uncertainties can help the owners to build safely and economically. Furthermore, actual state of existing buildings can be evaluated through retro-analysis.

8 OTHER APPLICATIONS

With the growing population and number of the megacities across the world, predicted to about 150 by 2025 in comparison to 25 such megacities of population more than 3 million in 2005 (Petrukhin et al 2010), a considerable infrastructure development is expected, wherein, value engineering may be a high demand area for the application of 'CEL' techniques. It is expected that the 'CEL' technique can be one of the tools for evaluation of the pragmatic asset value for insurance and real-estate transactions through risk involve in such infrastructures. Similarly, infrastructure developers can also ensure performance guarantee for the sustainability of structures using 'CEL' technique as one of the tools, particularly in context to various Build-Operate- Transfer schemes.

9 CONTINUING FURTHER DEVELOPMENTS

In this developing practice further improvement of the integrated exploration technique and 'CEL' are in progress for commercial application in Southern Africa and Australia. Mechanical design of the head-assembly is being improved for eliminating the intermittent actuating problem and better efficiency. The general correction necessary to simulate delay between the recorded energy and visual observation of any encountered material is being modelled considering various field conditions. The algorithm required for simultaneous penetration record and energy logging is being developed for constant monitoring and record through electronic database management system. Special provisions for efficient in-situ tests and collection of larger diameter undisturbed samples, without complete removal of the head-assembly, is also planned. Lastly, development of various relationships between 'CEL' and design parameters is progressing.

10 CONCLUSIONS

The integrated exploration technique, which was adopted to practice 'Continuous Energy Logging' (CEL), was found to be economical and advantageous in operation over conventional wash-boring and percussion drilling techniques due to its unique integrated facilities, namely, continuous sounding through energy logging, continuous collection of representative samples for visual identifications and classifications, and relatively simple undisturbed sampling and in-situ testing operations without withdrawal of boring/drilling tools from the exploration-hole. Further, potential human errors on visual identification of stratifications, choice of sampling, and in-situ testing, are considerably overcome in comparison to prevailing techniques. It is possible to carryout detailed investigation, adopting 'CEL' technique, without separate preliminary investigation programme. This integrated exploration technique has unique advantage of mobilising rotary drill for rock exploration without withdrawal of its boring/drilling tools and continue 'CEL'. Functional simulation of encountered subsurface is possible from the energy-log through characteristic modelling for various risks scenarios. Further, subsurface profiling through geostatistical approaches is possible modelling the spatial variability of subsurface parameters with greater level of confidence and accuracy for comprehensive geotechnical investigation for forensic investigation, risk and reliability analysis, and performance based design and analysis of

structures.

11 ACKNOWLEDGEMENT

Author acknowledges thanks to the following establishments on behalf of Diligent Group (India) for trusting him directly or indirectly in adopting 'CEL' technique for subsoil investigation of some important projects in northeast India, namely: Department of Telecom, Guwahati, for construction of 100m high super heavyweight tower foundation in northwest Assam, Guwahati Refinery for construction of OM&S Control and New Flare Towers, Central & Aviation Divisions of Central Public Works Department, Guwahati, for construction of Tezpur Central University, Indian Institute of Technology, Guwahati, and National Institute of Public Co-operation and Child Development, Guwahati, Coal India for construction of Guest House at Guwahati, Assam Industrial Development Corporation for construction of Export Promotion Industrial Park, North Guwahati (India).

12 REFERENCES

1) Aitch, P., Shee, N., and Das, S.C., 1999. Subsoil Characterisation by Heostatistical Methods, Proceedings Indian Geotechnical Conference 1999.
2) AS 1726, 1993. Geotechnical Site Investigations, Standards Australia.
3) BS 5930, 1999. British Standards Institution, Code of Practice for site investigations, British Standard Institute, p-29, 30, 90, 91.
4) CSRA, 1993. Committee of State Road Authorities, Standard Specifications for Subsurface Investigations, ISBN 1-874844-85-2, 1st Edition, Apr '93, Alkantrant, South Africa.
5) Gui, M.W., Soga, K., Bolton, M.D., and Hamelin, J.P., 2002. Instrumented Borehole Drilling for Subsurface Investigation, Journal of Geotechnical and Geoenvironmental Engineering, ASCE, Vol. 128, No 4.2007.
6) IS 1982, 1979. Code of Practice for subsurface investigation for foundations, Bureau of Indian Standards.
7) Issacs, E.H. and Srivastava, R.M., 1989. Applied Geostatistics, Oxford University Press.
8) Lahti, R.M., Hoekstra, P., 1991. Geophysical Survey for Mapping Migration of Brines from Evaporation Pits and Ponds, Proceedings of Symposium on the Application of Geophysics to Engineering and Environmental Problems, University of Tennessee, Knoxville, pp 65-7.
9) Petrukhin, V.P., Ulitsky, V.M., 2010. Preface, Proceedings of the International Geotechnical Conference, 7-10 June '10, Moscow, ISBN 978-5-9902005-2-4.
10) Sarma, D., 2008. Application of Continuous Energy Logging for Comprehensive Subsurface Characterisation, Proceeding of 2nd British Geotechnical Association International Conference on Foundations, 24-27 Jun '08, Dundee, IHS BRE Press, UK, ISBN-13: 978-1-84806-044-9, PP 1819-1828.

Sustainable Infrastructure

Sustainable Structural Solutions

Seismic fragility flow plots for risk assessment of reinforced concrete buildings with open ground storey

Choudhury, T.[1] and Kaushik, H.B.[2]

[1] Ph.D Student, Department of Civil Engineering, Indian Institute of Technology Guwahati, Guwahati – 781039, India.
[2] Associate Professor, Department of Civil Engineering, Indian Institute of Technology Guwahati, Guwahati – 781039, India.

ABSTRACT

Several past earthquakes in India and many other countries resulted in devastating impact on the reinforced concrete (RC) buildings with open ground storey (OGS). These buildings are highly vulnerable to earthquake forces because of inherent vertical irregularity arising from the absence of masonry infill walls in the ground storey that makes the ground storey highly flexible compared to the upper stories with infill walls. Thus, it is of utmost importance to assess the seismic risk associated with such buildings by categorizing their seismic vulnerability for affordable and sustainable housing development. This paper discusses the failure of several low to mid-rise RC buildings with OGS with the help of seismic fragility flow plot (FFP). Seismic fragility can be rapidly assessed using FFPs in combination with simplified demand models that are based on various structural parameters. If the displacement demand for a given seismic hazard is known for a structural system, its seismic fragility can be obtained using FFP for any value of displacement thresholds. The present study is an initiative for fragility based seismic design of buildings using the Fragility Flow Plots.

Keywords: Reinforced concrete buildings, Open ground storey, Seismic fragility, Fragility flow plot

1. INTRODUCTION

Reinforced concrete buildings with masonry infill walls are the most common construction methodology for buildings in different parts of the world. More usually, reinforced concrete buildings with an open ground storey are preferred where the ground storey is left open for various purposes, such as parking, shops, etc. The open ground storey (OGS) buildings are structurally one of the most vulnerable categories of buildings when seismic forces are considered. The relatively flexible ground storey attracts large forces, which the ground storey columns are unable to withstand. Unfortunately, in India and many other developing countries, earthquake-resistant construction standards have not been effectively applied, and special guidelines have not been considered even for important structures, such as school buildings and hospitals. The commercial use of the ground stories without masonry infill walls induces soft stories in reinforced concrete buildings and is one of the significant reasons for the hefty building collapses in an earthquake prone region.

It is not surprising, that each time an earthquake occurs; large damage and destruction of buildings are observed. Thus, it is of utmost importance to assess the seismic risk associated with such buildings by categorizing their seismic vulnerability. Specifically, the need of the time is large-scale seismic vulnerability assessment of buildings and categorizing them for detailed analysis and safety. Such large-scale assessment is only possible when simplified methods are available. The present paper considers several case studies related to the failure of open ground storey buildings in the past. A simple and rapid method is chosen for assessing the seismic demand and fragility of the case study buildings to verify the damage incurred.

2 SEISMIC RISK ASSESSMENT

Seismic risk assessment of a structure is to predict its probability of damage and economic losses subjected to a seismic hazard. Generally, it requires estimation of seismic fragility to assess structural vulnerability. Seismic vulnerability is a measure of the seismic strength or capacity of a structure with respect to some demand imposed on it. Calvi et al. 2006 defined seismic vulnerability of a structure as its susceptibility to damage by ground shaking of a given intensity. The aim of vulnerability assessment methodology is to obtain the probability of a given level of damage to a given building type due to a scenario earthquake. Major objectives of any large-scale vulnerability analysis generally involve:

i. Planning preventive interventions for the seismic risk mitigation,
ii. Helping the management of the emergency after a major earthquake, and
iii. Creating awareness of the impact of an earthquake on a group of buildings in an area.

In assessing the seismic vulnerability, the first step is to assess the building type. Next, vulnerability

models are utilized to represent mathematically these structural types. Vulnerability models are the tools to establish a correlation between seismic hazard and structural damage (Guéguen 2013). Seismic hazard may be represented in terms of peak ground acceleration (PGA) or any other seismic intensity measure. Damage is usually classified in terms of the performance level of buildings. The traditional way of representing the vulnerability of any structure is in the form of vulnerability curves. However, the use of such curves is limited as it represents a single parameter of interest only. More recently, seismic fragility flow plots (FFPs) are introduced (Choudhury and Kaushik 2018a), where, there is no discretization of damage states to obtain the seismic fragility. The use of these fragility flow plots has been appraised here in the present paper for rapid assessment of seismic vulnerability.

3 METHODOLOGY

In the past, severe earthquakes have caused extensive losses of life and property around the globe. Identification of seismically vulnerable buildings within the existing building stock is, therefore, a high priority task in the seismic risk reduction of the urban environment. Much effort has been devoted in recent years to the problem of how to develop reliable estimates, given the large uncertainties that exist. This section briefly talks about the methodology for the estimation of seismic performance (or demand) and evaluating the fragility for vulnerability assessment.

3.1 Seismic demand

Seismic performance (or demand) can be assessed with different levels of computational efficiency depending on available data and resources. The present study utilizes simplified equations (Eq. 1 to Eq. 3) developed through multiple linear regression (Choudhury and Kaushik 2017), also known as seismic demand model, to dedtermine the seismic displacement demand (S_d). It relates several parameters that do not require any complex analysis for rapid assessment of the seismic performance of OGS buildings. The demand models are classified for different range of PGA and are used for determining S_d of a few buildings (as discussed later) that suffered heavy damage as a consequence of past earthquakes.

For PGA > 0.02 to >= 0.3g:

$$S_d \text{ (m)} = 0.04 \times N_b^{0.1} \times N_s^{0.77} \times (1.5 - Op)^{0.3} \times PGA^{1} \quad \text{(R-squared: 0.994; SEE: 0.001 m)} \quad (1)$$

For PGA > 0.3 to >= 0.65g:

$$S_d \text{ (m)} = 0.058 \times N_b^{0.17} \times N_s^{0.94} \times (1.5 - Op)^{0.42} \times PGA^{1.64} \quad \text{(R-squared: 0.993; SEE: 0.004 m)} \quad (2)$$

For PGA > 0.65 to >= 1g:

$$S_d \text{ (m)} = 0.058 \times N_b^{0.2} \times N_s^{1} \times (1.5 - Op)^{0.5} \times PGA^{2} \quad \text{(R-squared: 0.99; SEE: 0.009 m)} \quad (3)$$

Here, N_b and N_s are the number of bays and stories, respectively. *Op* is the central opening size in masonry infill walls, and PGA is the peak ground acceleration.

3.2 Uncertainties

Uncertainties are associated in every step of probabilistic analysis. Uncertainty estimation requires a large number of parametric analysis to be carried out related to capacity and demand estimation of the concerned structure. However, generalized estimated values of different uncertainties for different building typologies are readily available for use in probabilistic seismic risk assessment methodologies (e.g., HAZUS 2013). A generalized uncertainty value of 0.7 is considered in the estimation of seismic fragility in the present study.

3.3 Seismic fragility using FFP

In simple terms, seismic fragility analysis is the comparison of seismic capacity and demand and to estimate whether the seismic capacity is exceeded for a well-defined performance level when the structural system is subjected to specified levels of ground motion intensity. A fragility curve represents a continuous curve representing fragility for a particular damage state. In contrast, fragility flow plots (FFP) can be used that gives a continuous representation of both damage state and seismic demand on the structure. Fragility Flow Plot is independent of discrete damage states, where results of the fragility analyses can be shown for different parameters, such as natural period of vibration, number of bays and stories, and openings in masonry infill walls (Choudhury and Kaushik 2018a).

4 CASE STUDIES: FRAGILITY FLOW PLOT

The details of the case study buildings and assessment of their seismic performance and fragility are discussed in this section.

4.1 Building damage database

Fig. 1 to Fig.3 show the various case study buildings that are partially or totally collapsed during past earthquakes. Most of these buildings had intact upper storeys, whereas, the open ground storey totally collapsed. The absence of masonry infill walls on the ground storey leads to a considerable difference in lateral strength and stiffness between the ground storey and the upper stories of the building. In the event of an earthquake, this difference introduces the ground storey to a large lateral force instead of distributing it over the height of the structure.

The performances of these buildings under seismic conditions are judged with the help of the seismic demand model (Eq. 1 to Eq. 3) and finally, seismic fragility is estimated with the help of FFP. Each of the considered buildings has a unique combination of number of bays, number of stories and opening size in infill walls. These characteristics are taken into consideration carefully and the seismic demand on the

buildings for different hazard conditions are estimated.

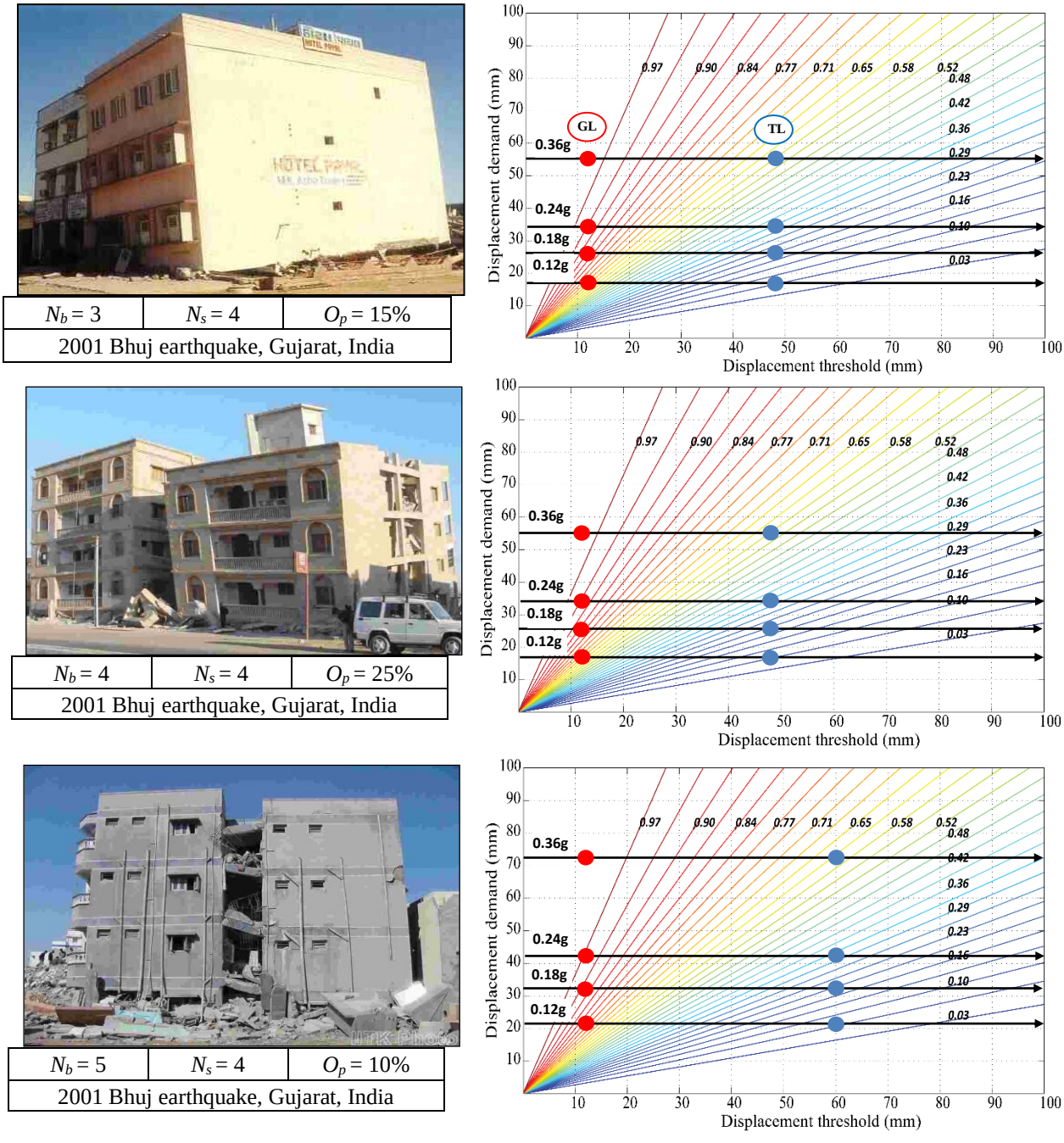

Fig. 1. (a) Collapsed four-storied RC open ground storey buildings, and (b) Fragility flow plot (FFP) showing seismic displacement demand at TL and GL for different PGA levels: 0.12g, 0.18g, 0.24g, and 0.36g.

4.2 Estimation of seismic demand

Determination of seismic demand for building frames based on Eq. 1 to Eq. 3 depends on their geometric configuration and seismicity of the site. For each case study buildings, a two-dimensional frame is judiciously taken and seismic demand is obtained for that frame. Here, seismicity is described in terms of PGA. Four different PGAs are chosen based on DBE and MCE levels as prescribed in Indian seismic code (BIS 2016), viz, 0.12g, 0.18g, 0.24g, and 0.36g. Seismic demand is determined in terms of displacement at the roof or top level (TL). However, it is known that in case of OGS buildings, the interstorey drift in the upper storeys is almost negligible; implying that the seismic demand at the ground level (GL) is more or less similar to that in the top level (TL). This happens due to the soft storey effect instigated by the absence of infill walls at the ground storey of open ground storey buildings. Also, the GL displacement gives a more realistic picture of the damage incurred in a vertically

irregular open ground storey buildings (Choudhury and Kaushik 2018b). Thus, the seismic displacement demands obtained at TL for different PGA levels are simultaneously used as GL displacement demand, and further seismic fragility is estimated as represented in Fig. 1 to Fig. 3 using FFP.

4.3 Seismic fragility

Seismic fragility of the case buildings is estimated with the aid of fragility flow plot (FFP). Fig. 1(a) shows four-storied buildings with open ground storey that collapsed during the 2001 Bhuj earthquake. Each building had small to large openings and number of bays varying from three to five that are considered appropriately for the estimation of seismic displacement demand. It is generally perceived that an increase in the number of bays should lead to an increase in global stiffness of the frame, thereby reducing the displacement demand on it, as well as the vulnerability to earthquake hazard. Surprisingly, observation during past earthquakes was not similar to this perception in case of open ground storey buildings. Buildings with different configurations of bays with the same number of stories, all suffered huge damage. None of the case study buildings considered here survived during the earthquake shaking (as can be clearly seen in the building photographs.

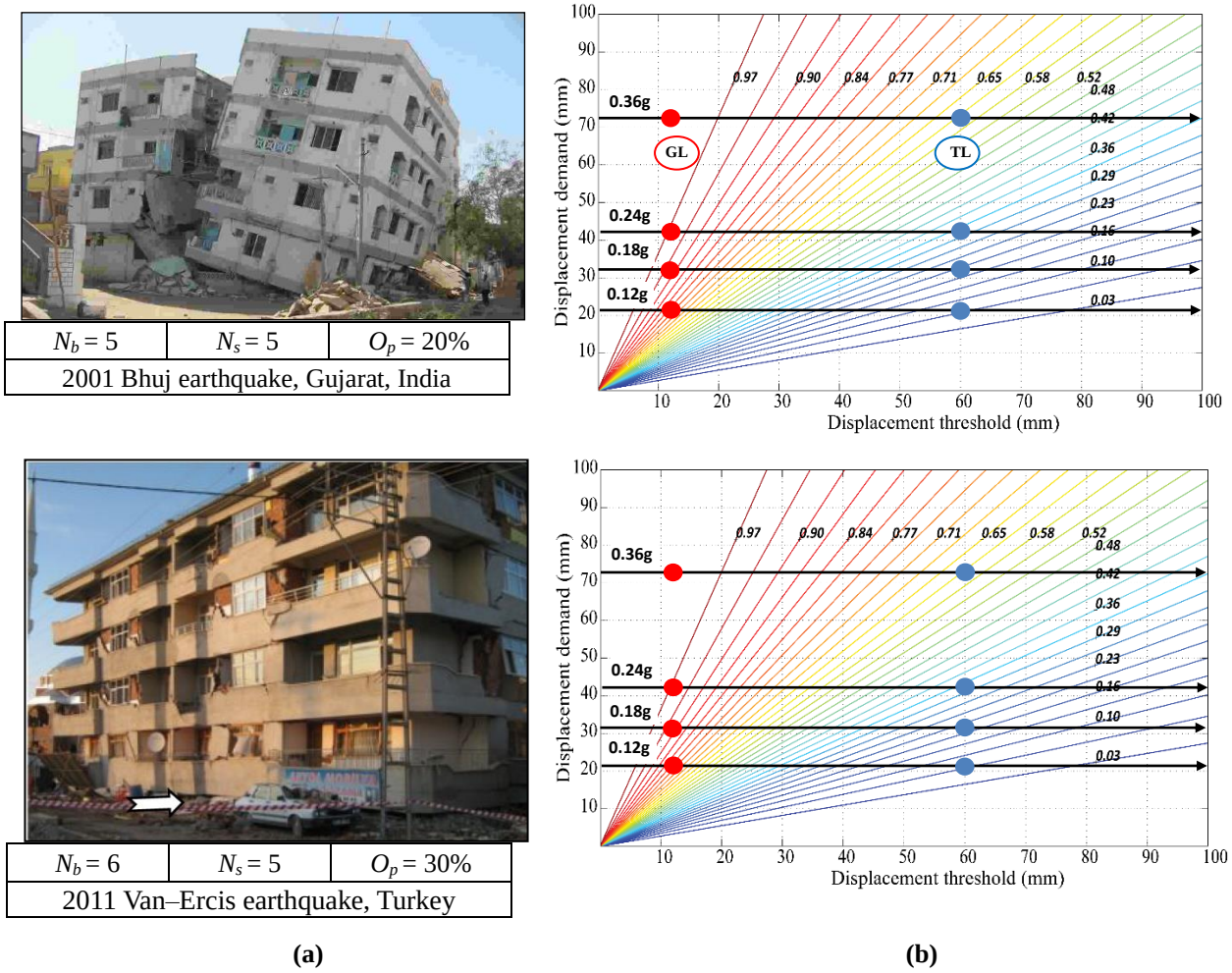

(a) **(b)**

Fig. 2. (a) Collapsed five-storied RC open ground storey buildings, and (b) Fragility flow plot (FFP) showing seismic displacement demand at TL and GL for different PGA levels: 0.12g, 0.18g, 0.24g, and 0.36g.

Seismic displacement demand and fragility using FFP for each of the buildings is shown in Fig 1(b) in which the demands are marked for two different limit states, i.e., the TL and GL. These refer to the drift limit as prescribed by the Indian seismic code (BIS 2016) as 0.4% of storey height. In case of the drift limit at TL, full building height is considered, whereas, for the GL, only the height of the ground storey is considered. At TL drift limit state, a highest value of 0.6 (or 60%) is indicated in the FFP as fragility for a PGA of 0.36g considering all the buildings. In contrast, the seismic fragility ranges from 0.7 (or 70%) to 1.0 (or 100%) when GL limit state is considered for a PGA ranging from 0.12g to 0.36g. Thus, the seismic fragility at the GL is very high as compared to the TL; as also indicated in the photographs of collapsed buildings. In all the cases (Fig. 1), the upper floors of the buildings incurred very less damage as compared to the ground

storey that was totally collapsed.

Similarly, Fig. 2(a) shows two different buildings that underwent failure during the 2001 Bhuj earthquake and 2011 Van–Ercis earthquake. Both the buildings had five number of stories but with different number of bays and opening size in infill walls. It was thus, observed that the seismic demand on the frames with a different number of bays and opening sizes does not vary much. Thus, it is the number of stories and the PGA of the site that is the chief factor for determining the seismic demand on the building. Secondly, failure is governed by the open ground storey configuration that leads to accumulation of all the damage in the ground storey itself. The seismic demand, as well as the fragility as determined from the FFP at the GL, gives the realistic picture of the damage.

A two-storey building with three bays collapsed during 2001 Bhuj earthquake is also considered in the present study (Fig. 3), that represents the class of low-rise buildings. The seismic fragility for such a low-rise building is also as high as 0.9 (or 90%) when a PGA of 0.36g is considered. Thus, the OGS building configuration is a highly vulnerable building category.

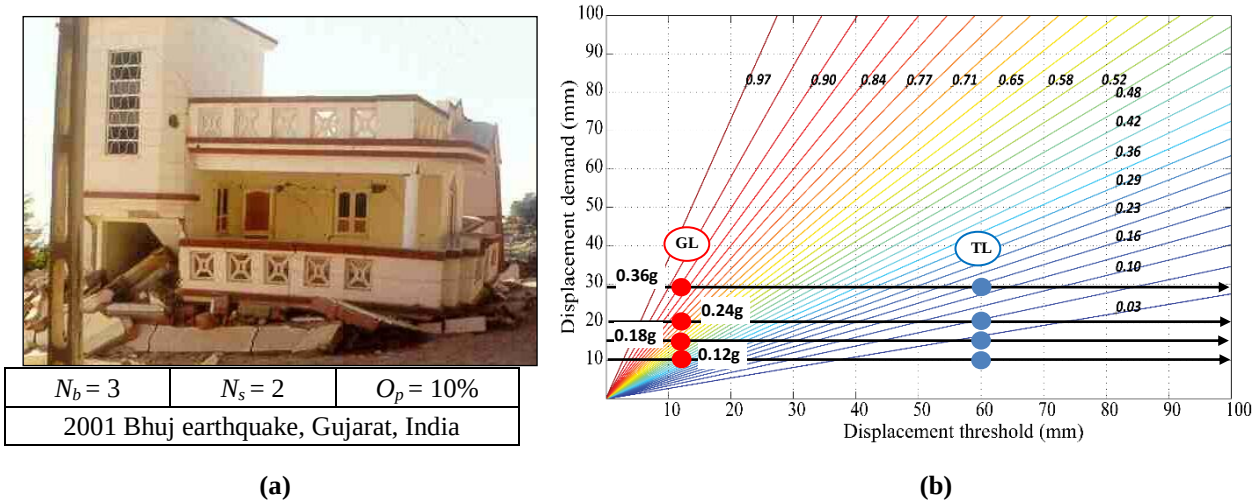

(a) **(b)**

Fig. 3. (a) Collapsed two-storied RC open ground storey building, and (b) Fragility flow plot (FFP) showing seismic displacement demand at TL and GL for different PGA levels: 0.12g, 0.18g, 0.24g, and 0.36g.

5 CONCLUSIONS

The present study validates the high seismic fragility of several low to mid-rise RC buildings with open ground storey that have suffered huge damage in past earthquakes using simplified methods. The considered case study buildings have a varied configuration of number of bays and stories and opening size in the infill walls that represents low to mid-rise buildings. Seismic demand based on the building configuration and seismicity is evaluated using a simplified seismic demand model. Seismic fragility of the buildings is obtained using fragility flow plots. It is concluded that for large-scale vulnerability assessment in an area, the FFP in combination with the seismic demand model can be reasonably used for an initial screening of vulnerable building typologies. It can be used as a rapid method for quantifying and categorizing the seismic vulnerability, and hence, the seismic risk of buildings for affordable and sustainable housing development.

ACKNOWLEDGEMENTS

The authors acknowledge the financial assistance provided by the Ministry of Human Resource Development (MHRD), Government of India.

REFERENCES

1) BIS (2016): IS 1893 (Part 1): 2002, Criteria for earthquake resistant design of structures: Part 1 General provisions and buildings." 5th Revision, *Bureau of Indian Standards, New Delhi, India*.
2) Choudhury, T., and Kaushik, H. B., (2018b): Component level fragility estimation for vertically irregular reinforced concrete frames, *Journal of Earthquake Engineering, Taylor & Francis*, DOI: 10.1080/13632469.2018.1453413
3) Choudhury, T., and Kaushik, H.B. (2017): A simplified method for seismic vulnerability assessment of RC buildings with open ground storey, *Proceedings of the 16th World Conference on Earthquake Engineering, Santiago, Chile*.
4) Choudhury, T., and Kaushik, H.B. (2018a): Seismic fragility of open ground storey RC frames with wall openings for vulnerability assessment, *Engineering Structures, Vol 155, Elsevier*, 345-357.
5) Gueguen, P. (2013): Seismic vulnerability of structures, *ISTE Ltd. and John Wiley & Sons, Inc, New Jersey*.
6) HAZUS (2013): Multi-hazard loss estimation methodology: Earthquake model, Technical Manual, *Developed by Federal Emergency Management Agency (FEMA), Washington, DC.*
7) Calvi, G.M., Pinho, R., Magenes, G., Bommer, J.J., and Crowley, H. (2006): Development of seismic vulnerability assessment methodologies over the past 30 years, *ISET Journal of Earthquake Technology, Vol. 43(472), 75–104*.

Effect of base width of concrete gravity dam and tail water presence on dynamic response of concrete gravity dam including soil-fluid- structure interaction

Khaund, P.K[1], Hazarika,M.[2]

[1] Professor, Department of Civil Engineering, Jorhat Engineering College, Gormur, Jorhat-785007, India.
[2] Student, Department of Civil Engineering, Jorhat Engineering College, Gormur, Jorhat-785007, India.

ABSTRACT

This paper presents a study on seismic analysis of a dam-reservoir-foundation system and evaluating the stresses in the dam and foundation body corresponds to the presence of dynamic time history analysis and analyzing its effect on the safety of the system. The dam is modeled as per the dimensional specifications of Mettur dam. One of the most important problems in evaluation of seismic behavior of concrete gravity dams is dam-reservoir-foundation interaction. Hydrodynamic pressure generated due to seismic forces and Fluid-Structure-Soil Interaction (FSS) are inevitable. Thus in this paper, the water-structure-foundation interaction is introduced. Dam-reservoir-foundation interaction has been investigated utilizing seismic analysis of a 3D dam-reservoir-foundation coupled system using ANSYS® WORKBENCH. Dam and foundation are modeled as concrete and rock foundation respectively, while reservoir water is considered acoustic and compressible. The modeling of reservoir has been carried out by fluid acoustic element and proper consideration of fluid boundary conditions. The effect of increase of base width of dam along with tail water presence on the dynamic response of the system is evaluated, by performing pseudo static analysis as per guidelines of IS: 1893-1984 (part-1) and dynamic time history analysis. The stress at toe and heel section of the dam is also checked against safety criteria of the dam concrete strength.

Keywords: fluid-structure-soil interaction, dynamic time history analysis, tail water

1. INTRODUCTION

A concrete gravity dam is a hydraulic structure of great importance which resists all external forces by its weight and therefore its analysis under the effect of earthquake force is highly significant. The purpose of dynamic analysis is not to determine dam stability in a conventional sense, but rather to determine what damage will be caused during the earthquake, and then to determine if the dam can continue to resist the applied static loads in a damaged condition with possible loading changes due to increased uplift or silt liquefaction. When a large structural system composed of many small components, subjected to transient loads, these structures interact with each other such that a continuous transfer of energy is established between them. For a dam-water-foundation system, the earthquake response is significantly influenced by the interaction of the dam with the impounded water and with the underlying foundation region, thus increasing the requirements for the analysis procedure to be used, and complicating a routine finite element analysis of a concrete cross-section.

2 LITERATURE REVIEW

Lofti and Zeng (2016) In this study Wavenumber approach is followed which is based on semi-infinite two dimensional fluid elements (hyper-element) for seismic analysis of dam-reservoir system. In this case very low value of L/H ratio is used for far field of reservoir where L represents length of reservoir and H represents water level in reservoir. **Zienkiewicz et al. (1988)** In this study one of the initial soil modeling technique, that is massless foundation model and its accuracy had been discussed. Massless foundation model has been proposed in the late seventies and has been used extensively for seismic analysis of concrete dams since then. The model assumes that the idealized foundation rock model is mass less. This results firstly, in a reduction in the number of dynamic DOF of the system. Secondly, the absence of mass makes the foundation rock function as a spring, in other words only the flexibility of the foundation rock is taken into account. As seismic response analysis of soil layer is an important part in seismic safety evaluation for key project sites (**Lou Menglin et al. 2004**), thus the practical site is assumed to be semi-infinite space, and the soil site is intercepted to limited range in the analysis with finite element method. Some studies have proved that, if the range of finite model reaches to a certain extent large enough, the boundary effect of incident waves and scattered waves can be ignored, and it can still obtain good approximate results (**Lou Menglin et al.2003).**

3 METHODOLOGY

The present study includes a model having three different systems as dam, reservoir water and rock foundation. The system is modeled in accordance with

the dimensional specifications of Mettur dam constructed over the Kaveri river in Salem district of Tamil Nadu. In the present study four dam models are used with four different base width specifications taken from the study of "*Effect of Static Seismic Loading and Uplift Parameters on the Stability of a Concrete Gravity Dam*" by **Khaund and Talukdar (2017).** The base widths that are considered in this analysis are the highest value of base widths corresponding to the stability criteria of overturning, sliding and shear friction factor and also corresponding to the highest value of seismic co- efficient (0.1g). The base width of model-1 is 37m and model-2 is 60m. The water reservoir is modeled with a maximum water level of 50m and the width of reservoir is taken according to the truncated boundary condition of fluid structure interaction. The originally the reservoir is constructed up to a length of 1700 m, but in this analysis the dam-reservoir-foundation system is 500 m long due to limited node capacity of the software. The tail water level is considered to be 10 m with a length of 500m.

3.1 Boundary conditions for FSI AND SSI

Some studies have proved that, if the range of finite model reaches to a certain extent large enough, the boundary effect of incident waves and scattered waves can be ignored, and it can still obtain good approximate results (Menglinet al.2003). According to the study in "*Transient analysis of dam-reservoir system by Wavenumber-TD approach*" by **Lotfi and Zenz (2016**), for good accuracy in results it is suitable to construct the far end boundary of reservoir at a minimum of twice the water height. By following the approach, the far end boundary of the reservoir is constructed at a distance equals to twice the height of the reservoir water level to behave as truncated boundary to satisfy the fluid structure interaction effect. The rock foundation is modeled considering the Soil Structure Interaction (SSI) boundary conditions. As mentioned in the study "*Nonlinear analysis of pine flat dam including base sliding and separation*" by **Viladkar and Al-Assady(2012**), by extending the soil foundation to a minimum of 1.5 times the base width of the dam, the amplification of excitation input due to radiation from far end boundaries can be nullify. In this study the SSI boundary conditions are applied by following this approach. The depth of the foundation is 1.5times the base width of the dam. The soil is extended in downstream direction equal to the height of dam. The reservoir end of foundation section is kept at distance twice the height of water level. According to the study "Iterative analysis of concrete gravity dam-nonlinear foundation interaction" by **Burman et al. (2010**), the vertical faces of the foundation along x-axis are restrained. By applying vertical roller (displacement in x and z direction is zero) the far end boundaries of foundation are restrained. It is done to reduce the modeling of soil section to a limited extent and to avoid the radiation of seismic waves at the far end boundaries of the foundation.

Table 1. Dimensional parameters of reservoir and foundation

MODEL NO	RESERVOIR WIDTH, W_R m	EXTENSIONOF SOIL D/S , W_E m	DEPTH OF SOIL, D, m
1	125		54
2	54		
	125		54
	90		

.

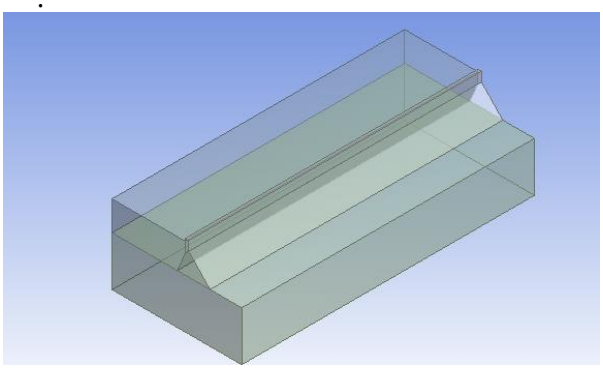

Fig.1. 3D view of a FEM model

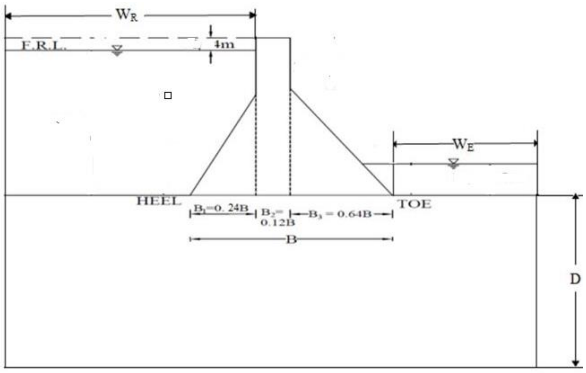

Fig.2. Model of dam reservoir foundation system

3.2 Material Properties

The reservoir section is assigned with common properties of water such as bulk modulus, mass density and sound speed of sound in water. Here density (ρ) and bulk modulus (K) of water are provided as 1000 kg/m^3 and 2250MPa respectively. The speed of sound in water is taken as 1440 m/sec. the mass density, Young's modulus of elasticity and the Poisson's ratio of the concrete are 2500 Kg/m^3, 29580 MPa and 0.2 respectively. The foundation soil is considered to be hard rock with density, Young's modulus and Poisson's ratio as 3300 Kg/m^3, 62054 MPa and 0.3.

3.3 Method of analysis

This analysis is performed with the help of

Static Structural tool. The hydrodynamic pressure is applied at the upstream face of the dam. The hydrodynamic pressure is calculated as per the procedure describe in of IS: 1893-1984 (part-1). Assuming the water to be incompressible, the hydrodynamic pressure at a depth y below the reservoir surface is given by

$$p_e = C_s \times \alpha_h \times \gamma_w \times y \quad [1]$$

C_s = coefficient which varies with shapes and angle of upstream face of the dam.
y= Depth below water reservoir
γ_w = Unit weight of Water.
α_h = Horizontal earthquake acceleration
The value of C_s can be approximately found for vertical or constant slope of upstream face of dam as given by

$$C_s = (C_m/2) \times [\{(y/H) \times (2-(y/H)\} + \{\sqrt{(y/H)} \times (2-(y/H)\}] \quad [2]$$

Where H is the water level of reservoir and C_m is the maximum value of pressure coefficient for a constant slope

In ANSYS® Workbench time history analysis can be performed through Transient Structural tool. El-Centro earthquake (1940) acceleration data is utilized for this analysis. The North-South component of El-Centro recorded at the Terminal Substation building is used. The El-Centro acceleration data have been scaled down to 0.1g in this present analysis

4 RESULTS AND DISCUSSION

4.1 Result data

Pseudo static analysis of the dam-reservoir-foundation system is conducted at the Static Structural tool of ANSYS® Workbench. The hydrodynamic pressure applied at the upstream face of dam is calculated as per the guidance of IS: 1893(Part 1)-1984. The stress profile generated from this process for the different models are shown below

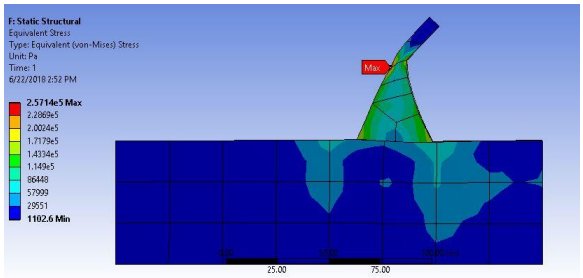

Fig.3. Stress profile of model-1 from pseudo static analysis

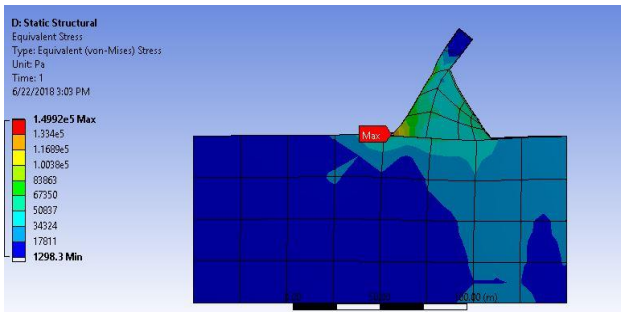

Fig.4. Stress profile of model-2 from pseudo static analysis

Time history analysis for scaled down (0.1g PGA) El-Centro earthquake acceleration data is done with Transient structural tool and the stress for every time step is represented in a graph. From the progress graph, the time period for maximum stress is found and then the stress profile obtained for that time period is studied.

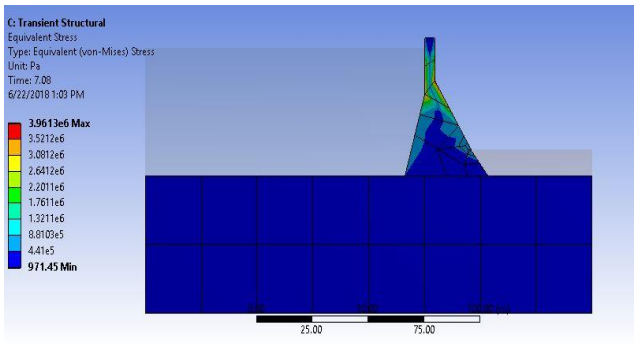

Fig.5. Stress profile of model-1 from Time History Analysis

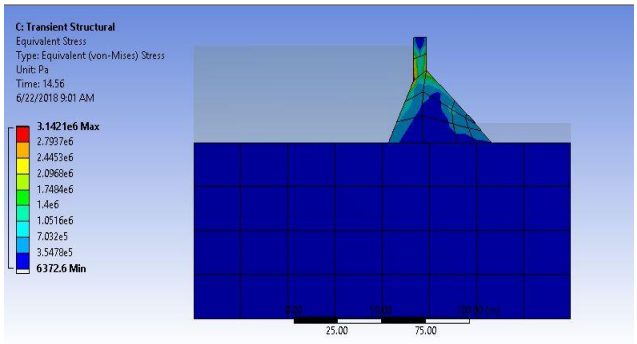

Fig.6. Stress profile of model-2 from Time History Analysis

4.2 Safety Evaluation

In this analysis the resultant of forces acting on the dam are towards the toe part of them and the toe and heel part of the dam are analyzed for compression and tensile strength criteria respectively. According to

IS: 6512-1984, the allowable compressive stress in the dam concrete shall not exceed, 7N/mm^2 and permissible tensile stress of concrete is taken to be 1 to 4 percent of compressive strength. In this analysis the permissible tensile stress is taken as 2% of compressive strength of concrete considering full reservoir condition and earthquake excitation.

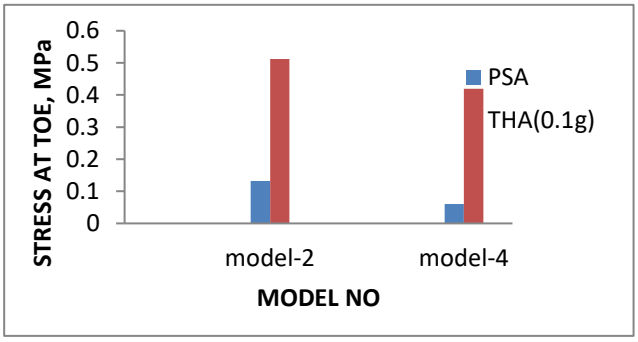

Fig.7. Stress at toe of dam obtained from pseudo static, time history method for different model

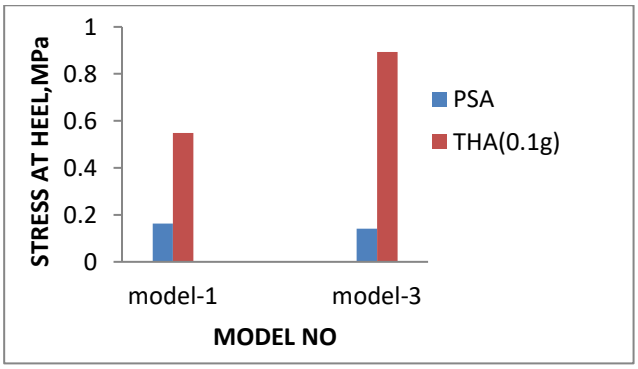

Fig.8. Stress at toe of dam obtained from pseudo static and time history method for different model

It can be observe that the stress at toe is under permissible limit of compressive stress whereas for heel section, the stress remains under limit for pseudo static method only. The stress at both toe decreases and at heel part of the dam increases with increase in base width of the dam in the presence of tail water for time history method. For pseudo static method, the stress decreases with increase in base width of dam.

5 CONCLUSIONS

In this present study, an attempt is made to present the results of the dynamic analysis of a concrete gravity dam with the effects from soil structure and fluid structure interaction. The purpose of the study is to investigate the stress developed in different models of dam-reservoir-foundation system against earthquake and to evaluate the safety of dam against the permissible limit. Pseudo static analysis as per the guidance of IS: 1893-1984(part 5) and time history analysis using El-Centro acceleration data are the different approaches of dynamic analysis used in this study.

In this present analysis brief overview of the FEM software ANSYS® Workbench is included. The software is used for modeling and different analysis of the dam using appropriate elements and material properties with appropriate boundary conditions. The stresses developed in the toe and heel of the dam which are obtained from different analysis procedure are found to be under permissible limit. It is observed that, with increase in base width of dam for tail water present condition, the stress at heel increases for time history method, whereas for pseudo static method, the stress follows a descending pattern with increase in base width of dam. Also the analysis of a dam in terms of safety should be done with proper dynamic methods as the stress obtained for pseudo static method in this analysis are insignificant as compared to the other method. Thus this study shows that the increase in base width of gravity dam increases stress rather than decapitating it to through lower enlarged portion

REFERENCES

1) Ahmed, A.R, and Wilfred, D.I, 1985, Dynamic analysis of short-length gravity dams, *Journal of Structural Engineering*, Vol. 111, No. 8, paper no- 19921.
2) Arabshahi, H., and Lotfi, V., 2008, Earthquake response of concrete gravity dams including dam–foundation-interface nonlinearities, Engineering *Structures 30*, 3065–3073.
3) Bilici,Y., Bayraktar, A.,Soyluk, K.,2009, Dynamic response of dam– reservoir– foundation systems to spatially varying earthquake ground motions, *Soil Dynamics and Earthquake Engineering 29*, 444–458.
4) Burman, A., Maity, D., Sreedeep, S., 2010,Iterative analysis of concrete gravity dam-nonlinear foundation interaction, *International Journal of Engineering, Science and Technology*,Vol. 2, No. 4, 85-99.
5) Chopra, A.K., 1996, *Dynamics of Structures: theory and applications to earthquake engineering*, Prentice Hall, Upper Saddle River, New Jersey, 635, 17.
6) Fenves, G., and Chopra, A.K., 1987, Simplified earthquake analysis of concrete gravity dams, *Journal of Structural Engineering*, Vol. 113, No. 8, paper no- 21717.
7) IS: 1893(Part 1)-2002, Criteria for earthquake resistance and construction of buildings, Bureau of Indian standards, New Delhi.
8) IS: 1893(Part 1)-1984, Criteria for earthquake resistance and construction of buildings, Bureau of Indian standards, New Delhi.
9) IS: 6512-1984, Criteria for design of solid gravity dam, Bureau of Indian standards, New Delhi.
10) Khaund, K.P, and Talukdar, S., 2017, Effect of Static Seismic Loading and Uplift Parameters on the Stability of a Concrete Gravity Dam, *Fifth Intl. Conf. Advances in Civil, Structural and Mechanical Engineering (CSM)*, 978-132.
11) Kramer, S.I., 1996, *Geotechnical Earthquake Engineering*, Prentice Hall, Upper Saddle River, New Jersey, 07458.
12) Lotfi, V., and Zenz, G., 2016, Transient analysis of concrete

gravity dam-reservoir systems by Wavenumber-TD approach, *Soil Dynamics and Earthquake Engineering* , 313-326.

13) Viladkar, N.M, and Al-Assady, S.M.K.A,2012, Nonlinear analysis of Pine Flat Dam including base sliding and separation, *15th World Conference of Earthquake Engineering*, LISBOA.

14) Rulin, Z., and Mengling, L., 2011, Substructure analysis method for dynamic response of large-scale soil site, Procedia *Engineering 14*, 417–1424

Plastic hinge length at RC shear wall and floor slab junction

Kaushik, S. [1], Dasgupta, K. [2]

[1] Assistant Professor, Department of Civil Engineering, GIMT, Guwahati 781017, India.
[2] Assistant Professor, Department of Civil Engineering, Indian Institute of Technology Guwahati, Guwahati 781039, India.

ABSTRACT

Conventionally, in seismic design of shear walls the region of inelastic behaviour is considered at the base of the wall, which represents the response of an isolated slender shear wall. However, in multistoried Reinforced Concrete (RC) wall-frame buildings with shear walls connected to the floor slabs at different levels, the wall-slab junctions also show extensive inelastic behaviour. Thus, slab-wall interaction contributes significantly to the overall seismic capacity of the building. Past studies have mainly focused on isolated slender wall specimens in which the zone of inelastic behaviour, i.e., the plastic hinge zone, is considered at the base of the wall under seismic actions. However, the extent of inelastic action in a wall connected with floor slabs has not been studied extensively in the past. In the present study, the extent of the zone of inelastic behaviour is studied at the wall-slab junction region by carrying out displacement based nonlinear static analysis of the wall-slab assemblages under monotonic as well as cyclic loads. A parametric study is carried out by varying the wall panel aspect ratio and axial load on walls. It is observed that unlike the concentration of inelasticity at the base of a wall without slab, the curvature demand increases significantly at the wall-slab junction, leading to the development of nonlinearity and damages at those locations. Based on curvature distribution and variation of tensile damage along the height of wall, analytical expressions for plastic hinge length are proposed.

Keywords: shear wall-slab junction, finite element analysis, nonlinear static analysis, plastic hinge length

1. INTRODUCTION

In multistoried RC frame buildings, typical material nonlinearity is observed in beams and columns during strong earthquake shaking. Along with beams and columns, similar nonlinear behaviour may get mobilized in shear walls for RC frame-wall buildings. The development of material nonlinearity along with possible tensile damages takes place in the plastic hinge region of each member. The extent of the plastic hinge zone is expressed in terms of plastic hinge length (L_p). Several researchers have developed various expressions estimating the plastic hinge length in RC members by conducting experiments and analytical studies on beams, columns and shear walls (Chan, 1995; Baker and Amarakone, 1964; Corley, 1966; Mattock, 1967). In isolated slender shear wall specimen, maximum nonlinearity and the plastic hinge zone develop at the base of the wall. Also, it is assumed that the maximum curvature at the bottom of the wall is uniform over the plastic hinge length which is considered within the range $0.5L_w$ - L_w, where L_w is the wall length. All the studies on shear wall specimens have been carried out on isolated slender specimens (Paulay, 1986; Wallace and Moehle, 1992; Paulay and Uzumeri, 1975; Paulay and Priestly, 1992; Panagiotakos and Fardis, 2001; Bohl and Adebar, 2011; Kazaz, 2013). However, in multistoried RC frame-wall buildings, the shear walls are usually slender in nature and are connected with slab at every floor level. Presence of slab at different floor levels influences the maximum curvature demand along the height of the wall. Hence, L_p determined from the studies on isolated shear wall without the presence of slab may not be applicable for the plastic hinge region at wall-slab junction. The objective of this study is to investigate the variation of curvatures and tensile damage in wall in the presence of floor slabs. The effect of axial load ratio, length of wall as well as wall panel aspect ratio on L_p is investigated. Based on the results of nonlinear static analysis, an expression of plastic hinge length is proposed as a function of wall length and storey height of wall for the junction region of shear wall and floor slab.

2. MODELLING AND ANALYSIS DETAILS

An exterior shear wall-slab assemblage from a five-storied RC frame-wall building is considered for investigation of plastic hinge length near the wall-slab junction region (Kaushik and Dasgupta, 2013). The concrete members and steel reinforcement of the assemblage are modelled using eight noded solid elements with reduced integration (C3D8R) and two noded truss element (T3D2) respectively, using Finite Element (FE) program ABAQUS (ABAQUS, 2010). The assemblage is modelled using solid elements with reinforcement embedded in the shear wall and floor slab region. The thickness of shear wall and slab are

300 mm and 120 mm, respectively. Two layers of vertical and horizontal reinforcement are provided in the shear wall. For all the cases, the shear walls and floor slabs are modeled using Concrete Damaged Plasticity (CDP) properties for concrete (Lubliner, et al., 1989; Lee and Fenves, 1998). The assemblage analyzed in the current study has a characteristic concrete compressive strength of 25 MPa. The tensile strength of concrete is assigned as 3.5 MPa. Steel reinforcement is modelled with the material property assigned using plasticity model in ABAQUS. The yield stress and ultimate stress are considered as 415 MPa and 527 MPa, respectively. The translational and rotational Degrees of Freedom (DoFs) are restrained at the bottom nodes of the wall. As the present study intends to investigate the nonlinear behaviour for in-plane analysis of wall, the outer edges of slabs are supported on rollers, and the out-of-plane bending of the shear wall is prevented.

For the parametric study, the length of the wall considered are 3 m, 4 m, 5 m, 6.7 m and 10 m. The height of the wall in between the floors (storey height, h_s) is kept constant as 5 m. To investigate the influence of axial compression on the plastic hinge region in the wall-slab assemblage, three different force levels of $10\%A_g f_c$, $40\%A_g f_c$ and $70\%A_g f_c$ are considered and they are applied on the top surface of the wall. Displacement based nonlinear static analyses are performed under monotonic as well as cyclic modes with varying axial load and length of wall. The gravity loads on the slab are kept constant during each analysis. For cyclic loading, the specimen is subjected to three cycles of applied displacement levels of 2.5 mm, 5.0 mm, 10.0 mm, 20.0 mm, 40.0 mm, 60.0 mm, 80.0 mm and 100.0 mm respectively (Fig. 1a). It is observed that the general trend of force-displacement response for different ratios of axial force on the assemblage is similar for both cyclic and monotonic analysis case when compared separately. Also, the extent of tensile damage at the junction region at the maximum drift level is similar for different axial load levels. Hence, the possible plastic hinge length in wall-slab junction region is not sensitive to the level of axial compression applied on the top surface of the wall. Thus, all further analyses (monotonic and cyclic) for different lengths of wall are carried out for axial compression of $10\%A_g f_c$. The assemblage is displaced up to a lateral displacement of 100 mm to study the behaviour under monotonic and cyclic loading.

3. EVALUATION OF RESULTS

Under cyclic loading, the peak lateral strength of slab-wall assemblage expectedly increases with reduction in aspect ratio of wall panel (Fig. 1(b)-(f)). The wall panel with the lowest aspect ratio also exhibits the maximum degradation in lateral strength as reflected from the backbone curves. As cracking of concrete is not explicitly modelled, the typical pinching characteristics of the force-displacement loops, is not observed.

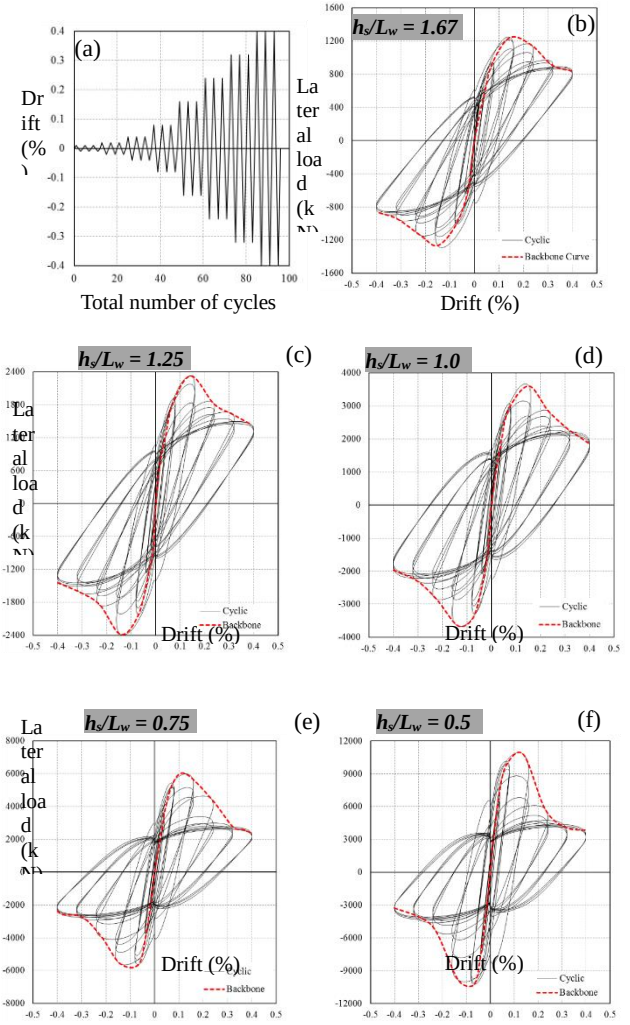

Fig. 1. Behaviour of wall-slab assemblage under cyclic loading with different panel aspect ratios: (a) Variation of drift level with loading cycles, (b) for aspect ratio 1.67, (c) for aspect ratio 1.25, (d) for aspect ratio 1.0, (e) for aspect ratio 0.75 and (f) for aspect ratio 0.5

Fig. 2 shows the similar trend of concrete strain at different drift levels at first floor wall-slab junction. One of the salient observations is that the strain profiles remain almost the same under the three different axial compression levels ($10\%A_g f_c$, $40\%A_g f_c$ and $70\%A_g f_c$), unlike slender isolated wall in which the effect of axial compression on strain profile in wall cross-section is significant. As the axial compression on wall is not observed to affect the stress-strain response of the wall-slab specimen, a compression of $10\%A_g f_c$ along with low reinforcement ratio of 0.25% are considered in the future studies.

Although the maximum compressive strain in

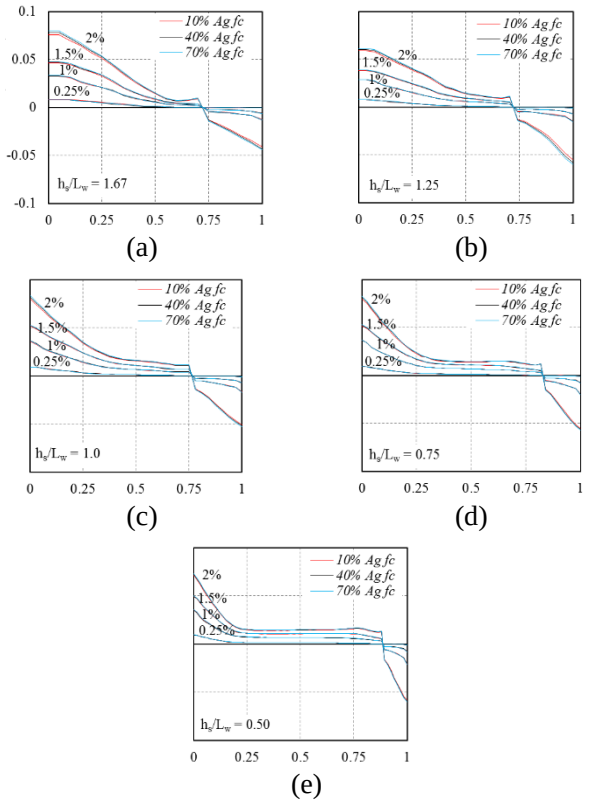

Fig. 2. Variation of strain in concrete at first floor level along the length of wall in wall-slab junction under different axial compression levels and aspect ratios: (a) for aspect ratio of 1.67, (b) for aspect ratio of 1.25, (c) for aspect ratio of 1.0, (d) for aspect ratio of 0.75 and (e) for aspect ratio of 0.5 (Compressive strain in mm/mm in Y-axis)

concrete is observed to be the same for the 2% drift level, the maximum tensile strain tends to increase with reduced aspect ratio of wall panel. This is due to the increase in the diagonal tension from the bottom wall panel with mobilization of more squat wall behaviour. Extensive cracking is expected towards the edge of the wall in the wall-slab junction region at the mentioned drift level. For all the drifts levels in the specimen, the strain profile cross the zero strain point at the same location. Similar trend was also observed for the strain variation along the web of an isolated slender wall in past studies (Thomsen and Wallace, 2004). However, the zero-strain point shifts towards the tension side of the wall with reducing panel aspect ratio (Fig. 2). Thus, the compression region reduces with increased wall length. The variation of longitudinal stress in reinforcement on the tension and the compression faces of the wall is shown in Fig. 3. It is observed that the vertical bar at the junction region reaches the yield value while the bar over the height of the wall remains unyielded. The floor slabs tend to partition the entire wall into different squat panels, and the strut-and-tie actions lead to tensile and compressive strain concentration in wall-slab junction at every floor level. These further cause yielding of vertical bars only at the junction region and not throughout the height of the wall. This highlights a significant deviation from the behaviour of vertical reinforcement in isolated slender shear walls in which the bars yield over a zone at the bottom of the wall under flexural deformations. Similar behaviour is observed for the stress distribution of longitudinal steel in wall panel with increased aspect ratio. The zone of yielding on the compressive face reinforcement towards the bottom of the wall tends to increase with the aspect ratio of wall panels. The curvature is obtained based on the strains obtained at the **tension and compressive faces of the wall for maximum drift level.**

Unlike isolated slender wall section having maximum curvature at the bottom of the wall, the slab-wall junction at every floor level is subjected to large curvature (Fig. 4) (Bohl and Adebar, 2011) With increasing distance from the junction, the curvature reduces sharply to a very small value along the storey height. The curvature profile is computed from element strains calculated at the two wall ends, at the same height and in the same row (Kazaz, 2013). The same procedure is adopted for obtaining the curvature profiles along the height of the wall for both monotonic and cyclic loadings considering different aspect ratio of shear wall panel.

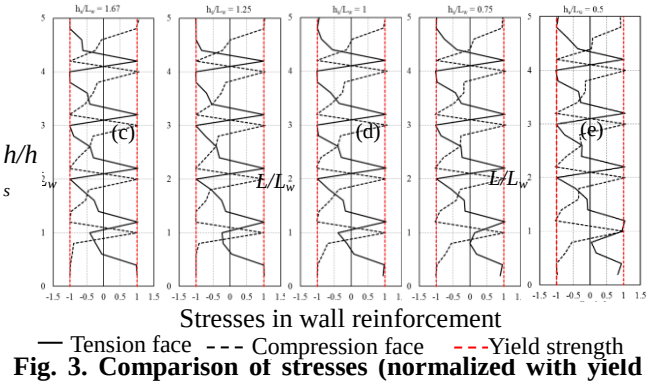

Fig. 3. Comparison of stresses (normalized with yield stress) in vertical reinforcement of wall for different wall panel at 2% drift ratio: (a) for aspect ratio of 1.67, (b) for aspect ratio of 1.25, (c) for aspect ratio of 1.0, (d) for aspect ratio of 0.75 and (e) for aspect ratio of 0.5

A similar trend is observed for tensile damage in wall in which maximum damages are observed in wall-slab junction region (Fig. 5). The tensile damage gets initiated at the base of the wall. However, it does not propagate along the height of the wall but tends to increase at the wall-slab junction at every floor level. This is due to the partitioning of the wall into a number of panels and the consequent strut and tie action. This is observed for all the specimens with different wall panel aspect ratios. However, along the height of each wall panel, insignificant damages are observed.

The presence of floor slab tends to reduce the flexural deformations along the height of the wall.

However, in each wall panel between two successive floor slabs, tensile and compressive damages accumulate at the wall-slab junction region (Fig. 5). So, along with curvature and compressive strain in concrete, tensile damage zone is also considered to express the plastic hinge region in the present study. For the specimens with wall panel aspect ratios of 1.67, 1.25, 1, 0.75 and 0.5, the possible plastic hinge regions are obtained by observing the variation of compressive strain in concrete, tensile damage in concrete and curvature in wall cross section. All the parameters show similar distribution across the height of the wall with higher values at each wall-slab junction (Figs. 5 and 6). By observing the distance over which each of these parameters reduces to zero on each side of the wall-slab junction, the possible extent of plastic hinge region is obtained.

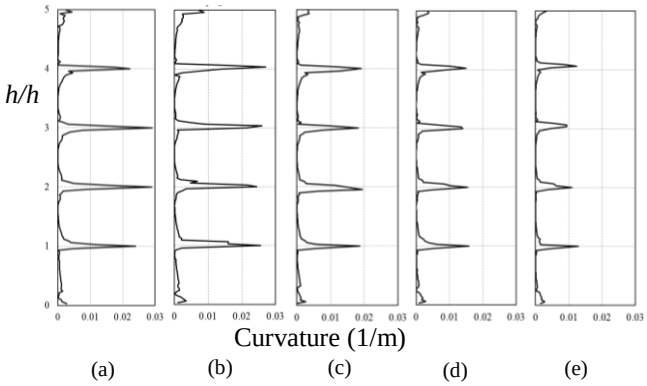

Fig. 4. Variation of curvature for different aspect ratios of wall panels at final drift level: (a) for aspect ratio of 1.67, (b) for aspect ratio of 1.25, (c) for aspect ratio of 1.0, (d) for aspect ratio of 0.75 and (e) for aspect ratio of 0.5

4. PLASTIC HINGE LENGTH

Based on the extent of tensile damage at wall-slab junction region, possible lengths of plastic hinge region are identified for different wall panel aspect ratios during monotonic and cyclic behaviours. Although conventionally inelastic curvature is directly used for expressing the plastic hinge length, the extent of tensile damage is also considered as a useful indicator for the present study.

In case of monotonic pushover analysis, the curvature profile considering the strains at the extreme tension and compressive faces of the shear wall is obtained at the maximum damage level. The curvature profile for cyclic loading is obtained at the maximum lateral load capacity of the shear wall. The variation in the vertical reinforcement stress over the height of the wall and possible yielding of reinforcement at the junction region are related to the maximum damage at the junction region. Although the observed maximum curvature reduces with increase in wall panel aspect ratio, the spread of tensile damage also decreases with the spreading out of strut-and-tie action in squat wall panels. This is observed for both monotonic and cyclic displacement-controlled analyses.

The spread of plasticity at the junction region decreases with an increase in the length of wall. Since the effect of axial compression is not contributing to the tensile damage and the compressive strains at the wall-slab junction region, the aspect ratio is considered as the key parameter affecting the possible plastic zone. For both monotonic pushover and cyclic pushover analyses, the identified L_p, normalized with respect to the length of the wall, is observed to increase with the wall panel aspect ratio (h_s/L_w) (Fig. 6). Considering L_p to be linearly varying with storey height and length of shear wall panel, the normalized plastic hinge length at the wall-slab junction is obtained using regression analysis and is expressed as,

For cyclic loading,

$$\frac{L_{p,cyclic}}{L_w} = 0.0546\left(\frac{h_s}{L_w}\right) + 0.0174 \quad (1)$$

For Monotonic loading,

$$\frac{L_{p,monotonic}}{L_w} = 0.0728\left(\frac{h_s}{L_w}\right) + 0.0234 \quad (2)$$

From Eqs. (1) and (2), it is observed that $L_{p,monotonic} \approx 1.34 L_{p,cyclic}$. To examine the accuracy of the proposed Eqs. (1) and (2), the plastic hinge length (L_p) at the wall-slab junction is estimated for five different lengths of shear wall and compared with the calculated values of L_p proposed in the various past studies on RC walls (Table 1).

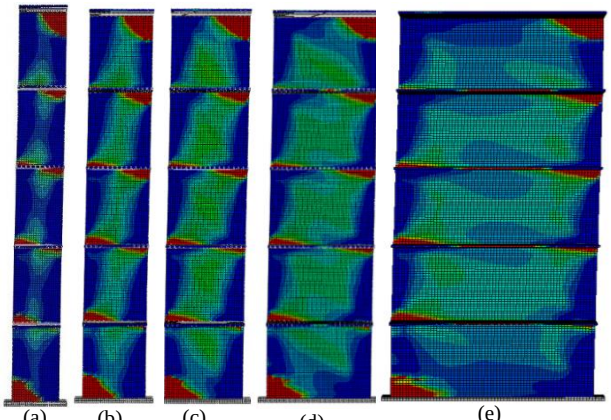

Fig. 5. Comparison of tensile damage for wall panel aspect ratios at 2% drift ratio: (a) for aspect ratio of 1.67 (b) for aspect ratio of 1.25, (c) for aspect ratio of 1.0, (d) for aspect ratio of 0.75 and (e) for aspect ratio of 0.5

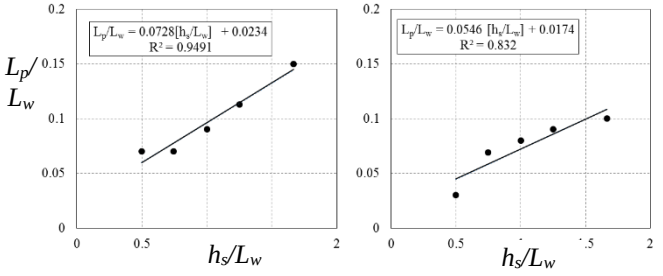

Fig. 6. Variation of normalized plastic hinge length with wall-panel aspect ratio for: (a) monotonic and (b) cyclic analysis cases

In the previous studies, it is mentioned that inelastic behaviour is observed mostly at the bottom of the isolated slender shear wall. However, the presence of slabs at every floor level in a multistoried building leads to inelastic behaviour at the wall-slab junction in addition to the inelastic behaviour at the base of the wall. The estimates of L_p, as per Eqs. (1) and (2), are obtained considering the possible zones of inelastic behaviour along the height of the wall and at wall-slab junction. Among the past studies, Panagiotakos and Fardis (2001) have proposed expressions for plastic hinge length under monotonic and cyclic loadings. On comparing the estimated plastic hinge lengths under monotonic and cyclic loadings, it is observed that the analytical estimates using the equations of Panagiotakos and Fardis (2001) are slightly lesser than the estimated values as per the proposed equation (Table 1). However, the proposed expressions are applicable only for the plastic hinge region adjacent to the wall-slab junction region. Between the two parameters, h_s and L_w, more weightage is given on h_s which reflects the increase in plastic hinge region with more slender wall panel.

Table 1: Comparison of plastic hinge length in terms of L_w for different lengths of shear wall

Model (L_w)		3 m	4 m	5 m	6.7	10 m
Baker and Amarakone (1964)		0.49	0.46	0.43	0.40	0.36
Corley (1966)		0.42	0.41	0.41	0.41	0.40
Mattock (1967)		0.44	0.43	0.43	0.42	0.41
Priestly and Park (1987)		0.08	0.06	0.05	0.04	0.02
Paulay and Priestly (1992)		0.09	0.07	0.05	0.04	0.03
Paulay and Priestly (1993)		0.24	0.23	0.22	0.22	0.21
Sasani and Der Kiureghian (2001)		0.36	0.35	0.35	0.34	0.34
Panagiotakos and Fardis (2001)	**Cyclic**	**0.10**	**0.08**	**0.06**	**0.04**	**0.03**
	Monotonic	**0.15**	**0.09**	**0.09**	**0.07**	**0.05**
Bohl and Adebar (2011)		0.24	0.22	0.21	0.20	0.19
Kazaz (2013)		0.16	0.17	0.18	0.19	0.20
Present study	**Cyclic**	**0.11**	**0.07**	**0.07**	**0.06**	**0.04**
	Monotonic	**0.14**	**0.10**	**0.10**	**0.08**	**0.06**

5. CONCLUSIONS

Expressions are proposed for estimation of possible plastic hinge length at the junction of shear wall and floor slab. The expressions are developed by observing variation in tensile damage pattern and curvature along the height of the wall under monotonic and cyclic nonlinear analyses for constant axial load. Due to the mobilization of the strut-and-tie mechanism in each partitioned wall panel, the concentration of tensile damage at each floor level plays an important role in identifying the extent of plastic hinge region. The proposed expression needs to be further validated through detailed experimental studies on RC wall-slab junction regions.

REFERENCES

1) ABAQUS. (2011): *ABAQUS analysis user's manual*, Hibbitt, Karlsson, and Sorenson, Pawtucket, R.I.
2) Baker, A.L.L. and Amarakone, A.L.M., (1964): Inelastic hyperstatic frame analysis, *Proceedings of the International Symposium of the Flexural Mechanics of the Reinforced Concrete ASCE-ACI*, Miami.
3) Bohl, A., and Adebar, P., (2011): Plastic hinge length in high rise concrete shear walls, *ACI Structural Journal*, 108(2), 148–157.
4) Chan, W.W.L., (1955): The ultimate strength and deformation of plastic hinges in reinforced concrete frameworks, *Magazine of Concrete Research*, 7(21), 121–132.
5) Corley, W.G., (1966): Rotational capacity of reinforced concrete beams, *Journal of Structural Engineering*, ASCE, 92(5), 121–146.
6) Kaushik, S., and Dasgupta, K., (2013): Seismic behavior of slab-structural wall junction in RC building, *Conference on Structural Engineering and Mechanics*, NIT Rourkela, India, Paper No. 054.
7) Kazaz, I., (2013): Analytical study on plastic hinge length of structural walls, *Journal of Structural Engineering*, ASCE, 139(11), 1938–1950.
8) Lee, J., and Fenves, G.L., (1998): Plastic-damage model for cyclic loading of reinforced concrete structures, *Journal of Engineering Mechanics*, ASCE, 124 (8), 892–900.
9) Lubliner, J., Oliver, J., Oller, S., and Onate, E., (1989): A plastic-damage model for concrete, *International Journal of Solids and Structures*, 25(3), 299–326.
10) Mattock, A.H., (1967): Discussion on rotational capacity of reinforced concrete beams, *Journal of Structural Engineering*, ASCE, 93(2), 519–522.
11) Panagiotakos, T.B., and Fardis, M.N., (2001): Deformation of reinforced concrete members at yielding and ultimate, *ACI Structural Journal*, 98(2), 135–148.
12) Paulay, T., (1986): Design of ductile reinforced concrete structural walls for earthquake resistance, *Earthquake Spectra*, 2(4), 783–823.
13) Paulay, T., and Priestley, M.J.N., (1992): *Seismic design of reinforced concrete and masonry buildings*." John Wiley and Sons Inc., New York.
14) Paulay, T., and Priestley, M.J.N., (1993): Stability of ductile structural walls, *ACI Structural Journal*, 90(4), 385–392.
15) Paulay, T., and Uzumeri, S.M., (1975): A critical review of the seismic design provisions for ductile shear walls of the Canadian code, *Canadian Journal of Civil Engineering*, 2, 592–601.

16) Priestley, M.J.N., and Park, R., (1987): Strength and ductility of concrete bridge columns under seismic loading, *ACI Structural Journal*, 84(1), 61–76.
17) Sasani, M., and Der Kiureghian, A., (2001): Seismic fragility of RC structural walls: Displacement Approach, *Journal of Structural Engineering*, ASCE, 127(2), 219–228.
18) Thomsen, J.H., and Wallace, J.W. (2004): Displacement-based design of slender concrete structural walls: experimental verification, *Journal of Structural Engineering*, ASCE, 130(4), 618–630.
19) Wallace, J.W., and Moehle, J.P., (1992): Ductility and detailing requirements of bearing wall buildings, *Journal of Structural Engineering*, ASCE, 118(6), 1625–1644.

Nonlinear analysis of R.C.C building considering soil structure interaction

Bharadwaj, K.

Assistant Professor, Department of Civil Engineering, Tezpur University, Napaam, Tezpur 784028, India.

ABSTRACT

In the last few decades, design of earthquake resistant structures have emerged enormously. Research works are being carried out to analyse the structures against seismic actions such that the economic loss and fatality rates can be minimized during and after an earthquake. Capacity Spectrum Method is an approximate method, which is a simple and effective procedure for nonlinear static analysis. In the present study, a four-storey hostel building is analysed and design for gravity loads and seismic loads as per provisions of IS 456:2000 and IS 1893:2016. A model of the hostel-building frame with fixed base is prepared in SAP2000 for performing nonlinear static analysis. Using Capacity Spectrum Method, a capacity curve as well as the performance point of the model is obtained. The effect of soil structure interaction is usually neglected during an analysis. With structural parameters similar to that of the model with fixed base, a model is prepared with flexible base to incorporate the soil flexibility (type II soil as per IS1893:2016). The stiffness values are calculated from ATC 40 and FEMA 356. The study shows that there is variation in the performance of building frame when soil flexibility is taken into consideration. Fragility curves are also developed to understand the performance variations.
Keywords: capacity spectrum method, soil structure interaction, soil flexibility, fragility curves

1. INTRODUCTION

Nonlinear static procedures are becoming a common practice in earthquake engineering field to analyze the seismic demands. The nonlinear static procedures involve less computation and complexity than the nonlinear time history analysis and hence gained popularity in the last few decades. In the nonlinear static pushover analysis, the capacity of a structure is determined using the lateral load and roof displacement, and is represented graphically by force displacement diagram. This capacity curve, popularly known as pushover curve, depicts the yielding of the structure beyond the elastic limit due to monotonically increasing predefined load patterns in the fundamental mode of the structure. The procedures for pushover analysis available in ATC40 do not take into consideration the effect of higher modes. Hence, these procedures are generally applicable for low-rise buildings where the fundamental mode is predominant.
The pushover curve obtained can be compared with the demand response spectra by converting the lateral load displacement plot to spectral acceleration and spectral displacement, which is obtained by using the dynamic characteristic of the fundamental mode to represent the structure as a SDOF system.

Although the nonlinear static pushover analysis is widely used, but this is mostly done considering the base of the structure as fixed. As per IS 1893:2016, the base can be considered as fixed only in case of hard soil or rock type soil which is soil type I, for the other two types viz. type II and type III, the flexibility of the soil should be considered in seismic analysis.

In the present study, an attempt is made to observe the variation of pushover curve for soil type I and II. In addition, the fragility curves are compared for both the soil types.

2 MODELLING OF THE BUILDING

In this study, a four-storey reinforced concrete 2D framed building is modelled in SAP 2000 version 20. Linear static analysis of the frame is performed. For nonlinear static analysis, the non linear (plastic) hinges are modelled for columns and beams from the moment rotation curve of the columns and beams respectively. The study is conducted for bare frames. The properties of infill wall is not taken into consideration. However, the infill load is included.

2.1 Building model with fixed base

As per IS 1893:2016, soil structure interaction (SSI) may not be considered for seismic analysis of structures constructed on rock type or hard soil i.e. type I. therefore, for soil type I, the base of the building model is considered as fixed with no translation or rotation at the supports.

2.2 Building model with flexible base

SSI study is preferred for medium and soft soil. In the present study, the building base is modelled for medium type soil only. Soft soil is not considered. For medium type soil, the supports no more behave like fixed base but have translational and rotational degrees of freedom due to the flexibility of the soil. The translational and rotational stiffness are determined using the Gazeta's equations as given in ATC 40. The dynamic shear

modulus (G) is obtained from the ratio of dynamic shear modulus and initial shear modulus, $\frac{G}{G_o}$ for different site class and effective peak acceleration, S_{DS}/.25 as given in IBC 2006.

The initial shear modulus,

$$G_o = \frac{\gamma V_s^2}{g} \quad (1)$$

$$= 5.4548 \times 10^4 \text{ kN/m}^2$$

Where, the soil density (γ) = 16 kN/m^3 and shear wave velocity (V_S) = 182.88 m/s for site class D which corresponds to medium type soil.
g is the acceleration due to gravity
Therefore, G = 3.1365 x 10^4 kN/m^2

Table 1: Soil Stiffness factors for medium type soil

Degree of freedom	Units	K_{sur}	Correction factor for embedment, β	K_{emb}
Translation along x-axis	kN/m	1.8034 x 10^5	2.369	4.272 x 10^5
Translation along y-axis	kN/m	1.8034 x 10^5	2.369	4.272 x 10^5
Translation along z-axis	kN/m	2.4569 x 10^5	1.399	3.437 x 10^5
Rotation along x-axis	kNm/rad	2.0910 x 10^5	2.014	4.212 x 10^5
Rotation along y-axis	kNm/rad	2.1077 x 10^5	2.227	4.694 x 10^5
Rotation along z-axis	kNm/rad	2.6095 x 10^5	2.493	6.506 x 10^5

2.3 Performance levels and limit states

The performance levels as adopted from FEMA356 are Immediate Occupancy (IO) with a global limit state of slight damage, Life Safety (LS) with a global limit state of moderate damage and Collapse Prevention (CP) with a global limit state of extensive damage and finally the limit state of collapse.

3. RESULTS AND DISCUSSION

3.1 Capacity curve

On plotting the data of capacity curve (fig 1)as obtained from pushover analysis of fixed base and flexible base, it is observed that for the same spectral acceleration (S_a) value the corresponding spectral displacements (S_d) are higher in case of flexible base than that of the fixed base. The performance point (S_a, S_d) for fixed base is observed at (.075g, 11.86mm) whereas for flexible base it is at (.075g, 13.41mm)

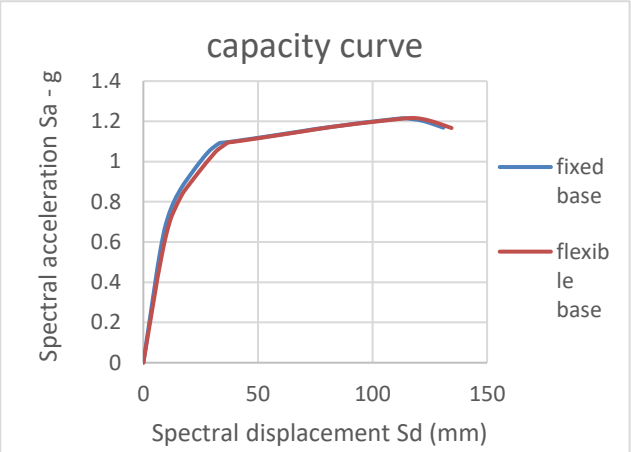

Fig.1. Capacity curve for fixed base and flexible base

3.2 Fragility curve

For better understanding of the variation in non-linear static pushover analysis due to fixed and flexible base, the fragility curves are developed for the different limit states.

Table 2: Soil Stiffness factors for medium type soil

Limit states	S_d (mm)	
	Fixed base	Flexible base
Slight damage	6.129	6.173
Moderate damage	14.876	14.819
Extensive damage	26.755	31.406
Collapse	27.94	32.509

From table 2, it is observed that there is very little variation for slight damage and moderate damage, but there is significant variation in case of extensive damage and collapse. Similar observations can also be derived from fig 2.

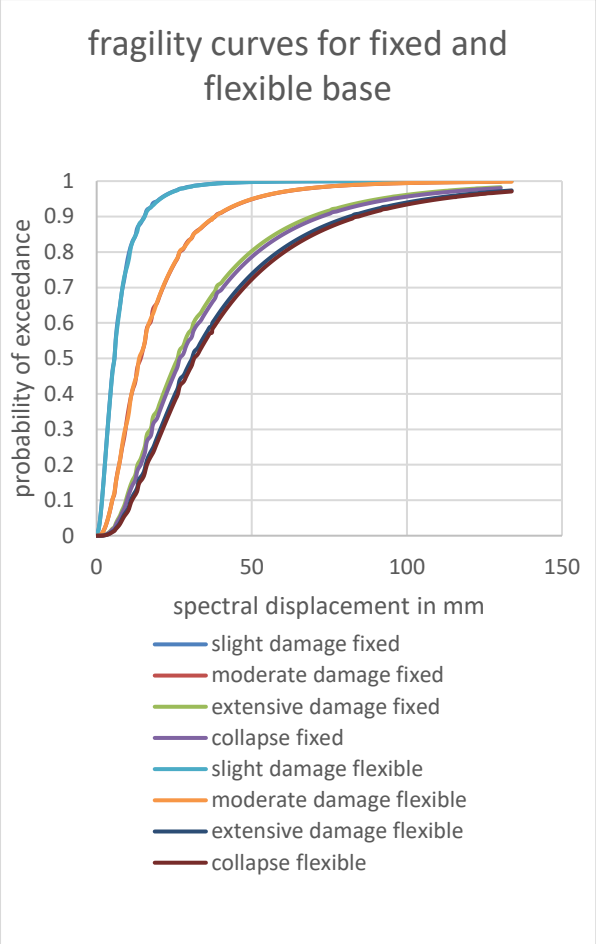

Fig.2. fragility curves for fixed base and flexible base

5. CONCLUSIONS

Non-linear static procedures are widely applied for seismic analysis due to its advantages over time history analysis even though time history analysis gives the most accurate results. In the present work, results of capacity spectrum method obtained from fixed base condition and flexible base condition are compared. Usually the effect of the flexibility of soil is neglected. This may be done for rock type or hard soil. But for medium type soil and soft soil, IS 1893:2016 recommends for soil structure interaction study. In this study the flexibility of medium type soil is considered and variation of results is observed when the building models are analyzed using SAP2000. The following conclusions can be drawn from the capacity curves and the fragility curves.

- The non-linear static pushover analysis may be carried out not only with fixed base but also with flexible base. There is variation in the spectral displacements obtained from fixed base condition and flexible base condition.
- From the study, it is observed that the performance point for flexible base is at a higher spectral displacement than that of the fixed base model. This shows that there is effect of soil flexibility on seismic analysis.
- The fragility curves show that at higher damage states, consideration of soil flexibility depicts a performance variation than that of the fixed base.

REFERENCES

1) ATC-40 (2002). "Seismic evaluation and retrofit of concrete buildings: Volume 1," Redwood City, California, 1996EFNARC
2) Chopra. A.K. (2012). "Dynamics of structures: theory andapplication to earthquake engineering", Prentice Hall, 2012.
3) Computers and Structures Inc., "SAP2000 – Integrated software for structural analysis and Design", Berkeley, California
4) Euro Code 8 part 3 (CEN 2004)
5) FEMA 356,(2000) "Prestandard and Commentary for the Seismic Rehabilitation of Buildings," Washington, D.C..
6) FEMA 440,(2005) "Improvement of Nonlinear Static Seismic Analysis Procedures," Washington, D.C.
7) Freeman, S.A., J.P. Nicoletti, and J.V. Tyrell, (1975), Evaluations of Existing Buildings for Seismic Risk – A Case Study of Puget Sound Naval Shipyard, Bremerton, Washington, Proceedings of the U.S. National
8) Conference on Earthquake Engineers, pp 113-122, Berkeley.
9) IS 1893 (part 1):2016, "Criteria for Earthquake Resistant Design of Structures", New Delhi
10) International Building Code 2006 by International Code Council, Inc

A study on effects of fire on reinforced concrete beams

Borgohain, A. [1], Bhattacharyya, Kumar, S.[2]

[1] U.G. Student, Department of Civil Engineering, NIT Silchar , Silchar,788010, India.
[2] Professor, Department of Civil Engineering, IIT Kharagpur, Kharagpur,West Bengal,721302,India.

ABSTRACT

Fire safety of structures has been of tremendous interest in last few decades particularly after the September 11 attacks on Twin Towers, New York in 2001. This has led to varied research in the field of evaluation of response of building and other structural systems under fire. Fire is one of the most severe risks to buildings and structures. A limited range of relevant research has been reported previously, especially for high performance concrete. In this paper a numerical study by three-dimensional modeling is developed for reinforced concrete beam exposed to fire conditions. Because of the changes in material properties and the large variations experienced in fire, both geometric and material properties are taken into account in this formulation. The three stages associated with the numerical procedure for evaluating fire resistance of RC beams; namely fire temperature calculation, thermal analysis and strength analysis are modeled using a finite element (FE) model. A FE model is prepared in ABAQUS software to study the response of an RCC beam under fire during loading conditions. In the beginning a simply supported RCC beam having constraints in one direction of roller support is analysed at 25°C .Then the uniform loading of one–third of the compressive strength of concrete is applied as a pressure loading in the beam(3D solid element).The other three faces of RCC beam have temperature boundary conditions that follows a temperature –time curve as per ASTM E119. The field output and the field history output are selected as required for post processing. The moment-curvature (M–k) relationships are developed for the beam at few critical positions of the RCC beam. These M-k relationships may be used to carry out the strength analysis of the beam member and draw significant conclusions.
Keywords: M–k relationships, fire temperature calculation, thermal analysis

1. INTRODUCTION

Fire is one of the most severe design situations as it not only affects the strength of concrete, but also the structural stiffness and stability. A reinforced concrete beam, compared to other structural members, has most often to cope with vertical forces and bending moments. In addition, the use of high strength concrete (HSC) is becoming more popular due to the improvements in structural performance such as higher strength and durability that it can provide compared to conventional Normal Strength Concrete (NSC). This paper presents the development of a computer model for predicting the fire behavior of RC beams under realistic fire loading scenarios. The model is based on a macroscopic finite element approach and a series of moment–curvature relationships for tracing the response of the beam.

2. LITERATURE REVIEW

Kodur V. et al.(1). Prepared batches of concrete with NSC , HSC(siliceous aggregate) , HSC (carbonaceous aggregate) , HSC(steel reinforcement), HSC(polypropylene) and found that deformation in beams are due to 3 factors namely load, thermal expansion and creep. NSC has a higher deformation rate than HSC due to the fact that HSC has higher young's modulus. Carbonate aggregate has less spalling than siliceous aggregates due to its higher specific heat value.

A. Lau (2) et. Al. studied concrete after being subjected to different elevated heating temperatures, ranging between 105 ℃ and 1200 ℃. The compressive strength, flexural strength, elastic modulus and porosity of concrete reinforced with 1% steel fiber (SFRC) and changes of color to the heated concrete etc were studied . For maximum exposure temperatures below 400 ℃, the loss in compressive strength was relatively small. Significant reductions in compressive strength are observed when temperature exceeds 400 ℃. When steel fibers are incorporated at 1%, an improvement of fire resistance and crack development was observed.

Jae H. Chung (3) developed a finite difference model that simulates coupled heat and mass transport phenomena in reinforced concrete structures exposed to rapid heating conditions such as fires. A mathematical and computational model for simulating the multidimensional, thermo-hydrological response of reinforced concrete structural elements is developed and used to study the effects of steel reinforcement on thermodynamic state variables. The effects of steel reinforcement on heat and mass transfer in the surface region of an R/C beam are found.

3. EXPERIMENTAL PROGRAMME

A reinforced concrete beam of 3-meter length and cross-sectional area 250mm×350mm used for the study . An attempt is made to compute the moment vs. curvature relationship at various locations of the beam. In the present study a roller–pinned support condition is considered and is subjected to a constant pressure load of 1.333E7 N/m^2. The beam is exposed to ASTM E119 standard fire for different exposure times. M40 grade of concrete and Fe 415 grade of steel have been used and geometric parameters of considered beam are described in given in Table-1**.**

Table 1. Geometric parameter of RCC beam

Beam length (mm)	3000
Concrete cross-section (mm^2)	350×250
Reinforcement diameter (mm)	20
Percentage reinforcement	1.795 %
Transverse reinforcement (mm)	12-8 dia. @250 mm c/c
Concrete cover (mm)	40
Support conditions	roller-pinned
Fire exposure method	ASTM E119 Standard fire
Exposure time in hours	0.5,1, 2, 3, 3.5

3.1 Reinforced concrete beam model

For the numerical analysis, on three faces of the referred RCC beam, model temperature boundary conditions are applied. Investigations done for the temperature, stress, strain, curvature distribution pattern as field output and at specific points as history output to characterize the beam exposed to fire. Modeling and analysis in finite elements software ABAQUS require the following steps such as part, property, assembly, interaction, step, load, mesh, job and visualization and those steps were performed. The number of element created were a) Concrete beam block 264 elements**;** b)Longitudinal reinforcement bar 33 elements .

3.2 Thermal conductivity

The thermal conductivity for siliceous concrete is a function of temperature and is expressed by equation (ENV 1992-1-2, 1995). Upper limit of thermal conductivity,

λ_c=2-0.2451(θ/100) +0.0107(θ/100)^2 W/mK

for $20^0C \le \theta \le 1200^0C$

lower limit of thermal conductivity

λ_c=1.36-0.136(θ/100) +0.0057(θ/100)^2 W/mK

for $20^0C \le \theta \le 1200^0C$

where λ_c is thermal conductivity in [W/m-K]

θ is the concrete temperature in [^{0}C]

The Thermal conductivity Vs temperature curve is presented in Fig 1.

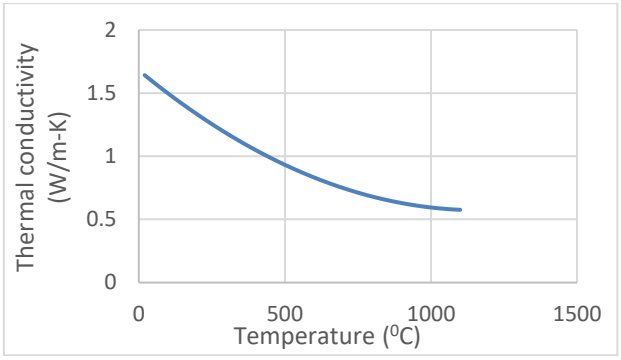

Fig. 1. Thermal conductivity as a function of temperature (ENV 1992-1-2, 1995)

3.3 Specific heat

The specific heat is a function of temperature and according to Euro code, it is valid to both siliceous and calcareous concrete (ENV 1992-1-2, 1995). The Specific heat Vs temperature curve is presented in Fig 2

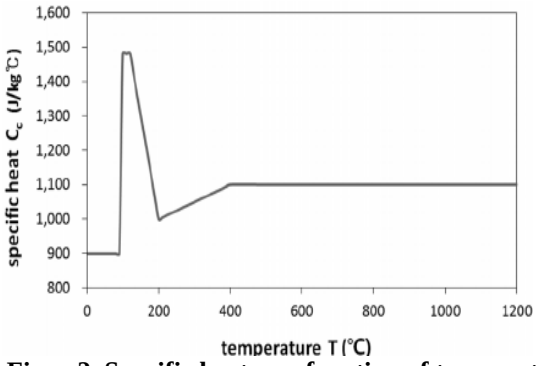

Fig. 2. Specific heat as a function of temperature for ordinary siliceous concrete (ENV 1992-1-2, 1995)

3.4 Thermal properties of steel

Steel is considered an isotropic material in temperature calculations and its thermal properties could be described by three different material properties: thermal conductivity, specific heat and thermal expansion co-eff and respective graphs are presented in Fig 3,4 and 5.

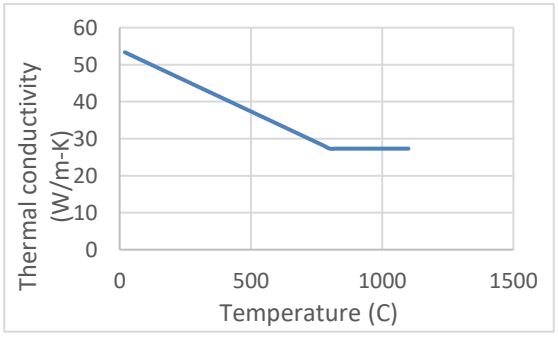

Fig.3.Thermal conductivity as a function of temperature for steel (ENV 1993-1-2, 1995)

Specific heat of steel is a function of temperature and expressed by the graph below(ENV 1993-1-2, 1995).

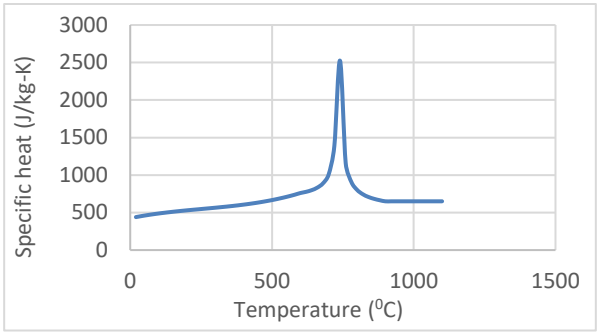

Fig.4. Specific heat as a function of temperature for steel (ENV 1993-1-2, 1995)

Density of steel and ordinary Siliceous concrete are considered a constant value 7850 kg/m^3 and 2400 kg/m^3 respectively.

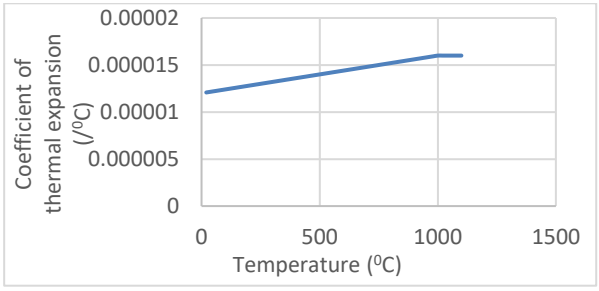

Fig.5 Thermal expansion co-efficient Vs temperature

3.5 Fire exposure methods

In this analysis ASTM E119 Standard fire method is considered.

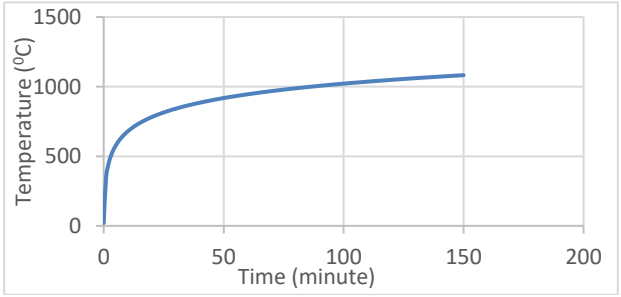

Fig 6. Temperature-time curve for the standard fire (ASTM E119, 2007)

The temperature-time relationship on the boundary member is defined by equation.

$T_f = T_0 + 750(1- \exp(-3.79553t_h^{1/2})) + 170.41t_h^{1/2}$

t_h, time (h);

T_0, initial temperature (° C); and

T_f, fire temperature (° C)

4 RESULTS AND DISCUSSION

4.1 Overview of the analysis

It is observed that initially the reinforced concrete beam is experienced a simultaneous contraction (at top fibres) and expansion (at bottom fibres) due to constant pressure load at the topmost surface. But when it is exposed to fire it experienced an expansion in elements and strain is developed . Due to the heating on the three surfaces curvature of the entire beam configurations changes and varies accordingly with time. Due to the cost of computation only data for some selected element of the beam is calculated such as 16(mid span), 25(quarter span) etc. Fig 7 shows A reinforced concrete beam of 3-meter length subjected to a constant pressure load of 13333.33 kN/m^2 on the X-Z surface and exposed to fire according to the fire curve ASTM E119 Standard fire (Transient) with exposure condition as three faces exposed to fire. The three other surfaces of the beam are kept at a constant temperature at 25°C.

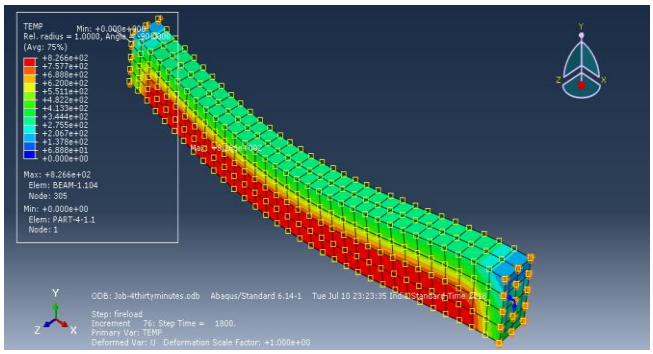

Fig.7 Fire load applied on three faces

Moment can be computed by the curvature at the desired elements on the beam. Even after simply applying the loading step with a uniform pressure load and not putting any heating step there are deformations in the RCC beam.

4.2 Results after 30 minutes fire loading:

Displacement in y direction for 30 minute duration fire loading is presented in Fig 8

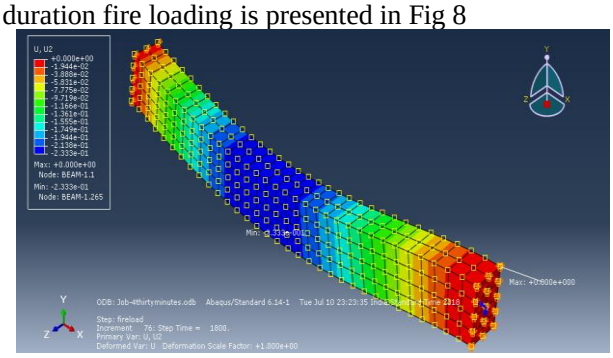

Fig 8: Displacement U2 (along global Y) contour

Initially the curvature is constant during the analysis of the loading step as there is no temperature

change during the loading step. Temperature changes monotonically only in the fire load step and both time and curvature magnitude keeps on increasing until heating stops. This is a condition which is observed at all the plots for curvature vs temperature as the static loading step is same in all the cases. Different durations for fire loading exposure for 0.5hr,1hr,2hr,3hr and 3.3 hr have been tried for. Maximum absolute value for U2 is 2.425e-1 m at element 1 solid beam part. The Curvature Vs temperature plot for wire beam element for 30 minute fire exposure has been presented in fig 9

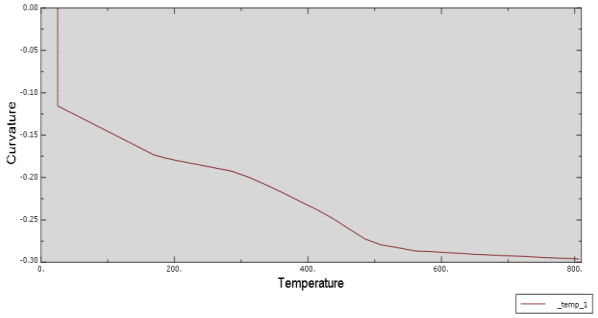

Fig 9: Curvature vs temperature plot for the central element of the RCC beam (wire-beam element 16)

4.3 Results for different durations of fire loading:

Analysis have been done for 5 different conditions of fire loading and deflected shape for all 5 cases have been extracted. Also curvature Vs temperature curves for all 5 cases for different elements have been extracted. Fig 10 represents vertical displacement contour 2 hour fire exposure.

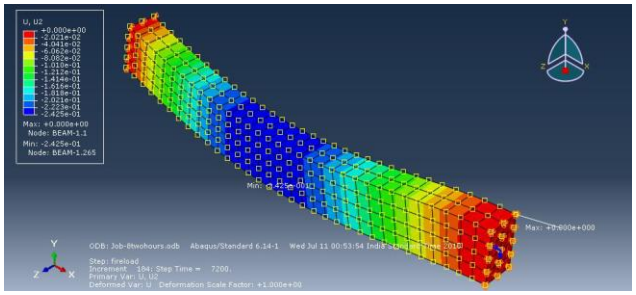

Fig 10 : Displacement U2 (along global Y) contour for entire beam at the end of the heating step

The Curvature Vs Temperature for different exposure durations have been presented in fig 11,12 and 13. From the curvature data, Moment curvature relationship have been obtained and presented in Fig

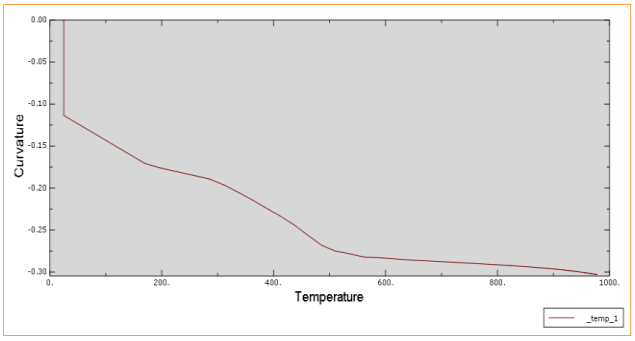

Fig 11: Curvature vs Temperature plot for 120 minute

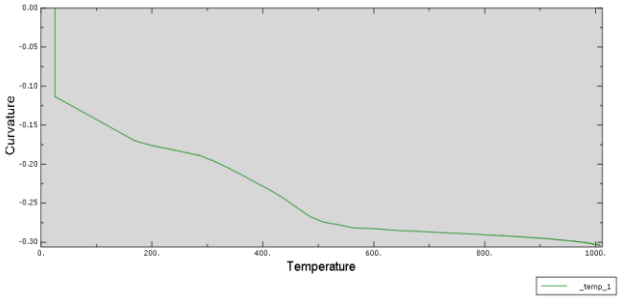

Fig 12: Curvature vs Temperature plot for element no. 16 (mid-point element) of the central embedded wire-beam element for a duration of 3 hours

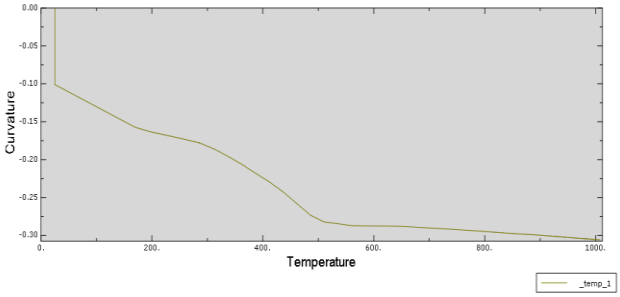

Fig 13: Curvature vs Temperature plot for element no. 8 (one fourth length element) of the central embedded wire-beam element for a duration of 3 hours

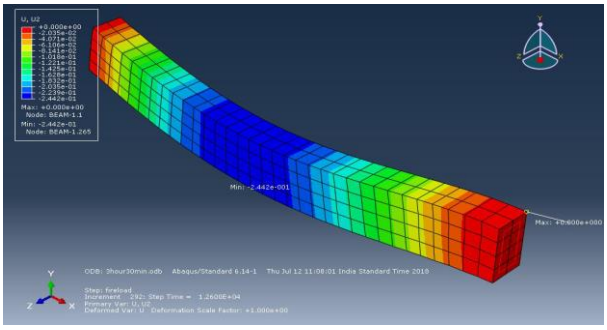

Fig 14: Displacement U2 (along global Y) contour for entire beam at the end of the heating step.

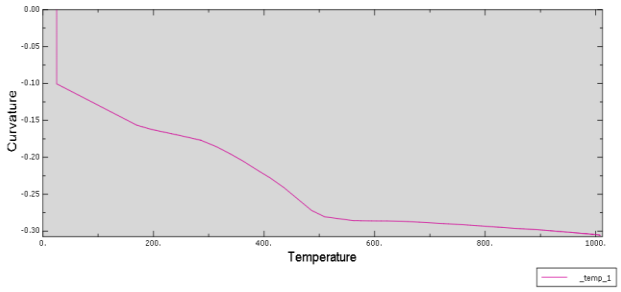

Fig 15: Curvature vs Temperature plot for element no. 8 (one fourth element) of the central embedded wire-beam element for a duration of 3 hours 30 minutes.

The moment curvature relationship for all durations were extracted. Fig 16 shows moment Vs curvature for 2 hr duration

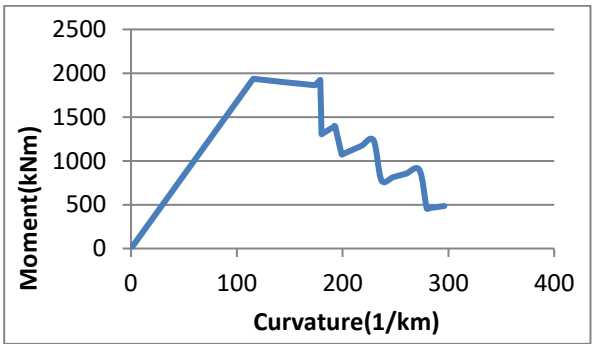

Fig 16: Moment vs curvature for element 16 (2hr duration)

From the moment Curvature relationships obtained, the values of respective moments have been presented in table 2.

Table 2. Moment and curvatures for salient points for different fire exposures

		Location 1 (Element 8)		Location 2 (Element 16)		Location 3 (Element 25)	
Sl. No.	Exposure time	Moment (kNm)	Curvature (/ km)	Moment (kNm)	Curvature (/ km)	Moment (kNm)	Curvature (/ km)
1	30 minutes	1664.293	99.26751	1936.96	115.5308	148.2866	8.844618
2	60 minutes	1664.266	99.2659	1903.005	113.5056	149.7022	8.929052
3	120 minutes	1695.789	101.1461	1903.984	113.564	151.2628	9.022137
4	180 minutes	1664.3	99.26794	1902.958	113.5028	151.0055	9.006794
5	210 minutes	1.66E+03	99.26599	1850.176	110.3546	149.7558	8.932252

The moment–curvature curve at any position in a beam has coincidental curves (at same locations for various times of exposures to fire). It is so because the loading step is same for all the different conditions and time of exposure to fire.

5 CONCLUSION

1. The maximum moment in moment curvature curve is at location 2(element 16) at time 120 minutes and is of magnitude 1903.984 kNm at curvature of 113.564 The next highest moment in moment curvature curve is at location 1(element 8) at time 120 minutes and is of magnitude 1695.789kNm at curvature of 101.1461
2. The moments at location 3 are very small in comparison. It is due to the non uniform boundary conditions applied at the cross-sections: hinge at one cross-section and a roller with constraints in any one direction in another direction.
3. The difference in the curves for Moment vs curvature for different times of exposure is very small due to the fact that after 30 minutes of fire exposure in fire loading step the increase in temperature is very gradual .Hence the effect in the moment vs curvature curve is very less making the difference between all the curves seemingly smaller.
4. The curve for lower time of exposure lies above the curve for higher time of exposure.
5. After exposure to fire for 120 minutes the peak Moment values and corresponding curvatures are reached for all the three locations elements 8, 16, 25 respectively in Table 2 .

6 ACKNOWLEDGEMENTS

I would like to express my special thanks to Prof. Sriman Kumar Bhattacharyya, IIT Kharagpur for his excellent guidance and encouragement. I would also like to thank
Prof. Arghya Deb, IIT Kharagpur for his valuable suggestions. I express my sincere gratitude to Indian Academy of Sciences for offering me this opportunity.

7. REFERENCES

1) Kodur VKR, Cheng F-P, Wang T-C, Sultan MA. Effect of Strength and Fiber Reinforcement on Fire Resistance of High-Strength Concrete Beams. J Struct Eng [Internet]. 2003;129(2):253–9.
2) Lau A, Anson M. Effect of high temperatures on high performance steel fibre reinforced concrete. Cem Concr Res. 2006;36(9):1698–707.
3) Chung JH, Consolazio GR. Numerical modeling of transport phenomena in reinforced concrete exposed to elevated temperatures. Cem Concr Res. 2005;35(3):597–608.

Steel bands: a sustainable strengthening technique to strengthen unreinforced masonry buildings

Choudhury, T.S.M. [1] and Kaushik, H.B. [2]

[1] Ph.D Student Department of Civil Engineering, Indian Institute of Technology Guwahati, Assam-781039, India.
[2] Associate Professor, Department of Civil Engineering, Indian Institute of Technology Guwahati, Assam-781039, India.

ABSTRACT

Past records of the building stocks in India ranging from the times of Harappa and Mohenjo-daro, through the medieval periods of Mughals and British till date, provides enough evidence that unreinforced masonry (URM) building has been a common construction practice. Recent census showed that large number of buildings in India, especially in rural areas, are still constructed using URM. Such building stocks include both important heritage buildings with complex architectures, government offices and houses. However, such buildings are susceptible to varying levels of damage during earthquakes due to improper maintenance and construction practice. Therefore, strengthening of such buildings has become an important motivation for study in order to save the heritage and other structures from further damage. Although recent strengthening interventions suggest use of fiber-reinforced polymer, such materials bear heavy cost and need skilled supervision. Hence, such interventions may not be feasible for use in most of the common URM buildings, except in case of important heritage structures. If not used properly, the polymer may incur further damage to the materials used in heritage buildings. On the other hand, steel bands, which are neither expensive nor react with the building material, can be conveniently used as a sustainable strengthening option for common buildings as well as heritage structures. The present paper reports results of a pseudo-static experimental study evaluating the effectiveness of a strengthening scheme for a URM building using steel bands. The strengthened building exhibited a significant improvement in the lateral load carrying capacity as well as deformability.

Keywords: Masonry, Seismic strengthening, Steel bands, Cyclic tests

1. INTRODUCTION

India has been one of the oldest users of masonry as a construction material. The construction practice of using masonry dates back since the time of Harappa and Mohenjo-daro. Even today, use of brick masonry has been a common construction practice in the country. Recent census showed that large number of buildings in India, especially in rural areas, are still constructed using URM.The main reason for such construction practice is that the construction materials are inexpensive and easily available. Despite its advantages, the unreinforced masonry (URM) buildings are highly vulnerable and may result into total or partial collapse during earthquakes. Besides, the earthquake reports by various authors cites that buildings constructed following the code provisions have survived even major earthquakes with repairable damages (Kaushik & Dasgupta, 2014; Kaushik, et al., 2006; Murty et al., 2006; National Disaster Management Authority, 2006). However, it is pretty unsure if the URM building stocks were constructed following the code provisions. This might be due to the fact that during the time the buildings were built, the seismic codes were not present. Strengthening of URM buildings is extremely important not only for saving large number of human lives residing in such buildings, but also for saving the monumental, heritage, and religious structures from severe damage during earthquakes. Such strengthening schemes should be simple, easily implementable, and cost effective. Hence, a sustainable solution to strengthen such structure has become a crucial issue particularly considering the case of those masonry buildings located in earthquake prone areas.

The existing codes like IS 13935 (BIS 1993) recommends grout or epoxy injection in existing weak wall and use of split and bandage technique using wire mesh as a strengthening solution. It also recommends tying the walls by pre-stressing techniques. Besides, the recent strengthening interventions suggest use of fiber-reinforced polymer; such materials bear heavy cost and need skilled supervision. And, the given strengthening solution by codes requires sophisticated equipment and skilled labour which one way or other does not seem to be sustainable.

It has also been observed that various strengthening schemes were adopted in the past to strengthen such buildings and steel has been a popular material for strengthening. For example, El-Borgi et al. (2005) proposed a retrofit scheme to strengthen a historical building at Tunisa that consists of a steel frame directly attached to the portrait room structure with added fluid viscous dampers. Recent studies indicate that tying wall with steel ties prevents

separation, disintegration of walls, and improves seismic behavior of the structure (Borri et al. 2009, Vincente et al. 2011). Besides Branco and Guerreiro (2011) in their work showed that use of steel ties can be less expensive and does not contribute to an excessive increase in the structure's weight and it minimizes the interruption of the normal functioning of the building. According to Tassios (2010), addition of steel elements as shear connectors, along transversal walls intersections, in case of cracks for stitching or in case of passing through connectors of three-leaf masonry, can be adopted to strengthen masonry wall. Therefore, due to various advantages of steel, use of steel bands to strengthening the unreinforced masonry buildings can be a sustainable strengthening methodology.

In the present work, two full-scale specimens of a single storey, single bay URM building are tested under pseudo-static slow cyclic lateral loading. One building is unstrengthened (Fig. 1), while the other is strengthened using horizontal and vertical steel bands both externally and internally (Fig. 2), and lateral load performance of both buildings are evaluated. One wall of the building has a door opening, while two adjacent walls have a central window opening. The fourth wall is constructed without any opening. Such a configuration will test the suitability of the strengthening scheme for walls with different opening sizes.

2. EXPERIMENTAL SETUP

The buildings are with the dimension 3m×3m×3m, with 0.1 m reinforced concrete slab on top. All the walls of the buildings are full brick thick (0.24 m). A full brick parapet wall of 0.9 m height is constructed over the top of the slab over each wall. An additional weight of 10 kN is applied on the slab to substitute the load due to floor finish. The URM building is strengthened using the steel flats of size 40 mm × 5 mm fitted horizontally at sill and lintel level. In addition, vertical steel bands are fitted vertically around the opening as shown in Fig. 2. The external steel bands are connected to the internal steel bands by drilling 10 mm dia. bolt of 30 cm long through the wall at 0.5 m interval. The cyclic loads are applied using displacement controlled servo-hydraulic actuator of 250 kN load and 250 mm displacement capacity. The cyclic loading is applied at the slab level of both the specimens with the help of steel plates connected at both the ends of the specimens using steel rods.

The material properties of the building models, some of which are obtained experimentally, are given in Table 1. The compressive strength of the masonry unit, mortar, and masonry prism are determined as per the relevant Indian standards (BIS 1992, BIS 1995 and BIS 1987). The tensile bond strength is determined using the method suggested by Khalaf (2005). The initial shear capacity of masonry units is determined following BS EN-1052 (2002).

Fig.1. Test Setup for URM Building

Fig. 2 Strengthened Building

Table 1. Material properties of the brick masonry

Property	Value
Brick Unit compressive strength	19.3 MPa
Compressive Strength of Mortar (1:6)	4.84 MPa
Masonry Prism compressive strength	3.18 MPa
Tensile bond strength (Z test)	0.129 MPa
Elastic Modulus of Masonry	1748 MPa
Shear Strength (Triplet Shear test)	0.165 MPa

3. RESULTS AND DISCUSSION

During the slow cyclic lateral load testing of the unstrengthened URM specimen, small cracks started initiating at the bottom layer of the wall corners at 1 mm displacement level as shown in Fig. 3. The corner diagonal cracks near openings are visible at 5 mm displacement level. These cracks gradually increased in the sizes with the increasing displacement levels. Cracks are also observed in the walls perpendicular to the direction of loading at 7 mm displacement level resulting in slight out-of-plane deformation of the

Fig. 3 Damage observed in the unstrengthened URM building in the form of cracks in different walls

Building.

By 12 mm displacement level, major cracks are visible throughout the walls and the cracks in the orthogonal walls are found to connect to each other at further displacement level. During the test, mixed failure mechanism is observed consisting of both shear and tensile failure in the bed joint along with torsional response at higher displacement levels (Fig 3). The hysteresis curves generated from the test show that the lateral capacity is nearly 80 kN as shown in Fig. 4.

The experimentally obtained hysteresis response and envelop curve for the Strengthened URM building specimen show the beneficial influence of using steel bands for strengthening as shown in Fig. 5. The specimen exhibited small cracks initiation near the openings at 4 mm displacement level. The corner diagonal cracks near openings started extending from 5 mm displacement level. Visible cracks are generated in the walls perpendicular to the loading direction at 6 mm displacement level, and at 12 mm displacement level these cracks became more prominent. By 15 mm displacement level, major cracks are visible in both exterior and interior sides of the walls (Fig. 6). Beyond 18 mm displacement the upper part of the structure is seen to be rocking on the lower part. At 28 mm displacement level the joints of steel flats snapped and major damage near the openings and corners is observed. During the test, mixed failure mechanism is observed consisting of both shear and tensile failure in the bed joint. However, the torsional response in the strengthened specimen is found to be significantly lesser than that of the unreinforced specimen. Fig. 5 shows that the lateral load carrying capacity of the strengthened specimen is about 110 KN. Capacity curve comparison of both the building models is shown in Fig. 7. It is seen that using steel band as a strengthening measure results in a significant increase of about 38% in load carrying capacity of the URM building. Similarly, the deformation capacity of the URM building also made a remarkable improvement.

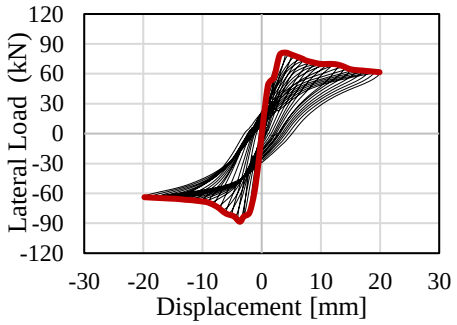

Fig. 4 Hysteresis and envelop curves for unstrengthened URM building

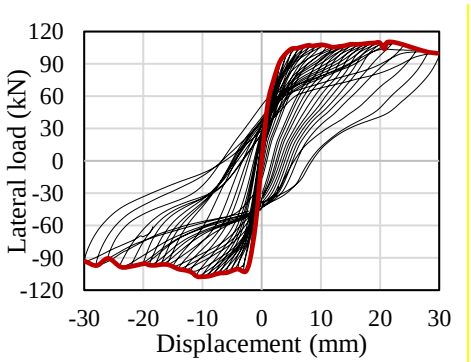

Fig. 5 Hysteresis and capacity curves for strengthened URM building

Fig. 6 Damage observed in the strengthened URM building in the form of cracks in different walls

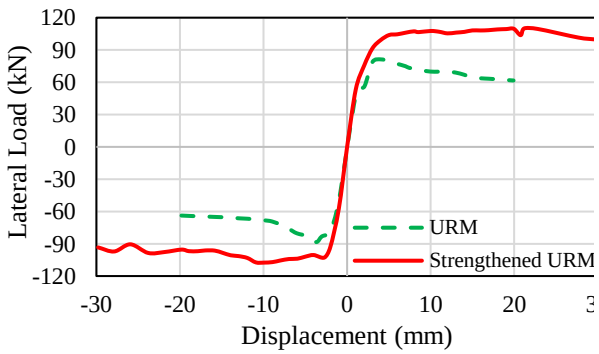

Fig. 7 Comparison of Capacity curves

About 61 strain gauges are attached on steel flats at various locations in order to measure the axial strain in the bands to know if any of the steel bands are subjected to nonlinear strains during the tests; the recorded strains are shown in Fig. 8. The points where comparatively large strain readings are recorded are corresponding to those where significant damage is observed. This signifies that the steel bands contribute to the lateral load resistance significantly and delay the formation of cracks and failure in the walls of the building. The strain gauges attached on the steel flats near the openings recorded high strain values confirming that these are the regions of high stress concentration. The final strain values recorded at 30 mm displacement level is shown in Fig 8. Even at the final displacement level, failure is not observed in the steel flats. However, at this level, point 29 recorded the highest strain value of 0.0027, which is slightly higher than the yield strain of 0.0023, marking the location of the highest damage area in masonry walls near the wall junction where two walls meet. This is the same location where failure is observed in the joint between steel flats in the wall junctions at two locations during experiments. Though, none of the other strain gauges are found to have exceed the yield strain value, the high linear strain values recorded in some of the steel flats in critical locations show that the steel flats are contributing to the lateral resistance of the building.

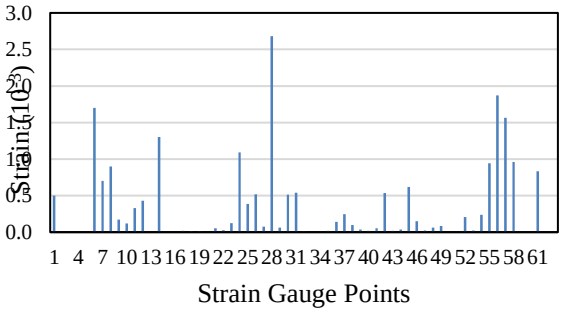

Fig.8 Axial strain in steel flats at various points

4. CONCLUSION

In the experimental study, pseudo-static cyclic tests on two URM buildings – one unstrengthened and another strengthened using steel bands – is carried out. Test results show that the lateral load carrying capacity of the unstrengthened specimen is 80 kN, which increased by about 38% to 110 kN after strengthening. In addition, the hysteresis response of the strengthened specimen is observed to be better and stable than the unstregthened specimen. The lateral deformability of the strengthened specimen is also found to be significantly better.

It is evident from the strain gauge readings that the corners of the openings are the most critical areas needing special attention. Results show that application of steel flats can significanrly improve the lateral load behavior of URM buildings, and hence, can reduce the vulnerabilty of the URM building substantially. The major advantage of using this strengthening scheme is its ability to be repaired and replaced easily when needed. Therefore, use of horizontal and vertical steel bands on both faces of the walls of URM building can be a sustainable strengthening solution for unreinforced masonry building, which can be used to strengthen both ordinary and heritage structures.

ACKNOWLEDGEMENTS

Authors gratefully acknowledge Department of Science and Technology, Government of India for providing research funding for the work under grant number SB/S3/CEE/0018/2014.

REFERENCES

[1] C. V. R. Murty, D. C. Rai, S. K. Jain, H. B. Kaushik, G. Mondal, and S. R. Dash, "Performance of structures in the Andaman and Nicobar islands (India) during the December 2004 Great Sumatra earthquake and Indian Ocean tsunami," *Earthq. Spectra*, vol. 22, no. SUPPL. 3, pp. 321–354, 2006.

[2] National Disaster Management Authority, *Guidelines on Repair, Restoration and Retrofitting of Masonry Buildings in Earthquake Affected Areas of Jammu & Kashmir*. Ministry of Home affairs, Government of India, 2006.

[3] H. B. Kaushik, K. Dasgupta, D. R. Sahoo, and G. Kharel, "Performance of structures during the Sikkim earthquake of 14 February 2006," *Curr. Sci.*, vol. 91, no. 4, pp. 449–455, 2006.

[4] H. B. Kaushik and K. Dasgupta, "Assessment of Seismic Vulnerability of Structures in Sikkim , India , Based on Damage Observation during Two Recent Earthquakes," vol. 27, no. December 2013, pp. 697–720, 2014.

[5] Bureau of Indian Standards (BIS)., "Repair and Seismic Strengthening of Buildings-Guidelines", IS 13935, New Delhi, India

[6] El-Borgi, S., Smaoui, H., Casciati, F., Jerbi, K., and Kanoun, F. (2005), "*Seismic evaluation and innovative retrofit of a historical building in Tunisia"*, Journal of Structural Control and Health Monitoring, Vol.12, Issue-2, pp. 179-195.

[7] Borri, A., Castori G., Grazini A. (2009), "*Retrofitting of Masonry Building with Reinforced Masonry Ring-beam"*, Journal of Construction and Building Materials, Vol.23, Issue-5, pp. 1892-1901

[8] Vincente, R., Rodrigues, H., Varum, H., Mendes, Da Silva, J.A.R. (2011), "*Evaluation of Strengthening Techniques of Traditional Masonry Buildings: Case Study of a Four-Building aggregate"*, Journal of Performance of Constructed Facilities, Vol.25, No3, pp. 202-216

[9] Branco, M., and Guerreiro L.M. (2011), "*Seismic Rehabilitation of Historical Masonry Building"*, Engineering Structures, Vol. 33, pp. 1626-1634.

[10] Tassios, T.P. (2010), "*Seismic Engineering of Monuments*", Earthquake Engineering, Springer, Vol.8, pp. 1231-1265

[11] Bureau of Indian Standards (BIS)., "Indian standard methods of test of burn clay building bricks—Part 1: Determination of compressive strength," *IS 3495*, vol. 3rd Revision. New Delhi, India, 1992.

[12] Bureau of Indian Standards(BIS), "Indian standard code of practice for preparation and use of masonry mortars," *IS 2250*, vol. 5th Revision. New Delhi, India, 1995.

[13] Bureau of Indian Standards (BIS), "Code of Practice for Structural use of Unreinforced Masonry," *IS 1905*, vol. 3rd Revision. New Delhi, India, 1987.

[14] F. M. Khalaf, "New Test for Determination of Masonry Tensile Bond Strength," vol. 17, no. December, pp. 725–732, 2005.

[15] BS EN, "Methods of test for masonry - Part 3: Determination of initial shear strength," *BS EN 1052-3*, 2002.

Sustainability of hospital building during earthquake in northeast india

Sachidananda, K.[1] and Victory, W.[2]

[1,2] Lecturer, Dept. of Civil Engineering, National Institute of Technology Manipur, Manipur, India.

ABSTRACT

Hospital played an important role for the safety of life and it needs to be fully safe even during the devastation time of earthquake. In the past earthquakes, buildings lying in the Northeast zone suffer damage or collapse, indicating the limitation of the design. Northeast India is the part of India which lies in the most earthquake prone zone (i.e., Zone V) and safety measures need to be taken for the sustainability of important buildings like hospital in this region. As per Indian standard (IS) code (i.e., Forced base design Method), buildings in India are usually designed for the safety purpose (i.e. under reinforced within the limitation of limit state design). The performance of the building as per FEMA (Federal Emergency Management Agency) 356 guideline have been categories into three stages i.e. immediate occupancy (IO), life safety (LS), Collapse prevention (CP) and the normal building design with Bureau of Indian standard (BIS) is at the CP level, which is the lowest level of performance level. The performances of the buildings are evaluated through Nonlinear Static Analysis (NSA) i.e. Push over analysis (ATC 40) using SAP 2000. The hospital building needs to be at the state of IO level to maintain the occupancy of building even during earthquake and its designed has been done with Displacement based design (DBD) with the consideration of performance of building. Even though the safety is ensured with DBD method, the economic consideration needs to be estimated as the DBD cost higher compared to the codal design.

Keywords: SAP 2000, push over, hospital, building, sustained

1. INTRODUCTION

Hospital is an institution, where all the needy and ill people used to get treatment. Many people used to assemble, irrespective of the types of community. As hospital is an essential structure for the existence of human kind, it is an important structure which needs to stand in all types of whether and climatic conditions. The importance of hospitals has been studied by many researchers i.e. Delavar. *et al.*, 2015; Maharjan *et al*., 2015; Kiranbala and Sandhyarani, 2016. They have studied the vulnerability assessment of hospital buildings. People have witnessed the devastation of hospital buildings during the past earthquakes. Bhuj earthquake (2001) have witnessed the failure of hospital buildings like Jubilee hospital, the Mental hospital, the Branch hospital etc leading to no place of habitation during the devastation time. Such important structure fall at the time of treatment for people. Other than the hospital buildings, many residential buildings also fall during the past earthquakes. So the design of hospital buildings

Based on the intensity of the earthquake, India is divided into four zones i.e. Zone II, III, IV, V as per IS 1893 (2016) shown in Fig. 1. Northeast India is a part of India and it lies in the earthquake prone area i.e. Zone V. Due to the past earthquakes in northeast india, many buildings, monumental structures got destroyed. During the past earthquakes in Imphal (M6.7, 4 January 2016), many buildings collapse or damage as reported in papers and journals (Rai *et al*., 2017; Ibotombi *et al*., 2018). Recently in Assam, an earthquake of magnitude 5.5 struck on 12 September 2018. The states of Sikkim, Mizoram, Shillong, Tripura, Nagaland, Manipur lies on the same belt of earthquake zone. Almost all the states had witnessed many shocks of earthquake in the past. The structures situated on this northeast zone of India needs to take special care from earthquake. As per Indian standard (IS) code (i.e., Forced base design Method), buildings in India are usually designed for the safety purpose (i.e. under reinforced within the limitation of limit state design). Depending on the importance of the structures, different performance level have been classified namely operational performance (OP) level , Immediate Occupancy (IO) level, Life Safety (LS) level, Collapse Prevention (CP) level as per FEMA 356 (2000). Usually the performance level of normal building as per IS code 456 (2000) is the collapse prevention (CP) level, which is the lowest level of performance. The hospitals in northeast India, needs to take special care as compared to other hospitals

situated in other lower earthquake zones. As per the literature review, no study has been made to compare the safety and the cost estimate of normal building and hospital buildings. In the present study, a plan of uniform structure with shear wall provision for providing more strength and stiffness of structure has been taken as it gives maximum stability to structure from seismic point of view. In the same plan of building, different performance level of design has been analyzed, following the performance based design of building (Priestley and Kowalsky, 2000). For the design of building, a finite element software namely SAP 2000 has been used. From Nonlinear Static procedure (NSP) generally known as Push over Analysis (ATC 40), performance point is evaluated through (a) Uniform load and (b) Mode proportional load. The target performance taken for the buildings are Immediate Occupancy (IO) with 1% drift, Life safety (LS) with 2% drift and Collapse prevention (CP) with 3% drift as per FEMA 356 (2000).

2. PERFORMANCE BASED DESIGN

The structures are generally designed on the basis of three main criteria namely- strength, stiffness and ductility. The strength is related to the damageability or ultimate limit state. For the earthquake resistant design of structures main demand is the ductility demand which is essential

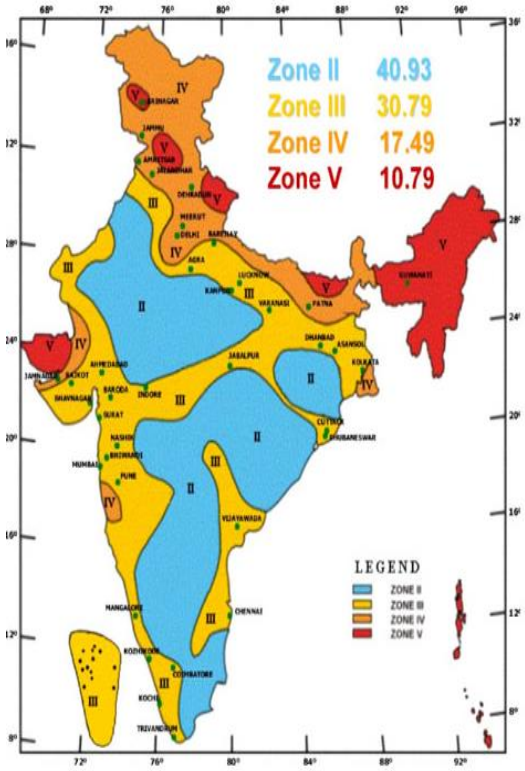

Fig. 1: Seismic zonation and intensity map of India (Pib.nic.in)

attribution of the structure that must respond to the strong ground motions. Performance-Based Design (PBD) is the method of design where a structure is designed to get the targeted performance of the structure under a specified hazard levels. The PBD methodology is the deformation based design rather than a force based design. Therefore due consideration is given to the nonlinear behavior of the structure. PBD methods differ from the codal method as it can specify a building individual performance. Performance based design generally follow the FEMA (Federal Emergency Management Agency) guidelines. Though FEMA-356 is a seismic rehabilitation document, it can be applied for new buildings as well. In this design method, strong column weak beam concept of IS 13920 is generally followed.

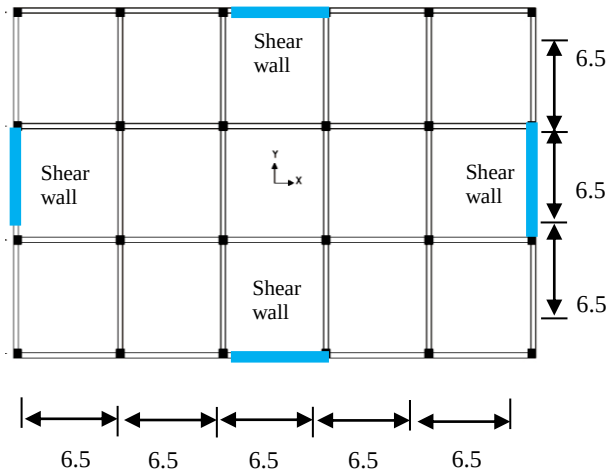

All dimensions are in 'm'

Fig. 2: Uniform Plan of typical building.

3. PUSH OVER ANALYSIS

Nonlinear static analysis (or Nonlinear Static Procedure, NSP) is a simplified analysis procedure that can be useful for obtaining approximate earthquake demands on building. This is popularly known as Pushover Analysis. Pushover analysis assumes that the structural response is dominated by the fundamental mode and that the mode shape remains unchanged after the structure yields. Therefore, the response of low to medium rise buildings, which is typically dominated by the first mode, can be predicted well by pushover analysis (Chopra, 2007).

A pushover analysis is performed by applying monotonically increasing pattern of lateral loads to a structure, representing the inertial forces which would be experienced by the structure when subjected to ground shaking. Under

incrementally increasing loads various structural elements may yield sequentially. At each event, the structure experiences a loss in stiffness. Using a pushover analysis, a characteristic nonlinear force displacement relationship can be determined. From the push over curve the performance point of the building frame can be found out through non-linear property of the material.

4. FINITE ELEMENT MODELLING

4.1 GENERAL

For the analysis of building structure, a plan shown in Fig, 2 has been taken for the analysis. The building of 10 storeys have been considered for the analysis, as hospitals usually have lifts and are big building in this modern days. The elevation of the building both on the longer side and shorter side are shown in Fig. 3. The same building will be analysed to find the different performance level of IO and CP levels through the Push over analysis in SAP 2000. The push over curve has been plotted both from uniform load and modal load. The sizes of building frames has been determined from different performance of the building, In the push over analysis, the performance level of the building has been determined. The foundation and slab design has not been studied in the present design, it has been neglected.

4.2 Modelling in SAP 2000

The RCC building has been modelled in SAP 2000 as a line diagram assigning different section sizes and finding the performance level of the building through Push over analysis. A series of trial has been made to determine the sizes of frames i.e. column and beams. From the trial and error, the frames sizes have been found out as shown in Table 1. The loading of the building as per IS 875 (1997) and the safety of the building has also been checked as per IS 456 (2000).

5. OBSERVATIONS

The non-linear static analysis has been performed to find the performance of building through push over analysis. The push analysis results using the frame sizes given in Table 1 has been plotted in Fig. 4 for the IO level building and Fig. 5 for the CP level buildings.

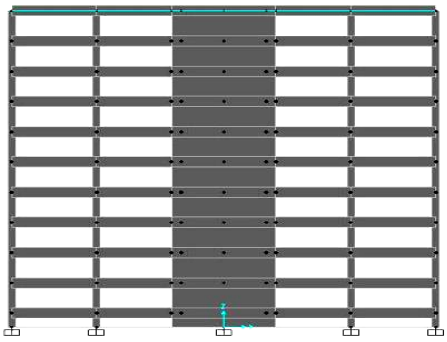

(a) Longer side of building

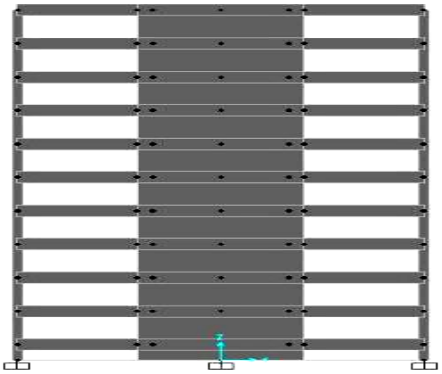

(b) Shorter side of building

Fig. 3: Elevation of building

The push over curve showed the difference in the performance level of the building considered. As the performance level of the building i.e. safety level increases, the frame size section of RCC structure increases in IO as compared to CP. As the sizes of the frame section increases the expenditure of construction also increases.

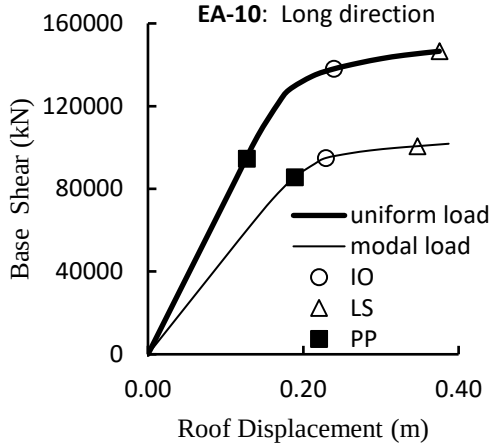

(a) Longer side

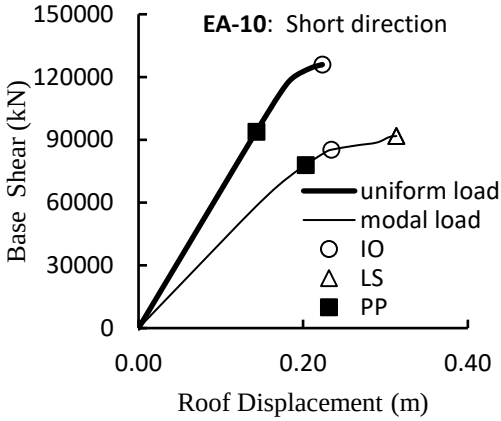

(b) Shorter side

Fig. 4: Push over curve of IO level

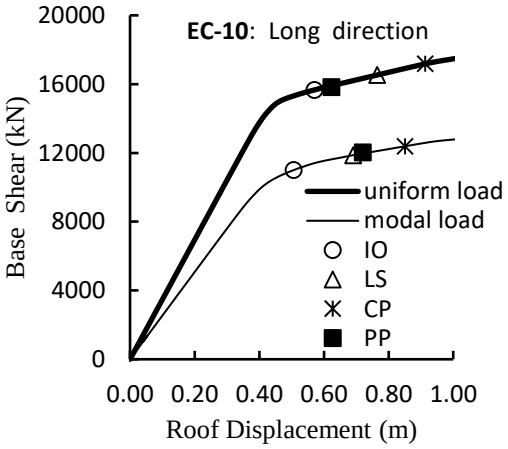

1. Longer side

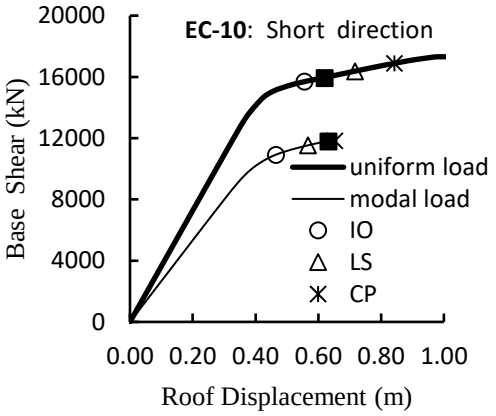

Fig. 5: Push over curve of CP level

6. CONCLUSIONS

Based on the studied building regarding the performance of building at IO and CP level, it has been found that the building at IO performance level require more money to meet the performance level. Since hospital occupy an important place for the safety of the society, all the hospital building need to be safe at seismic time. The hospital building at north-eastern regions needs to be design at the IO performance level, in order to sustain even in the devastating time of seismic.

Table 1: Member sizes of buildings

Performance level	Column size(mm)		Beam size (mm)	Shear wall size (mm)
	Inner column	Exterior column		
IO	550×550	700×700	1100×550	8000 × 450
CP	500×500	500×500	550×300	2500 × 300

REFERENCES

1) ATC 40 (1996) "Seismic evaluation and retrofit of concrete buildings", Report No. SSC 96–01, Seismic Safety Commission, State of California, Proposition 122 Program, prepared by *Applied Technology Council*.
2) Bhuj earthquake (2001). Earthquake rebuilding: Bhuj, the city that learnt its lesson. *The Indian Express*, Retrieved on 14/09/2018.
3) Chopra, A.K. (2007), "Dynamics of Structures, Theory and Applications of Earthquake Engineering", *Prentice-Hall* of India.
4) Delavar, M.R., Moradi M. and Moshiri B, (2015) Earthquake vulnerability assessment for hospital buildings using a GIS based group multi criteria decision making approach study of Tehran,Iran, *International Conference on sensors & Models in remote sensing & Photogrammetry*, 23-25 Nov, Kish Island, Iran.
5) FEMA 356 (2000): Prestandard and commentary on the seismic rehabilitation of buildings, *US Federal Emergency Management Agency*,Washington, DC.
6) IS 13920 (2016): Ductile design and detailing of reinforced concrete structures subjected to seismic forces - Code of Practice, (First revision), *Bureau of Indian Standards*, New Delhi.
7) IS 456 (2000): Plain and Reinforce Concrete –Code Practice (fourth Revision), *Bureau of Indian Standards*, New Delhi, 2000.
8) IS 1893 (2016): Criteria for Earthquake Resistant Design of structures: Part1 General Provisions and Buildings (sixth revision), *Bureau of Indian Standards*, New Delhi.
9) IS 875 (1997): "Code Practice for design loads (other than earthquake) for buildings and structures, (Part2) Imposed loads (second revision)," *Bureau of Indian Standards*, New Delhi.
10) Ibotombi S., Singh H.S., Singh T.J., Singh S.S. & Doungel T.S. (2018). January 4th, 2016 Manipur Earthquake and damages to some public engineering structures. *Journal of applied geochemistry*, 20(1), 140-149.
11) Kiranbala T. and Sandhyarani S., (2016), Seismic vulnerability assessment of existing hospital buildings in Imphal city.3rd *International Conference on Recent Innovations in Science, Technology, Management and Environment*, New Delhi.
12) Maharjan DK, Shrestha H., Guragain R (2015), Non-structural vulnerability mitigation in hospital and experience in recent medium intensity earthquake, *New technologies for urban safety of mega cities* in asia.
13) Priestley, M.J.N and Kowalsky, M.J. (2000): Direct Displacement-Based Design of Concrete Buildings, *Bulletin of the New Zealand National Society for Earthquake Engineering*, 33(4), 421-444.
14) Pib.nic.in.(2018). Earthquake zones of India. *Retrieved* on 14/09/2018.
15) Rai D.C., Kaushik H.B. & Singhal V. (2017). M 6.7, 4 January 2016 Imphal earthquake: dismal performance of publicly-funded buildings. *Current Science*, 113, 12, 2341-235.
16) SAP 2000. Structural software for analysis and design. *CSI documents*.

Selection of best pier cross-section of bridge for sustainable water flow

Sachidananda, K.[1] and Victory, W.[1]

[1]Lecturer, Dept. of Civil Engineering, National Institute of Technology Manipur, Manipur, India

ABSTRACT

The bridge piers represent an essential structure for the erection of bridge. The pier can be constructed in different shapes and the flow of water environment changes along with it. The selection of the best pier shape that minimizes the disturbance of water flow need to be investigated as it will have least disturbance to water environment and its subsequent bank. This paper present the experimental investigation of the best cross-section of bridge pier among the shapes of rectangular, hexagonal and oval shapes. From the study, it has been found that oval shape pier represents the best pier shape as it showed the least disturbance to water flow.

Keywords: pier, bridge, oval, rectangle, hexagonal

1. INTRODUCTION

Bridges are one of the important infrastructures for modern transport system. The stability of bridge piers depends mainly on the safety of the foundation, which ultimately depend on the phenomenon of scour around piers. Umesh (2007) has stated the detrimental effects that river flow can have on the stability of piers and abutments that support a bridge. The importance of the phenomenon of scouring on the stability of bridges had been studied from long time back by many researchers. Raudkivi AJ and Ettema R (1983); Raudkivi AJ (1986) studied about the importance of local scour depths in stability of bridges. Parola *et al*., (1996) reveals that considerable reduction in the scour depth may be observed if the foundation is located at or below the streambed. Melville (2008) described that the dependent parameters for scouring of bridges foundation are the flood flow and bed sediment characteristics, the geometry of the bridge pier and the rate of development of local scour. As per the literature review is concerned, the shape of pier played an important role in maintaining the stability flow of water. From the literature, it has been concluded that no one has experiment studied the effect of pier shape on water flow. The present study will experimentally studied three different shapes i.e. oval, rectangle, triangular, of piers that least disturbs the flow of water giving the minimum disturbance to its water flow. Apart from the experimental work, the finite element software, i.e. Ansys will be used for the analysis of the flow of water. The comparison between experimental and finite element software will enhance the accuracy of the result. The plotting of velocity with Ansys will enable to understand the water flow more effectively, it will enable to understand the flow lines of the water. From the results, the best shape of pier will be selected for the bridges.

2. EXPERIMENTAL INVESTIGATION

An experimental programme to find the most suitable pier shapes out of oval, rectangle, triangular shapes have been conducted in Civil Engineering Department of NIT Manipur, India using the model type specimen. Fig. 1, shows the top view of different shapes of piers namely as: a) Oval, b) Hexagonal, c) Rectangular. The water is allowed to flow through small channel. For maintaining the natural environment of water flow along the surface, small granular stone along with sand has been provided.

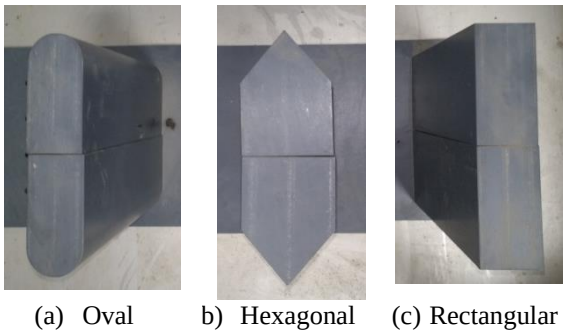

(a) Oval b) Hexagonal (c) Rectangular

Fig. 1: Different shapes of bridge piers.

For conducting the experiments, the disturbance of water flow and the amount of scouring needs to be investigated as to find the maximum water flow with the least disturbance of flow. Fig. 2 showed the channel, where the experiment has been conducted. Fig. 3 showed the points of measurement of velocity of water flow. The different points have been labelled as C for inlet; C' for outlet; F for right side; F' for left side. In conducting the experiment, two different conditions of water flow has been considered. First the velocity of free flow of water at the concerned points has been considered. Secondly, the water velocity at the surface of water with sediments of water and sand has been considered.

2.2 EXPERIMENT FOR FREE WATER FLOW

In this case the three piers i,e. Oval, hexagonal, rectangular cross-section shapes are kept one after another at the channel, with only free flow of water. The velocity of water at the specified points shown in Fig. 3 has been measured. The typical flow of water is shown in Fig. 4. The experiments have been repeated for all the three pier shapes.

2.3 EXPERIMENT OF WATER FLOW WITH SEDIMENTS OF SAND AND STONE

In this experiment, to provide the exact environment of water flow, the sediments mixture of stone and sand have been placed around the piers. Figs. 6 showed the experimental set ups. The experiment has been performed for all the pier shapes. As the water flow through the bed of the river, the sediments got transported. The distance of travel of the sediments also measured for all the different shapes of piers.

3. FINITE ELEMENT ANALYSIS

The finite element method is generally used to simulate the model of the water flow before making the prototype of the models. There are many FE softwares like Ansys, Abaqus etc. that are currently available. Out of these FE softwares, Ansys has been considered for the analysis of fluid flow as it can be used to simulate interactions of all disciplines of physics, structural, vibration, fluid dynamics, heat transfer and electromagnetic for engineer. It also has specific model of fluent. ANSYS has been used to plot the velocity of flow which will ultimately give the direction of flow and its disturbance to the surrounding areas.

4. OBSERVATIONS OF EXPERIMENTS

a) Water free flow in channel

When the water is allowed to flow freely without any sediments, the velocities at the observation points i.e. C (waterinlet), C'(outlet), F(leftside), F'(rightside) have been measured as shown in

Fig. 2: Channel for water flow

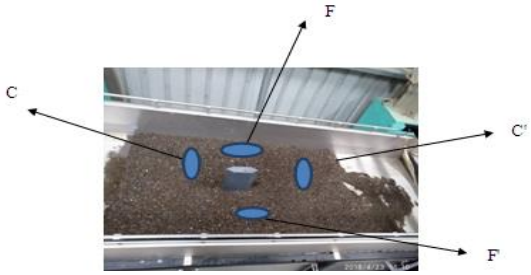

Fig. 3: Different positions where the head are measured (Top view of channel).

Fig. 4: Typical flow of free water in channel

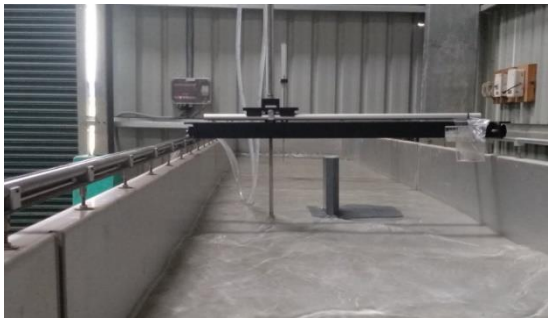

TABLE 1. Velocities of water around different pier shapes in free flow.

Points	Oval (m/s)	Hexagonal (m/s)	Rectangular (m/s)
C	0.306	0.316	0.314
C'	0.320	0.340	0.310
F	0.321	0.300	0.311
F'	0.308	0.309	0.280

Table 1. The results showed that the velocity of water got reduced in outlet point C' as compared to inlet point C in the rectangular pier. But incase of oval and hexagonal piers, the velocity of water increases from inlet to outlet showing the

negligible obstruction of the piers in water flow. The flowing of water is also plotted in Fig. 5 for all the pier shapes both experimentally as well as in finite element ANSYS.

a) Oval-shaped pier

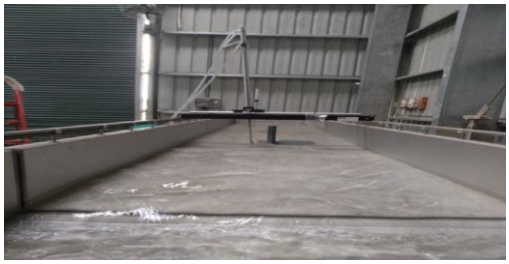

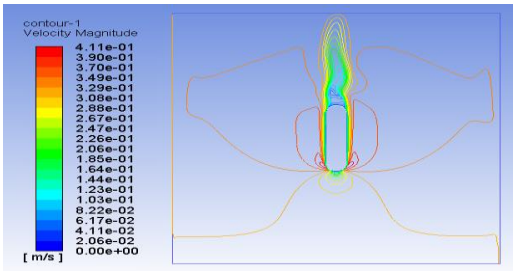

b)Hexagonal-shaped pier

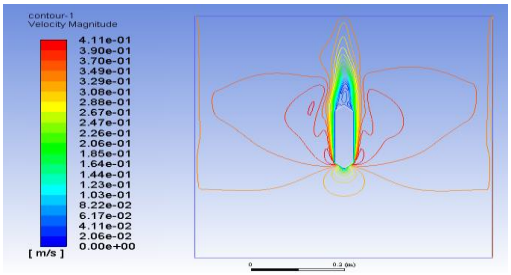

c) Rectangular-shaped pier

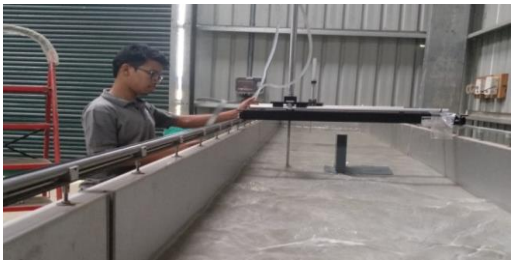

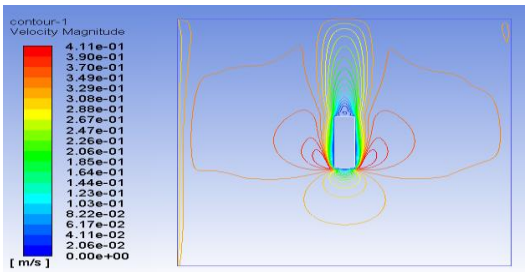

Fig. 5: Free Water flow in channel for different pier shapes (a) Oval , (b) Hexagonal, (c) Rectangular.

a) Oval-shaped pier

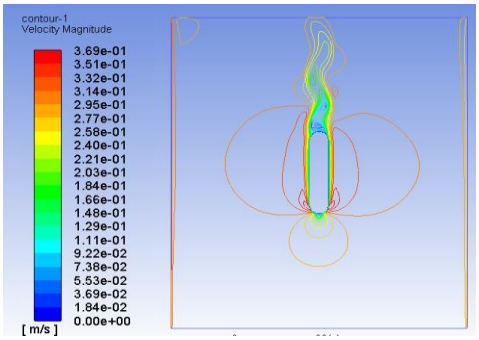

b)Hexagonal-shaped pier

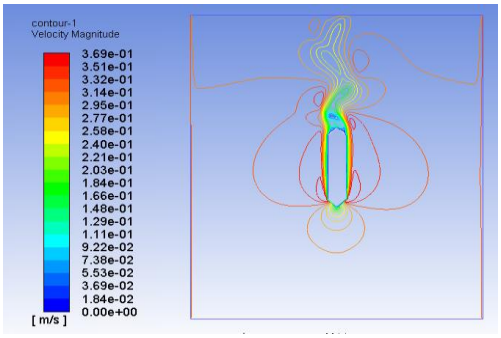

c) Rectangular-shaped pier

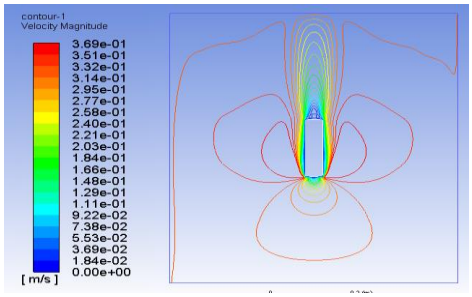

Fig. 6: Water flow in channel with sediments of sand and stone for different pier shapes (a) Oval , (b) Hexagonal, (c) Rectangular

In finite element plot, the flow lines of water are distinctly visible supporting the experimental result also.

b) Water flow in channel with sand and stone

The reading of the velocities of water are observed at points C, C', F, F' in Table 2. The reading shows that the reduction of velocities of water from inlet to the outlet side is the lowest at oval shape pier. The sediment transportation around the piers are also observed as in Table 3.The readings showed that the sediments transportation is also the lowest in case of
oval shape as compared to hexagonal and rectangular shaped piers. The experimental as well as the finite element plot are shown in Fig. 6. The pattern of water flow changes significantly from the case of free water flow with no sediments. From the finite element figures, it has been observed that the tails of water after crossing the obstruction due to sediments showed a zig-zag pattern showing the irregularities of the velocities of water.

TABLE 2. Velocities of water around different pier shapes with both sand and stone mixed.

Points	Oval m/s	Hexagonal m/s	Rectangular m/s
C	0.28	0.31	0.32
C'	0.27	0.28	0.30
F	0.32	0.33	0.32
F'	0.31	0.32	0.30

TABLE 3. Depth of sand around the piers before and after the water flow.

	Oval	Hexagonal	Rectangular
Before	3.9 cm	4.0 cm	4.0 cm
After	3.6 cm	3.4 cm	3.6 cm

5. CONCLUSIONS

Based on the experimental investigation of the model of bridge piers, with two different cases of studies, it has been concluded that the oval shape pier is the best shape among oval, hexagonal and rectangular pier shapes. The oval shape gives the lowest sediment transportation showing the most suitable pier for bridge stabilisation. Moreover, the oval shape pier gave the lowest obstruction to the flowing water thereby maintaining the sustainable flow of water.

REFERENCES

1) ANSYS. *ANSYS Engineering Analysis System User's Manual.*
2) Umesh C Kothyari (2007), "Indian practice on estimation of scour around bridge piers." *Sadhana Academy Proceedings in Engineering Sciences*, 32(3), 187-197.
3) Melville, B. (2008). "The physics of local scour at bridge piers." *Proceedings of Fourth International Conference on Scour and Erosion*, Tokyo, Japan.
4) Parola, A. C., Mahavadi, S. K., Brown, B. M., and El-Khoury, A. (1996)."Effects of rectangular foundation geometry on local pier scour."*Journal of Hydraulic Engineering*, ASCE, 0733-942, 122(1), 35-40.
5) Raudkivi, A. J. and Ettema, R. (1983). "Clear-water scour at cylindrical piers." *Journal of Hyd-raulic Engineering*, ASCE, 0733-9429 (1983) 109 :3 (338),111(4), 713-731
6) Raudkivi, A. J. (1986). "Functional trends of scour at bridge piers."*Journal of Hydraulic Engineering*, ASCE, 0733-9429, 112(1).

Response spectrum analysis including soil-fluid- structure interaction in concrete gravity dam

Parasor, A.[1], Dutta, A.K.[2]

[1] Student, Department of Civil Engineering, Jorhat Engineering College, Garmur, Jorhat, Assam 785007, India.
[2] Associate Professor, Department of Civil Engineering, Jorhat Engineering College, Garmur, Jorhat, Assam 785007, India.

ABSTRACT

This paper presents Soil-fluid-structure interaction of the Koyna dam, Maharashtra through response spectrum analysis of IS 1893(Part1):2002. Three numerical models have been considered to explore the soil fluid structure interaction issue: 3D dam with base fixed, 3D dam with reservoir with base fixed and 3D dam with reservoir and foundation. The Finite element model of the Dam, Foundation and Reservoir is done using ANSYS® with different elements and boundary conditions. A comparative study is carried out for the three models. It is found that the 3D dam with foundation and reservoir has the maximum stress value than the other two systems.

Keywords: soil-fluid-structure interaction, response spectrum analysis, numerical models

1 INTRODUCTION

Concrete gravity dam is a solid structure designed to hold back water primarily utilizing the weight of the material to resist all structural force. A dam is in direct contact with soil and water. When it is subjected to an earthquake, the dam interacts with the soil and water such that a continuous transfer of energy is established between them. The effects of dynamic behavior of dam are determined by the mechanical properties of all the elements of the system, the interaction mechanism and the type of dynamic loading. This soil-fluid–structure interaction problem in general is often too complex to solve analytically and so they have to be analyzed by means of numerical simulation.

This study focuses on the soil-fluid-structure interaction effect on concrete gravity dam due to ground motion.

2 LITERATURE REVIEW

Lotfi et al. (2016) did a comparative study on Wave number TD approach and Somerfield boundary condition for different normalized reservoir length. The study involved a special purpose finite element modeling of Pine flat against S69E component of Taft earthquake. The two type of reservoir bottom considered of full reflective as well as absorptive are adopted.

Viladkar et al. (2012) studied the possibility of sliding and separation at the base of Dam and study its effect on dynamic response of dam foundation system. The study involved non linear earthquake response of the tallest non overflow monolith of pine flat dam to Taft ground motion scaled to 0.5g. The interaction with both foundation and the reservoir has been considered. It has been found that both sliding and separation modes of the interface dominate the deformations as well as the principal stresses in the dam body. Sliding and rocking displacements have been found to be quite considerable at the heel.

Sarkar et al (2007) studied the response of a dam subjected to dynamic loading is a combined effect of the interaction among dam, reservoir and foundation systems. The profile of the Koyna dam has been adopted for the study of this investigation. Nonlinear concrete properties have been taken into account through concrete damaged plasticity model to simulate the damage induced in the dam body under a real-time earthquake motion. The study indicates that tensile damage of the dam structure occurred during the earthquake motion. Parametric studies, while varying the height of the reservoir and the Foundation modulus values have been conducted to show the influence of reservoir and foundation freedom at each node.

3 METHODOLOGY

In this work the soil, water and concrete gravity dam are modeled using ANSYS workbench® software with proper finite element. Three different numerical models have been considered to explore the soil fluid structure interaction issue: 3D dam with base fixed(S) system, 3D dam with reservoir with base fixed(FS) system and 3D dam with reservoir and foundation(SFS) system. The geometry of a typical non-overflow monolith of the Koyna dam-reservoir-foundation is illustrated in Figure 1, which is taken from Wang G *et al* (2016). This

monolith is 103 m high and 70 m wide at its base. The size of the reservoir is 206×96.5 m. The dam is assumed to rest on a 379×103 m foundation.

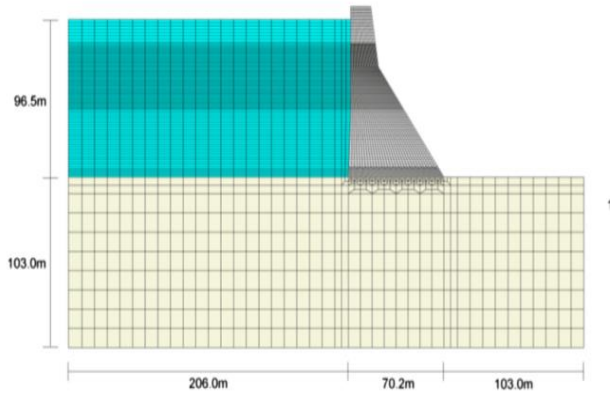

Fig. 1. Layout of Koyna Dam with reservoir and foundation, Maharashtra, India.

Different types of materials are used in modeling of dam soil foundation and water. Different engineering properties like density, Young's modulus and Poisson's ratio of these materials are listed in Table 1.M40 concrete grade is considered for modeling the concrete structure. In this table the following element properties are taken from Wang G *et al* (2016).

Table 1. Material properties for the Koyna dam-reservoir-foundation system

Property	DAM	FOUNDATION	WATER
Density (Kg/m^3)	2643	3300	1000
Young's Modulus (N/m^2)	31027	62054	-
Poisson's ratio	0.2	0.33	-
Bulk Modulus (N/m^2)	-	-	2250
Sonic Velocity (m/s)	-	-	1440

3.1 Description of modeling

Design modeler is used for building the geometry. Material and geometric properties are assigned. Appropriate mesh is generated. Depending upon the meshing method, sizing different solid elements are assigned by default. Boundary condition is assigned. Contact pair between different types of solid material is program controlled. SOLID187 is used in modeling the concrete dam and the soil mass, staging. While modeling this dam TARGE170 is taken as target element and CONTA174 is considered as contact element. These interfaces are able to perform fluid structure and soil structure interaction. The fluid element is capable able to exchange pressure and deformation properties with solid concrete dam and the foundation. As visualization of fluid-structure interaction is effective with sloshing effect of water during free mode vibration water inside the tank is modeled with FLUID220element.

3.2 Boundary condition

The three system i.e 3D dam with base fixed (S) system, 3D dam with reservoir with base fixed (FS) system and 3D dam with reservoir and foundation (SFS) system are modelled with different boundary conditions. Some studies have proved that, if the range of finite model reaches to a certain extent large enough, the boundary effect of incident waves and scattered waves can be ignored, and it can still obtain good approximate results (Menglinet al.2003). In S system and FS system the bottom of the dam is fixed. In FS and SFS for good accuracy in results it is suitable to construct the far end boundary of reservoir at a minimum of twice the water height. By following the approach, the far end boundary of the reservoir is constructed at a distance equals to twice the height of the reservoir water level to behave as truncated boundary to satisfy the fluid structure interaction as per Vahid L.$et\ al$ (2016). In SFS system the far end of the foundation is modelled at a distance of 1.5 times the base width of the dam to behave as truncated boundary to satisfy the soil structure interaction effect as per Viladkar N M *et al* (2012) the soil is restrained in horizontal direction with base fixed

3.3 Response spectrum analysis

The dam reservoir and foundation are stimulated against the response spectrum in reference with IS 1893(Part1):2002. The response spectrum is constructed by using the following equations of $\frac{Sa}{g}$ against different time interval with 5% damping is given by eq (1.1).

$$\frac{Sa}{g}=\begin{cases}1+1.5\,T & 0.00\le T\le 0.10\\ 2.50 & 0.10\le T\le 0.40\\ 1.00/T & 0.40\le T\le 4.00\end{cases} \quad (1.1)$$

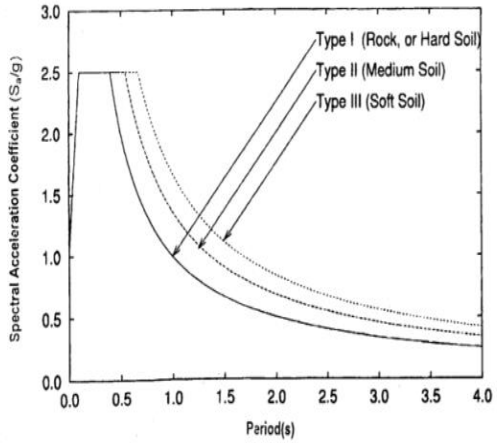

Fig. 2. Response spectrum for rock and soil sites for 5% damping

4 RESULTS AND DISCUSSION

The results obtained from modal analysis three system are compared in terms of modal frequencies as shown in table 2.

Table 2. Comparison between the frequencies the three systems

SYSTEM	Frequency (Hz)			
	First mode	Second mode	Third mode	Fourth mode
3D Dam	3.157	3.181	3.267	3.413
3D Dam with water	3.080	3.103	3.187	3.331
3D Dam with soil foundation and water	2.846	2.870	2.962	3.122

Response spectrum analysis is performed through "Response spectrum" tool in ANSYS Workbench®. The acceleration is applied in horizontal X direction to the whole geometry. The maximum principal stresses in concrete due to response spectrum analysis are computed. The details of the stress profile of the three models obtained from this analysis are shown below in Fig3 through Fig 5.

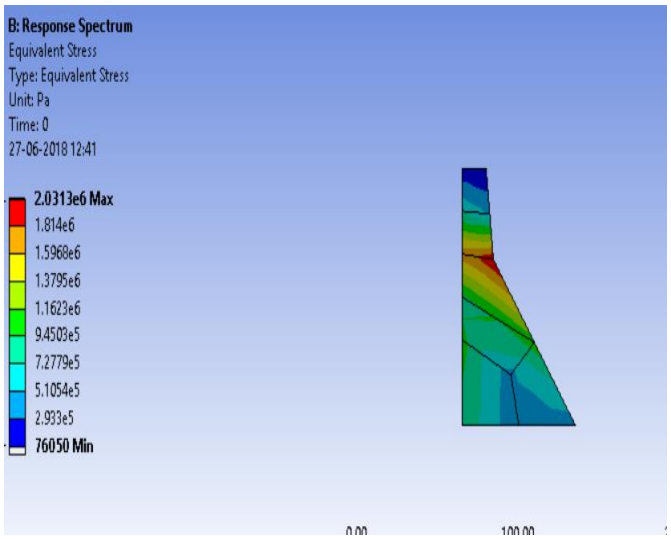

Fig. 3. Stress contour of 3D dam in response spectrum analysis

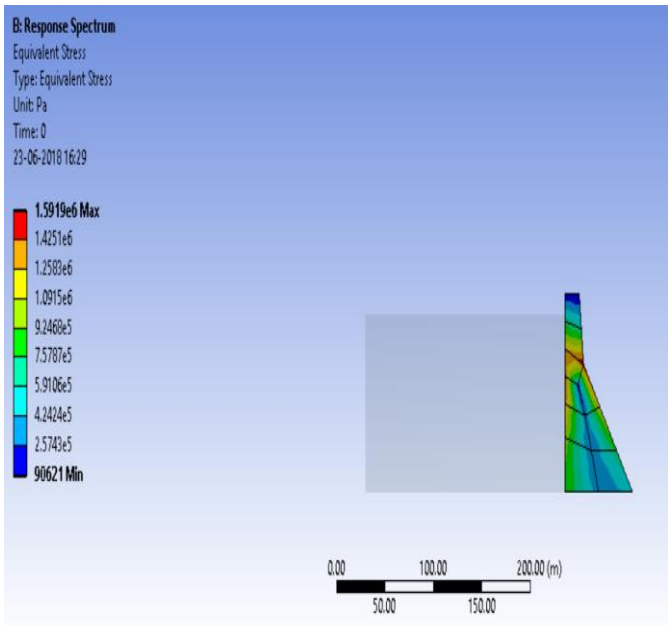

Fig. 4. Stress contour of Fluid - Structure system (FS) in response spectrum analysis

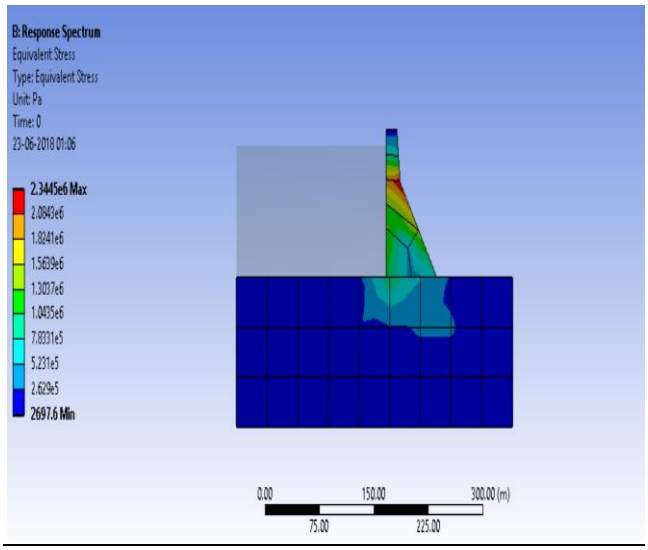

Fig. 5. Stress contour of Soil- Fluid - Structure system (SFS) in response spectrum analysis.

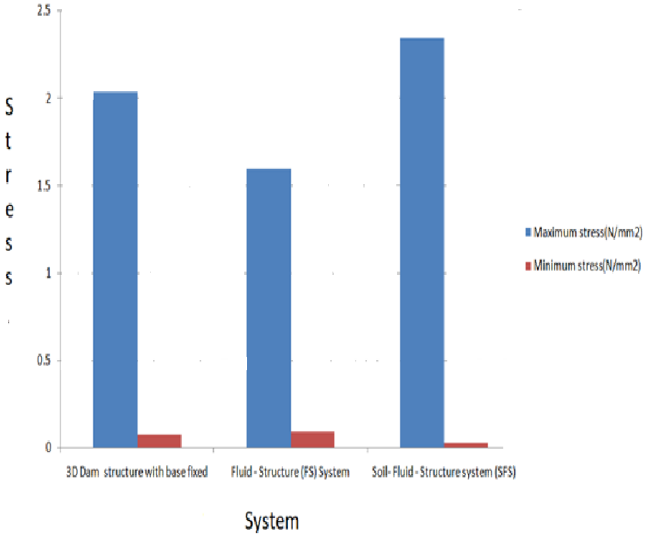

Fig. 6. Maximum Stress of dam obtained from, response spectrum analysis method for different models

Comparison between the maximum stresses in the concrete structures against response spectrum analysis is shown in shown in Table 3

Table 3. Comparison between the maximum stresses in the concrete structures

System	Maximum stress(N/mm^2)	Minimum stress (N/mm^2)
3D Dam structure with base fixed	2.03	0.076
Fluid - Structure (FS) System	1.59	0.090
Soil- Fluid - Structure system (SFS)	2.34	0.026

In this analysis the resultant of forces acting on the dam are compression and tensile strength criteria respectively. According to IS: 6512-1984, the allowable compressive stress in the dam concrete shall not exceed, 7N/mm^2 and permissible tensile stress of concrete is taken to be 1 to 4 percent of compressive strength. In this analysis the permissible tensile stress is taken as 2% of compressive strength of concrete considering full reservoir condition and earthquake excitation. The comparison of maximum and minimum stress is shown in the Fig 6

5 CONCLUSION

This study concludes the results of the dynamic analysis of a concrete gravity dam with the effects from soil-fluid-structure interaction. To solve the purpose, the stress developed in different models of dam-reservoir-foundation system against earthquake and to evaluate the safety of dam against the permissible limit. As per the guidance of IS: 1893-1984(part 5), response spectrum analysis with reference to IS: 1893-2002(part 1). The stresses developed in the dam are found to be under permissible limit. It can be observed that the presence of soil increases the stress values in dam as SFS system has the highest maximum stress value among all the systems.

6 REFERENCE

1) Arabshahi, H, and Lotfi, V, 2008, Earthquake response of concrete gravity dams including dam–foundation-interface nonlinearities, Engineering *Structures 30*, 3065–3073.
2) Burman, A., Maity, D., Sreedeep, S., 2010,Iterative analysis of concrete gravity dam-nonlinear foundation interaction, *International Journal of Engineering, Science and Technology*,Vol. 2, No. 4, 85-99.
3) Chopra, A.K., 1996, *Dynamics of Structures: theory and applications to earthquake engineering*, Prentice Hall, Upper Saddle River, New Jersey, 635, 17.
4) Fenves, G., and Chopra, A.K., 1987, Simplified earthquake analysis of concrete gravity dams, *Journal of Structural Engineering*, Vol. 113, No. 8, paper no- 21717.
5) IS: 1893(Part 1)-2002, Criteria for earthquake resistance and construction of buildings, Bureau of Indian standards, New Delhi.
6) IS: 1893(Part 1)-1984, Criteria for earthquake resistance and

construction of buildings, Bureau of Indian standards, New Delhi.
7) IS: 6512-1984, Criteria for design of solid gravity dam, Bureau of Indian standards, New Delhi.
8) Kramer, S.I., 1996, *Geotechnical Earthquake Engineering*, Prentice Hall, Upper Saddle River, New Jersey, 07458.
9) Lotfi, V., and Zenz, G., 2016, Transient analysis of concrete gravity dam-reservoir systems by Wavenumber-TD approach, *Soil Dynamics and Earthquake Engineering* , 313-326.
10) Viladkar, N.M, and Al-Assady, S.M.K.A,2012, Nonlinear analysis of Pine Flat Dam including base sliding and separation, *15th World Conference of Earthquake Engineering*, LISBOA.
11) Rulin, Z., and Mengling, L., 2011, Substructure analysis method for dynamic response of large-scale soil site, Procedia *Engineering 14*, 417–1424

Challenges of 3D modeling of the water tank using SAP2000® a case study

Nath, S.[1], Dutta A.K.[2]

[1] PG Student, Department of Civil Engineering, Jorhat Engineering College, Garmur, Jorhat-785007, India.
[2] Associate Professor, Department of Civil Engineering, Jorhat Engineering College, Garmur, Jorhat- 785007, India.

ABSTRACT

This paper presents the challenges of extrapolating a two-dimensional model of elevated water tank into three-dimensional model to check Fluid-structure interaction. Three dimensional modeling of the elevated water tank is done using SAP2000® software. The double spring-mass model suggested by Housner (1963) and IITK-GSDMA guideline is extended to 3-D modeling. Sloshing of water is attempted with 4 and 8 numbers of equivalent springs dividing the total spring constants of IITK-GSDMA guideline by 4 and 8 respectively. Dynamic characteristics are found

Keywords: double spring-mass model, SAP2000®, equivalent springs

1. INTRODUCTION

The elevated water tanks face severe damages during ground motions; one of the reasons for this failure is the interaction of fluid inside the tank. During ground motions, movable fluid inside the tank produces hydrodynamic pressure on the wall, which may cause permanent deformation of the tank. This interaction is known as fluid-structure interaction (FSI). In the seismic design of the tank, these effects should be minimized to make the structure safe. This FSI produces sloshing effect which may cause a serious failure like roof failure, damage to walls etc.

In this paper, the concept of spring-mass model is adopted to understand the effect of FSI. It is a challenge to extract a 2D model into 3D model, because there can be n numbers of springs in double spring mass modelling of the water. This is quite difficult to model. Sloshing of fluid is attempted with 4 and 8 numbers of equivalent springs. Also the effect of increasing spring stiffness is checked here.

2 LITERATURE REVIEW

The concept of fluid-structure interaction as a spring mass model is first introduced in the 1950s as shown in Fig. 1. Single spring mass model takes the completely filled tank as a lumped mass and the vertical shaft is considered as cantilever beam.. In 1963 Housner studied the behavior of Fluid-structure interaction as a double spring mass model for fixed base elevated tanks (Fig. 2). Fluid inside the tank divided into two parts, upper region of water is considered as convective mass and lower region is considered as impulsive mass. Sloshing of water takes place in convective mass of water and impulsive mass moves along with the tank. In this model convective mass of water is considered as lumped massconnected to the walls of tank by springs of stiffness K_c and impulsive mass as rigidly connected to the walls.

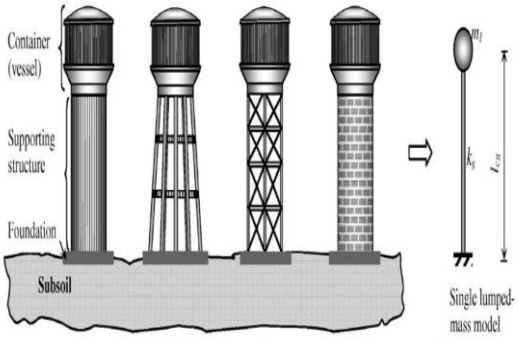

Fig.1. Elevated tanks and the single lumped-mass model after Dogangün and Livaoglu(2004)

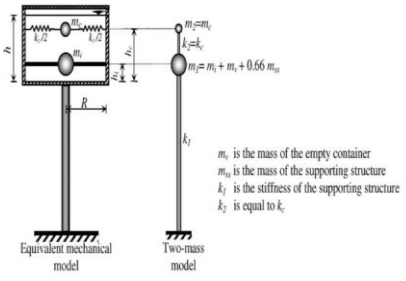

Fig.2. Two-mass model for the elevated tanks after Housner (1963)

Additional higher-mode convective masses may also be included for the ground-supported tanks, as shown in Fig.3. But for most accurate analysis higher modes of masses are neglected as higher modes of sloshing has negligible influence on the forces exerted on the container wall.

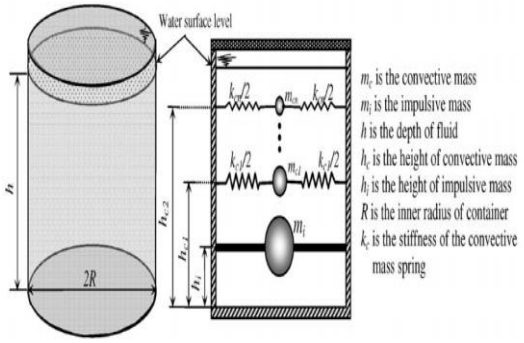

Fig.3. Spring-mass analogy for ground supported cylindrical tank after Dogangün and Livaoglu(2004)

IITK-GSDMA guideline (2007) issued the provisions for seismic analysis of liquid storage tanks. This guideline follows the concept of double spring mass model as per Housner(1963), considering impulsive mass ($m_{i)}$ and convective mass (m_c) to design the circular/rectangular water tank.

3 METHODOLOGY

In this work the water inside the tank is modeled as spring mass model to check the fluid-structure interaction following IITK-GSDMA guidelines (2007). As per the guideline impulsive mass and convective mass are calculated.

The model of frame staged elevated water tank is adopted from Krishna Raju N. (2015). The capacity of elevated water tank is 1 million liters supported on 16 meter long frame staging system with 8 columns and the Diameter of cylindrical section of tank is 12 meter. The dimensions of various components are given in Table1.

Table1. Sizes of various components

Components of Intz type tank	Dimensions
Top Dome	120 mm thick
Top Ring Beam	300 mm×300 mm
Cylindrical Wall	200 mm thick
Bottom Ring Beam	300mm×300mm
Circular Ring Beam	1200mm×600mm
Bottom Dome	300 mm thick
Conical Dome	600 mm thick
Braces	500mm×500mm
Radius of cylindrical Section	6000mm

M20 grade of concrete and Fe 415 grade for steel is used for design.

3.1 Description of modeling

The modeling of elevated water tank taken from Krishna Raju(2015) is done using SAP2000® software. The bases of the columns are considered to be fixed. Water inside the tank is modeled as double spring mass model following IITK-GSDMA guidelines. The impulsive mass and convective mass are calculated according to guideline. For tank shapes other than circular and rectangular (like Intze, truncated conical shape) the value of *h /D* shall correspond to that of an equivalent circular tank of same volume and diameter equal to diameter of tank at top level of liquid. Impulsive mass (m_i) and convective mass (m_c) can be calculated from the below figure 4. Also expressions are given to calculate the parameters. The flexible spring stiffness (k_c) connected to the convective mass is calculated according to the guideline. Value of the flexible spring stiffness can be found out from the Fig.4.

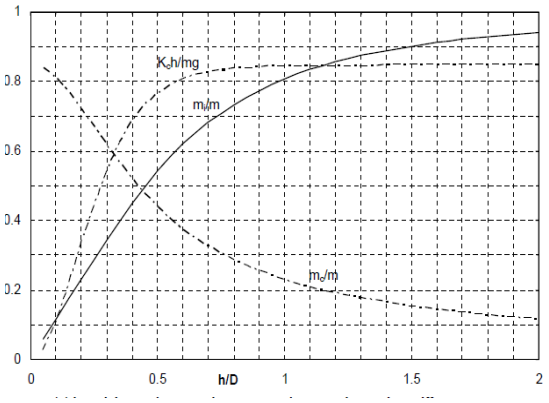

Fig.4. Impulsive and convective mass and convective spring stiffness after IITK-GSDMA guidelines (2007)

Convective spring stiffness, K_c =909.334 kN/m. The double spring mass model suggested by Housner (1963) is a two dimensional model as shown in Fig.2. But in case of three dimensional modeling there. In this study 4 and 8 numbers of flexible spring stiffeners are connected to the convective mass to check the effect of fluid-structure interaction. While considering 4 numbers of springs total spring stiffness is divided equally among the springs. Similarly in case of 8 numbers of flexible springs total stiffness is divided by eight. Fig.5. shows the first 3D model of elevated water tank

considering 4 numbers of flexible springs.

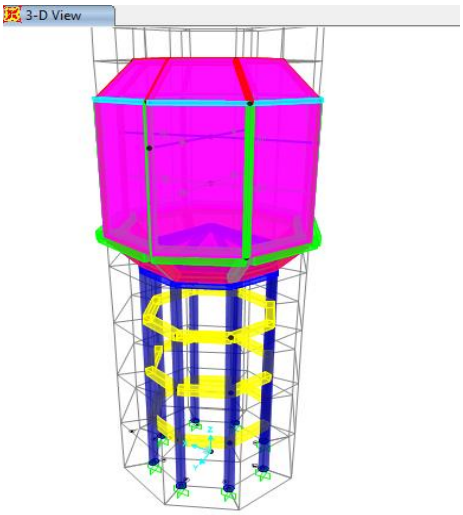

Fig.5.Elevated water tank considering 4 numbers of flexible springs

Fig.6. shows the second 3D model of elevated water tank considering 8 numbers of flexible springs connected to the convective mass.

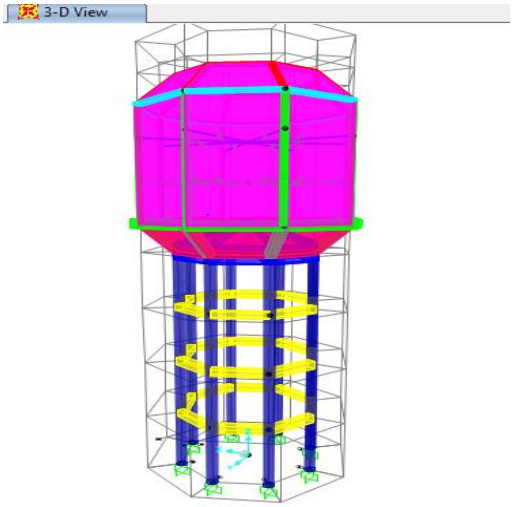

Fig.6.Elevated water tank considering 8 numbers of flexible springs

3.2 Time history data

Time history analysis is computed for three representitive earthquakes. These are El-Centro (18th May, 1940), Kobe (17th january,1995) and Kocaeli (18th May, 1999) earthquake, These ground motions are considered on the basis of their Maximum peak ground acceleration. Ground acceleration data for north-south component of El-Centro is obtained from http://www.vibrationdata.com/elcentro.htm.

Kobe and Kocaeli earthquake database are selected from Pacific Earthquake Engineering Research Next Generation Attenuation (PEER-NGA) strong motion database records available online at http://peer.berkeley.edu/nga. Table 2 shows the ground motion records.

Table 2. Gound motion characteristics

Different ground motions	Station	Magnitude	Time steps (sec)	Total time Period (sec)	PGA(g)
El-Centro (1940)	Imperial valley	M_w=6.9	0.02	31.14	0.319
Kobe (1995)	Takaraz uka, Japan	M_w = 7.2	0.02	40	0.8
Kocaeli (1999)	Sakaria station Turkey	M_w= 7.6	0.01	20	0.628

The input acceleration-time plot of El-centro earthquake, Kobe, Kocaeli earthquake are shown in Figure 7 through Figure 9.

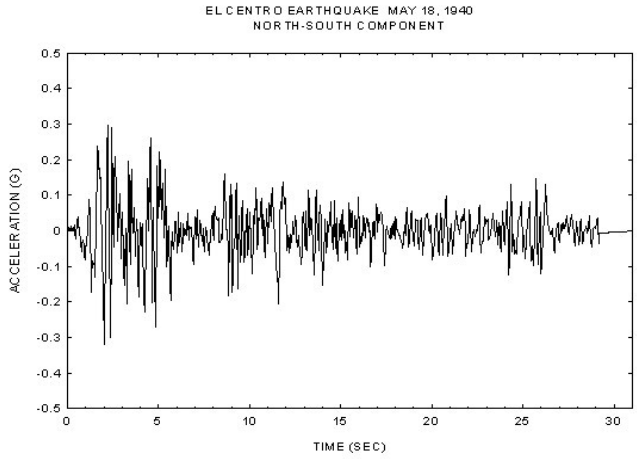

Fig.7.Accelerogram plot of El-centro(1940) earthquake

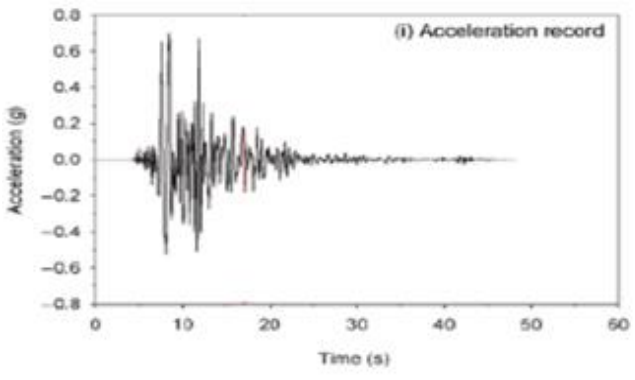

Fig.8. Accelerogram plot of Kobe (1995) earthquake

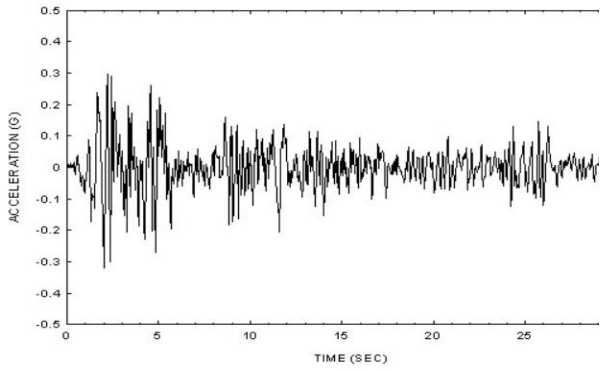

Fig.9.Accelerogram plot of Kocaeli (1999) earthquake

4 RESULTS AND DISCUSSION

The results obtained from modal analysis of both the systems are compared in terms of modal frequencies as shown in table 3.

Table 3. Comparison between the frequencies of both the systems

Mode shapes	Frequency in 1st system (Hz)	Frequency in 2nd system (Hz)
1	0.87073	0.87073
2	0.87073	0.87073
3	0.93904	0.93903
4	5.56944	5.57078
5	5.56944	5.57513

The result shows that increasing the stiffness of spring as double spring mass system does not change the modal frequencies.

To check the seismic effect on the tank, time history analysis done for both the systems with4 numbers of spring stiffeners and 8 numbers of spring stiffeners. Time history analysis are performed in SAP 2000® software against three representative earthquakes. The acceleration is applied in horizontal X direction. Comparison between the maximum axial stresses on frames in both the systems due to El-Centro (1940), Kobe (1995), Kocaeli (1999) earthquakes are shown in table 4.

Table 4. Structural behaviour of both systems under reprentative earthquakes

Earthquake	Axial stress in 1st system (N/mm^2)	Axial Stress in 2nd system (N/mm^2)
El-Centro(1940)	39.2	39.2
Kobe(1995)	154	154
Kocaeli(1999)	98	98

Considering maximum limit of stress in M20 grade of concrete under compression as $f_{ck}/ 1.5 = 13.33$ N/mm^2. It is observed that maximum axial stress on frame exceeds permissible limit for all the earthquakes for both the systems. However, for both the systems, axial stress values are equal. It shows that increasing spring stiffness considering double spring mass system does not affect the stress values on the system.

5 CONCLUSION

The paper presents the challenge of extrapolating a two-dimensional model formulation into three-dimensional considering fluid element as a double spring-mass model. It has been observed that the number of flexible spring stiffness does not affect the dynamic properties of the system. The axial stresses on frames due to three representative earthquakes are equal for both the systems.

REFERENCES

1) Structural Analysis Program SAP2000. "User's manual, Computers and Structures, Inc., Berkley, Calif.
2) Housner, G., W., (1957), "Dynamic pressures on accelerated fluid containers", *Bulletin of the Seismological Society of America,* 47, pp. 15-35.
3) Housner, G., W., (1963), "Dynamic analysis of fluids in containers subjected to acceleration. *Nuclear Reactors and Earthquakes*" Report No. TID 7024, U. S. Atomic Energy Commission, Washington D.C.
4) Livaoğlu, R., and Doğangün, A., (2004), "A simple seismic analysis procedure for fluid-elevated tank-foundation/soil systems" *In Sixth International Conference on Advances in Civil Engineering (ACE*), İstanbul, Turkey, v1; pp.570-580.
5) IITK-GSDMA,(2005) "Guidelines for seismic design of liquid storage tank ", *Indian Institute of Technology*, Kanpur.
6) Krishna Raju, N., (2015*),"Advanced Reinforced Concrete Design (IS: 456-2000) (English) 3rd Edition", CBS Publisher*.

2nd International Conference of Civil Engineering for Sustainable Development-Opportunities and Challenges
CESDOC-2018, 18th to 19th December, 2018, Assam Engineering College

Soil-structure-interaction problem in underground pipes-a dynamic approach

Barhai, P.[1] and Dutta, A.K.[2]

[1]P.G Student, Department of Civil Engineering, Jorhat Engineering College, Jorhat, Assam
[2]Associate Professor, Department of Civil Engineering, Jorhat Engineering College, Jorhat, Assam,

ABSTRACT

Soil-structure-interaction plays the key role in determining the response of underground structures such as pipelines. This paper analyses the response of buried pipes in terms of stresses and strains due to dynamic load. Three different types of soil media have been considered. A three dimensional finite element model is developed using ANSYS®. The soil is modeled by eight noded brick element and the pipe by four noded thin shell elements. The contact and sliding between the soil and pipeline is represented by 3-D nonlinear contact elements. The analysis is done considering the soil and pipeline to be linear, elastic, isotropic and homogenous. It has been observed that the stress in the pipe and the soil is dependent on their physical properties. Higher density and higher friction angle of soil influences higher stress.

Keywords: soil structure interaction, ANSYS®, contact elements, boundary conditions, modal analysis, response spectrum analysis

INTRODUCTION

Underground pipelines are damaged in earthquakes due to the forces and deformation imposed on them through interactions at the pipe-soil interface. This interaction between two different bodies (pipe and soil) is affected by many elements such as material nonlinearities, local and global buckling, soil settlement, pipe upheaval, among others (Rubio, et al., 2007).

This study attempts to analyze the interaction between the soil and pipe during earthquake. The response of a pipe or any underground structure is mainly dependent on the properties of soil it is buried in. Thus there can be considerable difference in the interaction between the soil and the pipe depending on the ground properties. Pipe in various soil media are selected for this study and tested against the response spectrum suggested by IS 1893 (part 1) 2002. The study will be carried out using Finite element software ANSYS®.

LITERATURE REVIEW

Different studies with varied approaches been done to study the soil structure interaction.

Wang (2005) explained that the most common analytical soil-structure interaction models are based on the assumptions that the soil domain may be represented by an elastic half space and that dashpots may be used to represent the transmitting boundary conditions. These boundary conditions are required to model both radiation damping of the foundation motion as waves propagate outward into the infinite domain and to prevent reflections back into the foundation from any artificially introduced finite domain of the half-space. IITK-GSDMA (2007) has stated that in general, the amplification is more in softer soils than stiffer soils**.** Hongjing et al. (2008) found that due to their easy deformation and absorbing more energy, buried pipeline has good performance to resist earthquake when buried depth is shallow. Lee (2010) found that boundary conditions have a lot of influence over a pipeline's performance. Infinitely long pipelines should be modeled by roller boundary conditions and finite pipelines such as those located between two buildings should be designed well especially at the ends of the pipeline. Saberi et al. (2014) found that the relative displacement between soil and pipe was maximum in the soil with a lower stiffness.

The analysis of the interaction between the soil and pipe in three different soil media will add a newer dimension in this field of study.

METHODOLOGY

In this work the soil and the structure are represented by respective finite elements in ANSYS®. A steel pipe of API 5L grade X65, with an outer diameter of 1.219 m and a wall thickness of 0.020 m and whose mechanical specifications are summarized in Table 1, is selected.

Table 1. Material properties of pipe (after J. Zhang et al, 2015)

Pipe material	Modulus of Elasticity (kN/m^2)	Poisson's ratio	Density (kg/m^3)
API 5L	210×10^6	0.3	7850

X65			

Soil properties

Three representative soil types are chosen for this study. These are:

(i) Fully saturated cohesive soil
(ii) Fully saturated sandy soil
(iii) Loess

The soil properties used are as in Table 2.

Table 2. Material properties of selected soil types (after Hyuk Lee, 2010 and J.Zhang, 2015)

Soil type	Modulus of elasticity (kN/m^2)	Poisson's ratio	Density (kg/m^3)
Fully saturated cohesive soil	48000	0.45	2000
Fully saturated sandy soil	96000	0.25	2160
Loess	33000	0.44	2460

Soil modeling

The scale of soil is created as a cuboid with buried pipeline on one centre line. The response of a pipe soil system analysis is accurate at a distance of four times the diameter from the centre of the pipe (Saberi et al. 2015). In this study, the aforementioned condition is considered for the near field modeling of soil region whereas, absorbing boundary conditions such as springs and dampers can be used to simulate the far field effect.

The length (L) of soil is considered as 50 m, width (B) as 10 m, and depth (H) as 15 m (Lee, 2010). According to IITK-GSDMA guidelines, the pipelines are typically buried at shallow depth (1 – 3 m) below ground surface. So keeping this in consideration the pipeline is taken to be buried at a depth (h) of 2.5 m from the top. The pipe is laid along the longitudinal direction as in Figure 1.

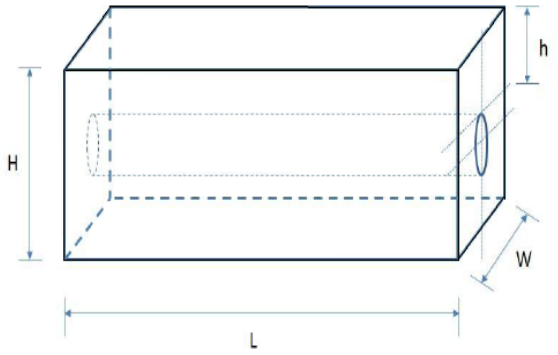

Fig. 1. Dimensions of soil model (redrawn after Lee, 2010)

Boundary conditions

In this study the bottom surface of 3D-Finite element soil model has been completely fixed. Four beside surfaces of 3D-finite element soil model are on rollers. The pipeline ends are on rollers too. In order to represent the continuity of soil media as an infinite half space, spring-damper element is being used.

Element types

Considering all aspects like the geometry in field, loading, required results etc., the best suited elements are chosen which will most efficiently represent the soil and the pipe and their interactions in this study. Elements SOLID185, a eight node structural solid suitable for modeling general 3-D solid structures and SHELL181, a four node element suitable for analyzing thin to moderately-thick shell structures are being used for representing the soil volume and the pipe element in the software respectively. TARGE170 and CONTA174 are used for interaction between the soil and the pipe. COMBIN14 is used as a spring damper element.

Modeling in ANSYS®

The meshed volumes are shown in Figure 2.

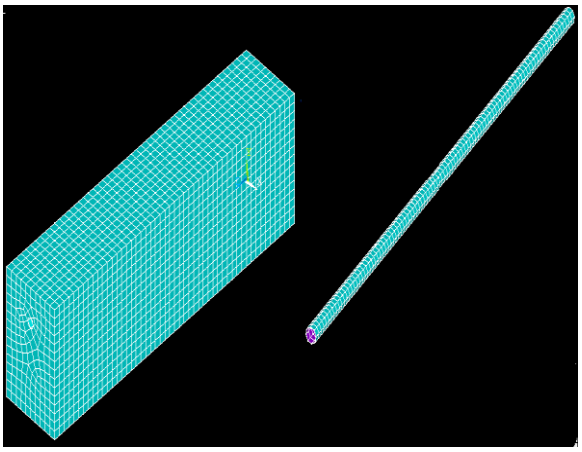

Fig. 2. Meshed soil and pipe

In studying the contact between the two bodies, the

surface of one body is conventionally taken as a contact surface and the surface of the other body as a target surface. The contact and target surfaces constitute a "Contact Pair" as shown in Figure 3.

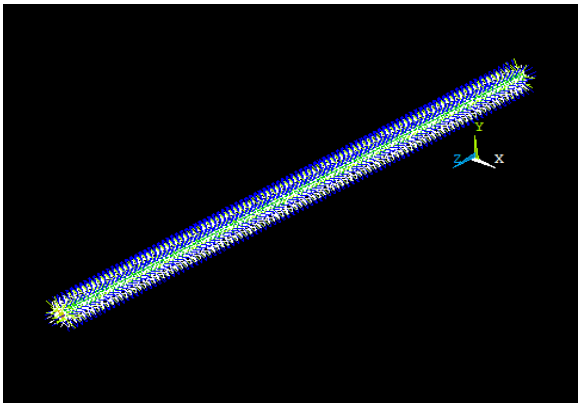

Fig. 3. Generation of contact pair

DYNAMIC ANALYSIS

Dynamic analysis comprises of the modal analysis and response spectrum analysis here. Modal analysis determines the natural frequencies and mode shapes of a structure. They can be a starting point for another more detailed dynamic analysis such as response spectrum analysis. This dynamic or seismic analysis is conducted against the design response spectra (Figure 4) curve in IS 1893 (Part 1) : 2002 for 5% damping in this study.

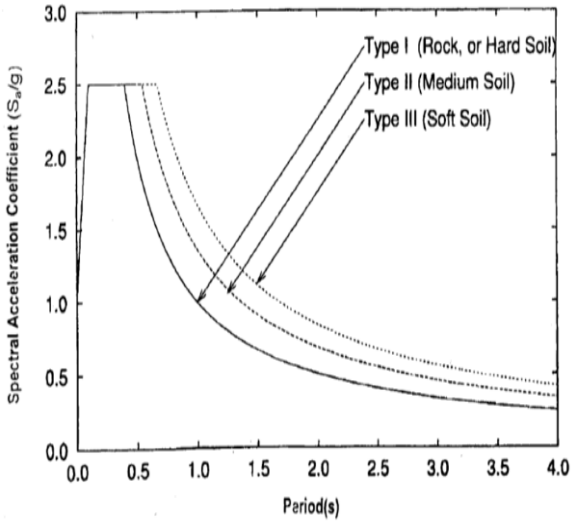

Fig. 4. Design response spectra curve as per IS: 1893 (Part-1) : 2002

Modal analysis

The purpose of a modal analysis is to find the shapes and frequencies at which the structure will amplify the effect of a load and these results of the analysis are used with the design response spectra curve in Figure 4 to calculate the stresses in the model.

The mode shapes of the three soil media corresponding to the first frequency of 0.388 Hz are shown in Figure 5, Figure 6 and Figure 7 respectively.

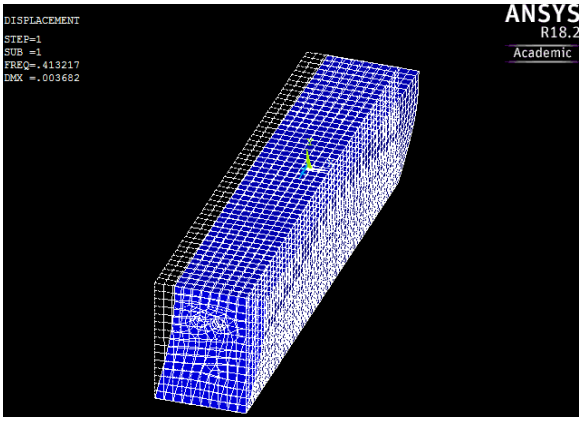

Fig. 5. First mode shape of fully saturated cohesive soil

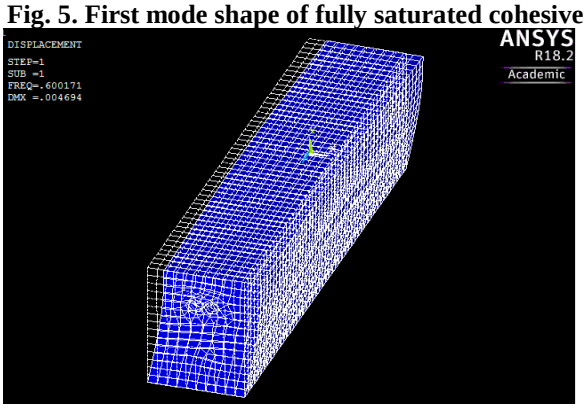

Fig. 6. First mode shape of fully saturated sandy soil

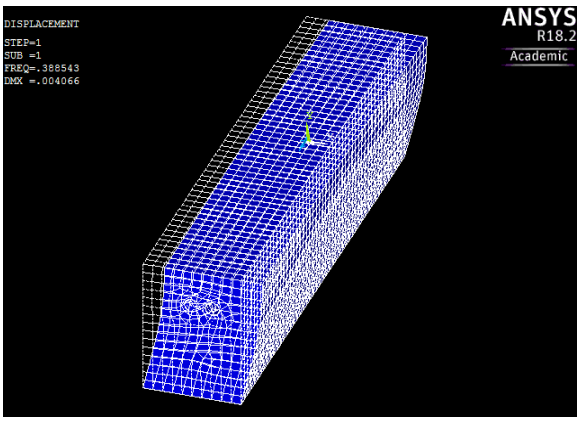

Fig. 7. First mode shape of loess

Response spectrum analysis

The stress generated in the three soil media and the respective pipes corresponding to the first mode shapes are shown in Figure 8, Figure 9, Figure 10, Figure 11, Figure 12 and Figure 13 respectively.

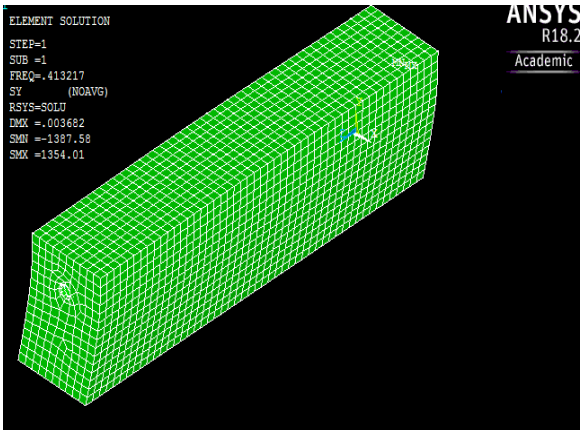

Fig. 8. Stress in the fully saturated cohesive soil

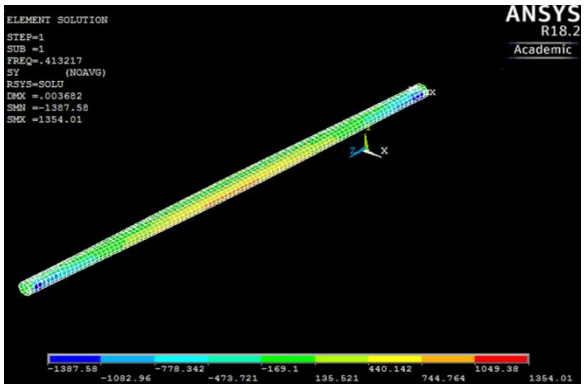

Fig. 9. Stress in the pipe in fully saturated cohesive soil

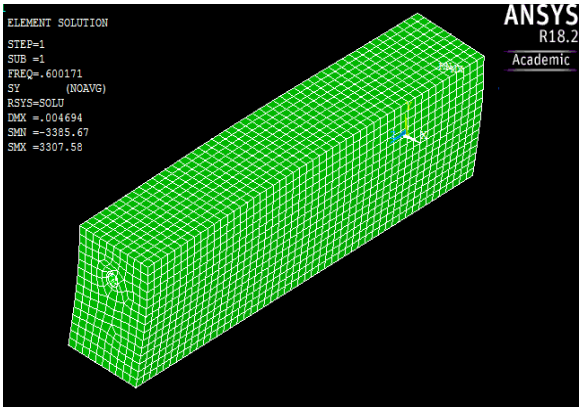

Fig. 9. Stress in the fully saturated sandy soil

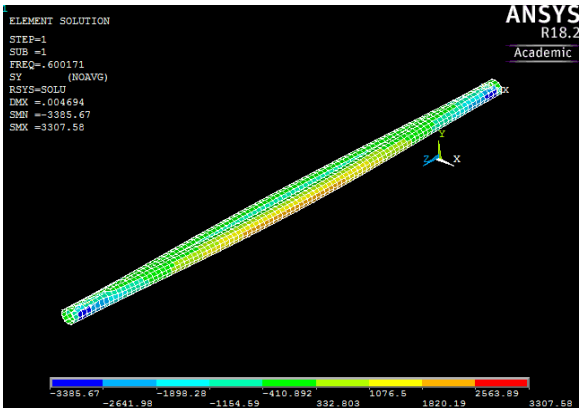

Fig. 10. Stress in the pipe in fully saturated sandy soil

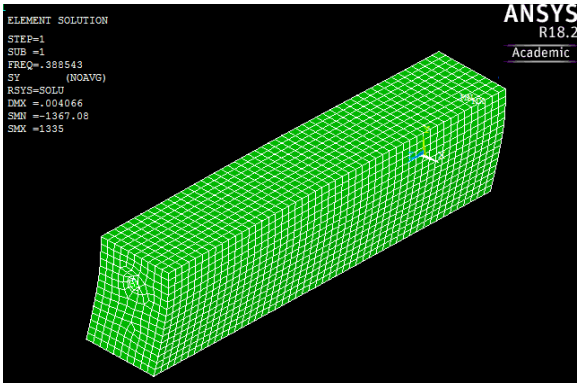

Fig. 11. Stress in Loess

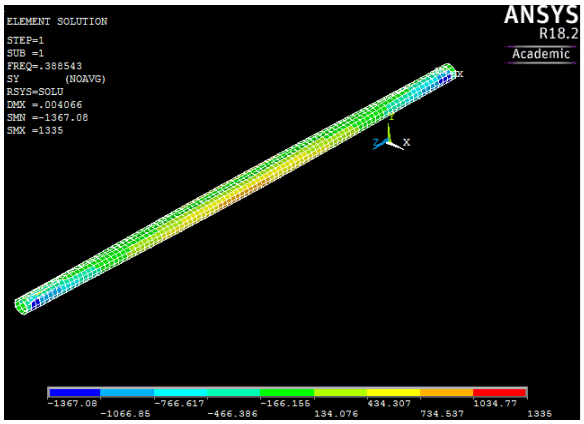

Fig. 12. Stress in the pipe in Loess

RESULTS AND DISCUSIONS

Fully saturated sandy soil has the highest stiffness among the three types of soil. This is the reason for its higher value of natural frequency.

Table 3 represents the comparison of the stress values in the three types of soil.

Table 3. Generated Stress in the pipe in Y direction

Parameters	Fully saturated cohesive	Fully saturated sandy soil	Loess

	soil		
Stress in Y-direction	1387.58 (-)	3385.67 (-)	1367.08 (-)
	1354.01 (+)	3307.58 (+)	1335 (+)

* Units are in KPa.

From Table 3, it can be observed that the pipe buried in fully saturated sandy soil has a higher stress value. This is because of the higher stiffness that the soil possesses.

CONCLUSION

The numerical results obtained gave a clear idea of the pipeline performance in different soil media. The properties of soil such as modulus of elasticity, Poisson's ratio, density has direct influence in the soil structure interaction. These properties and the possible influence they can have on an underground structure should be given utmost importance while designing.

REFERENCES

1) ANSYS® 18.5 Online documentation, Inc. Southpointe 275 Technology Drive Canonsburg
2) IS 1893 (Part 1) : 2002, Criteria for Earthquake Resistant Design of Structures, Part 1: General Provisions and Buildings.
3) IITK-GSDMA GUIDELINES for Seismic Design of Buried Pipelines (2007).
4) Hongjing LI., Liu JIN. and Baohua YAO.(2008): Response analysis of buried pipelines due to large ground movements, 14th World Conference on Earthquake Engineering, Beijing, China.
5) Lee Hyuk.(2010): Finite element analysis of a buried pipeline, a dissertation submitted to The University of Manchester for the degree of Master of Science by Research, In the Faculty of Engineering and Physical Science.
6) Rubio N P., Roehl D. and Romanel C.(2007): A three dimensional contact model for soil-pipe interaction, Journal of Mechanics of Materials and Structures, 2(8).
7) Saberi M., Behnamfar F. and Vafaeian M. (2015): A continuum shell-beam finite element modeling of buried pipes with 90-degree elbow subjected to earthquake excitations, IJE TRANSACTIONS C: Aspects 28(3), 338-349.
8) Wang J.(2005): Influence of different boundary conditions on analysis of SSI, 18th International conference on structural mechanics in reactor technology, Beijing, China.
9) Zhang J., Liang Z., Han C J. and Zhang H.(2015): Numerical simulation of buckling behavior of the buried steel pipeline under reverse fault displacement, Mech. Sci., 6, 203-210.

Dynamic response of an elevated intze tank for different staging configuration

Borkotoky, M.[1] and Chetia, N.[2]

[1]PG Student, Department of Civil Engineering, Jorhat Engineering College, Jorhat-785007, India.
[2]Assistant Professor, Department of Civil Engineering, Jorhat Engineering College, Jorhat-785007, India.

ABSTRACT

The paper entitled "***Dynamic response of an elevated intze tank for different staging configuration***" involves a 1000m^3 capacity RC elevated intze type tank supported on frame staging of 22m height. Initially the dynamic properties of the intze type tank are evaluated. The water inside the tank is modeled as mechanical spring mass analogue as per IITK-GSDMA (2007), which is based on the concept of George Housner (1963). The mass of water inside the tank is divided into two parts namely convective mass and impulsive mass due to the hydrodynamic pressure acting on the tank under dynamic loading. Hence two mass idealization of the tank is considered for finite element modeling of the tank in SAP2000. Parametric study is done where three types of bracing patterns and two types of fluid viscous dampers were applied on the tank staging such as conventional bracing, cross bracing, chevron bracing and long stroke and short stroke damper systems. Three different fluid level conditions such as tank empty, tank half and full tank conditions has been examined. Seismic responses of the tank in terms of tank roof displacement, base shear and base moment under different earthquake records for all the types bracing systems have been evaluated and compared.

Keywords: spring mass model, convective mass, impulsive mass, bracings, fluid viscous dampers

1. INTRODUCTION

All around the world water storage tanks are used extensively by municipalities and industries for water supply, firefighting systems etc. Elevated water tanks are considered as an important city services in many flat areas, and accordingly, their serviceability performance during and after strong earthquakes is of crucial concern. These structures has large mass concentrated at the top of slender supporting structure thus making them vulnerable to horizontal forces during earthquakes. Many of the elevated water tanks have suffered extensive damage during past earthquakes. The staging is one of the most difficult parts of an elevated water tank as failure in staging results in the failure of the whole tank. North Eastern region of India falls under the category of most severe seismic zone (Zone –V), which is the most vulnerable region prone to earthquakes. Thus a study dynamic behavior of such tanks must be taken into account considering their vulnerability to earthquakes in highly seismic regions.

2 LITERATURE REVIEW

Patel et al. 2012[1]; *Sloshing response of elevated water tank over alternate column proportionality*; It involves study of the seismic behavior of elevated water tank under alternate column proportionality under different earthquake records. It aims at checking the adequacy of water tank for seismic excitations. The response includes sloshing displacement under four different earthquake records and compared. The results show that the structural responses are exceedingly influenced by different column proportionality.

Patel et al. 2012[2]; *Seismic behavior of RC elevated water tank under different staging pattern and earthquake characteristics;* It involves study of the behavior of the supporting system which is more effective under different earthquake time history records in SAP2000. Two different supporting systems such as radial bracing and cross bracing are compared with basic supporting system for various fluid level conditions. Modeling is done as per IITK-GSDMA guidelines and Westergaard's added mass approach.

F. Omidinasab et al. 2011[3]; *Seismic response evaluation of RC elevated water tank with Fluid-Structure Interaction and earthquake ensemble;* This paper involves a RCC elevated water tank of 900 cubic meters and height 32 meters subjected to an ensemble of earthquake records. Finite element model of the tank has been employed in ABAQUS. Fluid-structure interaction for modeling is considered by Eulerian method. Seismic responses of the tank such as base shear, overturning moment, displacement and hydrodynamic pressure have been assessed for ensemble earthquake records. Responses of the tank are dependent with earthquake characteristics and

frequency of the tank. The maximum response of base shear force, overturning moment, displacement and hydrodynamic pressure occurred in different fluid level conditions.

3 METHODOLOGY

George W. Housner in 1963 after the Chile earthquake of 1960 proposed mechanical spring mass model to idealize an elevated water tank so as to characterize the dynamic behavior of the tank due to moving fluid masses inside it. Housner proposed certain provisions and guidelines for seismic behavior of elevated water tank, which are followed by most of the international codes including Indian code of standard IITK-GSDMA (2007). Modeling is done as two mass model as per IITK-GSDMA(2007): Guidelines for seismic design of liquid storage tanks and Draft Code IS 1893 (Part-2), where hydrodynamic pressure is considered and divided into two parts convective and impulsive hydrodynamic pressures and hence the fluid is divided into two masses as convective mass and impulsive mass respectively. The free surface liquid mass which undergoes sloshing motion known as convective mass and the bottom portion liquid of tank accelerates and moves along with the tank walls is impulsive mass. Previous IS 1893(part 2): 1984 suggested single mass model for elevated water tanks but later on IITK-GSDMA (2007) revised the provisions and recommended two mass model for elevated water tanks which was found to be more realistic as in many cases the tank is not completely full and it will result in sloshing of free surface water during an earthquake. FEM software SAP2000 is used for modeling the water tank. The parameters of the spring mass model are calculated as per the guidelines of the draft code IITK-GSDMA (2007): Guidelines for seismic design of liquid storage tanks.

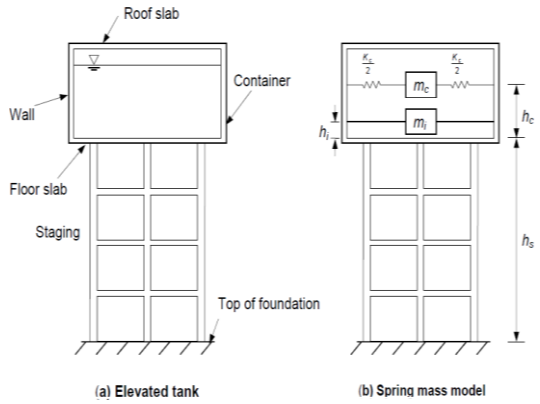

Fig.1. Spring mass model of elevated water tank; IITK-GSDMA (2007)

Table 1. Structural members of the tank

Top Dome, thickness	100 mm
Top Ring Beam; width and depth	200 mm X 400 mm
Cylindrical wall; thickness	300 mm
Bottom ring beam; width and depth	600 mm X 1200 mm
Conical Dome; thickness	600 mm
Bottom Dome; thickness	300 mm
Bottom Circular Girder; width and depth	600 mm X 1200 mm
Columns; diameter	650 mm
Beams; width and depth	500 mm X 500 mm
Bracings, width and depth	500 X 500
Long stroke fluid viscous damper	Damping force: 2000 KNm/sec; Stiffness : 3333.3 N/mm
Short stroke fluid viscous damper	Damping force: 1500 KNm/sec; Stiffness : 20000 N/mm

Shell elements are used in modeling the tank walls, top dome, bottom spherical dome and conical dome. Frame element used to model the columns and beams of the staging, top ring beam, bottom ring beam and bottom circular girder. Linear elastic spring elements are used to connect the convective mass with the tank walls and rigid link elements to connect the rigid mass with the tank walls. Thin shell elements (with four nodes and six degrees of freedom per node) are used in modeling the tank walls, top dome, bottom spherical dome and conical dome. Frame elements (with six degrees of freedom per node) are used to model the top ring beam, bottom ring beam, bottom girder and beams and columns of the staging. Also the bracings are modeled with frame elements. Both the long stroke and short stroke fluid viscous dampers are modeled with link elements.

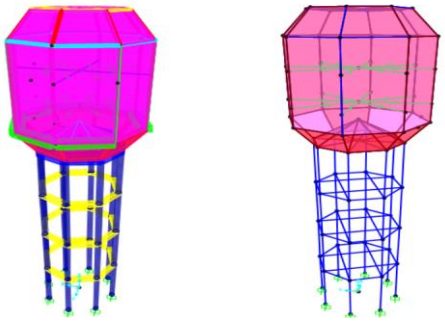

Conventional Braced **Cross Braced**

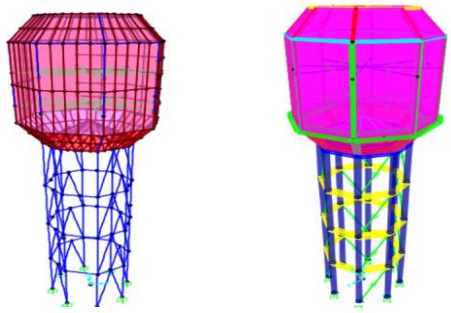

Chevron Braced **Fluid viscous damper braced**

Fig.2. FEM models for different bracing systems of the tank in SAP2000

4 TIME HISTORY ANALYSIS

Time history analysis is performed on the water tank where it is subjected to four different time history functions of previous earthquake records namely Imperial Valley earthquake (1979), Loma Preita earthquake (1989), Northridge earthquake (1994) and Whittier Narrows earthquake (1989). The acceleration data of each of the above earthquakes is given as an input data of ground motion in SAP2000. The peak ground acceleration (PGA) values of the above mentioned earthquakes are presented in Table.2

Table. 2 Peak Ground Acceleration of the earthquake records

EARTHQUAKE	PGA
IMPERIAL VALLEY (1979)	0.312 g
LOMA PREITA (1989)	0.368 g
WHITTIER NARROWS (1987)	0.34 g
NORTHRIDGE (1994)	0.26 g

5 RESULTS AND DISCUSSION

The seismic response of the tank is expressed in terms of roof displacement of the tank and base shear. From table 3 and the graphical representations it can be seen that in terms of roof displacement, chevron bracing system has the least response in all the tank fill conditions. Also both long stroke and short stroke fluid viscous dampers has reduced the response compared to the conventional bracing and cross bracing staging. On the contrary, in case of base shear the response is at the peak in chevron bracing system. However both the long stroke and short stoke dampers performed well in reducing base shear compared to the bracing systems and long stroke damper having the least response.

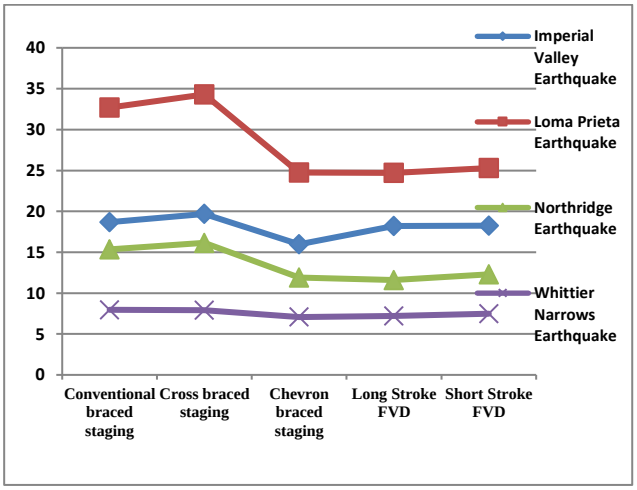

Full tank roof displacement

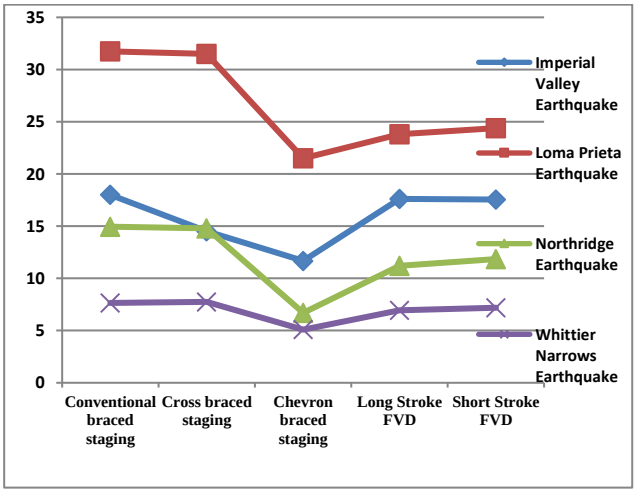

Half tank roof displacement

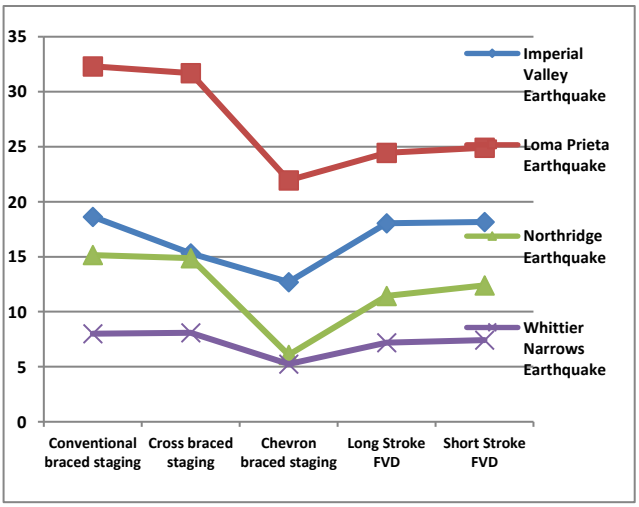

Empty tank roof displacement

Fig.3. Roof displacement due to different earthquakes records for different bracing systems in three tank fill conditions

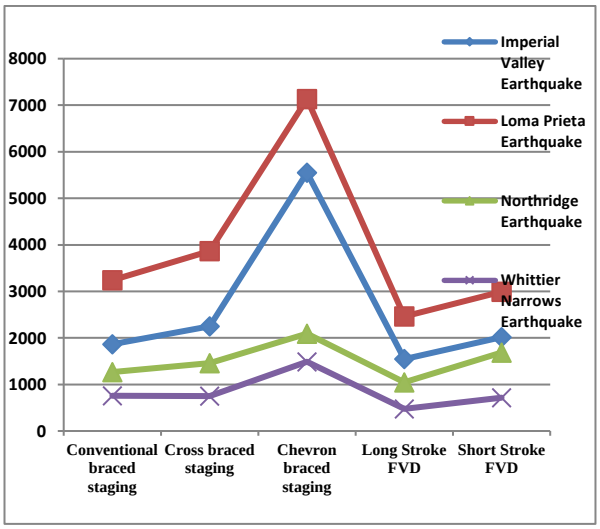

Full tank base shear (KN)

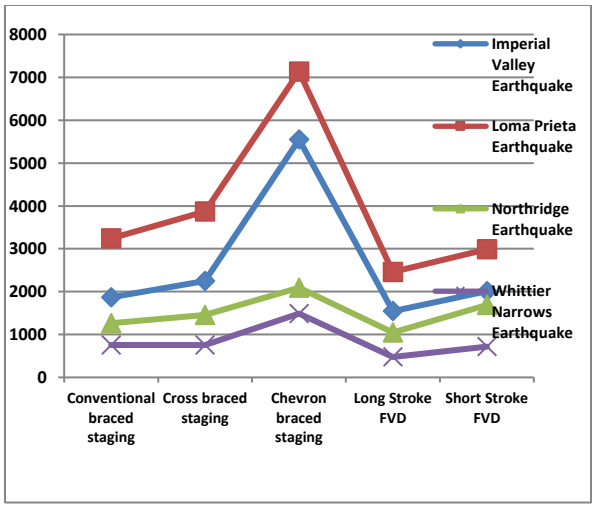

Half tank base shear (KN)

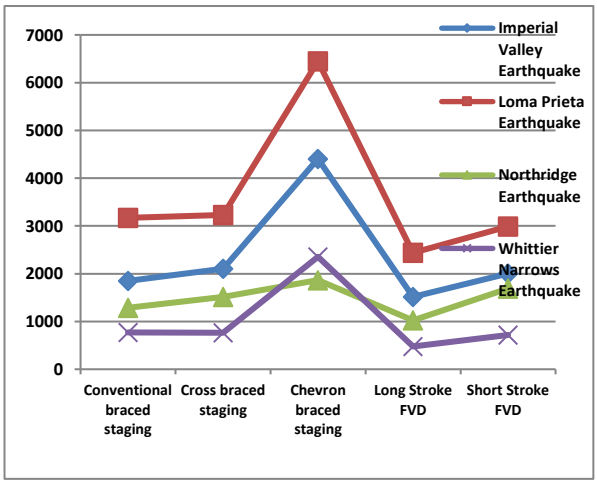

Empty tank base shear (KN)

Fig.4. Base Shear due to different earthquakes records for different bracing systems in three tank fill conditions

6 CONCLUSION

From this research work, it can be concluded that fluid viscous dampers may be a feasible solution for most of the cases compared to the conventionally used bracing systems. Out of dampers, long stroke fluid viscous damper may be more favorable.

REFERENCES

1) Patel, N, Chirag., Vaghela, N. Shashi and Patel, S, H. (2012a): Sloshing response of elevated water tank over alternative column proportionality, *International Journal of Advanced Engineering Technology, E-ISSN 0976-3945.*
2) Patel, S, H., Jabar and M, Ayazhussain. (2012a): Seismic behavior of RC elevated water tank under different staging pattern and earthquake characteristics, *International Journal of Advanced Engineering Research and Studies, E-ISSN2249-8974.*
3) Omidinasab, F and Shakib, H. (2011): .Effect of earthquake characteristics on seismic performance of RC elevated water tanks considering fluid level within the vessels, *Arab J Sci Eng(2011) 36:227-243.*
4) Omidinasab, F and Shakib, H. (2012): Seismic response evaluation of RC elevated water tank with Fluid-Structure Interaction and earthquake ensemble, *KSCE Journal of Civil Engineering, 16(3):366-376.*
5) Livaoglu, R., Dogangun, A. (2006): Simplified seismic analysis procedures for elevated tanks considering fluid-structure-soil interaction; *Journals of Fluids and Structures.*
6) Livaoglu, Ramzan., Dogangun, Adem. (2007): Seismic Behavior of cylindrical elevated tanks with frame supporting system on various subsoil; *Indian Journal of Engineering and Materials Science.*
7) Sorace, S., Terenzi, G., Mori, C.(2015): Analysis and seismic retrofit of a heritage-listed RC elevated water tower; *Sustainable Development, Vol.I.*
8) Swanson, B, David., Campbell, J, Daniel., Falkin, Bryce., Yamatsuka, K, Kylie. (2004): Use of friction dampers on elevated water tanks; *13th World Conference on Earthquake Engineering.*
9) IITK- GSDMA (2007): Guidelines for seismic design of liquid storage tanks.
10) IS 1893(Part –II): 2006.

Table 3. Seismic responses of the tank to different earthquake records for different staging configurations

		Roof Displacement (cm)					Base Shear (KN)				
Tank Fill	**Staging type** / **Earthquake records**	**Conventional brace**	**Cross brace**	**Chevron brace**	**Long stroke FVD**	**Short stroke FVD**	**Conventional brace**	**Cross brace**	**Chevron brace**	**Long stroke FVD**	**Short stroke FVD**
Empty	**Imperial Valley**	**18.64**	**15.3**	**12.7**	**18.04**	**18.16**	**1851**	**2107**	**4405**	**1515**	**2005**
	Loma Prieta	**32.31**	**31.70**	**21.95**	**24.46**	**24.9**	**3173**	**3228**	**6448**	**2438**	**2990**
	Northridge	**15.15**	**14.88**	**6.08**	**11.43**	**12.4**	**1288**	**1512**	**1866**	**1023**	**1687**
	Whittier Narrows	**8.01**	**8.09**	**5.25**	**7.20**	**7.43**	**770**	**763**	**2354**	**477**	**719**
Half	**Imperial Valley**	**18**	**14.52**	**11.68**	**17.61**	**17.55**	**1817**	**2052**	**4488**	**1500**	**1932**
	Loma Prieta	**31.74**	**31.50**	**21.50**	**23.80**	**24.40**	**3163**	**3338**	**6912**	**2381**	**2886**
	Northridge	**14.95**	**14.78**	**6.7**	**11.20**	**11.84**	**1230**	**1364**	**2041**	**1009**	**1627**
	Whittier Narrows	**7.66**	**7.75**	**5.09**	**6.94**	**7.18**	**731**	**702**	**1434**	**456**	**687**
Full	**Imperial Valley**	**18.68**	**19.84**	**15.97**	**18.2**	**18.23**	**1865**	**2249**	**5550**	**1545**	**2013**
	Loma Prieta	**32.70**	**34.3**	**24.74**	**24.7**	**25.31**	**3242**	**3868**	**7134**	**2461**	**2992**
	Northridge	**15.35**	**16.15**	**11.9**	**11.60**	**12.31**	**1263**	**1460**	**2092**	**1047**	**1688**
	Whittier Narrows	**7.96**	**7.91**	**7.07**	**7.21**	**7.47**	**756**	**753**	**1488**	**476**	**717**

Seismic rehabilitation of bridge pier using Fe-SMA: a review

Sarmah, M. [1], Deb, S.K. [2] and Dutta, A.[2]

[1] Ph.D Student, Department of Civil Engineering, IIT Guwahati, Guwahati-781039, India
[2] Professor, Department of Civil Engineering, IIT Guwahati, Guwahati-781039, India

ABSTRACT

Majority of the seismic rehabilitation techniques of severely damaged bridge piers currently at hand require a significant amount of time and labor along with specialized equipment. Although active confinement approach is superior to passive confinement, due to early application of confinement pressure before mobilization of concrete dilation, its widespread application has been hindered. The objective of applying active confinement onsite with minimal hardware and labor is fulfilled by the use of Shape Memory Alloys (SMAs) that are a class of *Smart Materials* which exhibit unique thermomechanical properties, namely shape memory effect (SME) and superelasticity. Most of the research work being carried out for active confinement involves ternary alloys with Ni and Ti as the base metals, which are very costly, thus imposing restrictions on the wide-scale practical use in civil engineering structures. Ease of production and economic consideration has been a major boost for the popularity of Fe-SMAs over NiTi and Cu-based SMAs, facilitating its use in applications that require large consumption rates. Heating of the prestrained alloy spirals, wrapped around the plastic hinge region of the damaged bridge pier, while being restrained, leads to the induction of large recovery stress in the SMAs owing to its SME. Results reported in the literature show that this rehabilitation technique is successful in restoring the as-built lateral strength, stiffness, flexural ductility and the energy dissipation capacity of the repaired RC bridge piers. Thus, application of Fe-SMA would improve the sustainability of rehabilitated bridge systems by extending the service life of structures with minimal maintenance or repairs against seismic events. This article presents an extensive review on the utilization of SMA spirals for seismic rehabilitation of bridge pier by active confinement approach.

Keywords: shape memory alloys, active confinement, reinforced concrete

1. INTRODUCTION

Bridges are among the most critical elements in any transportation infrastructure network. Modern seismic design practices for bridge structures involve the use of capacity design principles that locate plastic hinges in columns, while protecting against other locations of damage (Paulay and Priestley, 1992; Priestley, Seible, and Calvi, 1996). For large earthquakes, the formation of plastic hinges in columns can lead to buckling and rupture of longitudinal steel. Repair of severely damaged bridge elements following an earthquake is an advantageous alternative to replacement. The benefits include cost savings, reduction in construction time and decreased interruption for emergency services and the general public. The objective of bridge repair is to rehabilitate the damaged bridge elements to a performance level similar to the original performance by restoring the load and displacement capacity of the system.

Repair techniques for damaged bridge columns include the use of concrete jackets (Bett et al. 1988), steel jackets (Chai et al. 1991), externally bonded fiber reinforced polymer (FRP) jackets (Priestley and Seible 1993; Saadatmanesh et al. 1997; Elsouri and Harajli 2011; Rutledge et al. 2013). Previous studies (Nesheli and Meguro 2006) have shown that under the same confinement pressure, active confinement approach by prestressed steel/FRP jackets is superior to passive confinement in terms of increasing the concrete strength and ultimate strain, the key factor being delay in the damage sustained by the concrete due to early application of confinement pressure. However, in the case of passive confinement, the concrete would have to undergo dilation (i.e. deform laterally) in order to fully activate the confinement pressure.

Methods of active confinement to repair damaged RC columns require a significant amount of time and labor along with specialized equipment. Hence, despite its advantages, its widespread application has been hindered, and the passive confinement approach using steel or FRP jackets has become more popular over the last several decades. In order to allow active confinement to reach its full potential in the fields of seismic retrofit and repair, there is an urgent need for a simple and robust method to apply active confinement onsite with minimal hardware and labor. This objective is fulfilled by the use of shape memory alloys for active confinement of damaged RC bridge columns.

SMAs are a class of metallic alloys, which can undergo recovery of their original (undeformed) shape after being excessively deformed by heating the alloy to a temperature above the transformation temperature, A_f, which is a material property of the alloy predetermined by the user/manufacturer. This shape recovery is

associated with the induction of large recovery stress in the SMAs when the prestrained alloy is heated while restrained. This recovery stress is utilized to exert active confinement pressure externally on the plastic hinge zone of the columns. Economic consideration and ease of production have been the biggest factors for which Fe SMA systems are gaining popularity as they are much cheaper than Ni and Ti.

The current study is aimed at providing an assessment of the existing repair methods of RC bridge piers. In accordance with the challenges faced in repairing the damaged RC columns using traditional methods, the effectiveness of SMA repair scheme is explored.

2. REPAIR TECHNIQUES FOR RC BRIDGE COLUMNS

Various methods of repair of RC columns available in literature, is reviewed. Advantages and disadvantages associated with these repair techniques are also summarized emphasizing on the need for a simple yet effective method for on-site application.

2.1 RC jacketing

RC jackets have been used to repair earthquake-damaged columns for several decades. These usually involve enlarging the column cross-section with reinforced concrete, along part of or the entire length of the column, connecting the reinforcement in the jacket to the encased damaged column.

Bett et al. (1988), Ersoy et al. (1993), Rodriguez and Park (1994), Fukuyama et al. (2000) and Eduardo et al. (2005) conducted studies on the repair of RC columns with using concrete jacket. The columns were subjected to various loading schemes: uniaxial load, combination of uniaxial and cyclic lateral load, seismic load. The severely damaged columns were then repaired, by encasing the core in a reinforced concrete jacket. The repaired columns were stiffer and stronger than the original columns and performed nearly as well as columns retrofitted using the same technique as the repair, with significantly higher ductility capacity.

From the past research works, it was confirmed that this technique is labor intensive with a high operation cost owing to roughening, cleaning and dowelling of the existing damaged concrete section so as to ensure composite deformation between the jacket and the column surface. It increases the size of the structural element, which reduces the shear span ratio. Also, drilling of holes for addition of dowel bars or connectors leads to micro-cracking and subsequent weakness in the member.

2.2 Steel jacketing

Repair of RC columns using steel jacketing usually involves restoring the cross-section by casting new concrete, installing the steel jacket and filling the space between the jacket and column with cement based grout.

Chai et al. (1991), Fukuyama et al. (2000), Elsouri and Harajli (2011) reported repair of RC columns with steel jackets, which involved encasing the column plastic hinge region in a bonded steel jacket. These were then tested under constant axial load and cyclic lateral load. Results showed that the repair was able to enhance the strength and ductility compared to the as-built column. This resulted in achievement of considerably larger lateral loads and energy dissipation capacities than the as-built columns.

However, there are some drawbacks associated with this technique. The bonded plates are prone to corrosion and premature debonding. There is also difficulty in transportation, handling, installation and attainment of proper bond of theses plates with underlying concrete at remote locations.

2.3 Fiber-reinforced polymer (FRP) jacketing

FRP comprises of fibers (e.g. carbon, aramid, glass etc.) connected effectively with the help of resins, which provide the mechanism for load transfer between the fibers and are responsible for composite compressive strength. FRP with fibers oriented along the longitudinal axis of the column functions mainly to increase the flexural strength of the repaired column.

Priestley et al. (1993) and Saadatmanesh et al. (1997) conducted studies on repairing RC columns with glass FRP (GFRP) jacket that had been tested to failure under reversed cyclic loading and constant axial load. Test results indicated that this repair technique was effective in restoring both the flexural strength and displacement ductility, which were higher than those of the as-built columns. Sheikh and Yau (2002), Li and Sung (2003) and Chang et al. (2004) repaired RC columns with epoxy and non-shrink mortar which was strengthened with CFRP wrap. Retesting of the repaired columns under the same combined loading as that of the original columns revealed that the repair method was effective in improving the seismic performance of the column in terms of strength and ductility.

Excellent corrosion resistance with high strength and stiffness to weight ratios makes FRP's one of the most suitable alternatives for seismic repair as it does not alter the stiffness of the component which otherwise would impose additional seismic demand on the member. Several disadvantages associated with the use of FRP confinement are its need for experienced workmanship, high cost, ineffective functioning in the compression part of cyclic loads and delamination.

2.4 Pre-stressing Steel Reinforcement/FRP Jackets

Active confinement, as compared to passive confinement, effectively slows down the lateral expansion of concrete under compression because the pressure is applied before the concrete dilates; hence increasing the ductility and strength of concrete. These

attractive features encouraged many researchers to consider applying active confinement in the field. One such approach is to prestress/pretension steel strands, steel jackets, or FRP jackets/straps.

Saatcioglu and Yalcin (2003) and Miyagi et al. (2004) conducted series of tests on concrete columns retrofitted by individual seven-wire prestressing strand hoops and steel plates respectively and found that it was an effective way to improve shear capacity and ductility. Nesheli and Meguro (2006) and Janke et al. (2009) used pretentioned FRP belts to retrofit damaged concrete columns after an earthquake. Choi et al (2010) applied lateral pressure externally on steel jackets to tightly attach the steel jackets on concrete surfaces followed by welding lateral strip bands to protect the welding line from fracture. These retrofitted concrete columns were tested under cyclic lateral loading and constant axial compressive force. They concluded that pretentioned FRP belts helped to reduce or even close existing cracks and could be used for emergency retrofitting of damaged concrete columns. It was able to restore the flexural strength and shear capacity of the damaged columns. However, this technique requires heavy machinery to apply required external pressure.

Although the superiority of active confinement, in comparison to passive confinement, was well established by previous researchers, attempts to apply active confinement using the conventional materials such as steel strands or FRP straps were quite limited because of considerable labor and time to apply sufficiently high prestressing force in the field. To allow widespread application of active confinement onsite, there is an urgent need for a simpler method with minimal hardware and labor. This objective is fulfilled by the use of shape memory alloys. A brief background on shape memory alloys and its properties is presented in the next section.

3. SHAPE MEMORY ALLOYS (SMA)

3.1 Introduction

Shape Memory Alloys (SMAs) are basically metallic alloys, which undergo large deformation under external load at low temperature and can recover the same upon heating above a certain temperature. This capability of remembering its initial undeformed shape, gives these group of metallic alloys its name i.e. Shape Memory Alloy and this particular phenomenon is known as Shape Memory Effect (SME). Another unique thermomechanical phenomena that these groups of alloys exhibit, is known as Pseudo-Elasticity (PE) or Super-Elasticity (SE). Above a certain temperature, this material undergoes large deformation under the action of external load and is able to recover the same upon unloading. These distinct properties of the SMA materials, SME and SE are attributed to the special characteristics at the microstructural level which enables reversible solid-solid phase transformation among variants of its constituent phases, namely Martensite [M], and Austenite [A].

3.2 Thermomechanical properties of SMA materials

SMAs have two main crystallographic phases, the low-temperature phase is called Martensite [M], and the high-temperature phase is called Austenite [A]. As shown in Fig. 1(a), SMA is in the full martensite phase at a temperature below the martensite finish temperature (M_f). If the temperature increases above the austenite start temperature (A_s), the SMA enters the austenite phase and reaches the state of full austenite above the austenite finish temperature (A_f). In this phase, if the SMA is excessively deformed and then unloaded, it will return to its original, undeformed shape (SE) as shown in Fig. 1(b). The typical stress–strain behavior of the SMA loaded in the austenite phase exhibits hysteretic loop that has a flag-like shape, and brings the effects of energy dissipation and damping while still keeping its original shape. Many researchers have studied such phenomena for applications in civil structures such as dampers, base isolation devices, and reinforcement for concrete.

When the SMA loaded in its martensite phase, however, it will experience large residual strain even after the loading is removed. When the SMA is heated above A_f, the SME of the SMA allows recovery of its original shape. If the SMA is restrained, it is unable to recover its original shape, hence large recovery stress (prestress) would develop and maintain until the SMA is released. Researchers have made efforts to utilize this recovery stress of SMAs in the application of active confinement technique for concrete.

4. ACTIVE CONFINEMENT TECHNIQUE OF BRIDGE PIER USING SMA SPIRALS

Fig. 1(c) illustrates the active confinement technique of bridge pier using SMA. In this technique, pre-strained SMA wires are first wrapped around the plastic hinge region of the bridge pier, and then heated to a temperature above A_f to activate the shape recovery. Since the SMA spirals are restrained at both ends and the concrete pier around which they are wrapped is incompressible, the induced shrinkage causes the SMA spirals to squeeze the concrete column. This squeezing effect provides the active confinement pressure to the column. This recovery stress is highly dependent on the SMA material composition, manufacturing procedure, and the level of deformation experienced prior to shape

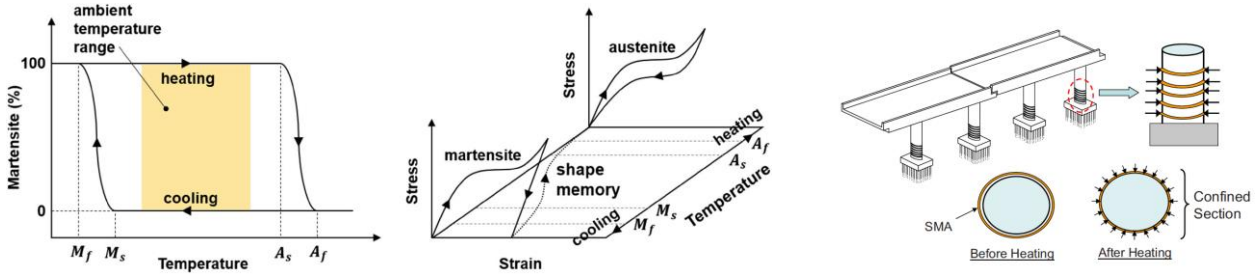

Fig. 1. (a) Thermal hysteresis & (b) Thermomechanical behavior of SMA (c) Active confinement concept (Andrawes et al. 2010)

recovery (Otsuak and Wayman 2002).

Andrawes et al. (2010) first carried out experimental and analytical work to explore the feasibility of the use of SMA spirals for active confinement of concrete through thermal prestressing. Uniaxial compression tests of concrete cylinders confined with NiTi SMA spirals showed a significant improvement in the concrete strength and ductility even under small confining pressure. The experimental results were then used to calibrate the analytical column model. Analytical models of bridge columns retrofitted with SMA spirals and CFRP were studied under displacement-controlled cyclic loading and a suite of strong earthquake records. Under cyclic loading, the SMA retrofitted column exhibited a maximum increase in strength relative to the CFRP wrapped columns by 38%. In addition, less damage was observed in the concrete core and longitudinal steel when the column was actively confined. On the other hand, under seismic excitations, using SMA spirals improved the seismic behavior of the columns significantly compared to CFRP wraps in terms of column strength, effective stiffness, and column residual drifts.

Shin and Andrawes (2011) conducted experiments on four large scale circular single-cantilever concrete columns 254 mm × 1270 mm with the same amount of internal longitudinal and transverse reinforcement, but using different retrofitting schemes. One of the four columns was tested as ‘as-built’ state. The other three used three different retrofitting schemes (Fig. 2.14): 10-layer of GFRP jackets, NiTiNb SMA spirals with 10 mm pitch and 20 mm pitch NiTiNb SMA spirals in addition to 5-layer of GFRP jackets outside the plastic zone. All four columns were tested under quasi-static lateral cyclic loading. It was concluded that although SMA confined and GFRP-SMA confined columns only improved the strength slightly compared to the ‘as-built’ column and GFRP confined column, using SMA spirals to provide active confinement, flexural ductility, drift capacity and the ability of dissipating seismic energy of concrete columns were all enhanced significantly. Besides, due to the active confining pressure applied to the column prior to loading, it can help to delay the dilation of concrete during loading, and hence limit the damage area of the concrete columns.

Shin and Andrawes (2011) reported an emergency repair method for RC columns with fractured longitudinal bars. The test specimen was a 1/3-scale circular RC column that was tested under constant axial load and cyclic lateral load. The damage after the original test included crushed concrete, fractured longitudinal bars, and excessive opening of transverse reinforcement. The repair was accomplished by replacing the damaged concrete with quick-setting mortar, injecting epoxy in the cracks, connecting the fractured bars using rebar couplers, and wrapping the NiTiNb SMA spirals at the repaired region. Retesting the repaired column revealed that the lateral strength was fully restored, and the stiffness was higher than that of the original column. The overall displacement ductility was increased. This was attributed to the ability of the SMA spirals to apply and maintain active confinement on the damaged region of the column and thus delayed the progression of damage.

Jung et al. (2018) studied the application of SMA confinement in seismic retrofitting and emergency repair of RC bridge columns, which was examined experimentally through a series of shake table tests. Two 1/6-scale RC columns, retrofitted and repaired with NiTiNb SMA spirals, were tested simultaneously under bidirectional test motions with varying intensity. Test results showed that SMA confinement is highly effective in mitigating the seismic damage and improving the seismic performance of retrofitted and repaired RC columns subjected to strong earthquakes.

5. FE-SMA FOR ACTIVE CONFINEMENT

Economic consideration has been a major stimulus for the attention Fe SMA systems are receiving as the base metals as they are much cheaper than Ni and Ti; also Fe based SMAs can be easily produced using traditional metal processing technologies. Once the Fe-SMA is activated through heating while contraction is inhibited, the recovered stress remains stable even if the temperature drops below the M_s. For structural concrete applications, it is also very important to consider the temperature at which the transformation occurs because high transformation temperature could deteriorate the mechanical properties of the surrounding concrete. In this sense, the reported SMA, (Leinenbach et al. 2012) Fe–17Mn–5Si–10Cr–4Ni–1(V,C) reached the recovery

stresses of 580 MPa after heating to only 130°C. This is important for civil engineering applications, where the prestressing force shouldn't be changed with the change in ambient temperature.

6. CONCLUSION

The thermally triggered recovery stress of prestrained Fe-SMAs exerts large external active confinement pressure on the concrete at the damaged region of the bridge pier. If Fe-SMAs are used for prestressing applications, they have several advantages compared to the traditional prestressing/posttensioning technologies, for example, there are no friction losses, no anchor heads or ducts are required, and no space is necessary for applying the force with a hydraulic device. The reason is that the prestressing of the SMA tendons is not performed mechanically, as in conventional prestressing steel, but with heating.

Studies carried out by several researchers revealed that the lateral strength of the SMA wrapped repaired column could be fully restored, and had stiffness higher than that of the original column. The overall displacement ductility, drift capacity and the ability of dissipating seismic energy of concrete columns could also be increased. This was attributed to the ability of the SMA spirals to apply and maintain active confinement on the plastic hinge region of the column. Ease of production, cost-effectiveness and ability to maintain constant recovery stress at ambient temperature after thermal activation at a comparatively low temperature, as compared to other SMA groups, make Fe-SMAs a promising material for seismic rehabilitation of bridge pier.

REFERENCES

1) Andrawes, B., Shin, M., & Wierschem, N. (2010). Active confinement of reinforced concrete bridge columns using shape memory alloys. *Journal of Bridge Engineering*, 15(1), 81-89.
2) Bett, B. J., Klingner, R. E., and Jirsa, J. O. (1988). Lateral load response of strengthened and repaired reinforced concrete columns, *ACI Structural Journal*, 85(5), 499–508.
3) Chai, Y. H., Priestley, M. J. N., Seible, F. (1991). Seismic retrofit of circular bridge columns for enhanced flexural performance, *ACI Structural Journal*, 88(5), 572–584.
4) Chang, S. Y., Li, Y. F., and Loh, C. H. (2004). Experimental study of seismic behaviors of as-built and carbon fiber reinforced plastics repaired reinforced concrete bridge columns, *Journal of Bridge Engineering*, 4(391), 391–402.
5) Choi, E., Park, J., Nam, T. H., Yoon, S. J. (2009). A new steel jacketing method for RC columns, *Magazine of Concrete Research*, 61(10), 787-796.
6) Eduardo, N.B.S., Fernando, A.B., Vitor, D.S. (2005). Reinforced concrete jacketing: Interface influence on monotonic loading response, *ACI Structural Journal*, 102 (2), 252–257.
7) Elsouri, A. M., and Harajli, M. H. (2011). Seismic repair and strengthening of lap splices in RC columns: Carbon fiber-reinforced polymer versus steel confinement, *Journal of Composite Construction*, 10.1061/(ASCE) CC.1943-5614.0000213, 721–731.
8) Ersoy, U., Tankut, A.T., Suleiman, R. (1993). Behavior of jacketed columns, *ACI Structural Journal*, 90, 288–293.
9) Fukuyama, K., Higashibata, Y., and Miyauchi, Y. (2000). Studies on repair and strengthening methods of damaged reinforced concrete columns, *Cement & Concrete Composites*, 22, 81–88.
10) Janke L., Czaderski C., Ruth J., Motavalli M. (2009). Experiments on the residual load-bearing capacity of prestressed confined concrete columns, *Engineering Structures*, 31(10), 2247–2256.
11) Jung, D., Wilcoski, J., Andrawes, B. (2018). Bidirectional shake table testing of RC columns retrofitted and repaired with shape memory alloy spirals, *Engineering Structures*, 160 (2018), 171–185.
12) Li, Y. F., and Sung, Y. Y. (2003). Seismic repair and rehabilitation of a shear-failure damaged circular bridge column using carbon fiber reinforced plastic jacketing, *Canadian Journal of Civil Engineering*, 30(5), 819–829.
13) Nesheli KN, Meguro K. (2006). Seismic retrofitting of earthquake-damaged concrete columns by lateral pre-tensioning of FRP belts, *Proceedings of the 8th U.S. National Conference on Earthquake Engineering*, 841.
14) Otsuak, K., & Wayman, C.M. (2002). Shape memory material, *Cambridge University Press*.
15) Priestley, M. J. N., and Seible, F. (1993). Repair of shear column using fiberglass/epoxy jacket and epoxy injection, *Report No. 93-04, Job No. 90-08, Seqad Consulting Engineers, Solana Beach, CA*.
16) Rodriguez, M. and Park, R. (1994). Seismic load tests on reinforced concrete columns strengthened by jacketing, *ACI Structural Journal*, 91 (2), 150–159.
17) Rutledge, S. T., Kowalsky, M. J., Seracino, R., and Nau, J. M. (2013). Repair of reinforced concrete bridge columns containing buckled and fractured reinforcement by plastic hinge relocation, *Journal of Bridge Engineering*, A4013001, 1-10.
18) Saadatmanesh, H., Ehsani, M., and Jin, L. (1997). Repair of earthquakedamaged RC columns with FRP wraps, *ACI Structural Journal*, 94(2), 206–215.
19) Saatcioglu, M. and Yalcin, C. (2003). External prestressing concrete columns for improved seismic shear resistance, *Journal of Structural Engineering*, 129(8).
20) Sheikh, S. A., and Yau, G. (2002). Seismic behavior of concrete columns confined with steel and fiber-reinforced polymers, *ACI Structural Journal*, 99(1), 72–80.
21) Shin, M., & Andrawes, B. (2011b). Lateral cyclic behavior of reinforced concrete columns retrofitted with shape memory spirals and FRP wraps, *Journal of Structural Engineering*, 137, 1282–90.
22) Shin, M., and Andrawes, B. (2011). Emergency repair of severely damaged reinforced concrete columns using active confinement with shape memory alloys, *Smart Materials and Structures*, 20(6), 065018
23) Leinenbach, C., Kramer, H., Bernhard, C., Eifler, D. (2012). Thermo-mechanical properties of an Fe–Mn–Si–Cr–Ni–VC shape memory alloy with low transformation temperature, *Advance Engineering Materials*, 14:62–7.

2nd International Conference of Civil Engineering for Sustainable Development-Opportunities and Challenges
CESDOC-2018, 18th to 19th December, 2018, Assam Engineering College

Seismic vulnerability assessment of the Jorhat Engineering College building

Kashyap, U. [1], Dutta, A. [2]

[1] Assistant Professor, Department of Civil Engineering, Assam Kaziranga University, Jorhat, Assam-785006, India.
[2] Associate Professor, Department of Civil Engineering, Jorhat Engineering College, Jorhat, Assam-785006, India.

ABSTRACT

This paper explores the seismic vulnerability parameters of the structural components of a G+3 building. The institute building of Jorhat Engineering College which lies in seismic zone V has been used as a case study. The dimension of the building is 33.36 m × 8.51 m. It also has a cantilevered projection of 2.30 m. Floor to floor height of the building is 3.6m (Ground storey) and 3.3m (Other floors). Evaluating the building for its vulnerability parameters will help check whether the institute building is seismically sound. The performance of the building is evaluated both qualitatively and quantitatively. For qualitative evaluation of seismic parameters of the building, Rebound Hammer test is performed on the structural components of the building while for quantitative evaluation Non-Linear Static Pushover Analysis and Non-linear Dynamic Time History Analysis is performed using SAP2000 by creating a model similar to that of the institute building. The results of the Rebound Hammer test were used in the modelling purpose. Also infill walls are modelled as equivalent concentric diagonal strut. Storey displacements, inter-storey drift ratios and plastic hinge locations were selected as response parameters for analysis. Displacement Coefficient Method according to ASCE 41-06 is used for calculating the target displacement. Yielding of the members was observed for 150% of the calculated target displacement of the structure. The building has been loaded with an invariant triangular load pattern along X-axis direction and Y-axis direction as well. Storey displacements, inter-storey drift ratios, plastic hinge locations, pushover curves were extracted from the pushover database at the calculated target displacements. The building in this study is a short period frame (3-storey RC frame); hence the triangular load pattern yielded almost same capacity curves for both X-axis and Y-axis load pattern applied to the building. The pushover curves for target displacements 23.25 mm and 30 mm are linear indicating that the deformation is within the elastic range and no hinges were formed for these two target displacements. But for time-history analysis, significant differences in storey displacements can be seen for X-axis loading and Y-axis loading for the input ground motions- El Centro, Kobe and Gebze unlike in pushover analysis. Hence the storey displacement profiles traced by time-history analysis are more accurate. The storey displacement profiles indicated clearly that the building is more vulnerable in the transverse direction, the stiffness of the building being less in that direction.

Keywords: pushover analysis, time-history analysis, storey displacements, inter-storey drift ratios, equivalent concentric diagonal strut, displacement coefficient method

1. INTRODUCTION

Jorhat Engineering College is one of the most important Government Engineering College of North-East India. The buildings of the college were designed using skeletal structural system. The college new building taken for this study is a three storey building designed considering the design factors of IS: 1893-2002. Jorhat, Assam, India is one of the largest towns in Assam with a population of 2.2 lakhs. Jorhat lies in ZONE V of Seismic Zone Map of 2002. According to Seismic Zoning Map of IS: 1893- 2002, this region is the highest earthquake risk zone. The performance of the building is evaluated both qualitatively and quantitatively.

1.1 Qualitative Analysis

For qualitative analysis of the building, Rebound Hammer test is performed on all the structural components of the building as per IS: 13311 (Part 2)-1992. The rebound hammer test is based on the principle that the rebound of an elastic mass depends on the hardness of the surface against which its mass strikes. When the plunger of the rebound hammer is pressed against the surface of the concrete, the spring-controlled mass rebounds and the extent of such rebound depends upon the surface hardness of the concrete. Thus the rebound is taken to be related to the compressive strength of the concrete. The rebound value is read from a graduated scale and is designated as the rebound number or rebound index. The compressive strength can be read directly from the graph provided on the body of the hammer. M-20 grade of concrete and Fe-415 grade of reinforcing steel are used for all members of the structure.

1.2 Quantitative Analysis

For quantitative analysis of the building, non-linear time-history method and non-linear pushover analysis are adopted. For time-history analysis, the ground

motion records used in this study include El Centro (Imperial Valley, 18 May 1940, NS component), Kobe (Hyōgo Prefecture, Japan, 17 January 1995, NS component) and Gabes (Kocaeli, August 17, 1999, EW component). The El Centro is a widely known ground motion utilized in many studies. Kobe is a very strong ground motion which is extremely important to study the performance of the building and map the damages. The damaging ground shaking intensities of the Gebze earthquake covered a 2000 square kilometre area and causes total collapse of thousands of un-engineered multi-storey apartment buildings. These ground motions are selected because of their uniqueness, difference in frequency content, amplitude etc. Static pushover analysis procedure is selected for its applicability to performance-based seismic design approaches and can be used at different design levels to verify the performance targets. Pushover analysis allows tracing the sequence of yielding and failure on member and structural level as well as the progress of overall capacity curve of the structure. Storey displacements, inter-storey drift ratios and plastic hinge locations were selected as response parameters for analysis. Displacement Coefficient Method according to ASCE 41-06 is used for calculating the target displacement.

2. MODELLING AND ANALYSIS PROCEDURE

2.1 Geometric Details

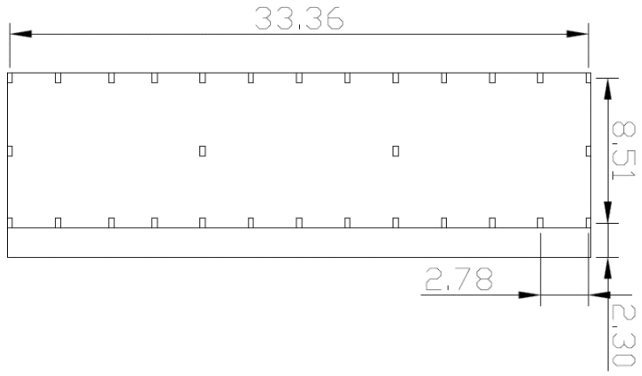

Fig 1: Plan of the study building

Geometric and material properties are as follows:

a) Plan of building = 33.360 m × 8.510 m

b) Floor to floor height = 3.6m (Ground storey) and 3.3m (Other floors)

c) Thickness of slab = 0.1m

d) Dead Load = 1× 0.1×20×1.5 kN/m2 = 3kN/m2

e) Live Load = 1.5 kN/m2 (for roof) & 3 kN/m2 (for floors)

f) Modulus of Elasticity (Ec) = 5000√fck = 5000 √20 N/mm2

=22360.68 N/mm2

g) Infill walls are modeled as equivalent concentric diagonal strut connected at the beam-column joints by pin joints.

2.2 Equivalent Strut Idealization of Infill Walls

A three-dimensional model of the building is created in SAP2000. The average compressive strength obtained from Rebound Hammer test (fck=20N/mm2) is used as an input for modeling. Equivalent Diagonal Strut Method is used for modeling the infill wall. In this method the infill wall is idealized as diagonal strut and the frame is modeled as beam or truss element. The idealization is based on the assumption that there is no bond between frame and infill [Tamboli H. R., Karadi U. N. (2012)]. The infill panel is represented by an equivalent diagonal strut of width a, and net thickness t_w as shown in Fig 2. The width (W_{eff}) of equivalent struts are calculated as per the following relations (Eqs. 1&2)

$$W_{eff} = 0.175(\lambda h \times H)^{-0.4} \times w' \quad (1)$$

$$\lambda_h = \left[\frac{\{E_w t_w sin(2\theta)\}}{4E_c I_c H_{in}}\right]^{\frac{1}{4}} \quad (2)$$

where, E_w and E_c are moduli of elasticity of the infill wall and the concrete (i.e. the frame material) respectively, $\theta = \tan^{-1}(\frac{H}{L})$ is the inclination of the diagonal, t_w is the thickness of the infill wall, and I_c is moment of inertia of the column of the frame, whereas H_{in}, H and L are the net height of the infill wall, the storey height, and the bay length of the frame. The thicknesses of the equivalent struts are the same as the thicknesses of the walls. [Tamboli H. R., Karadi U. N. (2012)]

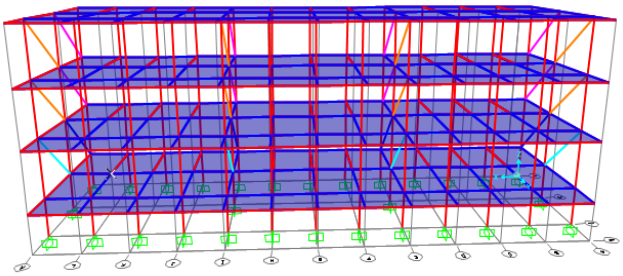

Fig 2: 3D view of the institute building modeled in SAP2000

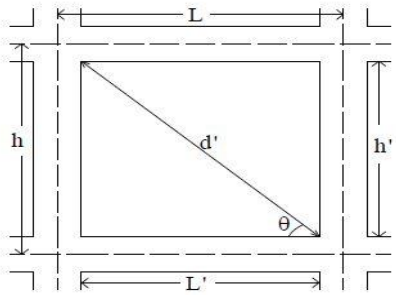

Fig 3: Equivalent strut idealization of infill walls.

2.3 Pushover Analysis

Gravity loads and inverted triangular lateral load pattern as per IS 1893:2002 for seismic zone V are applied to the structural model. Base shear and roof displacement are recorded at first yielding. Gravity

loads are then removed and a new lateral load pattern is applied to the structural members. A separate analysis is performed under each incremental lateral load. The results of each incremental lateral load analysis are super-imposed. The capacity curve of the building is obtained from the plot of base shear and roof displacement. The base shear is calculated as per IS: 1893(part 1):2000. Target displacement is the maximum displacement at the control node of the structure and is calculated by Displacement Coefficient Method as per ASCE 41-06. Pushover Analysis is performed until 1.5 times the target displacement is reached.

2.4 Time History Analysis

In SAP2000, the time history function is first defined and then a new time history load case is defined in addition to the gravity load case. The time history load is applied in the form of acceleration. A scale factor is added to this load type depending upon the units in the input file. The structure is then analyzed and required plots are obtained. The ground motion records used in this study include El Centro (Imperial Valley, 18 May 1940, NS component), Kobe (Hyōgo Prefecture, Japan, 17 January 1995, NS component) and Gabes (Kocaeli, August 17, 1999, EW component). The El Centro is a widely known ground motion utilized in many studies. Kobe is a very strong ground motion which is extremely important to study the performance of the building and map the damages. The damaging ground shaking intensities of the Gebze earthquake covered a 2000 square kilometre area and causes total collapse of thousands of un-engineered multi-storey apartment buildings. These ground motions are selected because of their uniqueness, difference in frequency content, amplitude etc.

2.5 Plastic Hinge Mechanism

During inelastic deformations, the plastic hinges are expected to format locations where the structural damage can be allowed to occur. The damages in the form of plastic hinges are expected to be formed in beams rather than in columns. In SAP2000® during modeling, the plastic hinges selected have an uncoupled moment hinges, an uncoupled axial hinge, an uncoupled shear hinge and a coupled axial force and biaxial bending moment hinges. Mechanism with beam yielding is characteristic of strong-column-weak-beam behaviour in which the imposed inelastic rotational demands can be achieved reasonably well through proper detailing practice in beams. Therefore, in this mode of behaviour, it is possible for the structure to attain the desired inelastic response and ductility.

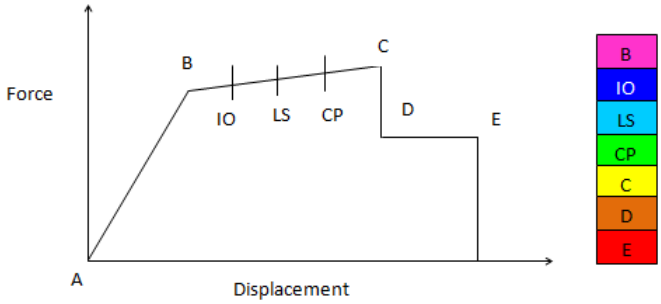

Fig 4: Different stages of plastic hinge formation

In order to obtain performance points as well as the location of hinges in different stages, we can use the pushover curve. In this curve, the range AB being the elastic range, B to IO is being the range of instant occupancy, IO to LS being the range of life safety and LS to CP being the range of collapse prevention.

When a hinge touches point C on its force-displacement curve then that hinge must start to drop load. The manner in which the load is released from a hinge that has reached point C is that the pushover force or the base shear is reduced till the force in that hinge is steady with the force at point D.

As the force is released, all of the elements unload as well as the displacement is decreased. After the yielded hinge touches the point D force level, the magnitude of pushover force is again amplified and the displacement starts to increase again.

If all of the hinges are within the given CP limit then that structure is supposed to be safe. Though, the hinge after IO range may also be required to be retrofitted depending on the significance of structure.

3. RESULTS

In this study, the behavior of the structure due to ground motions causing elastic and inelastic responses is predicted. The pushover capacity curve yielded almost same capacity curves for both X-axis and Y-axis load pattern applied to the building for the triangular load pattern applied to the building. This is because the building in the study is a short period frame (3-storey). The target displacement is calculated to be 23.5 mm for X-axis loading and 30 mm for Y-axis loading. The structure analyzed to the target displacement limit has shown no failure indicating that the deformation of the building is in the elastic range. The model is also analyzed for other monitored displacements such as 50 mm, 100 mm and 300 mm. Non-linearity in the building response can be observed clearly for roof displacement 50 mm. For the monitored displacement 100 mm, all hinges are within the collapse prevention range. Therefore, the structure is safe till a monitored displacement of 100 mm though retrofitting may be required. However the structure shows failure at monitored roof displacement of 300 mm.

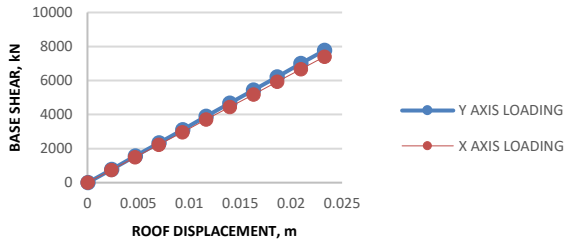

Fig 5: Pushover curve for 23.25 mm target displacement

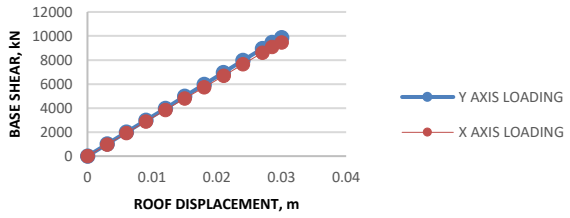

Fig 6: Pushover curve for 30 mm target displacement

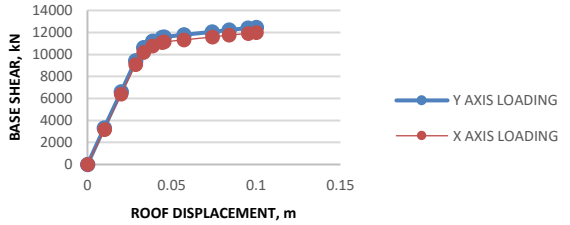

Fig 7: Pushover curve for 100 mm monitored displacement

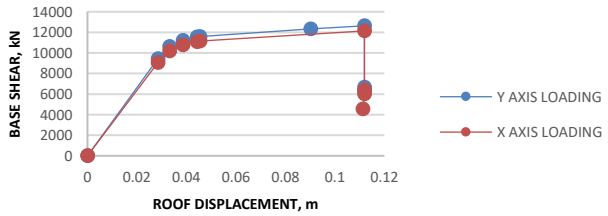

Fig 8: Pushover curve for 300 mm monitored displacement

The storey displacements of the study building are obtained by Non-linear Pushover analysis and Non-linear Time History analysis and the results obtained from both the analyses are compared. It is interesting to see that the storey displacement in X-axis loading and Y-axis loading are almost similar, although the stiffness of the skeletal frame is higher in the X-direction. It may be worth mentioning that infill walls are considered only in the Y-direction while the infill walls are neglected in the X-direction due to large openings.

This signifies that the presence of infill walls has increased the stiffness of the building in the Y-direction. Thus the displacement of the building in Y-direction is less than the displacement expected from the skeletal frame. Also the building is not allowed to displace freely as roof displacement is fixed in both the axis. Hence pushover analysis could not capture accurately the exact storey displacement profiles of the building. Significant differences in storey displacements can be seen for X-axis loading and Y-axis loading for the input ground motions- El Centro, Kobe and Gebze unlike in pushover analysis. Hence the storey displacement profiles traced by time-history analysis are more accurate. The storey displacement profiles indicated clearly that the building is more vulnerable in the transverse direction, the stiffness of the building being less in that direction.

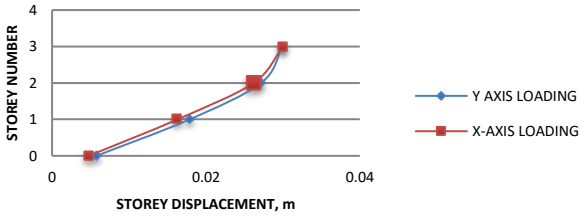

Fig 9: Storey number vs. Storey displacement curve for target displacement 22.5 mm

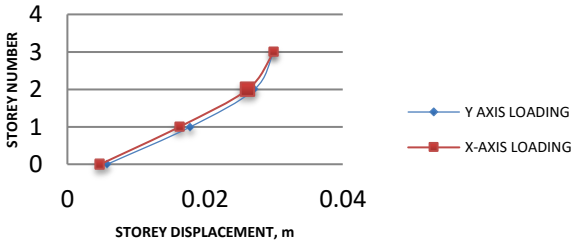

Fig 10: Storey number vs. storey displacement curve for target displacement 30 mm

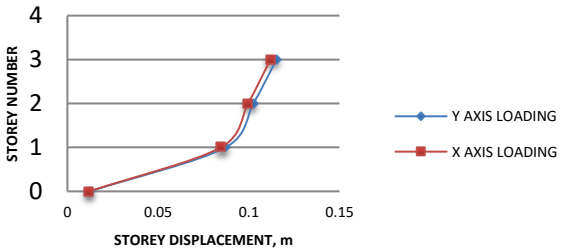

Fig 11: Storey number vs. storey displacement curve for monitored displacement 50 mm

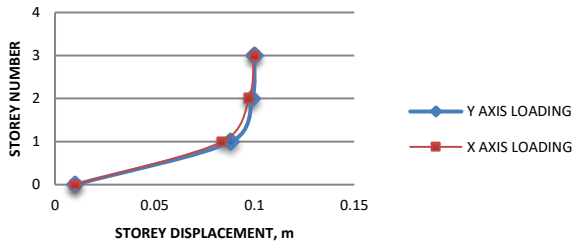

Fig 11: Storey number vs. storey displacement curve for monitored displacement 100 mm

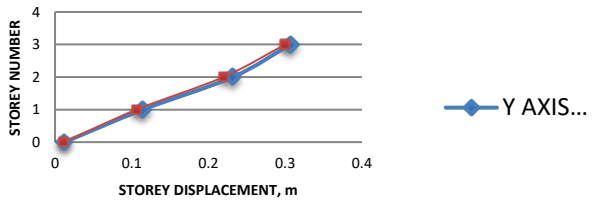

Fig 12: Storey number vs. storey displacement curve for monitored displacement 300 mm

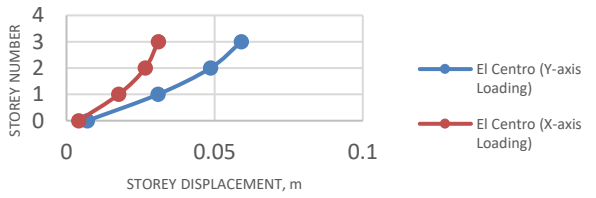

Fig 13: Storey number vs. Storey displacement curve for El Centro ground motion

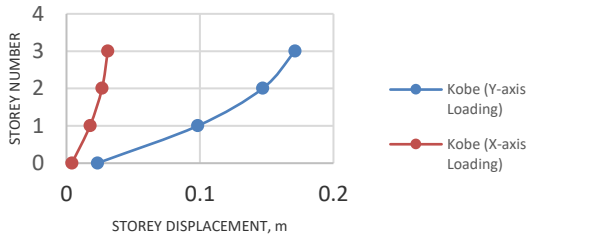

Fig 14: Storey number vs. Storey displacement curve for Kobe ground motion

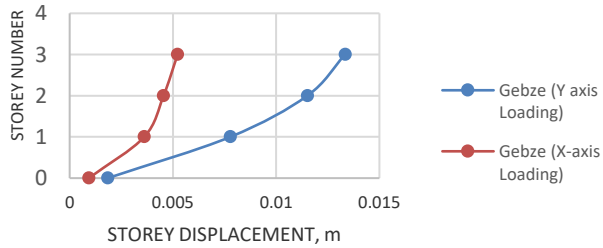

Fig 15: Storey number vs. Storey displacement curve for Gebze ground motion

4. CONCLUSION

In this study, the responses obtained for the 3-storey RC building for pushover analysis using an inverted triangular lateral load distribution are almost identical. Significant differences can be seen in the responses of time-history analysis. It can be concluded that dynamic time history analysis yield more accurate results. The pushover curves at the calculated target displacements are linear which indicate that the deformation of the building is in the elastic range. The building analysed to the target displacement limit has shown no failure. Hence according to this study, the building appears to be safe against such displacements. In this study the rebar position and rebar spacing of the structure could not be determined due to lack of proper instruments. Hence the conformation of the ductility requirement of the structure with IS 13920: 1993 could not be known. Also the grade of steel used could not be determined. Since the Jorhat Engineering College building lies in seismic zone V, the value of R is assumed to be 5. But this assumption may give approximate results and the safety of the building may not be predicted accurately.

REFERENCES

1) Duan Haijuan and Hueste Mary Beth D. (2012): Seismic performance of a reinforced concrete frame building in China, Engineering Structures, 41 (2012) 77-89, Elsevier
2) Cole Stephen W., Xu Yebang, Burton Paul W. (2007), Seismic hazard and risk in Shanghai and estimation of the expected building damage, Soil Dynamics and Earthquake Engineering,28 (2008) 778-794, Elsevier
3) Kadid A., Boumrkik A. (2008), Pushover Analysis of Reinforced Concrete Frame Structures, Asian Journal of Civil Engineering (Building and Housing), Vol. 9, No. 1 (2008), Pages 75-83.
4) Moreno Rosangel, Pujades G. Luis, Barbat H. Alex, Aparicio C. Angel (2004), Influence of Masonry Infill Walls on the Seismic Behaviour of Multi-Storey Waffle Slabs RC Buildings, 13th World Conference on Earthquake Engineering, Paper No. 209.
5) Tamboli H. R., Karadi U. N. (2012), Seismic Analysis of RC Frame Structure with and without Masonry Infill Walls, Indian Journal of Natural Sciences, ISSN: 0976 – 0997, Vol.3 / Issue 14/ October 2012.
6) Tan K.T. and Razak H. Abdul (2011): "Assessment of Risk to School Buildings Resulting from Distant Earthquakes", The Twelfth East Asia-Pasific Conference o Structural Engineering and Construction, Procedia Engineering 14(2011) 2196-2204.
7) Goel R. K. (2008), Evaluation of Current Nonlinear Static Procedures for Reinforced Concrete Buildings, The 14th World Conference on Earthquake Engineering, October 12- 17, 2008, Beijing, China.
8) Sattar S., Liel A. B. (2010), Seismic Performance of Reinforced Concrete Frame Structures with and without Masonry Infill Walls, 9th U.S. National and 10th Canadian Conference on Earthquake Engineering, Toronto, Canada, July 2010.
9) Tan K.T. and Razak H. Abdul (2011), Assessment of Risk to School Buildings Resulting from Distant Earthquakes, The Twelfth East Asia-Pasific Conference of Structural Engineering and Construction, Procedia Engineering 14(2011) 2196-2204.

3-Dimensional Finite Element Analysis of Piled Raft Under the Influence of Shallow Tunnel

Talukdar, P.[1],Goswami, D.[2]

[1]PG student, Department of Civil Engineering, Assam Engineering College,Jalukbari, Guwahati-781013, India.
[2]Associate Professor, Department of Civil Engineering, Assam Engineering College,Jalukbari, Guwahati-781013, India

ABSTRACT

This study aims to carry out to study the effect of shallow tunneling on the piled raft of a surface structure resting above it using a powerful finite element analysis software called PLAXIS 3D AE. The soil model considered in this study is Hardening soil model. A parametric study is being done first for the piled raft foundation by varying the position of tunneling below the existing structure. Based on the findings of the parametric study an attempt has been made to study the effect of tunneling on the pile, in terms of total displacement, skin friction, settlement and critical face pressure of tunnel.

Keywords: raft, piles,piled raft foundation, finite element analysis.

1. INTRODUCTION

Day by day competition is increasing for surface space, to fulfil the objective of sustainable development, use of subsurface space becomes very important. In heavily crowded areas, demand of public transportation is increasing day by day. But the overground space for construction of surface transportation mode decreases as a result of increased number of buildings and other structures above the ground. Also due to traffic congestion, the pollution have also increased to a significant extend. Owing to all these problems, requirement of underground tunnels for transportation becomes very important, as they provide effective means of transportation without disturbing the structures and natural habitats above the ground. The pollution above the ground surface also decreases significantly due to the underground tunnel transportation. Consequently, study of the effect of underground tunnel construction on the buildings above the ground and its settlement become very much important. This project mainly deals with the analysis of pile foundation under the influence of tunnel with the use of finite element analysis software plaxis-3d. For analysis purpose, a fully developed model was made and stimulated for various positions of tunnel with respect to the foundation of the building. Results were analysed to find the changes in the behaviour of pile in terms of displacement, skin friction, settlement etc. after thorough analysis of results of stimulation, it was found that pile foundation of building is influenced by tunnel when the tunnel is very close vicinity of pile and its influence is negligible if located far away from the structure. The distribution of internal forces induced by tunnel depends on the position of pile with respect to the tunnel horizontal axis. The critical position of tunnel is with a tip just below of the tunnel**.**

2. LITERATURE REVIEW

Brinkgreve R.B.J. et al (2003), studied the advancement of a tunnel boring machine in the ground. It was concluded that soil stiffness plays an important role in predicting the width of the settlement trough and consequently the influence on adjacent buildings. Huang X. and Schweiger H. F (2010) studied influence of deep excavations on existing tunnels in Shanghai using PLAXIS-GiD. The hardening soil constitutive model was used. Parameters studied were relative position of tunnel with respect to excavation, tunnel diameter, excavations dimensions and tunnel protection measures. Mroueh H. and Shahrour I. (2002) did analysis of the impact of construction of urban tunnels on adjacent pile foundations. It was carried out using an elastoplastic three-dimensional finite element modeling. Analysis was carried out for both single piles and groups of piles. Results of numerical simulations show that tunneling induces significant internal forces in adjacent piles. Analysis of the interaction between tunneling and a group of piles reveals a positive group effect with a high reduction of the internal forces in rear piles. Pornkasem Jongpradist et all.(October 2012) performed numerical simulations of geotechnical works in Bangkok subsoil using advanced soil models available in PLAXIS. Schweckendiek Timo(2007) studied structural reliability analysis of deep excavations using PLAXIS generic probabilistic toolbox called “Pro Box”, which performs reliability analysis automatically with output of PLAXIS. Stoel Van Der et all.(2007) studied risk management during

renovation of the new Rijksmuseum Amsterdam. The geotechnical design calculations are carried out by using the PLAXIS. Horizontal deformation of the sheet pile wall, horizontal and vertical deformations in a horizontal cross-section at surface level were determined from analysis.

3. PARAMETRIC STUDY

3.1 Geometry data and soil material properties

A soil model of 60m x 120 m x 50 m is created in PLAXIS 3D AE. A raft of size 7 m x 5 m and thickness 500 mm is modelled resting on the soil model. Six piles of diameter 1.5m and length 6m spaced at 3.5m and 4m are placed below the raft. The raft is modelled as a plate element and the piles as embedded beams. Hardening model is selected as the soil model. The material properties of the model are given in Table 1.

Property	Soil
Young's Modulus (kN/m^2)	38×10^3
Poisson's ratio	0.2
Unit weight (kN/m^3)	15.9
Angle of internal friction	32^0
Cohesion of soil (kN/m^2)	0.2

Table 1. Material Properties of the Model

3.2 Geometry data and building material properties

A G+2 storied building of 6m height is considered with a soil model of size 60 m x 120 m x 50 m and a raft foundation of size 7 m x 5 m in PLAXIS 3D AE. The material properties of the model are shown in Table 2.

Property	Concrete	Raft	Floor
Young's Modulus (kN/m^2)	40×10^6	30×10^6	30×10^6
Poisson's ratio	0.1	0.15	0.15
Unit weight (kN/m^3)	27	24	24
Shear Modulus	18.18×10^6	13.04×10^6	13.04×10^6

Table 2. Material Properties of the Structure

3.3 Geometry modeling of tunnel

A tunnel of diameter 6m and thickness 0.17m having jack pressure 634.5 kN/m^2, surface contraction 0.5, grout pressure 100 kN/m^2 and face pressure 90 kN/m^2.

Property	TBM	Beam	Column
Young's Modulus (kN/m^2)	250×10^6	31×10^6	30×10^6
Unit weight (kN/m^3)	250	24	24
Size	125×10^6	0.25x0.4	0.4x0.4

Table 3. Material Properties of the Structure

4. ANALYSIS OF PILED RAFT DUE TO TUNNELING

In this study 65 different cases of tunneling below the existing G+2 structure is considered.

4.1 Case 1 to Case 10

Tunneling at depth 15m from the top surface but at different horizontal distances from the center of the building. Variation of displacement on center and edge pile of the building is studied.

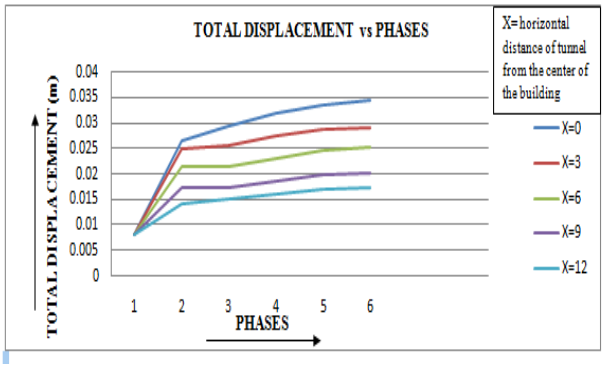

Figure 1. Displacement vs phases graph of middle pile

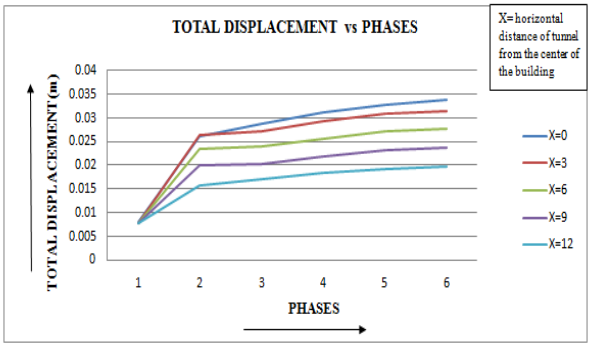

Figure 2. Displacement vs phases graph of edge pile

4.2 Case 11 to Case 20

Tunneling at different vertical depths from the top surface but vertically below the center of the building. Effect of tunneling on center and edge pile of the building is studied.

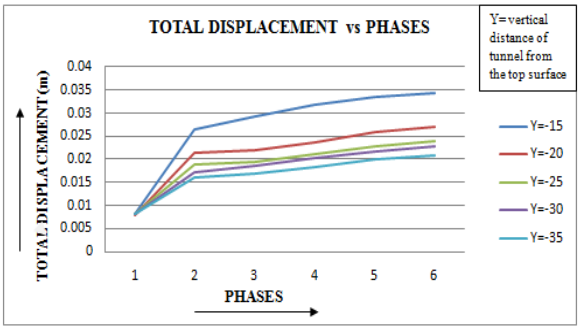

Figure 3. Displacement vs phases graph of middle pile

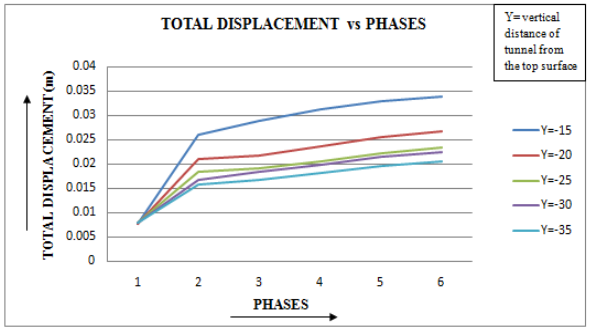

Figure 4. Displacement vs phases graph of edge pile

4.3 Case 21 to Case 30

Tunneling at depth 15m from the top surface but at different horizontal distances from the center of the building. Variation of skin friction with phases of center and edge pile of the building is studied.

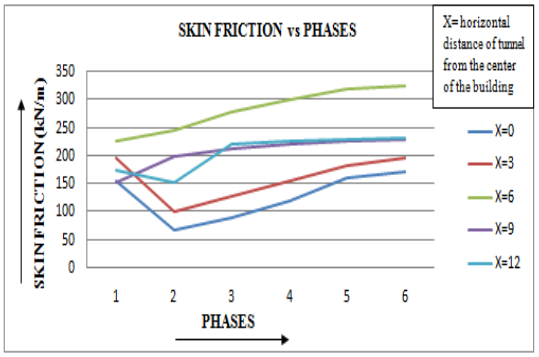

Figure 5. Skin friction vs phases graph of middle pile

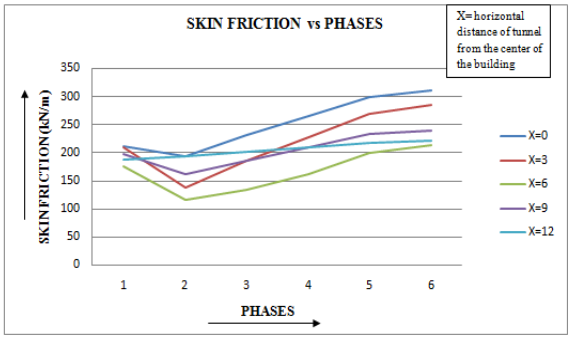

Figure 6. Skin friction vs phases graph of edge pile

4.4 Case 31 to Case 40

Tunneling at different vertical depths from the top surface but vertically below the center of the building. Effect of tunneling on center and edge pile of the building is studied.

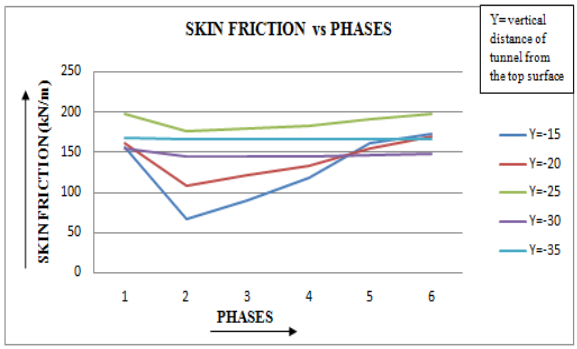

Figure 7. Skinfriction vs phases graph of middle pile

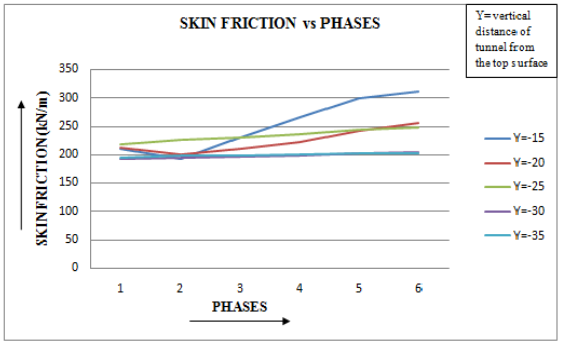

Figure 8. Skin friction vs phases graph of edge pile

4.5 Case 41 to Case 50

Tunneling at depth 15m from the top surface but at different horizontal distances from the center of the building. Variation of setttlement with phases of center and edge pile of the building is studied.

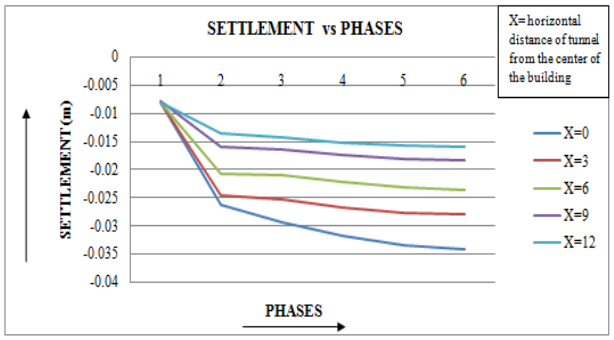

Figure 9. Settlement vs phases graph of middle pile

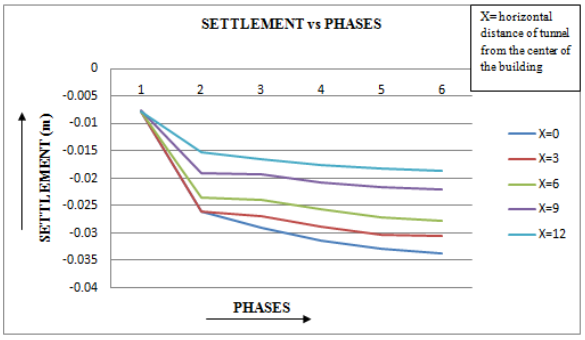

Figure 10. Settlement vs phases graph of edge pile

4.6 Case 51 to Case 60

Tunneling at different vertical depths from the top surface but vertically below the center of the building. Effect of tunneling on center and edge pile of the building is studied.

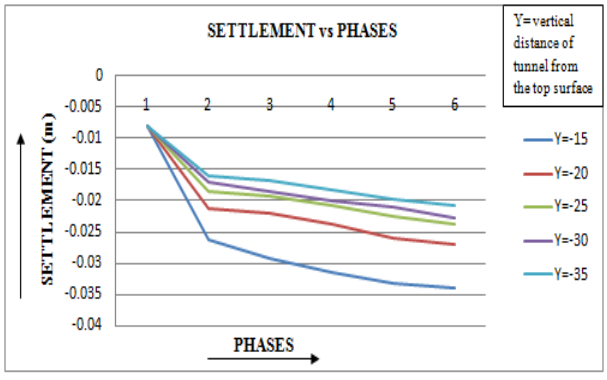

Figure 11. Settlement vs phases graph of middle pile

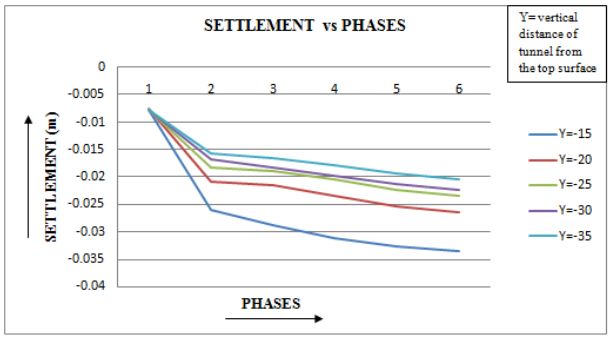

Figure 12. Settlement vs phases graph of edge pile

4.7 Case 61 to Case 65

Variation of face pressure required for tunneling at different vertical distance from center pile.

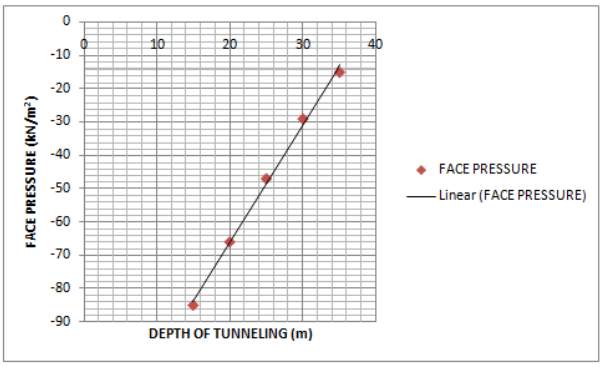

Figure 13. Face pressure vs depth of tunneling graph of center pile

5. FIGURES

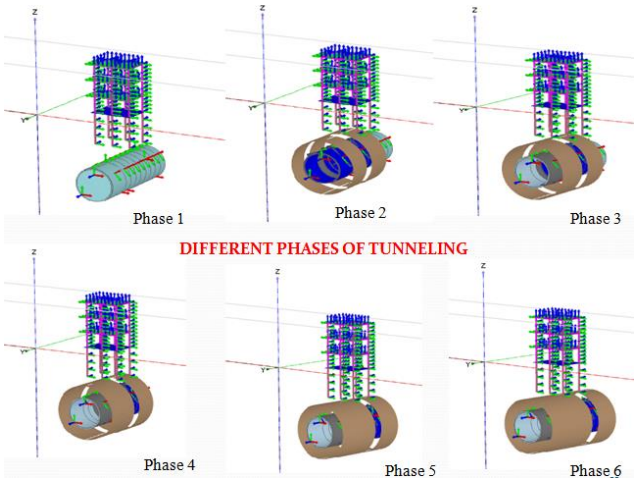

Fig. 14. Different Phases of Tunneling

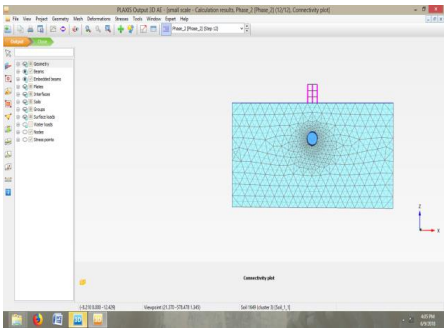

Fig. 15. Meshed Model

6. CONCLUSION

Pile foundation of building is influenced by tunnel only when tunnel is in very close vicinity of pile and its influence is negligible if located far away from the structure. The distribution of the tunnel induced internal forces strongly depends on the position of the pile tip with regards to the tunnel horizontal axis. The critical configuration corresponds to piles with a tip just below of the tunnel. when tunnel is located at various depths, the variation of total displacement with depth of pile depends upon position of tunnel and the tip of pile. The critical face pressure is tunnel decreases with increase in depth of tunneling. this is due to the arching effect of soil. The worst case of tunneling is when the tunnel passes through the center line of the existing building. The pile settlement is excessive in this case and so this case should be avoided.

REFERENCES

1) Akhaveissy A. H. (2010), "2D Numerical Analysis of Sao Paulo Tunnel", International Journal of Civil, Environmental, Structural, Construction and Architectural Engineering, Vol. 4, No. 3.
2) Brinkgreve R.B.J. et al (2003), "*The Influence of Tunnel Boring on Foundations and Buildings in Urban Areas – A Numerical Study*", Int. Workshop on Geotechnics of Soft Soils-Theory and Practice.
3) Chen S. L., Lee S. C., Wei Y. S. (2016), *"Numerical Analysis of Ground Surface Settlement Induced by Double-O Tube Shield Tunnelling"*, Journal of Performance of Constructed Facilities, ASCE, ISSN 0887-3828/04016012(10).
4) Huang X., Schweiger H. F.(2010) "*Study on influence of deep excavations on existing tunnels using PLAXIS-GiD*", Plaxis Professional, April 2010.
5) Kacar O. (2007), *"3D Finite Element Modelling of Surface Excavation and Loading over Existing Tunnels"*, Ms. Thesis, Middle East Technical University.
6) Keshuan M. (2008), *"Finite Element Analysis of Tunnel-Soil-Building Interaction Using Displacement Controlled Model"*, International Conference on Applied Computer and Applied Computational Science (ACACOS, 2008).
7) Moldovan A. R. (2012), *"Finite Element Modelling for Tunnelling Excavation"*, Acta Technica Napocensis: Civil Engineering & Architecture Vol. 55 No. 1.
8) Mroueh H. and Shahrour I. (2002), "*Three-dimensional finite element analysis of the interaction between tunnelling and pile foundations*", 'International Journal for Numerical and Analytical Methods in Geomechanics', 2002; 26:217–230.

A comparative study of raft and piled raft foundation using 3D finite element analysis

Choudhury, P.[1],Goswami, D.[2]

[1]PG student, Department of Civil Engineering, Assam Engineering College,Jalukbari, Guwahati-781013, India.
[2]Associate Professor, Department of Civil Engineering, Assam Engineering College,Jalukbari, Guwahati-781013, India

ABSTRACT

This study aims to carry out a comparative study for raft and piled raft foundation using a powerful finite element analysis software called PLAXIS 3D AE. A parametric study is being done first for the piled raft foundation by varying the parameters of raft and piles. Based on the findings of the parametric study an attempt has been made to suggest the most suitable type of foundation for a ten storied building resting on given soil conditions.

Keywords:raft, piles,piled raft foundation,finite element analysis

1. INTRODUCTION

In the conventional design approach, a raft is usually provided when the soil at a shallow depth has a low bearing capacity and the load from the superstructure is very high. The raft may not be able to withstand high stresses from the superstructure due to its large dimension, thus resulting in excessive settlement. The best option in this case is to provide piles under the raft in a systematic manner so that the settlement is under permissible limit. Such a composite foundation is called piled raft foundation. The load from the superstructure is shared because of the four interactions namely - raft and soil, pile and soil, raft and piles, pile and pile. As a result of these interactions the total and differential settlements experienced by the foundation are under permissible limits. Hence, an adequate design of piled raft foundation can lead to considerable economy without compromising the safety of the structure.Poulos (1991) has suggested that soil profiles consisting of stiff clay or dense sand are particularly favourable for piled raft foundation. On the other hand, he also suggested that soil profiles containing clay, loose soil or soil undergoing swelling movements are unfavourable for piled raft foundation.

2. LITERATURE REVIEW

Butterfield and Banerjee (1971) were the first to study the behavior of pile group in elastic half space continuum with rigid cap using Mindlin's solution. Sommer, Wittman and Ripper (1985) conducted a parametric study to study the variation of settlement in the piled raft foundation. Zhuang G.M. and Lee I.K. (1904) used a finite element method to understand the load sharing between the piles and raft. Cunha, Poulos and Small (2001) studied the influence of raft and pile characteristics on the design of piled raft foundation using a program called GARP6. Maharaj (2004) studied the influence of pile stiffness on the settlement of the piled raft system. Sharma, Vasanvala and Solanki (2011) modified the concept of piled raft by using short piles to reduce settlement at shallow depths and a cushion beneath the raft to redistribute the stresses. The analysis was carried out using a software called Midas GT. Joy and Hassan (2014) analyzed a ten storied building in STAAD PRO and the piled raft foundation was analyzed using PLAXIS 3D. They permuted the arrangement of piles and their diameter to study the effect on settlement of piled raft foundation.

3. PARAMETRIC STUDY

3.1 Geometry data and material properties

A soil model of 30 m x 30 m x 40 m is created in PLAXIS 3D AE having water table at the ground level. A raft of size 4 m x 4 m and thickness 300 mm is modelled resting on the soil model. Four Piles of diameter 500 mm and length 17 m spaced at 3 m are placed below the raft. The raft is modelled as a plate element and the piles as embedded beams. Mohr Coulomb is selected as the soil model. Point loads of 150 kN are applied at the corners spaced at 3m and a point load of 400 kN is applied at the centre. The material properties of the model are given in Table 1.

Table 1. Material Properties of the Model

Property	Soil	Raft	Piles
Young's Modulus (kN/m^2)	10×10^3	25×10^6	25×10^6
Poisson's ratio	0.4	0.15	0.15
Unit weight (kN/m^3)	18	25	25
Angle of internal friction	10^0	-	-
Cohesion of soil (kN/m^2)	10	-	-

3.2 Effect of raft thickness

Fig. 1. illustrates the variation of settlement with raft thickness which shows that with the increase in raft thickness settlement tends to decrease upto a particular raft thickness (500 mm) beyond which there is increase in settlement. This can be attributed to the fact that beyond a raft thickness of 500 mm self-weight of the raft increases which in turn increases the settlement.

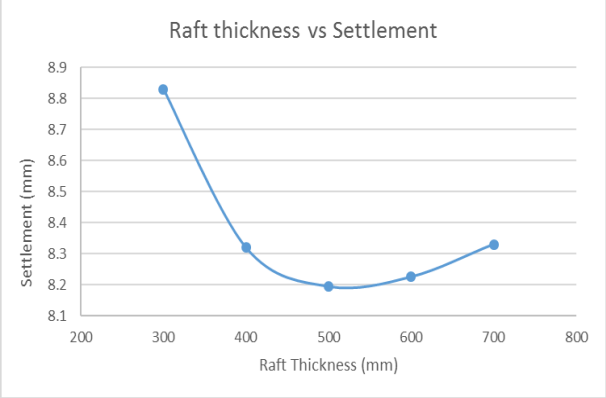

Fig. 1. Variation of Settlement with Raft thickness

3.3Effect of number of piles

Fig. 2. illustrates the variation of settlement with number of piles which shows that the settlement decreases with the increase in number of pilesupto a particular number and increases beyond it due to stress overlapping between the adjacent piles. In this case, the settlement is found to be minimum for five piles.

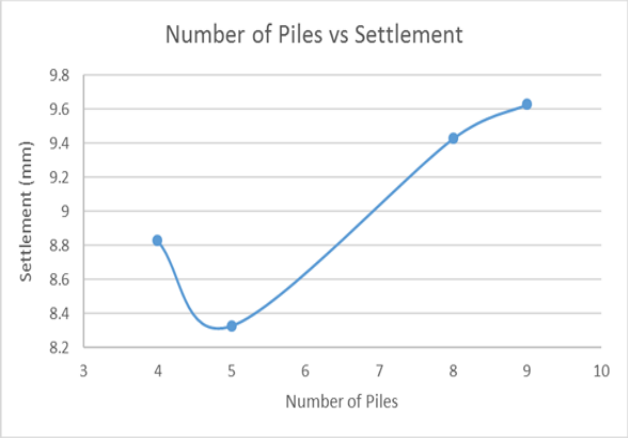

Fig. 2. Variation of Settlement with Number of Piles

3.4 Effect of spacing between piles

Fig. 3. illustrates the variation of settlement with spacing of piles which shows that the settlement decreases with the increase in spacing between piles.

3.5 Effect of length of piles

Fig. 4. illustrates the variation of settlement with length of piles which shows that the settlement decreases with the increase in length of piles

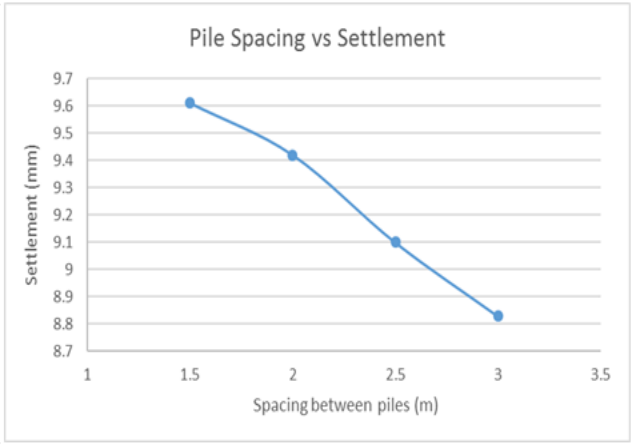

Fig. 3. Variation of Settlement with Number of Piles

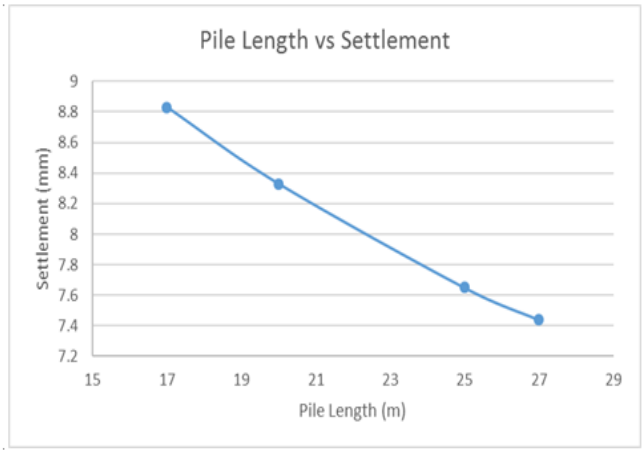

Fig. 4. Variation of Settlement with Pile Length

3.6 Effect of depth of raft from the ground level

Fig. 5. illustrates the variation of settlement with the variation of depth from the ground level which shows that the settlement decreases with the increase in depth from the ground level. This is because of lateral support from the surrounding soil.

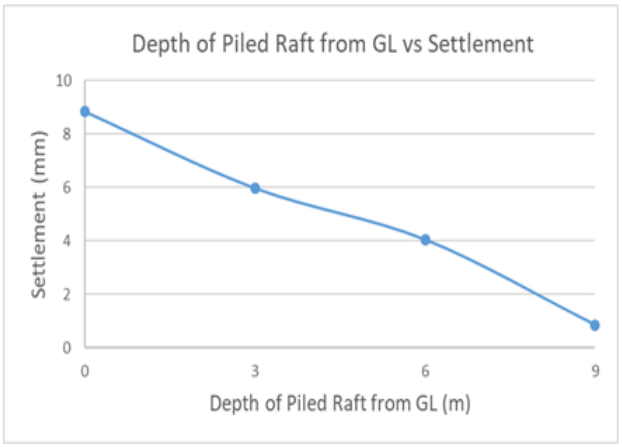

Fig. 5. Variation of Settlement with Depth from Ground

4. ANALYSIS OF A TEN STORIED BUILDING

A ten storied building of 30 m height is considered with a soil model of size 100 m x 100 m x 60 m and a raft foundation of size 15 m x 15 m in PLAXIS 3D AE. Based on the findings of the parametric study, three options are considered to bring the settlement of the raft foundation for the ten storied building under permissible limits. The three options are – increasing the thickness of raft foundation, increasing the depth of raft foundation from the ground level and providing a piled raft foundation. The material properties of the model are shown in Table 2.

Table 2. Material Properties of the Model

Property	Soil	Raft	Piles
Young's Modulus (kN/m^2)	7.5×10^3	25×10^6	25×10^6
Poisson's ratio	0.4	0.15	0.15
Unit weight (kN/m^3)	18	25	25
Angle of internal friction	20^0	-	-
Cohesion of soil (kN/m^2)	10	-	-

The cross sectional size of the beams and columns used in the building are 300 mm x 500 mm and 700 mm x 700 mm respectively. The thickness of the slab is considered as 120 mm. In addition to the self –weight of the members an additional surface live load of 5 kN/m^2 is applied across all the floors.

4.1 CASE I: Increasing the thickness of the raft

The thickness of raft is increased from 300 mm to 1000 mm. Fig. 6. illustrates the variation of maximum settlement with raft thickness which shows that with the increase in raft thickness settlement tends to decrease

upto a particular raft thickness beyond which there is increase in settlement. In this case, the lowest settlement is 90.85 mm for a raft thickness of 700 mm which is less than the permissible limit i.e. 75 mm.

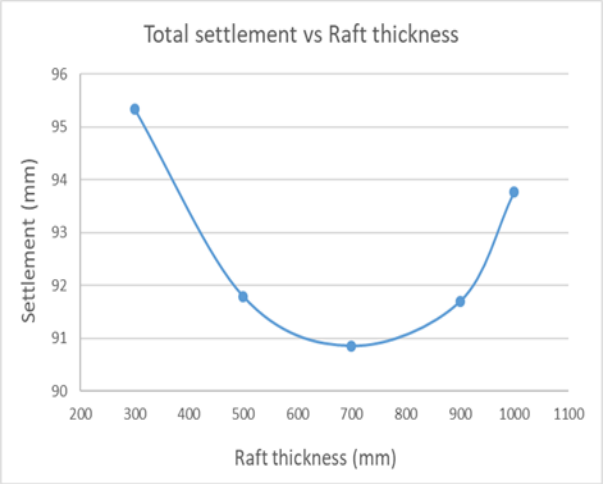

Fig. 6. Variation of Maximum Settlement with Raft thickness

The permissible differential settlement as per I.S. Code 1904-1986 is 0.0025 x L, where L is the centre-centre distance between the columns. The permissible differential settlement in this study turns out to be 16 mm. Fig. 7. illustrates the variation of differential settlement with raft thickness which shows that with the increase in raft thickness differential settlement tends to decrease. It can be observed that for a raft thickness of 900 mm the differential settlement is 14.39 mm which is below the permissible limit i.e. 16 mm.

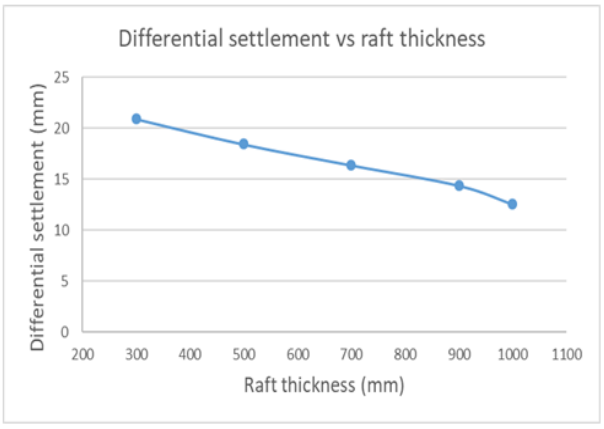

Fig. 7. Variation of Differential Settlement with Raft thickness

A cost analysis is being done for the raft foundation alone for a thickness of 700 mm as per the rates of Assam Public Works Department's Schedule of Rates 2013-14. The cost of construction for the raft foundation turns out to be Rs. 9,55,024.

4.2 CASE II: Increasing the depth of the raft from the ground level

The thickness of the raft is considered as 300 mm in this case at a depth of 0 m, 2 m, 4 m and 6 m from the ground level. Fig. 8. illustrates the variation of maximum settlement with depth of raft from the ground level which shows that with the increase in depth of raft from the ground level maximum settlement decreases. The maximum settlement is found to be 48.57 mm when the raft is at a depth of 6 m from the ground level.

Fig. 9. illustrates the variation of differential settlement with depth of raft from the ground level which shows that with the increase in depth of raft from the ground level differential settlement decreases. The differential settlement is found to be 3.73 mm when the raft is at a depth of 6 m from the ground level.

A cost analysis is being done for the raft foundation alone at a depth of 6 m from the ground level as per the rates of Assam Public Works Department's Schedule of Rates 2013-14. The cost of construction for the raft foundation turns out to be R.s. 4,99,831.

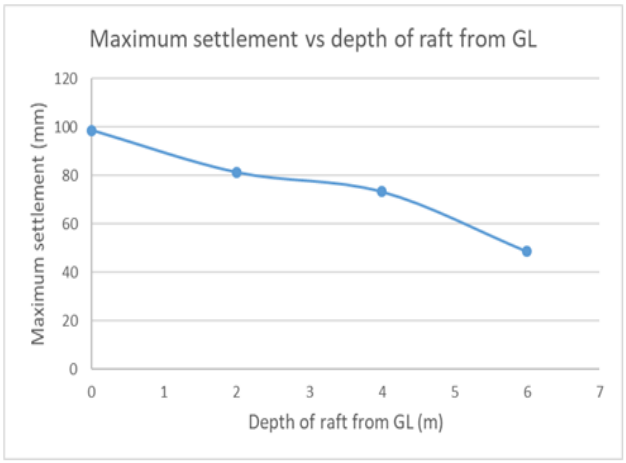

Fig. 8. Variation of Maximum Settlement with Depth of raft from the Ground Level

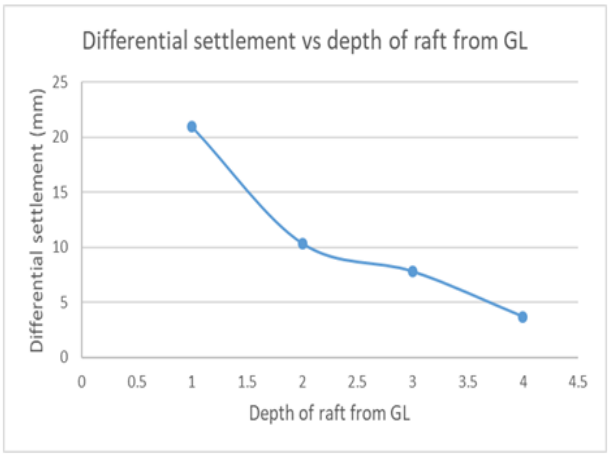

Fig. 9. Variation of Differential Settlement with Depth

of raft from the Ground Level

4.3 CASE III: Providing piled raft foundation

Four piles of 500 mm diameter are provided below the raft foundation with a spacing between the piles of 3 m.Fig. 10. illustrates the variation of maximum settlement with length of piles in a piled raft foundation which shows that with the increase in length of piles maximum settlement decreases. The maximum settlement is found to be less than the permissible limit (75 mm) for pile lengths of 15 m, 18 m and 20 m.

Fig. 11. illustrates the variation of differential settlement with pile length which shows that with the increase in length of piles differential settlement decreases.

A cost analysis is being done for the piled raft foundation alone for pile length of 18 m as per the rates of Assam Public Works Department's Schedule of Rates 2013-14. The cost of construction for the raft foundation turns out to be R.s. 4,94,975.

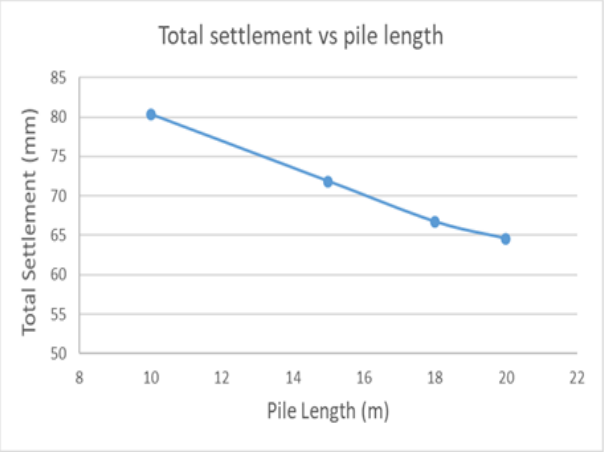

Fig. 10. Variation of Maximum Settlement with Length of Piles

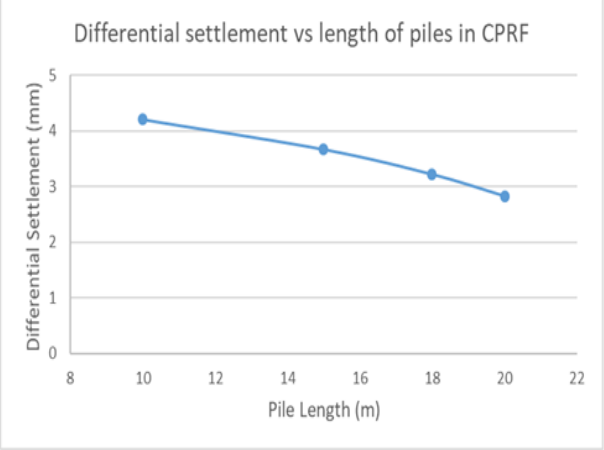

Fig. 10. Variation of Maximum Settlement with Length of Piles

5. CONCLUSION

On comparing all the three options for the foundation of the ten storied building, it can be seen that increasing the thickness of the raft is not a viable option as the maximum settlement exceeds the permissible limit and the cost of construction is also on the higher side. On the other hand increasing the depth of the raft from the ground level does keep the settlement values under permissible limits but there are many unseen expenses which are not accounted in this study. For example, the length of the columns gets increased beyond the ground level which will further add to the cost of construction. In addition to that, water below the ground level needs to be pumped out during the construction process. Hence, the most suitable option is to provide a piled raft foundation which keeps the settlement under permissible limits and is also the most economical option of the three.

REFERENCES

1) Butterfield, R. and Banerjee, P.K. (1971): The Problem of Pile Group-Pile Cap Interaction. Geotechmique, Vol. 21, Issue 2.
2) Cunha, R.P., Poulos, H.G., and Small, J.C. (2001): Investigation of Design Alternatives for a Piled Raft Case History, Journal of Geotechnical and Environmental Engineering, p.p. 635-641.
3) Joy, N. and Hassan, H. (2014): Study of Settlement Characteristics of Combined Pile Raft Foundation founded on Sand with various arrangements of Pile using Plaxis-3D, International Journal of Engineering Technology and Advanced Engineering, Vol. 4, Issue 10.
4) Maharaj, D.K. (2004): Three Dimensional Non-Linear Finite Analysis to Study the effect of Raft and Pile Stiffness on the Load-Settlement Behaviour of Piled Raft Foundation, The Electronic Journal of Geotechnical Engineering.
5) Poulos, H.G. (1991): Analysis of Piled Raft Foundations, Computer Methods and Advances in Geomechanics Journal, Vol. G2, No. 1, pp. 21-27.
6) Sharma, V.J., Vasanvala, S.A., and Solanki, C.H. (2001): Effect of Cushion on Composite Piled-Raft Foundation, Journal of Engineering Research and Studies, Vol. 2, Issue 4.
7) Sommer, H., Wittmann, P., and Ripper, P. (1985): Piled Raft Foundation of a Tall Building in Frankfurt Clay, Proc. 11 ICSMFE, pp. 2253-2257.
8) Zhuang, G., Lee, I., and Zhao, X. (1991): Interactive Analysis of Behaviour of Raft-Pile Foundations, Proc. Geo-Coast'91, pp. 759-764

Retrofitting solution for open ground storey building with strategically built masonry infill

Borpatragohain, H.S.[1];Sengupta, P.[2]; Pathak, J.[3]

[1] Project Assistant, Department of Civil Engineering, Assam Engineering College,Guwahati-781013, India.
[2]Assistant Engineer (Highway), LEA Associates South Asia Pvt.Ltd.,Guwahati-781006, India.
[3]Professor, Department of Civil Engineering, Assam Engineering College, Guwahati-781013, India.

ABSTRACT

Guwahati being a rapidly growing city, the demand of multi-storied buildings with open ground storey to accommodate parking has been increasing over last decade.Many such buildings were built during the last decade and a large stock of such buildings are found to be vulnerable to earthquake with soft ground storey. The open ground storey results dramatic change in lateral stiffness of the buildings with much stiffer upper storey compared to the ground storey. Though multi-storied buildings with open ground storey are inherently vulnerable to severe damage or even collapse during earthquakes, their construction is still largely practiced. In order to overcome the weaker open ground storey, a study has been carried out to provide a retrofitting solution using masonry infill walls instrategic location, without intervening or affecting the parking and increasing the global lateral stiffness of the structural system by providing in-plane shear stiffness in open panels with masonry. Nonlinear static analysis is carried out on the representative models their seismic performance is evaluated. It has been observed that, strategically placed masonry infill walls improve the stiffness distribution pattern to a large extent and the capacity of the structure is also enhanced substantially reducing the vulnerability of such open ground storey structures.

Keywords: open ground storey, seismic, lateral stiffness, retrofitting.

1. INTRODUCTION

Theadvent of urbanization indeveloping countries has led to the upsurge of several multi-storied buildings. The housing demand for the ever-increasing population density in the city of Guwahati is fulfilled by these multi-storied apartment buildings. Owing to high cost of land, small plot areas, the trend of Open Ground Storey (OGS), is an unavoidable feature. These types of buildings behave as an inverted pendulum, translating back and forth, in the event of an earthquake. The columns in the open ground storey are highly susceptible to severe damage due to large inter-storey drifts and may often lead to collapse when displacement demand is high. Several earthquakes in the past (1999 Turkey, 1999 Taiwan, 2001 Bhuj and 2003 Algeria) has shown the consistent weak performances of these buildings.

An attempt has been made in this paper to reduce the vulnerability of these existing open ground storied buildings by introducing masonry infills at strategic locations in the ground level, as a retrofitting measure.

2. LITERATURE REVIEW

Masonry infills are synonymous with RC framed buildings, all over the world. They are used to fill in the voids between vertical and horizontal resisting members. However, dubbed as non-structural elements, they are never designed nor their response is considered in computation of lateral stiffness of the structure. Earlier studies [1,2] concluded that, the presence of infills leads to a decrease in shear force in the columns, as “non-structural” infills takes part in resistance to seismic forces. Murty and Jain [3] carried out experimental studies to understand the effect of masonry infills on RC frame models. They found infills to have a very beneficial influence on the building, as it increases its strength, stiffness, overall ductility and energy dissipation. Furthermore, the deformation and ductility demand was seen to have decreased. However, they also coined out the detrimental effects of infills, such as soft storey and torsion, which are

of great concern and needs to be addressed with expertise.

Various researchers explained the reduction in lateral stiffness of infilled frames due to the presence of openings. Benjamin and Williams (1958), Mallick and Garg (1971), Ginnakus et al. (1987) showed the reduction to be 70-80% for an opening percentage of 20-30%. Asteris (2003)

Indian Code of Practice 1893-2002 [5] provides two formulae for computation of time period, for the case of bare RC frame and a RC frame with infills present. However, it has been seen that, in most of the cases the normalized spectral acceleration in both these scenarios differ only by small margins. Hence, there is very less change in the lateral force pattern in both the cases. In reality, however, the situation is quite different, as the displacement demand in the ground floor is large, which is often not met.

The need for accurate modeling of masonry infills lead to numerous experimental and analytical studies. Polyakov [6] was the first in replacing infills with an equivalent diagonal pin-jointed strut in steel frame. Smith [7] stressed on modeling infills as equivalent struts, considering elastic theory and proposed that, the effective width of the strut should be a function of infill stiffness with respect to that of the bounding frame. Stafford Smith [8] developed some empirical curves to relate stiffness parameters to effective width of a diagonal strut. Mainstone (1971) [9] proposed an empirical relation between effective width of strut and Smith‟s stiffness parameter. Pauley and Priestly (1992) [10] recommended a width of 0.25 times the diagonal length for modeling of equivalent concentric diagonal struts. Later on, Smith and his colleagues based on a experimental study conducted by steel infilled frames, reported that the width of the masonry infill strut was related to infill panel relative stiffness parameter and which includes modulus of elasticity of concrete and masonry respectively to estimate the width of the masonry infill strut.

The literature review establishes infill as vital structural elements providing lateral resistance to any frame, and absence of infills at any level renders a soft storey condition to a structure. Precisely, at that location, the structural elements (columns) fail, under seismic loading. The current research therefore, attempts in utilizing the lateral strength of infill in reducing seismic

[4] concluded that, the case of an infilled frame with soft ground storey could lead to higher shear forces in the columns as compared to the bare frame analysis. Reconnaissance study of the Bhuj earthquake by EERI credited the soft storey at ground level among the major factors to have triggered mass destruction in terms of lives and property.

vulnerability of open ground storey building in Guwahati city.

3. METHODOLOGY

3.1 Structural Modelling

A Reinforced Concrete (RC) frame with 3 bays and 4 stories (G+3) representing the most common practice of buildings in Guwahati city is considered. The frame is designed as weak column-strong beam frame system to reflect the current design procedure being practiced and adopted by designers all over India. The present study utilizes SAP2000 finite element program to for carrying out the non-linear static analysis of the building model. The beams and columns section material properties are considered as shown in Table 1.

Material non-linearity in RC members are incorporated in the elements at probable concentrated locations known as plastic hinges. It is calculated by using the equation given which is suggested by Paulay and Priestley (1992), where, L is the effective length of the member in m (taken at the point of contraflexure from the end), $d_b$is the diameter of longitudinal reinforcement in m, and $f_y$is yield stress of longitudinal reinforcement in MPa. Plastic hinges (only flexural) are assumed to form at a distance of $l_p/2$ from the face of beams and columns.

$$l_p = 0.08L + 0.022d_bf_y(\text{in m})$$

Material	Type	Strength (N/mm^2)	Elastic Modulus (N/mm^2)	Poisson's Ratio	Weight density (kN/m^3)
Concrete	Un-confined	20	22360	0.2	25
Rebar	HYSD	415 (f_{ye}=450)	200000	0.3	77

Table 1. Material properties considered in building frame model

3.2 Nonlinear Static (Pushover) Analysis

For the purpose of the study at first, nonlinear static (pushover) analysis of bare frame model and open ground storey model is carried out. The nonlinear static procedure normally called pushover analysis is a technique in which a computer model of a structure is subjected to a predetermined lateral load pattern (as shown in Fig. 1(a), which approximately represents the relative inertia forces generated by earthquakes at locations of substantial mass. The intensity of the lateral loading is increased, i.e., the structure is 'pushed', and the sequence of cracks, yielding, plastic hinge formations,and the load at which failure of the various structural components occurs is recorded as function of the increasing lateral load. This incremental process continues until a predetermined displacement limit. The outcome of the analysis of the structure is a base shear – roof displacement diagram or capacity curve of the structure (Fig. 1b). This capacity curve provides valuable information about the response of the structure because it approximates how it will behave after exceeding its elastic limit. During the inelastic stage, the system experiences a loss of stiffness and strength and a change in its vibration period.

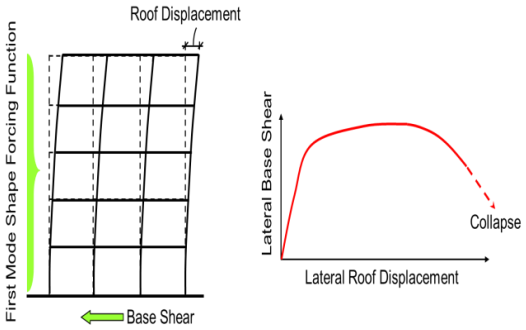

(a) (b)

Fig. 1(a) Pushover methodology for buildings based on first mode shape forcing function, (b) Pushover curve: lateral base shear force vs. lateral roof displacement.

Case I (Bare Frame): Building modeled as bare frame with wall loads taken as uniformly distributedloads and slabs (125mm thickness) modeled as per IS 875 (Part I & II) and IS 1893:2000. The thickness of the wall was taken as 5 inches (125 mm) as per the common practice in Guwahati city; Mander's confined model was used for defining beam and column sections. Diaphragms were assigned at each level.

Case II (Open Ground Storey): Infill in the upper stories was modeled as equivalent concentricdiagonal pin-jointed compression struts. Struts were placed in locations, where the openings (in form of doors, windows, ventilations) were less than 30%. The plan and sectional detailed properties are described in figure 2.

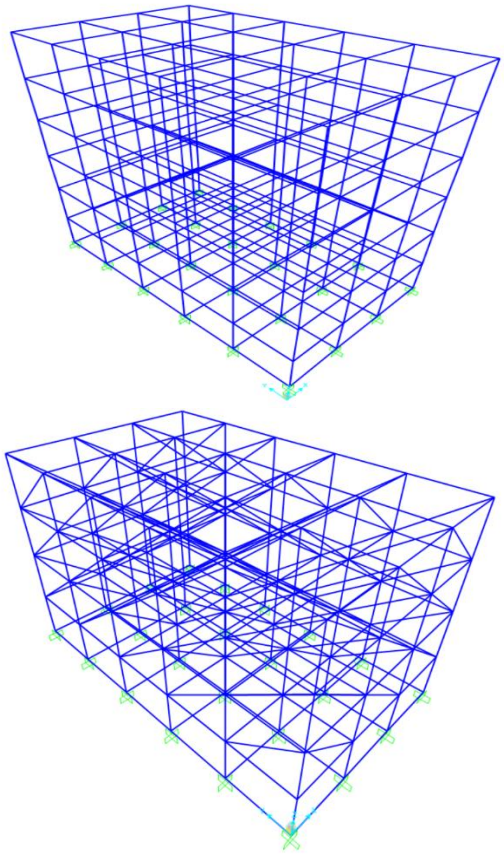

Bare Frame Model &Open Ground Storey Model

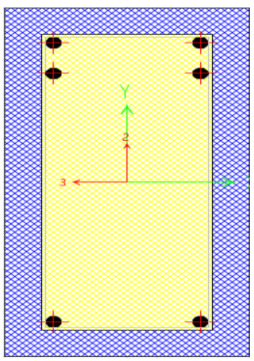

Beam Cross-Section

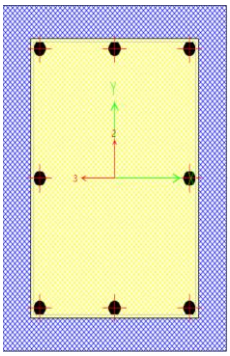

Column Cross-Section

Fig. 2 Plan and detailed sectional properties of the structure.

Modelling of Equivalent Strut:

The properties of the strut material have been derived from the formula stated by Smith BS, Carter C (A method for analysis for infilled frames)

$$\lambda_h = h\left[\frac{E_m t_m \sin 2\theta}{4E_c I_c h_m}\right]^{0.25} \quad (1)$$

where λ_h = width of strut; h= clear height of column; Ec and Em represents modulus of elasticity of concrete and masonry respectively; Ic represents the moment of inertia of column; h_m and t_m are the height and thickness of the infill wall respectively and θ is the angle between the horizontal and the panel diagonal

$$\frac{w_s}{l_d} = 0.175\lambda_h^{-0.4} \quad (2)$$

Here, w_s is the width of the strut and l_d is the diagonal length.

The material properties are given in table 2.

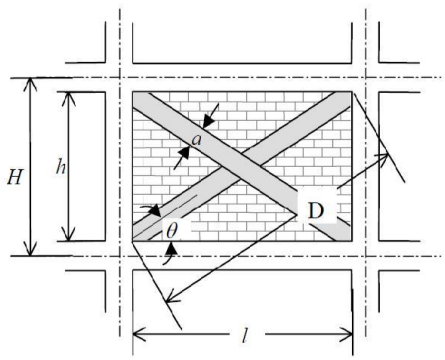

Fig. 3 Method - designing equivalent strut.

INFILL MATERIAL PROPERTIES	VALUES
Compressive Strength	4.63 MPa
Modulus of Elasticity	2200 MPa
Shear Modulus	1018 MPa
Thermal Coefficient	0.0000081/·C
Poissons Ratio	0.2

Table 2. Properties of Infill Masonry Wall

Analytical Result: It is observed that though the peak or ultimate strength of the bare and open ground storey buildings are almost similar in both X and Y directions (Fig 4(a) & (b)), the failure modes for the two buildings are completely different. The damage in bare frame building is found to be very well distributed in different members in all the stories. Therefore, though the lateral load carrying capacity of the bare frame building reduced significantly with incresing lateral drift, complete collapse of the building is not observed. Whereas in case of Open Ground Storey building, the damage is concentrated only in the ground storey columns resulting in complete collpase of the buidling due to failure of the ground storey columns. This contrasting behaviour in the two building typologies is observed along both the directions.

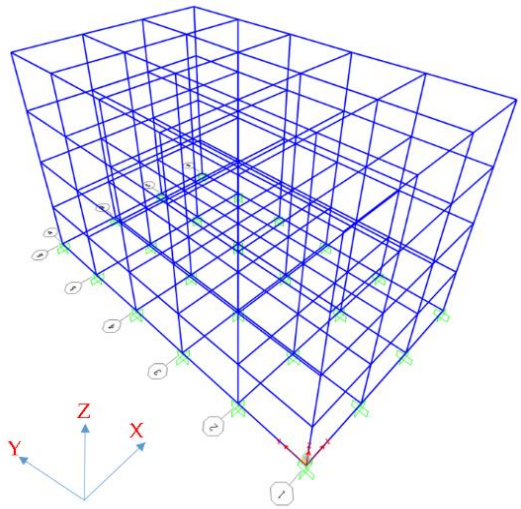

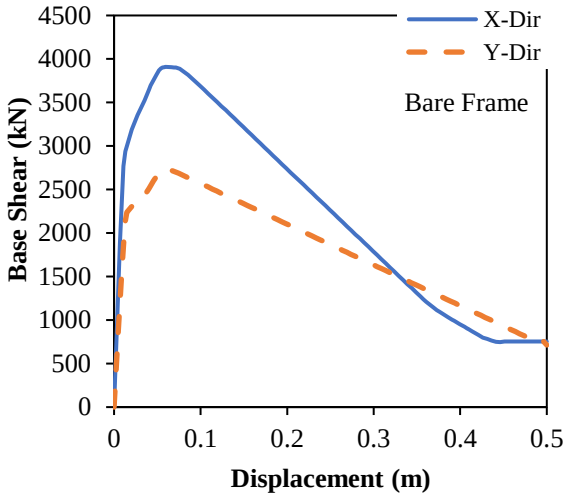

(a)

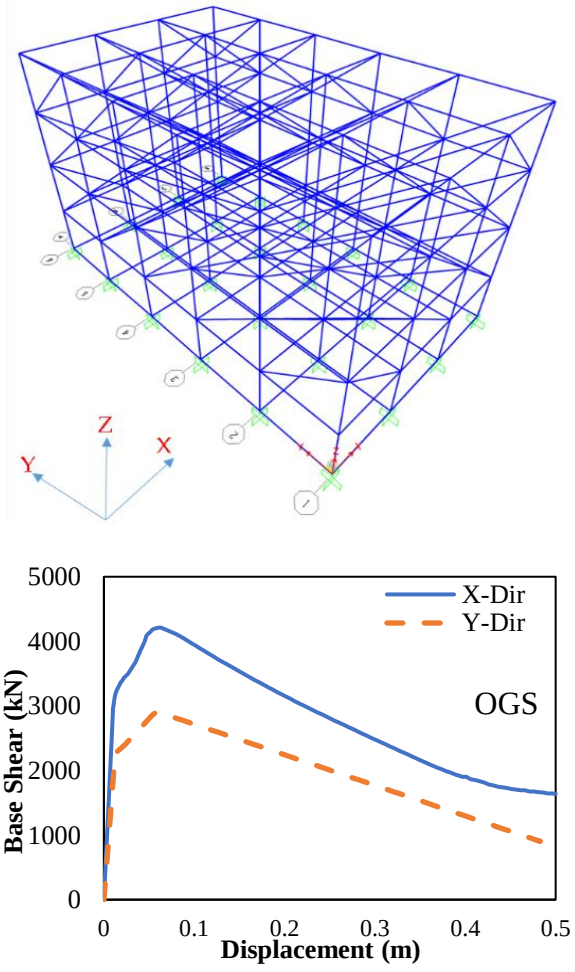

(b)

Fig. 4 3D view and the corresponding pushover curve in X and Y directions for (a) bare frame building, (b) Open Ground Storey frame building.

3.3 Strengthening Scheme: Addition of Strategically Built Masonry Infill Walls in Open Ground Storey

	Natural Period of Vibration (sec)					
	Bare	OGS	Fully Infill	Exterior Infill	Central Open Infill	Corner Infill
X	0.46	0.53	0.29	0.37	0.39	0.39
Y	0.58	0.65	0.29	0.36	0.38	0.45

Table 3 Natural period of vibration of different configurations of buildings

Infill walls provide an energy dissipation mechanismin structures subjected to the earthquake provided weak stories are avoided. This is a commonly adopted strengthening scheme for open first storey frames in which masonry infill walls are provided in the open ground storey also in different patterns as shown in Fig. 3, and all RC members are designed for regular design seismic forces. Fig. 5 shows plan of the (3×5) bay, 4 storied OGS building provided with masonry infills in different configurations at strategic locations. Self-weight, stiffness, and strength of infill walls were considered in all the stories. Table 3 shows the natural period of vibration of the OGS buildings retrofitted with masonry infill walls in the ground storey in comparison to bare and OGS buildings. Results of the pushover analyses in the form of pushover curves or the capacity curves for all the possibilities of placement of masonry infill walls in the open ground storey are shown in Fig. 6.

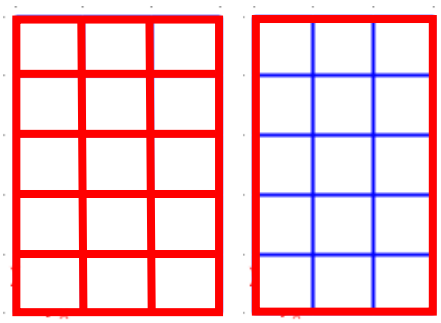

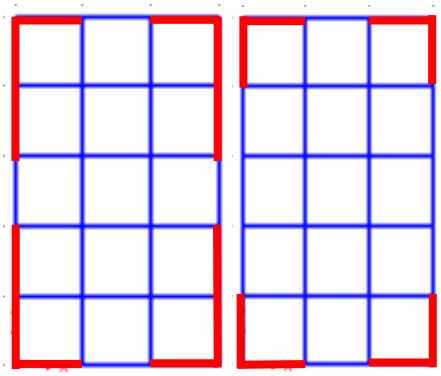

Fig. 5 Building plan-showing placement of infills at different locations in ground storey of the OGS building (Fully Infill, Exterior Infill, Central Open Infill, Corner Infill).

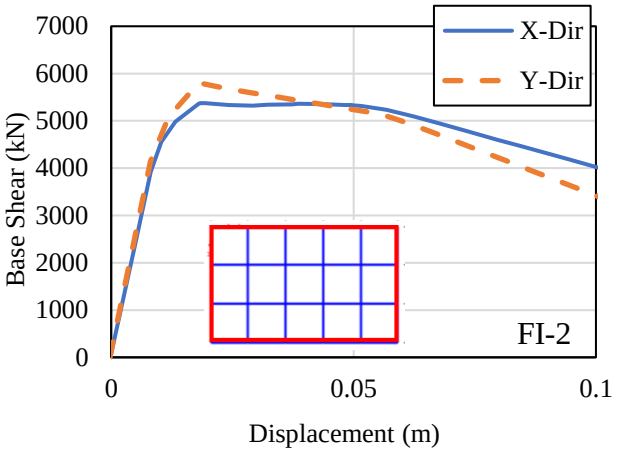

(b)

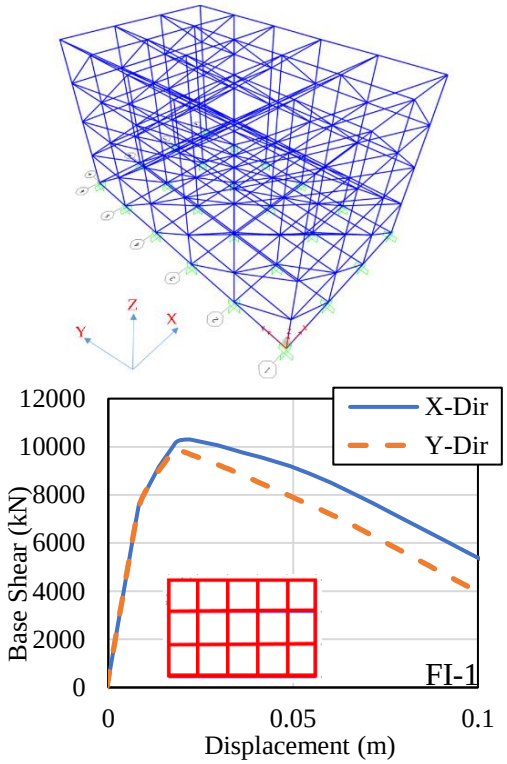

(a)

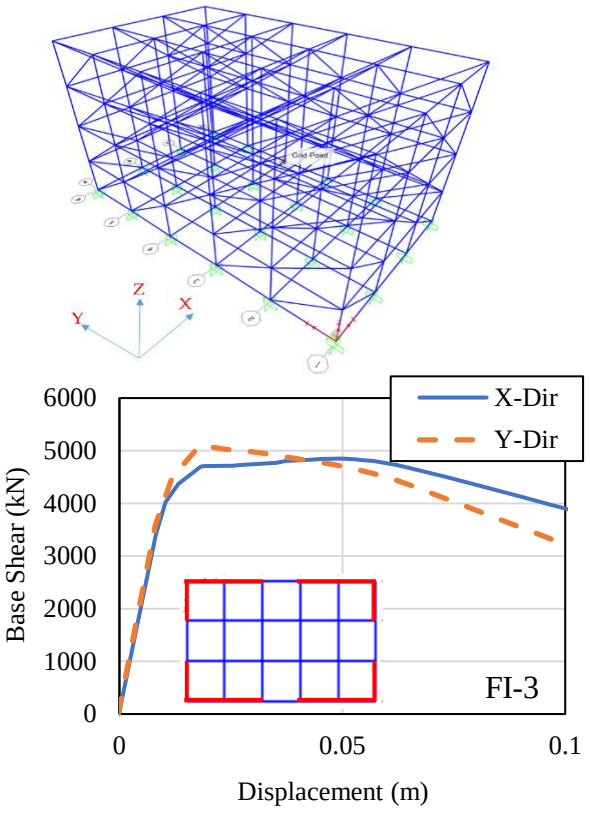

(c)

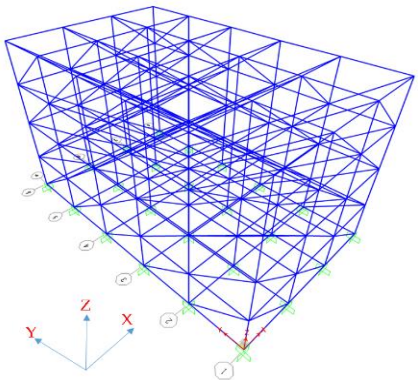

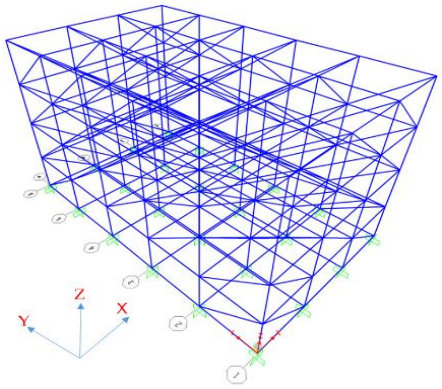

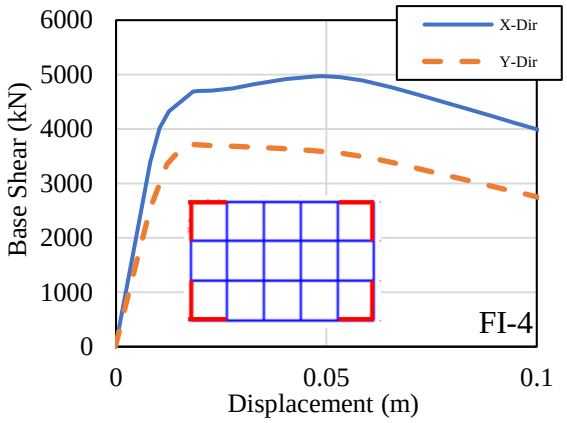

(d)

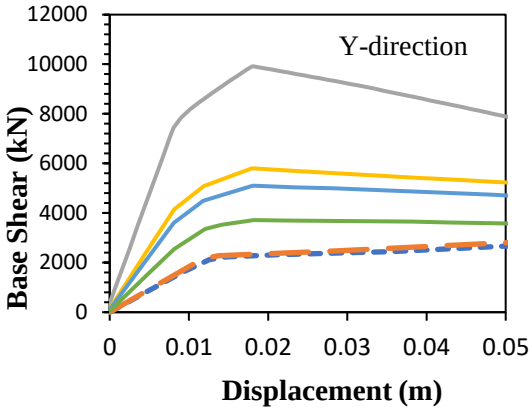

Fig. 6 3D Models for retrofitted OGS building and the corresponding pushover curve for (a) fully infill model, (b) exterior infill model, (c) central open infill model, (d) corner infill model.

Fig. 7 Comparative performance assessment of the 3D models for retrofitted OGS building.

4. RESULTS AND DISCUSSION

The comparative performance assessment of the OGS building retrofitted with additional infill walls in the ground storey is carried out in Fig. 7. It follows that buildings with masonry infill walls in any configuration have a lateral strength significantly higher than both the bare and the OGS building. Further, a fully infilled building shows the highest peak strength in terms of base shear.

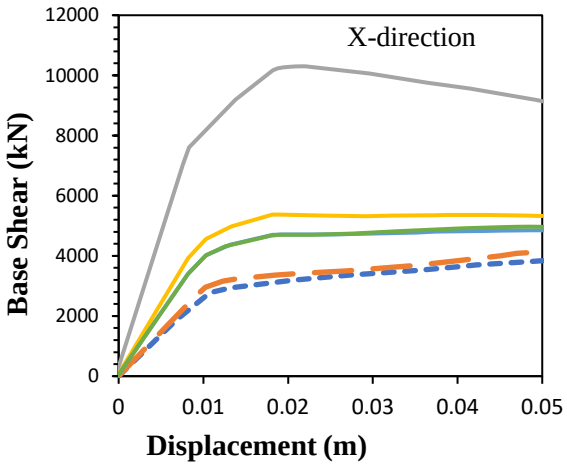

The non-linear static pushover analysis for the existing building showed a considerable increase in the lateral strength of the building with masonry infill as structural element. It has been observed that, for a given value of roof displacement, calculated horizontal base force is more for open ground storey (with masonry infill in upper levels) condition than bare frame condition. This establishes masonry infill as vital structural element contributing to lateral stiffness. However, on introducing masonry infill as retrofitting element at strategic locations in ground level, there is further increase in the horizontal base shear, which justifies the strategic introduction of masonry infill given location at ground storey.

5. CONCLUSION

The rapidly growing population in the Guwahati city has considerably increased the demand for housing in form of multi-storey apartments. The most of these buildings in Guwahati city constructed in the last decade have open ground storey as parking, which renders a soft ground storey condition. Most of these buildings are designed as bare frame without considering the masonry infill as structural elements. The study explored the opportunity to make this large mid rise building stock less vulnerable to earthquake by introducing a cost effective and quicker retrofitting solution in the form of masonry infill walls in the open ground storey at strategic locations. The study was carried out on few typical idealized building models and then

expanded to the analysis of an existing G+3 storied building in Guwahati. The results from the study is encouraging and has been found that, introduction of masonry infills at strategic locations at the ground level, enhances the performance of the structure in terms of increased lateral stiffness/resistance.

REFERENCES

1. Tassios, T. P. (1984), Masonry infill and R. C. walls ~ An invited state-of-the-art report.Proc., 3rd Int. Symp. on Wall Structures, Warsaw, Poland.
2. Murty, C.V., and Jain, S. K., (2000, Jan-Feb) "Beneficial Influence of Masonry Infill Walls on Seismic Performance of RC Frame Buildings", Proceedings of the Twelfth World Conference on Earthquake Engineering, held at Auckland, New Zealand, Paper No. 1790.
3. Asteris, P. G. (2003, August) "Lateral Stiffness of Brick Masonry Infilled Plane Frames," Journal of Structural Engineering, ASCE, 1071-1079.
4. Polyakov, S. V. (1960) "On the interaction between masonry filler walls and enclosing frame when loaded in plane of the wall," Earthquake Engineering, Earthquake Research Institute, San Francisco.
5. Smith, B.S. (1962)," Lateral Stiffness of Infilled Frames," Journal of Structural Division, Proc. of ASCE, 114, 183-199.
6. Smith, B., and C. Carter, (1969) "A Method of Analysis for Infilled Frames," Proceedings of the Institution of Civil Engineers, Vol. 44.
7. Mainstone,R.J. (1971) "On the stiffness and strength of infilled frames," Proc. of the ICE, 57-90.
8. Paulay, T. and Priestley,M.J. (1992)"Seismic Design of Concrete and Masonry Buildings," John Wiley & Sons Inc., New York, USA.
9. Bureau of Indian Standards (2002), "Indian Standard Criteria for Earthquake Resistant Design of Structures", New Delhi, India
10. Bureau of Indian Standards (1987), "Code of Practice of Design Loads (Other than Earthquake) Part I & II", New Delhi, India.

Sustainable Infrastructure

Sustainable Water Resources Development

Development of rainfall runoff model using cubic polynomial regression for Brahmaputra river basin, at Pandu location, Assam.

Borah, P. [1], Borah, T. [2]

[1] PG Student, Civil Engineering Department, Assam Engineering College, Guwahati, 781013, India.
[2] Associate Professor, Civil Engineering Department, Assam Engineering College, Jalukbari, Guwahati, 781013, India.

ABSTRACT

This study presents the development of rainfall runoff model by using cubic polynomial regression and it is compared with simple linear regression at Brahmaputra river basin at Pandu Location, Assam. The Brahmaputra watershed at Pandu area, Guwahati (42000 km^2) is divided into several hydrologic response units (HRU_S) that consist of homogeneous land use, topographical and soil characteristics. The objective of such models is to estimate the amount of runoff from the catchment with the help of Simple Linear and cubic Polynomial regression analysis and to studied comparison of predicted runoff of linear and cubic polynomial regression model with observed data. By studying the regression analysis, the Cubic Polynomial regression analysis produce the best predictions for this study area. All the calculations and graphs are prepared by using M.S. Excel for linear and cubic polynomial regression. In this study the average monthly rainfall data of 1993 to 2002 is considered as an input and on the basis of that, comparison is made for the observed discharged data which are used in Linear and Cubic Polynomial regression analysis. In this study, R^2 is considered as a goodness of fit in simple linear, and cubic polynomial regression model. Based on the results of the analysis it can be concluded that cubic Polynomial regression model is better than the Simple Linear regression. The values of co-efficient of determination (R^2) in simple linear and cubic Polynomial regression are 0.76, 0.69, 0.69, 0.60, 0.53, 0.51, 0.65, 0.70, 0.39, 0.58 and 0.76, 0.85, 0.81, 0.86, 0.68, 0.53, 0.85, 0.85, 0.66, 0.605 for the 10 years of 1993,1994, 1995, 1996, 1997, 1998, 1999, 2000, 2001 and 2002 respectively.

Keywords: regression analysis, linear regression, polynomial regression, co-efficient of determination

1. INTRODUCTION

Watershed management is an adaptive, comprehensive, integrated multi-resource management planning process that seeks to balance healthy ecological, economic, and cultural or social conditions within a watershed. Watershed management serves to integrate planning for land and water; it takes into account both ground and surface water flow, recognizing and planning for the interaction of water, plants, animals and human land use found within the physical boundaries of watershed.

Runoff from rainwater or snowmelt can contribute significant amounts of pollution into the lake or river. Watershed management helps to control pollution of water and other natural resources in the watershed by identifying the different kinds of pollution present in the watershed and how those pollutants are transported, and recommending ways to reduce or eliminate those pollution sources.

Rainfall-Runoff modelling is one of the most classical applications of hydrology. It has the purpose of simulating the peak river flow or the hydrograph induced by and observed or a hypothetical rainfall forcing. Rainfall-runoff models may include other input variables like temperature, information on the catchment or others. Within the context of this subject, we are studying rainfall-runoff models with the purpose of producing estimates of peak river flow, simulation of flood hydrographs or simulation of synthetic river flows in general, even for extended periods, for example for setting up water resources management strategies. Therefore, rainfall-runoff modelling is a cross cutting topic over several of the major issue this subject is focusing on. Rainfall-runoff models describe a portion of the water cycle and therefore the movement of a fluid, water and therefore they are explicitly or implicitly based on the laws of physics, and in particular on the principles of conservation of mass, conservation of energy and conservation of momentum. Depending on their complexity, models can also simulate the dynamics of water quality, ecosystems, and other dynamical systems related to water, therefore embedding laws of chemistry, ecology, social sciences and so forth.

Rainfall-runoff models can be classified within

several different categories. They can distinguish between event-based and continuous-simulation models, black-box versus conceptual versus process-based models, lumped versus distributed models, and several others. It is important to note that the above classifications are not rigid-sometimes a model cannot be unequivocally assigned to one category. We will treat rainfall-runoff models by taking into consideration models of increasing complexity.

2 REGRESSION ANALYSIS

In statistical modelling, regression analysis is a set of statistical processes for estimating the relationships among variables. It includes many techniques for modelling and analyzing several variables, when the focus is on the relationship between a dependent variable and one or more independent variables (or 'predictors'). Most commonly, regression analysis estimates the conditional expectation of the dependent variable given the independent variables – that is, the average value of the dependent variable when the independent variables are fixed. Less commonly, the focus is on a quantile, or other location parameter of the conditional distribution of the dependent variable given the independent variables. In all cases, a function of the independent variables called the regression function is to be estimated. In regression analysis, it is also of interest to characterize the variation of the dependent variable around the prediction of the regression function using a probability distribution. Regression analysis is widely used for prediction and forecasting, where its use has substantial overlap with the field of machine learning. Regression analysis is also used to understand which among the independent variables are related to the dependent variable, and to explore the forms of these relationships.

3. STUDY AREA

Brahmaputra is the one among the mightiest rivers of Asia. It is a transboundary river. River Brahmaputra is called Yarlung Transpo in Tibet. The Brahmaputra Valley has an average width of about 80 km. The main river of the valley, Brahmaputra is one of the largest rivers in the world and rank fifth with respect to its average discharge. The river originates from the Kailash ranges of Himalayas at an elevation of 5300 m after flowing through Tibet it enters India through Arunachal Pradesh and flows through Assam and Bangladesh before it joins Bay of Bengal. The catchments area of Brahmaputra in Tibet is 2,93,000 Sq. Km. in India and Bhutan is 2,40,000 Sq. Km. and in Bangladesh is 47000 Sq. Km. The Brahmaputra basin extends over an area of 5,80,000 Sq. Km. up to its confluence within Bangladesh. The maximum discharge of Brahmaputra at Pandu near Guwahati was recorded as 72,779 cumec on 23.08.62 and minimum discharge was recorded as 1757 cumec on 22.02.63. The average annual discharge is about 20,000 cumec and average dry season discharge is 4,420 cumec. The Water resources Department, Government of Assam established two gauge and discharge observation sites one at Pandu (near Guwahati, continuing) and the other at Bechamara (now discontinued). The chainage from Indo Bangladesh Border is 205 km at Pandu, near Guwahati. In this study, Pandu site has taken as a gauge and observation site. The watershed area extends from 25^0 N to 27^0 N latitude and 92^0E to 94^0E longitude and covers an area of 42000 km^2.

4. DATA COLLECTION

I. Monthly Rainfall data.
II. Monthly Runoff data.

Monthly rainfall and runoff data records of river Brahmaputra are available for 10 years from 1993 to 2002, gauged at Pandu, Guwahati. Data has been collected from the Water Resource Department, Basistha Charali, Guwahati.

5. METHODOLOGY

5.1 Simple Linear Regression.

Simple linear regression is a statistical method that allows us to summarize and study relationships between two continuous (quantitative) variables:

- One variable, denoted x, is regarded as the predictor, explanatory, or independent variable.
- The other variable, denoted y, is regarded as the response, outcome, or dependent variable.

Because he other terms are used less frequently, we'll use the "independent" and "dependent" terms to refer to the variables encountered in this study. Simple linear regression gets its adjective "simple", because it concerns the study of only one independent variable. In case of one explanatory variable is called simple linear regression. For more than one explanatory variable, the process is called multiple linear regression. In linear regression, the relationships are modelled using linear predictor functions whose unknown model parameters are estimated from the data. Such models are called linear models. Linear regression was the first type of regression analysis to be studied rigorously, and

to be used extensively in practical applications. This is because models which depend linearly on their unknown parameters are easier to fit than models which are non-linearly related to their parameters and because the statistical properties of the resulting estimators are easier to determine. The simplest form of the regression equation with one dependent and one independent variable is defined by the equation 3.1.

$$y = c + b * x \quad \text{--------} \quad (1)$$

Where, y = estimated dependent variable.

c = constant

b = regression coefficient

x = score on the independent variable.

5.2 Cubic Polynomial Regression

In statistics, polynomial regression is a form of regression analysis in which the relationship between the independent variable x and the dependent variable y is modelled as an n^{th} degree polynomial in x. Polynomial regression fits a nonlinear relationship between the value of x and the corresponding conditional mean of y, denoted E(y/x). Calculation instructions for many commercial assay kits recommend the use of a cubic regression curve-fit also known as 3^{rd} order polynomial regression. The cubic polynomial regression is:

$$y = a + bx + cx^2 + dx^3 \quad \text{----------} \quad (2)$$

Cubic regression is useful when the line through plotted data which curves one way and then the other. However, one problem with using cubic regression with assay analysis is that the determined curve might feature a turning point inside the range of the standards rendering parts of the curve unusable for concentration calculations.

6. RESULTS AND DISCUSSIONS

In this study, the goodness of fit was evaluated by one evaluation statistics, which is known as Co-efficient of Determination. It is denoted R^2 or r^2, a number that indicates the proportion of the variance in the dependent variable that is predictable from the independent variable. It is a statistic used in the context of statistical models whose main purpose is either the prediction of future outcomes or the testing of hypotheses, on the basis of other related information. It provides a measure of how well observed outcomes are replicated by the model, based on the proportion of total variation of outcomes explained by the model. The most general definition of the co-efficient of determination is:

$$R^2 = 1 - \frac{SS_{res}}{SS_{tot}} \quad \text{----------} \quad (3)$$

SS_{res} = Residual sum of squares = $\Sigma_i (y_i - f_i)^2 = \Sigma e_i^2$

SS_{tot} =Total sum of squares = $\Sigma (y_i - y)^2$

Where,

Observed data set = yi = $y_1, y_2, y_3 \ldots .y_n$

Predicted data set = fi= $f_1, f_2, f_3 \ldots \ldots f_n$

Mean of the observed data = $y = 1/n \ \Sigma$ yi

Residuals = $e_i = y_i - f_i$

R^2 gives the proportion of the variance in measured data explained by the model. R^2 ranges from 0 to 1, with higher values indicating less error variance, and normally values greater than 0.5 are considered acceptable. (Santhi et al., 2001; Van Liew and Garbrecht, 2003)

6.1 Simple Linear Regression

In this study simple linear regression analysis graphs are made in M.S. Excel sheet. Here 10 years monthly rainfall and runoff data are used from 1993 to 2002 in Brahmaputra watershed at Pandu observation site, Guwahati, Assam. In M.S. Excel the simple linear regression graphs are made by using scatter plot technique. Four years out of ten years simple linear regression plots are shown in figure 6.1 to 6.4.

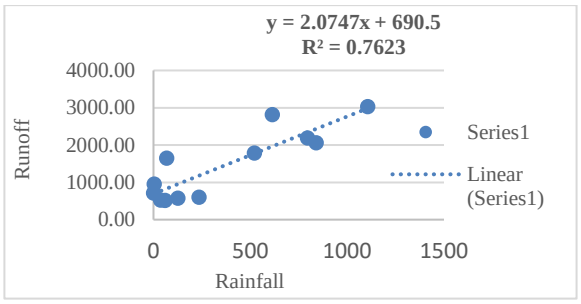

Figure 6.1. Linear Regression 1993

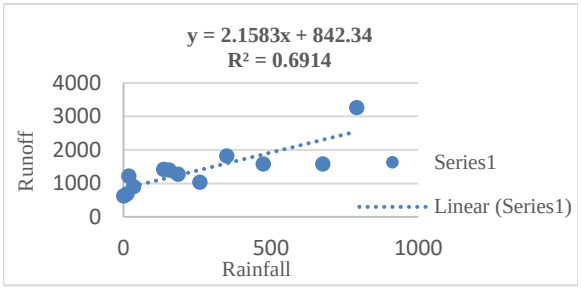

Figure 6.2. Linear Regression 1994

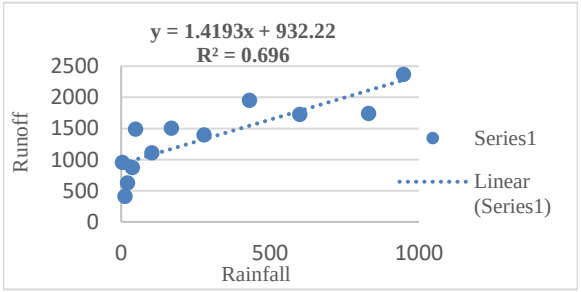

Figure 6.3. Linear Regression 1995

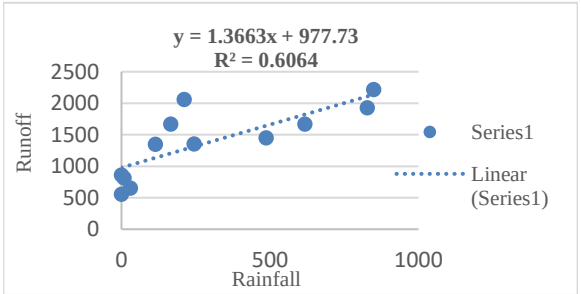

Figure 6.4. Linear Regression 1996

Figure 6.1., 6.2., 6.3., 6.4., shows the simple linear regression plots in M.S. excel for the year of 1993,1994,1995 and 1996 respectively. In this study, the data structure in M.S. excel, rainfall is in X-axis as an independent variable and runoff is in Y-axis as a dependent variable. The coefficient of determination R^2 is always a number between 0 and 1 which is explain in 6. From the calculation of simple linear regression, in figure 6.1. to 6.4. the co-efficient of determination (R^2) values for the year of 1993,1994,1995 and 1996 are 0.76, 0.691, 0.696 and 0.60 respectively. So, all four years of values are acceptable because its greater than 0.5. The co-efficient of determination (R^2) values in simple linear regression plots in M.S. excel for the year of 1997,1998,1999, 2000, 2001 and 2002 are 0.53, 0.51, 0.65, 0.70, 0.39, and 0.58 respectively. In 2001, R^2 value is less than 0.5 so this value is not acceptable.

6.2 Cubic Polynomial Regression.

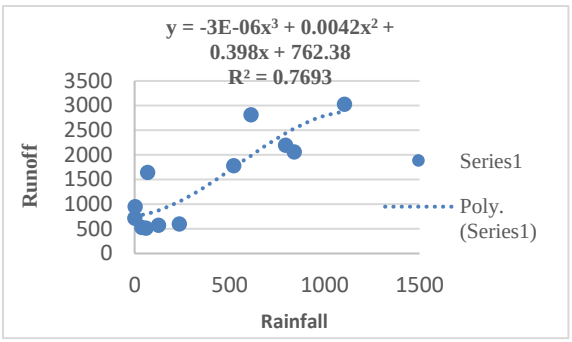

Figure 6.5. Polynomial regression 1993

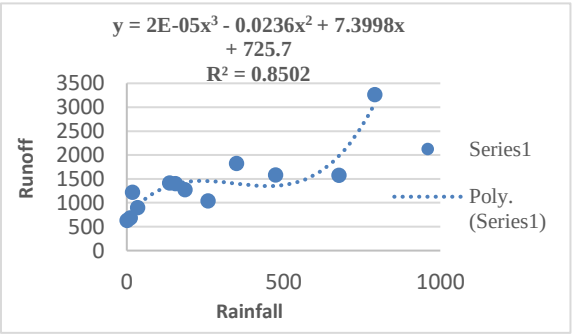

Figure 6.6. Polynomial regression 1994

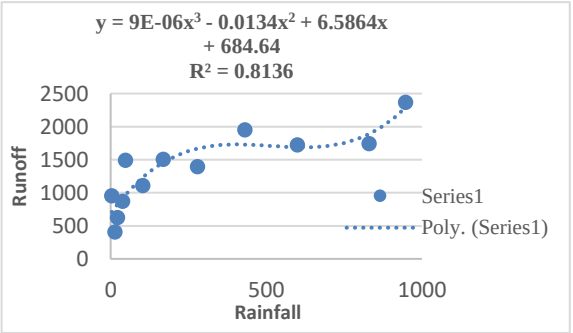

Figure 6.7. Polynomial regression 1995

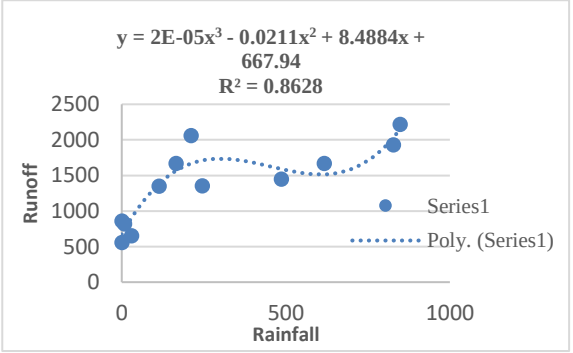

Figure 6.8. Polynomial regression 1996

Cubic Polynomial regression is done in M.S. Excel. The third order polynomial regression scatter plot graphs are shown in the figure 6.5, 6.6, 6.7 and 6.8 for the year of 1993, 1994, 1995 and 1996, respectively. In this study, rainfall is independent variable and runoff is dependent variable in X-axis and Y-axis respectively. Third order polynomial regression forms a cubic expression is y equal to $a + bx + cx^2 + dx^3$. From this equation, we have estimated the a, b, c and d values which are shown in figure 6.5, 6.6, 6.7 and 6.8. Coefficient of determination (R^2) values are calculated for the year of 1993,1994,1995 and 1996 in figure 6.5, 6.6, 6.7 and 6.8. In cubic form of polynomial regression, the R^2 values are more than the second order quadratic expression form of polynomial regression. In second order polynomial regression the shape of trend line is parabolic but in third order polynomial regression trend line shape is changed. A model which is consistent with the knowledge of data and its environment should be considered. It is always possible for a polynomial of order (n – 1) to pass through n points so that a polynomial of sufficiently high degree can always be found that provides a "good" fit to the data. The R^2 values calculated by third order polynomial regression in M.S. Excel are 0.76, 0.85, 0.81, 0.86, 0.68, 0.53, 0.85, 0.85, 0.66 and 0.605 for the year of 1993, 1994, 1995, 1996, 1997, 1998, 1999, 2000, 2001 and 2002 respectively.

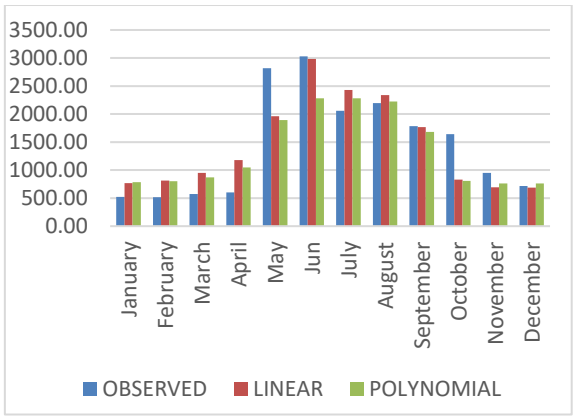

Figure 7.1 Comparison 1993

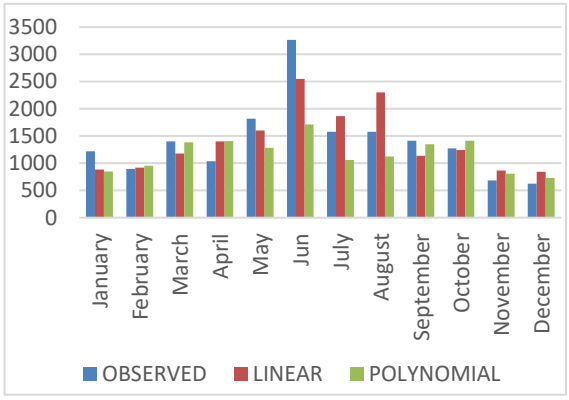

Figure 7.2 Comparison 1994

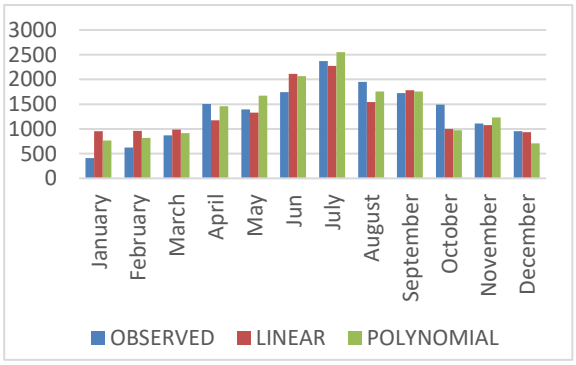

Figure 7.3 Comparison 1995

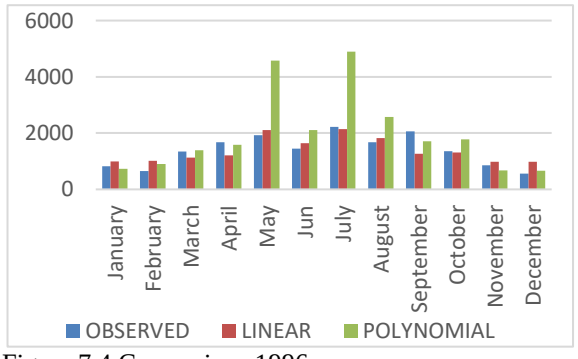

Figure 7.4 Comparison 1996

7. COMPARISON OF THE LINEAR AND CUBIC POLYNOMIAL REGRESSION MODEL.

An approximate comparison was made between the observed data and the predicted data of the LINEAR and cubic POLYNOMIAL (third order) regression models. Figure 7.1, 7.2, 7.3 and 7.4 show the comparison graphs between observed runoff and predicted runoff of the LINEAR and POLYNOMIAL third order models for the year of 1993, 1994, 1995 and 1996 respectively. As it can be seen from figure 7.1 to 7.4, the LINEAR monthly average results are inadequate as compared to that of POLYNOMIAL results. The LINEAR predicted values show the lack of consistency overall throughout the period. However, the POLYNOMIAL predictions are quite superior and they can effectively be used for the modelling applications. Issac, O. Ajao, Adedeji, A. Abdullahi (2012) carried out a similar study in mixed cost analysis where the performance criteria showed that cubic POLYNOMIAL regression was a better prediction model with a very high coefficient of determination than the usual LINEAR regression model

8 CONCLUSIONS

Regression analysis of rainfall runoff data is a very important aspect of Watershed Management and the demand for accuracy of the runoff predictions has been on an upward trend ever since. More specifically, regression analysis helps one understand how the typical value of the dependent variable changes when any one of the independent variables is varied, while the other independent variables are held fixed. In this study, R^2 is considered as a goodness of fit in simple linear, and cubic polynomial regression model. Based on the results of the analyses it can be concluded that cubic polynomial regression model is better than the simple linear regression, especially when analyzing data relating to rainfall and runoff functions. We can view polynomial regression as a particular case of multiple linear regression. Polynomial models are an effective and flexible curve fitting technique. It is obvious that Linear model is not too bad for prediction with respect to the data used in this research paper, but the Cubic polynomial regression is better. It is therefore recommended that data analysts should endeavor to always plot a simple scatter diagram before using any regression model in order to know the type of relationship that exists between the variable of interest. Here speculate that a distributed, process-based, simulation model will not be able to achieve this performance in predicting flow peaks and volumes or the same robustness of uncertainty analysis, using the same data set plus topography, land cover and soil data.

REFERENCES

1) Yawson, D.K., Kongo, V.M., and Kachroo, R.K. (2005), *Application of linear and nonlinear techniques in river flow forecasting in the Kilombero river basin, Tanzania*, Hydrological Science Journal, 50:5796, DOI: 10.1623/hysj. 2005.50.5.783
2) McIntyte, N., Qurashi, Al.A., and Wheater, H., (2007), Regression analysis of rainfall runoff data from an arid catchment in Oman. Hydrol. Sci.- Journal 52(6) Dec.2007
3) Ostertagova, E., (2012), Modelling using polynomial regression. Procedia Engineering 48 (2012) 500506. Faculty of Electrical Engineering and Informatic, Department of Mathematics and theoretical informatics 32. 04200, Slovak Republic.
4) Ajao, I.O., Abdullahi, A. A., and Raji, I.I., (2012*), Polynomial regression model of making cost prediction in mixed cost analysis.* Mathematical theory and modelling. ISSN 2224-5804 (paper) ISSN 2225-0522 (online) Vol.2, No.2, 2012.
5) Patel, S., Hardaha, M.K., Mukesh, K., Seetpal, Madankar, K.K., (2016), *Multiple linear regression model for stream flow estimation of Wainganga river.* American Journal of Water Science and Engineering, Volume 2, Issue1, January 2016, pages: 1-5
6) Ahmad Dar, L., (2017), *Rainfall-runoff modelling using Multiple Linear Regression Technique.* International Journal for Research in Applied Science and Engineering Technology (IJRASET) ISSN:

A study on the effect of permeable spur in velocity dissipation in near bank within the straight reach of an experimental field channel

Baruah, S.J.[1], Goswami, R.[2], Khaund, P.K. [3]

[1] Lecturer, Civil Engineering, Dibrugarh Polytechnic, Lahowal, Dibrugarh-10, Assam, India.
[2] Assistant Professor, Civil Engineering, Jorhat Engineering College, Jorhat-7, Assam, India.
[3] Professor, Civil Engineering, Jorhat Engineering College, Jorhat-7, Assam, India.

ABSTRACT

Most of the rivers of the north-eastern region of India originate from the foothills of the Himalayas and they usually carry huge sediment load during most of the time of the year. As these rivers enter the Assam valley, due to drastic reduction in bed slope, their velocities decrease rapidly and as a result they deposit these sediments on their respective beds, causing them to rise, reducing the waterway for the flow and form sandbars at the middle of the channels. During monsoon, when these rivers run in full discharge, the current hits the banks and erode them. Hence the use of effective river training works is a must in these rivers to counteract the problem of erosion. Different agencies are continuously applying mitigating measures for controlling riverbank erosion, by laying of porcupine screens. However, the success rates of such installations are very limited, which may be a result of lack of proper design procedure & specification and for the fact that the existing layout patterns of such structures are not dependent anyway on the factors like characteristics of flow and channel geometry etc of the sites where they are intended to be installed. In the present study, it was planned to critically compare the performance of different porcupine models on the basis of their capacity to reduce the flow velocity in near bank. During the study scaled down porcupine models were prepared based on characteristics like channel dimension and discharge. The models were installed in an experimental field channel and the changes in flow velocity data's in near bank were collected using Acoustic Doppler Velocimeter to find out the best performing porcupine models under different submergence ratios.

Keywords: porcupine, erosion control, permeable spur, velocity reduction, bank protection

1. INTRODUCTION

Riverbank and in-stream protection is becoming a necessity in many major rivers of India where scouring of the river bed and bank materials leads to change the river course and thereby flooding and causing losses to lives and properties in the nearby areas. Protection measures like dykes, impermeable spur embankments etc. associates with high labor and material cost. Thus in such reaches of the big Indian rivers it becomes necessary to employ some cost effective measures which are reliable as well as economical. Due to the increase in the demand of such economic measures many researchers have been studying different types of structures to reduce the problem of bed and bank erosion. Nowadays Porcupines have been also installed in many reaches of the big Indian rivers like Brahmaputra, kosi etc. and have yielded fairly good performance in erosion control.

2. MATERIALS USED AND THE METHODOLOGY ADOPTED

2.1 Materials description

2.1.1 Porcupine

***i*) Prototype (RCC Porcupine)**

RCC porcupines (Fig 1) consists of six members made-up of RCC, which are joined with the help of the iron nuts and bolts. Depending upon the field requirements the length of each members may vary from 2m to 3m and cross section is 15cm×15cm or 10cm x 10cm. Reinforcement is usually given using 4 numbers of MS bars of 6 mm diameter, with stirrups at 15 cm c/c.

Fig 1: RCC Porcupines laid in Majuli,Assam

ii) Model

The porcupine models used in this study are prepared in reducing scale(Fig 2) to match the dimensions of the field channel as per the guidelines of CWC manual 2012. The

models are prepared by bamboo sticks of size 5cm in length and 0.5 cm in thickness which were glued together. Extended lengths of 3cm for each member of the model are kept for embedding them into the simulated river bed in the field channel. Photograph of the model is shown below.

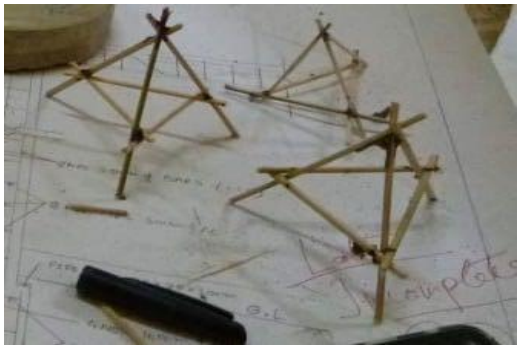

Fig 2: Prepared porcupine models

2.1.2 Bed material

The bed material was collected from river Bhogdoi, Jorhat. After collecting the river bed material sample, they were air dried for evaluating the particle size distribution and the material was found to be poorly graded fine sand. The bed of the field channel was filled with this collected sample up to a depth of 15 cm from the cut surface. This depth has been selected on the basis of trial runs in the channel without porcupine models with different discharges and observing the scouring level for such runs. A channel bed with a minimum thickness of 15 cm has been found to withstand significant scouring and subsequent exposure of the cut surface of the channel under any trial run.

2.2 THE FIELD CHANNEL

All the experiments for this study were carried out in a field channel that was developed inside the campus of Jorhat Engineering College, Assam. The field channel that was developed for the study is about 27.0 m long, 1.0 m wide and about 0.4m deep. Out of this 0.4m total depth of the channel, 0.2 m were kept available for flow ,after preparing he channel bed by filling up the bottom 0.15m with collected bed materials and considering a free board of 0.05m. Two 15 HP pumps were installed nearby to collect water from the JEC lake and feed the same into the experimental channel. The water from the pumps was first collected into a chamber (Fig 4). The water released from the collecting chamber then goes through some energy dissipaters (steps) for reducing the turbulence of the flow before entering the main channel. A foot valve was installed at the bottom of the channel near its u/s face to regulate the quantity of water to be fed to the channel in order to maintain different depths of flow inside it. The d/s of the channel is again fed to the JEC lake to complete the circle of flow .A steel trolley was installed to support the ADV; above the channel on the side walls (with rails on their tops) that were constructed on both the sides of the channel,as shown in Fig 5. A view of the prepared field channel is also shown in Fig 3.

Fig 3: The prepared field channel with porcupine models

Fig 4: The collecting chamber that receives the water from the pump

Fig 5:The ADV with probe installed inside the channel

2.3 ACCOUSTIC DOPPLER VELOCIMETER

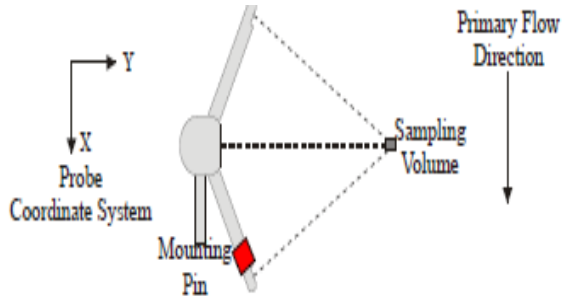

Fig 6: ADV probe orientation to stream flow

An Acoustics Doppler Velocimeter works on the principle of capturing change in frequency in acoustic waves .The ADV sends out a beam of acoustic waves at a fixed frequency from a transmitter probe. These waves bounce off a moving particulate matter in water and three receiving probes listen to change in frequency of the returned waves. The ADV then calculates velocities in x,y and z direction.

2.4 EXPERIMENTAL PROCEDURE

Before every experimental run, the channel bed was levelled and flow was introduced for a particular depth of flow. The required depth of flow for maintaining different submergence ratios was achieved by trying out different pump and valve combinations. achieved. Before installing the porcupine models into the channel, free run was conducted for about 20 minutes and the water was allowed to discharge completely after closure of the feed. After this free run; the porcupine models of required combinations were installed and flow was again introduced by maintaining the depths required to achieve the desired submergence Ratios. During each of such trial runs with different porcupine models, the flow velocity data were taken using the ADV at upstream and downstream of every porcupine spur installed within the screen and the change in velocity of flow is calculated after each screen.

After taking the flow velocity observations, the pumps were shut down and water was again allowed to discharge completely out of the channel. In this manner several trials were conducted using porcupine screens comprising of 3, 4 and 5 no.s of spurs spaced apart c/c by 3, 4 and 5 times their length. Submergence ratios of 1.7, 2.0 and 2.5 for each of the screen modals were found to be achievable with the available set-up of feeding pumps and foot valve combinations.

The models used are listed below:

Model	Combinations	Submergence Ratio
1	3 spur with 3L spacing	1.7
	3 spur with 3L spacing	2.0
	3 spur with 3L spacing	2.5
2	3 spur with 4L spacing	1.7
	3 spur with 4L spacing	2.0
	3 spur with 4L spacing	2.5
3	3 spur with 5L spacing	1.7
	3 spur with 5L spacing	2.0
	3 spur with 5L spacing	2.5
4	4spur with 3L spacing	1.7
	4spur with 3L spacing	2.0
	4spur with 3L spacing	2.5
5	4 spur with 4L spacing	1.7
	4 spur with 4L spacing	2.0
	4 spur with 4L spacing	2.5
6	4spur with 5L spacing	1.7
	4spur with 5L spacing	2.0
	4spur with 5L spacing	2.5
7	5spur with 3L spacing	1.7
	5spur with 3L spacing	2.0
	5spur with 3L spacing	2.5
8	5 spur with 4L spacing	1.7
	5 spur with 4L spacing	2.0
	5 spur with 4L spacing	2.5
9	5spur with 5L spacing	1.7
	5spur with 5L spacing	2.0
	5spur with 5L spacing	2.5

Where,L=Length of spur

3. RESULTS AND DISCUSSIONS

3.1 Effect of submergence ratio on flow velocity:

After compilation of the collected velocity data's from the ADV, the percent reduction in velocity after the flow crosses each spur is calculated and plotted against the respective submergence ratios for all the models as shown in the figures below.

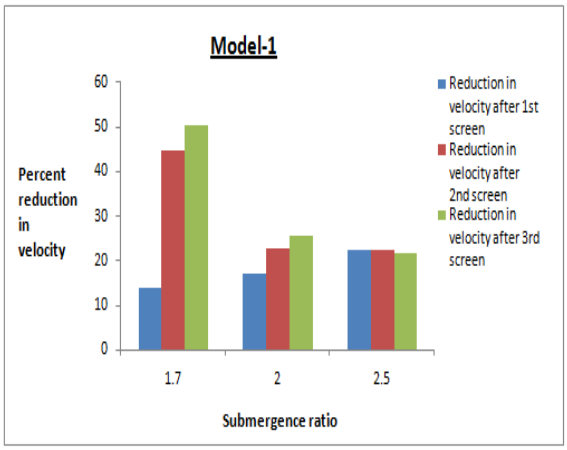

Fig 7:Reduction in velocity due to installation of Model 1 with different submergence ratios

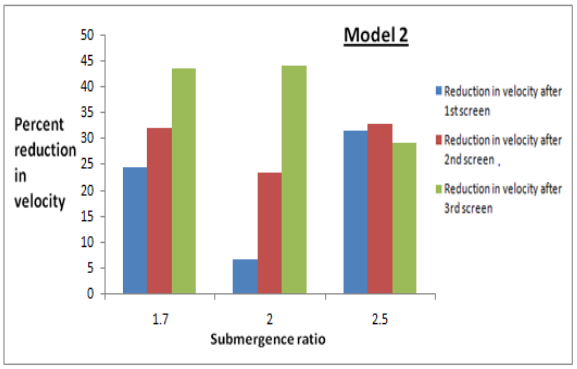

Fig 8:Reduction in velocity due to installation of Model 2 with different submergence ratios

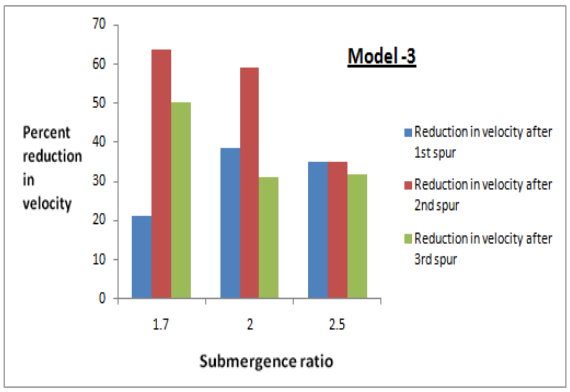

Fig 9:Reduction in velocity due to installation of Model 3 with different submergence ratios

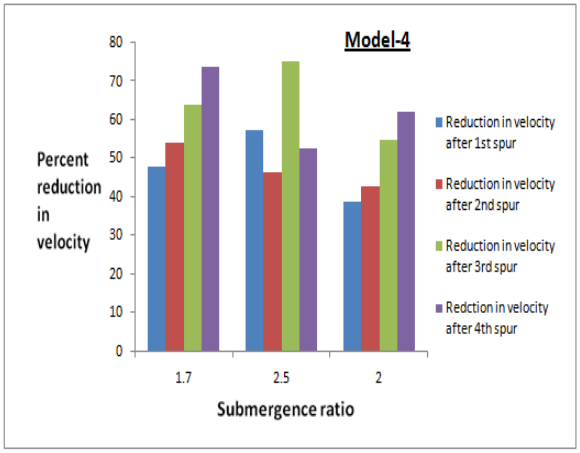

Fig 10:Reduction in velocity due to installation of Model 4 with different submergence ratios

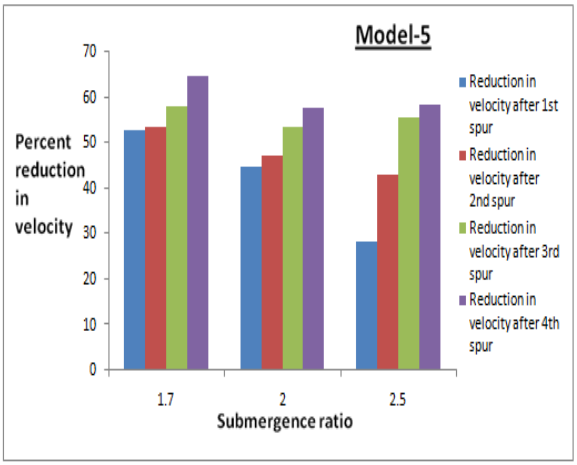

Fig 11:Reduction in velocity due to installationof Model 5 with different submergence ratios

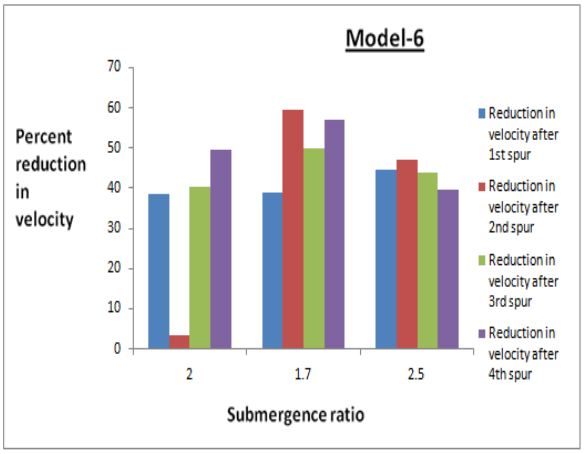

Fig 12:Reduction in velocity due to installationof Model 6 with different submergence ratios

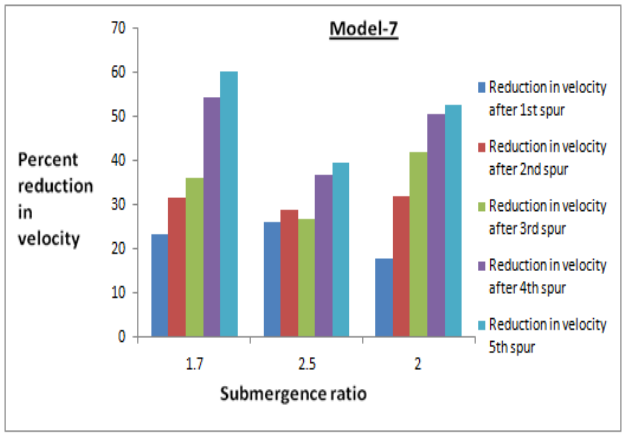

Fig 13:Reduction in velocity due to installationof Model 7 with different submergence ratios

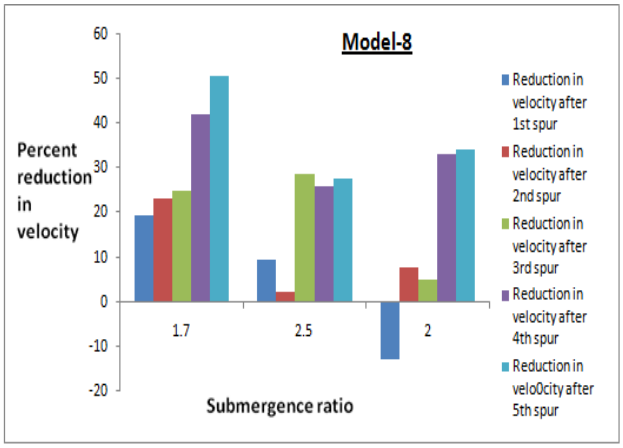

Fig 14:Reduction in velocity due to installationof Model 8 with different submergence ratios

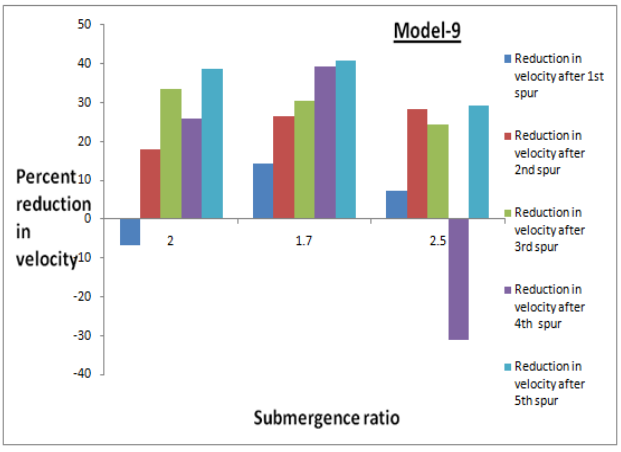

Fig 15:Reduction in velocity due to installationof Model 9 with different submergence ratios

As it can be seen from the above figures that in almost all the cases maximum reduction in velocity is achieved with lower submergence ratios and the best performing ratio is found to be 1.7.

3.2 Effect of spur spacing on flow velocity reduction:

Considering the submergence ratio of 1.7 the percent reduction in velocity after the flow crosses each spur is plotted against all the different models as shown below in fig 16.

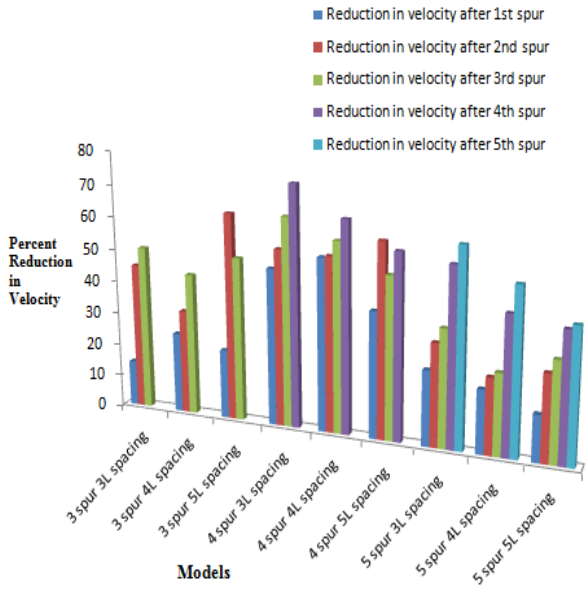

Fig 16: Variation in percent reduction in velocity for different models for a submergence ratio of 1.7.

It can be observed from the above figure that the models are performing better with less spacing between them, hence increase in amount of velocity reduction can be achieved with less spacing.

3.3 Effect of no of spurs on flow velocity reduction:

From figure 16 it has been observed that increase in no of spurs does not necessarily guarantee more reduction in velocity, as it is seen that maximum percentage of velocity reduction is achieved with 4no's of spurs and the best performing model happens to be the one with 4no's of spur with minimum spacing. Beyond 4no's of spurs the increase in velocity reduction does not seem to be very prominent, hence the installation of a 5thspur does not seem very essential.

4. CONCLUSIONS

The following conclusions have been drawn from the present study:

1) The rate of increase in reduction in flow velocity is inversely proportional to submergence ratio of the porcupine models. Hence with less submergence ratios better reduction in velocity in near bank can be achieved.

2) For a particular model, reduction in spur spacing will result in better reduction in flow velocity in the near bank.

3) From increase in spur no's from 3 to 4 has resulted in better performance ,but beyond spur no 4 ,the percent reduction in velocity is not very prominent.

REFERENCES

1. Baishya S. J (2013) **.** "A Study on Bank Erosion by the River Baralia (Bhairatolajan) in Melkipara Village of HajoRevenue".International Journal of Scientific and Research Publications, Volume 3, Issue 9, September 2013
2. .B. F Pramod, Oak R.A (2012) "Relation between spur spacing and safety margin of protected bank: a field verification".International Journal of Advanced Engineering Research and Studies, E-ISSN2249–8974.
3. Devmurari. R.K , Gandhi H.M , Ramanuj P.S , Chudasama M.K , Acharya N (2015) ."River Training: A Brief Overview".IJSRD - International Journal for Scientific Research & Development| Vol. 2, Issue 12, 2015.
4. Dingorkar N.A ,Kulkarni D, Hirave P (2017) "Study of river training works on permeable groynes". International Journal of Civil Engineering and Technology (IJCIET)Volume 8, Issue 6, June 2017
5. Khaund P.K , Goswami R, Das G (2015) "A study on the effect of Porcupine on the flow velocity in a laboratory tilting type channel using physical model".Proceedings of 4th IRF International Conference on 19th April 2015, Cochin, India
6. Kulkarni D, Oak R.A , Nimbalkar P.T (2013)." Verification Studies for Effect of Blockage in Permeable Structures. INDIAN JOURNAL OF APPLIED RESEARCH Volume : 3 | Issue : 8 | Aug 2013.

Study of sediment behavior and river flow characteristics in the Brahmaputra river using HEC RAS software

Talukdar, B. [1] and Koch, D.[2]

[1] Associate Professor, Department of Civil Engineering, Assam Engineering College, Guwahati 913-2018, India.
[2] PhD Student, School of Water Resources, IIT Kharagpur, Kharagpur 302-20158, India.

ABSTRACT

The Brahmaputra River is one of the biggest rivers of the world. It carries immense load of sediment acquired from the heavy erosion of the Himalayan slopes. Sediment generated per year in the Brahmaputra River is alarmingly high at about 1 billion tones, five times as much as in China's Huang Ho. The hydrology of this river is, therefore, characterized by its significant rate of sediment discharge, the large and variable flows, along its rapid channel aggradations and accelerated rates of basin denudation. In this study a sediment transport analysis is carried out with the help of the HEC RAS software along a reach of the Brahmaputra River for a reach length of 83.5kilometres. In the selected reach, the width of the river in the upstream is 1.2kilometres and in the downstream, near Gumi, it is around 18 kilometers. The main objective here is to study the sediment carrying behavior of the river. After performing 1D quasi unsteady flow analysis and sediment transport analysis, the difference in the depths of erosion and deposition has been observed in the various cross sections along the reach. Some of the other parameters such as shear stress variation and flow velocity variation is also analyzed here. In conclusion, it can be said that the downstream of the reach is in need of deposition control measures to restrict the flow of the river and stabilize it within a shorter width.

Keywords: sediment transport, erosion and deposition, quasi-unsteady flow.

1. INTRODUCTION

The Brahmaputra basin covers an area of about 580,000 sq. km spanning over an area of 293,000 sq.km in Tibet, 45,000 sq. km in Bhutan, 194,413 sq. km in India and 47,000 sq. km in Bangladesh. In India, the basin covers the states of Arunachal Pradesh, Assam, Nagaland, Meghalaya, Sikkim and West Bengal. This river carries one of the highest sediment loads of the world. The dynamics of sediment transport of this river is unique and unpredictable. It has affected the ecology as well as the geomorphology of the entire region through which it flows.

Estimation of the amount of sediment material, which a specific flow can carry, is one of the major issues of sedimentation research. Many scientists such as Einstein, Colby and Engelund-Hansen have proposed analytical and graphical procedures for the computation of sediment discharge of alluvial streams (Garde, R.J. and Ranga Raju, K.G. Mechanics of Sediment Transportation and Alluvial Stream Problems). Usually, mathematical models of alluvial hydraulics are used for the evaluation of the bed deformation and bank erosion of natural channels. Even though there are a large number of theories regarding transfer of sediment in an alluvial river, very few are able to predict correct or accurate sediment discharge. But with the help of software, this drawback can be overcome. Software allows the user to input certain data and can model those data to actually analyse the real conditions existing or occurring in a river. These models are developed using software like HEC-6 and QUASED.

Barbe et al. (1998) developed a HEC-6 model to present the development, calibration and use of a model to analyze the long term effects on dredging due to freshwater diversions along the lower Mississippi river. **Dade (2000)** examined some existing approaches and focused on some analytical predictions to discriminate between the two and present new, quantitative constraints for channel form. This new analysis reconciles existing empirical and theoretical approaches to predict alluvial channel geometry. **Stanford Gibson et al. (2006)** "explicitly coupled" hydraulic computations with transport, erosion, deposition, bed mixing and cross section change computations using the set of initial value-boundary value equations used in HEC-6.

Matt Fleming et al. (2008) studied the effects of surface erosion and stream sediment loading in watersheds using HEC-HMS and modelled the translation and attenuation of the sediment load along with deposition and erosion processes occurring in the channel. **Fischer et al. (2016)** synthesized reported peer-reviewed data relevant to sediment transport and performed a sensitivity analysis to identify sensitive and uncertain parameters, using the one-dimensional model HEC-RAS, considering both present and future climatic conditions. The HEC RAS software has also been used to study sediment flow and unsteady flow problems extensively (**G. Brunner et al. (2017)** and **Stanford et al. (2005)**) by taking up several case studies (**Z Corum et al. (2017)).**
Keeping in mind these problems, in this study a sediment transport analysis is carried out with the help of the HEC RAS software along a reach of the Brahmaputra River for a length of 83.5kilometres. The reach selected for sediment transport analysis extends from Guwahati (North Bank: 26011'.07"N, 91041'22.58"E, South Bank: 26010'16.15", 91041'20.77"E) in the upstream to Barpeta (North Bank: 26014'57"N, 90059'57.5"E, South Bank: 26011'26.41"N, 9100'49.20"E) in downstream. The width of the river in the upstream is 1.2kilometres and in the downstream, near Gumi, it is around 18 kilometres. The analysis is carried out to study the changes in sediment behaviour of the river bed.

2. AIM OF THE STUDY

The aim of this study is to analyse the sediment behaviour of the Brahmaputra River using the HEC-RAS software for a reach length of 84 kilometres starting from Guwahati in the upstream to Barpeta in the downstream. 1D quasi unsteady sediment transport analysis is carried out in the existing condition of the Brahmaputra River in the selected reach. The software analyses around 14 different parameters, of which, 5 parameters have been studied in details here.

3. HEC-RAS SOFTWARE AND 1D ANALYSIS

3.1 Model Description

The HEC-RAS modeling system was developed as a part of the Hydrologic Engineering Center's "Next Generation" (NextGen) of hydrologic engineering software. The NextGen project encompasses several aspects of hydrologic engineering, including rainfall-runoff analysis (HEC-HMS), river hydraulics (HEC-RAS), reservoir system simulation (HEC-RecSim), flood damage analysis (HEC-FDA and HEC-FIA) and real time river forecasting for reservoir operations (CWMS).

3.2 Governing Equations

3.2.1 1D steady flow analysis

HEC-RAS can perform 1D water surface profile calculations for steady gradually varied flow in natural or constructed channel. Sub critical, super critical and mixed flow regime water surface profiles can be calculated. The basic equations used for profile calculations are:

$$Z_2 + Y_2 + \frac{a_2 V_2^2}{2g} = Z_1 + Y_1 + \frac{a_1 V_1^2}{2g} + h_e \quad (1)$$

Where Z1, Z2 = elevation of the main channel inverts
Y1, Y2= depth of water at cross sections
a1, a2= velocity weighting coefficients
g= gravitational acceleration
he = energy head loss
The equation for energy **head loss** is given by:

$$h_e = L\bar{S}_f + C\left|\frac{a_2 V_2^2}{2g} - \frac{a_1 V_1^2}{2g}\right| \quad (2)$$

Where L = discharge weighted reach
$\bar{S}_f$ = representative friction slope between two sections
C = expansion or contraction loss coefficient

3.2.2 1D unsteady flow analysis

HEC-RAS can also perform 1D unsteady flow hydrodynamics governed by principle of conservation of mass and momentum. The basic equations used are:

$$\frac{\partial A_T}{\partial t} + \frac{\partial Q}{\partial x} - q_l = 0 \quad (3)$$

$$\frac{\partial Q}{\partial t} + \frac{\partial QV}{\partial x} + gA\left(\frac{\partial z}{\partial x} + S_f\right) = 0 \quad (4)$$

3.2.3 Sediment continuity equation

The HEC-RAS sediment routing routines solve the sediment continuity equation also known as the Exner's equation:

$$(1-\lambda_p)B\frac{\partial \eta}{\partial t} = -\frac{\partial Q_s}{\partial x} \quad (5)$$

Where B = channel width
h = channel elevation
lp= active layer porosity
t = time
x = distance
Qs = transported sediment load

3.2.4 Sediment load calculating equations

The Tofaleti equation of sediment transport is considered here keeping in mind the unique sediment carrying characteristics of the river. The Brahmaputra River is a very dynamic river. It has a very high sediment transport capacity and discharge carrying capacity and it is not possible to describe this capacity in terms of an empirical equation. Toffaleti is a total load function developed primarily for sand sized particles, which followed the basic principles of the Einstein approach, replacing some of the empirical assumptions. Toffaleti is usually applied to large rivers. The function is not driven by excess shear velocity or bed shear. Instead it describes the relationship between sediment, hydraulics and water temperature with a set of regressions. This function has been successfully applied to large systems like the Mississippi, Arkansas, Amazon,etc.

Toffaleti breaks the water column down into four vertical zones and computes the concentration of each zone separately with a simple approximation of a Rouse concentration profile. It uses the zones as a coarse integration of vertical concentration profiles and assumes that the grain class is evenly mixed and in equilibrium in the zone. This function also uses two different grain sizes, d50 and d65 in an attempt to quantify transport dependence on the gradational deviation from the mean.

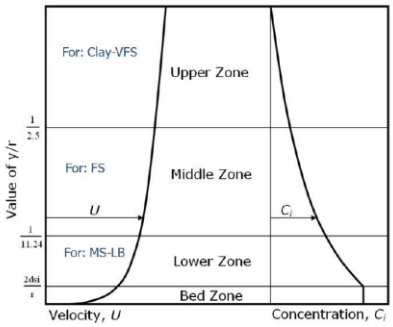

Fig1: Toffaleti's Zones for Computing Transport

This approach has limitations too. It distributes sediment evenly throughout the zone at the beginning of each time step. This assumption simplifies the concentration gradients. Also, assuming the effective depth is only a function of grain size ignores the Rouse dependence on shear velocity. Despite these limitations, this is a very effective function for sediment transport analysis.

4 1D QUASI UNSTEADY SEDIMENT TRANSPORT MODEL

For sediment transport analysis in a large and dynamic river like the Brahmaputra, quasi-unsteady flow is more suitable than unsteady flow. Here, 1D quasi unsteady sediment transport analysis is carried out in the existing condition of the Brahmaputra River in the selected reach extending from Guwahati (North Bank: 26011'.07"N, 91041'22.58"E, South Bank: 26010'16.15", 91041'20.77"E) in the upstream to Barpeta (North Bank: $26^0$14'57"N, $90^0$59'57.5"E, South Bank: 26011'26.41"N, 9100'49.20"E) in the downstream. This reach is selected because the width of the river in the upstream is 1.2kms and downstream near Gumi, it is around 18 kms. It is seen that in a short span of 84 kilometres the river undergoes heavy braiding and its width expands up to a great extent.

4.1 Assumptions

In this condition, the data used for quasi-unsteady flow are the actual data reflecting the existing conditions of the river. The assumptions made before performing the quasi unsteady flow analysis are:

a) The Manning's roughness coefficient is assumed to be constant throughout the reach for both the river banks and all the cross sections.

b) Same bed material gradation is used for all the cross sections.

c) Interpolated values of discharge data and temperature data have been used in the locations where actual data is unavailable.

d) Toffaletti equations are used in the calculation of sediment transport capacity of the river bed.

4.2 Basic Data Requirements

The HEC-RAS software is basically used to compute water surface elevations at all locations of interest for either a given set of flow data (steady flow simulation) or by routing hydrographs through the system (unsteady flow simulations). The data needed to perform these computations are divided into the following categories: Geometric data, Steady flow data, Unsteady flow data and Sediment data. In this condition, the data used for quasi-unsteady flow are the actual data reflecting the existing conditions of the river. The cross section data has been obtained from a GIS map, discharge and water level data from the Water Resources Department, Assam for two successive years.

4.2.1 Geometric data

The geometric data required for this analysis mainly consists of river schematics and cross section data (Elevation Vs River Station). First of all a base map of the reach of the Brahmaputra River is generated using the Google earth software.

The various cross sections are also specified along the reach in the base map itself with their respective coordinates. The geometric data obtained from Water Resource Department, Assam is then geo-referenced using the HEC Geo RAS tool in the Arc GIS software.

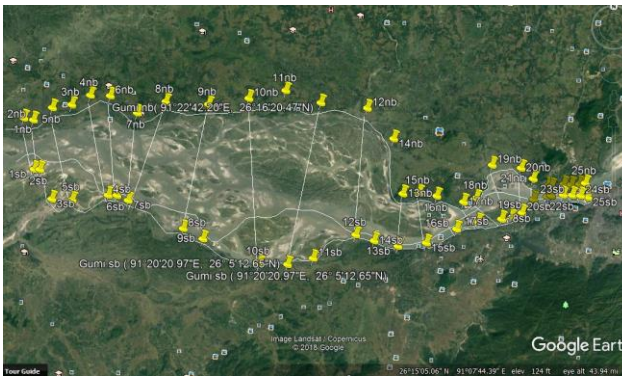

Fig 2: Base Map of the Reach

The figure above shows the base map of the reach. The cross sections are taken as per the availability of data and requirement of the study. This entire length has been divided into 19 cross sections taken at right angles to the centreline of the river. The Digital Elevation Model (DEM) used in the Arc GIS software is obtained from BHUVAN satellite imagery (Dated December, 2015). The HEC Geo RAS toolbar allows the user to superimpose the flow-lines, centre line of the main channel, bank lines and cross section lines from the base map on the DEM. The geo-referenced data is then extracted in GIS format to use in the HEC-RAS software.

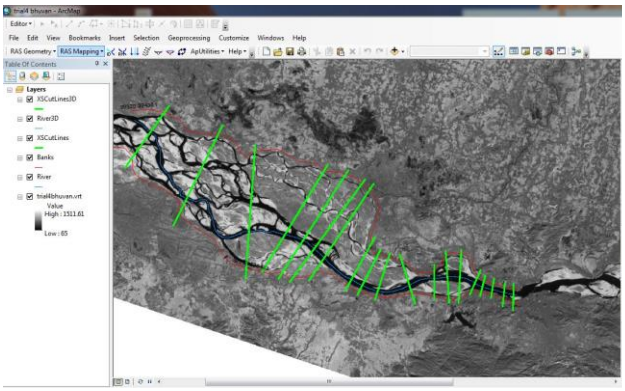

Fig 3: Geo-referencing in Arc GIS Using HEC Geo RAS tool

In the HEC-RAS software, the cross section data in GIS format is then extracted to get a geometry file as shown in the figure below.

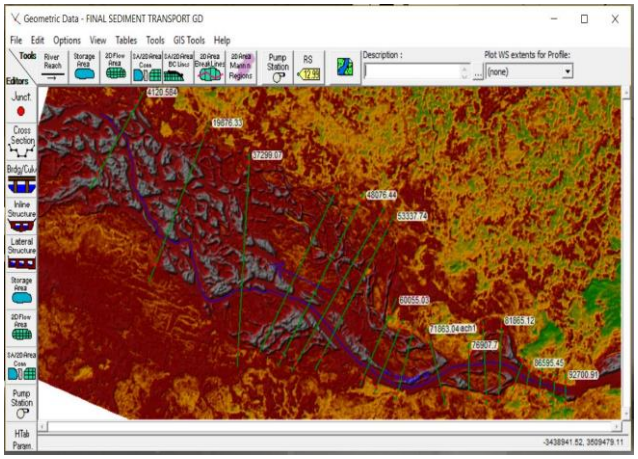

Fig 4: Geometric Data Representation Along the Reach

In the geometric data editor, the elevation data for each cross section is plotted individually. Manning's coefficient, expansion and contraction coefficients along with reach lengths are also specified here.

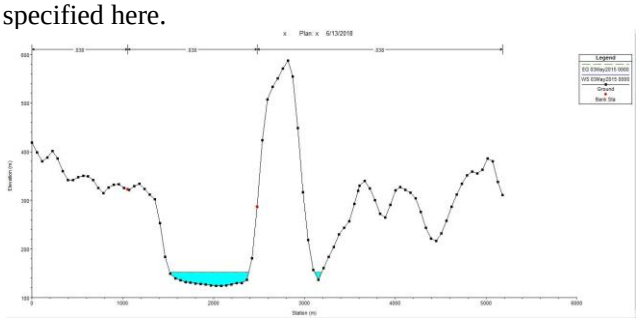

Fig 5: First Cross Section

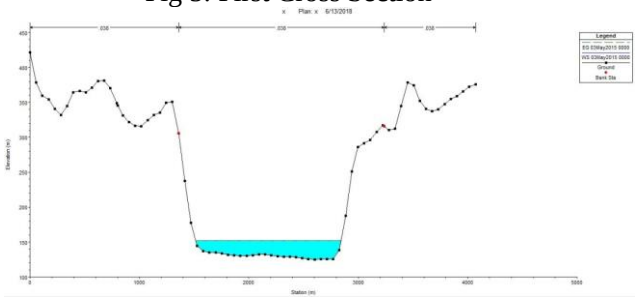

Fig 6: Fourth Cross Section

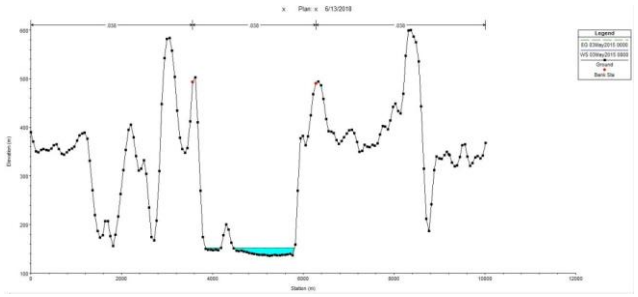

Fig 7: Seventh Cross Section

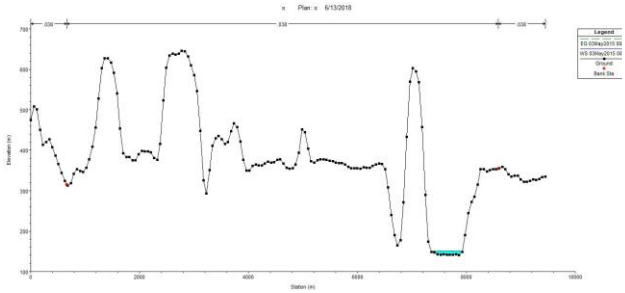

Fig 8: Tenth Cross Cection

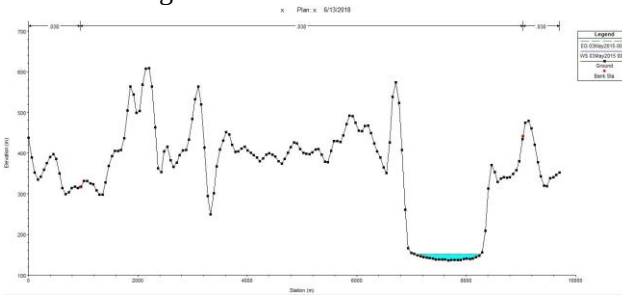

Fig 9: Eleventh Cross Cection

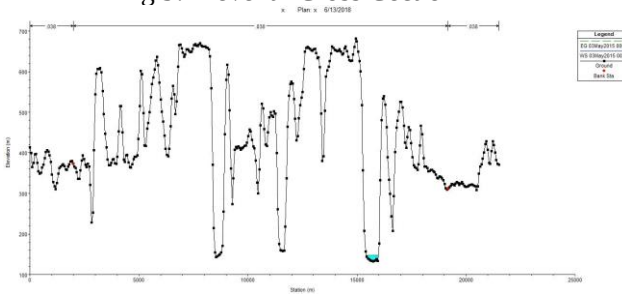

Fig10: Eighteenth Cross Section

4.2.2 Quasi unsteady flow data

The quasi unsteady flow editor needs to specify boundary conditionsat both upstream and downstream of the reach. In the upstream, a flow hydrograph for a period of two years (2012 and 2013 data; discharge data obtained from WRD, Assam) is used as a boundary condition. A temperature series data also needs to be specified for the same period. (Temperature data is obtained from Regional Meteorological Centre, Assam)

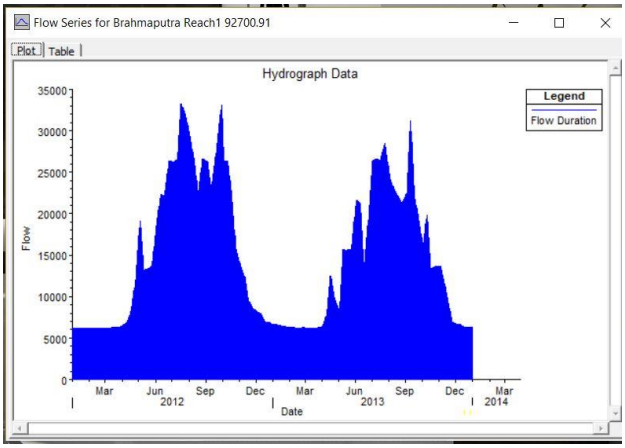

Fig 11: Flow Hydrograph as Boundary Condition in the Upstream of the Reach for Two Years (2012 & 2013 respectively) (Source: WRD, Assam)

In the downstream, normal depth is used as a boundary condition. Only one data is required here i.e. critical slope from which the software back calculates the normal depth using the Manning's equation. Here critical slope of value 0.00025 is used. (Source: Literature)

4.2.3 Sediment Data

The data required in the sediment data editor includes mainly gradation of the river bed material and sediment properties. The transport capacity function also needs to be specified along with the method of sorting and armoring and the method to compute fall velocity of the sediment particles. For sediment transport capacity computations, the Toffaleti equation is specified as it is found to be the most suitable equation.

In the sediment data editor, each cross section requires a different bed gradation as per the varying reach characteristics. Due to unavailability of data for the downstream cross sections, only one bed gradation (on bed materials collected from Pandu, Guwahati) has been used in all the cross sections. Moreover, heavy braiding occurs in the downstream region of the reach but no separate assumptions have been made for that. The analysis is carried out considering the centreline of the main channel and allowing the software to simulate the flow in the adjacent braids.

5. RESULTS AND DISCUSSIONS

5.1 Erosion and Deposition Changes Along the River Bed.

a)Second cross section

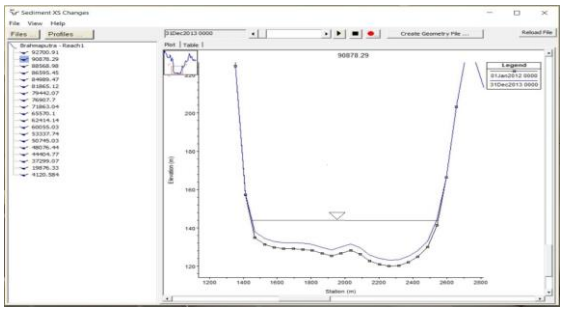

Fig 12: Second Cross Section

From the above graph, it is very clear that deposition of around 4metres depth has occurred in this cross section.

b) Fourth cross section

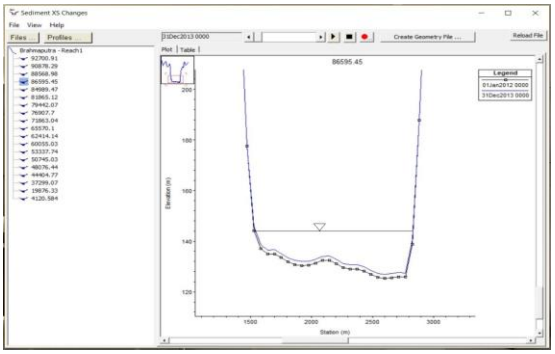

Fig 13: Fourth Cross Section

c) Eighth cross section

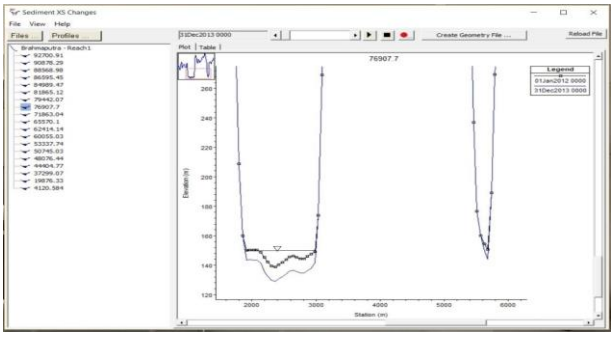

Fig 14: Eighth Cross Section

From the above graph, it is very clear that erosion of around 12metres depth has occurred in this cross section.

d) Tenth cross section

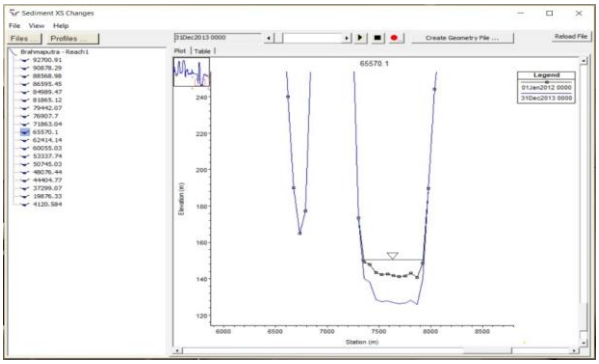

Fig 15: Tenth Cross Section

From the above graph, it is very clear that erosion of around 18metres depth has occurred in this cross section.

e) Twelfth cross section

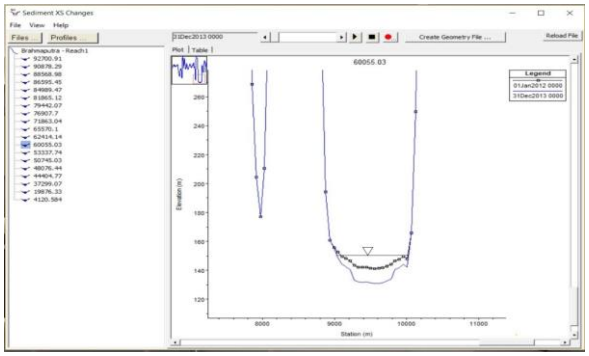

Fig 16: Twelfth Cross Cection

From the above graph, it is very clear that erosion of around 10metres depth has occurred in this cross section.

f) Fourteenth cross section

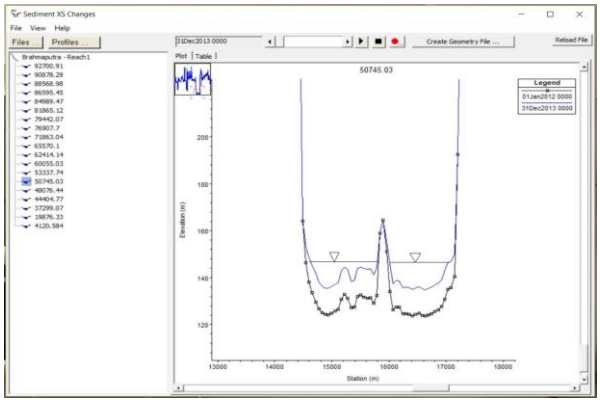

Fig 17: Fourteenth Cross Cection

From the above graph, it is very clear that deposition of around 10metres depth has occurred in this cross section.

g) Seventeenth cross section

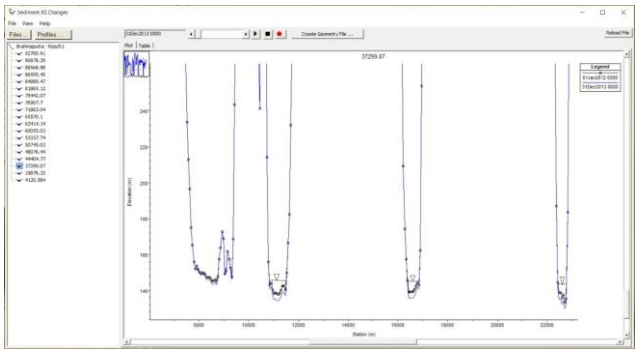

Fig 18: Seventeenth Cross Section

From the above graph, it is very clear that erosion of around 3metres depth has occurred in this cross section.

5.2 Variation of Flow Velocity Along the Reach

In the figure below, the variation of flow velocity along the different cross sections of the reach is shown. Here also, five curves have been considered to show the variation of flow velocity

longitudinally across the reach for duration of six months each.

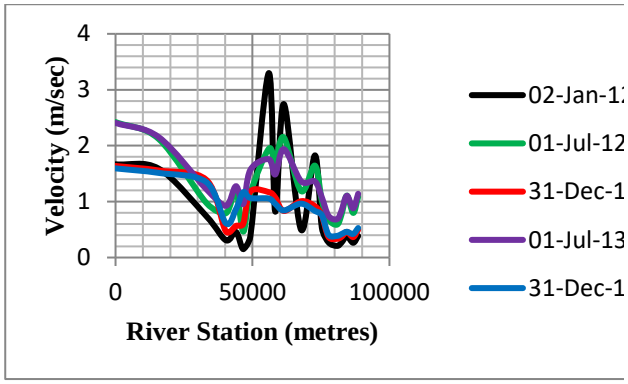

Fig 19: Variation of Flow Velocity Along the Reach

5.3 Variation of effective depth along the reach

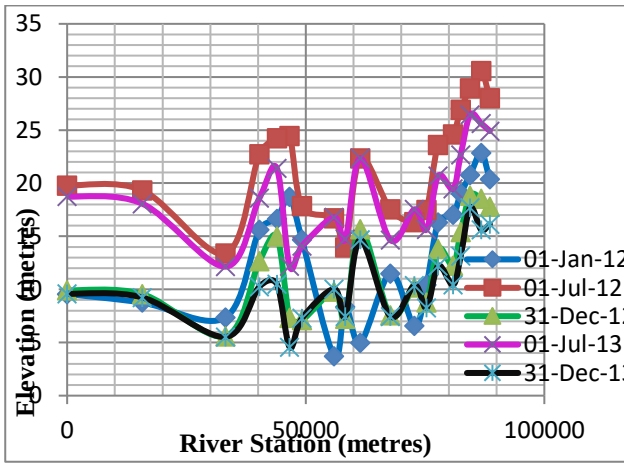

Fig 20: Variation of Effective Depth Along the Reach

In the figure above, the variation of effective depth along the different cross sections of the reach is shown. Here also, five curves have been considered to show the variation longitudinally across the reach for duration of six months each.

5.4 Variation of Shear Stress Along the Reach

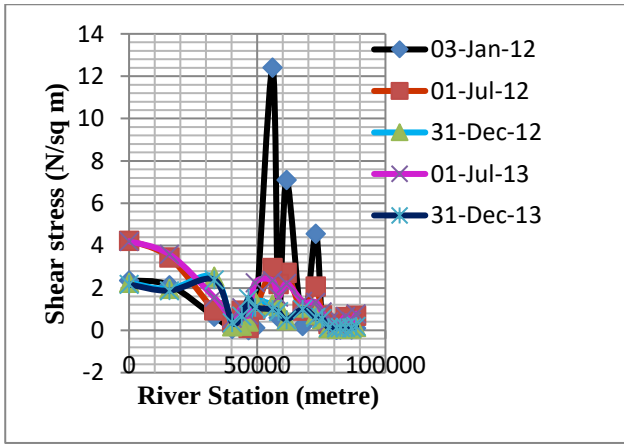

Fig 21: Variation of Shear Stress Slong the Reach

In the above figure, the variation of shear stress along the reach is plotted. Five curves are taken into consideration, each for duration of six months.

5.5 Mass Bed Change (cumulative) (tonnes)

Fig 22: Mass Bed Change (cum) 3 Jan 2012

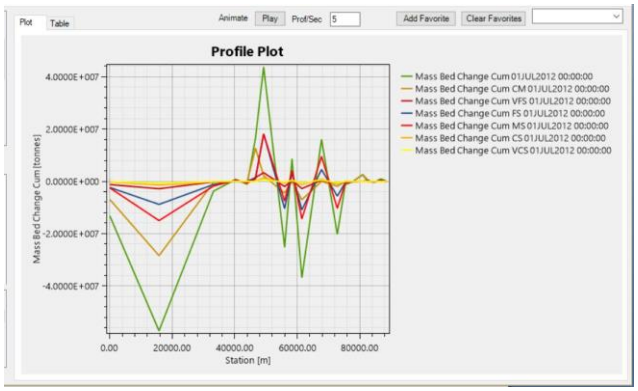

Fig 23: Mass Bed Change (cum) 1July 2012

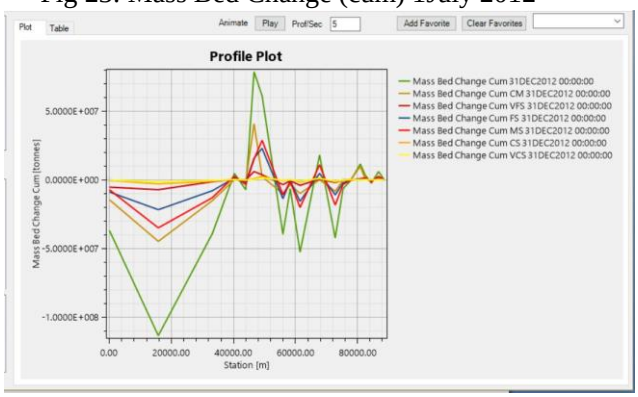

Fig 24: Mass Bed Change (cum) 31 December 2012

Fig 25: Mass Bed Change (cum) 1July 2013

Fig 26: Mass Bed Change (cum) 31Dec 2013

The five different parameters studied are: depth of erosion and deposition, effective channel depth, shear stress, flow velocity and cumulative mass bed change. After analysing the above mentioned five parameters, it has been observed that maximum erosion and maximum deposition of 18 metres and 10 metres has occurred at Palasbari and Gumi respectively. In the cross sections near Palasbari, erosion of varying depths has occurred whereas in the cross sections near Gumi, where the river is heavily braided, huge depositions have taken place. The same is reflected in the variation of velocity graphs. In the cross sections where erosion has taken place, the velocity has peaked and near Gumi the graph has assumed a minimum value.

In the variation of shear stress, it is highest where the velocity has peaked and lowest where the velocity is also low. In the later graphs of cumulative mass bed change, the distribution of sediments along the reach as per their size and gradation has been shown.

The results obtained above shows the need to remove the excessively deposited sediment to reduce braiding of the river in the downstream. In order to stabilise the river and to restrict the flow of the river in one single channel, it is, thus, imperative that some measures are carried out.

6. CONCLUSION

From the above results and discussion, it can be seen that the Brahmaputra river deposits as well as erodes huge amount of sediment along the reach that has been studied. However, the reach taken under consideration is of length 83.5kilometres only. The Brahmaputra river reach is much larger and more complex than this span of 83.5 kilometres. As such a more detailed and extensive study of the entire reach of the river needs to be done to derive a more reasonable conclusion.

It is very difficult to replicate the exact condition of a river in a software model. There are numerous variables and limited data available. Therefore, there are also limitations to this study such as:

a) Only single bed gradation of bed materials collected from Pandu site is available and it is used in all the cross sections till downstream for sediment analysis.
b) The choice of sediment transport equation. There is no proper equation specified for computing sediment transport capacity of the Brahmaputra River.
c) The Manning's roughness coefficient is kept constant for all the cross sections and both the banks of the river.
d) A very important limitation of this project is the unavailability of recent data. The flow hydrograph used in the study are from 5 years ago i.e. 2012 & 2013.

A thorough geo-morphological investigation of the Brahmaputra River basin, along with recording of discharge data and sediment transport load is of utmost importance for any kind of research work to obtain genuine results.

ACKNOWLEDGEMENT

I would like to express my heartfelt gratitude to my guide Dr. Bipul Talukdar, Associate Professor of Civil Engineering Department, Assam Engineering College for his advice, support and able guidance.

I am also very grateful to Mr. Tapodhan Das, Additional Chief Engineer, Water Resources Department, Assam and Dr. Rajib Kumar Bhattacharjya, Professor, IIT Guwahati for their kind cooperation, help and valuable advice regarding the project.

I am also indebted to the Civil Engineering Department, Assam Engineering College, Gauhati University for giving me the opportunity to carry out this work.

REFERENCES

1. Barbe, Donald E., Fagot K. and McCorquodale, J.A. "Effects on dredging due to diversions from the lower Mississippi River." Published on Journal of Waterway, Port, Coastal and Ocean Engineering, Vol 126, No 3. (2000) ASCE.
2. Dade, W. B. "Grain size, sediment transport and alluvial channel pattern." Institute of Theoretical Geophysics, University of Cambridge. Published in May, 2000.
3. Gibson, S., Brunner, G., Piper, S. and Jense, M., Research Hydraulic Engineer, US Army Corps of Engineers, Hydraulic Engineering Centre, Davis 95616.
4. Fleming, M.J., Pak, J.H. and Gibson, S.A. "Modeling Watershed and Riverine Sediment Processes with HEC HMS and HEC RAS." Watershed Management Conference, ASCE(2010).
5. Fischer, S., Pietron, J., Bring A. and Thorslund, J. "Present to future sediment transport of the Brahmaputra river: reducing uncertainty in predictions and management." Published in August, 2016.
6. Jensen, M. R., Piper, S.S. and Brunner, G.W. "Lateral Weir and Split Flow Optimization with the Hydrologic Engineering Center's River Analysis System (HEC-RAS)" Joint Conference on Water Resource Engineering and Water Resources Planning and Management, 2000.
7. Corum, Z., Comport, B. and Gibson, S. "Calibrating a Sediment Transport Model through a Gravel-Sand Transition: Avoiding Equifinality Errors in HEC-RAS Models of the Puyallup and White Rivers." World Environmental and Water Resources Congress 2017.

Trap efficiency of porcupine system in alluvial rivers

Gayan A.[1] and Talukdar B.[2]

[1]PG Student, Department of Civil Engineering, Assam Engineering College, Jalukbari-781013, India.
[2]Associate Professor, Department of Civil Engineering, Assam Engineering College, Jalukbari-781013, India.

ABSTRACT

A common problem faced during floods is scouring of the river bed and bank, subsequently leading to a change in the course of the river along with losses to both land and property. A number of riverbank protection measures have been engineered. Porcupine has been developed as a preventive measure which traps the sediments, thereby controlling scouring. In this study, an attempt has been made to study the deposition pattern and sediment trap efficiency of porcupine systems with laboratory experiments. Various configurations of layout of porcupines have been investigated. The velocity at upstream, mid and downstream has been measured with the help of Acoustic Doppler Velocimeter (ADV) for every configuration. Some dimensionless indices have been developed and comparison between them and trap efficiency has also been shown graphically. Moreover, the contour plots of the sediment deposition pattern have been shown.

Keywords: Scouring, Porcupine, Trap efficiency, Acoustic Doppler Velocimeter

1. INTRODUCTION

RCC porcupine is a prismatic type permeable structure, comprises of six members made of RCC, which are joined with the help of iron nuts and bolts. Porcupines can make the river deposit its silt in and around the porcupine, slow down the velocity of flow of the river, stop riverbank erosion, reclaim land, i.e., build up scoured or a low area to utilizable level, stop bed scour, maintain bed level etc.

The objective of the proposed study is to logically study the pattern of sediment deposition caused by various configurations of porcupine field layout and to make critical comparisons between the performance of various models of porcupine fields (defined on the basis of some dimensionless parameters) in terms of their sediment trapping efficiency.

2 METHODOLOGY AND PROCEDURE

2.1Experimental channel

All the experiments for this study were carried out in the Hydraulics Laboratory Channel of Assam Engineering College, Guwahati. The channel is 19.14 m long, 0.96 m wide, 1.275 m deep with 0.49 m thickness of sand bed. Three pumps of 7.5 HP, 10 HP and 15 HP are used to feed water into the channel. The bed and bank materials used in the laboratory channel were collected from the River Brahmaputra, Pandu Port of Maligaon, Guwahati, Assam.

Fig. 1. Experimental Channel

2.2 Porcupine model

The models are prepared with MS Rods, circular in diameter (6mm) and 12 cm in length which are anchored together by welding. Extended lengths of 3 cm for each member of the model are kept for embedding them into the simulated river bed in the experimental channel.

Fig. 2. Model of Porcupine made of MS Rod

2.3 Experimental procedure

First, the bed of the channel is levelled and the flow is gradually introduced into it by releasing the discharge valve slowly until a point at which the bed materials just tend to lift representing incipient motion condition. The valve was then readjusted back a little so that the velocity of flow remains a little less than the critical velocity (that corresponds to incipient motion condition). Before starting of experimentation with the porcupine field models, this clear water run was continued for half an hour. Then the motor was shut and the rectangular weir was removed which allowed the water to drain out gradually from the channel without disturbing the sand bed. The position of the discharge valve (that regulates the quantity of flow into the channel) was thus fixed and was kept constant for the rest of all experiments. Sand bed levels were measured with the help of point gauge.

After placement of the first trial model of the porcupine field, the sediment bed of flume was again levelled around the field and the flow was introduced in the channel. The discharge was kept same as the clear water run. Once the flow came into steady state condition, a fixed quantity of sediment was injected into the channel 2 m upstream of the porcupine field for 45 minutes. Then the motor was shut down and the rectangular weir was removed which allowed the water to drain out gradually from the channel. After the water was drained completely, sand bed levels were again measured with the help of point gauge. The same procedure was followed for the rest of the model porcupine fields studied in this work.

2.4 Measurement of velocity

The velocity was measured with the help of Acoustic Doppler Velocimeter (ADV). The velocity was measured at three points for each trial i.e., at the upstream, mid and downstream.

Fig. 3. Acoustic Doppler Velocimeter (ADV)

2.5 Initial test results

The specific gravity and porosity of the bed material was found to be 2.58 and 34% while that of the bank material was 2.78 and 35% respectively. From the Direct Shear Test, the values of Φ and c were found to be 29^0 and 0 respectively.

2.6 Indices

Some indices were coined in this study in order to differentiate between various porcupine field models in their terms. These indices are defined as under:

a) Porcupine Field Density Index (PFDI)
= Length of one retard / Spacing between the two retards = L_r / L_s

b) Porcupine Compartment Density Index (PCDI)
= Length of retard / Total length of compartment = L_r / L_c

c) Porcupine Field Length Factor (PFLF)
= Length of one compartment of porcupine field / Total length of compartments= L_s / L_c

d) PFVI (Porcupine Field Velocity Index) = (Upstream velocity – Mid velocity)/ (Mid velocity – Downstream velocity)

Table 1. Range of Dimensional Parameters for the Trial Porcupine Field Models.

Trial No.	Length of Retards (L_r)	Spacing of Retards (L_s) (cm)	No. of compartment	Weight of sand injected (kg)	Length of compartment (L_c) (cm)	PFLF ($\frac{L_s}{L_c}$)	PCDI ($\frac{L_r}{L_c}$)	PFDI ($\frac{L_s}{L_c}$)
1	24	15	2	3	30	0.5	0.8	1.6
2	24	15	2	6	30	0.5	0.8	1.6
3	24	15	3	3	45	0.33	0.53	1.6
4	24	15	3	6	45	0.33	0.53	1.6
5	24	30	2	3	60	0.5	0.4	0.8
6	24	30	2	6	60	0.5	0.4	0.8
7	24	30	3	3	90	0.33	0.27	0.8
8	24	30	3	6	90	0.33	0.27	0.8
9	36	15	2	3	30	0.5	1.2	2.4
10	36	15	3	3	45	0.33	0.8	2.4
11	36	30	2	3	60	0.5	0.6	1.2
12	36	30	3	3	90	0.33	0.4	1.2

Using the dimensional parameters as listed in Table 1, trial porcupine field models were prepared and laid on the channel with the simulated river bed. Relevant observations were made to study the sediment deposition of these trial field models. Length of each porcupine field was started from a distance of 6 m from the upstream end of the simulated bed in the channel and the width started from the bank of the channel. After each experimental run, the bed profiles were measured in the form of 0.30 m x 0.48 m grid with point gauge along three imaginary lines (A, B & C) on the channel bed along the flow, as shown in figure 4.

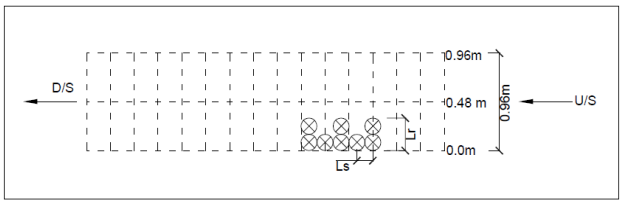

Fig. 4. Line Diagram of Channel Grid

The sediment deposition in the porcupine field with every dimensional variation is shown by contour plots drawn with the help of SURFER@13 software. These plots clearly show the deposition of sand around the porcupine fields. Length of the porcupine field is indicated starting from the point nearest to the upstream end of channel and width is indicated starting from the wall of the channel. The color legend shows sediment deposition in m.

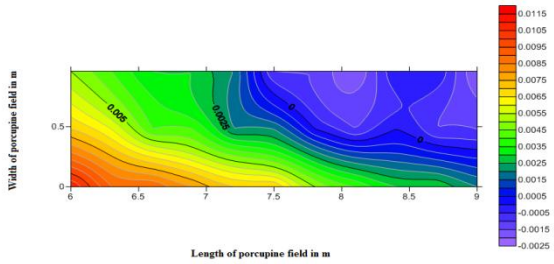

Fig. 5. Contour Plot for 1stTrial of Porcupine Field for PFDI= 1.6, PCDI= 0.8 and PFLF= 0.5

3 RESULTS AND DISCUSSIONS

3.1 Trap efficiency calculation

Table 2. Velocity Index and Trap Efficiency Calculation

Trial No.	PFVI = $(\frac{u/s-mid}{mid-d/s})$	Water Depth (cm)	Sediment Concen-tration q_s (ppm)	Weight of sand deposited (kg)	Trap Efficiency (%)
1	2.68	15	300	0.030358	1.01
2	2.35	15	600	0.099392	1.65
3	1.19	15	300	0.0443717	1.48
4	2.64	15	700	0.1023051	1.70
5	3.76	15	300	0.0358119	1.19
6	4.51	15	600	0.0883257	1.47
7	1.20	15	300	0.0376264	1.25
8	3.16	15	700	0.0911562	1.52
9	1.58	15	600	0.1417063	2.36
10	1.05	15	700	0.159361	2.66
11	1.44	14	600	0.146330	2.44
12	0.84	14	600	0.175195	2.92

3.2 Comparison of Trap Efficiency with different indices and their graphical representation

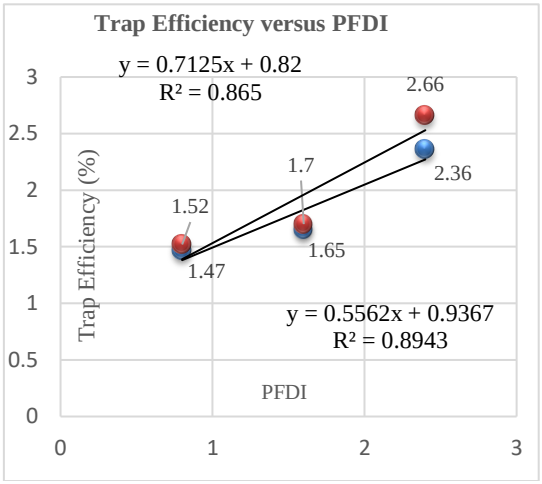

Fig. 6.Plot of Trap Efficiency versus PFDI when 6 kg of Sediment was Injected

Series 1 represents plot of trap efficiency versus PFDI for PFLF = 0.5, when 6 kg of sediment was injected
Series 2 represents plot of trap efficiency versus PFDI for PFLF = 0.33, when 6 kg of sediment was injected.

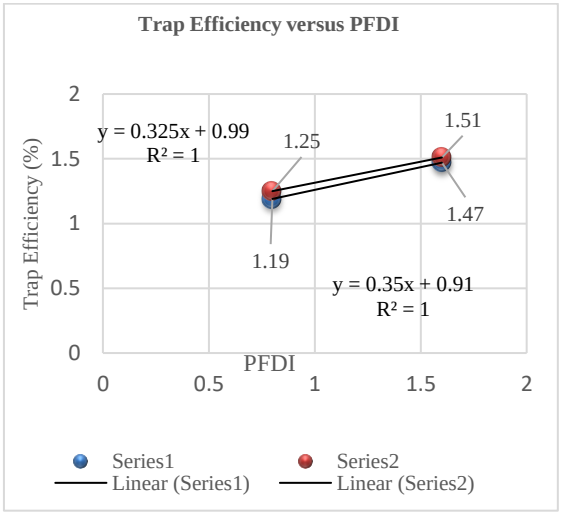

Fig. 7.Plot of Trap Efficiency versus PFDI when 3 kg of Sediment was Injected

Series 1 represents plot of trap efficiency versus PFDI for PFLF = 0.5, when 3 kg of sediment was injected
Series 2 represents plot of trap efficiency versus PFDI for PFLF = 0.33, when 3 kg of sediment was injected

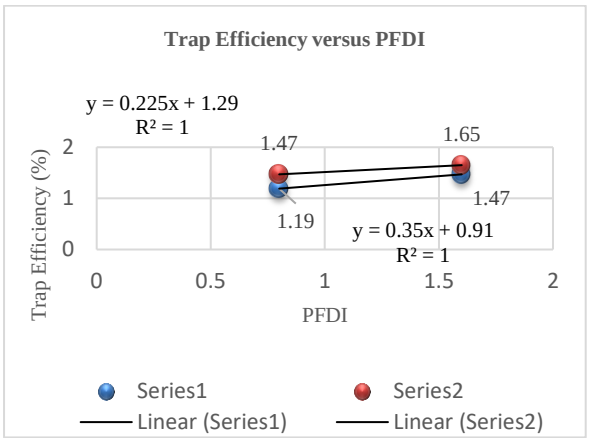

Fig. 8. Plot of Trap Efficiency versus PFDI for PFLF = 0.5

Series 1 represents plot of trap efficiency versus PFDI for PFLF = 0.5, when 3 kg of sediment was injected
Series 2 represents plot of trap efficiency versus PFDI for PFLF = 0.5, when 6 kg of sediment was injected

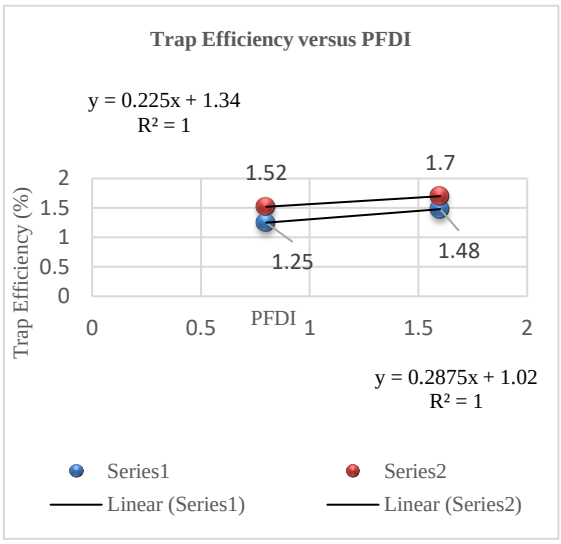

Fig. 9.Plot of Trap Efficiency versus PFDI for PFLF = 0.33

Series 1 represents plot of trap efficiency versus PFDI for PFLF = 0.33, when 3 kg of sediment was injected
Series 2 represents plot of trap efficiency versus PFDI for PFLF = 0.33, when 6 kg of sediment was injected

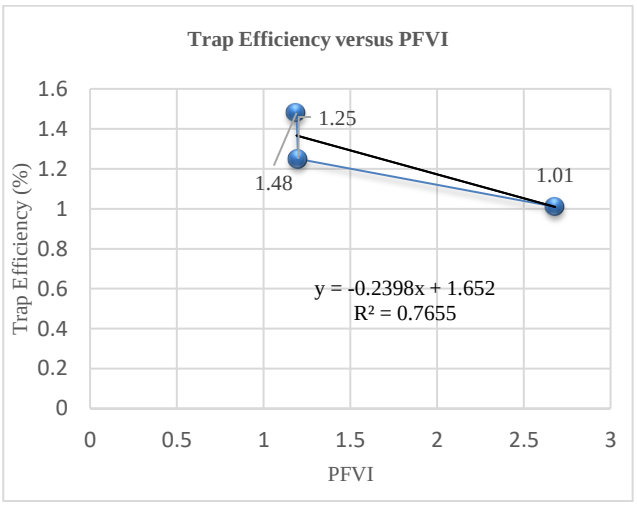

Fig. 10. Plot of Trap Efficiency versus PVFI for q_s= 300 ppm

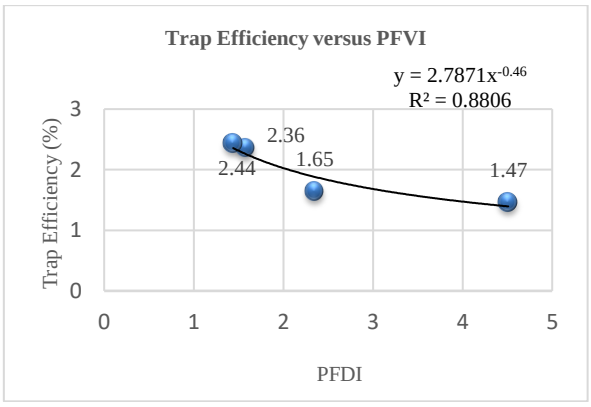

Fig. 11. Plot of Trap Efficiency versus PVFI for q_s= 600 ppm

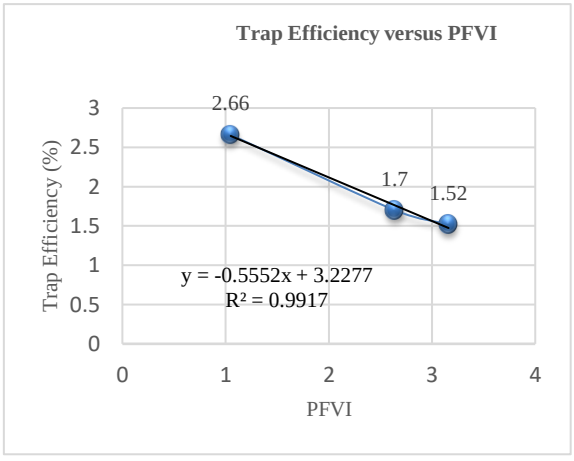

Fig.12. Plot of Trap Efficiency versus PVFI for q_s= 700 ppm

.

4 CONCLUSION

A total of twelve experimental trials were conducted in which the length of retards, spacing of retards and sediment concentration were changed. The contour plots of each of the twelve trials were then drawn using Surfer and the sediment deposition pattern for each experimental trial was calculated. The velocity for each trial was measured using Acoustic Doppler Velocimeter (ADV). The graphical representation of the different indices versus trap efficiency was done and it was found that trap efficiency is inversely proportional to Porcupine Field Length Factor (PFLF), directly proportional to amount of sediment injected and inversely proportional to Porcupine Field Velocity Index (PFVI). Further it was found that Porcupine Field Velocity Index (PFVI) is inversely proportional to sediment concentration. The application of porcupine system is an effective and economic method for river training purpose. It serves the purpose of prevention of scouring by deposition of sediments facilitated by the significant decrease in intensity of flow caused by a decrease in the velocity of flow by the porcupines. The fabrication of these structures is simple and easy, requiring only concrete and steel rods, with a few numbers of nuts and bolts only. Their installation can be done by just placing them successively and connecting them together using wire rope, thus needing no skillful labour.

REFERENCES

1) Aamir M. and Sharma N. (2014): Sediment Trap Efficiency of Porcupine Systems for Riverbank Protection,ISH-HYDRO 2014 INTERNATIONAL.
2) Aamir M. and Sharma N. (2015a): Efficiency of Triangular and Prismatic Porcupines in Capturing Sediment for River raining,HYDRO 2015 INTERNATIONAL. 20th International Conference on hydraulics, Water Resources and River Engineering.
3) Aamir M. and Sharma N. (2015b): Riverbank Protection with Porcupine Systems: Development of Rational Design Methodology,ISH Journal of Hydraulic Engineering, April 2015.
4) Brahmaputra Board, Guwahati (2012): Protection of Majuli Island from Floods and Erosion,Technical report.
5) Das M.M. (2011): Open Channel Flow,PHI Learning Private Limited.
6) Garde R.J. and Rangaraju K.G. (1977): Mechanics of Sediment Transportation and Alluvial Stream Problems,University of Roorkee, Roorkee.Kalita S. (2017): A Comprehensive Study on the Sediment Trapping Efficiencies of Various Riparian and Aquatic Vegetations on Open Channel flow Environment,HYDRO-2017, The 22nd International conference on Hydraulics, Water Resources and Coastal Engineering. L.D. College of Engineering, Ahmedabad.
7) Punmia B.C., Jain A.K. and Jain A.K. (2011): Soil Mechanics and Foundations, LAXMI PUBLICATIONS (P). LTD.
8) Sarkar M.H., Akter J. and Ferdaous R. (2011): Riverbank Protection Measures in the Brahmaputra-Jamuna River: Bangladesh Experience,Center for Environmental and Geographic Information Services (CEGIS), Dhaka, Bangladesh.
9) Sinha T. (2017): Effect on Permeable Spurs (Porcupines) and their Dimensional Variations on the Erosion/Sedimentation Pattern of Open Channel Flow,HYDRO-2017, the 22nd International conference on Hydraulics, Water Resources and Coastal Engineering. L.D. College of Engineering, Ahmedabad.

Threshold velocity of geo-mega bag revetment failure for bank protection works

Barman, R. [1] and Talukdar, B.[2]

[1] Guest Faculty, Department of Civil Engineering, Assam Engineering College, Jalukbari-781013, India
[2] Associate Professor, Department of Civil Engineering, Assam Engineering College, Jalukbari-781013, India

ABSTRACT

Bank revetment with sand filled geotextile bags is one of the methods of river bank protection carried out in Assam. However, till now, lots of revetments have been failed after some period of application of the revetment. In the previous study, laboratory experiments as well as theoretical study was carried out to analyse the stability of geobag revetment for conventional bag size (1.03 m x 0.7 m) of 126 kg weight for 1:10,000 and 1:500 bed slope. This paper reports the second part of the study dealing with the geo mega bags for high slope (1:500) as the conventional size was found to be safe for mild slope (1:10,000). Here, the behaviour of geo mega bags under submerged conditions has been studied experimentally and theoretically to check the suitability of geobags, for different situations. The experiments are conducted with two different arrangements of geo mega bags with different percentage of sand filing in 1:500 bed slope. Failure modes and failure velocities for each case is observed in the experiments and the causes of failure and probable remedial measures have been discussed. In theoretical analysis, stability analysis from sliding and uplift displacement criteria is done to find the theoretical safe velocities for different situations. The laboratory results are compared with the theoretical calculations and it has been found that the results from both the analysis are almost matching.

Keywords: bank revetment, geo mega bags, failure modes, sliding, uplift, hydraulic stability

1. INTRODUCTION

To prevent the huge amount of financial and other losses that occurred in the past years because of riverbank erosion, the Assam Government developed several riverbank protection measures. Out of those, a very popular one is to use sand-filled geotextile bags (commonly called geobags) in the riverbanks, to save the lives and properties of citizens from flood and erosion. Geobags are polyester-made geosynthetic products, that are specially designed for good soil tightness and high seam efficiency. However, due to the lack of detailed scientific studies, there is little technical understanding about them. In the previous study, stability of geobag revetment for conventional bag size (1.03 m x 0.7 m) of 126 kg weight for 1:10,000 and 1:500 bed slope was carried out. In that study, it was concluded that size and weight of the geobags should be increased. In this particular study, stability analysis is carried out with geo mega bag revetment with an approximate bag size (2.7 m x 1.3 m) of 1638 kg weight for 1:500 bed slope. To understand the hydrodynamic forces related to geo mega bag failure, we are going to use a distorted scale model with an artificial open channel and miniature geo mega bags, in a laboratory. The main objectives of this study are:

1. To understand the performance of a geo mega bag revetment in submerged conditions.
2. To observe the stability of different percentages of sand filled geo mega bags under different flow parameters.
3. To determine the causes of failure and discuss a few probable remedial measures.

Several scholars have performed a few similar studies. Neil et al (2008) performed tests on small-scale bags to examine their various design and placement aspects, and tried to compare their behaviour with that of rock riprap. Recio and Oumeraci (2009) analysed multiple aspects of Sand Filled Container (SFC) stability, by performing laboratory experiments to investigate the stability of geotextile containers arranged in a variety of configurations, and over a wide range of wave conditions.

Akter et al (2009) observed the failure modes of a geobag structure using a series of physical model tests, and established that overtopping, sliding, puncturing, pullout/dislodgement, and toe scour are the most common failure modes for geobags. Oumeraci et al (2012) investigated the hydraulic stability of geotextile sand container (GSC) structures to better understand the processes and failure-causing parameters of GSCs.

Again, using both fixed bed and mobile sediment bed configurations, Akter et al (2013a) performed laboratory experiments to study their failure modes. They also modelled the relevant hydrodynamic

forces with the Conveyance Estimation System software, by using a distorted scale model. The CES results found in this study were used to further develop a mapped velocity field, for a coupled DEM simulation of geobag revetment failure (Akter et al., 2013b).

2. METHODOLOGY AND PROCEDURE

2.1. Flume channel

The laboratory experiments were carried out in the flume channel of the hydraulics laboratory of Assam Engineering College having dimension of 20000 mm X 960 mm X 1240 mm. A mobile sediment bed of locally available sand with average thickness 400 mm above concrete floor of the channel has been used for the tests.

2.2. Model geo mega bags

Distorted scale geo mega bags are used made up of combination of needle punched Non-woven PP Geotextile and slit film tape yarn PP woven geotextile having an outer layer of Geo-textile woven fabric and an inner layer of non-woven geotextile of 300 GSM manufactured from poly propylene conforming to relevant ISO standard and conforming to technical specification. The bags are filled with locally available sand of characteristic grain size 0.2 to 0.25 mm, porosity 40% and Cu 1.3 with different percentage of filling (100% filled, 80% filled and 60% filled). In tables 1 and 2 below, scale ratio for experimental set up, actual size, and size of model geo mega bags with different percentage of filling used are shown. This actual size of the bag is taken from the erosion control project taken up by the Water Resource Department of Assam Government, at Nimatighat.

Table 1. Scale Ratio of Model Bags.

Quantity	Dimensions	Scale Ratio
Length, Breadth	L	1:12
Bag volume / mass	L^3	1:1728
Velocity	$L^{1/2}$	1:3.46
Discharge	$L^{5/2}$	1:498.83
Shear stress	$L^{3/2}$	1:41.57

Table 2. Size of Geo mega Bags.

Bag Type	Bag Size	Filled L	Filled B	Filled H	Weight (kg)
Actual size	3.2 m X 1.7 m	2.7 m	1.3 m	0.3 m	1638
Model size (100% filled)	-	225 mm	105 mm	25mm	0.95
Model size (80% filled)	-	235 mm	115 mm	22 mm	0.77
Model size (60% filled)	-	240 mm	125 mm	18 mm	0.58

100% filled bags are filled with sand up to full capacity which is a model of the bag used in the field of filled dimension 2.7 m x 1.3 m. The geo mega bags are nearly completely saturated with water as they are mostly placed below the waterline. If ρ_b, ρ_s, ρ_w are the densities of model bags, sand and water respectively, the mass density of the bags is calculated with the equation (1), shown below. n is the porosity of sand, depending on where the bag is located.

$$\rho_b = \rho_s(1-n)+ \rho_w(n) \quad (1)$$

2.3. Test section

A two-metre long test section is prepared for the experiments. The test section has a side slope of 1V:2H within the test flume as seen in figure 1. The width and height of the banks are 300mm and 150mm respectively. Along the upstream and downstream of the test section, also in its opposite side, a bank is constructed with river bank material maintaining the same slope (1:500).

Fig 1. Laboratory Model Set-up.

2.4. Experimental criteria

The experiments are performed for two different arrangements of geobags.

1. AM1 Running bond: The geo mega bags are laid longitudinally in a typical brick wall pattern, with the geobag joints lying in the middle of the bags in the layers directly above and below. The running bond is displayed in figure 2.

Fig 2. Running Bond.

2. AM2 Half-basket weave: The AM2 bond comprises of alternate layers of bags aligned with their longer and shorter axes parallel to the flow direction as shown in figure 3.

Fig 3. Half-basket Weave Bond.

The experiments are conducted in the bed slope 1:500 for three conditions of depth stated below.

1. Depth A : Up to 50% of the structure height.
2. Depth B : 50% - 80% of the structure height.
3. Depth C : 80% - 100% of the structure height.

The experiments are performed individually with 100% filled, 80% filled and 60% filled geo mega bags. For 60% filled bags, another experiment is performed confining the revetment structure with wire mesh for 1 m. Each experiment is run for 3 hours such that all physical processes can occur. Different failure modes in the revetment are observed and studied. Also the theoretical analysis is carried out and compared the results from both the analysis.

3. OBSERVATIONS AND INTERPRETATIONS

3.1. Observations in the revetment

For the two arrangements with 100% filled bags, similar types of observations are made. No change in the revetment is seen for all three depth ranges, as shown in figure 4 and 5.

Fig 4. Observation in AMI (100% filled).

Fig 5. Observation in AM2 (100% filled).

For 80% filled bags, sliding and displacement in the bottom layer is seen in the highest depth range for both the arrangements, but no bag is pulled out which can be seen in figure 6 and 7.

Fig 6. Observation in AMI (80% filled).

Fig 7. Observation in AM2 (80% filled).

The experimental tests with 60% filled bags are run with only one depth range i.e. 50% of the structure height as failure is seen in the 1st range itself which is seen below. For AM1, uplifting of bags and displacement from the entire layer occurs. For AM2, sliding of the bags occur, many are pulled out and carried away. For the two arrangements mode of failure is shown in figure 8 and 9.

Fig 8. Observation in AM1 (60% filled).

Fig 9. Observation in AM2 (60% filled).

In the test for confined revetment with 60% filled bags, void flow and no change in the revetment is seen for both the arrangements and all three depth ranges as shown in figure 10 and 11.

Fig 10. Observation in AM1 (60% filled, confined).

Fig 11. Observation in AM2 (60% filled, confined).

3.2. Interpretations

- It has been observed that 100% and 80% filled large bags are found to be safe against the flow while 60% filled bags are washed away. If the bags are covered by wire mesh, then the revetment behaves as one structure which is found to be safe against the flow.
- After the failure of revetment, the displaced bags get deposited in the downstream of the channel. This creates an obstruction for the waterway and a hydraulic jump is formed in the downstream, as shown in figure 12.

Fig 12. Formation of Hydraulic Jump.

3.3. Causes of failure

- In the laboratory revetment, there is a high water-pressure difference between the channel side and the geobag lee side. This introduced

turbulent bursting-induced flow through the revetment voids.

- Higher stream wise velocities influenced the bag pull-out processes.
- Internal sliding, combined with other modes, characterized the failure process in almost all cases.

4. THEORETICAL ANALYSIS

The flow is associated with hydrodynamic forces, i.e. drag force, lift force, buoyancy force and the self-weight of the geobags. The drag and lift forces are calculated with the equations (2) and (3) respectively where F_D and F_L are the drag and lift force, C_D and C_L are the drag and lift coefficients. A is the cross sectional area perpendicular to the flow and u is the velocity of flow.

$$F_D = 0.5C_D\rho_w Au^2 \quad (2)$$

$$F_L = 0.5C_L\rho_w Au^2 \quad (3)$$

The stability of the bag is lost from uplift displacement criteria if the wave induced vertical forces exceed the weight of the bag expressed by equation (4).

$$F_L \leq (\rho_b - \rho_w)\, gV_m \quad (4)$$

Where g is the acceleration due to gravity and V_m is the volume of the bag. Again when wave-induced horizontal forces exceed the resisting forces, then sliding of the bags occur. The stability criteria from sliding force is seen in equation (5).

$$F_D \leq [(\rho_b - \rho_w)gV_m - FL\,]\mu \quad (5)$$

Where μ is the friction factor taken as 0.53. For 1:500 bed slope the coefficients C_D and C_L are calculated as 3 (C_D) and 4.8 (C_L) from the equation (6), based on the findings of Wu et al. (1999), considering C_D and C_L as 0.8 and 0.5 from the findings of Recio and Oumeraci (2009) (Ref no 6) for 1:10,000 bed slope.

$$C_D = 2DgS/TV^2 \quad (6)$$

D is the depth of flow, S is the bed slope, T is the height of vegetation.

Theoretical safe velocities for a single geo mega bag from uplift and sliding displacement criteria for all experimental arrangements are calculated using all the equations mentioned above and compared with the laboratory results.

5. RESULTS AND DISCUSSIONS

Results from both experimental and theoretical analysis is shown in table 3, 4 and 5 for 100% filled, 80% filled and 60% filled bags respectively.

Table 3. Results for 100% Filled Bags.

Analysis	Failure modes	Model Velocity (m/s)	Prototype Velocity (m/s)
Laboratory observations	Void flow	0.4	1.38
	No change in the revetment	0.5	1.73
	No change in the revetment	0.6	2.08
Theoretical safe velocities	For uplift force	0.66	2.30
	For sliding force	0.45	1.56

Table 4. Results for 80% Filled Bags.

Analysis	Failure modes	Model Velocity (m/s)	Prototype Velocity (m/s)
Laboratory observations	Void flow	0.4	1.38
	Sliding starts	0.5	1.73
	Sliding and uplifting	0.6	2.08
Theoretical safe velocities	For uplift force	0.607	4.10
	For sliding force	0.41	1.42

Table 5. Results for 60% Filled Bags.

Analysis		Failure modes	Model Velocity (m/s)	Prototype Velocity (m/s)
Laboratory observations	For one bag	Sliding of bags, displacement of bags	0.4	1.38
	Considering whole revetment	Void flow	0.4	1.38
		No change in the revetment	0.5	1.73
		No change in the revetment	0.6	2.08
Theoretical safe velocities	Considering one bag	For uplift force	0.53	1.84
		For sliding force	0.36	1.25
	Considering whole revetment	For uplift force	1.085	3.75
		For sliding force	0.73	2.54

From the above tables the results from the analysis can be compared and certain discussion can be pointed out.

- In the laboratory tests for 100% filled bags, no change in the revetment was seen for model

velocities up to 0.6 m/s (prototype velocity 2.08 m/s). Again safe velocity for uplift force validates the laboratory data while safe velocity for sliding force is lower than the highest velocity in the channel.

- For 80% filled bags, sliding starts above 0.4m/s model velocity and uplifting occurs for model velocity 0.6 m/s which is almost validated by theoretical analysis.
- For 60% filled bags, sliding and displacement of bags occurs for unconfined revetment for model velocity 0.4 m/s and from theoretical analysis safe model velocity from sliding is 0.36 m/s.
- For confined revetment of 60% filled bags, safe theoretical velocities from both the criteria are higher than laboratory model velocities which validates the laboratory results as no change in the revetment takes place for model velocity up to 0.6 m/s.

5. CONCLUSIONS

It is seen that failure starts with sliding and proceeds with uplifting. The failure modes in the revetment structures are same for both the arrangements of bags in the revetment and both the arrangements (running bond and half basket weave bond) are suitable for geo mega bag application in field. The 100% filled geo mega bags can sustain in the field up to 2 m/s prototype velocity at 1:500 bed slope. But even 60% sand filled bags also can be used if the revetment is confined as the whole revetment behaves as one structure. The theoretical safe velocities also increase for 100% and 80% sand filled bags for confined revetment. Therefore, to resist velocity greater than that, the confinement of the revetment can be done.

REFERENCES

1) Akter, A., Wright, G., Crapper, M. and Pender, G. (2009): Failure Mechanism in Geobag Structure, *Proceedings of the 4th IASME/WSEAS International Conference on Water Resources, Hydraulics & Hydrology,* 25-30
2) Akter, A., Pender, G., Wright, G. and Crapper, M. (2013a): Performance of a Geobag Revetment I: Quasi-Physical Modelling, *Journal of Hydraulic Engineering, American Society of Civil Engineers*, 865-876
3) Akter, A., Pender, G., Wright, G. and Crapper, M. (2013b): Performance of a Geobag Revetment II: Numerical Modelling, *Journal of Hydraulic Engineering, American Society of Civil Engineers*, 877-885
4) Neill, C., Mannerström, M. and Azad, A.K. (2008): Model Tests on Geobags for Erosion Protection, *Fourth International Conference on Scour & Erosion*, pp. 404-411
5) Recio, J. and Oumeraci, H. (2009): Process based stability formulae for coastal structures made of geotextile sand containers. *Coastal Engineering V56*, 632 – 658
6) Recio, J., and Oumeraci, H. (2009): Processes affecting the hydraulic stability of coastal revetments made of geotextile sand containers. *Coastal Eng.,56(3),* 260–284
7) Soysa, V.A.N., Dassanayake, D.M.D.T.B. and Oumeraci, H. (2012): Hydraulic Stability of Submerged GSC Structures, ENGINEER - *The Institution of Engineers, Sri Lanka, Volume XXXXV, No. 04*, 31 - 40
8) Wu, F.C., Shen, H.W. and Chou, Y.J. (1999): Variation of Roughness Coefficients for Unsubmerged and Submerged Vegetation, *Journal of Hydraulic Engineering*, 934-942

WQI and Statistical Analysis Approach for Sustainable Management: A Case Study of Three Urban Lakes Situated in Delhi

Chakma, S. [1] and Sinha, V. [2]

[1] Chakma, S. Department of Civil Engineering, IIT- Delhi, Hauz Khas, New Delhi: 110016, India.
[2] Sinha, V. Department of Civil Engineering, IIT- Delhi, Hauz Khas, New Delhi: 110016, India.

ABSTRACT

The present work aims at assessing the water quality index (WQI) of Hauz Khas Lake (HKL), Sanjay Lake (SL) and National Zoological Park Lake (NZP) situated in Delhi urban district. The study of physico-chemical parameters such as pH, TDS, COD, BOD, DO, conductivity, several cations, anion, and heavy metals (iron, cadmium) analysis have been carried out. The assessed physico-chemical parameters for the three lakes have been statistically compared and correlated. The WQI value of HKL, SL, and NZP was found to be 102.9, 112.44, and 122.29 respectively. The results suggest that the origin of dissolved ions is from carbonate weathering. The study indicates that among the three studied lakes SL was found to be the most polluted. Moreover, the WQI calculated reveals that the water quality of the lakes under study is unsuitable and highly contaminated. The present study may be helpful towards framing sustainable management policies to contain the sources of pollutant for these urban lakes.

Keywords: Water Quality Index, Delhi, Physico-chemical parameters, Carbonate weathering, Sustainable management.

1. INTRODUCTION

Water quality refers to the physico-chemical, radiological and organic characteristics of water. The increasing environmental stress and the consequent rise in pollution load of water bodies is a global cause of concern. The deteriorating water quality parameters of rivers and inland water bodies like lakes needs immediate attention since it directly affects all aspects of ecosystems (Parmar et al., 2013). WHO report suggests that 80% of health related issues are due to contaminated water. This problem is more serious especially in developing countries like India, due to the exponential rise in urbanization in urban cities. Due to poor socio-economic growth associated with the exploitation of existing water resources, water is considered as the highest risk to the world for future due to increase in demand and decrease in freshwater sources (Chauhan and Singh, 2010); Srinivasamoorthy et al., 2013). Therefore, water quality needs to be periodically monitored, to locate major sources of contributing factors to minimize or contain pollutants at the point source itself.

Water quality index (WQI) is an important parameter for qualitative and quantitative assessment of contaminated water bodies. WQI is defined as a rating reflecting the composite influence of different water quality parameters and is calculated from the point of view of the suitability of water for human consumption (Tyagi et al., 2013). It provides a numerical figure that expresses general water quality at a certain location and time, based on numerous water quality parameters. The benefits of an index include its ability to conglomerate various measurements in a range of different measurement units in a single metric and its efficiency as a communication tool. (Yogendra and Puttaiah, 2008; Kangabam et al., 2017; Singh et al., 2015).

The present investigation was aimed at assessing and fitting the complex water quality data of three lakes in Delhi (Hauz Khas Lake, Sanjay Lake, and National Zoological Park Lake) into patterned information that is comprehensible and usable by the public based on WQI. This study will help in framing proper management strategies to minimize pollutant load in the lakes studied.

2. METHODOLOGY

Study Area

For the present study three lakes of Delhi (Hauz Khas Lake, Sanjay Lake, and National Zoological Park Lake) were studied and samples were collected from all these lakes from various strategic points (Fig.1).

Study Area I

Hauz Khas Lake is located in Hauz Khas village in District Park of urban south Delhi and has a water spread of 6 hectares, with its latitude being 28° 32'

58" N and longitude being 77° 12' 13'' E. Hauz Khas is a historic place and the lake inside it is 700 years old. The lake itself is 1.5 km long and is 26 km far from the Yamuna.

Increasing and haphazard urbanization led the catchment area of Hauz Khas Lake in Delhi to come down from 10 sq km in 1936 to less than 2 sq km today, which is more than an 80 % reduction.

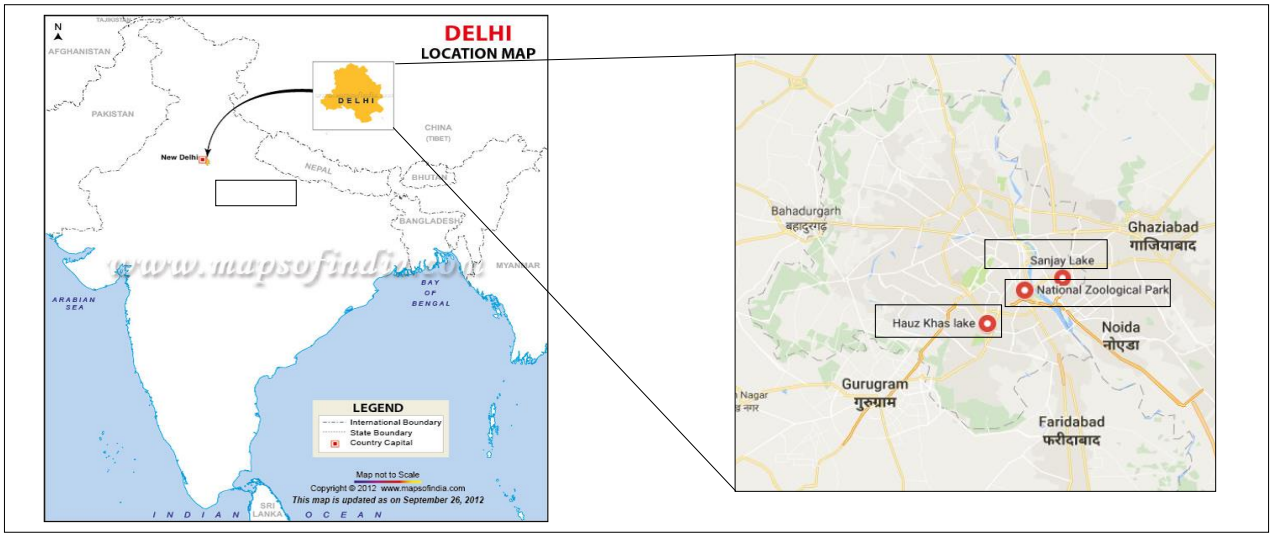

Fig 1. Location map of Hauz Khas Lake, Sanjay Lake, and National Zoological Park Lake

Study Area II

Sanjay Lake is an artificial lake located in Trilokpuri in East Delhi, between 28.6148° North latitude and Longitude being 77.3041° East longitude. The lake covers an area of approximately 17 hectares (42 acres) in the middle of a 69 hectares (170 acres) forest cover in Sanjay Lake Park. The lake draws its water from the rains and sewage.

Study Area III

The lake is present inside the National Zoological Park (originally Delhi Zoo) is a 176-acre (71 ha) zoo near the Old Fort in Delhi, India. The latitude of the lake is 28.6030° N and longitude is 77.2465° E.

Collection of water samples

The surface water samples were collected from Hauz Khas Lake, Sanjay Lake and National Zoological Park Lake. All the surface water samples were collected in acid washed, 2 L pre-cleaned polyethylene bottles for an in the month of January 2018 during the morning hours. The samples were taken from 15 to 20cm below the water surface and away from the banks of the lakes (where the water is less turbid) to avoid unpredictable changes in characteristic. These samples were later stored in an incubator at 4oC before testing. Monitoring involved comprehensive physico-chemical analyses encompassing estimation of major cations (Cd2+, Fe2+), anions (HCO3−, Cl−, NO3−, F−) besides general parameters (pH, EC, TDS, alkalinity, total hardness, DO, BOD, COD, colour).

Experimental procedures

In situ parameters like pH, EC, TDS, dissolved oxygen, etc. were measured immediately after sampling. The standard analytical procedures as recommended by the American Public Health Association (APHA, 2005) were employed in the present study. BOD, DO, pH,

TDS, EC is done as per Indian Standard manuals, other parameters like chloride, nitrate, COD, ammonia, fluoride and heavy metals like iron and cadmium were determined by Hach DR1900 spectrophotometer. Sample from each site (lakes) were analyzed thrice for each parameters (i.e., triplicate results) to obtain concordant values.

Water quality index (WQI)

WQI is calculated from the point of view of the suitability of lake water for human consumption. Hence, for calculating the WQI in the present study, 12 parameters namely, pH, electrical conductivity, BOD, COD, total dissolved solids, chloride, sulphate, nitrate, fluorides, cadmium and iron have been considered (Table 2, 3, 4).

The water quality data are recorded and transferred to a weighting curve chart, where a numerical value of Qi is obtained. The overall WQI of samples were calculated using the following expression:

$$WQI=\sum_{i=1}^{n} W_i Q_i \qquad (1)$$

Where, Qi = sub-index for ith water quality parameter;

Wi = weight associated with ith water quality parameter;

n = number of water quality parameters

3. RESULTS AND DISCUSSIONS

In this study, samples have been collected from Hauz Khas Lake, Sanjay Lake, and National Zoological Park's lake. The physiochemical parameters and quality analysis of the lake water are summarized in Tables 1, 2, 3 and 4.

Table 1 Observations of the physiochemical parameters of the three lakes

Sr. No.	Parameter	Std. Value	Concerned Agencies	HKL Lake	NZP Lake	SL lake
1	pH	8.5	BIS	8.41	7.9	7.68
2	TDS	500	BIS	483.38	546.86	585.86
3	Chloride	250	BIS	148.27	302.49	542.74
4	Nitrate	45	BIS	11.4	2.52	1.51
5	BOD	5	ICMR	22.6	7.91	6.833
6	DO	5	ICMR	6.2	9.04	4.66
7	COD	10	ICMR	249.67	199.4	170.67
8	Ammonia	0.5	BIS	0.154	0.08	0.14
9	Fluoride	1	BIS	0.446	0.506	0.45
10	EC	750	ICMR	743.67	841.34	901.34
11	Iron	0.3	BIS	0.11	0.113	0.16
12	Cadmium	0.003	BIS	0.0031	0.0034	0.0037

Table 2: Water Quality Index calculation of Hauz Khas Lake

Sr. No.	Parameters	Concerned Agencies	Observed Value	Standard Value	Unit Wt. (Wn)	Quality Rating Qi	Qi×Wi
1	pH	BIS	8.41	8.5	0.218	98.941	21.650
2	TDS	BIS	483.38	500	0.003	96.676	0.359
3	Chloride	BIS	148.27	250	0.007	59.308	0.441
4	Nitrate	BIS	11.4	45	0.0413	25.333	1.047
5	BOD	ICMR	22.6	5	0.372	452	168.144
6	DO	ICMR	6.2	5	0.372	124	46.128
7	COD	ICMR	249.67	10	0.186	2496.7	464.3862
8	Ammonia	BIS	0.154	0.5	3.72	30.8	114.576
9	Fluoride	BIS	0.446	1	1.86	44.6	82.956
10	EC	ICMR	743.67	750	0.002	99.156	0.245
11	Iron	BIS	0.11	0.3	6.2	36.666	227.333
12	Cadmium	BIS	0.0031	0.003	620	126.666	64066.6667
					ΣWn = 632.9837		ΣQnWn = 65193.9347

WQI= ΣQnWn/ ΣWn= 65193.9347/632.987 = **102.9**

Table 3: Water Quality Index calculation of NZP Lake

Sr. No.	Parameters	Concerned Agencies	Observed Value	Standard Value	Unit Wt. (Wn)	Quality Rating Qi	Qi×Wi
1	pH	BIS	7.9	8.5	0.218	92.941	20.337
2	TDS	BIS	546.86	500	0.003	109.372	0.406
3	Chloride	BIS	302.49	250	0.007	120.996	0.900
4	Nitrate	BIS	2.52	45	0.0413	5.6	0.231
5	BOD	ICMR	7.91	5	0.372	158.2	58.850
6	DO	ICMR	9.04	5	0.372	180.8	67.257
7	COD	ICMR	199.4	10	0.186	1994	370.884
8	Ammonia	BIS	0.08	0.5	3.72	16	59.52
9	Fluoride	BIS	0.506	1	1.86	50.6	94.116
10	EC	ICMR	841.34	750	0.00248	112.177	0.278
11	Iron	BIS	0.113	0.3	6.2	37.666	233.533
12	Cadmium	BIS	0.0034	0.003	620	113.333	70266.666
				ΣWn= 632.983		ΣQnWn = 71172.982	

WQI= ΣQnWn/ ΣWn= 71172.982/632.987 = **112.44**

Table 4: Water Quality Index calculation of Sanjay Lake

Sr. No.	Parameters	Concerned Agencies	Observed Value	Standard Value	Unit Wt. (Wn)	Quality Rating Qi	Qi×Wi
1	pH	BIS	7.68	8.5	0.218	90.352	19.771
2	TDS	BIS	585.86	500	0.003	117.172	0.435
3	Chloride	BIS	542.74	250	0.007	217.096	1.615
4	Nitrate	BIS	1.51	45	0.041	3.355	0.138
5	BOD	ICMR	6.833	5	0.372	136.66	50.837
6	DO	ICMR	4.66	5	0.372	93.2	34.670
7	COD	ICMR	170.67	10	0.186	1706.7	317.446
8	Ammonia	BIS	0.14	0.5	3.72	28	104.16
9	fluoride	BIS	0.45	1	1.86	45	83.7

10	EC	ICMR	901.34	750	0.024	120.178	0.298
11	Iron	BIS	0.16	0.3	6.2	53.333	330.666
12	Cadmium	BIS	0.0037	0.003	620	123.333	76410.406
				ΣWn= 632.983		ΣQnWn = 77410.4066	

WQI= ΣQnWn/ ΣWn= 77410.4066/632.987 = **122.29**

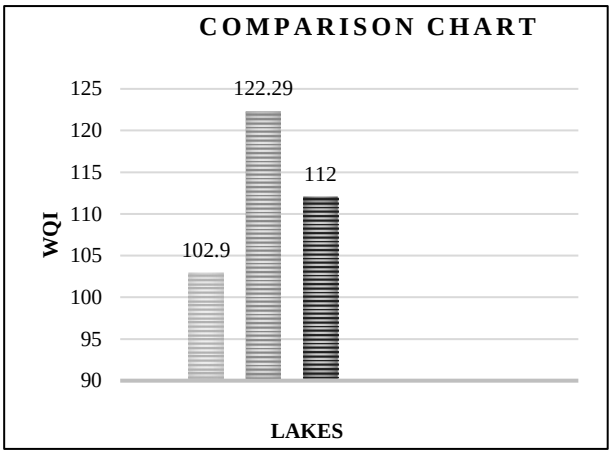

Fig 2. WQI Comparison of all lakes studied

The computed WQI values are classified into five types namely, excellent water (WQI<50), good water (50>WQI<100), poor water (100>WQI<200), very poor water (200>WQI<300) and water unsuitable for drinking (WQI >300). In the present study, the computed WQI values in Hauz Khas Lake and NZP Lake 102.9 and 112.44 respectively and while in Sanjay Lake water, it was 122.29. It is evident from the results that Sanjay Lake water fall under poor water category and the most polluted among the lakes studied (Fig. 2)

4. CONCLUSION

After water quality assessment of the three lakes, it was concluded that the water quality of all the lakes were in poor category based on WQI value. It was observed that Sanjay Lake was more polluted than other lakes. The water quality of Sanjay Lake is deteriorated concerning some of the major water quality determining parameters like Dissolved oxygen, Biological oxygen demand, iron, chloride and electrical conductivity due to heavy discharge of industrial and domestic sewage. NZP Lake was relatively more polluted than Hauz Khas Lake, though the water of all these lakes was in the same category i.e. unsuitable for drinking purposes.

Thus, it is quite clear from the experimental data that present practices of waste disposal adopted by the urban dwellers are responsible for the deterioration in water quality making it unfit for various purposes. However, sound practices based on scientific methods can help solve the problem of pollution and sustainable utilization of this important water resource. Though there are many studies for lake pollution around the country, there are not many done on Delhi lakes. We need to urgently address the lake pollution of Delhi. The capital is already facing water shortage challenges. So, we need a more comprehensive study on these lakes. There is urgent policy intervention needed.

ACKNOWLEDGMENTS

The authors are thankful to Water Resources Laboratory, Environmental Laboratory, IIT Delhi for providing us lab facility.

REFERENCES

7) Chauhan, A., & Singh, S. (2010). Evaluation of Ganga water for drinking purpose by water quality index at Rishikesh, Uttarakhand, India. Report and Opinion, 2(9), 53-61.
8) Kangabam, R. D., Bhoominathan, S. D., Kanagaraj, S., & Govindaraju, M. (2017). Development of a water quality index (WQI) for the Loktak Lake in India. Applied Water Science, 7(6), 2907-2918.
9) Parmar, K. S., & Bhardwaj, R. (2013). Water quality index and fractal dimension analysis of water parameters. International Journal of Environmental Science and Technology, 10(1), 151-164.
10) Singh, S., Ghosh, N. C., Krishan, G., Galkate, R., & Thomas, T. (2015). Development of an overall water quality index (OWQI) for surface water in Indian context. Development, 5000(50000), 50000.
11) Srinivasamoorthy et al. (2013), "Hydrochemical characterization of various surface water and groundwater resources available in Matahara areas, Fantalle Woreda of Oromiya region", Journal of Hydrology: Regional Studies, Vol. 3.
12) Tyagi, S., Sharma, B., Singh, P., & Dobhal, R. (2013). Water quality assessment in terms of water quality index. American Journal of Water Resources, 1(3), 34-38.
13) Yogendra, K., & Puttaiah, E. T. (2008). Determination of water quality index and suitability of an urban waterbody in Shimoga Town, Karnataka. In Proceedings of Taal2007: The 12th World Lake Conference (Vol. 342, p. 346).

Sustainable Urban Development

Sustainable Urban Development

Urban transport system

Road network analysis of Guwahati city using GIS

Das, D.[1], Ojha, A. K.[1], Kramsapi, H.[1], Baruah, P.P.[1], Dutta, M.K.[2]

[1]Student, Department of Civil Engineering, Jorhat Engineering College, Jorhat 785007, Assam, India.
[2]Associate Professor, Department of Civil Engineering, Jorhat Engineering College, Jorhat 785007 Assam, India.

ABSTRACT

Starting from the past or medieval period to the present day situation, history clearly indicates that the development of a region was and even today is a function of a good transportation network. In the present day, society demands for an efficient and unobstructed road network after experiencing major issues or problems like traffic congestion, delay, pollution, increased vehicle operating cost and road accidents. Keeping in mind the above needs and constraints to traffic movement, an analysis of a digitized road network of the concerned city/town can be one of the best remedy to solve the problems. Such analysis is best suited in ArcGIS, Geographic Information System (GIS) software for creating, analyzing and compiling maps for obtaining information. In the present study an effort has been made to prepare a road network map of Guwahati city and to find the shortest route between two places by proper analysis and digitization of its existing road network system in order to solve the traffic related problems to great extent. Network Analyst is a special analysis tool in ArcGIS which not only scrutinize the closest facility available in network of digitized interconnected lines but also facilitates in optimizing route during floods and emergency responses. One of the best models that can be prepared through Network Analysis is the shortest route between required origin and destination points. The analysis is done based on input of certain network attributes like traversing distance, time and cost of travel, barriers, vehicle restrictions etc. All the important roads connecting each other within the Guwahati City were digitized in the GIS environment and proceeded further to serve the purpose.

Keywords: ArcGIS, digitization of maps, road network, network analysis, shortest route

1. INTRODUCTION

The Indian highway network (IHN) is one of the busiest road networks in the world, constituting 2% of all roads in India but handling 40% of the total road traffic as of 2010 (Mukherjee, 2012). Traffic congestion occurs in certain parts and stretches of roads in Guwahati. Inadequate parking space, exorbitant bus, auto rickshaw, rickshaw and taxi fares, time consuming and uncomfortable journey, frequent accidents are the causes and consequences related to traffic in the city. Flood inundation and water-logging problems are also faced in several ward of Guwahati Municipal Corporation area during the rainy season. Rapid urbanization with increased housing more rooftops, driveways, streets and other impervious or hard surfaces (Barman & Goswami, 2009). Hence to overcome the problems and to maintain sustainability, proper analysis of the present road network is very much crucial to help mankind to reach their destination with ease, reduced cost and time etc.

A GIS is an organized collection of computer hardware, software, geographic data, and personnel to efficiently capture, store, update, manipulate, analyze, and display all forms of geographically referenced information. ArcGIS Network Analyst enables users to dynamically model realistic network conditions, including turn restrictions, speed limits, height restrictions, and traffic conditions, at different times of the day (Kumar & Kumar, 2016). ArcGIS proves to be one of the most user friendly, effective and time saving tool in the field of both traffic engineering and transportation planning.

2. METHODOLOGY

For the network analysis of Guwahati City, a street basemap was added in ArcGIS software from the Google Earth satellite imagery and geo-referenced to get the co-ordinates. Geo-referencing involves image alignment in a co-ordinate system (Herbei et al., 2010). The study area is being enlarged to a easily workable scale as shown.

Fig.1. Image showing the enlarged study area (Guwahati City) marked as red color.

Layers are the mechanisms used to display geographic datasets in ArcGIS (ESRI, 2018a). For the analysis, the layers were being categorized as major road (mainly the Highways) and minor road (city roads connecting the highways and other urban localities), lanes and by-lanes in addition to wards. The table of contents lists all the layers on the map and shows what the features in each layer represent (Laixing et al., 2008). After successful creation, the base map digitization for each layer was done to form a skeleton of the prevailing road network. Digitization is process of making an electronic version of a real world object or event, enabling the object to be stored, displayed and manipulated on a computer, and disseminated over networks and/or the www (Manjula et al., 2010). The entire GMC area is divided into 31 municipal wards and each municipal ward is further divided into 2, 3 or 4 Area Sabhas (GMC, 2017a). A ward map was drawn as a layer over the Guwahati city based on the official GMC map (GMC, 2017b).

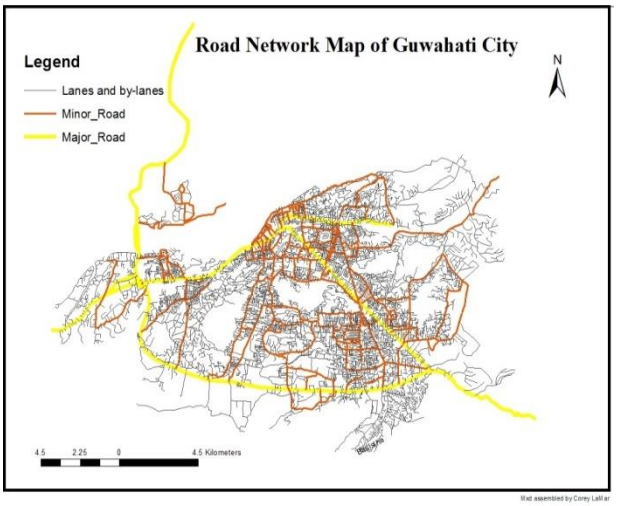

Fig. 2. Road Network Map of Guwahati City

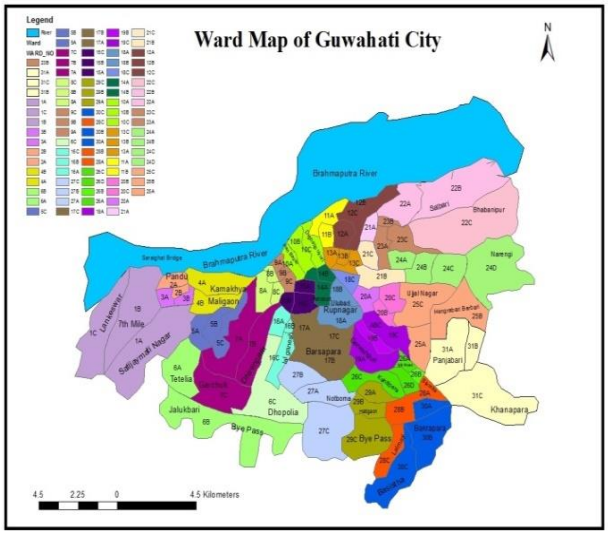

Fig. 3. Ward Map of Guwahati City

To run the analysis over the digitized road network, a network geo dataset was created which resulted in a layer consisting of the junctions and edges connected topologically to each other. Ward analysis was done using Intersection tool to get the statistics of all the categorized roads created as layers. The origin and destination points were selected to solve the network for determination of the shortest route and to serve the purpose of our study.

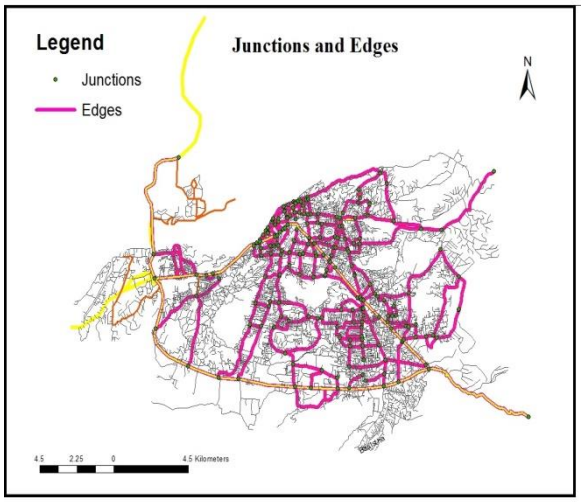

Fig.4. Junctions and edges of the digitized road network generated by Network Analyst toolbar.

3. RESULTS AND DISCUSSIONS

Table 1. Statistics obtained on ward analysis

Sl. No.	Description	Results
1	Total no. of major roads	3
2	Total no. of minor roads	135
3	Total no. of lanes and by-lanes	4476
4	Total length of major roads (in km)	75.971
5	Total length of minor roads (in km)	919.499
6	Total length of lanes and by-lanes (in km)	1298.834

Guwahati city has been divided into 31 main municipal wards which are further subdivided forming a total of 90 wards. From the ward-road network analysis, it has been seen that ward 22C has the largest area (9.954 km^2) and ward 12B has the smallest area (0.103 km^2). The 3 major roads pass through the 44 wards of Guwahati city out of which the ward 1B covers the maximum number of major roads (2) with a total length of 7.873 km.

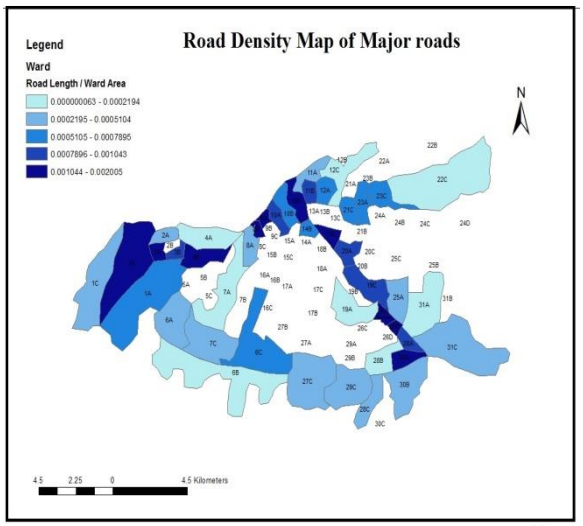

Fig.5. Map showing density of major roads ward wise.

Again, all the minor roads pass through 85 wards of the city out of which the ward 10A holds the maximum number of minor roads (9) with a total length of 4.554 km. The lanes and by-lanes cover up all the wards among which ward 6C has highest number of lanes (148) traversing throughout with a total length of 37.305 km.

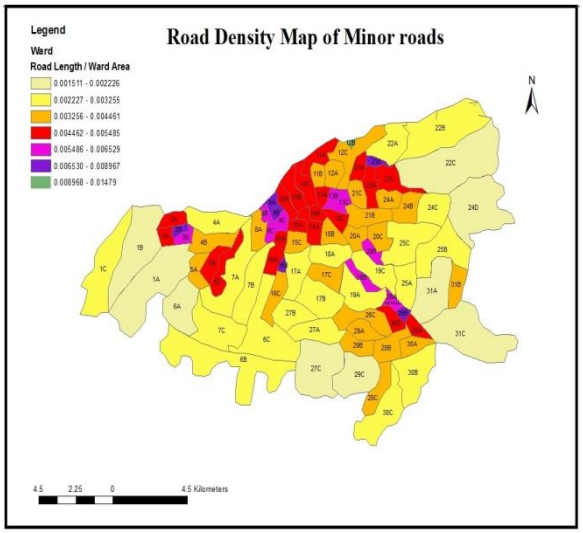

Fig.6. Map showing density of minor roads ward wise.

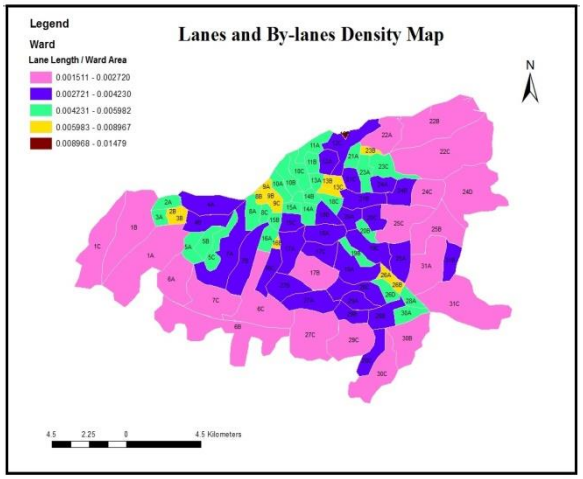

Fig.7. Map showing density of lanes and by-lanes ward wise.

A network analysis layer stores the inputs, properties, results of a network analysis and is always performed on network dataset (ESRI, 2018). Network analysis in GIS rests firmly on the theoretical foundation of the mathematical sub disciplines of graph theory and topology (Curtin, 2007). This paper is presented taking into account the route analysis layer and the analysis is based on real time network problems independent of the hierarchy (major roads, minor roads and lanes).GIS networks consist of interconnected lines (known as edges) and intersections (known as junctions) that represent routes upon which people, goods, etc. can travel (Wikipedia contributors, 2018a). Network Analysis helps in modeling as well as planning and management of moderate to heavy traffic routes. One common type of network analysis is finding the shortest path between two points (Wikipedia contributors, 2018b). Junctions (or nodes) and edges have certain attributes affixed to them which help in modeling. Edges and junctions are topologically connected to each other-edges must connect to other edges at junctions, and the flow from edges in the network is transferred to other edges through junctions (ESRI, 2018b).

Determination of the shortest route between the origin and destination using the GIS Network Analyst will not only help the tourists or business entrepreneurs to access the tourist places or the trade centers with ease but it will also reduce cost and avoid traffic congestion resulting in less emission of pollutants. Dijkstra (1959) proposed a graph search algorithm that can be used to solve the single-source shortest path problem for any graph that has a non-negative edge path cost (Akpofure & Paul, 2017). Network attributes are properties of the network elements that control movement over the network and helps in finding the shortest route based on type of attribute such as distance, vehicle restrictions, turn restrictions etc. This paper presents the shortest route based on the assumptions that traffic congestions are not considered and the calculations are based on road distances.

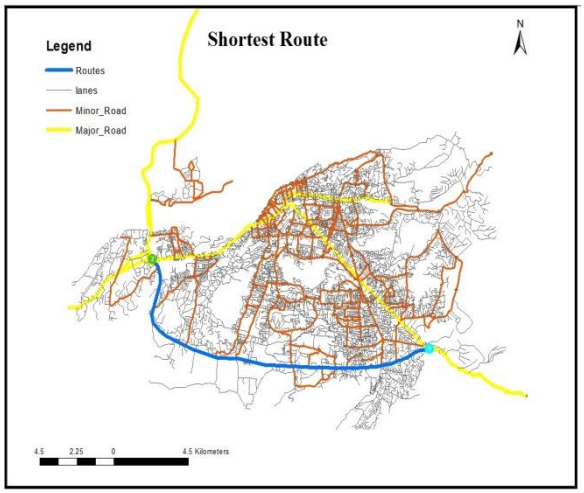

Fig. 8. Image showing the shortest route between old ASTC point to flyover point (shown by blue color)

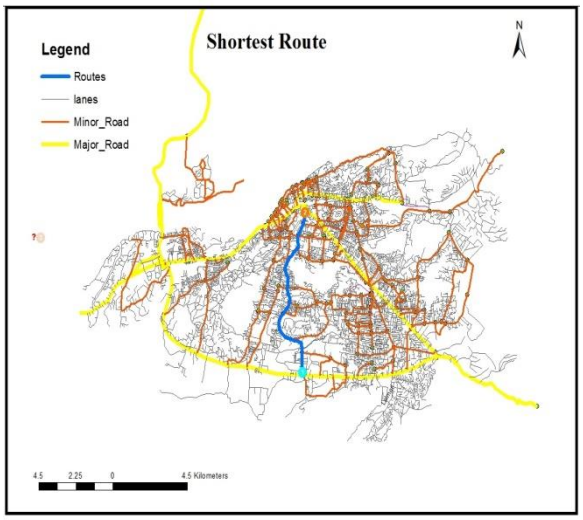

Fig. 9. Image showing the shortest route between Paltan Bazar to Lokhra Bamunpara Chowk (shown by blue color).

Table 2. Shortest distance measurements.

To traverse		Shortest route is via	Total distance (km)
From	To		
Khanapara old ASTC point	Jalukbari flyover point	Guwahati Bypass, NH 37	18.779
Paltan Bazar	Lokhra Bamunpara	Lokhra Road	8.775

Chowk

4. CONCLUSION

Thus Network Analysis is one of the most powerful tool to deal with the real time transportation problems. It is reliable, user friendly and efficiently solves the network problems. It has replaced the conventional methods of analyzing and saves lot of time and work. It emerged out as the helping hand in the field of transportation planning, origin and destination studies. It has high potentiality in analyzing the closest facility and service areas in a network. Ward analysis is a another easiest way to know the present density and number of roads in service which in turn would help in transportation planning keeping in consideration the various aspects. An information about the shortest route would help the drivers and road users to save the transportation cost, time and avoid traffic congestions in commuter routes by diverting the excess flow through less travelled shorter routes. As a whole, it can also be concluded that GIS has a lot of applications directly or indirectly in the field of transportation as the studies about the existing road network problems as their solutions can enhance the economy of a locality to a great extent. Implementation of the advanced technologies can be beneficial to maintain the sustainability and transportation related GIS tasks should be preferred for better output in future.

REFERENCES

1) Akpofure, O.N., & Paul, A.N. (2017). Anapplication of Dijkstra's Algorithm to shortest route problem. *IOSR Journal of Mathematics (IOSR-JM) e-ISSN: 2278-5728*, Volume 13, Issue 3 Ver. 1 (May. - June. 2017), 20-32.
2) Barman, P. & Goswami, D.C. (2009). Floodzone of Guwahati Municipal Corporation Area using GIS Technology. 10th *ESRI India User Conference 2009*.
3) Curtin, K.M. (2007). Network Analysis in Geographic Information Science: Review, Assessment and Projections. *Cartography and Geographic Information Science*, Vol. 34, No. 2, 2007, 103-111.
4) ESRI. (2018a). ArcMap. Retrieved from ArcGIS Desktop:http://desktop.arcgis.com/en/arcmap/10.3/map/working-with-layers/what-is-a-layer-.htm.
5) ESRI. (2018b). ArcMap Extensions- Network Analysis Workflow. Retrieved from ArcGIS Desktop:http://desktop.arcgis.com/en/arcmap/latest/extensions/network-analyst/network-analysis-workflow.htm.
6) GMC. (2017a). About Us. Retrieved from GMC:http://gmc.eodbassam.in/category/aboutus/ .
7) GMC. (2017b). Guwahati Municipal Corporation Map (pdf). Retrieved from http://www.gmcportal.in/gmc-web/uploads/GMC-MAP.pdf.
8) 8. Herbei, M.H., Ciolac, V., Smuleac, A., Nistor, E., & Ciolac, L. (2010). Georeferencing of topographical maps using the software ArcGIS. *Research Journal of Agricultural Science*, 42 (3),595-606.
9) Kumar, P. & Kumar, D. (2016). Network Analysis using GIS Techniques: A case of Chandigarh City. *International Journal of Science and Research (IJSR)*, Volume 5 Issue 2,409-411.
10) Laixing, L., Deren, L., & Zhenfeng, S. (2008).Research on Geospatial Information Sharing Platform based on ArcGIS Server. *The International Archives of the Photogrammetry, Remote Sensing and SpatialInformation Sciences*, Vol. XXXVII, Part B4. 791-795.
11) 11. Mukherjee, S. (2012). Statistical analysis of the road network of India. *Pranama Journal of Physics*, vol 79, No.3, 483-491.doi: 10.1007/s12043-012-0336-z, ePublication: 10 August 2012.
12) 12. Manjula, K.R., Jyothi, S. andSUD Varma, A.K. (2010). Digitzing the Forest Resource Map Using ArcGIS. *IJCSI International Journal of Computer Science* Issues, Vol 7, Issue 6, 300-306.
13) 13. Wikipedia contributors. (2018a). Network analysis. In Wikipedia, The Free Encyclopedia. Retrievedfromhttps://en.wikipedia.org/w/index.php?title=Network_analysis&oldid=837669905
14) 14. Wikipedia contributors. (2018b). Network analysis. In Wikipedia, The Free Encyclopedia. Retrievedfrom https://en.wikipedia.org/w/index.php?title=Network_analysis&oldid=837669905.

Sustainable Urban Development

Urban traffic management system

Dynamic data collection of staggered-following behavior in non-lane based traffic streams

Das, S. [1], Maurya, A.K. [2]

[1] PhD Student, Department of Civil Engineering, Indian Institute of Technology Guwahati, Assam, 781039, India.
[2] Associate Professor, Department of Civil Engineering, Indian Institute of Technology Guwahati, Assam, 781039, India.

ABSTRACT

Different maneuvering patterns of vehicles, the absence of lane discipline and interactions of a large number of vehicles with each other and with roadway features make the traffic phenomena of non-lane based traffic streams more complex. Vehicles' movement in weak lane discipline traffic is rather two-dimensional because they always tend to evaluate possible available gaps on the road while progressing longitudinally. Recent literature has underlined the importance of centerline separation of traffic in modelling the staggered-following behavior. However, the requirements for staggered-following trajectory data are indeed stringent. Although recent advancements in new digital technology have expedited new horizons in the field of traffic engineering, proper estimation of microscopic car-following data has still proven to be challenging. Understanding the staggered-following behavior, a proper evaluation of car-following behavior in non-lane based traffic environments requires an accurate characterization of the microscopic traffic variables and reliable experimental data. This study describes an image-based in-vehicle trajectory data collection system to process the microscopic variables (such as longitudinal gap, centerline separation, vehicle speeds, accelerations, etc.), using camera calibration and in-vehicle GPS information on straight roads. Improved accuracy in the experimental data collection, proper extraction and estimation of data can substantially enrich the understanding of riders' behavioral phenomena from a microscopic perspective and the realism of traffic models, which will result in a better prediction of microscopic simulation models.

Keywords: heterogeneous, car-following, centerline separation, data collection

1. INTRODUCTION

Recent advancements in the development of microscopic simulation models and Intelligent Transportation Systems (ITS) have spurred a growing interest in the transport modellers of many countries. Achieving a detailed understanding of how drivers react to the surrounding traffic, how they control the vehicles in the car-following process and different factors affecting their behaviour will essentially enhance the realistic replication of riders' behaviour in simulation modelling.

The peer-reviewed literature has supported the development of car-following theories and its subsequent sub-models since decades. In particular, car-following condition refers to that state in which the subject vehicle assigns full leadership to the immediate vehicle in-front. Unlike in homogeneous and lane-based traffic conditions where car-following behaviour mostly prevails, vehicles in non-lane based traffic environments not only interact with the front leading vehicle but also with the surrounding vehicle in the lateral direction. Due to the differences in the static and operational characteristics of diverse vehicle types in non-lane based traffic streams, they often tend to look for possible available gaps in the surrounding traffic while progressing longitudinally. Therefore, the subject vehicles do not always fully follow the leading vehicles in the longitudinal direction, rather they maintain some centreline separation (CS) with the preceding vehicle laterally, commonly termed as 'staggered-following behaviour' in the literature (Gunay, 2007; Asaithambi et al., 2016; Das and Maurya, 2018) either to perceive the forward visual field with more confidence or to anticipate the behavioral response of the front vehicles.

Although the advancements in new digital technology have expedited new horizons in the field of traffic engineering, however, the collection and processing of accurate, unbiased, time-series data for empirical verification of staggered-following behaviour in non-lane based traffic streams, has still proven to be challenging. Different researchers have demonstrated the advantages of satellite-based Global Positioning System (GPS) technology in modelling the car-following behavior (Gurusinghe et al., 2002; Punzo and Simonelli, 2005; Mathew and Ravishankar, 2012). However, the data requirements of staggered following behavior are indeed stringent. While the longitudinal spacing between the two vehicles can be obtained from the recorded GPS positions with 1m accuracy, the

estimation of lateral separation from the GPS receivers may produce unreliable results. It is therefore envisaged that an integration of satellite-based GPS technology with an image-based trajectory extracting system can prove to be suitable in the collection and estimation of staggered-following data.

This paper, therefore, attempts to establish an image-based in-vehicle data collection methodology using camera calibration and satellite-based GPS receivers on straight roads of non-lane based traffic streams, to process the microscopic parameters (such as longitudinal gap, centerline separation and speed) in the staggered-following scenario.

2 METHODOLOGICAL FRAMEWORK

A discussion on the experimental set-up, data collection process and calibration of the video data is provided in this section.

2.1 Data collection process

The in-vehicle experimental setup consists of a GPS device (Racelogic Video V-box) with 10Hz data logging frequency and a video camera attached at the windshield of the following vehicle, allowing real-time monitoring of the forward visual field. The GPS device provides the vehicle position and speed with 1m and 0.1km/h accuracy respectively while the video recorder captures continuous video data at 25 frames/s. For this study, two cars were equipped with GPS receivers and experiments were conducted along straight rural roads on NH-27 in Guwahati. Both the vehicles were then allowed to move in the following state so that the car-following (or, staggered-following to be more precise) data could be further processed and analyzed. In this process, it was ensured that the vehicles were not involved in any lane-changing or overtaking processes and for any intrusions in between the two GPS equipped vehicles, the corresponding data were discarded from further analysis.

2.2 Calibration

While information on speeds and accelerations of both the vehicles are obtained from the GPS receivers, the longitudinal and lateral separations between the two successive vehicles can be extracted from the video footage. Camera calibration of the recorded video is conducted by a vanishing point technique, where image coordinates of the four corners forming a perfect rectangle in the real field need to be captured (Fung et al., 2003). With an aim to extract and analyze the longitudinal and lateral spacing, a semi-automated trajectory extractor is developed, where the image/screen coordinates of the video footage are obtained by using mouse clicks at different time stamps and the corresponding screen coordinates are then converted to real-world coordinates by utilizing Fung et al's (2003) calibration equations. The camera calibration technique used in this study is depicted in Fig. 1.

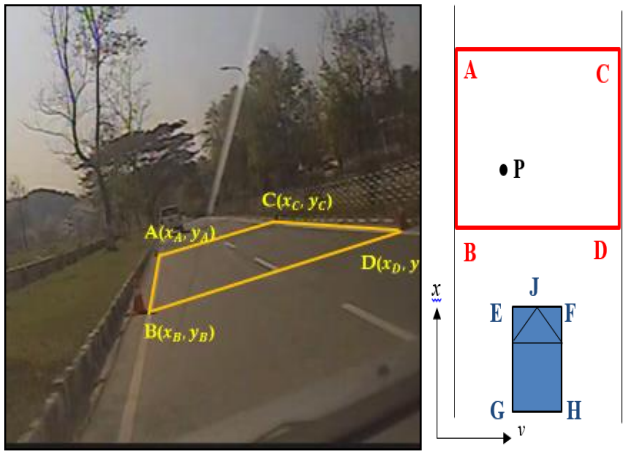

(a) (b)

Fig. 1. Camera calibration technique (a) rectangle *ABCD* viewed from the camera (b) representation of the calibration pattern.

Before starting the experiment, four end-points of the road (ABCD as shown in Fig. 1a) representing an exact rectangle of known dimensions are marked on the road. The corresponding end-points are further extracted from the video footage by manual mouse clicks on the screen to obtain its respective screen coordinates. For the estimation of inter-vehicle longitudinal and lateral separations, let us consider the test vehicle (EFGH) with its front center (point J) parked parallel to the road edge (AB). The lateral and longitudinal distance of one of the marked end-points from one corner of the test vehicle also needs to be known (Say, point B from point E). For any point P lying in the plane ABCD (i.e. plane of the road) its camera co-ordinates (x_P, y_P) can be calculated and subtracted from coordinates of point B and E so as to obtain the lateral and longitudinal offset of point P. In other words, lateral offset or centerline separation $= y_P - (y_E - y_B) + (y_J - y_E)$, longitudinal offset= $(x_B - x_P) + (x_E - x_B)$. The distances $(x_E - x_B)$, $(y_E - y_B)$ and $(y_J - y_E)$ are accurately measured in the field. The screen coordinates are extracted at every 0.2s and are then transformed into real coordinates as discussed before. The recorded vehicle positions from the GPS receivers are then synchronized with the positional data extracted from the video footage at every 0.2s intervals.

3 RESULTS AND ANALYSIS

3.1 Preliminary analysis

In the staggered-following scenario, several variables were extracted from the video recorders and the GPS receivers such as vehicle speeds, acceleration, longitudinal gap and centerline separation. A

representation of longitudinal gap (LG) and centerline separation (CS) considered in the study is presented in Fig. 2.

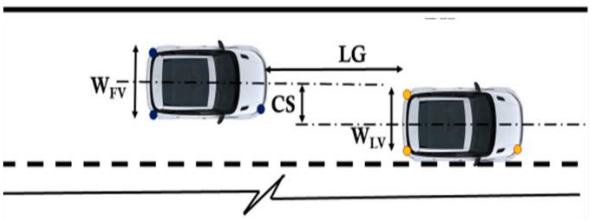

Fig. 2. Variables considered in the study (Das and Maurya, 2018).

In total, 7200 cases of time-series data for staggered car-following scenario is obtained in this study. As already discussed, CS is usually considered as an indicator of lateral interaction in the car-following process of non-lane based traffic. Essentially, CS<0.34m represents a car-following state (Gunay, 2003) while 0.34<CS<3m depicts a staggered-following case where the subject vehicles interact with the leading vehicles maintaining certain centerline separation between them.

The obtained trajectory data indicated a wide range of longitudinal gap, speeds and centerline separation varying from a range of 3.4-29.89m, 10-78km/h and 0-3m respectively. The observed range for longitudinal gap (<30m) further justifies the longitudinal interaction region for car-following-car cases, as indicated in the previous car-following research work.

3.2 Univariate modelling of the traffic variables

Proper estimation of probability distribution models for longitudinal gap, vehicle speeds and centerline separation can provide a better understanding of the stochastic uncertainties in the car-following processes. The probability distributions of these variables are also considered as dominant input parameters for generating vehicles in microsimulation modelling.

Several statistical models were used to fit longitudinal gap, centerline separation and vehicle speed data. The candidate distributions selected for the study are logistic, Weibull, lognormal, normal and gamma. The maximum likelihood technique is employed to estimate the parameters of the univariate models while the suitability of a distribution is evaluated using log-likelihood values and two goodness-of-fit statistics such as Kolmogorov-Smirnov (K-S) and Anderson-Darling (A-D) tests. Hence, a particular distribution is considered to be the best-fitted one if the log-likelihood value is the largest and the selected distribution passes the goodness-of-fit tests (i.e. the statistic values are lower than the critical values at 5% significance level). Table 1 presents the log-likelihood (LL) values and the goodness-of-fit statistics of the selected distributions for longitudinal gap, centerline separation and vehicle speeds.

Table 1. Log-likelihood and goodness-of-fit statistics for each microscopic traffic variable.

Distribution type	LG			CS			Speed		
	LL	KS	AD	LL	KS	AD	LL	KS	AD
Lognormal	-6486.0	0.05	12.25	-1494.5	0.06	24.37	-7154.04	0.08	41.74
Weibull	-6469.0	0.09	25.67	-1563.3	0.11	41.56	-7352.6	0.16	91.71
Logistic	**-6426.9**	**0.04**	**7.87**	-2285.9	0.21	153.5	**-7091.07**	**0.10**	**35.8**
Normal	-6451.0	0.05	9.62	**-1508.2**	**0.10**	**34.31**	-7169.28	0.12	56.29
Gamma	-6481.2	0.05	12.25	-1899.6	0.06	24.37	-7111.13	0.08	41.74

Note: Bold features indicate the best-fitted distribution
LG- Longitudinal gap; CS- Centerline separation

Based on the LL values and goodness-of-fit results, logistic distribution provided the best-fits for longitudinal gap and speed data while normal distribution was found to the best-fitted one for centerline separation. The distribution profiles of the best-fitted statistical models for LG, CS and vehicle speeds are presented in Fig. 3.

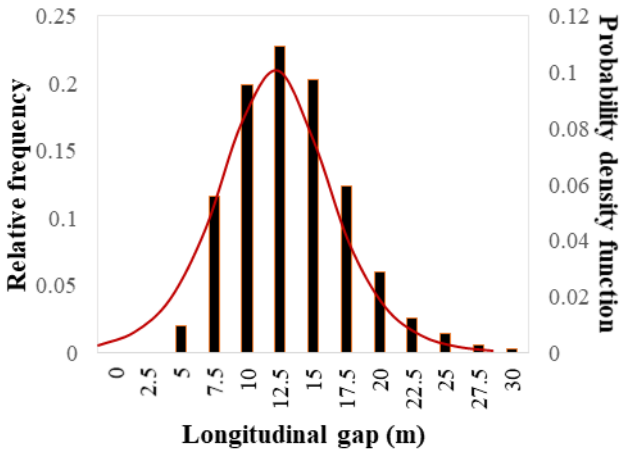

(a)

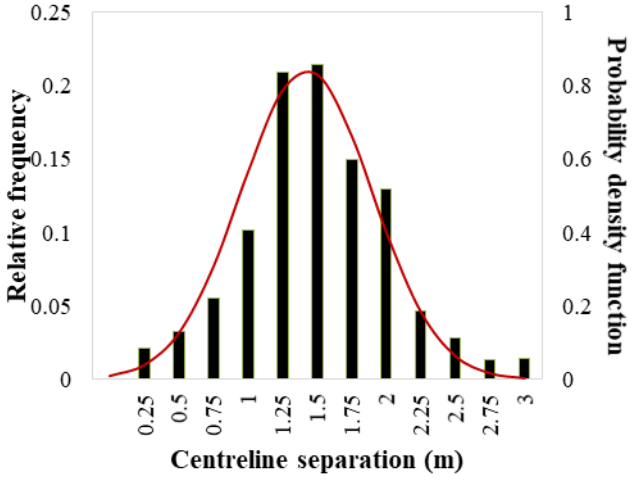

(b)

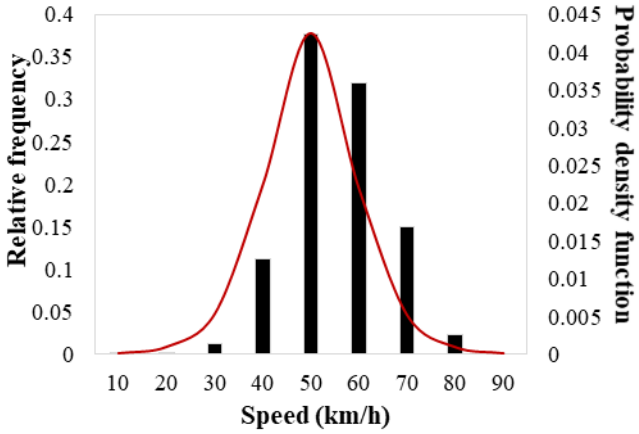

(c)

Fig. 3. Best-fitted probability density curves for (a) longitudinal gap, (b) centerline separation and (c) vehicle speeds.

The histogram plots of Fig. 3 indicate that inter-vehicle longitudinal spacing range from 5m to a maximum of 30m, while the peaks of the distributions lie at 12.5m, 1.5m and 50km/h for LG, CS and speeds respectively. As importantly, lower values of LG may not actually imply an unsafe car-following event as the following vehicles have the flexibility to move laterally maintaining large CS even at even lower longitudinal gaps. The variation of LGs with CS and speeds may provide a better understanding of the car-following events of non-lane based traffic streams.

3.2 Relationship among LG, CS and speed

Firstly, to understand the inter-relationship between LG and speed in staggered-following conditions, the variations of longitudinal gaps with different speed ranges are presented in a box-plot as shown in Fig. 4.

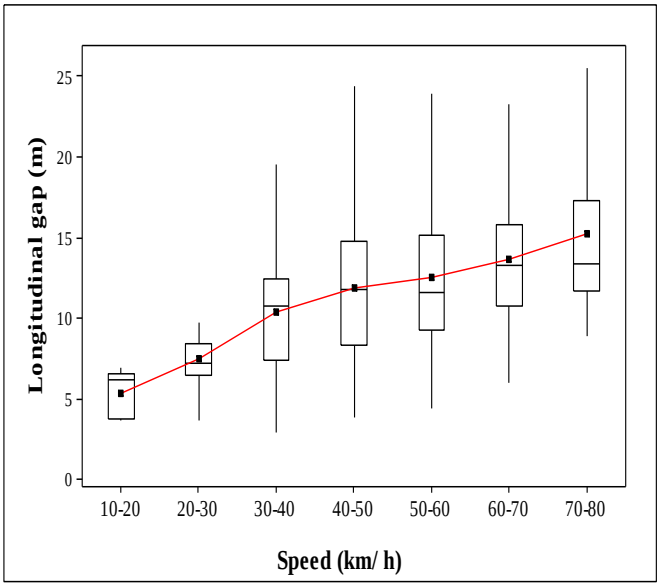

Fig. 4. Box plot showing variations of LG with speeds

The connecting line in Fig. 4 represents the mean values of LG at each speed range and it clearly depicts an increasing relationship between the two variables. As expected, significant statistical differences in the variances of longitudinal gaps were observed across all speed ranges at 5% significance level ($Fstat = 381.89, p < 0.001$). This indicates that as longitudinal gap between the interacting vehicles increases, the following vehicles will accelerate and proceed at higher speeds to avail the gap. Moreover, the consideration of lateral descriptor of vehicle interactions (that is, centerline separation) in car-following events will provide additional insights into the variations of LG with speeds. The descriptive statistics of LGs and speeds at different CS ranges are therefore evaluated and a summary of the values is presented in Table 2.

Table 2. Descriptive statistics of LG and speed for different CSs

CS (m)	LG (m)			Speed (km/h)			Sample
	Mean	Median	SD	Mean	Median	SD	
0-0.5	17.76	18.51	4.99	54.66	56.3	10.29	387
0.5-1	14.36	13.84	4.71	53.84	53.09	8.72	1024
1-1.5	12.48	12.26	3.91	50.68	49.92	10.17	2424
1.5-2	11.16	11.07	3.47	47.33	44.71	9.51	2622
2-2.5	9.31	8.49	2.80	47.56	44.60	10.23	539
2.5-3	7.68	6.88	2.47	54.02	54.13	8.32	198

Note: SD-Standard deviation

It can be observed from the table that the mean and median values of longitudinal gaps follow a decreasing trend as centerline separation increases. This implies that vehicles at large CS feel lesser obstruction of the leading vehicles, have wide visual field of view and can anticipate the leading vehicle's behavior due to which

they tend to follow the leading vehicles closely, resulting in lower longitudinal gaps. However, the mean and median values of speeds reveal a decreasing relationship till 2m CS while the speed values increase beyond 2m CS. This can be attributed to the fact that the following vehicles reduce their speeds when they interact with the leading vehicle below 2m CS whereas at CS greater than 2m, the extent of influence of the leading vehicles comparatively reduces and the following vehicles feel less constrained. As a result, they tend to proceed at higher speeds at larger CS (>2m).

4 CONCLUSIONS

Although GPS technology can prove to be a promising technique in vehicle tracking, yet the collection of real-time trajectory data for staggered car-following conditions has still proven to be challenging. While the longitudinal spacing between the two vehicles can be obtained from the recorded GPS positions with 1m accuracy, the estimation of lateral separation from the GPS receivers may produce unreliable results. This study therefore, attempts to provide an in-vehicle data collection methodological approach using camera calibration and satellite based GPS receivers, to process reliable dynamic time-series data (longitudinal gap (LG), centerline separation (CS) and vehicle speeds) for staggered car-following conditions of non-lane based traffic streams.

Preliminary analysis on LG, CS and speed data indicated that logistic distribution provided the best-fit for longitudinal gap and speed data while normal distribution was found to the best-fitted one for centerline separation in staggered car-following conditions of non-lane based traffic streams. As expected, the results further indicated a positive dependent relationship between LG and CS and a reciprocal relationship between LG and CS. This implies that vehicles at large CS feel lesser obstruction of the leading vehicles, have wide visual field of view and can anticipate the leading vehicle's behavior due to which they tend to follow the leading vehicles closely, resulting in lower longitudinal gaps. It was further observed that the following vehicle speeds increase when CS exceed 2m.

The results of this study can substantially enrich the understanding of riders' behavioral phenomena from a microscopic perspective and the realism of traffic sub-models, which will result in a better prediction and development of microscopic simulation models.

REFERENCES

1) Asaithambi, G., Kanagaraj, V., & Toledo, T. (2016): Driving Behaviors: Models and Challenges for Non-Lane Based Mixed Traffic. *Transportation in Developing Economies*, *2*(2), 19. doi: 10.1007/s40890-016-0025-6
2) Das, S., and Maurya, A. K. (2018): Multivariate analysis of microscopic traffic variables using copulas in staggered car-following conditions, *Transportmetrica A: Transport Science*, 1-26. doi: 10.1080/23249935.2018.1441200
3) Fung, G. S., Yung, N. H., and Pang, G. K. (2003): Camera Calibration from Road Lane Markings, *Optical Engineering*, 42(10): 2967-2977. doi:10.1117/1.1606458.
4) Gunay, B. (2003): Methods to quantify the discipline of lane-based driving, *Traffic Engineering and Control*, 44(1), 22-27.
5) Gunay, B. (2007): Car Following Theory with Lateral Discomfort, *Transportation Research Part B: Methodological* 41(7), 722-735.
6) Gurusinghe, G. S., Nakatsuji, T., Azuta, Y., Ranjitkar, P., and Tanaboriboon, Y. (2002): Multiple Car-Following Data Using Real-Time Kinematic Global Positioning System, In *Transportation Research Record: Journal of the Transportation Research Board, No. 1802*, Transportation Research Board of the National Academies, Washington, D.C., 166–180.
7) Mathew, T. V., and Ravishankar, K. V. R. (2012): Neural network based vehicle-following model for mixed traffic conditions, *European Transport / Trasporti Europei*, 52, 1-15.
8) Punzo, V., and Simonelli, F. (2005): Analysis and comparison of microscopic traffic flow models with real traffic microscopic data, *Transportation Research Record: Journal of the Transportation Research Board*, (1934), 53-63.

Design of signalized traffic intersections on Guwahati bypass road

Bhardwaj, B. B.[1], Devi, H. C.[2], Boruah, B. B.[2], Borah, R.[2], Hazarika, B. J.[2], Agarwalla, S.[2], Terang, B.[2]

[1]Assistant Professor, Department of Civil Engineering, Assam Engineering College, Guwahati, 781013, India.
[2]UG student, Department of Civil Engineering, Assam Engineering College, Guwahati, 781013, India.

ABSTRACT

Traffic congestion is a reflection of infrastructure planning and development of a city. Since, infrastructure development is dynamic, capacity of roads is built to accommodate a certain threshold at a time; once that threshold is reached, congestion occurs. As the economy grows and more people can afford to buy cars, the roads slowly fill up, worsening the condition of traffic congestion. However, irrespective of the reasons of increasing traffic congestion, the same needs to be eradicated or reduced to ensure that the vehicle operating cost of the user doesn't get severely affected. At microscopic level, a jam can be caused by bottlenecks, moving bottlenecks or inefficient intersection management. From construction of fly-overs to construction of rotary, there are many solutions to traffic jam at intersection. But, traffic signal, because of its advantages is mostly preferred over the other options. But designing a traffic signal invites a lot of data collection and analysis too. Guwahati, as a city has crossed the blooming stage and now is exploding in terms of road traffic. The arterial roads of the city viz. G.S. road, R.G.B. road, M.G. road etc. reach saturation state during daytime and hence are avoided by most of the travelers who commute through the city and not within the city. The bypass road i.e. NH-27 is primarily used by those commuters. But traffic congestion problem has become a serious concern from the last couple of years on that road too. This is mainly because, none of the intersections on that road is scientifically controlled. Manual control not only, complexifies the situation but sometimes increases cost too. An attempt to signalize and coordinate three important intersections on the bypass road is made and comparative cost and time analysis with the present condition is also carried out in this study.

Keywords: traffic, congestion, jam, signal, intersection, coordination

1. INTRODUCTION

Traffic congestion is a regular phenomenon in the big cities and towns in India and across the globe. In case of our country the rapid increase in population the number of vehicles of different types for the movement and transport of the people has increased by leaps and bounds but the likewise increase of dimensions of the already available roads has not been at the pace as that of the former. Such inequity in supply and demand is causing an unprecedented level of safety challenges. Considering the statistics of the recent years' escalation in motorization, infrastructure development and snowballing mobility of people in Indian cities, the same inclination is expected to endure in the coming years. Reddy et al. (2016) said that traffic consists on Indian roads of bi-directional freedom traffic such as two or three wheeled vehicles and uni-directional vehicles such as four wheelers.

Overall traffic flow depends on the performance of the intersections. It also affects the capacity of the road. Therefore, both from the accident perspective and the capacity perspective, control of traffic at intersections is of utmost necessity. The essence of the intersection control is to resolve these conflicts at the intersection for the safe and efficient movement of both vehicular traffic and pedestrians. Two methods of intersection controls are there: time sharing and space sharing. Control using traffic signal is based on time sharing approach. At a given time, with the help of appropriate signals, certain traffic movements are restricted whereas certain other movements are permitted to pass through the intersection. Two or more phases may be provided depending upon the traffic conditions of the intersection. When the vehicles traversing the intersection are very large, then the control is done with the help of signals.

2. BACKGROUND

Assam being the gateway state to the rest of North East of India and amongst that Guwahati being the busiest city of the entire North-East India, the problem of traffic contestations inside the metropolitan city and also the bypassing National Highway 27 has been a problem ever since road traffic grew up sizably as shown in Fig. 1. The traffic congestion affects the daily lives of the people who ever commute through the roads.

To add to the concern the National Highway-27 bypassing the city of Guwahati is the primary lifeline of all the districts of Upper and Middle Assam including

that to neighboring states of Meghalaya, Arunachal Pradesh, Tripura and Nagaland too had intersections that are manually controlled till this date. Such aspects add up to the road being of strategic importance to the Nation. Along with all of that the recent North-South and East-West corridor project being implemented in the county and its far east end being located at Silchar in the state of Assam, the successful implementation of the same requires for the respective intersections to remain decongested, as such these vitalities associated with these locations were the key aspects in our choice of the respective locations for the project.

Fig. 1. Photograph of Basistha Traffic Intersection during peak traffic flow

After analyzing of the road intersections, three intersections have been chosen viz. Basistha Chariali, Lokhora Chariali and Gorchuk Chariali as shown in Fig. 2.

Fig. 2. Locations of the intersections on the road

Traffic congestion is observed frequently at the above-mentioned intersections, primarily due to lack of a proper traffic management as these intersections are considered amongst the busiest intersections in the entire Guwahati city.

3. METHODOLOGY

In order to design the traffic signals, accurate information and continuous monitoring of traffic by appropriate methods is necessary. It is essential to know the magnitude of traffic data required or to be collected, which will then determine its quality and type of vehicle classification to be adopted. In this Project a mix-method has been adopted for data collection. Here vehicles are manually counted from recorded video clips. For this, three video cameras (cell phone camera) have been mounted in every intersection. Videos are recorded from the top of the nearby buildings which gave the bird eye views of the intersections that helped in precise counting of the same.

After collection of data, manual counting of vehicles is done through careful inspection of the video recordings taken at the three different sites. The first step in analysis of traffic data is to determine the different directions in which the flow of traffic is occurring in a complete cycle. Twelve different directions of flow have been observed as shown in Fig. For each direction of flow, a counting sheet is prepared where the numbers of different class of vehicles are entered separately in the form of a tally count. Thus, in a given cycle twelve sheets are prepared to record the vehicle count in the twelve different directions and the same is followed for all the cycles observed.

When counting is completed for all the cycles, the numbers of different types of vehicles are converted to standard unit values known as the Passenger Car Unit (or PCU) values since it is essential to bring all the different classes of vehicles to a common unit to make way for easy analysis of traffic data. The numbers of different classes of vehicles are, thus, converted to equivalent passenger car units by multiplying with their PCU values as shown in Table 1 and are recorded.

Table 1. PCU factors for different vehicle types.

Sl No.	Vehicle Type	PCU Factor
1	Motor Cycle/Scooter	0.5
2	Passenger Car	1
3	Auto Rickshaw	1.2
4	Light Commercial Vehicle	1.4
5	Truck (up to dual rear axle)	2.2
6	Truck (multi rear axle)	4
7	Bus	2.2
8	Agricultural Tractor -Trailer	4
9	Bicycle	0.4
10	Cycle Rickshaw	1.5
11	Horse drawn vehicle	1.5
12	Hand cart	2

The PCU values for each direction in a cycle are added and this gives the total PCU count for the cycle. In this way, the total PCU counts for the different cycles are worked out simultaneously. Next, a continuous period of 1 hour is chosen from the 1.5 hours taken such that the sum of PCUs of the cycles, within this period, is the maximum. The value of PCU thus obtained within this period is used in the design of traffic signals for the intersections.

Webster Method of Signal design is adopted-

Optimum cycle length C as suggested by Webster is:

$$C = \frac{1.5L+5}{1-\sum_{i=1}^{P}(V/S)_i} \quad (1)$$

Where,

C: Optimal cycle length, in seconds

L: Lost time during a cycle. Sum of the start-up lost time and the clearance lost times.

p: total number of phases in the cycle

V: volume of a particular movement

S: saturation flow for movement, can be taken as 1400 PCU/lane for urban roads

Further L can be calculated as:

$$L = \sum_{i=1}^{P}(\alpha + \beta + \mu) \quad (2)$$

α : startup time loss

β : movement time loss or clearance lost time

μ: all red time loss

P: No. of phases

4. RESULTS AND DESIGN OF SIGNALS

The data collection of vehicle count was done by means of capturing videos at the respective intersection. The same was categorically reorganized into 12 directions of flow as shown in Fig. 3 at those respective intersections as per cycle completion. From that the time duration with the maximum vehicle flow was found out, by means of calculating the maximum PCU during those cycles. The four design phases for the Basistha Chariali intersection are illustrated in Fig 4.1. For Basistha, Lokhra and Gorchuk intersection, the peak flows are found to be 4242.29 PCU/hr, 6862.8 PCU/hr and 5384.1 PCU/hr respectively.

It is also observed that the normal flow is 60% of peak traffic flow for Basistha Chariali intersection, 40% for Lokhra intersection and 34% for Garchuk intersection.

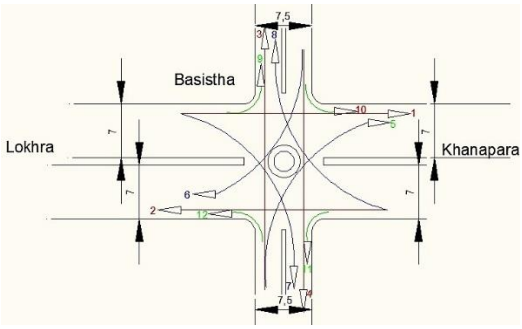

Fig. 3. Directions considered at Basistha Chariali intersection.

Four phases are considered for designing of the signals as shown in Fig. 4.

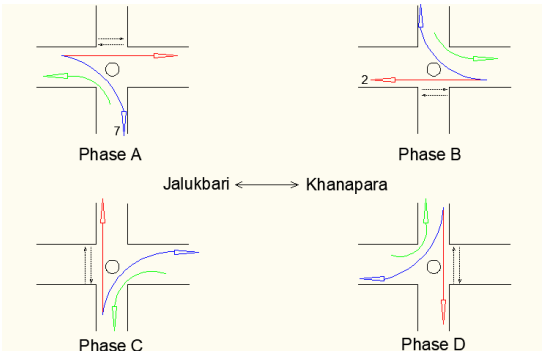

Fig. 4. Phases considered for the intersections.

After designing the signal timings for all the intersections, Table 4 is summarized.

Table 4. Summary of phase timings.

Phases	Basistha		Lokhra		Garchuk	
	Green	Amber	Green	Amber	Green	Amber
Phase A	72	3	61	3	23	3
Phase B	77	3	57	3	51	3
Phase C	26	3	54	3	36	3
Phase D	33	3	26	3	58	3
Total time	220s		210s		180s	
Distance	4.83 km between Basistha and Lokhra		4.13 km between Lokhra and Garchuk			

Now, in order to increase the efficiency of the traffic signals they need to be coordinated with each other.

CASE I: Direction- Khanapara to Jalukbari

Assuming, average velocity of the vehicles = 60 kmph = 16.67 m/s

Table 5. State of the traffic signals at phase B.

Intersection	Green signal time	Amber signal time	Red signal time	Offset Distance from X (m)
Basistha (X)	77	3	143	0
Lokhra (Y)	57	3	153	4830
Garchuk (Z)	51	3	129	8960

Since, the signals will be coordinated in the direction of Khanapara to Jalukbari and Basistha is the 1st intersection in the direction, so efficiency will be 100% at Basistha intersection.

Basistha to Lokhra:

Let us assume that the *first* vehicle from X starts at time *t*=0

It will reach Y at = $0 + \frac{4830}{16,67} = 290^{th}$ sec

Again, Let the *last* vehicle leaves X at *t*=77s

It will reach Y at $=77 + \frac{4830}{16,67} = 367^{th}$ sec

So, green signal should start at X from time, *t*=0s to *t*=77s

At Y from time, *t*=290s to *t*=290+57=347s

Efficiency at Lokhra intersection will be $= \frac{347-290}{367-290} \times 100\ \% = 74.02\ \%$

Similarly, the *first* vehicle from Y starts at $=290^{th}$ sec

It will reach Z at $=290 + \frac{4130}{16.67} = 538^{th}$ sec

Last vehicle Starts at $t=347^{th}$ sec

It will reach Z at $=347 + \frac{4130}{16.67} = 594^{th}$ sec

So, green signal should start at Z from time $t=538^{th}$ to $t=589^{th}$ sec

Efficiency at Lokhra intersection will be $= \frac{589-538}{594-538} \times 100\ \% = 91.1\ \%$

Table 6. Offset in time for Phase-B.

Green time	Basistha	Lokhra	Garchuk
Starts at (sec)	0	290	538
Ends at (sec)	77	347	589

Since the cycle will start with Phase A, so the difference

in timing of starting the signals at these three intersections calculated from Table 6 will be 0 sec, 299 sec (4 min 59 sec), 587 sec (9 min 47 sec) with respect to the time of starting at Basitha intersection.
That means, if the traffic signal is switched on at 8:00:00 am in the Basistha intersection, then the traffic signal at Lokhra should be switched on at 8:04:59 am and that of Garchuk intersection at 8:09:47 am exactly to ensure maximum efficiency of operation.

CASE II: Direction- Jalukbari to Khanapara
Phase-A
At Basistha, Green starting time = Initial time+ $\sum_{k=phaseB}^{phaseD}(\text{green} + \text{amber})$ = 0 + (77+3) + (26+3) + (33+3) = 145s
Ending time = 145+72 = 217s
At Lokhra, Green starting time = Initial time+ $\sum_{k=phaseB}^{phaseD}(\text{green} + \text{amber})$
= 299 + (57+3) + (54+3) + (26+3) = 445s
Ending time = 445+61 = 506s
At Garchuk, Green starting time = Initial time+ $\sum_{k=phaseB}^{phaseD}(\text{green} + \text{amber})$
= 587 + (51+3) + (36+3) + (58+3) = 741s
Ending time = 741+23 = 764s

Table 7. State of the traffic signals at phase B.

Green time	**Basistha**	**Lokhra**	**Garchuk**
Starts (s)	145	445	741
Ends (s)	217	506	764

Gorchuk to Lokhra
The *first* vehicle reaches at = 741+$\frac{4130}{16.67}$ =989th sec
The *last* vehicle reaches at = 764+$\frac{4130}{16.67}$ = 1012th sec
At Lokhra, green starts at: 445+210×3 =1075th sec
and ends at: 1075+61 =1136th sec
So, waiting time at Lokhra intersection for the first vehicle is = 1066 – 989 =77 sec = 1 min 17 sec

Lokhra to Basistha
The *first* vehicle reaches at = 1075+$\frac{4830}{16.67}$
= 1365th sec
The *last* vehicle reaches at = 1136+$\frac{4830}{16.67}$
=1426th sec
At Basistha, green Time Starts at: 145+220×6 =1465th sec
and Ends at: 1465+72 =1537th sec
So, waiting time at Basistha intersection for the first vehicle will be 1465 – 1365 =100 sec = 1 min 40 sec
Since, the Green time at Basistha intersection is more than that of Lokhra and Green time at Lokhra is more than that of Garchuk, so efficiency at all the intersections will be 100% but they had to stop at both the intersections for a period of 177 seconds i.e. 2 min 57 sec.

5. ANALYSIS OF COST AND TIME

Adhering to the basic principle of trying to implement a project that is in terms of investment being made from public exchequer; true value would only be realized only if it is economically viable enough. In view of this aspect, a detailed survey work was conducted at those respective intersections collecting detailed data of various aspects of traffic control from the traffic policeman in duty. Those included questions such as the investment of government (in terms of salaries being given to the traffic police), their training facilities, the work shifts etc.
After analyzing the financial expenses incurred on part of the government in terms of traffic policeman salary for a 5-year period per intersection, the amount equals to Rs. 1,28,58,000/-. This is the cost incurred assuming that there is no hike in the salaries.
The main signal proposed by the authors at each of the three intersections will be as shown in Fig. 5 the proposed pedestrian signals as shown in Fig. 6.

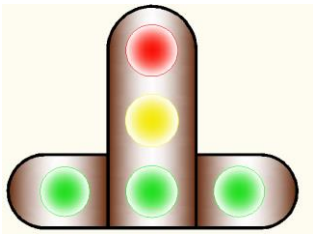

Fig. 5. Proposed main signals at each of the three intersections.

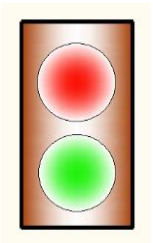

Fig. 6. Proposed sub signals (for pedestrian traffic flow) at each of the three intersections.

Considering four such combinations of signals at each intersection, the total installation cost per intersection comes to Rs. 2,29,320/-
The power consumption cost of Rs. 13,204 is obtained and assuming one home guard will be appointed to switch on the traffic signals at the specific time from a common place and four constables are appointed to ensure smooth vehicular flow, the total cost in signalized intersection equals Rs. 20,52, 524/- per month
At the rate of current cost, for the next 5 years the government has to spend Rs. 1,28,58,000/-
If, the intersections get signalized the cost incurred for the next 5 years will be Rs. 20,52, 524/-
So, total saving in next 5 years = Rs. 1,08,05,476/-
% of money saving = 100× (10805476/12858000) = **84.04 %**

After taking 10 nos. of trips from Jalukbari to Khanapara and vice versa during different times of a normal day at a maximum speed of 60 km/hr, it is found that the average time taken by a vehicle to travel

from Khanapara to Jalukbari is 36.62 minutes and from Jalubari to Khanapara is 36.84 minutes. But if, traffic signals are installed and coordinated, the optimistic time taken by a vehicle at 60 km/hr speed to cover the same distance will be as shown in Table 8-

Table 8. Optimistic travel time calculation.

Direction	Calculation	Time taken
Khanapara to Jalukbari	Total distance between Khanapara and Jalukbari/Speed of the vehicle = (2.62+4.83+4.13+7.09) km/ 60 kmph = 0.311 hour	18 minutes 40 seconds =18.67 minutes
Jalukbari to Khanapara	Waiting Time at all the intesections + Total distance between Khanapara and Jalukbari/Speed of the vehicle = 2 min 57 sec + 0.311 hour	21 minutes 37 seconds =21.62 minutes

The pessimistic time (assuming that the vehicle gets stopped at all the intersections for the maximum possible amount of time) taken by a vehicle at 60 km/hr speed to cover the same distance will be as shown in Table 9-

Table 9. Pessimistic travel time calculation.

Direction	Calculation	Time taken
Khanapara to Jalukbari	Optimistic Time + (Phase-A + Phase C + Phase D) of all the intersections =18 minutes 40 seconds + 416 seconds	25 minutes 36 seconds = 25.6 minutes
Jalukbari to Khanapara	Optimistic Time + (Phase-B + Phase C + Phase D) =21 minutes 37 seconds + 445 seconds	29 minutes 2 seconds =29. 03 minutes

So, the average time taken can be taken as average of optimistic and pessimistic time and adding 20% for loss due to interaction with other vehicles.

i.e. time taken from Khanapara to Jalukbari= 26.57 minutes

Similarly, time taken from Jalubari to Khanapara = 30.4 minutes

So, % time saving in the direction of Khanapara to Jalukbari will be **27.4 % and that** in the direction of Jalukbari to Khanapara will be **17.5 %**

6. CONCLUSION

It is found that after installing the traffic signals at the three major intersections of the Guwahati bypass road i.e. NH-27

- The users can save 27.4% of their time while commuting from Khanapara to Jalukbari
- The users can save 17.5% of their time while commuting from Jalubari to Khanapara
- The government can save 84.04% of the taxpayers' money

7. REFERENCES

1) Reddy, B.S., Reddy, N.V. (2016): S*ignal design for T-intersection by using Webster's method in Nandyal town, Kurnool district of Andhra Pradesh*, 3(4), 1124-1131.
2) Indian Road Congress- 93 (1985): *Specification for Signal Poles.*

Sustainable Urban Development

Urban waste management

Urban waste management: Situation in Guwahati, Assam

Kalita, D.[1] and Wahab, S.W.[2]

[1]Guest Lecturer, Civil Engineering Department, Goalpara Polytechnic, Goalpara-783121, India.
[2]Master Student, Department of Civil and Environmental Engineering, University of Stuttgart, Stuttgart-70569, Germany.

ABSTRACT

Guwahati is the gateway to the seven sisters of the northeast region of India. With an exponentialpopulation growth every year, the city has a high generation of waste primarily due to non-availability of proper waste management techniques to dump or recycle all the wastes generated by an approximately two million people (2017). Often, it is seen that the wastes end up in the drainage systems leading to clogging up of drains.

The under-capacity waste containers, irregular emptying of the bins, non-availability of secured dumping grounds, lack of incineration facilities, inefficiency of the city waste management techniques create havoc at times and as a result the waste management system collapse under the load which were designed inadequately without considering the population density, locality, type of waste generated, economic condition of the people, mentality and various other factors. The purpose of this study is to identify innovative, feasible and more practical solutions taking into account the present scenario of Guwahati area and working on the development of a sustainable urban waste management system and mitigate the undesirable consequences from the unplanned waste management system in certain localities.

Keywords: clogging, dumping grounds, incineration, sustainable urban waste management, mitigate

1 INTRODUCTION

Guwahati is the gateway to the North Eastern part of India. It is the biggest city in the state of Assam. It is located at 26.1445° N latitude and 91.7362° E longitude and covering an area of 216 sq. km with a population of two million. The population density of Guwahati is 4400 persons per square kilometer. Guwahati lies between the banks of river Brahmaputra and at the foothills of the Shillong plateau.

The current scenario of solid waste management is very unorganized and uncategorized. Despite the entire awareness program “Swachh Bharat”, still all kind of solid waste i.e. wet, dry, renewable, plastic, hazardous wastes are collected and dumped together

pplication of various techniques that have not been previously used in the area.

2 PRESENT SCENARIO IN GUWAHATI

The method of disposal by the people differs in many ways. For example, out of the households sampled, 40 percent used the municipal bins for disposal of waste, 35 percent dispose it in their own campus, 11 percent throw it on the road side and only 6 percent give it to private parties on a payment basis. The remaining 2 percent burn it and 6 percent use other methods of disposal.During the study, various solid waste typeswerecollected and differentiated as biodegradable, plastic, glass and metal waste which comprised the total generation; contributing as 57%, 1%, 14% and 28% respectively in the total waste in West Boragaon Dumpsite. This dumping is done without any pre- treatment, processing and precautions, which has become amajor health risk for the people in the neighboring area. The purpose of this study is to identify a possible solution considering the present scenario of Guwahati area and working on the development of a sustainable urban waste management system that would be sufficient enough to accommodate the whole of waste generated without causing any nuisance in the area and treating them efficiently. This study also focuses on ways to mitigate the undesirable consequences from the unplanned construction of sewage systems and on ways to utilize and reuse waste in the area by

generation scenario.

Figure 1 Methods of Waste Disposal

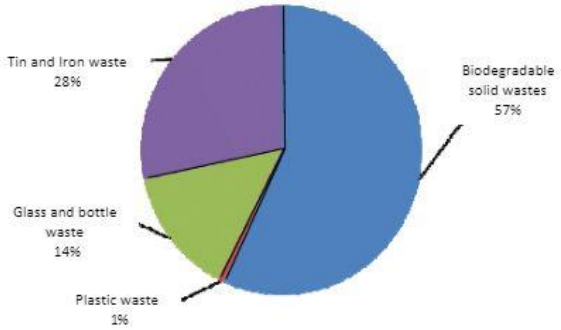

Figure 2 Types of Waste Generated

3 PROBLEMS IN GUWAHATI DUE TO INEFFICIENT WAYS OF HANDLING SOLID WASTE

1. Irregularity in emptying of waste containers in some of the busiest locations of the city lead to piling up and littering of waste in the surrounding areas.
2. Under- capacity bins are installed at places where the requirement of the bin size is much larger.
3. Improper dumping of wastes away from the demarcated area (Boragaon Landfill).
4. Unscientific way of dealing with hazardous waste.
5. Hazardous medical wastes are seen to be disposed of together with domestic wastes.
6. Unawareness of the people concerning waste treatment, sorting and disposal.
7. Unethical ways of disposing waste without caring about the environment.
8. Lack of pretreatment of waste before dumping it into the landfills.

4 SOLID WASTE MANAGEMENT TECHNIQUES

When people think about managing solid waste, they likely associate it with garbage being dumped in landfills or incinerated. But there comes associated consequences with it if not handled properly. There are various methods for solid waste management that are used worldwide considering the population density, type and amount of waste generated per annum. Few methods are listed here.

1. Landfills: This is the most common method to dispose solid waste and the least preferred method in the waste management hierarchy. This method could only be implemented when proper care is taken so that dumping sites are completely sealed and there is no scope of pollution of land, water and air.
2. Incineration: It is one of the most effective ways to treat solid waste. It reduces mass of the waste greatly. In places where there is scarcity of dumping sites, incineration is a good waste management option. Also, the energy generated could be used for various purposes.
3. Recycling and reuse: This is one of the most popular methods to treat solid waste. Materials such as paper, glass, plastic, metals can be recycled and reused. This method also aims at reduction of consumption of new materials and energy.
4. Composting: The biodegradable waste can be turned into manure for agriculture, and at the same time reduce the load on landfills. This is an environmental friendly way to deal with the waste generated.
5. Pyrolysis: This method could also be applied to reduce solid waste by chemically burning them in the absence of oxygen. The main products obtained from this process have a high calorific value such a syngas, biofuel which can be further used.

   The above mentioned are some of the few procedures that are performed in some developed nations all over the world. Considering the present scenario of waste management in Guwahati, Assam, this paper focuses on how these techniques can be utilized according to the needs, economic viability, amount and type of waste generated.

5 WAYS TO IMPROVE SOLID WASTE MANAGEMENT IN GUWAHATI, ASSAM

The possible ways are as follows:

1. The first step towards an efficient way to handle solid waste is proper sorting and separation of biodegradable waste from the non- biodegradable ones. Strict rules should be implemented by the Guwahati Municipal Corporation (GMC) to sort out waste separating plastics, glass, paper, metals and biodegradable wastes.
2. The landfill areas of West Boragaon should be enclosed completely so that the waste does not lie exposed in the surrounding areas which are a major problem at present. The waste ends up in drains ultimately clogging them.
3. The underlying soil of the dumping grounds should be properly lined and structured so that the leachate does not end up polluting the ground water.
4. The solid waste generated from Guwahati which is mainly urban waste has the potential to be recycled and reused.
5. The biodegradable waste can be efficiently transformed into compost which can be used as manure. People having sufficient space in their compounds can chose to do it on their own as it would reduce the load and cost.
6. Guwahati, having a lot of medical institutions generate a large amount of hospital wastes.

These wastesshould be incinerated instead of dumping in order to prevent spreading of hazardous materials.

7. The waste generated from industries should be pyrolysed (chemically treated) and converted into other reusable forms.
   Incineration and Pyrolysis being expensive ways to treat solid wastes should be used efficiently and GMC should take necessary steps to implement these ways to deal with hazardous wastes.

6 CONCLUSIONS

Considering the rapid growth of population in Guwahati, and with it, the high amount of waste being generated, it is the need of the hour to deal with the waste in an efficient manner. Mishandling of waste often leads to various other health and hygienic problem and at the same time affecting the quality of life. Improper management of waste leads to various soil and water borne diseases. The solid wastes often end up in drains, heavily clogging them which are one of the major causes of flash flood. In order to solve this problem of flash flood, authorities need to first take care of waste disposal methods. The problem requires scientific planning by the responsible authorities of the government of Assam for effective waste disposal and reuse techniques by taking into account the type and amount of waste, location, economic condition of the people in Guwahati. The Government must come up with innovative schemes and ideas to protect, maintain and preserve the land and natural water bodies from the pollution of solid wastes.

6 REFERENCES

1) Kashyap, A. , Kalita, J.,Kalita, S., and Mazumdar, K.,Environ, Guwahati, Assam, India-781 006
2) Chakraborty, A., Goswami, A., Deb, A., Das, D., Mahanta, J. (2014): Management of waste generated in Guwahati city and the Incorporation of Geocells in the landfill site
3) Master Plan Guwahati 2025, Guwahati Development department, Government of Assam
4) Draft, Assam Urban Solid Waste Management Policy, 2018
5) Gogoi, L., Municipal solid waste disposal: A Case Study in Guwahati City to Mitigate Man Made Disaster.

Grey water recycling and its applications

Paul, S.R.[1], Medhi, S.K.[1] and Upadhyaya, C.[2]

[1]UG Student, Department of Civil Engineering, Royal Global University, Guwahati-781035, India.
[2]Assistant Professor, Department of Civil Engineering, Royal Global University, Guwahati-781035, India.

ABSTRACT

The main purpose of this report is to perform the test or experiments for the sullage water that is chloride test, pH test, bod, cod etc. The report presents typical grey water characteristics that can be applied in areas where there is scarcity of water for regulations of grey water reuse. The tests are presented where treated grey water can be justified whether it can be used for flushing, gardening etc.

This report is not a plea to implement grey water management systems unconditionally and since it is cost effective, it can be aimed at providing for small house-holds and not for large scale or industrial purposes. This report focuses on the future benefits for using the model, so that it becomes economical for the people who live in Areas scarcity to water.

Keywords: sullage, grey water, reuse, cost effective

1. INTRODUCTION

Grey water is wastewater generated from bathrooms (shower and basin), laundries and kitchens, those components of household sewage that do not come from a toilet, urinal. Kitchen wastewater must not be reused as untreated grey water. It may be reused after treatment, but it is recommended that since bathroom and laundry water is relatively uncontaminated compared to kitchen water, and can be generated in higher volumes, grey water should be primarily sourced from the bathroom and laundry.

The characteristics of grey wastewater depend firstly on the quality of the water supply, secondly on the type of distribution net for both drinking water and the grey wastewater (leaching from piping, chemical and biological processes in the bio film on the piping walls) and thirdly from the activities in the household. The compounds present in the water vary from source to source, where the lifestyles, customs, installations and use of chemical household products will be of importance.

2. METHODOLOGY OF STUDY

Grey water recycling filter is an extremely effective filter media because of its ability to hold precipitates containing impurities. The filter is easy to assemble and no energy is required. Water is poured in the upper storage which is filled with three layers gravel, fine sand and charcoal. Sand & Gravel removes the bacteria and other small particles from water &charcoal is used to absorb odours and toxins from the water. The medical use of activated charcoal is mainly the adsorptions of poison. The filter net is also being used for protecting the sand from falling through the holes of the bucket. As the water travels through the sand and gravels small impurities and pathogens get trapped in the sand & gravel. The slower the water travels the more impurities are taken out. Once the water has passed through the middle storage where ceramic candles is being used to remove the suspended particles , pathogens & the fine charcoal particles that comes out with the water from the upper storage. Finally the filtrated water falls in the lower storage and to be collected from faucet for reuse.

3. OBSERVATION, RESULTS AND GRAPHS

3.1 pH, colour and odour test

Table no.1

Sample	Raw sample	Using Charcoal filtered sample	Using(Charcoal + Ceramic candle) filtered sample
pH test	8	9	9
Colour test	Grey	Translucent	Transparent
Odour test	Strong Pungent Smell	Slight Pungent Smell	Odour less

3.2 Alkalinity test

The sample is already alkaline in nature as the pH of raw sample, charcoal filtration sample and (charcoal + ceramic candle) is 8, 9 and 9.

.

3.3 Acidity test

The sample is already basic in nature hence there will be no presence of acidity.

3.4 Chloride test

There will be no presence of chloride as ceramic candle and charcoal are used which absorbs all the minerals especially chloride.

3.5 Hardness test

Graph no. 1

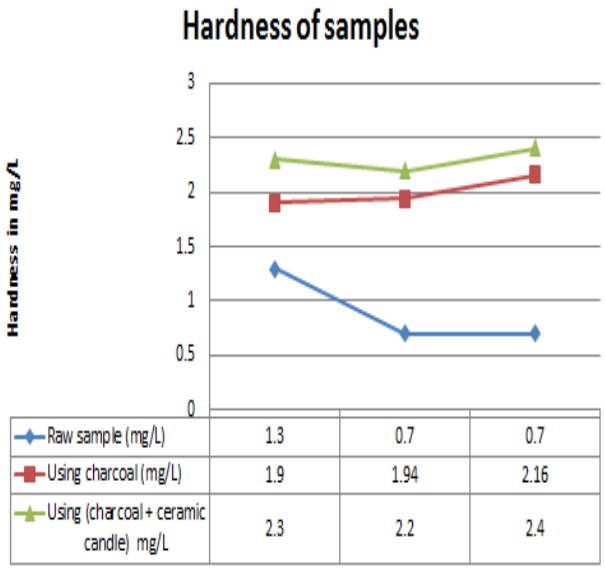

Raw sample (mg/L)	1.3	0.7	0.7
Using charcoal (mg/L)	1.9	1.94	2.16
Using (charcoal + ceramic candle) mg/L	2.3	2.2	2.4

Graph no. 2

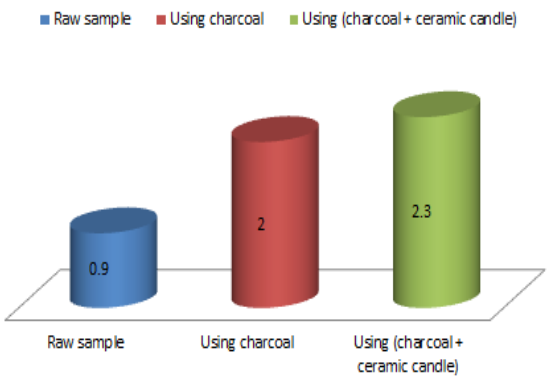

The hardness of raw sample is 0.9mg/L.
The hardness of sample using charcoal is 2mg/L.
The hardness of sample using (charcoal + ceramic candle) is 2.3mg/L.

3.6 Turbidity test

Graph no. 3

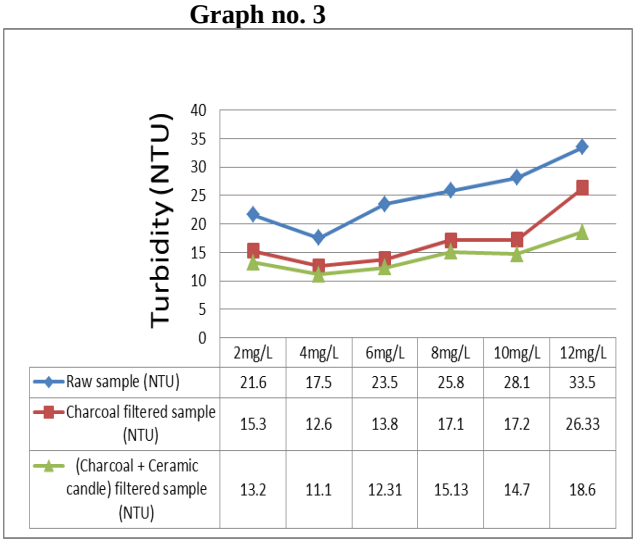

	2mg/L	4mg/L	6mg/L	8mg/L	10mg/L	12mg/L
Raw sample (NTU)	21.6	17.5	23.5	25.8	28.1	33.5
Charcoal filtered sample (NTU)	15.3	12.6	13.8	17.1	17.2	26.33
(Charcoal + Ceramic candle) filtered sample (NTU)	13.2	11.1	12.31	15.13	14.7	18.6

Optimum coagulant dosage of Raw sample is 4mg/L.
Optimum coagulant dosage of Charcoal filtered sample is 4mg/L.
Optimum coagulant dosage of (Charcoal + Ceramic candle) filtered sample is 4mg/L.

3.7 Total solids, Total dissolved solids and Total suspended solids test

Graph no. 4

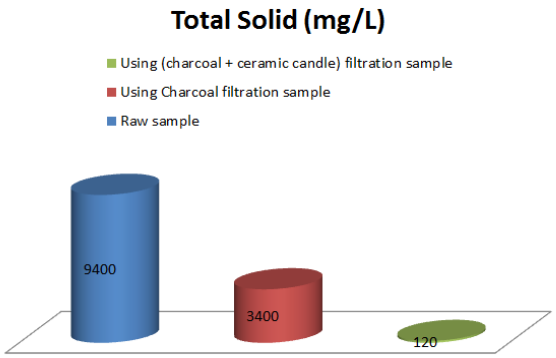

Graph no. 5

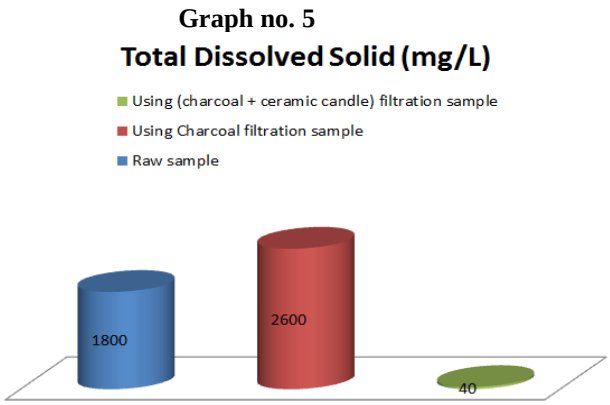

Graph no. 6

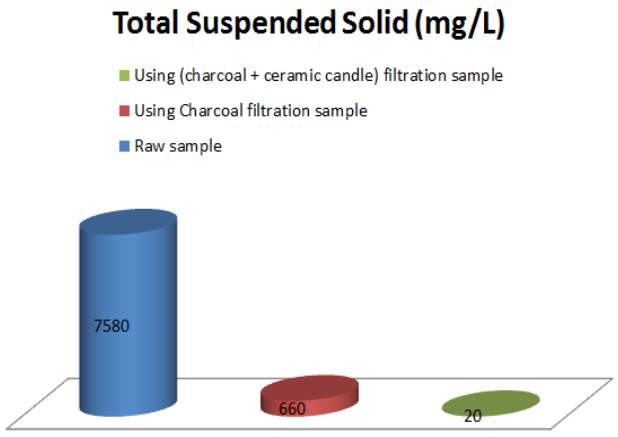

3.8 Dissolved oxygen test

Graph no. 7

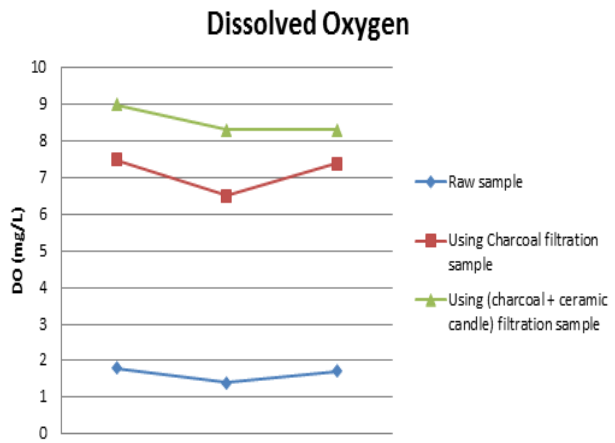

Graph no. 8

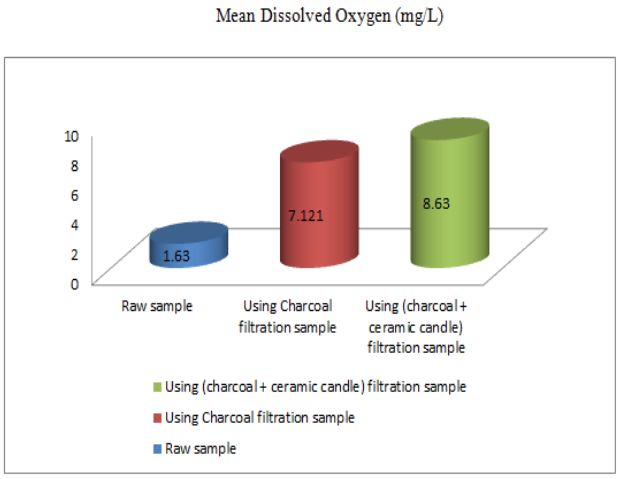

DO of Raw Sample is 1.63mg/L.
DO of Using Charcoal filtration sample is 7.121mg/L.
DO of Using (charcoal + ceramic candle) filtration sample is 8.63mg/L.

3.8 Biochemical Oxygen Demand (BOD) test

Graph no. 9

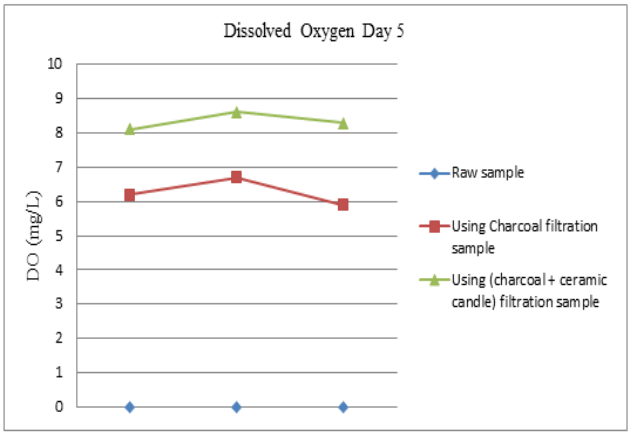

Graph no. 10

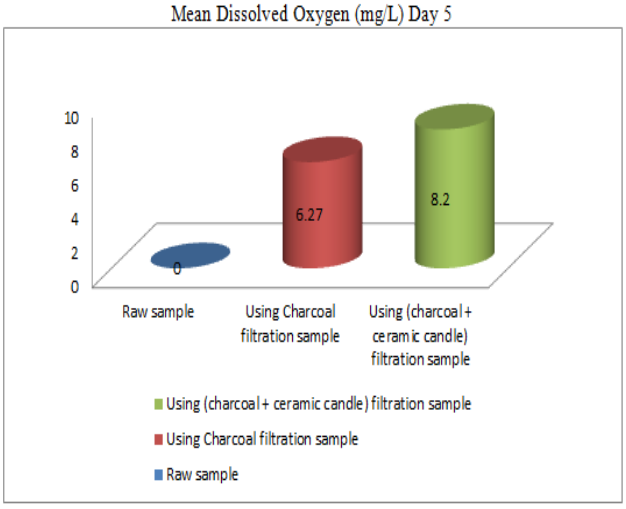

Graph no. 10

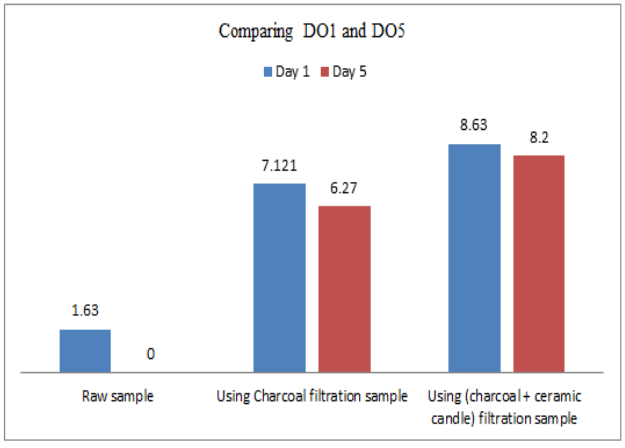

Graph no. 11

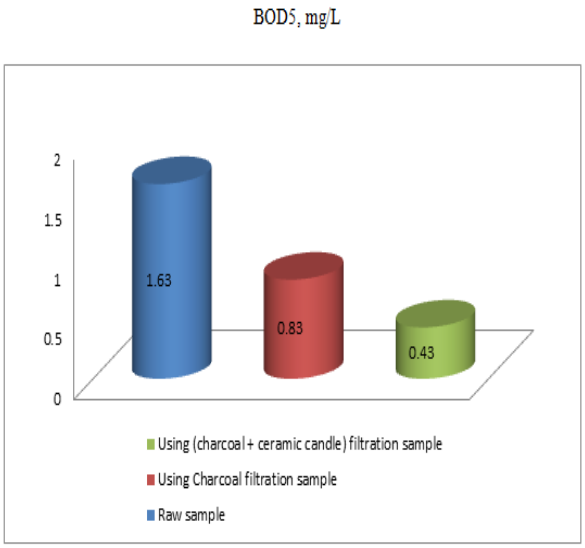

BOD5 of raw sample is 1.63 mg/L

BOD5 of charcoal filtration sample 0.83 mg/L

BOD5 of (charcoal + ceramic candle) filtration sample 0.43 mg/L

3.9 Chemical Oxygen Demand (COD) test

Graph no. 12

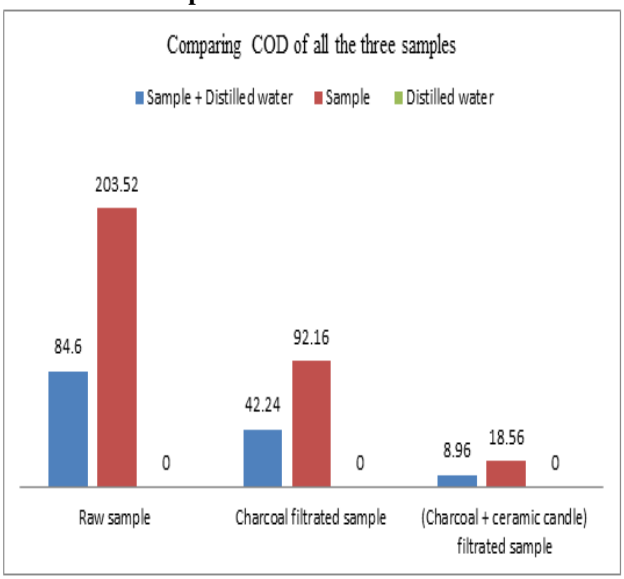

The COD value of raw sample is203.52 mg/L.

The COD value of Charcoal filtrated sample is 92.16 mg/L.

The COD value of (Charcoal + ceramic candle) filtrated sample is 18.56 mg/L.

4. CONCLUSION

The filtrated grey water has low BOD & COD value. The CPCB range for BOD is3-5mg/L & COD should be less than 20 mg/L for drinking purposes. pH of the water increases due to presence of charcoal. The filtered grey water has high amount of DO which is good for aquatic life. It means it is useable. The hardness we found in filtered sample is way more greater than the raw sample because charcoal and ceramic candle both absorbs minerals from water. The hardness we found in filtered sample is temporary hardness. Based on the criteria of hygienic safety, aesthetics and environmental tolerance, the filtered grey water is found to be usable for flushing and irrigation purposes.

5. ACKNOWLEDGEMENTS

The satisfaction of completing a project successfully would remain incomplete without the mention of people whose constant encouragement and guidance has been a great source of inspiration throughout the course of this project.
We would like to take this opportunity to express our sincere and heartfelt gratitude to our H.O.D Sir Dr. Arnab Sarma for giving us the opportunity to do the project work. We would also like to thank our project guide Chandra Upadhyaya, Assistant Professor, Department of Civil Engineering, Royal School of Engineering and Technology, for supporting and guiding us through the completion of the project work. We would also like to thank our civil engineering laboratory assistants and staff for providing us the required instruments which were required in our project work and helping us throughout the duration of the project.
I would like to thank my fellow friends Swagat Kumar Medhi, Sivanga Pratim Sarma and Zeshan Zakaria as without their support and help it is impossible to complete this project.
Finally, we would like to extend our gratitude to beloved parents for supporting and helping us in the completion of this project work.

6. REFERENCES

1) J. S. LAMBE(2005) Greywater - Treatment and Reuse, *IOSR Journal of Mechanical and Civil Engineering (IOSR-JMCE) ISSN: 2278-1684, PP: 20-26*
2) Kamal Rana(2014) INTERNATIONAL JOURNAL OF ENGINEERING SCIENCES & RESEARCH TECHNOLOGY Integrated Approach towards Grey Water Management
3) SaeedGovahi(2014) Studying of treatability of Gray Water Using Slow Sand Filter, Department of

Civil, Behbahan Branch, Islamic Azad University, Behbahan, Iran
4) R.Saranya (2017) Experimental Study On Treatment Of Sullage Waste Water Using Coagulants,SSRG International Journal of Civil Engineering
5) KarnapaAjit(2016) A Review on Grey Water Treatment and Reuse International Research Journal of Engineering and Technology (IRJET)
6) Radin Maya SaphirabteRadinMohamed(2011), ENVIRONMENTAL IMPACTS OF GREYWATER USE FOR IRRIGATION ON HOME GARDENS
7) RadinAbabuTeklemariamTiruneh, A Grey Water Dam Design for the Treatment
and Reuse of Grey Water from Single and
Multiple Households, Journal of Water Resource and Protection, 2014, 6, 1259-1267
8) Parameshwara Murthy P. M, Greywater Treatment & Reuse: A Technological Review, Parameshwara Murthy P. M., Research Scholar, Department of
Environmental Engineering, SJCE, Mysore, India
9) Sara Finley(2008), Reuse of Domestic Greywater for the Irrigation of Food Crops
10) Othman A. Al-Mashaqbeh(2012), Grey Water Reuse for Agricultural Purposes in the Jordan Valley: Household Survey Results in DeirAlla
11) KirstyCarden(20017), The use and disposal of greywater in the non-sewered areasof South Africa: Part 1 – Quantifying the greywater generated and assessing its quality

Waste management in Guwahati city- challenges ahead and ways to achieve sustainability.

Sharma, N.J.

Former Adviser (IFC&WM) NEC currently Adviser (WR) GeoKno India Pvt. Ltd.

ABSTRACT

Waste generation in any form and its inadequate collection, transportation, treatment and finally its disposal are the major environmental concern and challenges in every big cities of the world. Guwahati city in the North East part of India is no exception. Present system handled by the Municipal Corporation is not enough to cope with the volume of waste generated due to increasing population day by day, which is creating not only the environmental pollution but also affecting badly on public health. Priority needed now in waste segregation at source and use of specialized waste processing facilities to separate recyclable materials and disposal of the residual waste in a proper landfill site or create waste-to-energy facilities. This paper will review the challenges and barriers associated with the waste management in Guwahati city and shall find the ways and means to overcome the barrier to achieve a sustainable solution.

Keywords: waste management, sustainable, segregate, recyclable, waste-to-energy

1. INTRODUCTION

Millions of Tonnes of wastes are being generated every year in our country. Looking at the enormous challenges that is being faced by almost all urban cities in India, there is an urgent need to move beyond the linear production-consumption-disposal approaches, which is widely adopted at present. Most of the dumping grounds or landfills in India have not been built according to accepted specification. Owing to the decomposition of inorganic waste the ground water is contaminated. A study by the scientists at the School of Environmental science in JNU, New Delhi reveals that high level of Zinc, Nickel, Arsenic, Lead, Chromium and other metals are present in the solid waste at landfills of all metro cities. Over and above, most of the methane gas emissions is caused by landfills as a result of which a great spiral of smoke climbing the horizon is seen from the fire that catches due to heat generated by the decomposed waste. Another biggest urban challenges in India is the menace of sewage. According to a report of Centre for Science and Environment, CSE, 80% of sewage in Indian cities is integrated and flows directly into the drains and tribulets polluting the water

Therefore there is a need to critically examine the present practice of waste collection and disposal together with evacuation of untreated sewage. The present study is aimed to use both primary and secondary data collected from various sources of the GMC to arrive at a decisive solution.

2. WASTE GENERATION AND ITS CHARACTERIZATION

Generation of waste in the city is directly proportional to the growth of population. Per capita per day waste generated in Indian cities on average is 0.41 kg. Population of Guwahati city as per 2017 record (obtained from Google cloud data) is about 2.05 million which is expected to be 2.8 million by the end of 2025. Geographical area of the city under the Guwahati Municipal Corporation is about 219 sqkm. Having a population density of 4393 persons per sqkm. There are 31 wards in the city and the quantum of solid waste generation varies from ward to ward according to population density. As per one study (Lakhimi Gogoi) the average waste generation in Guwahati city is 2.66 kg per day per households. The waste generation is therefore 1090.60 Tons per day. Considering waste generation from other sources like Markets, Commercial establishments, Hotels and Restaurants, Schools and Institutions etc. which is around 25% of the domestic waste, the total solid waste generation in the city will be around 1363.10 Tonnes per day.

Impact of economic growth is generally seen on the composition of waste in India. As high income groups use more packaged products

resulting in higher consumption of plastics, paper, glass, metals and textiles etc. Municipal solid waste also includes some hazardous waste like pesticides, paints, used medicine, batteries and some compostable organics like fruits. vegetables and food waste. Most organic waste generated from households and inert waste is generated from construction, demolition and road sweeping.

3. EXISTING SYSTEM OF WASTE COLLECTION, TRANSPORTATION AND DISPOSAL IN GUWAHATI

Guwahati Municipal Corporation (GMC) is the only authority for collection, transport and disposal of solid waste in Guwahati city. As per record the status of GMC"s waste management system consists of the following facilities.

Table 1. Status of GMC, SWMS.

Sl No.	Description	Present status
1	Total number of wards	31
2	Total Number of dustbins	200
3	Total Quantity of solid waste collection per day	500 TPD(Aprx.)
4	Total number of workers Road sweepers------- Garbage Collectors----- Drivers & Handymen--- Supervisory staffs------	 720 650 200 80
5	Total number of vehicles for carrying the waste Garbage compactor----- Excavator cum loader---- Mini loaders------ Dumpers---------	 22 15 6 22
6	Place of Landfill covering 120 Bighas	West Boragaon
7	Total Number of NGOs engaged & equipped with Auto Tippers	58

According to the Solid Waste Management (SWM) rules 2016 of India, all the Urban Local Bodies (ULB) are responsible for SWM activities within their respective jurisdiction. In the Guwahati Municipal Corporation area under the Guwahati Development Department (GDD) ,the GMC takes up the following SWM activities.

3.1 Primary Collection

GMC is divided into 31 wards and these wards are assigned to 58 NGOs for the job of house to house collection of solid waste and street sweeping. The NGO deposits these waste to nearby Secondary collection bins. The work of primary collection is being supervised and monitored by the JTOs and Sanitary Supervisors of the wards. NGOs are responsible for collection of monthly user charges fixed by the GMC. NGOs use Tri cycles, Thelas, Hydraulic mounted trailer, Auto Tippers etc. for collection of waste from households and commercial establishments.

3.2 Secondary Collection

The Secondary Collection and Transportation is being handled by a fleet of modern Compactors, Tippers etc. by the GMC itself. This is looked after by Zonal engineers, JTOs and Supervisors with a fleet of hand carters and Sweepers. There are three functional transfer stations in Guwahati. One at RGB road near Nurshery, Ganeshguri, one at Chatribari and the other near GMCH, Bhangagarh. Approximately 85 to 90% waste being transported daily to Boragaon landfill point.

Fig. 1. Secondary Transfer Station at Zoo Road

Fig.2. Vans used for transporting waste to Secondary Transfer Station at Zoo Road

Fig.3.Loading of waste from the Primary Collection Point into the truck with the help of JCB

3.3. Processing and Disposal

GMC has taken up the job of segregation of dry waste at source as well as at the Functional Transfer Stations. There is adequate facility of waste cleaning and sanitization inside the station along with the provision of Leachate treatment facilities. GMC has also set up a compost plant at Boragaon in 2010 with an installed capacity of 50 TPD. However, its present production is only 5 TPD.

4. ENVIRONMENTAL AND HEALTH PROBLEM FROM ITS DUMPING SITE

Waste dumps have adverse impacts on the environment and public health. Open dumps release methane gas from decomposition of biodegradable waste under anaerobic conditions. Methane causes fire and explosions and is a major contributor to global warming. Therefore, solid waste management if not done properly will cause harmful problems to both human health and the natural environment. As per norms solid waste should be managed through a number of activities like waste prevention, recycling, composting, controlled burning etc. In Guwahati there is no recycling units near the dumping ground and the recycling business is running in an unorganized manner. Due to lack of willingness of the Govt. and the lack of awareness about the ill effects of the solid waste management among the citizens of Guwahati,not a single planned project of SWM has come up so far.

Fig.4. Present Landfill site at West Boragaon

Present dumping ground of GMC at west Boragaon has not only created a health hazard but also becoming a threat to aquatic animals like fish in the nearby Deepar beel. It has been seen that no proper disposal method is followed in the west Boragaon dumping site.The municipal trucks simply carry the wastes to the site and dispose it off without processing, which has created a health risk and air as well as water pollution in the locality.

Although GMC has been engaging NGOs to collect all the solid wastes from every nook and corners of the city, about 10 to 15% of the wastes are still remained uncollected and are strewn on the road sides and drains, which become a breeding place for mosquitos and other insects that encourage spreading of diseases like malaria, encaphelities, dengue, dihaeria etc.

5. HURDLES IN MANAGEMENT OF WASTE IN THE CITY

One of the biggest hurdles in the city of Guwahati is the absence of a planned sewage system. About eighty percent of the sewage in the city is untreated and flows directly into the drains and then to the river Bharalu flowing through the south-east and central part of the city, polluting its fresh water as well as the environment with bad odor.

The next hurdle is the lack of awareness among the citizens about the dangers of dumping or throwing of domestic wastes contain mostly

plastic pouch pack, aluminum foils etc. into the road side drains Instead of designated dustbins. GMC's role in providing separate dustbins for dry and wet wastes in sufficient numbers is another hurdle in effective management of solid waste. As a result, domestic waste, construction and demolition waste, medical waste all end up together.

Last but not the least, is the absence of an Integrated Waste Management Authority that ensures segregation and recycling of all waste, so that there shall be no necessary of landfill. The authority also need to be empowered for creating awareness among the citizens and enforcement of environmental laws enacted by the Govt.

6. MODIFICATION REQUIRED IN THE MANAGEMENT SYSTEM FOR FURTHER IMPROVEMENT

6.1. Recovery and Recycling

Recycling process to convert waste products into new products should be adopted effectively to prevent energy usage and consumption of fresh raw materials This will also reduce volume of landfills, reduce greenhouse gas emissions and preserve natural resources for future use.

6.2. Plasma Gasification

This is one of the methods of waste management used presently in various other countries. Plasma is a primary electrically charged or a highly ionized gas. Lighting one type of plasma which produces temperatures that exceed 12000 degree Fahrenheit which creates a gasification zone till 3000 degree Fahrenheit for conversion of solid or liquid wastes into syngas,that provide renewable energy and other benefits.

6.3. Waste to Energy

Waste to Energy process involves converting of Non-recyclable waste into usable heat, electricity or fuel through variety of processes. However, there is a need to import economically feasible and proven technologies. Apart from this, suitably characterized and segregated waste needs to be provided to waste-to-energy plants as per its requirement.

7. CONCLUSIONS AND RECOMMENDATIONS

(i) Number of NGOs should be increased to more households for collection of wastes.

(ii) Number of Secondary Transportation Station need to be increased at convenient locations.

(iii) Facilities of equipment and techniques in the Secondary Transfer Stations for recovery of reusable or recyclable materials from the waste should be improved and modernized as these transfer stations are the perfect solution to help create a clean environment.

(iv) No Government in the State, whichever party is in power had taken Solid Waste Management as their priority action in the annual plan. It should be wise if the political parties include the Solid Waste Management in their election manifesto and give assurance to the citizens that they will take up this job as a top priority after coming into power.

(v) Without creation of a separate department or agency for the solid waste management in the Guwahati city, the problem will never be solved.

(vi) Preventing some wasteful expenditures like holding various 'Utsavas', the Govt. should allocate sufficient fund to improve and modernize the waste management system, even by engaging efficient National and International experts or consultants.

(vii) The Guwahati Municipal Corporation should widely use the method of disposal of solid waste through Incineration or Combustion instead of dumping the waste in the landfills. The biggest advantage of this type of method is that it can reduce the volume of the solid waste to 20 to 30 percent. This process is also known as Thermal treatment which can be very well be used to generate heat leading to generation of electricity through steam turbine.

(viii) Composting plant with modern technology should be installed as per the guidelines of the Govt. of India so that all the unsafe organic waste can be turned into safe compost.

(ix) Finally, we the citizens of Guwahati should also know the waste management technique and method of disposal of different waste, in order to ensure

ourselves safe as well as keep our environment free from pollution.

(x) Government should take initiative to encourage Universities, technical Institution to take up waste management in its curriculum. Assistance of academic institutions should be solicited in characterization of waste in their vicinity.

8. ACKNOWLEDGEMENT

Solid Waste Management Division of Guwahati Municipal Corporation.

9. REFERENCES

1) P. K. Pradhan, C. R. Mohanty, A. K. Swar and P. Mohapatra Urban Solid Waste Management of Guwahati City in North-East India Source: Journal of Urban and Environmental Engineering, Vol. 6, No. 2 (July to December2012).

2) Audit Report (Civil) for the year ended 31 March 2011 of Guwahati Development Department on Performance Audit of Public Private Partnership (PPP) in Solid Waste Management (SWM) in Guwahati.

3) Gogoi,Dr. Lakhimi Geography Department Narangi Anchalik Mahavidyalaya, Assam, India. Municipal solid waste disposal: a case study in Guwahati city to mitigate the man made disaster, IOSR Journal Of Humanities And Social Science (IOSR-JHSS) Volume 9, Issue 3 (Mar. - Apr. 2013).

4) Chariar, Vijayaraghavan, Academician at IITD,Waste Management in India Perspectives and Challenges, published in September,21,2015.

5) Top 10 Things to know about Indias Waste Management Woes, Highlights of BANEGA SWATCH INDIA SEASON 5 ,LAUNCH by Swatch Bharat Abhiyan, Govt. of India ,May,2018

6) Sunil Kumar,[1] Stephen R. Smith,[2] Geoff Fowler,[2] Costas Velis,[3] S. Jyoti Kumar,[4] Shashi Arya,[1] Rena,[1] Rakesh Kumar,[1] and Christopher Cheeseman[2] Challenges and opportunities associated with waste management in India, Published online in the Journel of Royal Society Open Science, March, 2017.

7) Padmanabhan, Kavita, Solid Waste Management in Guwahati City. An Interview published in the Telegraph on August,12,2012.

8) Rajkumar Joshi1 and Sirajuddin Ahmed2 Environmental Chemistry Pollution & Waste Management. A Review Article.Status and challenges of municipal solid waste management in India: Reviewed in,Feb.2016

Sustainable Urban Development

Sustainable solutions for urban flood problems

Unsteady flow analysis of Brahmaputra river at an urban stretch of Guwahati using HEC-RAS

Choudhury, R.S. [1]and Borah, T. [2]

[1] Student, Department of Civil Engineering, Assam Engineering College, Jalukbari, Guwahati 781013, India.
[2] Associate Professor, Department of Civil Engineering, Assam Engineering College, Jalukbari, Guwahati 781013, India.

ABSTRACT

An approach has been proposed for unsteady flow simulation for the river Brahmaputra considering the flow from Uzanbazar to Palashbari area of Assam. The present study focuses on calculation of surface water elevations on the part of Brahmaputra River flowing through Guwahati city for different amount of discharges, and also includes determination of flooding area at different amount of the discharge for different time series. Hence, stimulate the critical situation of flood and its impact on the study area of Brahmaputra River. USACE Hydrologic Engineering Center's River Analysis System (HEC-RAS 4.1.0) model of the given study area was prepared. This software allows us to perform both steady and unsteady flow river hydraulic calculations. This software uses either the energy equation or the momentum equation for calculating the water surface profiles from one cross-section to the next. HEC-RAS is based on implicit finite difference method which uses courant number condition for time step to avoid instability problems. The unknowns in the entire analysis are computed by governing equations, boundary and initial conditions. The study reach consists of 17 cross-sections. Hydraulics model HEC-RAS is employed to evaluate flood conveyance performance and also non-uniform flow computation is carried out. The output from the model shows that at cross-section 1 and 7 for steady and unsteady flow condition are critical and subjected to flooding of the adjoining areas disturbing the normal life, for reducing the losses protective measures needs to be taken.

Keywords: unsteady flow analysis, Brahmaputra, HEC-RAS, flood, uniform flow computation

1. INTRODUCTION

In the study of natural ecosystems, often many variables simultaneously change with time and location due to anthropogenic influences (urban, industrial and agricultural activities, increasing consumption of water resource) as well as natural processes (changes in precipitation inputs, erosion, weathering or mineral dissolutions) systematically or otherwise. Surface waters such as rivers, lakes and oceans provide humans with food, transportation and recreation; however, they are also critical recipients for the waste. Around 77% of pollution in the ecosystems comes from the human activities. There are two types of chemical contaminations that enter the ecosystems; inorganic (phosphates, nitrates and metals) and organic (pesticides and hydrocarbons). Understanding the water quality pattern is necessary to identify the distribution, growth and physiological function of aquatic ecosystems.

The Brahmaputra River is a large river system with a catchment occupying an area of 580,000 km^2 passing through four south Asian countries and characterized by a dynamic fluvial regime with unique physiographic setting spread along the eastern Himalayan region (Goswami, 1985; Sharma, 2005). The relatively recent industrial growth and urbanization leading to pollution caused by industrial and municipal waste in and around Guwahati city has created increasing threat to the Bharalu tributary and consequently to the river Brahmaputra.

For performing unsteady flow analysis, implicit finite difference scheme is used. Implicit finite difference scheme: The most successful and accepted procedure for solving one-dimensional unsteady flow equations is the four point implicit scheme, also known as the box scheme.The simultaneous solution is an important aspect of this scheme because it allows information from the entire reach to influence the solution at any one point.

Most of open channel flows are in steady state flow condition. In steady state flow, the velocity at any location does not change with time, whereas in the unsteady flow; the velocity changes with time. Also, the flow called uniform if the depth of flow and the velocity remain the same along the channel. In this case, the depth is called normal depth. On the other hand, for non-uniform flow condition the flow depth and velocity vary along the channel. In nature, most of the open channels experience steady or unsteady and

non-uniform flows. Natural channels tend to be non-prismatic where the cross section, alignment and slope are not consistent along the channel. The non-uniform flow can be classified in: (a) Gradually varied flow which requires the analysis of the energy equation and (b) Rapidly varied flow which requires the analysis of the momentum equation.

The flood affects human lives, destroying their home and livelihood, moreover affecting the countries business, economy and industry. As the research and development continues to overcome this vulnerability, the study made in this project tries to focus on the use of HEC-RAS. The objective of the study is to analyse the stability of a segment of Brahmaputra River by evaluating its carrying capacity in response to peak discharge and slopes.

2. STUDY AREA

The Brahmaputra is one of the major rivers of Asia, a trans-boundary river which flows through China, India and Bangladesh. About 3,848km long, the Brahmaputra is an important river for irrigation and transportation. At Guwahati the Brahmaputra cuts through the Shillong plateau and is at its narrowest at 1km. Guwahati is a sprawling city beside the river Brahmaputra in the northeast Indian state of Assam. In the present study 15 km long Brahmaputra river reach is selected along Guwahati city. The study area is located 26^{O}12’06.04’’N to 26^{O}10’43.98’’N and 91^{O}45’22.88’’E to 91^{O}37’18.46’’E. It covers the area from Uzanbazar upto Palasbari. There are large residing populations along this river which necessitates the extensive study of potential threats arising from the deterioration of quality of water. Figure 1 shows the map of the study area comprising the part of Brahmaputra river adjoining Guwahati city.

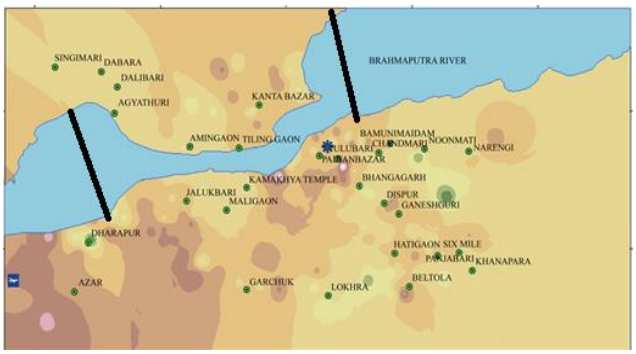

Figure 1: Image showing the study area of brahmaputra river

3. METHODOLOGY

This software used was HEC-RAS system, which is a product of Corps’ Civil Works System Wide Water Resource Research Programme (SWWRP). The HEC-RAS system was developed at the Hydraulic Engineering Centre (HEC), which is a division of the institute for water resources (IWR), U.S. Army Corps of Engineers. The software was designed by Mr. Gary W. Brunner, leader of the HEC-RAS development team.

3.1 Geometric information

The main objective of HEC-RAS is to calculate the water surface elevations for all the required locations either for steady or unsteady state simulations. The basic geometric data needed for analyses are cross-section information; reach length, energy length coefficients that include friction loss, contraction and expansion losses, and stream junction data. In the case that the widths or depths are varying significantly between the cross-sections, the interpolation can be used through HEC-RAS geometric option.

3.2 Cross sections information

Cross sections are representatives for the locations along the river, and they indicate the changes of slopes and roughness of river section. The spacing between channels is important depending on the type of the study. The cross section is defined by entering the station and elevation (X-Y coordinates) with a given station number. Normally the given station numbers will be numerically reduced from the upstream to downstream in order to identify the exact location within the software. Reach lengths which defines the distance between two consecutive cross-sections should be entered as well. The distance between the left banks and right banks of two consecutive cross sections represent how the river reaches’s meanders. Energy loss coefficients, which are roughness, expansion and contractions, should be included.

3.3 Unsteady state flow simulation

Time dependent boundary conditions and initial conditions are required to be entered in HEC-RAS in order to simulate the constructed model in unsteady state condition. Each model needs certain boundary conditions for upstream and downstream. Flow hydrograph, stage hydrograph or flow and stage hydrograph can be considered as an upstream boundary condition whereas the rating curve, normal depth, flow hydrograph, stage hydrograph or known flow and stage can be considered as the downstream boundary conditions. On the Other hand, the internal boundary condition can be lateral inflow hydrograph, uniform lateral inflow hydrograph, groundwater inflow hydrograph, and internal in stage and flow hydrograph. In addition, the initial condition can be done by entering the flow data for each reach. The principles of conservation of continuity and momentum are used to calculate the flow of water in terms of differential equations.

4. DATA ANALYSIS

4.1 Geometric data

For analysis, at first we add the map of the traced river as the background image in the geometric data editor. Then by using the river reach tab we draw the river over the map. While drawing the river in the geometric data editor we have straighten many curves of the actual river profile for our convenience. After that, we have added the calculated cross sections, naming them as RS1 at downstream end to RS17 on the upstream end, along with their profile elevation data. After entering the required geometric data, the HEC-RAS window will be as shown in Figure 2.

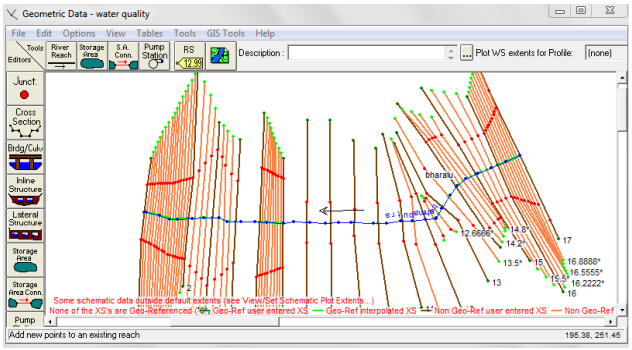

Figure 2: The HEC-RAS window showing the geometric data editor along with cross sections

4.2 Cross-section data

The cross-section data includes the station and elevation data of each section. Reach length, manning's value of floodplain and main channel and contraction and expansion coefficients are the data which are to be entered in the cross-section data editor. Figure 3 gives the HEC-RAS window showing the cross-section data editor.

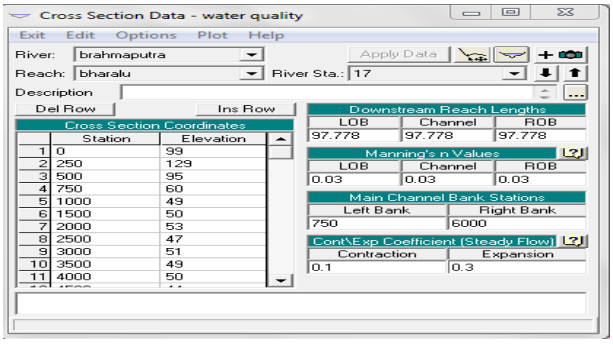

Figure 3: HEC-RAS window showing the cross-section data editor

4.3 UNSTEADY FLOW DATA

Unsteady flow data are required in order to perform an unsteady flow analysis. Unsteady flow data consists of boundary conditions (external and internal), as well as initial conditions. In this present work, flow hydrograph is used as upstream boundary condition and normal depth is used as downstream boundary condition. The flow hydrograph entered in the software is shown below in Figure 4. The flow hydrograph entered is from January 2010 to December 2011. The data collected was on weekly basis. It was collected from Brahmaputra Board, Bashishta.

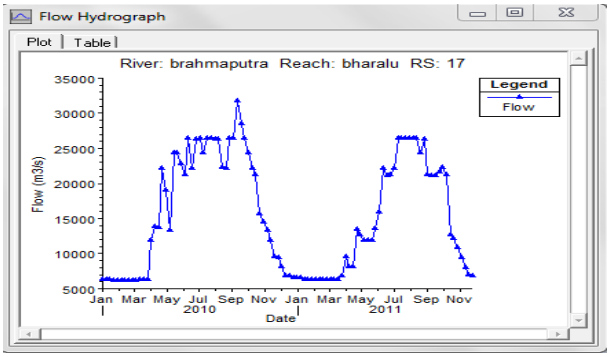

Figure 4: Flow hydrograph at cross-section 17

5. RESULTS AND DISCUSSION

5.1 Water surface profile

The Brahmaputra river water surface profiles are computed for a technical issue like rain water during the monsoon season. Profiles are computed for flood insurance studies, flood hazard mitigation investigations, other similar design needs. The water surface profile can be computed using step profile (standard step method) for unsteady flow. The method is based on solving the unsteady flow equations using a cross section to cross section. Figure 5 shows the water surface profile of the entire study reach.

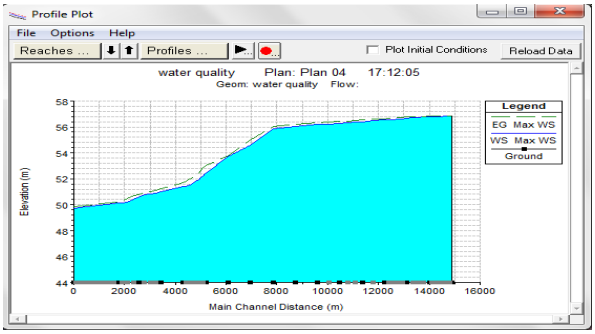

Figure 5: Water surface profile plot of the study area of brahmaputra river

5.2 Cross- section geometry

Boundary geometry for analysis of flow in natural streams is specified in terms of ground water profiles (cross section 15 km reach) and the measured distances between them (reach length). Each cross-section in an HEC-RAS data set is identified by a river, reach and river station label. The cross-section is defined by entering the station and elevation (X-Y data) from left to right, with respect to looking in the downstream

direction. Cross-section data are used to determine the conveyance and storage of a river channel and overbank areas (Figure 6). Storage area and top width can also be determined from cross-section data.

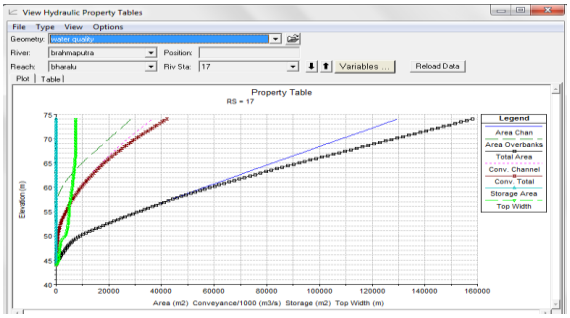

Figure 6: Hydraulic condition of the study area of brahmaputra river

5.3 Velocity profile of the study area of Brahmaputra River

The velocity profile of the study area of Brahmaputra River for the main channel is different from the velocity profile of left and right channel. The velocity is seen to be maximum in between cross-section 6 and 7. Figure 7 shows the velocity profile of the whole channel.

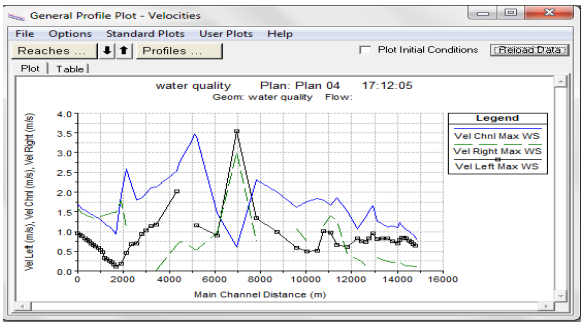

Figure 7: Velocity profile of the study area of brahmaputra river

5.4 General Profile Plot

In the general profile plot, we can plot hydraulic depth, surface area, shear, top width etc. versus main channel distance. Figure 8 shows hydraulic depth versus main channel distance. Figure 9 shows the general profile plot of surface area throughout the main channel distance for maximum water surface profile.

5.5 Rating curve of the study area of Brahmaputra River

In hydrology, a Rating curve is a graph of discharge versus stage for a given point on a stream, usually at gauging stations, where the stream discharge is measured across the stream channel by HEC-RAS model. Numerous measurements of stream discharge are made over a range of stream stages. The rating curve is usually plotted as discharge on x-axis versus stage (surface elevation) on y-axis. An example of Rating curve of cross-section 1 is shown in Figure 10.

The rating curve plotting window has the ability to plot other variables besides discharge versus water surface elevation. Any variable that is computed at any cross section can be displayed against another computed variable (or variables). An example of this capability is shown in Figure 11. In this example, Discharge (x-axis) is being plotted against total flow area and main channel flow area (y-axis).

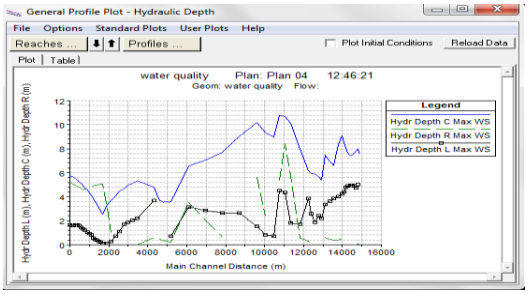

Figure 8: General profile plot showing hydraulic depth

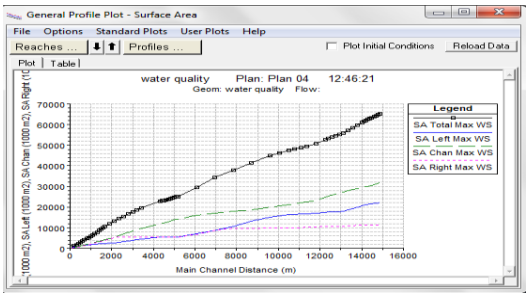

Figure 9: General profile plot showing surface area of the channel for maximum ws

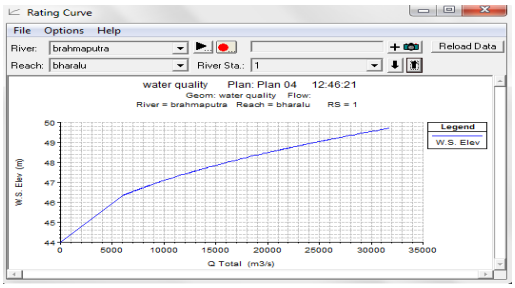

Figure 10: Profile plot showing the rating curve for cross-section 1

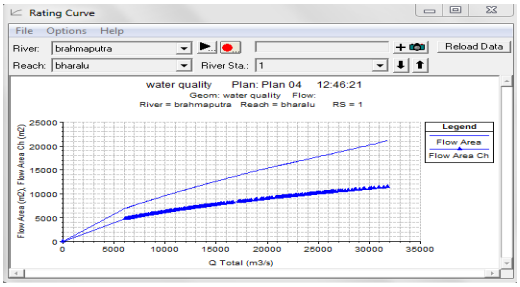

Figure 11: Rating curve showing discharge versus flow area

5.6 Stage and flow hydrograph

The stage and flow hydrograph option is available only when unsteady flow analysis is performed. Statistics about the hydrographs (peak stage and flow, time of peak and volume) can also be viewed in the stage and flow hydrograph window. There is an option in the unsteady flow analysis window for the user to specify the locations where we want to have hydrographs computed and available for display. Figure 12 shows the stage and flow hydrograph of cross-section 17 of the Brahmaputra River. The graph indicates that the model run was stable. The output stage and flow hydrograph can also be viewed in the tabular form.

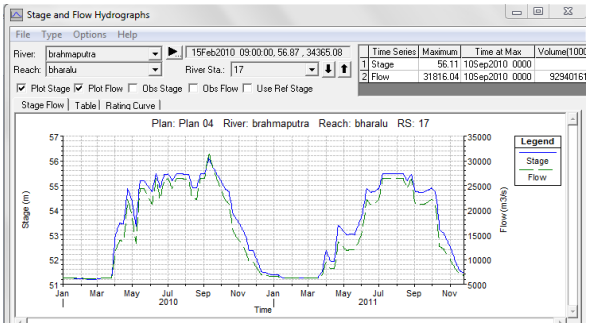

Figure 12: Stage and flow hydrograph of the study area of brahmaputra river

5.7 Computation Level Output

An additional feature that has been added to HEC-RAS to help user's find model stability problems, is the "Computational Level Output" option. Visualization of computation level output can be accomplished with either **Spatial Plots** or **Time Series Plots.** This type of output is often very useful in debugging problems with flow run. Figure13 shows the unsteady flow spatial plot of the model where we can view either a profile, a spatial plot of the schematic or tabular plot. The variables that can be plot are: water surface elevation (XS WSEL); Flow (XS flow); computed maximum error in the water surface elevation (XS WSEL ERROR); computed maximum error in the flow (XS FLOW ERROR); and maximum depth of water in the channel (DEPTH). Each of the plots can be animated in time by using the video player buttons at the top right of the window.

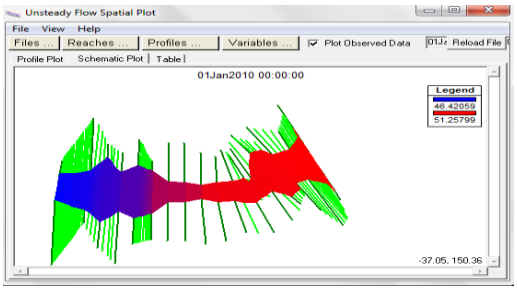

Figure 13: Schematic plot of cross-section ws elevation on unsteady flow spatial plot

6. CONCLUSIONS

The flood analysis is carried out by using the HEC-RAS model by giving the input of river cross-section and hydrologic data of river. The unsteady flow is carried out successfully for Brahmaputra River located in Guwahati city for all cross-sections of a reach. Among them cross-section 1 and 7 are overflowed and cross-sections 14, 15 and 16 are at critical condition. It is necessary to provide some prevention such as separating rainwater from sewage system, install water infiltration, impermeable surfaces replaced with permeable materials, provide protection wall to the city. Different cross-sections with different water levels of a stream help to provide preventive measures for respective cross-section and prevent them from damage. It can be concluded that:

- Flow depth, velocity, shear stress etc. can be determined from flood hydraulics by the model.
- River flow data from the one dimensional model was critical in the development of the physical model to define the modelled flow rate, in the development of two-dimensional numerical model to define the downstream boundary condition.
- One-dimensional models require many assumptions including the accurate representation of a river using selected cross-section data, and neglecting of some orthogonal and vertical velocity of Brahmaputra River.

REFERENCES

1) Beavers (1994). "*Hydraulic modelling of river channels using GIS based tools named HEC.*
2) Garde R J, Raju Ranga K. G. (2000). "*Mechanics of Sediment Transportation and alluvial stream problems"* New Age International publishers (P) Ltd. New Delhi, India
3) Jensen M. (2002), "*Using HEC-RAS to model canal systems"*. Journal of Engineering, 2, 607-616
4) Dyhouse Gary R.(2003) " *Floodpain Modelling using HEC-RAS*" Haested Methods First Edition
5) Fleenor, William E. '*Evaluation of Numerical Model, HEC-RAS and DHI-MIKE 11*." (2003).
6) Subramanya K. (2006). *"Flow In Open Channels" Tata McGraw-Hill Publishing Company Limited. New Delhi, India.*
7) Daniel E. Christiansen and David A. Eash (2008) "*Flood-Plain Study of the Upper Iowa River in the vicinity of Decorah, Iowa*" USGS Report.
8) US Army Corps of Engineers, (2010) *"HEC-RAS, Hydraulic Referance Manual,"* Hydrologic Engineering Center, Version 4.1.
9) US Army Corps of Engineers, (2010) *"HEC-RAS, User Manual,"* Hydrologic Engineering Center, Version 4.1.
10) Timbadiya P. V., Patel P., Porey Prakash D., (2011) "*Calibration of HEC-RAS model on Prediction of Flood for lower Tapi river India,"* Journal of Water Resource and Protection.

A study of soil loss behaviour of hilly urban watershed of Guwahati city for various surface cover scenarios of steep hill cuts

Patowary, S. [1] and Sarma, A.K. [2]

[1]Associate Project Engineer, Department of Civil Engineering, IIT Guwahati, Guwahati-781039, India.
[2]Professor, Department of Civil Engineering, IIT Guwahati, Guwahati-781039, India.

ABSTRACT

Excessive removal of vegetative covers caused by incessant urban growth in the hilly watersheds of Guwahati city is a prime reason for the increasing urban flood in the city. Since residents of Guwahati city are not typical hill dwellers, they prefer to live in a flat land than in a raised platform in the form of a stilt house. Hence, they cut the natural slope into bare standing hill cuts to get some additional flat area for housing. The soil erosion from these near-vertical hill cuts contributes to the water-logging in the drainage system of the city. However, these steep hill cuts are not detectable in ortho-rectified satellite images, resulting in the erroneous soil loss estimation. Therefore, in this study, the soil loss from a watershed of the city has been estimated by using GIS-based RUSLE by incorporating the hill cut factor which considers the soil loss from those standing hill cuts. In order to analyse the variation of annual sediment loss from hills with the variation of conditions of the steep hill cuts, four different surface cover conditions were considered and compared with the present condition obtained from a field survey. It is found that if all the steep hill cuts are in bare condition, there will be a 16.5% increase in annual soil loss from the watershed. Similarly, if those are well-maintained by grass or creepers, the soil loss will decrease by almost 25% in comparison to the present condition. This reveals that if steep hill cuts of hilly watersheds will be well-maintained, the urban flash flood problem of the city caused by sediment deposition in the drains will be mitigated to a large extent. Hence, the soil loss estimation with the consideration of the hill cut factor is essential for efficient and sustainable management of hilly terrains.

Keywords: urban settlement, soil loss, GIS, RUSLE, hill cut factor

1. INTRODUCTION

Soil erosion by rainwater has become a worldwide environmental problem due to the increasing deforestation or diminishment of natural land cover (De Graaff, 1996). Effect of soil loss can be categorised into two types: on-site and off-site effects (Morgan, 2009). The on-site effect mainly deals with soil quality and health. Whereas, the off-site effect includes the sedimentation in watercourses and reservoirs, increase in downstream flood, disturbance in downstream eco-system etc., which are mainly caused by the movement of the sediments to downstream. For such multi-dimensional side effects, soil loss information has become a basic need of management plans. However, the field observation of soil loss is very time consuming. Besides, by this method, it is also not very easy to quantify how the soil loss behaviour of an area is depending on its topography and climate (Morgan, 2009, Syahli, 2015). Hence, numerous models are available for estimation of soil erosion. WEPP (Nearing et al., 1989), GUEST (Ciesiolka et al., 1995; Rose et al., 1997), EUROSEM (Morgan et al., 1998) etc. are some process-based soil loss estimation models. These models can't be applied to ungauged watersheds having no observed sediment loss data (Bhattarai and Dutta, 2007). On the other hand, empirical models like Universal Soil Loss Equation (USLE, Wischmeier and Smith, 1961) and its improved versions- MUSLE (Modified Universal Soil Loss Equation; Williams, 1975) and RUSLE (Revised Universal Soil Loss Equation; Renard et al., 1991) are simple in input data requirement. Several past studies are found to use these empirical models on GIS platform (Dabral et al., 2008; Biswas and Pani, 2015).

In developing countries like India, urban settlements are expanding in a much-unplanned way. Guwahati, the most developed city in Northeast India experiences frequent urban floods due to the blockage of drains by sediments coming from the hilly urban watersheds (Desai et al., 2014). The inhabitants of Guwahati city are not typical hill dwellers residing in raised platforms in the form of a stilt house. They often cut the natural slope into bare standing hill cuts to get some additional plain area for housing. The soil erosion from these near-vertical hill cuts is also contributing to the water-logging of the drainage system in the city. On the other hand, these steep hill cuts are not detectable in ortho-rectified satellite images, resulting in the erroneous soil loss estimation. Patowary and Sarma

(2018) introduced the hill cut factor (H_f) to take account of the soil loss from those standing hill cuts associated with the urban settlements in hills. It was well-validated that due to non-consideration of this factor, the soil loss can be underestimated by 28% than the observed value. Due to the increasing urban flood issue, the accurate estimation of soil loss from the inhabited hills of Guwahati city is highly desirable. Hence, in this study, the soil loss from a hilly watershed of the city has been estimated by using GIS-based RUSLE with the incorporation of H_f into the cover management factor. The incorporation of H_f into RUSLE makes feasible to analyse how the annual sediment loss from hills varies with the variation of surface cover conditions of the steep hill cuts.

2. STUDY AREA

The study area is a mini-watershed of Japorigog hill in Guwahati city covering an area of 0.74 km^2 (Fig. 1). As it is lying in the core city area, it is experiencing a high rate of urban settlement in the recent period. The watershed, covering both plain and hilly area, has been delineated by using an SRTM (Shuttle Radar Topography Mission) DEM (Digital Elevation Model) of approximately 30 m resolution. Its elevation varies from 59 m to 177 m.

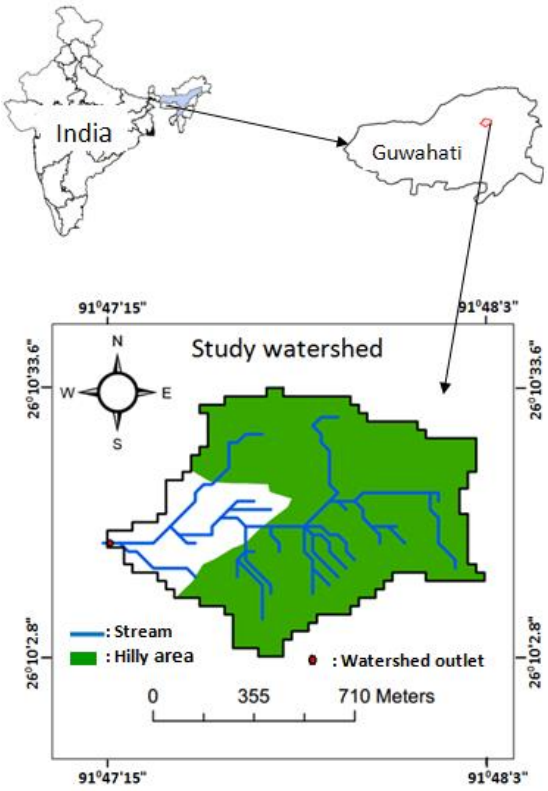

Fig. 1. Location of the study watershed.

3. METHODS AND MATERIALS

The RUSLE is given by:

$$A = R \times K \times LS \times C \times P \quad (1)$$

where, A is the average annual soil loss per unit area (tons ha^{-1}year^{-1}); R is the rainfall erosivity factor (MJ mm ha^{-1} h^{-1}year^{-1}); K is the soil erodibility factor (ton h MJ^{-1} mm^{-1}); L is the slope length factor; S is the slope steepness factor; C is the cover management factor and P is the support and conservation practices factor.

For the study area, R factor value is taken as 9259 MJ mm ha^{-1} h^{-1} year^{-1} (Sarma et al., 2005). It is having clay loam type of soil. So, the K factor is equal to 0.032925 t h MJ^{-1}mm^{-1} for the soil texture class and organic content (2%) as given in Stewart et al. (1975). LS factor has been calculated in ArcGIS platform by using Eq. (2) (Moore and Burch, 1986; Desmet and Govers, 1996a).

$$LS = (A_c/\ 22.13)^{0.6}\ (\sin\theta/0.0896)^{1.3} \quad (2)$$

where, A_c and θ are the specific catchment area (m^2) and natural slope angle (degree), respectively. In the study watershed, no support practices are found. Hence, the P factor is taken as 1. C factor values are taken based on the LULC map of the study watershed prepared from a LISS IV satellite image of capture date 4 December 2015. These are shown in Table 1.

Table 1. C factor values for LULC of the study watershed.

LULC type	C factor
Bare soil	1 (Sarma et al., 2005; Sarma, 2011)
Forest	0.01 (Sarma et al., 2005; Gelagay and Minale, 2016)
Scrub land	0.014 (Wishmeier and Smith 1961; Gelagay and Minale 2016)
Impervious area	0 (Sarma, 2011)
Urban settlement in plain area, C_g (60% impervious, 40% bare)	0.4 (=0x0.60+1x0.4)
Grass/creepers	0.01 (Sarma, 2011)
Retaining wall	0 (impervious; Sarma, 2011)

Here, C-factor for urban settlement in plain area of the watershed has been assigned by considering 60% of the settlement area is impervious and the remaining 40% is bare [According to GMDA Building By-Laws (2006), the maximum coverage area including the area for infrastructural facilities in the urban settlement area is 60%]. In this study, the soil loss from steep hill cuts associated with urban settlements in the hilly portion is also to be considered. Therefore, the C-factor for urban settlements in the hilly area will be higher than that for urban settlement lying in the plain area of the watershed. After the incorporation of H_f (Eq. 3), the C-factor for urban settlements in the hilly area of the study watershed is given by Eq. (4). The detail

derivation of H_f and C_{hu} are found in Patowary and Sarma (2018).

$$H_f = \frac{\sin\theta}{\sin(\beta-\theta)} \quad (3)$$

$$C_{hu} = \left(\sum_{i=1}^{n} a_i C_i\right) \times H_f + C_g \quad (4)$$

where, i = 1, 2, 3,....., n be types of surface covers in steep hill cuts

a_i= Fraction of the total steep hill cut area covered by the i^{th} type of surface cover.

$$\sum_{i=1}^{n} a_i = 1$$

C_i= Cover management factor of the i^{th} type of surface cover.

θ= Natural slope of the hill. Here, the average slope angle of the hilly portion of the watershed is taken from the slope map of the hilly area prepared from DEM in ArcGIS.

β= Average steep hill cut angle.

Patowary and Sarma (2018) performed a sample field survey in Guwahati city to get information regarding the present condition of steep hill cuts. It was obtained that average 1% of the total steep hill cut area is covered by retaining wall, 39% area has natural vegetations like grass or creepers and the remaining 60% area is in bare condition. Again, the average hill cut angle is obtained as 70^0 (=β). This information has been used to indicate the present scenario of hill cuts. Apart from this, four other scenarios are also assumed for the hill cuts in order to analyse the variation of sediment loss from hills as a response to conditions of the hill cuts associated with urban settlement in hills. Therefore, the five different scenarios considered here are:

Scenario 1: Present condition representing average 1% area of hill cuts being protected by retaining wall, 39% area being covered by grass or creepers and the remaining 60% area of hill cut being in bared condition.

Scenario 2: All hill cuts are completely bared.

Scenario 3: All hill cuts are completely protected by retaining wall.

Scenario 4: All hill cuts are completely covered by grass/creepers.

Scenario 5: Lower 50% area of all the hill cuts being protected by retaining wall and the upper 50% area of all the hill cuts being covered by grass/creepers.

4. RESULTS AND DISCUSSIONS

The hill cut factor, H_f for the study watershed is calculated as 0.2959. Maps of soil loss rate (in t ha^{-1} $year^{-1}$) are prepared for all the five scenarios by multiplying raster maps of RUSLE parameters in ArcGIS and an average rate of soil loss is calculated for all scenarios. The cover management factor C_{hu} for the urban settlement in the hilly area and average rates of soil loss for all the scenarios are shown in Table 2. From the table, it is clear that if all the steep hill cuts will be in bare condition (scenario 2), the soil loss rate will increase by 16.52% from the present value. On the other hand, soil loss can be significantly decreased by implementing the scenarios 3, 4 and 5. The maximum decrease in soil loss rate can be obtained by replacing the present condition (scenario 1) of the hill cuts with scenario 3. This is as expected since in scenario 3 all hill cuts are well protected by retaining wall. Again, scenarios 3, 4 and 5 are decreasing the soil loss from the study watershed almost equally (~25%). Therefore, from environmental as well as economic point of view, for management purpose, scenario-4 is more enviable. It is worth to mention that in this study soil loss only due to the rill and inter-rill erosion has been considered. It does not include the substantial amount of soil loss due to the potential landslide and channel/gully erosion.

Table 2. Cover management factor of urban settlement in hill and soil loss rate for different scenarios

	Scenarios				
	1	2	3	4	5
C_{hu}	0.5787	0.6959	0.4	0.4030	0.4015
Soil loss rate (t ha^{-1} $year^{-1}$)	402.95	469.52	301.46	303.14	302.32
Change (%) in soil loss w.r.t. senario-1		+16.52	-25.19	-24.77	-24.98

5. CONCLUSIONS

This study attempts to determine the amount of soil loss from a hilly urban watershed located in Guwahati city by using GIS-based RUSLE incorporating the hill cut factor. In addition to the present scenario, five different scenarios have been assumed for the surface cover conditions of steep hill cuts. The comparison of soil loss for these scenarios with that of the present scenario indicates that the amount of soil loss from the study watershed is highly dependent on the surface cover condition of the steep hill cuts. If all the steep hill cuts are in bare condition, there will be a 16.5% increase in annual soil loss from the watershed. Similarly, if those are well-maintained by grass or creepers, the soil loss will decrease by almost 25% in comparison to the present condition. This reveals that if the steep hill cuts of hilly watersheds will be well-maintained, the urban flash flood problem of the city

caused by sediment deposition in the drains will be mitigated to a large extent. Soil erosion rate has a stronger relationship with land cover change than that with the variability in rainfall or slope (Kosmas et al., 1997). That's why in the recent period, land-use based watershed management techniques are quite well-accepted and the information derived in this study can be very useful for such management schemes.

REFERENCES

1) Bhattarai, R., & Dutta, D. (2007): Estimation of soil erosion and sediment yield using GIS at catchment scale, *Water Resources Management*, *21*(10), 1635-1647.
2) Biswas, S. S., & Pani, P. (2015): Estimation of soil erosion using RUSLE and GIS techniques: a case study of Barakar River basin, Jharkhand, India, *Modeling Earth Systems and Environment*, *1*(4), 42.
3) Ciesiolka, C. A., Coughlan, K. J., Rose, C. W., Escalante, M. C., Hashim, G. M., Paningbatan Jr, E. P., & Sombatpanit, S. (1995): Methodology for a multi-country study of soil erosion management, *Soil Technology*, *8*(3), 179-192.
4) Dabral, P. P., Baithuri, N., & Pandey, A. (2008): Soil erosion assessment in a hilly catchment of North Eastern India using USLE, GIS and remote sensing, *Water Resources Management*, *22*(12), 1783-1798.
5) Desai, R., Mahadevia, D., and Mishra, A. (2014): City Profile: Guwahati (CUE Working Paper 24), *Centre for Urban Equity (CUE), Ahmedabad.*
6) Desmet, P. J. J., & Govers, G. (1996): A GIS procedure for automatically calculating the USLE LS factor on topographically complex landscape units, *Journal of soil and water conservation*, *51*(5), 427-433.
7) Gelagay, H. S., & Minale, A. S. (2016): Soil loss estimation using GIS and Remote sensing techniques: A case of Koga watershed, Northwestern Ethiopia, *International Soil and Water Conservation Research*, *4*(2), 126-136.
8) GMDA (2006): Building By-Laws for Guwahati Metropolitan Area, *Guwahati Metropolitan Development Authority, Guwahati.*
9) Kosmas, C., Danalatos, N., Cammeraat, L. H., Chabart, M., Diamantopoulos, J., Farand, R., ... & Mizara, A. (1997): The effect of land use on runoff and soil erosion rates under Mediterranean conditions, *Catena*, *29*(1), 45-59.
10) Moore, I. D., & Burch, G. J. (1986): Physical Basis of the Length-slope Factor in the Universal Soil Loss Equation 1, *Soil Science Society of America Journal*, *50*(5), 1294-1298.
11) Morgan, R. P. C., Quinton, J. N., Smith, R. E., Govers, G., Poesen, J. W. A., Auerswald, K., ... & Styczen, M. E. (1998): The European Soil Erosion Model (EUROSEM): a dynamic approach for predicting sediment transport from fields and small catchments, *Earth surface processes and landforms*, *23*(6), 527-544.
12) Patowary, S. and Sarma, A. K. (2018): GIS-based estimation of soil loss from hilly urban area incorporating hill cut factor into RUSLE, *Water Resources Management*, *32*(10), 3535–3547.
13) Renard, K. G., Foster, G. R., Weesies, G. A., & Porter, J. P. (1991): RUSLE: Revised universal soil loss equation, *Journal of soil and Water Conservation*, *46*(1), 30-33.
14) Rose, C. W., Coughlan, K. J., Ciesiolka, C. A. A., & Fentie, B. (1997): Program GUEST (Griffith University Erosion System Template), *A New Soil Conservation Methodology and Application to Cropping Systems in Tropical Steeplands, KJ Coughlan and CW Rose, eds., ACIAR Technical Report*, 34-38.
15) Sarma, A. K., Chandramouli, V., Singh, B., Goswami, P., & Rajbongshi, N. (2005): Urban flood hazard mitigation of Guwahati city by silt monitoring and watershed 211 modeling, *Report submitted to ministry of human resources department (MHRD) by Department of Civil Engineering, IIT Guwahati.*
16) Sarma, B. (2011): Optimal ecological management practices for controlling sediment and water yield from a hilly urban system within sustainable limit, *Doctoral dissertation, IIT Guwahati, India*.
17) Stewart, B. A., Woolhiser, D. A., Wischmeier, W. H., Caro, J. H., & Frere, M. H. (1975): Control of Water Pollution from Cropland, *Volume 1--A Manual for Guideline Development.*
18) Williams, J. R. (1975): Sediment routing for agricultural watersheds, *JAWRA Journal of the American Water Resources Association*, *11*(5), 965-974.
19) Wischmeier, W. H., & Smith, D. D. (1961). A universal equation for predicting rainfallerosion losses–An aid to conservation farming in humid regions. *US Dept. of Agric., Agr. Res. Serv. ARS Special Report*, 22-66.
20) Wischmeier, W. H., & Smith, D. D. (1961): A universal equation for predicting rainfall erosion losses–An aid to conservation farming in humid regions, *US Dept. of Agric., Agr. Res. Serv. ARS Special Report*, 22-66.

Sustainable Rural Development

Sustainable Rural Development

Affordable housing

Study of seismic performance of traditional Assam-type wooden house

Chand, B. [1], Kaushik, H.B. [2] and Das, S.[3]

[1] PhD Student, Dept. of Civil Engineering, Indian Institute of Technology Guwahati, Guwahati 781039, India.
[2] Associate Professor, Dept. of Civil Engineering, Indian Institute of Technology Guwahati, Guwahati 781039, India.
[3] Assistant Professor, Dept. of Civil Engineering, Indian Institute of Technology Guwahati, Guwahati 781039, India.

ABSTRACT

Assam-type wooden houses were popular structural systems in north-eastern region of India as they performed exceptionally well during past earthquakes. These houses are also commonly known as *Ikra* houses as the walls and roof of houses are sometimes made of locally available reed named *Ikra*. Alternatively, bamboo mesh is used in walls and CGI sheets on wooden truss is used as roof. The housing is known to have a number of features that contribute to the safety of the house during an earthquake; these include light mass of walls and roof, good wall-to-wall connection, and good quality and strength of materials used. Another unique feature of these houses is flexible connections used for different wooden elements at different levels. In spite of these exceptionally good features, these houses have not received due attention and their performance under seismic action has not been studied so far. In this paper, a brief discussion of the construction methodology and dynamic performance of a full-scale Assam-type house under shake table excitation is presented. The house exhibited an excellent performance under the action of ground motions without significant damage despite extreme level shaking. The connections between various members of the house remained intact during the tests. The excellent performance exhibited can be attributed to the unique type of construction with flexible connections and light-weight material used in the construction. Results of the study will help in developing an analytical model for study of seismic performance of such houses.

Keywords: Assam-type house; shake table testing; traditional wooden house; *Ikra* house

1. INTRODUCTION

Traditional wooden type of houses are found in most parts of the world. These timber frame buildings are characterized by a timber frame infilled with variety of materials (masonry, wood products, etc.). The seismic performance of these traditional timber-braced frame systems has been found to be exceptionally resilient to earthquake shaking (Ali et al. 2012, Rai and Murty 2005, Cardoso et al. 2004). The excellent performance of these systems can be attributed to the closely spaced vertical posts, horizontal and diagonal bracing, light weight infill, and the inherent flexible property of wood. Assam-type house is one of such traditional houses, found in north-eastern region of India, which has light weight infill besides other good properties (Jain 2016).

Assam-type houses are one of the very few housing systems in India that have performed exceptionally well during past earthquakes compared to other popular structural systems, such as, reinforced concrete frame buildings and masonry buildings. Due to the historical high seismicity of the north-eastern region of India, the local people have developed a unique housing system in terms of both its construction technique and the material used in the structural components. This type of construction has been in practice for many decades, and is mostly seen in the north-eastern part of India, where the local people mostly use the local resources in construction of such houses. This makes Assam-type houses easy to construct, maintain, and an economical housing construction typology. The walls of Assam-type houses are made of *Ikra* (locally available reed found in river beds) or bamboo mesh material that makes it light weight due to which it does not require extensive foundations, and therefore, can be constructed in varied geotechnical conditions. It has excellent ability to withstand seismic events which has been proven in past earthquakes (Jain 2016, Kaushik and Ravindra Babu 2012, Kaushik and Dasgupta 2013). Also, these walls have good thermal and acoustic qualities. This type of construction does not require commercially processed materials or a skilled labour force; rather unskilled local labour can conveniently construct an Assam-type house. A typical Assam-type house is shown in Fig.1 (Kaushik and Ravindra Babu 2012).

Fig. 1. A typical Assam-type house (Kaushik and Ravindra Babu 2012).

In spite of all these exceptionally good features, these houses have not received due attention and their performance under seismic action has not been studied so far. The uniqueness of this type of house from other traditional wooden houses lies in its construction methodology, framing members, special type of connection between framing members, light-weight walls, and foundation. In the present study, a description of typical construction methodology adopted in such houses is presented, and dynamic load behaviour of a full-scale Assam-type house specimen is discussed.

2 CONSTRUCTION METHODOLOGY OF ASSAM TYPE HOUSE

Due to high seismicity in the north-eastern region of India, the local people have developed a unique construction typology using locally available materials to construct their dwellings that are highly earthquake resistant and commonly known as Assam-type houses or *Ikra* houses. The name *Ikra* given to such housing typology is derived from a reed, locally known as *Ikra*, used extensively in walls and roof of such houses. This type of housing construction is commonly found in both rural and urban areas. The housing is known to have a number of features that influence earthquake safety of the house. These include: (a) Architectural aspects: regular plan, small openings, central location of openings, and small projections and overhangs, (b) Structural features: light mass of walls and roofs, good wall-to-wall connection, good quality and strength of materials used, (c) Flexible connections (using bolts, nails, grooves, etc.) between various wooden elements at different levels (Kaushik and Ravindra Babu 2012).

Several modifications in the construction methodology and materials used in Assam-type housing have been observed at various places to suit the local requirements. The frames and panels of the windows and doors are made of locally available wood material. The door and windows are small in size and are generally placed in the center of the walls. The main wooden posts of the house are supported on plain concrete pedestals constructed over the ground up to plinth and the connections between wooden posts with foundation are achieved through steel L-clamps. An important aspect of this housing type is its connection between various elements: main posts, intermediate horizontal and vertical studs, wall plate beams, infill wall panels, roof trusses, and roofing elements. Typical Assam-type houses may have false ceilings made of timber and bamboo mats, while in modern construction, plywood or gypsum sheets are used. Nowadays, pitched CGI (Corrugated Galvanized Iron) sheet roofing over timber trusses is the most common form of roofing used in these houses. However, in older days and in some rural areas even in the present day, Ikra (river reed) is used as roofing. Further, a detail description of the Assam-type house are discussed in the next section.

3 DESCRIPTION OF FULL-SCALE TEST SPECIMEN

A full-scale single room house specimen of a typical Assam-type house was tested under dynamic loads as shown in Fig. 2. The house specimen (main posts and walls) was constructed on rigid steel frame consisting of channel sections after filling concrete in the web of the channels. The main posts of the specimen were supported over the concrete using steel L-clamps, which were inserted in the concrete and welded with the channel sections. A detail description of the construction methodology is shown in one wall of the house specimen with various connections and their locations in Fig. 3. Joints A and B (bottom of main posts) were mutually provided such that Joints A resists the rotation of the main post along its own plane, while Joints B allows the rotation as shown in Fig. 4 (a and b). In this type of constructions, main posts are first erected and connected to the top wall plate beam through open tenon-mortise connection reinforced with the help of steel flats and bolts to prevent sway in the joints (Fig. 4c).

Fig. 2. A full-scale Assam-type house specimen.

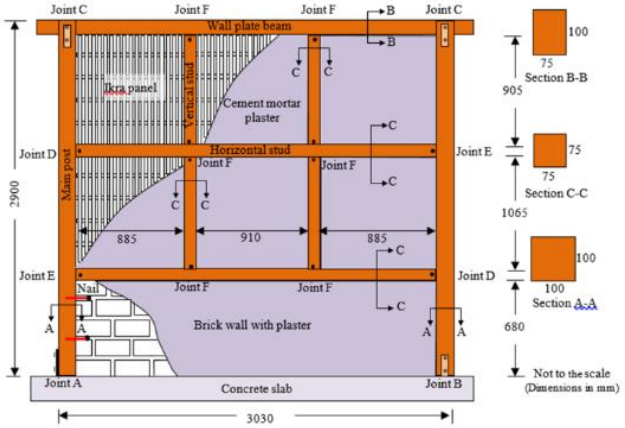

Fig. 3. Details of a wall of Assam-type house specimens.

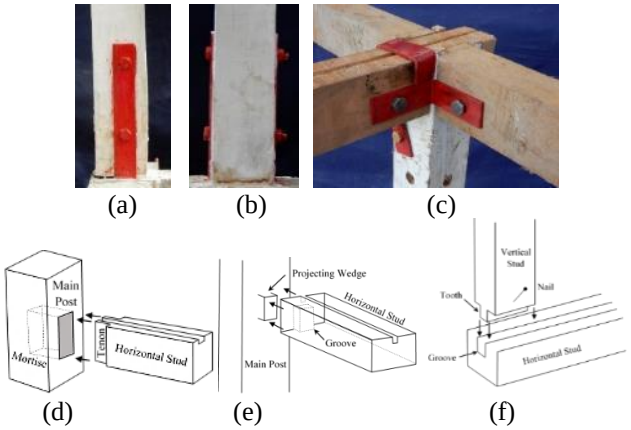

Fig. 4. Connections in Assam-type house specimen: (a) Joint A, (b) Joint B, (c) Joint C, (d) Joint D, (e) Joint E, and (f) Joint F.

The main posts and top beam are then joined with horizontal and vertical frame members with help of different connections as shown in Fig. 3. One end of the horizontal studs is connected to the main post (Joint D) using mortise and tenon joint (Fig. 4d), and the other end is connected using a shear key type of arrangement (Joint E) as shown in Fig. 4(e). The vertical studs are toothed on both the ends to facilitate insertion into the grooves (5 mm wide and 15 mm deep) cut along the length of the horizontal studs or the beams (Joint F), and a nail is driven in these connections to reduce the sway (Fig. 4(f)). The timber frame (main posts and wall plate beam) of the specimen is made of *Sal* wood (shorea robusta) and secondary horizontal and vertical studs are made up of *Jam* wood.

Brick masonry of about 75 mm thickness is used as infill up to sill level, and two long nails (150 mm) are driven in each main post through the mortar joints of the masonry wall to provide out of plane stability to the wall (Fig. 3). Above the sill level, the panels (*Ikra*) are meshed using locally available bamboo and plastered using cement mortar in two layers making the total thickness of *Ikra* panels to be about 45 mm. The bamboo strips (25 mm wide) used in *Ikra* walls are also supported vertically by inserting them into grooves in the horizontal studs. The bamboo strips are also inserted into the holes made in the main posts and vertical studs to provide out of plane stability. The clay brick infill (below the sill) is also plastered with cement mortar.

The specimen had a central window opening in one face of the wall above the sill level, and a central door opening in adjacent wall of the house specimen (Fig. 2). As per the prevalent construction practice, the connections of window panels with the frame are mortise and tenon type, whereas, doorposts are little inserted into the plaster of the floor without any connection. However, in the present study, the doorposts were inserted into the foundation of the specimen (concrete). The House specimen was a single story, single room Assam-type house with a room size of about 2.83 m × 2.83 m and a height about 3.6 m. The main posts were made of about 100 mm square sections and the wall plate beams had section of about 75×100 mm. The intermediate stud frame sections had about 75 mm square section. The rafter sections were about 75×65 mm and purlins about 75×50 mm in section. The roof of the specimen comprised of three wooden trusses connected to the top wall plate beams through long nails and covered with tin sheets. The ceiling surfaces of the house specimen were covered with gypsum sheet panels fixed through nails on the grids of wooden battens.

Unidirectional shake table tests were performed on the house specimen along the weaker direction, since the purpose of the study was to evaluate the critical in-plane behavior of these houses. Along the shaking direction, the house specimen had a wall with central door opening and a fully infill wall. In the direction perpendicular to the shaking direction (out-of-plane direction), the specimen had a central window opening and a fully infill wall (Fig. 2).

4 EXPERIMENTAL PROGRAM

The dynamic behaviour of the full-scale house specimen was studied with the help of four recorded ground motions and one simulated ground motion. The ground motions were selected based on different frequency range and optimizing shake table capabilities. All the ground motions are scaled to peak ground acceleration (PGA) of 1g. The specimen was subjected to multiple excitations of 5%, 10%, 20%, 30%, 40%, 50%, 60%, 70%, 80%, 90%, and 100% of PGA of selected ground motion. In the present study, the results of 1994 Northridge ground motion are presented and discussed only. Fig. 5 shows the input acceleration history at the shake table for 100% excitation of 1994 Northridge ground motion. The primary objective of the shaking table tests was to assess the seismic performance of the Assam-type houses. To assess the seismic performance, acceleration, displacement, and strain measuring sensors were employed at different location of the specimen. Fig. 6 shows the locations of the accelerometers in the specimens.

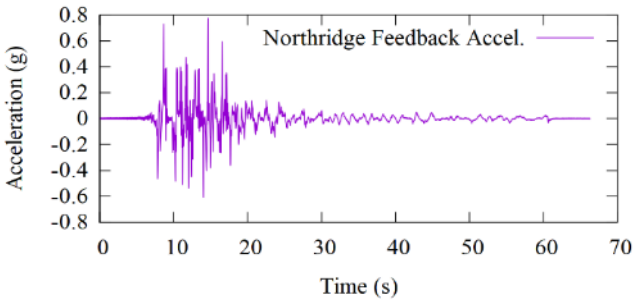

Fig. 5. 1994 Northridge earthquake ground motion considered in the shake table testing at 100 % excitation level.

The specimen was subjected to band-limited white noise with frequency 0.25-8.0 Hz and an RMS of 0.03g every time before and after the application of each seismic excitation for determining frequency drop in the structure and the destructiveness of the seismic excitation. At the end of each test run, the specimen was carefully examined for any damage. In each test event, the input and output accelerations were measured in the shaking table and in the specimen, with a sampling rate of 200 Hz. Recordings from the accelerometers and displacement transducers were carefully processed for base-line correction and noise removal from acceleration time histories. The signals were first processed by removing the DC components (0 Hz) and by employing 0.1 Hz to 10 Hz band pass filter for noise removal from acceleration time histories.

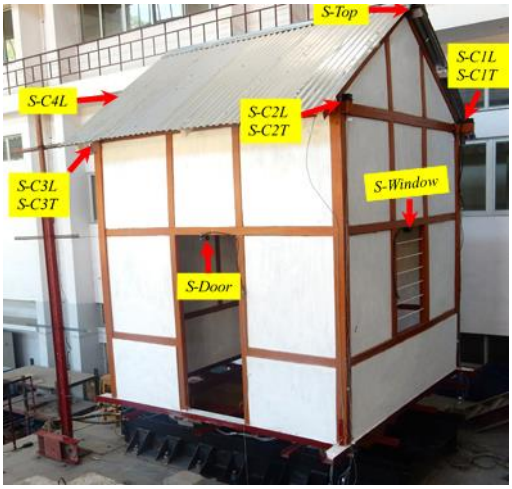

Fig. 6. Location of accelerometers in the specimen.

5 EXPERIMENTAL RESULTS AND DISCUSSION

The results presented in this section intend to identify the global seismic behavior of the specimen. The test structure behaved well during the sequence of seismic test events even though five earthquake signals with high energies were introduced to perform the shake table tests on the same specimen.(As already mentioned above, the results discussed in the present study are of Northridge ground motions only.) No damage was observed on the walls of the specimen. However, interface cracks along the framing members of the walls were visible towards to higher excitation levels.

Fig. 7 shows the reduction in the natural frequency of vibration of the first mode of the specimen obtained from the white noise base excitations. The frequency of the first longitudinal mode is 7.42 Hz at the undamaged state, i.e., at the beginning of the test. The frequency of the first mode decreases to 5.89 Hz after the completion of the entire testing sequence. The downward trend of frequencies of the vibration modes is a result of increased seismic action imposed on the specimen and resulting damage in the specimen. This damage corresponds mainly to the separation of interface connections of infill panels with the timber members (main posts, horizontal studs, vertical studs, top plate beam, and sill level beam), and loosening of nails in different connections of the timber frames as shown in Fig. 8.

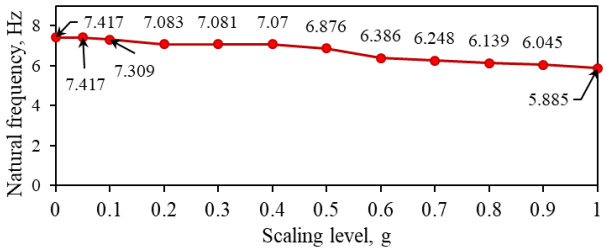

Fig. 7. Frequency degradation in the specimen with increment of PGA levels.

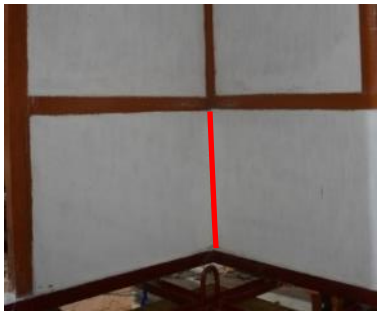

Fig. 8. An interface crack between the masonry wall and the main post after the entire testing events.

Fig. 9 shows the maximum acceleration response of the house specimen to maximum table acceleration at different excitation levels of Northridge ground motion recorded at different locations. The acceleration response of the specimen obviously increased with the increase in the excitation of the shake table. As it can be observed from Fig. 9 that the maximum acceleration response at top of the specimen was more than 2 g at about 0.77 g level of base excitation.

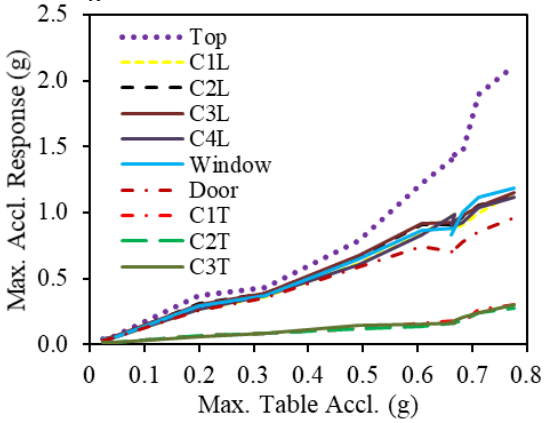

Fig. 9. Maximum acceleration response of the specimen with increment in PGA levels of Northridge ground motion at different locations.

The acceleration recorded along the shaking direction at wall plate beam level in different main post locations (at C1L, C2L, C3L, and C4L in Fig. 6) and at lintel level (at window and door in Fig. 6) was similar and more than 1 g except at door location (0.96 g). The

highest acceleration response in transverse direction (at C1T, C2T, and C3T in Fig. 6) was about 0.3 g. Fig.10 (a) shows the acceleration response at the top level in shaking direction at 100 % excitation. In order to compare the acceleration response at various levels, Fig.10 (b) shows the acceleration response of the specimen at wall plate beam level along the direction recorded at C1L location (Fig. 6), and Fig. 10 (c) shows the acceleration response of the specimen at wall plate beam level along the transverse direction (at C1T location). Due to unavailability of recording of displacement response at 100 % excitation, Fig. 10 (d) shows the displacement response at wall plate beam level along the direction of shaking at 60 % excitation level of input motion.

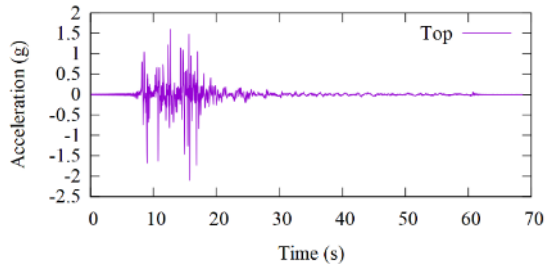

(a)

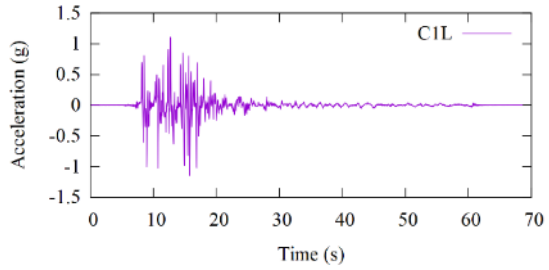

(b)

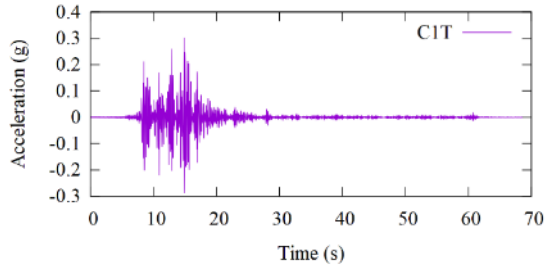

(c)

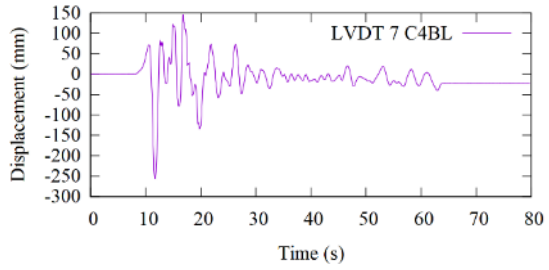

(d)

Fig. 10. Response of specimen at different locations for Northridge ground motion: (a) at top level in shaking direction, (b) at wall plate beam level in shaking direction, (c) at wall plate beam level in transverse direction, and (d) absolute displacement response history at 60% excitation in shaking direction.

10 CONCLUSIONS

The shake table testing of a full-scale, single-story wood frame Assam-type house was carried out to assess the seismic response of such houses under extreme dynamic loading. The natural frequencies were determined by white noise excitation, and the damage was estimated through the change of natural vibration frequencies of the specimen. It was observed from a sequence of shake table testing that the natural frequency of the Assam-type house reduced by about 25% due to minor damage in the masonry wall of the house and loosening of different connections of the house. Even after a sequential application of dynamic loads with high PGA values, the house performed really well with no visible damage to the main framing system of the house. The *Ikra* walls of the house also did not suffer any visible damage, though the interface between the *Ikra* walls and the timber members was lost. The main connections at the bottom of the main posts did not suffer any damage, and therefore, the house specimen continued to resist the dynamic loads. The test results showed that the excellent performance of Assam-type house under shake table testing was primarily due to low seismic mass of the house and flexible connections in different members.

ACKNOWLEDGEMENTS

Authors acknowledge the financial assistance provided by the Ministry of Human Resource Development (MHRD), and a research grant (DST/TSG/STS/2012/65-G) provided by Department of Science and Technology, Government of India.

REFERENCES

1) Ali, Q., Schacher, T., Ashraf, M., Alam, B., Naeem, A., Ahmad, N., and Umar, M. (2012): "In-Plane Behavior of the Dhajji-Dewari Structural System (Wooden Braced Frame with Masonry Infill)." Earthquake Spectra, 28(3), 835−858.

2) Rai, D.C., and Murty C.V.R. (2005): Preliminary report on the 2005 North Kashmir Earthquake of October 8, 2005, *Indian Institute of Technology Kanpur*, India.

3) Cardoso, R., Lopes. M., and Bento. R. (2004): Earthquake resistant structures of Portuguese old "Pombalino" buildings, *13th World Conference on Earthquake Engineering*, Vancouver, BC, Canada.

4) Jain, S.K. (2016): Earthquake safety in India: Achievements, challenges and opportunities. *Bull Earthquake Engineering*, 14, 1337–1436.

5) Kaushik, H. B, and Ravindra Babu K.S. (2012): Assam-type House. *World Housing Encyclopedia*, Report no. 154

6) Kaushik, H.B., and Dasgupta, K. (2013): Assessment of seismic vulnerability of structures in Sikkim, India,

based on damage observation during two recent earthquakes. *Journal of Performance of Constructed Facilities*, 27(6), 697−720.

Sustainable housing using confined masonry buildings

Borah, B.[1], Singhal, V.[2] and Kaushik, H.B.[3]

[1] Ph.D. Student, Department of Civil Engineering, IIT Guwahati, Guwahati 781039, India.
[2] Assistant Professor, Department of Civil Engineering, IIT Patna, Bihta 801106, India.
[3] Associate Professor, Department of Civil Engineering, IIT Guwahati, Guwahati 781039, India.

ABSTRACT

Much of India is prone to substantial earthquakes and vulnerability associated with both unreinforced masonry (URM) and improperly built reinforced concrete (RC) frame construction have been unmasked by past earthquakes. URM structures present a severe hazard in earthquake prone regions. As well as non-engineered RC structures can lead to devastating consequences. Therefore, housing for families in the economically weaker sector and lower income group is really challenging to such events. Regardless of residing in a city or village, everyone desires a house with masonry walls and RC roof, just like the buildings in larger urban areas. Confined masonry (CM) construction, which is a popular building system in many countries, can fulfil this need of the society. Though CM building started informally, the seismic performance is found to be really well in several destructive earthquakes. This type of construction combines the advantages of URM and RC structures and does not need sophistication required in RC construction. In this paper, seismic response of URM, infilled RC frame and CM buildings is compared using past seismic performance and literature. It is concluded that confined masonry is a better alternative for sustainable housing in seismic prone regions of India.

Keywords: unreinforced masonry, reinforced concrete, confined masonry, seismic response

1 INTRODUCTION

In recent years, earthquakes occurring in India and other countries have unveiled many weaknesses associated with both unreinforced masonry (URM) and reinforced concrete (RC) frame construction. Both URM buildings and non-engineered RC frame buildings continue to be the major cause of human and economic losses during past earthquakes as observed during Bhuj (2001), Kashmir (2005), Sikkim (2011) and Nepal (2015) earthquakes. Confined Masonry (CM) has emerged as an improved masonry structural system, where the unreinforced masonry walls are confined with nominally-reinforced concrete tie-elements (tie-columns and tie-beams) at the perimeter and other salient locations. Though a finished CM building looks like a RC fame building with infill walls, CM building does not need sophistication required in RC construction (Meli et al. 2011). Here, the confining elements are not designed to act as load bearing elements as in case of RC frame buildings with masonry infill, however these are provided to tie together the walls, floors and roofs as well as to strengthen walls with openings. Because of these small tie-elements, the ductility of the structure under lateral load improves compared to URM structure, which translates into better seismic performance. Therefore, CM structure combines the advantages of URM and RC structure and utilizing the masonry strength in the main load-bearing element, the structure provides economical advantage. The past seismic performance of CM structure in comparison to other type is described in the next section.

2 PAST SEISMIC PERFORMANCE

The first reported use of CM construction was in the reconstruction of buildings destroyed by the 1908 Messina, Italy earthquake of magnitude 7.2. After that its practice started in Chile and Colombia in the 1930's, and is currently widely used for housing construction, from low-rise (one to two-storey) dwellings to multistory (up to six storeys high) apartment buildings in several countries of high seismic risk (Brzev 2008). CM structure has been subjected to many devastating earthquakes. Table 1 includes some countries where CM buildings have been used for housing construction and the history of remarkable earthquake experienced by them (Moroni et al. 2004, Brzev et al. 2010, Schultz 1994, Jimenez et al. 1999, Alcocer et al. 2006, Gallegos 1994, Asfura and Flores 2000, Hashemi et al. 2003, Yang and Jian 1988, Bilek et al. 2007, Meisl et al. 2006). As mentioned in the past literature, the overall performance of CM building in these earthquakes was very satisfactory. For example, in the earthquake performance report of 1939 Chile earthquake, 1999 Tehuacan earthquake, 2003 Tecomán earthquake, and 2007 Pisco earthquake, CM structures showed far better

performance than URM structure. Large majority of CM buildings remained undamaged while the adjacent URM building (especially adobe construction) damaged severely or collapsed in these earthquakes. Also, in 1985 Guerrero-Michoacán earthquake, CM buildings showed better performance than even infilled RC frame buildings. Several reports of the past earthquakes have identified the out-of-plane collapse of URM and infilled RC wall as one of the predominant modes of failure. In the infilled RC frames due to construction difficulties, loose fitting of masonry beneath the concrete beam are quite common, which resulted in the out-of-plane collapse of these panels during the past earthquakes. However, a superior integration between the masonry and adjacent RC tie elements is naturally developed in CM walls because of the construction sequences. As the concrete is casted after the masonry wall, a good bond is developed between the wall and surrounding frame in CM building. Therefore, in these earthquakes CM buildings were less vulnerable in the out-of-plane direction compared to URM or infilled RC frame buildings.

Table 1. CM building performance during past notable earthquakes

Country	Year	Earthquake Location	Magnitude
Chile	1939	Chillán	7.8
	1985	Llolleo	7.8
	2010	Coast of Maule	8.8
Mexico	1985	Guerrero-Michoacán	8.0
	1999	Tehuacan	6.5
	2003	Tecomán	7.6
Peru	1970	Chimbote	7.8
	2007	Pisco	8.0
Colombia	1983	Popayan	5.5
	1999	El Quindio	6.2
Iran	1990	Manjil	7.6
	2003	Bam	6.6
El Salvador	2001	Offshore El Salvador	7.7
China	1976	Tangshan	8.2
Indonesia	2004	Northern Sumatra	9.3
	2005	Northern Sumatra	8.7
	2007	Bengkulu	8.4
Haiti	2010	Port-au-Prince	7.0

In general, because of the main concept, i.e., load bearing masonry wall tied by small RC elements, CM structures showed very good resistance to seismic events occurred in worldwide. A few CM buildings suffered severe damage, especially high-rise buildings but most low and medium rise dwellings did not experience any damage. The damage in CM buildings was found to be mainly due to omission of tie-columns, discontinuity in tie-beams, inadequate diaphragm connections, and inappropriate structural configuration. Therefore, if it is properly constructed, it is able to sustain earthquake effects without collapse. As a result, CM structure has attracted considerable interest in the research field. Studies have been carried out to understand the behaviour of CM building system in order to transform it to a proper engineered construction. In the next section, behaviour of CM structure under experimental study is discussed.

3 REVIEW OF PAST LITERATURE

Seismic behaviour of CM structure has been a subject of experimental studies from many years. Past experimental studies have contributed to the comprehensive understanding of the seismic behaviour of CM walls in terms of their damage pattern and failure modes. From the investigation of experimental test studies and past earthquake damage reports, the general failure modes of CM structures can be broadly categorized into in-plane failures, out-of-plane failures, diaphragm failures, connection failures, and non-structural failures as shown in Fig. 1 (Matthews et al. 2007). Among these, the in-plane performance of CM walls has attracted considerable interest in the seismic research, as it is the primary load path for transferring lateral seismic forces to the foundation.

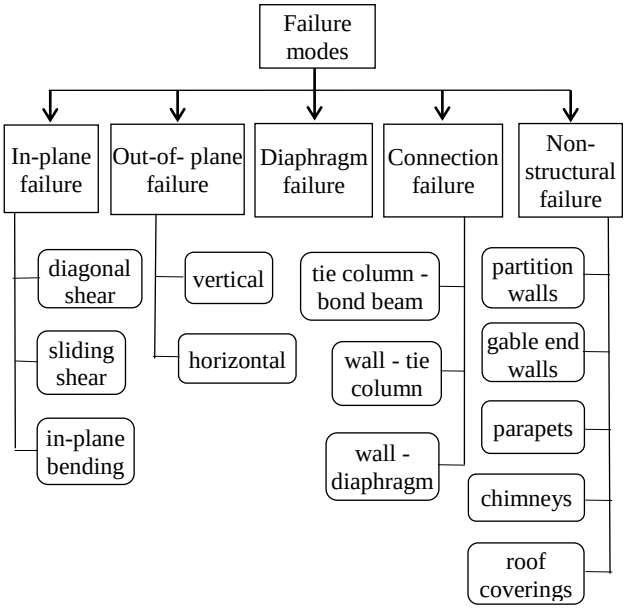

Fig. 1. Different failure modes of CM structure.

The summary of experimental studies conducted to understand the in-plane behaviour of CM walls in the past three decades is presented by Meli et al. (2011). It was observed that initially in a CM wall, the masonry panel resists the effect of lateral earthquake loads while the confining elements do not play a significant role. Once the cracking takes place in masonry units or mortar joint, the panel becomes less effective in transferring the forces. If the lateral force continues to increase, the masonry panel typically begins to lose strength and at this stage the vertical reinforcement in tie-columns becomes engaged in resisting tensile and compressive stresses. Thus, even if the lateral loads on

the wall exceed its capacity, because of tie-elements, the walls will stay together and continues to deform or stretch until the lateral loads lessen. In this way, the wall got somewhat higher strength and considerably higher deformation capacity than URM walls and is prevented from collapse. These additional deformations cause further damage in the masonry and tie columns. In many cases, ultimate failure occurs when the tie columns completely fail in shear by the extension of diagonal shear failure of the panel. Meli et al. (2011) also concluded that the maximum in-plane resistance of CM wall could be considered as the sum of the shear resistance provided by the plain masonry wall and the tie-columns. Further, the load -deformation behaviour depends on various factors, i.e., aspect ratio (height-to-length) of wall, type of masonry, type of wall-to-tie-column interface, detailing of tie-columns, openings, axial stress etc. (Riahi et al. 2009, Kuroki et al. 2010, Gavilán et al. 2015, Singhal et al. 2016).

The improvement in the in-plane performance of CM walls in comparison to URM walls was confirmed by Tomaževič and Klemenc (1997a, 1997b) as shown in Fig. 2. From their study it was observed that by confining the wall with RC tie-columns, lateral resistance of a URM wall is improved by more than 1.5 times and deformation capacity by almost 5 times in addition to enhancing the energy dissipation capacity by 6-7 times.

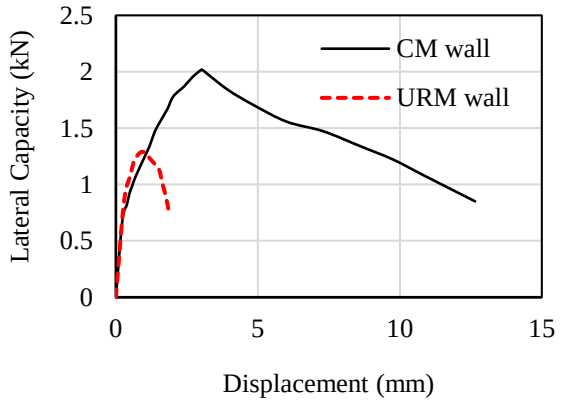

Fig. 2. Comparison of in-plane response of CM and URM walls (Tomaževič and Klemenc 1997a, 1997b).

During lateral loading, masonry walls may be subjected to out-of-plane lateral loading and vertical compression due to self-weight and overburden loads. Out-of-plane lateral loading creates bending and shear stresses in wall, and because of the low tensile strength of masonry, cracks may appear in walls leading to possible collapse by overturning. However, when the masonry panels are tightly attached with the RC frame elements (as in case of CM structure), it exert thrust on the beams and columns and forms effective arching mechanism. Several factors like aspect ratio (height/length ratio), slenderness ratio (height/thickness ratio), diaphragm type, boundary condition, panel thickness, material characteristics of masonry, overburden pressure, etc. affect the out-of-plane capacity of masonry wall (Drysdale and Essawy 1988, Dawe and Seah 1989b, Al-Chaar et al. 1994, Bashandy et al. 1995, Abrams et al. 1996, Henderson et al. 2003, Griffith et al. 2007, Tu et al. 2010, Komaraneni et al. 2011, Derakhshan et al. 2013). In masonry buildings, in many case URM walls are intersected by the cross walls normal to their plane at regular intervals. Also, now-a-days RC diaphragms are used instead of flexible diaphragm. These cross walls and the rigid diaphragms provide sufficient confinement to the URM wall, which is comparable to the confinement provided by the frame to infill in the out-of-plane direction in infilled RC frame structure. However, the out-of-plane capacity of URM wall and infilled RC wall are less compared to CM wall.

Tu et al. (2010) conducted shaking table tests on two full-scale single-story structures to investigate the out-of-plane behaviour of CM walls of different thicknesses. The out-of-plane performance of these confined walls was also compared with infilled RC frames. The test results suggest that CM walls can sustain significant out-of-plane loads. The composite action between wall and confining frames prevented the masonry panels from falling out of the frame and helped reducing the influence of inertia forces caused by their self-weight. On contrary, infill panels separated from the boundary frame and collapsed due to the out-of-plane inertia forces.

Practically, a seismic event can cause a masonry panel to experience both in-plane and out-of-plane loads simultaneously. The in-plane force causes damage to the wall by forming diagonal cracking, shear sliding or bending depending on the geometry of the wall. The in-plane damage of the wall affects the arching mechanism and reduces the out-of-plane capacity of the wall. Hence, the combined effect of in-plane and out-of-plane forces aggravates the extent of damage. Singhal et al. (2016) tested half-scaled CM wall specimens with different connection at wall-to-tie-column interface as shown in Fig. 3 and considered the successive applications of out-of-plane and in-plane loading. The seismic performance of CM wall in comparison with that of a typical infilled RC frame wall was also studied. It was observed that the CM walls with or without toothing exhibited improved in-plane and out-of-plane responses in comparison to infill masonry panels as shown in Fig. 4 and 5. The increased density of toothing caused significant improvement in post-peak behavior under in-plane loads, however, it didn't have significant effect on out-of-plane behavior. Under lateral loads, CM walls acted as shear walls and due to the composite action between the wall and the tie-column, the out-of-plane failure was delayed and the wall could safely sustain large in-plane drifts up to 1.75%. However, the RC frame with infill masonry

showed separation of the wall panel at its interface with the framing element at in-plane drifts as low as 0.5%, which led to excessive out-of-plane deflection and increased risk of dislodgement from the frame.

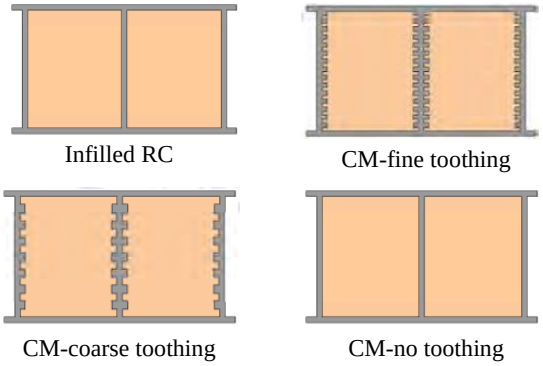

Fig. 3. Wall specimens prepared for the experimental investigation (Singhal et al. 2016).

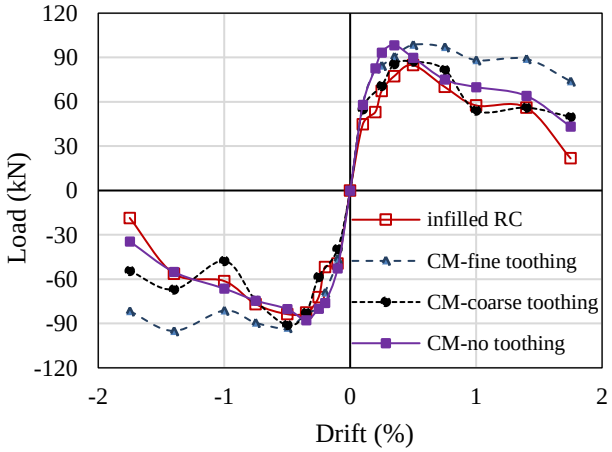

Fig. 4. Comparison of seismic response of infilled RC frame and CM walls (Singhal et al. 2016).

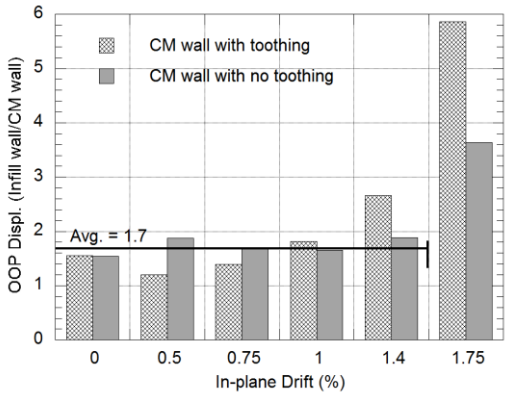

Fig. 5. Normalized out-of-plane displacement of infill wall with respect to CM walls at different in-plane drift (damage) levels.

4 CONCLUSION

In this paper, seismic performance of CM building in comparison to URM and RC frame building with infill walls is examined. From the study it is clear that low-rise CM wall exhibits better in-plane and out-of-plane resistance in comparison to URM and infilled RC frame wall under any seismic event. URM walls provide very less lateral strength in comparison to CM wall and because of the brittle behaviour, they have no reserved strength after cracking. Again to construct a proper RC frame building with infill walls requires technical skills and finances. To study the economic aspect, Marques and Lourenço (2014) estimated the costs associated to the construction of dwellings with RC, URM and CM typologies. Increase of 33% in the total cost was observed for the CM structure when compared to the URM structure. However, it allows a total cost reduction of 16% when compared to the RC structure. Much of India is prone to substantial earthquakes and construction of earthquake resistant housing for families in the economically weaker sector and lower income group is really challenging. Confined masonry can be an effective construction technology because this practice does not require new or advanced construction skills or equipment. Same materials are used which are available in the country, that is, concrete, masonry, and steel. It only requires nominal care in design and construction and yet performs very well in earthquakes. Medium-rise CM building had its first formal application in India in the form of a large-scale project involving construction of 36 CM buildings in the new campus of IIT Gandhinagar, Gujarat. Preliminary cost estimates indicated that adoption of CM technology resulted in a cost saving of 10 to 15% over alternative RC frame construction (Jain et al. 2014). The cost savings are mainly due to a smaller amount of concrete and steel because of smaller member sizes in CM buildings compared to RC frame buildings. Therefore, confined masonry is a better alternative for sustainable housing in seismic prone regions of India.

REFERENCES

1) Abrams, D.P., Angel, R., and Uzarski, J. (1996): Out-of-plane strength of unreinforced masonry infill panels. *Earthquake Spectra*, 12(4), 825-844.
2) Al-Chaar, G., Angel, R., and Abrams, D.P. (1994): Dynamic testing of unreinforced brick masonry infills. *Structures Congress XII: Proceedings of papers presented at the Structures Congress, Atlanta, GA, American Society of Civil Engineers, Reston, VA*, 791–796.
3) Alcocer, S.M. and Klingner, R.E. (2006b): The Tecomán, México Earthquake January 21, 2003. An EERI and SMIS Learning from Earthquakes Reconnaissance Report, *Earthquake Engineering Research Institute, Oakland, California*.
4) Asfura A. and Flores P. (2000): El Quindio, Colombia Earthquake, January 25, 1999: Reconnaissance Report. An EERI Learning from Earthquakes Project. *Earthquake*

Engineering Research Institute, California.

5) Bashandy, T., Rubiano, N.R., and Klingner, R.E. (1995): Evaluation and analytical verification of infilled frame test data. *Report 95-1, Department of Civil Engineering, University of Texas, Austin, TX, USA*.
6) Bilek, S., Satake, K., Sieh, K. (2007): Introduction to the Special Issue on the 2004 Sumatra–Andaman Earthquake and the Indian Ocean Tsunami. *Bulletin of the Seismological Society of America*; 97 (1A), S1–S5.
7) Brzev, S. (2008): Earthquake-Resistant Confined Masonry Construction. *National Information Center for Earthquake Engineering, Kanpur, India*.
8) Brzev, S., Astroza, M., and Moroni, O. (2010): Performance of Confined Masonry Buildings in the February 27, 2010 Chile Earthquake, *Earthquake Engineering Research Institute, Oakland, California*.
9) Dawe, J.L., and Seah, C.K. (1989b). Out-of-plane resistance of concrete masonry infilled panels. *Canadian Journal of Civil Engineering*, 16(6), 854-864.
10) Derakhshan, H., Griffith, M.C., and Ingham, J.M. (2013): Airbag testing of multi-leaf unreinforced masonry walls subjected to one-way bending. *Engineering Structures*, 57, 512-522.
11) Drysdale, R.G., and Essawy, A.S. (1988): Out-of-plane bending of concrete block walls. *Journal of Structural Engineering*, 114(1), 121-133.
12) EERI (1999): The Tehuacan, Mexico, Earthquake of June 15, 1999. EERI Special Earthquake Report. Newsletter. *Earthquake Engineering Research Institute, California*.
13) EERI (2001): Preliminary Observations on the El Salvador Earthquakes of January 13 and February 13, 2003. EERI Special Earthquake Report. Newsletter. *Earthquake Engineering Research Institute, California*.
14) Gallegos, H. (1994): Masonry in Peru. Masonry in the Americas, *ACI Publication SP-147, American Concrete Institute, Detroit*, 307-331.
15) Gavilán, Pérez J. J., Flores, L. E., Alcocer, S. M. (2015): An experimental study of confined masonry walls with varying aspect ratios. *Earthquake Spectra*, 31(2), 945-968.
16) Griffith, M.C., Lam, N.T.K., Wilson, J.L., and Doherty, K. (2004): Experimental investigation of unreinforced brick masonry walls in flexure. *Journal of Structural Engineering*, 130(3), 423-432.
17) Hashemi, B.H., Alemi, F., and Ashtiany, G. (2003): Confined Brick Masonry Building with Concrete Tie-Columns and Beams. *Iran, Report 27, World Housing Encyclopedia, Earthquake Engineering Research Institute*.
18) Henderson, R.C., Fricke, K.E., Jones, W.D., Beavers, J.E., and Bennett, R.M. (2003): Summary of a large-and small-scale unreinforced masonry infill test program. *Journal of Structural Engineering*, 129(12), 1667-1675.
19) Jain, S. K., Basu, D., Ghosh, I., Rai, D. C., Brzev, S., and Bhargava, L. K. (2014): Application of Confined Masonry in a Major Project in India. *Proceedings of the 10th National Conference on Earthquake Engineering. Earthquake Engineering Research Institute, Anchorage, Alaska, USA.*
20) Jimenez, J. I., Villarreal, J. I., Centeno, M. R., Gonzalez, B. G., Correa, J. J. G., Acevedo, C. R., Salazar, I. S. (1999): Tehuacan, Mexico, Earthquake of June 15, 1999. *Seismological Research Letters*, 70 (6), 698–704.
21) Komaraneni, S., Rai, D.C., and Singhal, V. (2011): Seismic behavior of framed masonry panels with prior damage when subjected to out-of-plane loading. *Earthquake Spectra*, 27(4), 1077-1103.
22) Kuroki, M., Kikuchi, K., and Nonaka, H. (2010): Experimental Study on Reinforcing Methods for Window Openings in Confined Masonry Walls. *Proc., 35th Conference on Our World in Concrete and Structures, CI-Premier PTE LTD, Singapore.*
23) Marques R, Lourenço PB (2014): Unreinforced and confined masonry buildings in seismic regions: validation of macro-element models and cost analysis. *Engineering Structures*, 64, 52–67.
24) Matthews, T., Riahi, Z., Centeno, J., Charlet, A., Garcia, H., Hoffman, C., Safaie, S., and Elwood, K.J. (2008): Evaluation of Confined Masonry Guidelines for Earthquake-Resistant Housing, *Confined Masonry Network*,
25) , K.J., Gupta, R., and Kowsari, R. (2006): Housing Reconstruction in Northern Sumatra after the December 2004 Great Sumatra Earthquake and Tsunami. Special Issue on the Great Sumatra Earthquakes and Indian Ocean Tsunamis of 26 December 2004 and 28 March 2005, *Earthquake Spectra*, 22(S3), S777-S802.
26) Meli, R., Brzev, S., Astroza, M., Boen, T., Crisafulli, F., Dai, J., Farsi, M., Hart, T., Mebarki, Ahmed, Moghadam, A.S., Quinn, D., Tomaževič, M., Yamin L. (2011): Seismic Design Guide for Low-Rise Confined Masonry Buildings, *Earthquake Engineering Research Institute and International Association for Earthquake Engineering, Oakland, CA, USA (www. confinedmasonry.org)*
27) Moroni, M.O., Astroza, M., and Acevedo, C. (2004): Performance and Seismic Vulnerability of Masonry Housing Types used In Chile. *Journal of Performance of Constructed Facilities, ASCE*, 18(3), 173-179.
28) Riahi, Z., Elwood, K. J., & Alcocer, S. M. (2009): Backbone Model for Confined Masonry Walls for Performance-Based Seismic Design. *Journal of Structural Engineering*, 135(6), 644-654.
29) Schultz, A. E. (1994): Performance of Masonry Structures during Extreme Lateral Loading Events. Masonry in the Americas, *ACI Publication SP-147, American Concrete Institute, Detroit*, 21-55.
30) Singhal, V., & Rai, D. C. (2016): In-plane and out-of‐plane behavior of confined masonry walls for various toothing and openings details and prediction of their strength and stiffness. *Earthquake Engineering & Structural Dynamics*, 45(15), 2551-2569.
31) Singhal, V., and Rai, D. C., (2012): Role of Toothing on Out-of-Plane Behavior of Damaged Confined Masonry Wall. *15th World Conference on Earthquake Engineering, Paper no. 4850, Lisbon, Portugal.*
32) Singhal, V., and Rai, D. C., (2014): Role of Toothing on In-Plane and Out-of-Plane Behavior of Confined Masonry Walls. *Journal of Structural Engineering* 140(9), 04014053.
33) Singhal, V., and Rai, D. C., (2014): Seismic Behavior of Confined Masonry Walls when Subjected to In-Plane and Out-of-Plane Loading. *10th US National Conference on Earthquake Engineering, Paper no. 675, Anchorage, Alaska*.
34) Tomaževič, M., and Klemenc, I. (1997a). Seismic behavior of confined masonry walls. *Earthquake Engineering and Structural Dynamics*, 26(10), 1059–1071.
35) Tomaževič, M., and Klemenc, I. (1997b). Verification of seismic resistance of confined masonry buildings. *Earthquake Engineering & Structural Dynamics*, 26(10), 1073-1088.
36) Tu, Y.H., Chuang, T.H., Liu, P.M., and Yang, Y.S. (2010): Out-of-plane shaking table tests on unreinforced masonry panels in RC frames. *Engineering Structures*, 32(12), 3925-3935.
37) Yang, W., and Jian, Z. (1988): Functions of Tied Concrete Columns in Brick Walls. *Proceedings of the Ninth World Conference on Earthquake Engineering, Tokyo, Japan*, 6, 139-144.

Sustainable Rural Development

Rural sanitation, water supply and waste management

Performance monitoring of indigenous household water filter of Amingaon, North Guwahati for iron and fluoride removal from groundwater

Kanoo, B.[1], Soni, A.[2], Jawed, M.[3]

[1] Ph.D. Student, Department of Civil Engineering, IIT Bombay, Powai – 400076, India.
[2] Ph.D. Student, Centre for Rural Technology, IIT Guwahati, Guwahati – 781 039, India
[3] Professor, Department of Civil Engineering, IIT Guwahati, Guwahati 781039, India

ABSTRACT

Amingaon – a rural locality in North Guwahati, Assam has very limited municipal water supply. Hence majority of people rely on the groundwater for their domestic needs. A field survey reveals that groundwater from this area contains excessive amount of dissolved iron (0–11.3 mg/L) whereas the fluoride concentration (0.13–0.66 mg/L) is within the permissible limits. The household level treatment for removal of iron from the groundwater includes use of indigenous water filter comprising of sand, gravel and wooden charcoal. The filter units fabricated using RCC rings is the most commonly used but its effectiveness in iron and fluoride removal is neither evaluated by government agencies nor reported in literature. The present study aims to investigate the efficiency and effectiveness of the selected RCC water filter unit in removal of iron and fluoride. Water quality parameters viz. iron, fluoride, pH, temperature, turbidity, conductivity and dissolved oxygen are monitored over a period of 3 months. It is observed that the raw groundwater contains iron and fluoride in the range of 8.13–11.63 and 0.51–1.17 mg/L respectively which on passage through the filter gets reduced to 0–0.08 mg/L for iron and 0.33–0.77 mg/L for fluoride. The mechanism of iron removal appears to be conversion of ferrous iron to ferric iron and its subsequent precipitation over the filter media.

Keywords: Groundwater, Iron, Fluoride, Amingaon, Indigenous household water filter

1 INTRODUCTION

More than 80% of rural population in Assam depends on groundwater for drinking and irrigation purposes (CGWB, 2014). Unfortunately iron and fluoride concentrations in the groundwater of Guwahati is observed to be in the range of 1-10 mg/L (Ahamad, 2005) and 0.3-7 mg/L (Das et al., 2003) respectively. The permissible limits for drinking purposes are 0.3 mg/L and 1-1.5 mg/L for iron and fluoride respectively (IS 10500, 2012). Even higher concentrations of fluoride in the range of 0.2-18.1 mg/L have been reported from Karbi Anglong and Nagaon districts (Das et al, 2003). Amingaon is a rural locality in North Guwahati (Assam), alongside river Brahmaputra. Till now there is very limited municipal water supply in North Guwahati, hence majority of people rely on the groundwater for their domestic needs. However, there are no literatures available to indicate level of fluoride and iron concentrations in the groundwater of Amingaon (Das et al., 2003; NIH, 1998).

The methods of iron removal basically involve oxidation, precipitate settling and filtration (DRDO, 2002; NEERI, 2011) whereas fluoride removal involves coagulation, flocculation and filtration or adsorption alone (NEERI, 1987). These methods are sophisticated and needs costly chemicals or adsorbents. The lack of education, ignorance and poor economic conditions of rural population residing in Amingaon area appears to be the main reasons for the non-applicability of these techniques in treatment of groundwater. The people of Amingaon rather use different types of indigenous household water filter units (also known as traditional filters). These units basically use sand, gravel, wooden charcoal as filtering medium and a mesh (net) arranged vertically in reinforced cement concrete (RCC) rings for the treatment of groundwater. The filter material, its percentage in the filter and its arrangement varies from place to place and house to house. A mesh or net with small openings is provided below the filtering media to prevent escape of sand from the filter unit. The groundwater is applied to the

indigenous filter as and when there is requirement of potable water. These filters are fabricated and operated solely based on experiences of local population gained over past generations.

The performance of these indigenous household water filters in removing iron and fluoride from groundwater has not been assessed till now. Therefore, the objectives of this study are (a) to assess the iron and fluoride concentrations of groundwater of Amingaon area, (b) to obtain first-hand information of 8-10 households using indigenous household water filter units, (c) to understand the fabrication/refabrication, operation and maintenance of a selected filter unit, and (d) to monitor the performance of the selected filter unit for its potential to remove iron and fluoride from the groundwater.

2 MATERIALS AND METHODS

2.1 Field survey

A field survey up to a distance of 600 m from the boundary of IIT Guwahati campus was undertaken to identify the household which were using indigenous household water filter unit for their drinking and cooking purposes. Face-to-face interaction with the house-owner provided information regarding personal experiences on using groundwater for their daily activities. In addition, groundwater samples were also collected to assess the levels of iron and fluoride present in the groundwater.

2.2 Monitoring of a selected indigenous household water filter unit

The filter unit located in the house of Mr. Pawan Das near Faculty School gate, Amingaon (GPS location: 26° 11' 11.2" N and 91° 42' 02.6" E) was selected for monitoring. The reasons for selecting this filter unit were: (a) the source of groundwater was located at some distance from the bank of river Brahmaputra with possibly minimum infiltration of river water, (b) the assessed groundwater iron concentration of 11.30 mg/L was the highest in the area, and (c) filter location was close to the Environmental Engineering Laboratory of the Department of Civil Engineering, IIT Guwahati (at a distance of 500 m) which was necessary for the quick analysis of water quality parameters of the collected water samples.

The samples collected from the source groundwater (i.e. tubewell) and the filter unit were analyzed for temperature, pH, conductivity, turbidity, dissolved oxygen (DO), iron and fluoride – taken as important water quality parameters for monitoring of filter performance. The water samples were collected during July-November, 2017 once in three-four days and analyzed.

2.3 Methods

Temperature and pH were measured using a digital pH meter (Model: µpH System 361, M/S Systronics India Ltd., India). Turbidity was measured using a digital turbidity meter (Model: 123, M/S Systronics India Ltd., India). Conductivity was measured with a digital conductivity meter (Model: LT-51, M/S Labtronics, India). DO was measured by Azide Modification method (APHA, 2012). Iron concentration in water was analyzed by 1, 10-Phenanthroline method (APHA, 2012) using spectrophotometer (Model: Spectro V-11D, M/S MRC Ltd., UK). The concentration of fluoride was analyzed by SPADNS method (APHA, 2012) using spectrophotometer. GPS locations were obtained using a smart mobile phone (Model: PA4C0020IN, M/S Motorola, India).

3 RESULTS AND DISCUSSION

3.1 Field survey

A field survey of 10 households using indigenous household water filter units was carried out outside the campus of IIT Guwahati in Amingaon area. The relevant information was obtained through face-to-face interaction with the house-owner (or the landlady). The groundwater samples were collected from the surveyed household for the assessment of concentrations of iron and fluoride. A brief summary of the surveyed household is presented in Table 1. The ranges of iron and fluoride concentrations in the groundwater of the surveyed locations are in the range of 0-11.30 mg/L and 0.13-0.66 mg/L respectively.

Table 1. Summary of surveyed household using indigenous household water filter units in Amingaon (North Guwahati)

Location	Left of Faculty Gate facing Faculty School			Lothia Bagisa, Bodogaon			Near Main Gate	Near ASEB Gate	Right of Faculty Gate facing Faculty school	
Village	Ghoramara, North Guwahati			Lothia Bagisa, Bodogaon			Kating Pahar	Abhaypur Shishugram	Ghoramara, North Guwahati	
Taluka	GMC (North Guwahati circle)			GMC (North Guwahati circle)			GMC (North Guwahati circle)	GMC (North Guwahati circle)	GMC (North Guwahati circle)	
District	Kamrup			Kamrup			Kamrup	Kamrup	Kamrup	
Latitude	26°11’11.6” N	26°11’10.1” N	26°11’09.6” N	26°10’59.5” N	26°11’01.7” N	26°10’58.6” N	26°11’49.1” N	26°11’59.5” N	26°11’11.2” N	26°11’11” N
Longitude	91°42’08.2” E	91°42’04.3” E	91°42’04.9” E	91°41’40.3” E	91°41’38.7” E	91°41’40.6” E	91°41’40.6” E	91°42’12.8” E	91°42’02.6” E	91°42’02.4” E
Distance from IITG campus (m)	400	100	100	100-200	300-400	100-200	100-200	600	500	50
Main livelihood	Electric Maintenance works in IITG	Govt. Service (Irrigation Department)	Agriculture, Rented house	Puffed rice business	IITG mess worker	Pig business	Dairy business	Welding and farming	Rented houses, Conductor in bus, Grass cutter in IITG	Labour
House-owner Name + family size	Ajanta Thakuria	Brajmohan Kalita	Satish Thakuria	Jogen Bodo	Ganesh Bodo	Bhadra Bodo	Tilu Prasad Sarmah	Rajeev Das	Pawan Das	Tarani Rajbangshi
Age of house-owner	40	51	43	65	35	34	81	31	40	72
No. of family members	12	4	10	9	9	2	18	8	4	3
Educational qualification of house-owner	Higher secondary	Higher Secondary	Higher Secondary	Lower Primary	Class 7	Higher Secondary	Bachelor of arts	Uneducated	Class 5	Higher Secondary
Water for drinking purpose	Double compartment RCC ring filter and then candle filter	Candle filter and then boil	Direct	Traditional filter	Traditional filter	Direct	Well-Filter-Boil	Direct	Double compartment RCC ring Filter	Traditional filter
Water for other uses	Direct	Direct	Direct	Direct	Direct	Direct	Direct	Direct	Direct	Direct
Odour problem	Slight	Slight	Yes	Yes	Slight	No	No	No	Yes	Slight
Color problem	Slightly muddy	Reddish	Reddish	Slight reddish	Slight reddish	Clean	Clear	Muddy	Reddish	Slightly Reddish
Pale teeth	Yes	No	No	No	No	Slight	No	No	Yes	No
Agriculture water supply system	Yes, in small quantity	No	Yes	Yes	No	No	Yes	Yes (By pond and tubewell)	No	Yes
Cleanliness near the water resource	Yes	Yes	Yes	Yes	Yes	Yes	Yes	No	No	Yes
Groundwater Iron concentration (mg/L)	0.22	1.21	1.53	2.31	1.11	1.56	0.00	0.52	11.30	3.73
Groundwater Fluoride concentration (mg/L)	0.44	0.51	0.36	0.43	0.59	0.56	0.13	0.35	0.66	0.62

ASEB: Assam State Electricity Board, GMC: Guwahati Metropolitan Corporation, IITG: Indian Institute of Technology Guwahati

3.2 Fabrication/refabrication, operation and maintenance of a selected filter unit

The selected indigenous household water filter unit at the house of Mr. Pawan Das is made of two compartments of RCC rings (as shown in Fig. 1) – the upper compartment contained the filter media while the lower compartment is used for storage of the filtered water. In the upper compartment, a mesh (net) is put at the bottom, and then a sand layer of around 10-12 cm and a layer of gravel of around 14-16 cm at the top. Later on, a layer of wooden charcoal is also included as a filtering medium with a depth of 2-4 cm at the top. The heights of compartments are 36 cm each with total height of the unit as 72 cm.

(a) Front View

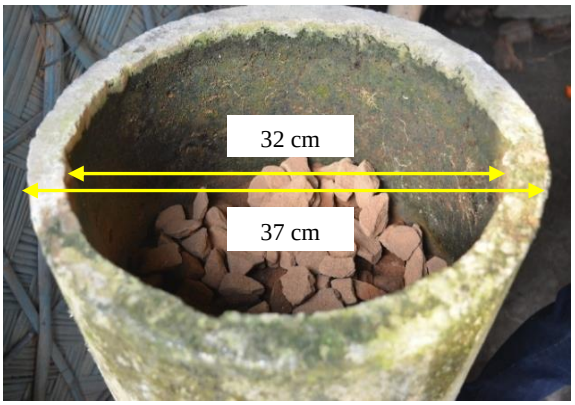

(b) Top View

Fig. 1. Indigenous household water filter unit located at the house of Mr. Pawan Das.

Approximately 8-10 L of the groundwater collected from the tubewell is directly poured into the filter unit in one go for filtration. The filter unit produced approximately 50-60 L of filtered water daily and the unit is operated for 3-4 months continuously. After 2-3 months of continuous use, the filtration output decreases due to formation of reddish cake or layer of precipitated iron on the top of the filter media (as shown in Fig. 2) which indicated clogging of the filter unit. This necessitates the dismantling, washing and refabrication of the filter unit.

Fig. 2. Reddish layer formed on top of the filter media of the selected filter unit.

The filter media and mesh (net) is removed from the upper compartment. Then both upper and lower compartments of the filter unit are washed and cleaned 5-6 times using a scrubber before reinstalling it again. The sand is distributed equally in two buckets of 10 L capacity. Each bucket with sand is then washed thoroughly using tubewell water 5 times for 5 min. each. Whole processing of washing sand takes around 40-45 min. Washed sand is then placed into the upper compartment of the filter unit above the plastic net to form a layer of height 10-12 cm. Gravels are washed by tubewell water and are put on the top of the washed sand layer. After the reinstallation of indigenous household water filter unit, it is poured with groundwater 3-4 times until the colour of filtered water fades away.

3.3 Performance monitoring of the selected filter unit

The performance of the selected filter unit was monitored from July to November 2017. The filter unit performance was assessed by estimating water quality parameters such as iron and fluoride concentrations, pH and temperature, conductivity and turbidity as well as DO levels on regular basis for water samples collected from the source

groundwater and filtered water. The variation in iron and fluoride concentrations of groundwater and filtered water is presented in Fig. 3.

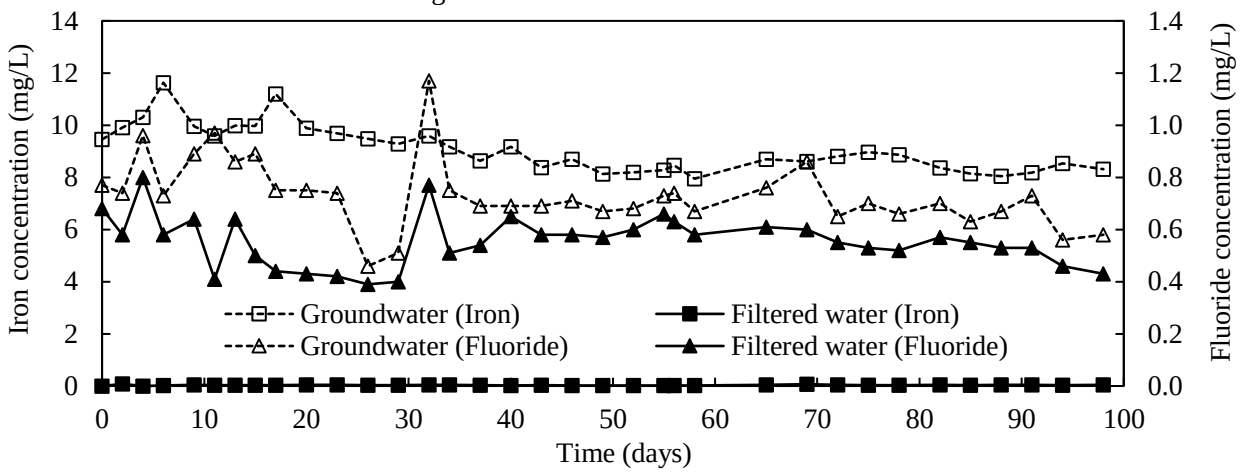

Fig. 3. Variation in iron and fluoride concentration during monitoring period of the selected filter unit.

The monitored performance related parameters of the selected indigenous household water filter unit are summarized in Table 2. The iron concentration varied in the range of 8.13-11.63 mg/L whereas fluoride concentration varied in the range of 0.51-1.17 mg/L in the groundwater samples. The groundwater after being filtered through the filter unit had iron concentration in the range of 0-0.08 mg/L while fluoride concentration was in the range of 0.39-0.77 mg/L. The concentration of fluoride in the filtered water was always within the permissible limit for drinking and cooking purposes. The removal of iron is taking place possibly due to oxidation of ferrous iron to ferric iron forming a reddish colour cake on the top of the filter unit. It is believed that this ferric layer might be able to reduce the concentration of fluoride a bit.

The pH of the groundwater was measured immediately after the sampling to represent the true picture. The pH of the groundwater sample varied in the range of 6.17-6.81. The pH of the filtered water from the unit is in the range 6.82-7.51 which is within the permissible limit of 6.5-8.5 for domestic use (IS 10500, 2012). It is observed that the increase in pH is favourable for the precipitation of iron. The temperature keeps on varying and is dependent on the weather conditions for that particular sampling day. The conductivity of the groundwater samples collected from the tubewell and the filtered water did not show major changes and is almost same ranging within 0.4-1.1 mS/cm. The turbidity of the groundwater varied in the range of 0.7-1.5 NTU and is directly proportional to the time gap between sampling and analysis for turbidity, the

reason being formation of ferric precipitates by the oxidization of ferrous ion. The turbidity of the filtered water ranged within 0-0.2 NTU which is lower than the permissible limit of 1 NTU (IS 10500, 2012).

The collected groundwater samples from the tubewell were devoid of DO. However, when the groundwater was poured into the top of the filter unit, it absorbed oxygen from the air and showed DO in the range of 1.0-2.4 mg/L. This level of DO might have helped in conversion of ferrous iron into ferric iron and its retention on top of the filter media as precipitate. Therefore, the mechanism of iron removal from the groundwater is conversion of ferrous iron to ferric iron and its filtration through the filter media. The filtered water contained DO levels of 5.9-6.7 mg/L.

4 CONCLUSION

The groundwater in Amingaon has a high concentration of iron (0-11.3 mg/L), often exceeding the acceptable range of 0.3 mg/L whereas the concentration of fluoride in the range of 0.13-0.66 mg/L is within the acceptable limit of 1-1.5 mg/L for domestic purposes. The local population of Amingaon, irrespective of educational qualification and age, livelihood and occupation; invariably use an indigenous household water filter units fabricated using RCC rings with filtering media comprising

of sand, gravel and wooden charcoal in layered form. The monitoring of a selected filter unit reveals that the groundwater iron concentration of 8.13-11.63 mg/L is reduced to 0-0.08 mg/L in the filtered water. The selected filter unit is also able to reduce the fluoride concentration from 0.51-1.17 mg/L to 0.39-0.77 mg/L. The DO level in the groundwater increases as the same is poured into the filter unit thereby converting ferrous iron to ferric form. The ferric form of iron is filtered out as precipitate in the filter unit.

Water quality parameters		Monitoring Period		
		0 - 34 days (28 July 2017 to 31 August 2017)	35 - 62 days (01 September 2017 to 31 September 2017)	63 - 98 days (01 October 2017 to 06 November 2017)
Iron (mg/L)	Groundwater	9.94±0.67 (15)	8.43±0.40 (09)	8.50±0.31 (11)
	Filtered water	0.03±0.02 (15)	0.02±0.01 (09)	0.04±0.01 (11)
Fluoride (mg/L)	Groundwater	0.80±0.18 (15)	0.70±0.02 (09)	0.68±0.08 (11)
	Filtered water	0.55±0.14 (15)	0.60±0.04 (09)	0.53±0.05 (11)
pH	Groundwater	6.59±0.13 (15)	6.47±0.17 (09)	6.33±0.08 (11)
	Filtered water	7.17±0.07 (15)	7.12±0.18 (09)	7.25±0.04 (11)
Temperature (°C)	Groundwater	28.53±0.49 (15)	28.47±0.67 (09)	28.20±0.53 (11)
	Filtered water	31.30±0.52 (15)	31.14±0.7 (09)	30.53±0.40 (11)
Conductivity (mS/cm)	Groundwater	0.51±0.06 (07)	0.61±0.20 (09)	0.62±0.11 (11)
	Filtered water	0.48±0.05 (07)	0.54±0.09 (09)	0.45±0.05 (11)
Turbidity (NTU)	Groundwater	1.11±0.21 (07)	0.97±0.15 (07)	1.05±0.38 (11)
	Filtered water	0.07±0.05 (07)	0.08±0.07 (07)	0.33±0.55(11)
Dissolved oxygen (mg/L)	Groundwater	0.00±0.00 (15)	0.00±0.00 (09)	0.00±0.00 (11)
	Influent water above filter media	1.93±0.40 (15)	2.18±0.11 (09)	2.25±0.16 (11)
	Filtered water	6.23±0.26 (15)	6.24±0.21 (09)	6.46±0.12 (11)

Table 2. Summary of monitored performance parameters for the selected water filter unit.

[The data is presented in xx±yy (zz) format where xx is the average value, yy is the standard deviation, and zz is the number of data points considered for obtaining average and standard deviation]

ACKNOWLEDGEMENTS

The authors would like to acknowledge the family of Mr. Pawan Das for their cordial support during the filter monitoring phase of the research work.

REFERENCES

1) APHA (2012): Standard Methods for the Examination of Water and Wastewater, 21st Ed., American Public Health Association, American Water Works Association and Water Environment Federation, Washington, DC, USA.
2) Ahamad, K. U. (2005): Iron (II) Adsorptive Capacity Evaluation of Wooden charcoal and Sand Media used in Indigenous Household Iron Filtration Units of Rural and Semi-Urban Assam, Masters Thesis, Department of Civil Engineering, Indian Institute of Technology Guwahati, Guwahati, India.
3) CGWB (2014): Groundwater Year Book 2013-14, Ministry of Water Resources, Government of India, New Delhi.
4) Das, B.; Talukdar, J.; Sarma, S.; Gohain, B.; Dutta, R. K.; Das, H.B. and Das, S. C. (2003): Fluoride and other inorganic constituents in groundwater of Guwahati, Assam, India, *Current Science*, 85(5), 657-661.
5) DRDO (2002): Water Iron Removal Unit, Technology Focus, Bulletin of Defense Research and Development Organization, 10(1), ISSN: 0971-4413. (https://www.drdo.gov.in/drdo/pub/techfocus/2015/TF_Mar_2015_WEB.pdf) (website last accessed on 21 September 2017).
6) IS 10500 (2012): Specification for Drinking Water, Bureau of Indian Standards, New Delhi.
7) NEERI (1987): Defluoridation technology mission on drinking water in villages and related water management, National Environment Engineering Research Institute, Nagpur, India
8) NEERI (2011): Handbook on drinking water treatment technologies, Ministry of Drinking Water and Sanitation, Government of India, New Delhi.
9) NIH (1998): Groundwater Water Quality Monitoring and Evaluation in and around greater Guwahati, Assam, National Institute of Hydrology, Roorkee, CS (AR) 10/97-98.

Swachh Bharat mission (gramin): target versus achievement in Lakhimpur district

Kalita, T.[1] and Lahkar, H.[2]

[1] Assistant Engineer, Public Health Engineering Department, North Lakhimpur Division, North Lakhimpur, 787001, India.
[2] Technical Officer, Public Health Engineering Department, North Lakhimpur Division, North Lakhimpur, 787001, India.

ABSTRACT

The rural sanitation programme in India was first introduced in 1954 as a part of First Five Year Plan of Government of India. The 1981 census showed that the rural sanitation coverage was nearly 1%. The government has started giving emphasis on rural sanitation after the declaration of International Decade for Drinking water and Sanitation during 1981-90. In 2008, 88% of total population in India had access to an improved water source but only 31% had access to improved sanitation. In rural areas where 72% of India's population lives, the respective share is 84% and 21%. In the light of the above, on 2nd October, 2014, The Prime Minister of India launched a nationwide largest cleanliness campaign called Swachh Bharat Mission (Gramin). The main objectives of SBM (G) are to eliminate open defecation through construction of individual household, cluster and community toilets. The concept of SBM (G) is to provide sanitary facility to every family which includes toilet, solid and liquid waste disposal system, village cleanliness and safe and adequate drinking water. Under the SBM (G), nearly 11 crore toilets will be constructed by 2nd October 2019. Since the launch of SBM (G), nearly 8.28 crore toilets (nearly 75% of the target) have been built till August 2018. In order to accelerate the pace of work and aspect of behavioral change, it was envisaged that the Self Help Groups (SHGs)/ Non Government Organizations (NGOs) have to be associated in the implementation of the mission in the rural area. They are considered for active involvement in Information, Education and Communication (IEC) activities including demand generation, capacity building assistance in construction and ensuring sustained use of facilities. This paper highlights the present target versus achievement of Individual Household Latrines (IHHLs) in Lakhimpur district of Assam. As the district is highly flood affected, hence the rate of construction is slightly slower in comparison to the other districts of the state. However to overcome this problem the modular structure concept is implemented. Also to speed up the process of construction of IHHLs Direct Beneficiary Transfer (DBT) mode of construction is also appreciated.

Keywords: Swachh Bharat Mission (SBM), Individual Household Latrines (IHHLs), Sanitation, Flood.

1. INTRODUCTION

The focus on sanitation was initiated in 1954 in First Five Year Plan as "The National Water Supply and Sanitation Program". In 1972 "Accelerated Rural Water Supply Program (ARWSP)" was implemented to provide funds for villages with tribal peoples, Scheduled Caste and backward classes people. The government has begun giving more emphasis on rural sanitation after declaration of International Decade for Drinking water and Sanitation during 1981-90. In 1986 "Central Rural Sanitation Program (CRSP)" was launched to focus on supply of toilets in subsidy. After this in 1999 the "CRSP" was restructured as "Total Sanitation Campaign (TSC)". In 2012 "TSC" was renamed as "Nirmal Bharat Abhiyan (NBA)" with a view of covering 100% sanitation in rural areas by 2020. Presently "NBA" is replaced by "Swachh Bharat Mission (SBM)" on 2nd October 2014 with a new target of making India "Open Defecation Free (ODF)" by 2nd October 2019 as a fitting tribute on 150th Birth Anniversary of Mahatma Gandhi. Lakhimpur district is situated in north bank of Brahmaputra River. The district lies between 26º48' and 27º53' northern latitude, 93º42' and 94º81' eastern longitude. The mighty river Brahmaputra touches all along the southern and south eastern boundary of the district. The district is bounded on north by Arunachal Pradesh and on east by Dhemaji district of Assam. South portion is touches by Majuli district of Assam and Biswanath district on west. The district consist of 9 blocks namely Narayanpur, Bihpuria, Karunabari, Telahi, Nowboicha, Lakhimpur, Boginadi, Dhakuakhana, Ghilamara, which consists of 81 gram panchayat and 1146 villages. This study shows the present target versus achievement of Individual Household Latrines (IHHLs) in Lakhimpur district of Assam under Swachh Bharat Mission (SBM).

2 OBJECTIVES OF SBM

The Swachh Bharat Mission has the following objectives:

1. To eliminate the open defecation.

2. To eradicate the Manual Scavenging.

3. Modern and Scientific Municipal Solid Waste Management.

4. To aware the people about health and hygiene through Information Education Communication (IEC) and Inter Personal Communication (IPC)

5. To effect behavioural change regarding healthy sanitation practices.

6. To generate awareness about sanitation and its importance with public health.

3 OPEN DEFECATION

Open defecation (OD) is the practice of defecating outside or in public. This may be done as a result of cultural practices or having no access to toilets. Open defecation is practiced all over the world in nature or camping type situations and represents no health and environmental problems when done in sparsely populated settlements and when the "cat method" is used, i.e. covering the feces with some soil, leaves or sand. However, open defecation becomes a significant health problem and an issue for human dignity when it occurs in more densely populated areas, such as in larger villages or in urban informal settlements in developing countries. Here, the practice is usually associated with poverty and exclusion.

Of the 1 billion people around the world that still practice open defecation today, almost 600 million, or around 60 percent, reside in India alone. Under Swachh Bharat Mission, 111 million toilets will be built by 2019. However, simply building toilets and sanitation infrastructure will not stop open defecation in India. Proper behavioral change, habit and personal preference should also affects with regards to toilet use.

The battle to end open defecation in India needs to be fought on two fronts: one on the ground with toilets and sanitation infrastructure, and second in the hearts and minds of the people by repositioning toilets so that latrine use becomes the norm.

4 IMPACTS OF OPEN DEFECATION

Open defecation leads to affect the health and personal safety of women.

4.1 Health Impacts

Open defecation or lack of sanitation is a major factor in causing various diseases, most notably diarrhea and intestinal worm infections, but also typhoid, cholera, hepatitis, polio, trachoma and others. Those countries where open defecation is most widely practiced have the highest numbers of deaths of children under the age of 5, as well as high levels of malnourishment (leading to stunted growth in children), high levels of poverty and large disparities between the rich and poor.

4.2 Safety and Gender Impacts

Open defecation also impacts on human safety and dignity - in particular women are more vulnerable to gender-based violence and sexual assault when they defecate in the open.

5 DISEASES OCCUR BECAUSE OF POOR SANITATION

Human excreta have been implicated in the transmission of many infectious diseases including cholera, typhoid, infectious hepatitis, polio, cryptosporidiosis, and ascariasis. Undernutrition, pneumonia, worm infestations, are also associated with unsafe water, poor sanitation and hygiene resulting in reduced physical and mental growth, weakened physical fitness and impaired cognitive function, particularly for children under the age of five.

6 PROGRAM CONDUCTED FOR AWARENESS OF SWACHH BHARAT MISSION

1. Swachh Bharat Summer Internship: This is a school level program where the students are enrolled to adopt one or more villages and conduct activities of their choices to contribute to the cause of rural sanitation in India. The duration of internship is 100 hours which is categories into two cluster namely Information Education Communication (IEC) and Solid Liquid Waste Management (SLWM) activities.

2. Swachh Sarvekshan Gramin: Under this program, Rural community, Non Government Organization (NGO) and Self Health Group (SHG) were engaged in improvement of their sanitation status through an intensive and holistic IEC campaign along with the cleaning campaign of their respective villages. Higher officials including DC/DM/BDOs are to lead the campaign for its built up, publicity and roll out strategy and field visit.

3. Gram Sabha: The main objective of this awareness is to promote safe sanitation and clean environment in the village. The programs encourage organizations to play a catalytic role in the implementation of Swachh Bharat Mission (SBM).

Fig. 1. Awareness Campaign for Swachh Bharat Mission in Lakhimpur.

7 TECHNOLOGY USE IN SBM TOILET

The estimated cost of one IHHL is Rs 12000, in which the central government provide Rs 10800 (90%) and state government provide Rs 1200 (10%). Highly advance and economic toilet have been designed, which consists of two cylindrical (leach) pit of 1.05 m outside diameter each with 1.20 m depth, having a number of honeycombs in each leach pit to release blackwater in the surrounding soil. The depth of leach pit has kept 1.20 m which is above the ground water table, so that the blackwater does not contaminate the ground water table. The two pits have a very unique versatile function.

Fig. 2. 3D Model of IHHLs.

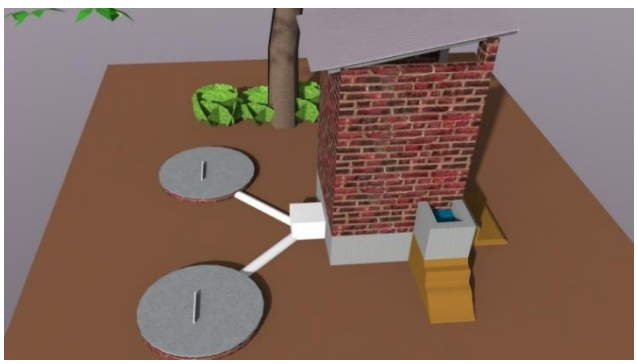

Fig. 3. 3D Model of IHHLs Showing Two Pit.

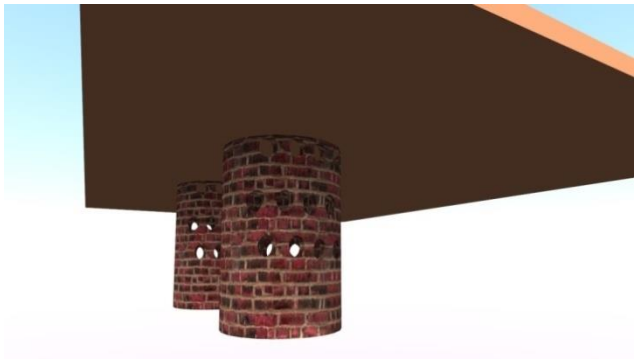

Fig. 4. 3D Model of IHHLs Showing Honeycomb in Both Pits.

The two pits get converged at a "Y" junction which has a locking key, the key facilitate for movement of blackwater to one particular leach pit keeping the other unused. After 2 year or so when the leach pit gets filled, then the key should be directed in opposite direction so that the blackwater moves to the next leach. After some year when the excreta get dried and decomposed by action of anaerobic bacteria, this material will be taken out and can be use as very good manure.

The Pan Trap used in Swachh Bharat Mission (SBM) has slightly different specification, as the pan have a gradient of 25º to 30º which is higher than the gradient of pan use in urban toilet, for easy movement of human excreta to the siphon and then to the leach pit with less requirement of water.

As the leach pits have honeycombs structure and open bottom, the black water can easily flows into the soil and hence the pits have to be constructed at least at a distance of 10 m away from the drinking water source.

8 COMPONENTS OF SBM

The Swachh Bharat Mission has the following components:

1. Household toilets, including conversion of insanitary latrines into pour-flush latrines.

2. Community toilets.

3. Public toilets.

4. Solid waste management.

5. IEC & Public Awareness.

Fig. 5. Construction of IHHLs in Lakhimpur district.

9 PROBLEM FACED DURING CONSTRUCTION OF IHHL IN LAKHIMPUR DISTRICT

This paper highlights the present target versus achievement of Individual Household Latrines (IHHLs) in Lakhimpur district of Assam. As the district is highly affected by flood and has poor communication facilities, the rate of construction of IHHL is slightly slower in comparison to the other districts of the state. However to overcome this problem, the modular structure concept can be used in flood prone area as shown in Figure 6.

Fig. 6. Modular Structured of IHHLs used in Lakhimpur.

i.e. the superstructure is made up by steel frame covered by colour coated roofing sheet. Also to speed up the process of construction of IHHLs Direct Beneficiary Transfer (DBT) mode, i.e. the beneficiary will have to construct the latrine on their own and then the Public Health Engineering Department on behalf of Swachh Bharat Mission will credit Rs 12000 to the beneficiary account directly.

10 CONCLUSIONS

The total target of IHHL in North Lakhimpur is 119990. The total number of IHHL constructed in 2014-2015 are 4411, in 2015-2016 are 13348, in 2016-2017 are 26511, in 2017-2018 are 30832, in 2018-2019 are 22626. The total coverage of IHHL in Lakhimpur is 87.03% till August 2018. The work of Swachh Bharat Mission in Lakhimpur district is going on with full momentum and till date 97728 number of IHHLs has been constructed and 22262 number of IHHLs is yet to be constructed. The Mission is expected to be completed well before 2nd October 2019. After achieving Open Defection Free (ODF) status in the district, it can be expected to have very less diseases to the people of the district and people can go to their own latrine with dignity.

ACKNOWLEDGEMENTS

The authors would like to acknowledge Dr Jeevan B. (IAS), Deputy Commissioner of North Lakhimpur, Er Dilip Kumar Gogoi, Executive Engineer (PHE), North Lakhimpur Division, Er Apurba Kumar Hazarika, Assistant Executive Engineer (PHE) Cum Nodal Officer SBM(G), Er Prasenjit Dutta, Assistant Engineer (PHE), Er Banashri Gogoi, Assistant Engineer (PHE), North Lakhimpur Circle, Er Prachurjya Saikia, Techinal Officer SBM(G) and Mr. Dipankar Saikia, MIS Consultant for their active participation in Swachh Bharat Mission (Gramin) in Lakhimpur district.

REFERENCES

1) Badra, S., and Sharma, V. (2015); Management lessons from Swachh Bharat Mission, *International Journal of Advance Research In Science And Engineering, IJARSE, Vol. No.4, Special Issue (01), March 2015,* 214-220.
2) Jangra B., Majra, J.P., and Singh, M., (2016): Swachh bharat abhiyan (clean India mission): SWOT analysis, *International Journal of Community Medicine and Public Health, 2016 Dec;3(12):*3285-3290.
3) http://swachhbharatmission.gov.in/sbmcms/index.htm
4) Pradhan, P., (2017): Swachh Bharat Abhiyan and the Indian Media, *Journal of Content, Community & Communication, Amity School of Communication, Vol. 5 Year 3, June – 2017,* 43-51.
5) Tiwari, S.K., (2014): To Study Awareness of A National Mission: Swachh Bharat: Swachh Vidyalaya in the Middle School Student of Private and Public Schools, *International Journal of Research, Volume 3, Issue 12,* 23-24.

Sustainable Energy Solutions

Sustainable Energy Solutions

Sustainable energy development

Concept of hybrid solar electric boat: a renewable water transportation

[1]Bharadwaj, S. [2]Mena, S.

[1]Graduate Student, Indian Institute of Information Technology, Guwahati-781015, India.
[2]Undergraduate Student, Assam Down Town University, Guwahati-781026, India.

ABSTRACT

Conventional fuels are being replaced by the renewable energy sources that are replenished and environment-friendly. In the paper, authors introduced a modern concept of hybrid boat cascading two sources of energy such as solar energy and electric energy stored in the battery bank. The roof of these boats consists of solar photovoltaic (PV) panels arranged in arrays that charge the battery during day hours. Paper prototypes the idea of installing charging boots in the bank of the river, charging the battery during inappropriate weather, sunset and off hours of the day. The idea enlightened a new dimension to develop solar-electric water transportation that reduces the cost of water transportation and dependence of conventional fuels.

Keywords: SOx and NOx emission, charging boots, battery storage, charging circuit, boost circuit, solar panel arrays

1. INTRODUCTION

Modern transportation is potentially dependent on the renewable energy source including solar PV, fuel cell and electricity. The initiation led to a gradual reduction in the SOx and NOx emission from the vehicles, but still in a developing stage in airways and waterways. In this regard, a number of researchers proposed the concept of developing the water transports that run on renewable energies. Therefore, it is a challenge to build up renewable boats cascading a number of alternative energy sources

Authors introduced the concept of a hybrid boat that is powered by regular charging of batteries that are installed in the boat Fuels including diesel, petrol, alcohol, and compressed natural gas (CNG) are used as alternatives in these boats to energize the mechanical system. The paper is being distributed into a number of sections; section one is the preliminary overview of hybrid vehicles, section two describes the idea of hybrid solar electric vehicle and section three describes the constraints of the hybrid system [3,4].

2. HYBRID BOAT: A NEW AGE OF FUTURE TECHNOLOGY

Hybrid vehicles are the modern energy efficient and cost-effective roadway motors. A number of modern companies manufactures road vehicles including cars, trucks, and busses that run of electricity and environment fuels. The concept of the hybrid boat is represented in the paper considering two main energies; solar and electricity that is responsible for producing power using the gasoline engine [5,6].

Hybrid boat structure is similar to general diesel-fuelled motor-driven boats and undergoes a major modification of replacing the diesel engine with a generator, motor and rechargeable batteries. Rechargeable batteries are charged by solar PV panels and the boots located at the ports. However, the charging current of the PVs decreases in the days of less intense sunlight and cloudy weathers. Therefore, the alternative electric charging from port boots plays an important role in turning the system efficient and cost-effective as the operating cost reduces drastically in comparison to conventional fuels. Electric motors are coupled to the propellers and rotated at a higher speed to improve the power-to-weight ratio. It improves the acceleration and relatively constant torque of the electric motor. Boats are charged from the power grids overnight and the electricity to the grid is supplied from the neighbouring hydro-power plants as most of the commercial and household loads turn off (Figure 1 and 6)

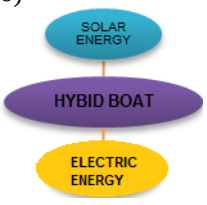

Fig. 1 Energy Sources in Hybrid Model

3. SYSTEM COMPONENTS AND OPERATIONS

3.1 Solar Module

A solar module consists of solar panels that are arranged in arrays to trap maximum heat over the area of the boat. Solar heat is converted into electrical energy by photoelectric cells fabricated in huge panels. The number of solar panels required in the boat depends on the power required to drive the boat, area

of the roof and other parameters including the types of loads (Figure 2).

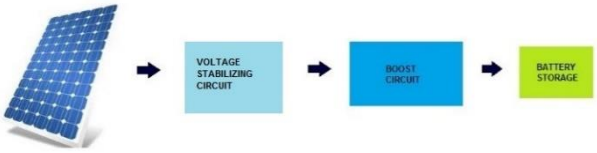

Fig. 2 Solar Panel Module for Voltage Stabilization

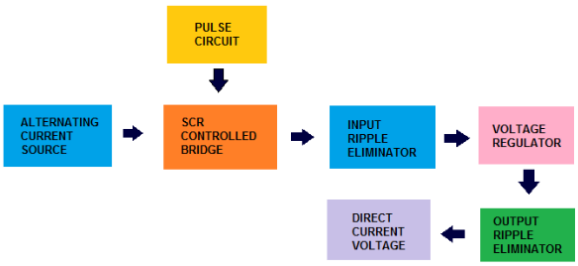

Fig. 3 Model of Charging Boot

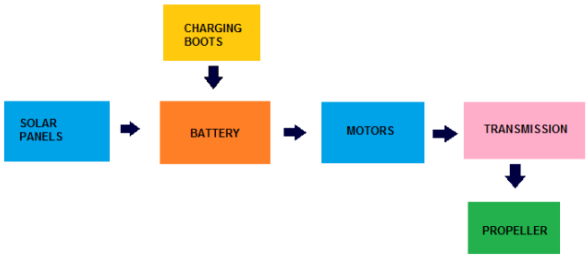

Fig. 4 Model of Hybrid Boat

3.2 Chargers on the Ports

Boats are being charged by electrical charging boots located at the port each at a certain distance away. The basic structure of these chargers is similar to the rectifiers. Power consumed from the electric grids is being rectified by controllable semiconductor switches. Input ripples are removed by connecting a capacitor in parallel across the Zener or regulator circuit. Output direct current (DC) voltage is filtered by the capacitor connected in between the Zener and charging terminals (Figure 3)

3.3 Hybrid Vehicle

The hybrid vehicle consists of mainly solar panels, battery, electric motors, transmission system, and wheels. Energy from the solar panels and charging boots are stored in the battery and provided to the motor and driving control system after stabilizing the flow of power. These speed controlled motors are used in the transmission system to control and brake the boat propellers (Figure 4 and 6).

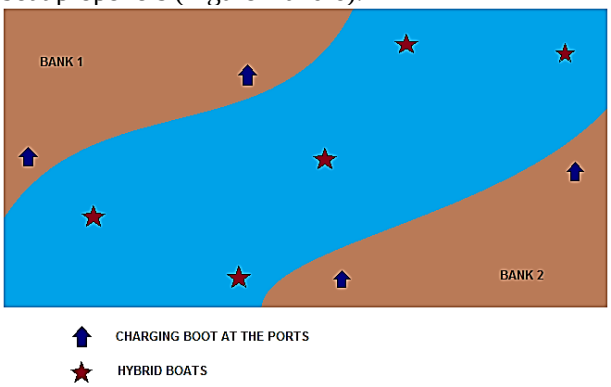

Fig. 5 Charging Boots and Hybrid Boats

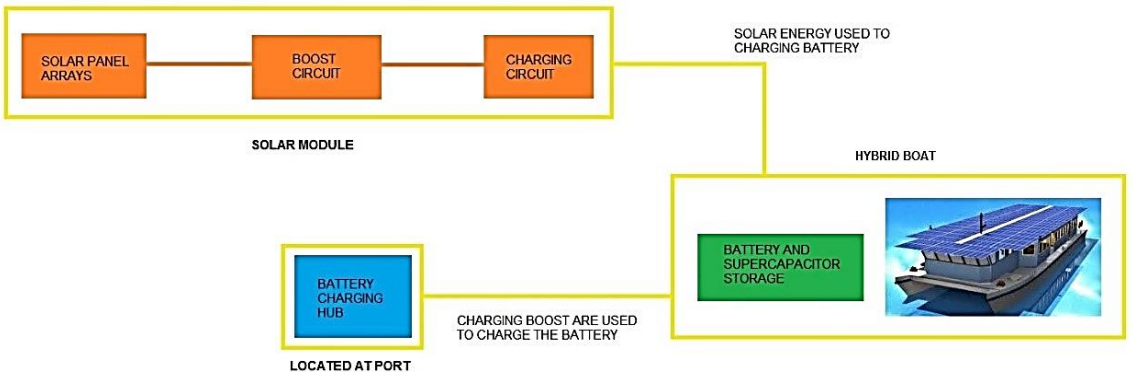

Fig. 6 Concept of Hybrid Vehicle

4. CONSTRAINTS OF THE HYBRID SYSTEM

A number of physical constraints present in the hybrid system need to be controlled within a defined range. Power and frequency of the electrical system should be regulated that reduces the fire hazard. An accurate battery alert system needs to be installed as these charged boats can move only to a certain distance. Boats cannot be efficiently be driven in seas and oceans as it fails to overdrive the high-speed waves. These are heavier after the installation of battery bank, chargers and controllers. The initial cost of these vehicles is high and the spare parts seem to be more expensive as a less number of manufactures are present in the market. These limiting constraints and disadvantages need to be overcomed as it will be the future vehicular technology around the globe [10,11].

5. CONCLUSIONS

Energy from different sources is sustained and utilized in various applications including vehicular technology. In water transportation, a number of issues create huge challenges to be overcome i.e. the risk of

fire, safety system and grounding of electrical systems. The paper illustrated the modern technically advanced idea of hybridizing all ways of transportation especially waterways to connect two isolated places disconnected by lands.

REFERENCES

1) Emadi A, Lee Y J, Rajashekara K. Power electronics and motor drives in electric, hybrid electric, and plug-in hybrid electric vehicles. IEEE Transactions on Industrial Electronics. 2008 Jun;55(6):2237-45.C
2) Yilmaz M, Krein PT. Review of battery charger topologies, charging power levels, and infrastructure for plug-in electric and hybrid vehicles. IEEE Transactions on Power Electronics. 2013 May;28(5):2151-69.
3) Hori Y. Future vehicle driven by electricity and control-research on four-wheel-motored" UOT Electric March II". IEEE Transactions on Industrial Electronics. 2004 Oct;51(5):954-62.
4) Wang CS, Stielau OH, Covic GA. Design considerations for a contactless electric vehicle battery charger. IEEE Transactions on industrial electronics. 2005 Oct;52(5):1308-14.
5) Moreno J, Ortúzar ME, Dixon JW. Energy-management system for a hybrid electric vehicle, using ultracapacitors and neural networks. IEEE transactions on Industrial Electronics. 2006 Apr;53(2):614-23.
6) Sakai SI, Sado H, Hori Y. Motion control in an electric vehicle with four independently driven in-wheel motors. IEEE/ASME Transactions on mechatronics. 1999 Mar;4(1):9-16.
7) Taylor J, Maitra A, Alexander M, Brooks D, Duvall M. Evaluations of plug-in electric vehicle distribution system impacts. InPower and Energy Society General Meeting, 2010 IEEE 2010 Jul 25 (pp. 1-6). IEEE.
8) Hori Y, Toyoda Y, Tsuruoka Y. Traction control of electric vehicle: basic experimental results using the test EV" UOT electric march". IEEE transactions on Industry Applications. 1998 Sep;34(5):1131-8.
9) Callon M. The sociology of an actor-network: The case of the electric vehicle. InMapping the dynamics of science and technology 1986 (pp. 19-34). Palgrave Macmillan, London.

Sustainable Energy Solutions

Sustainable design and economic development

Assessment of impact of infrastructural growth and development on bio-diversity in Indian context

Shiva, J. [1], and Punekar, R.M.[2]

[1] Assistant Professor, Department of Design, Indian Institute of Technology Hyderabad, India.
[2] Professor, Department of Design, Indian Institute of Technology Guwahati, India.

ABSTRACT

The growth and development of a country is measured by the growth and development of construction sector. In a way it is an indicator of the health of economy. The expansion of constructed footprint by humans is taking its toll on nature and its other species from flora and fauna. The shrinking virgin reserves of forest land and pollution has posed serious danger to the bio-diversity in various parts of India. The guidelines for a responsible design and construction could lower the impact from the present scenario. Various methods for such effort are being framed. One such tool is Green Rating for Integrated Habitat Assessment by The Energy and Resources Institute and Ministry of New and Renewable Energy, Government of India. Many such tools are available to provide pre and post construction guideline to minimize impact of built-environments on the biodiversity of a place, such as LEED India. The evaluation of these tools was taken up to assess provisions made to serve the cause. Similar recommendations from NBC of India were taken into account to draw a parallel in effectiveness achieved in these tools. Further a case study was undertaken in and around the campus of IIT Guwahati to understand the impact of growth and development on a virgin greenfield. The industrial units established around the campus and other infrastructural developments has made impacts in various ways affecting water, soil, air, animal, bird and aquatic life of the place. The changes were observed and a comparison was drawn to assess the effectiveness of provisioned criteria in the tools. Several lacunae were identified and a set of points were observed which may help in strengthening the next editions of such tools.

Keywords: biodiversity, sustainability assessment methods, GRIHA, LEED, CASBEE, BREEAM, national building code of India

1. INTRODUCTION

The construction sector is the single largest world energy consumer between 30% — 40% of total world energy. The awareness regarding this issue has been taken up by various research agencies and governments from all over world. Lately we have various Sustainability Assessment (SA) methods as a guidelines for pre-construction design exercises and post-construction evaluation and assessments. Green Rating for Integrated Habitat Assessment (GRIHA) is the Indian version of such SA methods which is being adopted by Architects, Planners, Designers, Builders, Project Owners and various agencies involved in construction sector. This research intends to study the adequacy of addressing Biodiversity issues by SA methods. As the biodiversity has been threatened by development activities, it is imperative to check the effectiveness of SA method being applied. India is a country with major geographies like deserts, coastal, plains, mountains, hills, cold, temperate, humid regions with variety of distinct socio-cultural groups. This variety offers a wide range of nature evolved species of flora and fauna which are set in a fragile ecological environments.

2 THE IMPORTANCE OF BIODIVERSITY AS OUTLINED IN NBC PART 11

2.1 Ecological design/conserving bio-diversity

Diverse ranges of flora fauna species such as animals, birds, insects, reptiles, plants, ferns, moths, trees, algae, and aquatic plants and animals, and pollinator species, etc. hence in order to protect these the following considerations may be taken up:

2.1.1 Protection and use of existing vegetation Minimum disruption to the existing species and their habitat. Relocation of trees shall be done to retain old and mature trees from site.

2.1.2 Use of vegetation that promotes a regional identity and a sense of place plants and other species of native origin, non-invasive species which conserve water and do not dominate over local species shall be used on site, which promotes regional and place based identity.

2.1.3 Conservation of native endangered species endangered local species shall be promoted to plant on and off site to conserve bio-diversity.

3. BIODIVERSITY CRITERIA GIVEN IN SA METHODS TITLE

3.1 GRIHA

No existing trees should be cut, transplant mature trees, plant 3 trees for every 1 tree cut of the same species. Increase total number trees by 25%. Preserve top soil, maintain its fertility and use for landscape.

3.2 LEED

On site restoration of trees using native or adapted vegetation. Vegetated roof surfaces in 1.5 density of floor-area ratio buildings. Restore disturbed soil. Top soil must be taken care for its organic matter, compaction, infiltration rates, soil biological function and chemical composition.

3.3 CASBEE

Preservation and conservation of Biotope. Protection and restoration of natural habitat inhabited by animals and support the growth of plants. Creation of high quality green spaces.

3.4 BREEAM

Long term impact on biodiversity shall be reduced. Principal contractor is given charge to take action on site to protect biodiversity. Development of full biodiversity management plan shall be done to ensure control on site.

4 EMPIRICAL FINDINGS

Campus of IIT Guwahati was chosen to make this study and observe on ground. The research intends to understand the impact of development on a green fields site hence the campus of IIT Guwahati was found to be suitable as it has been a marshy / swamp area for always with variety of aquatic, insect, reptile, animals and birds. The area was used for mainly fishing as it has remained water logged since it is known.

Inferences from NBC Part 11 which talk about certain inclusions which are required to tackle social and environmental impacts on the green field sites and their former inhabitants. Construction has changed virgin landscapes forever and the biome of that place has been forced to be displaced or in many cases be damaged need attention. The research intends to study the impacts of setting up of institutional campuses on such stakeholders.

The Earth mapping technology from Time Machine Library of CREATE Lab, Carnegie Mellon University enables us to study the time lapse shots/videos from year 1984 till 2016. The same was used to map the time-lapse of IIT Guwahati campus and surroundings

4.1 Key Findings

Shrinkage in swamp cover. (See Figure 1 for Point 1 to 5)

2. **Land reclamation** by sand filling, earlier there were bamboo houses in swamp waters.

3. **Pollution** by nearby industrial units like, soil, noise, air, water, etc. **Fine pollutants** are flagging the campus and nearby residential areas of Amingaon. Blaring horn by trains which passes from near main gate creates terrible noise problem for residential quarters, even in odd hours. LPG bottling plant which shoots fine particles and gas.

4. Industrial corridor developed in the back side of Kali Pahar (hill) near Digholi Bill (lake).

5. Rainwater streams linked with artificial lakes to not to disturb the natural course of waters.

- Uncontrolled construction practices spilled cement mixes to waters which has resulted into poisoning of water for aquatic life.
- Animal life (jackal, foxes, etc.) displaced due to light and noise pollution.
- Loss of habitat for reptiles.
- Urban spread has increased along the national highway around area of Amingaon as it was established as the district headquarters of Kamrup rural district. Various administrative offices, hospitals, roadside restaurants, petrol pumps, service centres and industrial units have come up.
- Large scale land reclamation has been done in vicinity for setting up residential, commercial and industrial units by sand filling which has permanently changed the water levels and green cover. This has resulted into silent killing of aquatic animal and plant species. Drainage of grey water in the water bodies has taken lives of amphibians, insects and reptiles. Detergent water and various household cleansers have eradicated small species which silently fall prey to such industrial chemical based products.
- The significant loss of swamps can be seen in comparative satellite images from year 1994 and 2017.

Fig. 1. Time-lapse satellite image from above IITG campus shows how the landscape has changed over 27 years. Source: Google Earth Engine

Fig. 2. Loss of swamp cover between 1994 to 2017

Fig. 3. Cement slurry seepage - loss of aquatic habitat between 1996 to 2016

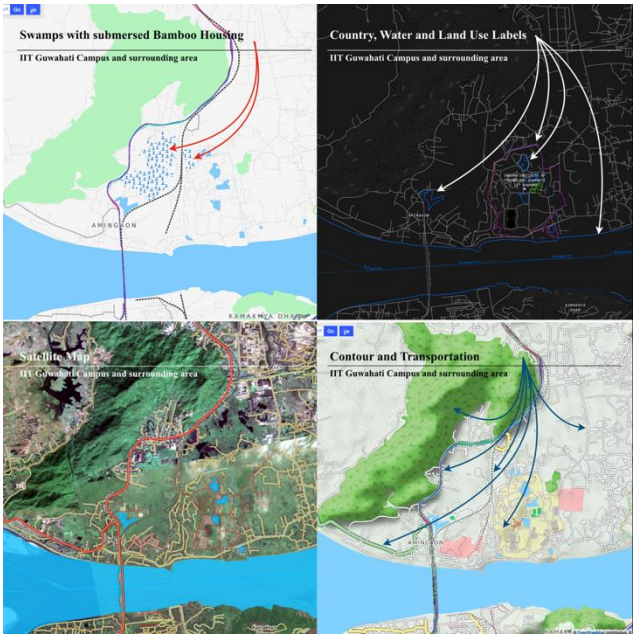

Fig. 4. Changes observed have had adverse effect from external forces also such as highways, change in land-use from agricultural to industry/commercial, heavy transportation, etc.

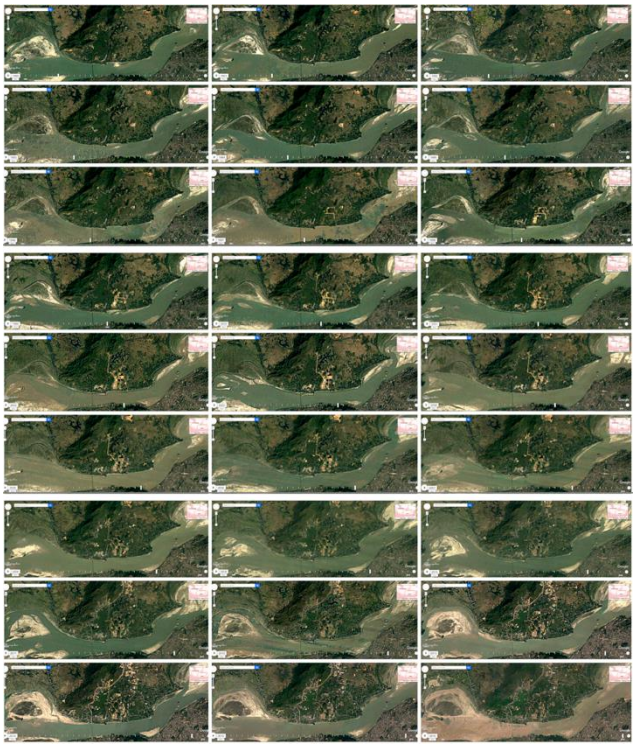

Fig. 5. Yearly time lapse of IIT Guwahati campus site and surroundings in 26 years, from year 1990 to 2016

5 RESULTS

The lack of control on impact from infrastructure development is seen very clearly on site and surrounding locations. The growth along the highways and change of land-use from agrarian to industrial or commercial has ended up in a total change of landscape and existing biodiversity. Swamp cover on the face of earth has gone down. Significant land is filled with sand, levels are raised high and no longer retains rain water. Rather rain water can't be retained and flows to the river and then ocean. Time-lapse shows increase in brown areas and reduced green cover on the site land and in surroundings. The level of river water has also shown scattered and scarce dispersion in the river bed. The same can be seen by increasing sand islands and sand bank from either side of river Brahmaputra.

Fig. 6. Tree Cover Loss during 2001 to 2016, Courtesy: https://www.globalforestwatch.org/map/

6 CONCLUSIONS

After seeing the existing provisions in SA Methods and their enforcement in growth and development of built-environments, the efficacy and sufficiency of criteria become questionable. The provisions of NBC Part 11 of 2016 has pointed out regional species protection, promotion to local wild life to not to make them vulnerable to the impact. SA Methods of GRIHA, LEED, CASBEE and BREEAM have certain criteria set to monitor few components of diverse scope of biodiversity. Starting from individual footprint of a building to which may be called as a green building, to energy efficient building, to environment friendly building, to sustainable building, comes to landscape and biodiversity conservation, before much larger sustainable development and climate change mitigation level. It increases in progression of scope and inclusion of various components of biosphere and human intervention in it.

The first hand observations show the movement of animal and aquatic life from the site and surroundings. Loss of tree cover and receding water cover from the ground surface are evident on and off site.

7 SUMMARY

As the pace of growth and development is growing exponentially, the corresponding impact on land, water and air is crucial. Development has started penetration into regions and places where there have been only jungles, inhabited lands, agricultural fields, water bodies and other remote places where nature has its own ways of sustaining life sans humans. The change is visible and predominantly becoming harsher by the day. The SA Methods has some provisions to check but geography specific criteria needs to be framed to make SA Methods more relevant in changed scenarios. Frameworks shall be reinforced with more local considerations and include criteria for micro-environment. To cope up with the pace of development, the SA Methods need to evolve to match.

REFERENCES

1) National Building Code (NBC) of India 2016, Volume 2, ICS 01.120; 91.040.01, Bureau of Indian Standards, New Delhi, India
2) Green Rating for Integrated Habitat Assessment (GRIHA) Version 2015, Abridged Document, GRIHA Council and The Energy and Resource Institute, New Delhi, India
3) Leadership in Energy and Environmental Design (LEED) v4 for Building Design and Construction 2017, US Green Building Council, Washington, United States of America
4) Comprehensive Assessment System for Built Environment Efficiency (CASBEE) 2016, Institute for Building Environment and Energy Conservation (IBEC), Tokyo, Japan
5) Building Research Establishment Environmental Assessment Method (BREEAM) 2014, Building Research Establishment (BRE) Global, Hertfordshire, United Kingdom
6) https://earthengine.google.com/timelapse/ Accessed : July 2017 (07/11/2017)
7) NASA Landsat Program, Landsat 4 (1984-1993), Landsat 5 TM (1984-2012), Landsat 7 ETM+ (1999-2013), Landsat 8 OLI (2013-2016), courtesy of the U.S. Geological Survey, Sioux Falls, South Dakota, United States of America
8) https://www.globalforestwatch.org/map/ Accessed : May 2018 (05/30/2018)

Sustainable Ecosystem Management

Sustainable Ecosystem Management

Sustainable management and restoration of rivers and wetlands

Assessment of spatial and temporal water quality variation of river Bharalu in Guwahati city, Assam, India

Das, M.[1], Sarma, J.[2] and Bhattacharjya, R.K.[3]

[1]Ph.D student, Department of Civil Engineering, Indian Institute of Technology Guwahati, Guwahati-781039, India.
[2] Former Junior Research Fellow Department of Civil Engineering, Indian Institute of Technology Guwahati, Guwahati-781039, India.
, [3] Professor, Department of Civil Engineering, Indian Institute of Technology Guwahati, Guwahati-781039, India.

ABSTRACT

In this study, the water quality of the river Bharalu is monitored for three years to understand its spatial and temporal variation. Physiochemical analysis of water samples such as Turbidity (NTU) , Total Dissolved Solids (mg/L), pH , Alkalinity (mg/L), Electrical Conductivity (EC), Total hardness (mg/L), Dissolved Oxygen (mg/L), Biochemical Oxygen Demand (mg/L), Chemical Oxygen Demand (mg/L), Iron (mg/L), Sulphate (mg/L), Fluoride (mg/L), Chloride (mg/L), Na, K, Ca and Mg (mg/L) are analyzed as per standard methods prescribed by (APHA,1995). From the whole investigation, it is observed that the water of river Bharalu is thickly polluted with different inorganic and organic waste, metals, and ions. Further, the concentration of the physical and chemical parameters increases significantly towards the downstream site of the river with some variation in the middle course. The primary sources of pollution of the river are dumping of domestic, municipal, commercial and industrial waste into the river.

Keywords: water quality; concentration; Bharalu river; physio-chemical analysis

1. INTRODUCTION

Guwahati, the gateway of Northeast is considered as one of the fastest growing cities in India. As a major city of the region, the population of the city is increasing at an alarming rate, which as a result increase the demand for drinking water. Though the river Brahmaputra is flowing through the heart of the city, the major source of water for the people of Guwahati city is the groundwater extracted from shallow unconfined aquifer or from deeper confined aquifer. The water distribution network of the city is not yet developed and as a result only a few percentages of the city population get the municipal supply of water. Therefore, most of the people depend on open well and tube well to meet their daily water requirements.

The river Bharalu, a small tributary of the river Brahmaputra is flowing through the heart of Guwahati city. In early days, it was used as a source of potable water. However, time has converted the river as a main drainage channel of the city. During the monsoon season, the water level of the river Bharalu rises up to the ground level and sometimes even it flooded the areas near the river.

It has been noticed that the waste material of the city including domestic, commercial, industrial, biomedical wastes are directly disposed into the Bharalu river. There is no integrated system for sewage disposal in the city and due to lack of scientific disposal method, all the biodegradable, and non-biodegradable wastes are discarded together in and around the river bank.

A study was carried out on the water quality of river Bharalu at IIT Guwahati and it was observed that the concentrations of phosphorous, iron, sulphate of the river water are more than the permissible limits (Girija et. al 2007). High phosphorous content in drinking water may cause osteoporosis and may lead to damage to the arteries of the human body. The Central Pollution Control Board of India has also reported 'the river Bharalu' as one of the most polluted rivers in India. In the year 2013 Erec Indian Research Laboratory, has carried out an experimental study on the water quality of river Bharalu for a short duration of time for eight different locations. They observed that the river water was highly turbid and rich in organic matters. Therefore, the water quality of the river Bharalu is a major concern for the people living on the banks of the river. In order to examine the present scenario of the river Bharalu a physicochemical analysis of water quality is carried out in this study.

2 METHODOLOGY

2.1 Study area

The study is carried out through the longitudinal section of the river Bharalu in the greater Guwahati city of Kamrup Metro district, Assam, India. The river Bharalu is basically divided into two parts. The upper part of the river is found in the hilly catchment areas of Meghalaya from where it originates. This is known as river Bahini, which covers the area of approximately 60

km^2. The downstream part is known as river Bharalu which is flowing through the Guwahati city. The catchment area covered by river Bharalu is approximately 40 km^2.The whole sewage, untreated effluent, municipal solid wastes, domestic wastes of Guwahati city are carried out by river Bharalu and are released at Bharalumukh, to the river Brahmaputra. The catchment area of the river lies between of 25°59′ to 26°11′ North and 91°43′ to 91°51′ East. Topographically this study area consist of hills and plains with some bloated hillocks. The southern and the eastern parts of the city are bounded by rows of hills which are the extensions of the Khasi Hills of Meghalaya. Geologically, Guwahati rests upon the typical Precambrian rock units which are overlain by young and recent alluvium. Fig.1 shows the river Bharalu and its drainage system along with its sampling locations.

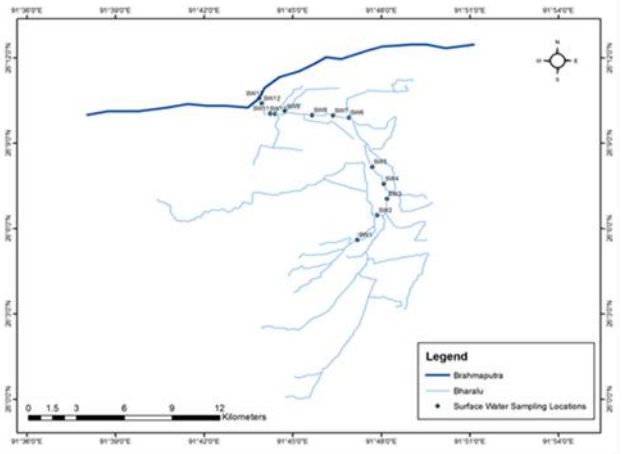

Fig. 1. Map of river Bharalu showing the sampling location.

2.2 Field sampling &Laboratory Analysis of water samples from Surface water of Bharalu River

Collection of the samples

The surface water samples are collected from thirteen different sampling stations along the longitudinal section of Bharalu River. The sampling locations (Fig. 1) are starting from Basistha Mandir to Bharalumukh. Table 1 listed the sampling locations. Water samples are collected within the time interval of three months from 2014 to 2016. Total four samples examined for dry season and three samples for wet season. The equipment that is used for the collection of water samples and for analysing the physiochemical parameters are cleaned plastic bottles, thermometer, PH meter, YSI Professional Plus Multiparameter water testing probe, GPS for identification of the location, Winkler's A and Winkler's B reagent, BOD bottle (300ml capacity).

Table 1. Sampling location along the river Bharalu.

Sampling point	Locations
SW1	Basistha Mandir
SW2	Natun bazar, Basistha
SW3	Bhetapara
SW4	Beltola
SW5	Rukminigaon
SW6	Jonali
SW7	Anilnagar
SW8	Ulubari
SW9	Chabipool
SW10	Athgaon
SW11	Fatasil
SW12	Sluicegate
SW13	Bharalumukh

2.3 Methodologies for analysis of physico-chemical parameters of water samples

The experimental study is carried out as per standard methods prescribed by (APHA, 1995). The parameters that are examined is given in Table 2. Among them Dissolved oxygen (mg/L), Electrical Conductivity (µmho/cm) and pH were measured on the sampling spot by using the YSI Multi parameter water testing probe.

Table 2. The water quality parameters considered in this study.

Parameters	Symbols	Units
Turbidity	~	NTU
Total Dissolved Solids	TDS	mg/L
pH	pH	mg/L
Alkalinity	~	mg/L
Total hardness	TH	mg/L
Dissolved Oxygen	DO	mg/L
Biochemical Oxygen Demand	BOD	mg/L
Chemical Oxygen Demand	COD	mg/L
Iron	Fe	mg/L
Sulphate	SO_4^{-2}	mg/L
Fluoride	F^-	mg/L
Chloride	Cl^-	mg/L
Sodium	Na^+	mg/L
Potassium	K	mg/L
Calcium	Ca^{+2}	mg/L
Magnesium	Mg^{+2}	mg/L

The observed concentration of all the parameters is compared with the standard permissible limit as given by IS: 10500-2012 for drinking water, given in Table 3. The maximum acceptable limit of COD is considered as 10 ppm. This is as set by W.H.O., I.S.I., I.C.M.R., Govt. of India for drinking water standard. The maximum value of BOD for fresh river water should be below 1 mg/L (Connor 2016).

Table 3. Standard value of the water quality parameters for drinking water as per IS: 10500: 2012.

Water quality parameters	Requirement (acceptable limit)	Permissible Limit in the absence of alternate sources
pH	6.5-8.5	No relaxation
TDS	500 mg/l	2000 mg/l
Total	200 mg/l	600 mg/l

Hardness		
Alkalinity	200 mg/l	600 mg/l
Iron	0.3 mg/l	No relaxation
Sulphate	200 mg/l	400 mg/l
Chloride	250 mg/l	1000 mg/l
Fluoride	1 mg/l	1.5 mg/l
Calcium	75 mg/l	200 mg/l
Magnesium	30 mg/l	100 mg/l
Turbidity	1 NTU	5NTU

3 RESULTS AND DISCUSSION

The physiochemical analysis of the water samples of river Bharalu is carried out with seasonal and spatial variation. From the analysis, it is observed that the sodium, sulphate, and magnesium content are within the permissible limits as per the drinking water standards. The remaining other parameters having its concentration more than its permissible limit are presented graphically to understand the seasonal and spatial variation.

3.1 Dry season

To examine the longitudinal variation, four samples were collected from all the thirteen locations in the dry season. Among the four, the samples having the maximum concentration of the parameters is considered to compare the longitudinal variation.

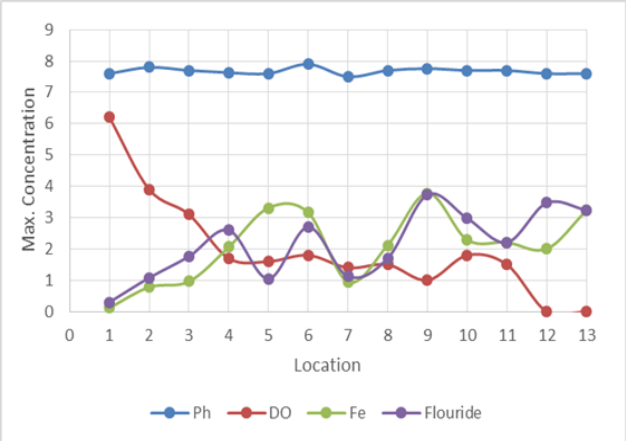

Fig. 2. Variation of pH, DO (mg/L), Fluoride (mg/L) and Iron (mg/L) with the sampling locations in dry season.

Fig. 2. Shows the variation of pH, DO (mg/l), Fluoride (mg/l) and Iron (mg/l) concentration with the sampling locations. From the figure, it can be observed that the pH level in the river water is within the permissible limit during the dry season. The DO level of the water samples are continuously decreasing from upstream to downstream and the value of DO is almost zero at the downstream. High concentration of Fluoride is also observed on some of the sampling locations. As seen in the figure, the Fluoride concentration is in between 0.3 and 3.73 mg/l with an average value of 1.42 mg/l. The Fluoride concentration is high in almost all the samples but the samples collected from the upstream site near Basistha Mandir is within the permissible limit. The high value (3.78 mg/l) of Fluoride was recorded in the Chabipool location. The lowest value (0.12 mg/l) was recorded near Basistha Mandir. It may be noted that the concentration of Iron is also showing a similar trend that of fluoride. The maximum concentration of iron has been recorded at Chabipool location and minimum concentration has been recorded near Basistha Mandir.

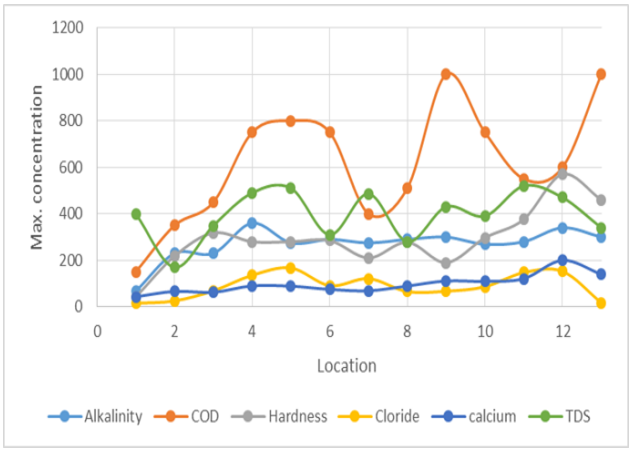

Fig. 3. Variation of Alkalinity (mg/L), TDS, Hardness (mg/L) and COD (mg/L), Chloride and calcium with the sampling locations in dry season.

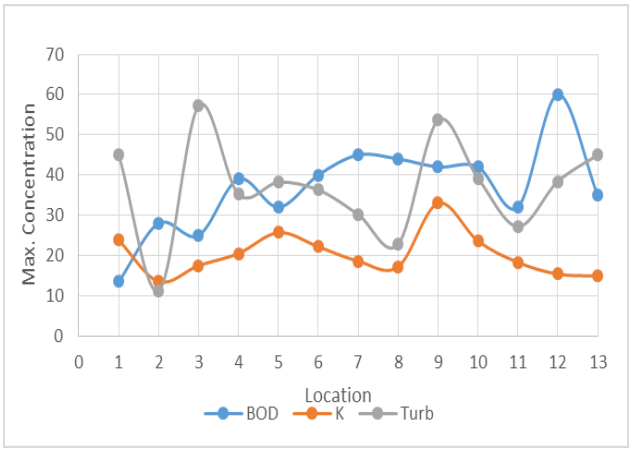

Fig. 4. Variation of BOD, Potassium (K) and Turbidity (NTU) with the sampling locations in dry season.

Fig. 3. shows the variation of Alkalinity (mg/l), Total Dissolved Solid (TDS), Hardness (mg/l), COD (mg/l), Chloride and calcium with the sampling locations. The observed mean value of alkalinity is 269.69 mg/l and it ranges from 67 to 340 mg/l. The cause of total alkalinity in water is due to the presence of various ions. As such Potassium and Chloride ion content is also found to be more than its permissible limits. As shown in Fig. 3. chloride ion value is increasing towards the downstream site of the river. Its value ranges from 15-167.25 mg/l. The concentration of

Potassium shows (Fig. 4) distinct point to point variation along the river with highest values at the downstream site. The average value of Potassium ion present in Bharalu water is 20.73 mg/l (range 12.7-29.1 mg/l). The water of the river Bharalu has large BOD and COD concentrations in comparison to other natural river systems. Thus, it results in decrease of dissolved oxygen. The Dissolved oxygen found in the water sample is very low throughout the river and this leads to zero dissolved oxygen content at the downstream (Fig.3.). The Total Dissolved solid (TDS) is high in Chabipool location (720 mg/l). The water of river Bharalu is also highly turbid due to the presence of suspended and colloidal matter such as clay, silt, finely divided organic and inorganic matter, and other microscopic organisms in the river water. The average value of hardness of the water samples is 292.6 mg/l. The highest value of 570mg/l was recorded in sluice gate location, which is located in the downstream region of the basin (Fig. 3.). Thus, considering the average value of the total Hardness the Bharalu water can be termed as "very hard" in the dry season.

3.2 Wet season

In case of the wet season, three samples were examined from all the thirteen locations. Among the three, the samples having the maximum concentration of the parameters are considered to compare the spatial variation.

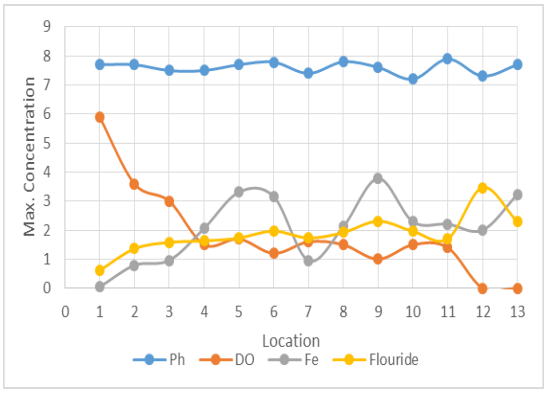

Fig. 5. Variation of pH, DO (mg/L), Fluoride (mg/L) and Iron (mg/L) with the sampling locations in wet season.

The observed pH value of the river water is within its permissible limit during the wet season as shown in Fig. 5. During the wet season, the Fluoride content of river water ranges from 0.61-3.47 mg/l with an average mean of 1.86 mg/l. The Fluoride concentration is high in all the locations except in the upstream site, near Basistha Mandir where the concentration of Fluoride is within the permissible limit (Fig.4). Both in the dry and the wet season, the highest value of fluoride content is recorded in the Chabipool location. In case of Iron, the average iron concentration is recorded to be 2.06 mg/l with the highest value of 3.78 mg/l was recorded in sluicegate location. The lowest value of 0.04 mg/l was recorded during wet season near Basistha Mandir.

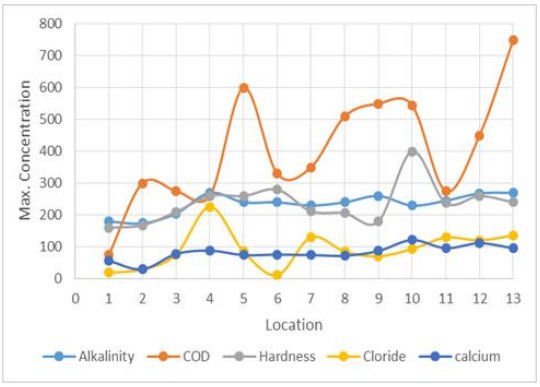

Fig. 6. Variation of Alkalinity (mg/L), Hardness (mg/L) and COD (mg/L), Chloride and calcium with the sampling locations in wet season.

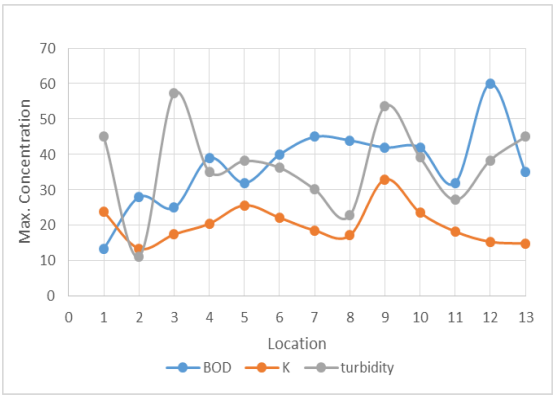

Fig. 7. Variation of BOD, Potassium (K) and Turbidity (NTU) with the sampling locations in wet season.

The observed mean value of alkalinity is 234.7 mg/l and it ranges 180-270 mg/l (Fig.6). The concentration of Potassium and Chloride is found to be more than its permissible limit. As shown in Fig. 6, the concentration of chloride ion is increasing toward the downstream site of the river. Its value ranges from 11-225.93 mg/l. In case of Potassium ion, it increases at the downstream site of the river with the highest value in Chabipool location as shown in Fig. 7. Its average value is 20.32 mg/l and ranges from 13.5-25.7 mg/l. Although the BOD and COD concentration of river Bharalu is low in the wet season than the dry season, it is more as compared to other natural river systems. Thus, it results in a decrease in the dissolved oxygen of the river water. The Dissolved oxygen found in the water sample is very low throughout the river and this leads to zero dissolved oxygen content at the downstream (Fig. 5). The total suspended solids present in the river water is more which may be responsible for high turbidity (Fig.6). Due to rich calcium content in the river water, hardness observed in the water sample is also very high. It is observed that the average hardness is 23.6 mg/l.

4 CONCLUSIONS

From the investigation, it is observed that the water of river Bharalu is thickly polluted with different inorganic and organic waste, metals, and ions. As the river flows it carries lots of pollutants from industrials, commercial, municipal sites through the interconnected drains and creates surface water pollution at the downstream section of the river. The Bharalu water may be termed as 'very Hard, as its hardness level is more than 200mg/L in almost all the sample locations both in dry and wet season. The Bharalu water is highly contaminated with Fluoride and Iron. The water of the river Bharalu has large BOD and COD concentration in comparison to other natural river systems. This may produce high organic contamination and growth of algae. As a result, the dissolved oxygen will reduce further. It has also been observed that the DO level of river Bharalu water is very low and the DO content is zero at the downstream. Since the Bharalu River is connected to the Brahmaputra, it is contributing water pollution to the river Brahmaputra also. Thus, proper remediation techniques should be adopted for controlling the surface water pollution of river Bharalu.

ACKNOWLEDGEMENTS

This work was been carried out with the research grant received from NRDMS division of Department of Science and Technology, Govt. of India.

REFERENCES

1) APHA (1995) Standard Methods for the Examination of Water and Wastewater. 19th Edition, American Public Health Association Inc., New York.
2) Bureau of Indian Standards, Indian Standards (IS:10500:2012) Drinking Water Specification: New Delhi (2004).
3) Connor, R., (2016). The United Nations World Water Development Report 2016: Water and Jobs, chapter 2: The Global Perspective on Water. Paris: UNESCO. p. 26. ISBN 978-92-3-100155-0.
4) Girija TR, Mahanta C, Chandramouli V (2007):Water quality assessment of an untreated effluent impacted urban stream: the Bharalu tributary of the Brahmaputra River, India Environ Monit Assess, 130(1-3), 221-36

Evaluation of river course change detection using remote sensing & GIS

Mishra, D. [1] and Mazumdar, M. [2]

[1]Ph.D Scholar, Civil Engineering, Assam Engineering College, Guwahati 781013, India.
[2]Assistant Professor, Department of Civil Engineering, Assam Downtown University, Panikhaiti, Guwahati781026, India.

ABSTRACT

The Brahmaputra is one of the largest alluvial rivers in the world characterized by frequent bank erosion leading to channel pattern changes and shifting of bank lines. This study was aimed at quantifying the changes of river course along the Brahmaputra for a period of different years and months. A course of about 56 kms has been studied using an integrated approach of Remote Sensing and GIS. The channel configuration of the Brahmaputra has been mapped for a period (1985-2018) using USGS and Landsat 8 OLI/TIRS C1 Level 2 satellite image respectively. The analysis of satellite data has provided not only channel configuration of the river system but also significant facts about the changes in river morphology, stability of the river banks and changes in the main channel.

Keywords: remote sensing, GIS, landsat, river morphology

1. INTRODUCTION

The Bhramaputra has braided channels in most of its course in the alluvial plains of Assam. The lateral changes in channels cause severe erosion along the banks leading to a considerable loss of good fertile land each year. Bank oscillation also causes shifting of outfalls of its tributaries bringing newer areas under waters. Thousands of hectares of agricultural land continuously suffers from severe erosion along the Brahmaputra covering important parts of Assam and Arunachal Pradesh.

The present paper briefly describes a study of some portions of Brahmaputra river for a stretch of around 56 kms for a period of (1985-2018) using an integrated approach of Remote Sensing and GIS. The satellite data have provided the information on the channel configuration of the river system, river morphology, erosion and deposition patterns.

1.1 Study Area

The Brahmaputra termed a moving ocean, is an antecedent snowfed river which flows across the rising young Himalayan Range. Geologically, the Brahmaputra is the youngest of the major rivers of the world. The gradient of the Brahmaputra is as steep as 4.3 to 16.8 m/km in the gorge section upstream of Pasighat, but near Guwahati it is as flat as 0.1 m/km. For the present study, a reach of 56.192 kms of Brahmaputra from Palasbari near Guwahati International Airport (Lat: 26 07’ 17”N, Lon: 091 32’ 14”E) to Barpeta (Lat:26 19’ 49”N, Lon: 091 00’ 20”E) has been considered.

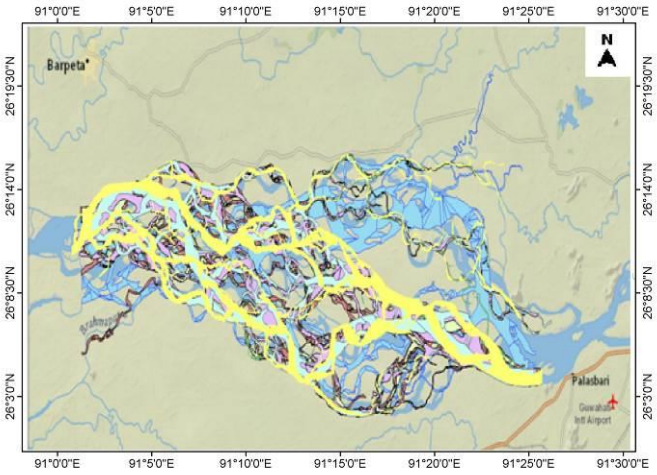

Fig. 1. Study area observed by base map ARGIS

2. LITERATURE STUDY

Satya Prakash Maurya and Akhilesh Kumar yadav (2016) studied Evaluation of river Course change detection of Ramganga River using remote sensing and GIS. They studied the visibility of Ramganga river course change detection was made using Remote Sensing and GIS in study area among period of forty one years from 1972, 1989, 2000, 2006 and 2013 respectively were used to delineate the historical changes of the river course. They found that for a long time this area has been suffering due to erosion problemand shifting characteristics of the Ramganga River. G.Jeba Sweetline and Sangeetha Identified Manimuthar River Course Changes And Estimated Command Area In Ambasamudram Taluk Using Remote Sensing And GIS. Based on the observations

statics is generated to provide an overview of the modifications in the river channel and irrigated agriculture land. Manual method of demarcation of channel changes is very tedious. Integration and co relation of the information related to the factors considered for water monitoring, which is very complex, can be handled easily with GIS. The ability of GIS based overlay analysis helps us to make decision about the identification of areas that has been susceptible to course and command area change over a period of 12 years.

Sainath P. Aher, Shashikant I. Bairagi, Pragati P. Deshmukh and Ravindra D. Gaikwad(2012) in their work River Change Detection And Bank Erosion Identification Using Topographical And Remote Sensing Data is related to Pravara River which channel is continuously changing due to Geomorphic, Climatic agents and Human activities influence in the surrounded region of present river. This changes identification is the main objective of paper with constructive suggestion for control the bank erosion and shifting of Pravara River. An attempt has been made here, to apparatus the GIS and Remote Sensing techniques for river change detection using traditional to advance geographical data sources. The advance Remote Sensing data and Topographical data are to be implementing for obtaining 35 years change result in river stream. The comparatively result explains the 35 years changes in the river bank due to various natural and manmade like flood, water velocity, sand excavation, removal the vegetation cover and fertile soil excavation for the various purpose of local surrounded regions people.

Amna Butt, Rabia Shabbir,Sheikh Saeed Ahmad and Neelam Aziz(2015) studied Land use change mapping and analysis using Remote Sensing and GIS. They applied supervise classification maximum likelihood algorithm in ERDAS imaging to detect land cover/land use changes observed in Simly watershed, Pakistan using multi spectral satellite data obtained from Landsat 5 and Spote for the years 192 and 2012 respectively. The watershed was classified into five major land cover/use classes like Agriculture , Bare soil/rocks Settlement , Vegetation and Water. Resultant land cover/land use and overlay ,maps generated in ArcGis 10 indicated a significant shift from Vegetation and Water cover to Agriculture, Bare soil/rock and settlements cover, which shrank by 38.2% and 74.3% respectively. These land cover/use transformations posed a serious threat to Watershed resources. Hence, proper management of Watershed is required or else these resources will soon be lost and no longer be able to play their role in socio-economic development of the area.

3. METHODOLOGY

3.1 Geo-referencing

Firstly , we have chosen a site area of about 56.192 kms along the Brahmaputra river from palasbari to barpeta. Satellite images of 1985, 2013, 2014, 2015, 2016, 2017, 2017 and 2018 have been used through USGS earth explorer and processed by Arcgis to observed the information related to the site area, as other dated back year maps were not available on search. ArcGis contains the ArcTool box, which has all the tools required for modifying, reading, determining and viewing maps. Shape files (.shp) are the files created in ArcCatalog and edited in ArcMap.

3.2. Digital processing of the satellite data

The maps of different years are edited by processing the satellite images into bands and raster form and coordinated with coordinate system setting in WGS 1984 of the project raster tool (data management) in ArcGIS so as to merge the maps altogether form point to point for better results of detection. Maps are then classified accordingly to distinguish each year map separately for analyzing the change that had occurred. Each year maps shows the clear view of the river course change of their respective years as shown below.

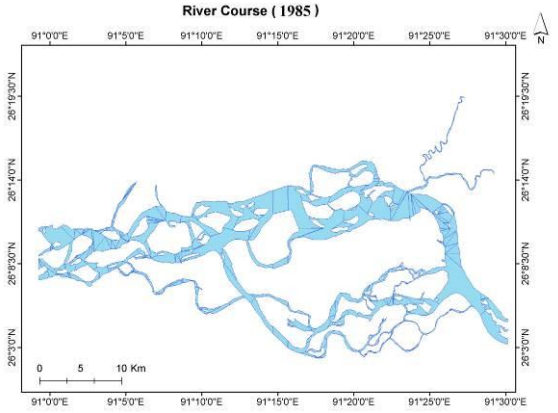

Fig. 2. River course in 1985

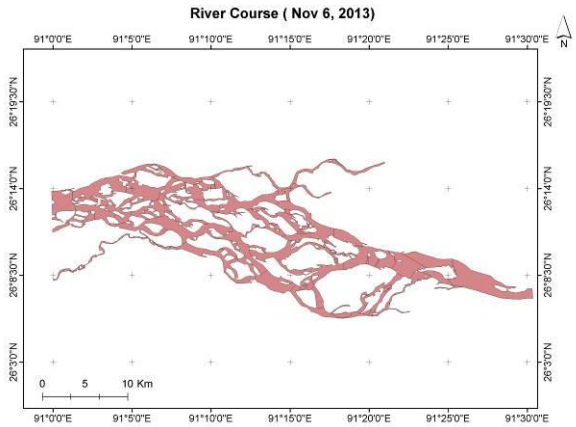

Fig. 3. River course in 6 November 2013

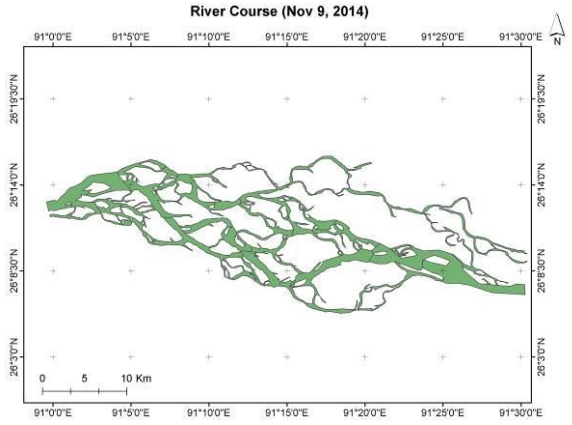

Fig. 4. River course in 9 November 2014

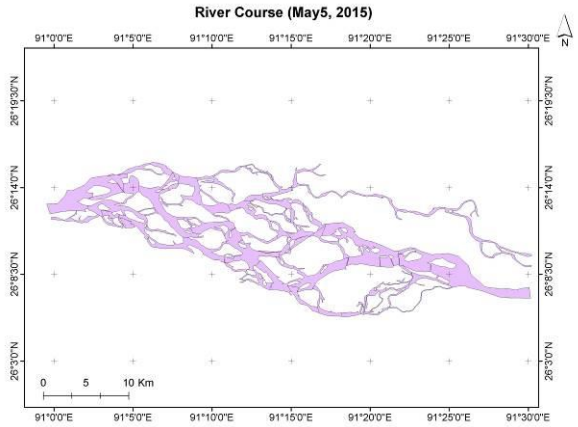

Fig. 5. River course in 5 May 2015

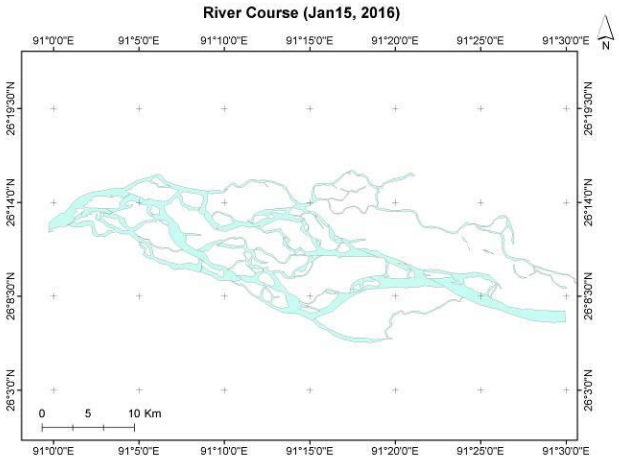

Fig. 6. River course in 15 January 2016

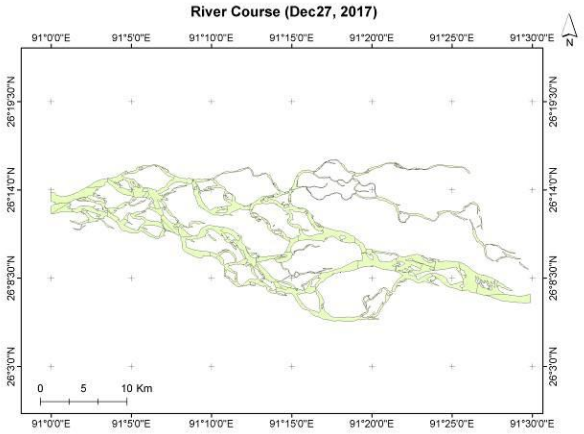

Fig. 7. River course in 27 December 2017

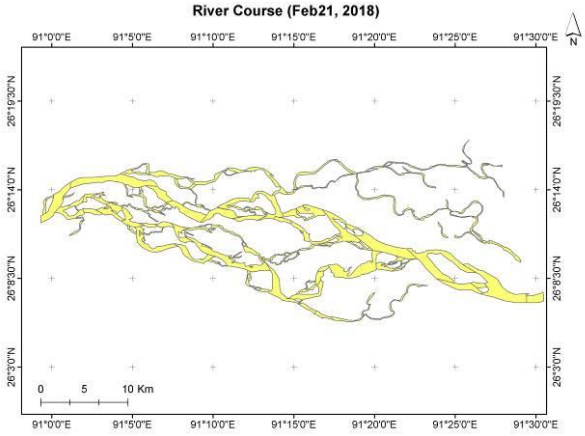

Fig. 8. River course in 21 February 2018

4. PURPOSE AND OBJECTIVE

4.1 Purpose of the Study:

Since the River Brahmaputra is one of the largest rivers in India so its course widely affects the nearby surrounding areas within it and also the habitant. So its sudden change in course during the years can cause problem like

1. Floods
2. Soil Erosion
3. Deforestation
4. Scarcity of drinking water
5. Loss of Agricultural area

But if we are able to detect the river course changes, then we could avoid or take measures against the odds. Moreover by detecting the change we can predict the course and accordingly in future we can know the areas which are safe or unsafe.

The safe areas can be used to construct buildings, bridges and also for Agricultural purposes.

4.2 Objective of the Study

1. To detect the river course change from the period 1985 to 2018.
2. To find out how much change occurred in the study area.

5. RESULTS AND DISCUSSION

5.1 Observation

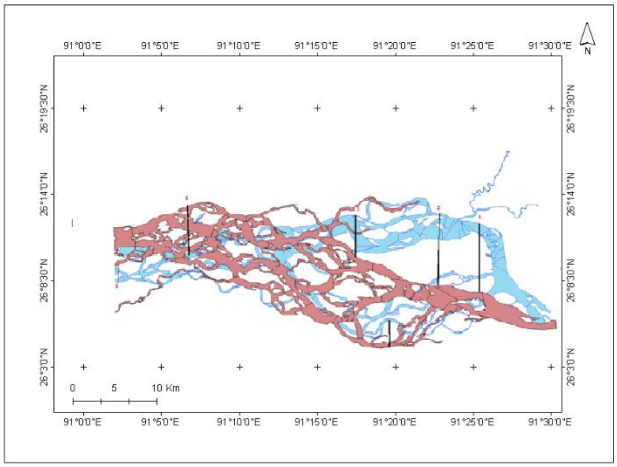

Fig.9. Comparison between 1985 and 2013 river course

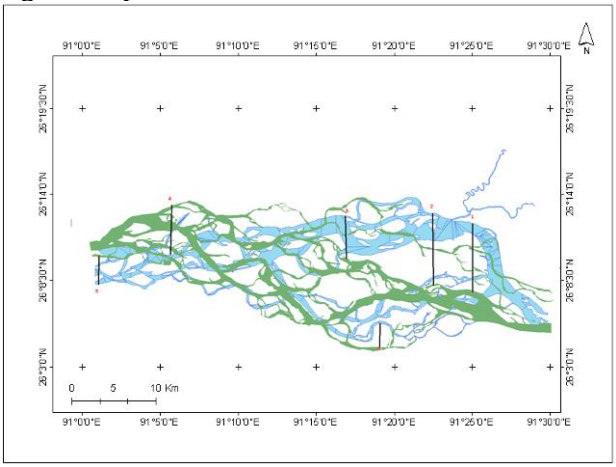

Fig. 10. Comparison between 1985 and 2014 river course

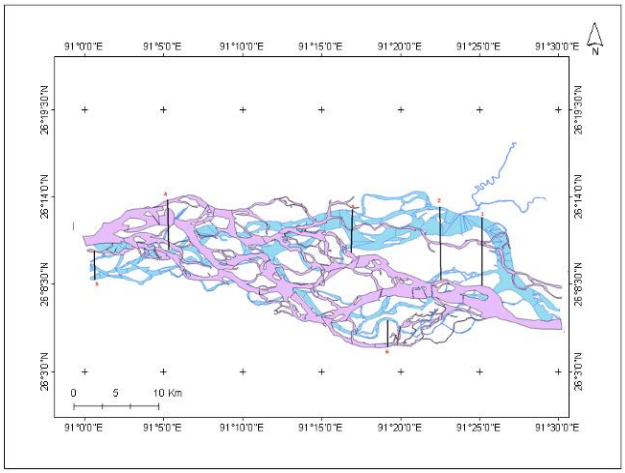

Fig. 11. Comparison between 1985 and 2015 river course

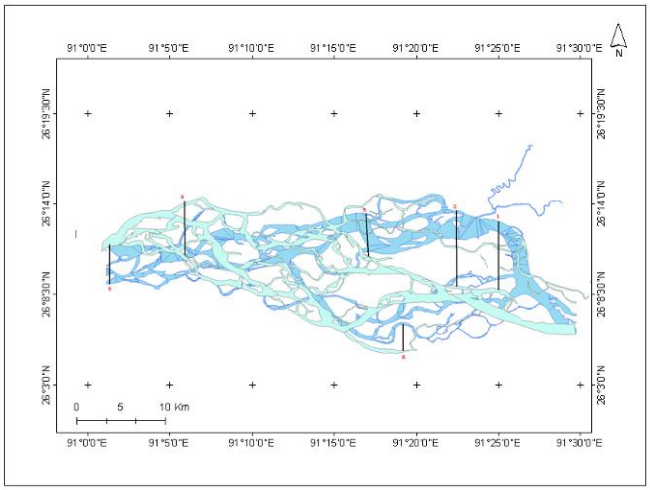

Fig. 12. Comparison between 1985 and 2016 river

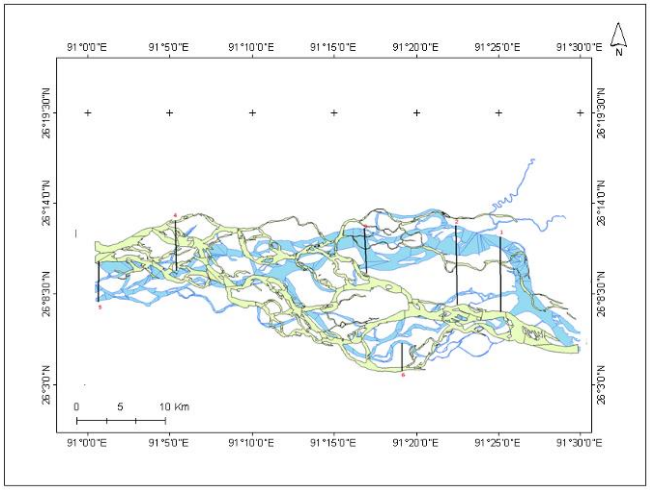

Fig. 13. Comparison between 1985 and 2017 river course

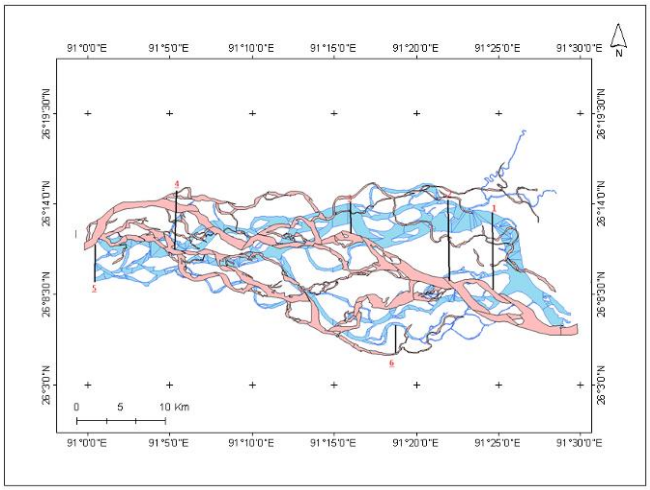

Fig. 14. Comparison between 1985 and 2018 river course

Table 1 Data Table for change detection

Year	Position 1(km)	Position 2(km)	Position 3(km)	Position 4(km)	Position 5 (km)
1985- 2013	9.526	10.190	5.584	7.330	2.881
1985- 2014	9.271	9.563	5.773	6.450	3.676
1985- 2015	9.087	9.475	5.628	6.447	3.721
1985- 2016	8.842	9.856	5.591	7.008	4.654
1985-2017	9.437	10.082	5.563	6.455	4.897
1985- 2018	8.497	9.579	3.757	6.475	4.687

According to the above data table and figures, we came to determine that the river bank which we took as a position for checking the evolution of the course shifted drastically over age. Also all the positions taken for the detection of change are at the exact same location for each and every comparison map.

5.2.1 For 1985 and 2013

• It can be seen that in position 1, the river course had changed and shifted downwards approximately about 9.536 Km.
• At position 2, the river course had changed and shifted downwards approximately about 10.190 Km.
• At position 3, the river course had changed and shifted downwards approximately about 5.584 Km.
• At position 4, the river course had changed and shifted upwards approximately about 7.330 Km.
• At position 5, the river course had changed and shifted upwards approximately about 2.881 Km.
• At position 6, the river course had changed and shifted downwards approximately about 3.401 Km.

5.2.2 For 1985 and 2014

• It can be seen that in position 1, the river course had changed and shifted downwards approximately about 9.271 Km.
• At position 2, the river course had changed and shifted downwards approximately about 9.563 Km.
• At position 3, the river course had changed and shifted downwards approximately about 5.773 Km.
• At position 4, the river course had changed and shifted upwards approximately about 6.450 Km.
• At position 5, the river course had changed and shifted upwards approximately about 3.676 Km.
• At position 6, the river course had changed and shifted downwards approximately about 3.127 Km.

5.2.3 For 1985 and 2015

• It can be seen that in position 1, the river course had changed and shifted downwards approximately about 9.087 Km.
• At position 2, the river course had changed and shifted downwards approximately about 9.475 Km.
• At position 3, the river course had changed and shifted downwards approximately about 5.628 Km.
• At position 4, the river course had changed and shifted upwards approximately about 6.447 Km.
• At position 5, the river course had changed and shifted upwards approximately about 3.721 Km.
• At position 6, the river course had changed and shifted downwards approximately about 3.501 Km.

5.3.4 For 1985 and 2016

• It can be seen that in position 1, the river course had changed and shifted downwards approximately about 8.842 Km.
• At position 2, the river course had changed and shifted downwards approximately about 9.856 Km.
• At position 3, the river course had changed and shifted downwards approximately about 5.591 Km.
• At position 4, the river course had changed and shifted upwards approximately about 7.008 Km.
• At position 5, the river course had changed and shifted upwards approximately about 4.654 Km.
• At position 6, the river course had changed and shifted downwards approximately about 3.249 Km.

5.3.5 For 1985 and 2017

• It can be seen that in position 1, the river course had changed and shifted downwards approximately about 9.437 Km.
• At position 2, the river course had changed and shifted downwards approximately about 10.082 Km.
• At position 3, the river course had changed and shifted downwards approximately about 5.563 Km.
• At position 4, the river course had changed and shifted upwards approximately about 6.455 Km.
• At position 5, the river course had changed and shifted upwards approximately about 4.897 Km.
• At position 6, the river course had changed and shifted downwards approximately about 3.665 Km.

5.3.6 For 1985 and 2018

• It can be seen that in position 1, the river course had changed and shifted downwards approximately about 8.497 Km.
• At position 2, the river course had changed and shifted downwards approximately about 9.579 Km.
• At position 3, the river course had changed and shifted downwards approximately about 3.757 Km.
• At position 4, the river course had changed and shifted upwards approximately about 6.475 Km.
• At position 5, the river course had changed and shifted upwards approximately about 4.687 Km.
• At position 6, the river course had changed and shifted downwards approximately about 3.504 Km.

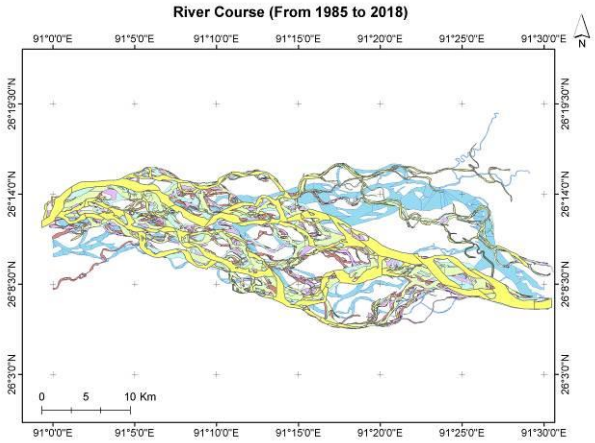

Fig. 15. Comparison of all different year of maps

6. CONCLUSION

Based on the work using remote sensing and GIS based approach with different year's satellite data (1985, 2013, 2014, 2015, 2016, 2017, and 2018) it has revealed sharp changes in river course in recent years resulting in considerable shift of river flow. The Brahmaputra River within the study reaches exhibits differential rate of erosion and deposition during the years (1985, 2013, 2014, 2015, 2016, 2017, and 2018). It is observed that in general the river has eroded both the banks throughout its course except at a few sites. The reaches have been prioritized with respect to the land area lost in different years. This study has proved the utility and application of satellite remote sensing which allows us to determine, analyze viewing of large area and so provides the opportunity for a better and detailed assessment of changes in river course during the years. This study has further shown how the use of GIS has been useful in organizing geo-spatial databases and viewing of channel position mapping and measurement.

REFERENCES

1. Amna Butt, Rabia Shabbir, Sheikh Saeed Ahmad and Neelam Aziz(2015)." Land use change mapping and analysis using Remote Sensing and GIS"- https://doi.org/10.1016/j.ejrs.2015.07.003
2. G.Jeba Sweetline and Sangeetha. "Identification of Manimuthar River Course Changes And Estimation Of Command Area In Ambasamudram Taluk Using Remote Sensing And GIS". *IOSR journal of Mechanical and Civil Engineering (IOSR-JMCE)* e-ISSN:2278-1684, p-ISSN: 2320-334X PP 104-115-www.iosrjournal.org
3. M. R. H. Kauser, H.S. Alam and M.K Islam(2015) ."Bank Shifting and Land use Change of Jamuna River Due to Construction of Multipurpose Bangabandhu Bridge Using Remote Sensing and GIS"-*International Conference on Recent Innovation in Civil Engineering for Sustainable Development (IICSD-2015)-* www.duet.ac.
4. Sainath P. Aher, Shashikant I. Bairagi, Pragati P. Deshmukh,And Ravindra D. Gaikwad(2012)."River Change Detection And Bank Erosion Identification Using Topographical And Remote Sensing Data". *International journal of applied information system (IJAIS) foundation of computer science* FCS, New York, USA Volume 2-NO.3,My 2012- www.ijis. org
5. Satya Prakash Maurya and Akhilesh Kumar yadav (2016)." Evaluation of river Course change detection of Ramganga River using remote sensing and GIS" https://doi.org/10.1016/j.wace.2016.08.001
6. Tingneyuc Sekac and Sujoy Kumar jana(2014)."Change Detection Of Busu River Course In Papua New Guinea-Impact On Local Settlements Using Remote Sensing And GIS Technology"- *International Journal of Scientific and Engineering Research,* Volume 5, Issue 8, August-2014 ISSN2229-5518- www.ijser.org

Victor Klemas(2015)."Remote Sensing of Floods and Flood-Prone Areas" *School of Marine Science and Policy, University of Delaware,* Newark, DE 19716, U.S.A. klemas@udel.edu

Sustainable Ecosystem Management

Sustainable environmental impact management

Analysis of soil hydraulic properties in unsaturated soil

Bora, B.[1], Borah, T.[2]

[1]PG student, Department of Civil Engineering, Assam Engineering College, Guwahati-781039, India.
[2]Associate Professor, Department of Civil Engineering, Assam Engineering College, Guwahati-781039, India.

ABSTRACT

The knowledge of soil hydraulic properties (the soil water retention and hydraulic conductivity) is indispensable for predicting or managing the migration of water and dissolved constituents in unsaturated soil, but the hydraulic properties are difficult to determine experimentally. As an alternative to direct measurement of hydraulic conductivity, statistical pore-size distribution models have been developed to indirectly estimate the hydraulic conductivity from the more easily measured soil water retention curve. In this study soil hydraulic properties of different areas of Guwahati city is determined using RETC program. van Genuchten retention model and Burdine m=1-2/n conductivity is used to determine soil water retention and hydraulic conductivity respectively. From the study it is found that soil water retention curve is different for different areas due to the different shape parameters. Soil having higher fine particles have higher water retention property. But hydraulic conductivity is highest for coarse grained soils.

Keywords: RETC, unsaturated soil, soil water retention, hydraulic conductivity

1. INTRODUCTION

Interest in the unsaturated (vadose) zone has dramatically increased in recent years because of growing evidence and public concern that the quality of the subsurface environment is being adversely affected by industrial, municipal and agricultural activities. Computer models are now routinely used in research and management to predict the movement of water and chemicals into and through the unsaturated zone of soils. Such models can be used successfully only if reliable estimates of the flow and transport properties of the medium are available. Current technology of developing sophisticated numerical models for water and solute movement in the subsurface seems to be well ahead of our ability to accurately estimate the increasing number of parameters which appear in those models. This is especially true for the unsaturated soil hydraulic properties which by far are the most important parameters affecting the rate at which water and dissolved chemicals move through the vadose zone. While a large number of laboratory and field methods have been developed over the years to measure the soil hydraulic functions, most methods are relatively costly and difficult to implement. Accurate in situ measurement of the unsaturated hydraulic conductivity has remained especially cumbersome and time-consuming. Thus, cheaper and more expedient methods for estimating the hydraulic properties are needed if we are to implement improved practices for managing water and chemicals in the unsaturated zone.

2. STUDY AREA

Guwahati is the premier city of North-East India. It may be called as the hub of political administration, education, commerce and many other activities of not only the state of Assam but also the entire north eastern region of India. Geographically the present Guwahati area or the Greater Guwahati area lies in both the sides of the mighty Brahmaputra. The area extends latitudinally from $26^0 5^/$ N to $26^0 12^/$ N and longitudinally from $91^0 24^/$ E to $91^0\ 51^/$ E. It covers a geographical area of 358 km^2. Being a part of North –East India and moreso of the Brahmaputra valley falls under the influence of the region's monsoonal climates. While the physiographic controls and orographic structures of the region have their macro effects on the climate of the area, local topographic factors have also impact on the micro variation in the climate of the area.
Hengrabari is located in the capital city of Guwahati of Assam, a state on the north-east of India. It is located in Latitude $26^0 09^/ 06.2^{//}$ North and Longitude $91^0 47^/ 33.2^{//}$ East. Hatigaon is a locality in the southern part of Guwahati, Assam, India. It is surrounded by the localities of Ganeshguri, Bhetapara, Sijubari, and Survey. It is located in Latitude $26^0 08^/ 18.6^{//}$ North and Longitude $91^0 46^/ 40.6^{//}$ East. Percentage of sand, silt and clay for this area is 2%, 48% and 50% respectively and textural class of soil is silty clay.Panjabari area of Guwahati. Panjabari is located south east of Guwahati, it is sparsely populated area of the city.

3. METHODOLOGY

3.1 RETC

RETC (Retention Curve) computer program is used to describe the hydraulic properties of unsaturated soils. The program may be used to fit several analytical models to observed water retention and/or unsaturated hydraulic conductivity data. As before, soil water retention data are described with the equations of Brooks and Corey [1964] and van Genuchten [1980], whereas the pore-size distribution models of Burdine [1953] and Mualem [1976a] are used to predict the unsaturated hydraulic conductivity function. New features in RETC include (1) a direct evaluation of the hydraulic functions when the model parameters are known, (2) a more flexible choice of hydraulic parameters to be included in the parameter optimization process, and (3) the possibility of evaluating the model parameters from observed conductivity data rather than only from retention data, or simultaneously from measured retention and hydraulic conductivity data.

The RETC code provides several options for describing or predicting the hydraulic properties of unsaturated soils. These properties involve the soil water retention curve, $\Theta(h)$, the hydraulic conductivity function, K(h),and the soil water diffusivity function, $D(\Theta)$. The soil water retention function contains 5 independent parameters, i.e., the residual water content Θ_r, the saturated water content Θ_s, and the shape factors α, n and m. The predictive equations for K and D add two additional unknowns: the pore connectivity parameter l, and the saturated hydraulic conductivity, K_s. Hence, the unsaturated soil hydraulic functions contain up to 7 potentially unknown parameters. The restrictions n-∞ (i.e., the BC restriction), m = l-l/n and m = 1-2/n will reduce the maximum number of independent parameters from 7 to 6. The RETC code may be used to fit any one, several, or all of the 6 or 7 unknown parameters simultaneously to observed data.

3.2 Parametric Models for the Soil Hydraulic function

Water flow in unsaturated or partly saturated soils is traditionally described with the Richards Equation (1) [Richards, 1931] as follows

$$C.\partial h/\partial t = \partial/\partial z\,(K.\partial h/\partial z - K) \qquad (1)$$

Where h is the soil water pressure head (with dimension L), t is time (T), z is soil depth (L), K is the hydraulic conductivity (LT^{-1}), C is the soil water capacity (L^{-1}) approximated by the slope ($\partial\Theta/\partial h$) of the soil water retention curve, $\Theta(h)$, in which Θ is the volumetric water content(L^3 L). Equation (2) may also be expressed in terms of the water content if the soil profile is homogeneous and unsaturated ($h \leq 0$).

$$\partial\Theta/\partial t = \partial/\partial z\,(D.\partial\Theta/\partial Z - K) \qquad (2)$$

Where D is the soil water diffusivity (L^2T^{-1}), defined as

$$D = K.dh/d\Theta \qquad (3)$$

The unsaturated soil hydraulic functions in the above equations are the soil water retention curve $\Theta(h)$, the hydraulic conductivity function K(h) or $K(\Theta)$, and the soil water diffusivity function $D(\Theta)$. Parametric models of these functions are reviewed in detail below.

Soil water retention model

Several functions have been proposed to empirically describe the soil water retention curve. One of the most popular functions has been the equation of Brook and Corey [1964], further referred to as the BC-equation:

$$\Theta = \Theta_r + (\Theta_s - \Theta r)\,(\alpha h)^{-\lambda} \qquad (\alpha h > 1)$$
$$= \Theta_s \qquad (\alpha h \leq 1) \qquad (4)$$

Where Θr and Θ_s are the residual and saturated water contents, respectively; α is an empirical parameter (L^{-1}) whose inverse is often referred to as the air entry value or bubbling pressure, and λ is a pore-size distribution parameter affecting the slope of the retention function. For notational convenience, h and a for the remainder of this report are taken positive for unsaturated soils (i.e., h denotes suction).

Following van Genuchten and Nielsen [1985] and Luckner et al. [1989], Θ_r and Θ_s in this study are viewed as being essentially empirical constants in soil water retention functions of the type given by (4), and hence without much physical meaning.

Equation (4) may be written in a dimensionless form as follows

$$S_e = \{\,(\alpha h)^{-\lambda} \qquad (\alpha h > 1)$$
$$= \{\,1 \qquad (\alpha h \leq 1) \qquad (5)$$

where S_e is the effective degree of saturation, also called the reduced water content ($0 < S_e < 1$).

Because of their simple form Equ (4) and (5) have been used in numerous unsaturated flow studies.

A related smooth function with attractive properties is the equation of van Genuchten [1980], further referred to as the VG-equation in Equ (6) as follows

$$Se = l/\,[l + (\alpha h)^n]^m \qquad (6)$$

Where α, n and m are empirical constants affecting the shape of the retention curve.

3.3 Burdine's hydraulic conductivity model

$$K(S_e) = K_s S_e^{l}\ .\ g(S_e)/\,g(1)$$

3.4 Hydrometer Test

Texture in the present experiment is determined by the hydrometer method. The standard hydrometer with Bouyoucos scale in g/L is used in an aquous suspension of the pre measured pre treated soil.

The dominant size fraction is used to describe the texture. If no fraction is dominant, the soil is described as loam. A triangular diagram (fig 3.1) is commonly used to set the limits for each texture class.

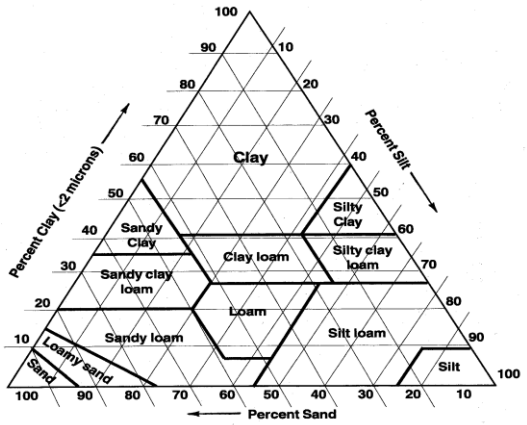

Figure 3.1 Triangular Diagram for Textural Class

4. RESULTS AND DISCUSSIONS

4.1 Results from Hydrometer Test

Hydrometer test is done for grain size analysis of fine grained soils. In this study sand, silt and clay percent for different area of Guwahati. From the hydrometer test the textural class for Hengrabari, Hatigaon and Panjabari are silty clay loam, silty clay and clay respectively.

4.2 Soil water retention curve from RETC

Figure 4.1,4.2 and 4.3shows the water content vs. pressure head curve for silty clay loam, silty clay, sandy clay and clay for Hengrabari, Hatigaon, and Panjabari respectively. For Silty clay loam, silty clay and clay saturated water content (Θ_s) is 0.45, 0.49 and 0.48 at a Pressure head of 0.05m. Air entry values for silty clay loam, silty clay and clay are found as 1 m, 1m, 0.5m, 0.5m respectively. The residual water content (Θ_r) values are found for silty clay loam, silty clay and clay are as 0.378, 0.42, 0. 3862 respectively at a pressure head of 100 m. With the increase in finer particles the saturated water content and residual water content increases. This finding from the study resembles the results from the literature (Fredlund 2000; Aubertin et al. 2003). That justify the result obtained from RETC programme. Li et al. (2009) have observed that soil type affects air entry value (AEV) and slope of SWCC. As the clay content increases, the slope of the curve becomes gentle. Thus justify our results from RETC.

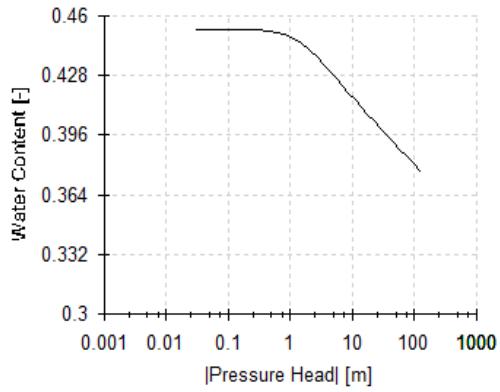

Figure 4.1 water content vs pressure head for Hengrabari area

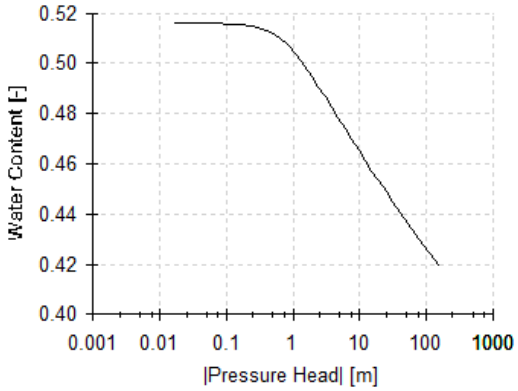

Figure 4.2 water content vs pressure head for Hatigaon area

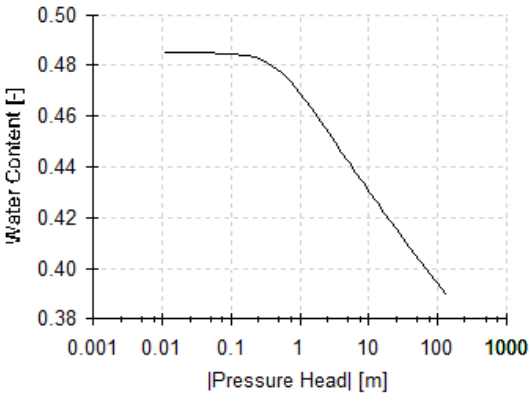

Figure 4.3 water content vs. pressure head for Panjabari area

4.3 Prediction of Hydraulic Conductivity

Figure 4.4,4.5 and 4.6 shows the hydraulic conductivity versus pressure head curve for silty clay loam, silty clay and clay for Hengrabari, Hatigaon and Panjabari respectively.

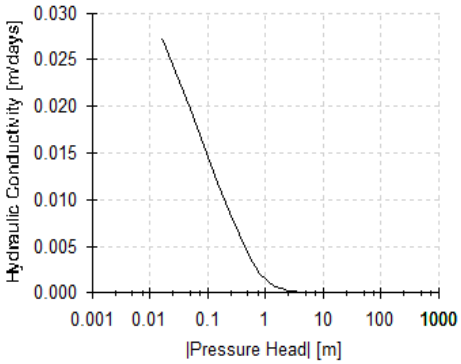

Figure 4.4 Hydraulic conductivity vs. Pressure head for Hengrabari area

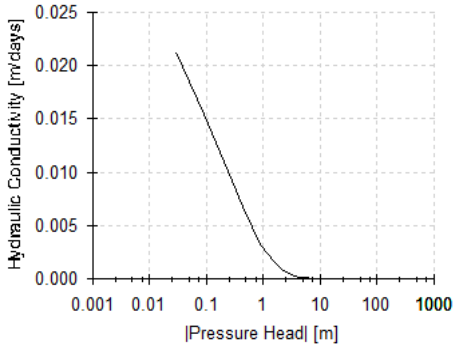

Figure 4.5 Hydraulic conductivity vs. Pressure head for Hatigaon area

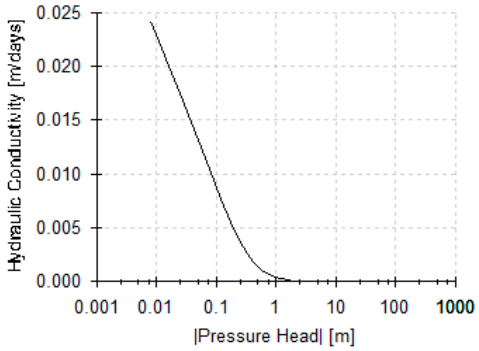

Figure 4.6 Hydraulic conductivity vs. Pressure head for Panjabari area.

From the figure 4.4, 4.5 and 4.6 it is shown that hydraulic conductivity for Silty clay loam hydraulic conductivity is saturated just after the pressure head of 0.01m. Saturated hydraulic conductivity at that point is 0.0265 m/days. Hydraulic conductivity ceases at a pressure head of 5m.For silty clay soil is 0.021 m/days at a pressure head of 0.05 m. with increase in pressure head hydraulic conductivity decreases linearly. Beyond 0.01 m of pressure head a non linear variation of hydraulic conductivity is observed and finally hydraulic conductivity ceases at a pressure head of 9m. For sandy clay hydraulic conductivity is 0.030m/days at a pressure head of 0.01 m, hydraulic conductivity decreases linearly up to 0.010 m/days at a pressure head of 0.12 m. beyond this point hydraulic conductivity ceases at pressure head of 5m.For clay saturated hydraulic conductivity is 0.0249 m/days at a pressure head of 0.01m. Hydraulic conductivity decreases linearly up to 0.005 m/days at suction head of 0.5 m of pressure head. Finally hydraulic conductivity ceases at a pressure head of 2 m. From the figure it is seen that saturated hydraulic conductivity is highest for coarse grained soil compared to fine grained soil which resembles the literature Sarki et al.Thus justify our result.

5. CONCLUSIONS

Soil hydraulic properties constitute the basis for understanding flow and transport processes and are of important input properties in any simulations of vadose zone properties. In this focus methods are presented that allow prediction and characterization of soil hydraulic properties, with an emphasis on the moisture retention characteristics, unsaturated hydraulic conductivity and diffusivity.

This report describes the hydraulic properties of unsaturated soils using RETC computer program. The soil water retention curve ϴ (h), in the program can be represented by the equations of van Genuchten, while the unsaturated hydraulic conductivity K (h) or K (ϴ), and diffusivity D (ϴ), functions are formulated in terms of the statistical pore-size distribution models of Burdines. From the study it is found soil retention property is highest for soils having high percentage of fine particles .VG-Burdine model it holds water upto 0.01m of pressure head.

REFERENCES

1)Burdine, N.T.1953. Relative permeability calculations from pore-size distribution data. Petrol. Trans; Am. Inst Min Eng. 198:71-77

2)Fredlund, D. G. (2000). " The 1999 R.M. Hardy lecture: the implementation of unsaturated soil mechanics into geotechnical engineering", Canadian Geotechnical Journal, Vol. 37,pp. 963-986.

3)Aubertin, M; Mbonimpa, M; Bussiere, B. and,Chapius, R.P. (2003). " A model to predict the water retention curve from basic geotechnical properties", Canadian Geotechnical Journal, Vol. 40, No. 6, pp. 1104-1122.

4)Li, J; Yang, Q; Li, P; and Yang, Q. (2009). " Experimental research on soil-water characteristic curve of remolded residual soils", Electronic Journal of Geotechnical Engineering, Page count: 12.

Sustainable Ecosystem Management

Sustainable environmental impact management

Modeling extreme PM_{10} concentration using Generalized Pareto Distribution: an extreme value approach

Hazarika S. [1], Borah P. [1] and Prakash A. [2]

[1] Ph.D Student, Department of Environmental Science, Tezpur University, Tezpur, Assam, India.
[2] Assistant Professor, Department of Environmental Science, Tezpur University, Tezpur, Assam, India.

ABSTRACT

The extreme concentration of particulate matter (PM) in the atmosphere constitutes a major concern due to its harmful effects on human health and the surrounding environment. In recent decades, high level of PM_{10} concentration has been recorded mostly in urban areas. A statistical model based on extreme value theory (EVT) has been used to predict the probability of extreme PM_{10} pollution episodes. EVT allows estimation of the probability of occurring extreme values greater than the values, observed during a period of record. Modeling extreme pollution events is helpful for the decision makers to plan effective abatement measures on time, preventing air pollution episodes while avoiding useless restrictions of economic activities. In the present work, the Generalized Pareto Distribution (GPD) has been fitted to high PM_{10} levels over a threshold limit, for six locations in the Guwahati city namely Bamunimaidam, Khanapara, Boragaon, Gopinath Nagara, Pragjyotish College and Guwahati University. The threshold limit has been chosen according to the National Ambient Air Quality Standards (NAAQS) as prescribed by the Central Pollution Control Board (CPCB), India. The possible intensity of the extreme pollution level is predicted by estimating the return level for 2, 3, 4, and 5 day return period. The estimated value of shape parameter indicates that the extreme PM_{10} concentrations follow Beta distribution for all locations in Guwahati except Bamunimaidam where, it follows distribution of GPD family.

Keywords: PM_{10}, GPD, return level.

. INTRODUCTION

Respirable particulate matter (RSPM) concentration in the atmosphere of South and East Asia exhibit a progressive trend in recent decades. The increasing concentration of anthropogenic RSPM in the megacities of this region are often associated with rapid environmental changes (Soni et.al., 2014). RSPM (PM_{10}) is a serious air pollutant as it can induce health impacts like cardiovascular, respiratory problems and premature mortality etc. (Guo et.al., 2014; Qin et. al., 2014). Guwahati one of the major city of North-East (NE) India, with a high rate of urbanization, has witnessed increasing particle load in its ambient atmosphere (Tiwari et.al., 2017). Modeling extreme PM_{10} concentration is an integral task to take control measures in time and it will help to improve the sustainability of megacity life (Gurjar et.al., 2010). The limiting distribution models provide efficient mechanism for modeling extremes, inferences and make prediction. The present study aims to predict the extreme PM_{10} level recurrence probability at 6 different locations namely Head office, Bamunimadam (HO), Khanapara (KH), Boragaon (BR), Gopinath Nagara (GN), Pragjyotish College (PC) and Guwahati University (GU) in Guwahati city. To model extreme PM_{10} concentration events in the above mentioned locations, extreme value theory (EVT) has been applied and their probable return levels are computed, that has potential to better urban management.

2 METHODOLOGY

2.1 Site and Data description

Guwahati city is the gateway of NE India with a fast growing urban sprawl. It is located at latitude of $26^0$10’45” North and the longitude of $91^0$45’0” East.in Kamrup Metropoitan District.

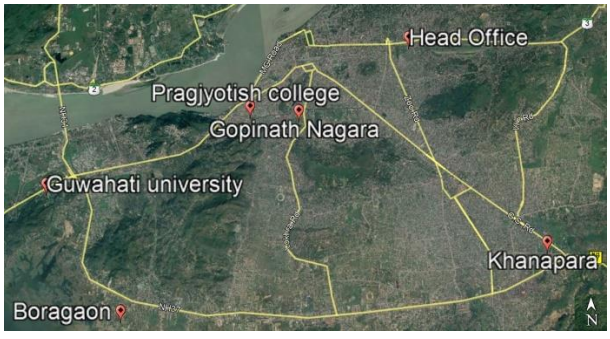

Fig. 1. Map of Guwahati city. Study locations are pin pointed. [Source: Google Earth]

The daily data for PM_{10} concentrations were obtained from State Pollution Control Board Assam for mentioned locations.

2.2 Modeling Extreme Events

Extreme value analysis (EVA) is statistical tool

based on extreme value theory (EVT). EVA allows estimation of the probability of occurring extreme values greater than the values observed during a period of record (Coles, 2001). Extreme value analysis can be done through three processes, namely Generalized extreme value distribution (GEV), Generalized Pareto distribution (GPD), Poisson Point process. In the present study GPD model has been fitted to predict the return of extreme PM_{10} concentration.

2.2.1 Sampling extreme PM_{10} level

There are two standard approaches to describe extreme events, block maxima approach and point over threshold approach. First one deals with maximum value of a specific block size for example daily maxima, weekly maxima etc. Whereas, the second approach gives the maximum values over a threshold limit (Chavez-Demoulin et.al., 2016). Extreme value theory assumes that the distribution of the extreme events from second approach will follow a Generalized Pareto Distribution (GPD) (Coles, 2001; Young et al., 2012). According to National Ambient Air Quality Standard (NAAQS) prescribed by Central Pollution Control Board of India (CPCB), the daily PM_{10} concentration greater than 100 $\mu g/m^3$ affect the environment and human health as well. Therefore, in the present work, the selected threshold level is 100 $\mu g/m^3$.

2.2.2 Generalized Pareto Distribution

If daily ambient PM_{10} concentrations for n number of days, denoted as $x_1,x_2,...,x_n$, is independently and identically distributed and with common cumulative distribution function (cdf), then concentrations exceeding the threshold limit (u), i.e. $y_i=x_i-u$, follows a generalized Pareto distribution (GPD) (Mondal and Mujumdar, 2015). The generalized Pareto distribution (GPD) is a family of continuous probability distributions and often used to model the tails of another distribution. It is specified by two parameters: scale σ, and shape ξ. The standard cumulative distribution function (cdf) of the GPD is defined by:

$$H_x = 1 - \left[1 + \xi\left(\frac{y}{\sigma_u}\right)^{\frac{-1}{\xi}}\right], y > 0, 1 + \xi\frac{y}{\sigma_u} > 0 \qquad (1)$$

Where, u is a high threshold, x > u, scale parameter $\sigma_u > 0$ (depending on the threshold u), and shape parameter $-\infty < \xi < \infty$. ξ determines three types of distributions: heavy tail when $\xi > 0$ (Pareto), upper bound when $\xi < 0$ (Beta) and exponential in the limit as $\xi \to 0$. The GPD is an approximation of the upper tail of a parent distribution function. The return level (x_m) with the selected threshold level (u) is

$$x_m = \begin{Bmatrix} u + \frac{\sigma_u}{\xi}\left[(m\zeta_u)^{\xi} - 1\right], \xi \neq 0 \\ u + \sigma_u ln(m\zeta_u), \xi = 0 \end{Bmatrix} \qquad (2)$$

Where, $\zeta_u = Pr(x>u)$, x_m is exceeded on average once every m observation.

3. RESULTS AND DISCUSSION

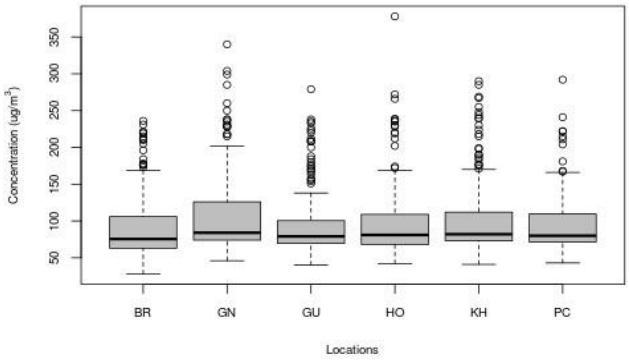

Fig. 2. Box and whisker plot for ambient PM_{10} concentrations at different study locations of Guwahati

The median, first quartile, third quartile, minimum and maximum values of PM_{10} concentration at each location is presented by the box and whisker plot (Fig. 2). PM_{10} data for each location contains outlier values more above maximum value. The median of the data is farther from third quartile for each study location, indicating the parent distributions of the data are positively skewed. Presence of outliers and positive skewness indicates that parent distributions PM_{10} concentration have heavier right tail (Hubert and Vandervieren, 2008).

Table 1: GPD distribution parameters for each study location

Locations	Scale	Shape
Head office	44.78	0.11
Khanapara	74.38	-0.25
Boragaon	80.83	-0.55
Gopinath Nagara	73.34	-0.19
Pragjyotish College	40.68	-0.04
GU	69.13	-0.29

Distribution parameters are obtained through maximum likelihood method. Extreme PM_{10} concentrations in Khanapara, Boragaon, Gopinath Nagara, Pragjyotish College and GU follows beta distribution as ξ is negative (Table 1). But in Head Office, high levels of PM_{10} follows a heavy tailed Pareto distribution.

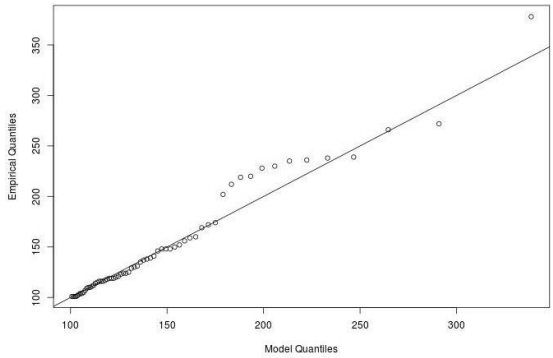

Fig. 3. QQ plot for extreme ambient PM_{10} level in Head Office, Bamunimadam

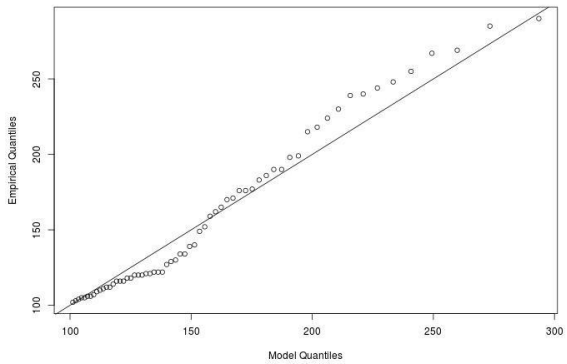

Fig. 4. QQ plot for extreme ambient PM_{10} level in Khanapara

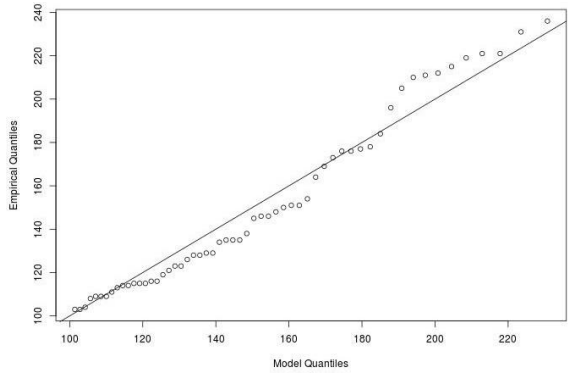

Fig. 5. QQ plot for extreme ambient PM_{10} level in Boragaon

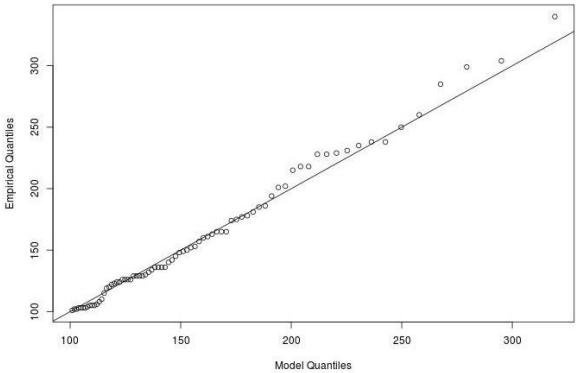

Fig. 6. QQ plot for extreme ambient PM_{10} level in Gopinath Nagara

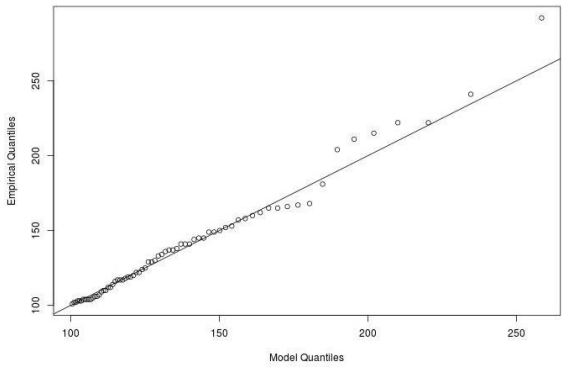

Fig. 7. QQ plot for extreme ambient PM_{10} level in Pragjyotish college

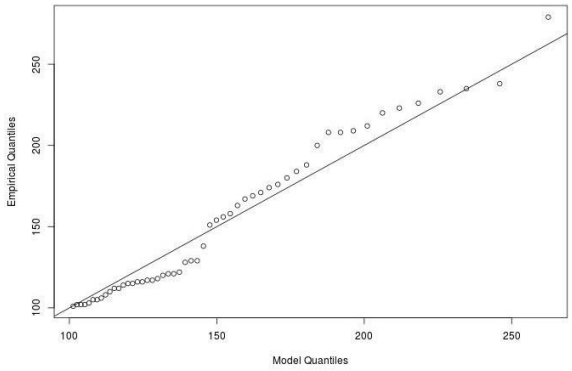

Fig. 8. QQ plot for extreme ambient PM_{10} level in Guwahati University

The model performance is evaluated by model diagnostic plots. Quantile-Quantile (QQ) plot of model quantile and empirical quantile has been generated, where, a good fit should yield a straight line (Gyarmati-Szabo et.al., 2016). Inspection of QQ plots for each site indicates that the model performance is better for Head Office, Gopinath Nagara and Pragjyotish college (Fig. 3-8). For other locations the quantiles are deviated from the straight line. It may be because of large outliers present in the data. The fitted models are further extended to predict the probability and return levels of extreme PM_{10} concentrations.

Table 2: Probability of crossing standard and return levels of extreme PM_{10} concentration for different return periods

Location	Probability	2 day	3 day	4 day	5 day
HO	0.978	309.20	337.55	358.48	375.18
KH	0.987	281.68	293.10	300.55	305.97
BR	0.988	226.67	230.61	232.91	234.46
GN	0.968	305.02	318.83	328.02	334.82
PC	0.976	244.09	257.95	267.64	275.07
GU	0.968	252.75	262.02	267.96	272.24

The probability of crossing the standard level i.e. 100 $\mu g/m^3$ at each location is very high for each location. Return levels estimated for Head office is

showing

maximum values for each respective return periods compared to other site. The boxplot (Fig. 2) indicates that highest maximum PM_{10} level also has been recorded for Head office. The return level for respective return periods at each site is above the permissible limit prescribed by CPCB (Table 2).

.

4. CONCLUSION

to model the extreme conditions. Analyzing extreme air pollution episodes in different weather conditions is the future scope of the study and it will help the urban planners to enforce suitable abatement programme on time.

ACKNOWLEDGMENTS

We acknowledge the Department of Environmental Science, Tezpur University for supporting us throughout the study.

REFERENCES

1) AQI Bulletin, November 2017, Central Pollution Control Board, India. http://cpcb.nic.in/cpcbold/aqiv.php.
2) Chakraborty, A., Bhattu, D., Gupta, T., Tripathi, S.N. and Canagaratna, M.R., 2015. Real-time measurements of ambient aerosols in a polluted Indian city: Sources, characteristics, and processing of organic aerosols during foggy and nonfoggy periods. Journal of Geophysical Research: Atmospheres, 9006-9019. (doi: https://doi.org/10.1002/2015JD023419).
3) Chavez-Demoulin, V., Embrechts, P. and Hofert, M., 2016. An Extreme Value Approach for Modeling Operational Risk Losses Depending on Covariates. The Journal of Risk and Insurance, 83(3): 735-776.
4) Coles S., 2001. An introduction to statistical modeling of extreme values, Springer, Bristol, UK.
5) Guo, Y., Li, S., Tawatsupa, B., Punnasiri, K., Jaakkola, J.J.K. and Williams, G., 2014. The association between air pollution and mortality in Thailand. Scientific Reports, 4: 5509.
6) Gurjar, B.R., Jain,A., Sharma, A., Agarwal, A., Gupta, P., Nagpure, A.S. and Lelieveld, J., 2010. Human health risks in megacities due to air pollution. Atmospheric Environment, 44: 4606-4613.
7) Gyarmati-Szabó, J., Bogachev, L.V., and Chen, H., 2016. Non-stationary POT modelling of air pollution concentrations: Statistical analysis of traffic and meteorological impact. Environmetrics 28(430). (doi 10.1002/env.2449).
8) Hubert, M. and Vandervieren, E., 2008. An Adjusted Boxplot for Skewed Distributions. Computational Statistics and Data Analysis 52(12), 5186-5201.
9) Mondal, A. and Mujumdar P.P., 2015. Modeling non-stationarity in intensity, duration and frequency of extreme rainfall over India. Journal of Hydrology, 521: 217–231.
10) Pant, P., Shukla, A., Kohl, S.D., Chow, J.C., Watson, J.G. and Harrison, R.M., 2015. Characterization of Ambient PM2.5 at a Pollution Hotspot in New Delhi, India and Inference of Sources. Atmospheric Environment, 109: 178-189.
11) Qin, S., Liu, F., Wang, J. and Sun, B., 2014. Analysis and forecasting of the particulate matter (PM) concentration levels over four major cities of China using hybrid models. Atmospheric Environment, 98: 665-675.
12) Soni, K., Kapoor, S., Parmar, K.S., Kaskaoutis, D.G., 2014. Statistical analysis of aerosols over the Gangetic–Himalayan region using ARIMA model based on long-term MODIS observations. Atmospheric Research, 149: 174–192.
13) Tiwari, S., Dumka, U.C., Gautam, A.S., Kaskaoutis, D.G., Srivastava, A.K., Bisht, D.S., Chakrabarty, R.K., Sumlin, B.J., Solmon, F. 2017. Assessment of $PM_{2.5}$ and PM_{10} over Guwahati in Brahmaputra River Valley: Temporal evolution, source apportionment and meteorological dependence. Atmospheric Pollution Research 8(1): 13-28.
14) Young, I. R., Vinoth, J., Zieger, S. and Babanin, A.V., 2012. Investigation of trends in extreme value wave height and wind speed. Journal of Geophysical Research, 117:C00J06. (doi:10.1029/2011JC007753).

Extreme pollution episodes due to particulate matter has been a serious concern for the urban society. Concentration of ambient PM_{10} in the urban atmosphere is increasing significantly specially in developmental countries (Chakraborty et al., 2015; Pant et. al., 2015; AQI Bulletin, November 2017, CPCB). A rapidly growing city like Guwahati may have high pollution episodes in near future. Extreme value technique is a suitable statistical tool

Effect of waste tire addition on geotechnical properties of soil – A Critical Review

Kakati, N.[1], and Chetia, M.[2]

[1]Former PG Student, Department of Civil Engineering, Assam Engineering College, Guwahati-781013, India.
[2]Assistant Professor, Department of Civil Engineering, Assam Engineering College College, Guwahati-781013, India.

ABSTRACT

Scrap tire disposal has been a critical environmental problem in many urban cities due to the huge increase in the number of vehicles. Significant research efforts have been devoted in recent years to explore the use of scrap tires in civil engineering application, as reuse or recycling of scrap tires is the preferred option from a waste management perspective. Civil engineering applications for scrap tires include lightweight fill, conventional fill, retaining wall and bridge abutment, insulation layer and drainage applications (Young et al., 2003). The objective of this study is to assess the geotechnical properties of the different processed used tires. Detailed literature study is conducted on geotechnical properties of different processed used tires as tire shreds, tire chips and tire buffing's and their mixture with sand. Properties like specific gravity, adsorption, compacted density, void ratio, slope stabilization, triaxial determination, direct shear tests, CBR values, bearing capacity of sand reinforcement, earthquake protection, compaction of cohesive soil, unconfined strength of cohesive soil has been reviewed. Disposal scrap tires are environmental dilemma. However, they can improve the characteristics of soil which is an essential material of construction.

This technical paper is a state of art of literature review regarding tire shreds as a construction material. The main focus is to present the technical properties of tire shreds focusing on the use of the material in geotechnical engineering application

Keywords: scrap tire, environment, reuse, geotechnical properties, engineering application.

1. INTRODUCTION

Waste tires are being generated at an increasing rate in quickly growing markets like India due to fast growth of the number of vehicles plying on their roads. In more industrialized nations, approximately one waste tire per capita is generated every year. One such option is the use in various geotechnical engineering applications especially in earthwork projects.

Scrap tire disposal has been a critical environmental problem in many urban cities due to the huge increase in the number of vehicles. Significant research efforts have been devoted in recent years to explore the use of scrap tires in civil engineering application, as reuse or recycling of scrap tires is the preferred option from a waste management perspective. Civil engineering applications for scrap tires include lightweight fill, conventional fill, retaining wall and bridge abutment, insulation layer and drainage applications (Young et al., 2003). The civil engineering applications, in which tires are shredded for applications such as leachate collection in landfills and for highway embankments, account for about 15% of scrap tires. The major reuse application is crumb rubber, also known as ground rubber. In 1994, only about 2% of scrap tires generated in the US were reprocessed as crumb rubber, but by 2001 this had jumped to about 12%. Of all scrap tire reuse options, crumb rubber is probably the most complex but least studied, in terms of both production and markets. (Sunthonpagasit and Duffhey, 2004).

2. EFFECT OF WASTE TIRE ON GEOTECHNICAL PROPERTIES OF SOIL

The review paper gives a clear view on effect of waste tire on geotechnical properties of soil. Properties like specific gravity, adsorption, compacted density, void ratio, slope stabilization, triaxial determination, direct shear tests, CBR values, bearing capacity of sand reinforcement, earthquake protection, compaction of cohesive soil, unconfined strength of cohesive soil has been reviewed.

2.1 Specific Gravity

The specific gravity was determined by using AASHTO T 85-85(10), the samples were air dried rather than oven dried at the start of the tests. The apparent specific gravity of the tire chips is slightly greater than that of water and ranged from 1.14 – 1.28 tire chips composed of glass belted tires have a lower specific gravity than those composed of a mixture of glass and steel belted tires. (Humphrey et al. 1993)

Specific gravity (G) values of mixtures are measured using a large size pycnometer (1,000 ml) as per ASTM C128-12 (ASTM 2012), for sand, tire chips, and STC mixtures. Fig.1 shows the average of the three G values obtained for various samples. For STC mixtures, the specific gravity values were also calculated using G values of sand, tire chips alone, and the corresponding weights used in the mixtures, Fig. 1 presents the measured and calculated specific gravity values of the different STC mixtures, which are well matched. Hence, for any targeted STC mixture, the specific gravity can be calculated using the specific gravity values of S and TC alone, along with the proposed weights (S and TC) for that mixture.

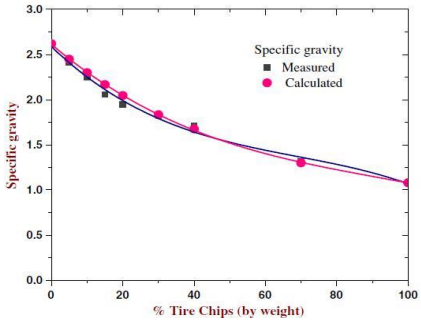

Fig. 1 Specific gravity values of sand tire chip mixtures (Data source: Humphrey et al. 1993)

2.2 Absorption

The absorption capacity was determined by using AASHTO T 85-85(*10*) of tire chips are found to be around 2% - 4%. We can say that the absorption capacity of tire chips are relatively low. (Humphrey et al. 1993)

2.3 Compacted Density

Compaction is the process by which the bulk density of an aggregate of matter is increased by driving out air. For any soil or other material, for a given amount of compactive effort, the density obtained depends on the moisture content. At very high moisture contents, the maximum dry density is achieved when the soil or the material is compacted to nearly saturation, where (almost) all the air is driven out. At low moisture contents, the particles interfere with each other; addition of some moisture will allow greater bulk densities, with a peak density where this effect begins to be counteracted by the saturation of the soil.

The compacted density of air dried tire chips ranges from (.615 - .645) Mg/m^3 or (38.5 - 40) pcf. The low compacted density would potentially result in low horizontal pressure in the walls. It also helps in reducing the settlement of underlying compressible soil and would increase the global stability of the walls. In some case this would allow the wall to be placed on a spread footing rather than a pile foundation, which would significantly reduce construction costs. This clearly shows that the tire chip has the potential to be used as lightweight fill. (Humphrey et al. 1993).

2.4 Void Ratio

The void ratios of the mixtures were calculated which are plotted in Fig. 2. In Fig. 2 the void ratios at the compacted and loose states of the mixtures followed a decreasing trend up to 40% tire-chip content and then an increasing trend beyond 40%. The sand particles filled the voids between the tire chips, and the minimum–maximum void ratio of the mixture decreased. This would continue until all the voids between the tires chips are completely filled with sand particles. When all voids between the tires chips filled with sand particles, any further addition of tire chips would increase both the overall volume of the mixture and consequently its minimum– maximum void ratio. (S. Bali Reddy et al. 2015)

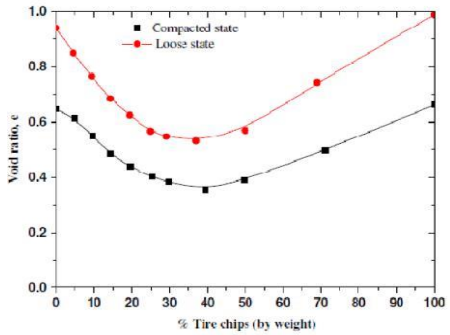

Fig. 2 Total void ratio of STC mixture (Data source: S. Bali Reddy et al. 2015)

2.5 Slope Stabilization

An innovative and inexpensive slope-stabilization scheme is present that uses old rubber tires and woven geotextile to arrest the deterioration of a hill slope. The two main considerations in the selection of a rubber tire wall to prevent further erosion of the steep slope were low costs and ease of construction. The internal stability and the sliding resistance, as well as the hearing capacity were checked. Rubber tires that were filled with granite aggregate and quarry waste were used to protect the fabric against direct sunlight and vandalism. The wall was constructed in 5 m (16 ft.) long sections. The toe of the slope was trimmed back first, and quarry waste was mixed in situ with the sandy silt below the wall. The soil was compacted to form a hard base for the rubber tires. The bottommost row of tires was then placed and filled with 20 mm (0.75 in.) granite aggregate and quarry waste. The soil was backfilled to the height of the tires and compacted. This was followed by a second layer of tires. The procedure was repeated until the third layer of tires was in place. The slope was then trimmed back further to accommodate the bottom geotextile layer. The fabric was folded back around a drainage core of 20 mm (0.75

in.) granite aggregates next to the tires. The procedures were repeated until the required height of the wall had been reached. A reinforced-concrete beam was cast at the top of the wall so that it would not be possible to remove the tires by hand. Creeper plants were planted at the top of the wall to improve the appearance. Unskilled labor was used for the construction of the wall and of the fill. The total cost was less than 40% of the estimated cost of a conventional retaining wall. (Paul S. H. Poh and Bengt B. Broms 1995)

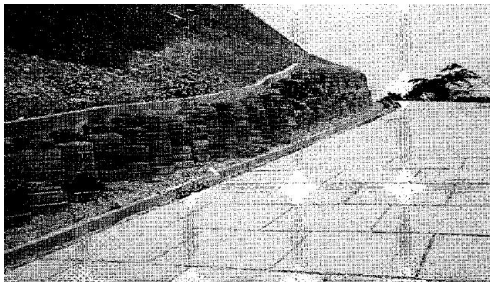

Fig. 3 View of rubber tire wall (Data source: Paul S. H. Poh and Bengt B. Broms 1995)

2.6 Direct shear determination

The objective of this study was to investigate the feasibility of using shredded waste tires to reinforce sand. Direct shear tests were conducted on mixtures of dry sand and shredded waste tires. The following factors were studied to evaluate their influence on shear strength: normal stress, sand matrix unit weight, shred content, shred length, and shred orientation. From results of the tests, three significant factors affecting shear strength were identified: normal stress, shred content, and sand matrix unit weight. A model for estimating the strength of reinforced soils was also evaluated to determine its applicability to mixtures of sand and tire shreds. When the model is calibrated using results from one shred content, it may be useful for estimating the friction angle for other shred contents. In all cases, adding shredded tires increased the shear strength of sand, with an apparent friction angle is as large as 67 being obtained. Shred content and sand matrix unit weight were the most significant characteristics of the mixes influencing shear strength. Increasing either of these variables resulted in an increase in friction angle. Tests were also conducted on specimens consisting of only shredded tires (no sand), and the friction angle obtained was 30°.

Shredded waste tires and mixtures of sand and shredded waste tires may be useful as soil reinforcement in highway fills, leachate collection systems on steep slopes, and other applications where strong and lightweight fill is needed. (G.J Foose et al. 1996)

An optimization of aspect ratios of shreds having widths of 2, 3, and 4 cm can increase f_1 on average by 25%. It has been found that regardless of compaction level and shred contents in the mixtures, for a given width; there is only a certain length that gives the greatest value of ϕ. The absolute greatest value of about ϕ_1=67° was obtained by using 50% shreds with dimensions of 438 cm at γ_m=16.8 kN/m3. (Mahmoud Ghazavi and Masoud Amel Sakhi 2005)

2.7 Cbr values

The advantage of optimizing aspect ratio (length to width) of waste tire shreds on California Bearing Ratio (CBR) of sand-tire shred mixtures is investigated in this paper. The mixtures were composed of a relatively uniform sand and tire shreds with 2, 3, and 4cm widths and various lengths. Shred contents of 15, 30, and 50% by volume were mixed with sand at two sand matrix unit weights of 15.5 kN/m^3 and 16.8 kN/m^3. The CBR value of sand-tire shred mixtures increases with increasing shred contents. With adding 15% tire shreds to the sand, the CBR value increases from 14 % to 485 %, depending on the compaction degree and shred dimensions. In samples compacted at γ_m = 15.5 kN/m^3, if the shred content increases to 30 %, the CBR increases in the range of 88.2 – 595 %. By adding 50% shreds to the sand, the CBR increases from 180 to 850 %. For specimens compacted at γm =16.8 kN/m^3, these quantities account for 14 – 45.6%, 32.4 – 61.8%, and 56.6 – 90.4 %, respectively, depending on shred dimensions. The optimization of tire shreds leads to an average increase of 161% in the CBR value. For samples compacted at γ_m =15.5 kN/m^3 and γ_m = 16.8 kN/m^3, the average values of increased CBR are about 284% and 38 %, respectively. (Mahmoud Ghazavi and Masoud Amel Sakhi 2005)

2.8 Bearing capacity of sand reinforced

Shred content and shreds aspect ratio are the main parameters that affect the bearing capacity. Tire shreds with rectangular shape and widths of 2 and 3 cm with aspect ratios 2, 3, 4 and 5 are mixed with sand. Five shred contents of 10%, 20%, 30%, 40% and 50% by volume were selected. Addition of tire shreds to sand increases BCR (bearing capacity ratio) from 1.17 to 3.9 with respect to shred content and shreds aspect ratio. The maximum BCR is attained at shred content of 40% and dimensions of 3x12 cm. It is shown that increasing of shred content increases the BCR. However, an optimum value for shred content is observed after that increasing shreds led to decrease in BCR. For a given shred width, shred content and soil density it seems that aspect ratio of 4 gives maximum BCR. (N. Hataf , M.M. Rahimi , 2006)

Table 1. Bearing capacity for reinforced sand (Data source: N. Hataf , M.M. Rahimi 2006)

Tire shreds content (%)	Size of shreds						
	2×4 cm	2×6 cm	2×8 cm	2×10 cm	3×6 cm	3×9 cm	3×12 cm
10	1.17	1.46	1.46	1.56	1.56	1.73	1.83
20	1.6	2.03	2	1.97	1.9	2.13	2.2
30	2.15	2.73	2.8	2.84	2.69	2.8	3
40	-	3.2	3.4	-	-	-	3.9
50	-	2.95	3.3	-	-	-	3.9

2.9 Effect on Unconfined Strength of Cohesive Soil

The stress–strain relationships of cohesive soil-tire specimens as obtained from unconfined compression tests are depicted in Fig. 4. The results show that the stress-strain behavior of the soil is markedly affected due to the addition of tire chips. The initial stiffness of the reinforced soil is decreased, and a greater peak compressive strength is obtained at higher axial strains. Due to the reinforcement, there is less reduction in strength beyond peak value, and the ultimate strength remains substantial. This trend confirms that the addition of chips imparts resilient property to the mixes.

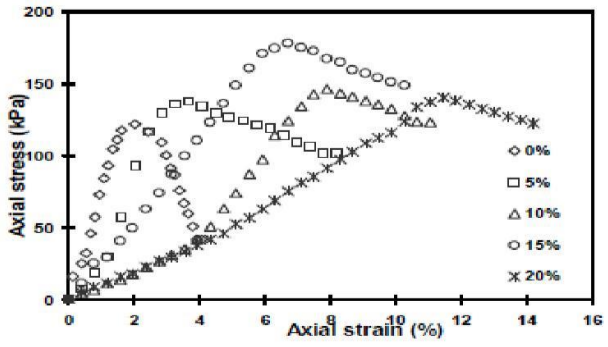

Fig. 4 Stress-strain response of cohesive soil-tire chip mixtures in UC tests (Data source : Baleshwar Singh and Valliapan Vinot 2011)

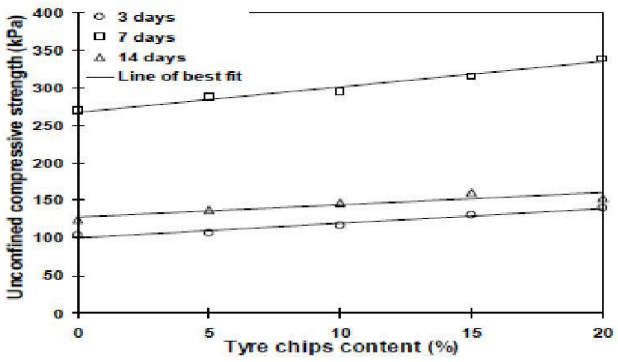

Fig. 5 Variation of unconfined compressive strength of cohesive soil-tire chip mixtures with curing period(Data source : Baleshwar Singh and Valliapan Vinot 2011)

The study has demonstrated the benefits of reusing chips of scrap tires to reinforce a cohesive soil and a cohesion less soil. From the test results, it can be concluded that tire chips mixed in a compacted fine-grained soil can result in greater strength and improved ductility. On the other hand, the addition of tire chips to sand increases the shear resistance at higher displacement although the magnitude and nature of this increase are affected by normal stress, chips content and aspect ratio, which are statistically significant at 95% confidence level. Additionally, a model has been developed to predict the shear strength of the reinforced sand. On the whole, the results reveal that the addition of 13% and 30% chips content can be considered as optimum to reinforce the cohesive soil and the cohesionless soil, respectively. (Baleshwar Singh and Valliapan Vinot , 2011)

Table 2. Compaction parameters and unconfined compressive strength of cohesive soil-tire chip mixtures(Data source : Baleshwar Singh and Valliapan Vinot 2011)

Tire chips content (%)	OMC (%)	MDD (kN/m^3)	UCS (kPa) after curing periods of		
			3 days	7 days	14 days
0	20.3	16.3	105.9	268.8	124.3
5	20.1	16.2	107.1	288.1	137.7
10	19.9	15.5	116.7	293.9	146.4
15	18.6	14.9	131.1	315.8	178.3
20	20.1	14.6	140.5	338.8	140.5

3 CONCLUSIONS

This study presents a comprehensive review of effect of tire content on the geotechnical properties of soils. This review highlights that using scrap tires as a recycled material, either as whole or shredded into small pieces, the potential impact on geotechnical properties have been studied by several investigators. It is found that the geotechnical parameters of soils are improved substantially by the addition of tire waste.

- The specific gravity of tire is found slightly greater than that of water and ranged from 1.14 – 1.28 ; tire chips composed of glass belted tires have a lower specific gravity than those composed of a mixture of glass and steel belted tires.
- The absorption capacity of tire chips was found to be low; which ranges from 2% - 4%.
- With an increase in tire content up to 40% of the STC mixture, void ratio is decreased by approximately 50%, which indicates better compressibility behavior.
- The tire chip can be used as lightweight fill as the compacted density of air dried tire chips ranges from (.615 - .645) Mg/m^3

- The interparticle friction angle ϕ_f was calculated to be 44°-56°. All the tire sample products have similar frictional behaviors with a negligible cohesion intercept when the confining pressure is less than about 40 kPa .
- The initial friction angle ϕ_1 ; increased as the shred content was increased. Adding shredded tires increased the shear strength of sand, with an apparent friction angle ϕ' as large as 67° being obtained.
- The tire shreds cause ϕ_1 to be increased by about 10–94%, depending on shred width and aspect ratio, shred content, and mixture compaction. An optimization of aspect ratios of shreds having widths of 2, 3, and 4 cm can increase $\phi 1$ on average by 25%. The absolute greatest value of about $\phi_1 = 67°$ was obtained by using 50% shreds with dimensions of 438 cm at γ_m =16.8 kN/m^3.
- Addition of tire shreds to sand increases BCR (bearing capacity ratio) from 1.17 to 3.9 with respect to shred content and shreds aspect ratio. The maximum BCR is attained at shred content of 40% and dimensions of 3x12 cm. It is shown that increasing of shred content increases the BCR.

The addition of tire chips to sand increases the shear resistance at higher displacement although the magnitude and nature of this increase are affected by normal stress, chips content and aspect ratio, which are statistically significant at 95% confidence level.

REFERENCES

1. Das, T., and Singh B. (2012).. "Benefits and impacts of scrap tyre use in geotechnical engineering." *Environ. Res Develop*., 7(3), 1262-1271
2. Das, T., and Singh B. (2012).. "Benefits and impacts of scrap tyre use in geotechnical engineering." *J. Environ. Res Develop*., 7(3), 1262-1271.
3. Foose, G., Benson, and Bosscher, P. (1996) " Sand reinforced with shredded waste tires." J. Geotech. Engrg., 1996, 122(9): 760-767.
4. Ghazavi, M., and Sakhi, M., (2005) "Optimization of aspect ratio of waste tire shreds in sand-shred mixtures using CBR tests." *Geotechnical Testing Journal,* Vol. 28, No. 6.
5. Hataf, N., and Rahim, M. (2006) "Experimental investigation of bearing capacity of sand reinforcedwith randomly distributed tire shreds" Department of Civil Engineering, Shiraz University, hiraz, Iran_ 2005 Elsevier Ltd. Humphrey, D., Sandford, T., Cribbs, M., and Manion,
6. W. (1993) "Shear strength and compressibility of tire chips for use as retaining wall backfill." University of Maine, Orono, Maine.
7. Paul, S., Poh, I., and Bengt B., Broms. (1995) "Slope stabilization using old rubber tires and geotextiles." ASCE J. Perform. Constr. Facil. 1995.9:76-79.
8. Reddy, S., Pradeep Kumar, D., and Krishna, A. (2015) "Evaluation of the optimum mixing ratio of a sand-tire chips mixture for geoengineering applications." © 2015 American Society of Civil Engineers.
9. Singh, B., and Vinot,V. (2011) "Influence of waste tire chips on strength characteristics of soils" Sep. 2011, Volume 5, No. 9 (Serial No. 46), pp. 819-827 Journal of Civil Engineering and Architecture, ISSN 1934-7359, USA.

Optimal heavy metal removal in a multi-ion scenario for sustainable water and wastewater treatment using adsorption techniques

Zaman, D.[1], Jawed, M.[2]

[1] Ph.D. student, School of Water Resources, Indian Institute of Technology Kharagpur- 721302, India.
[2]Professor, Department of Civil Engineering, Indian Institute of Technology Guwahati, 781039, India.

ABSTRACT

Adsorption techniques have been increasingly used in advanced water and wastewater treatment for the uptake of heavy metal ions. In the present study, adsorption kinetics of binary-ion systems of Cr(III) and Pb(II) is carried out using granular activated alumina (GAA) as adsorbent, under conditions of controlled as well as uncontrolled pH value of 5 by taking different proportions of individual ions in the binary systems, but keeping the initial metal ion concentration constant. Concentration of ions is taken on the basis of its equivalent weights so that the difference in electrovalence and atomic weight of individual ions is accounted for. Comparative analysis of the experimental data reveals several properties pertaining to the interaction between individual ions in multi-ion systems and also with the adsorbent. It further establishes that concentration gradient (expressed in equivalent weight) of a particular metal ion dominates its uptake over all other properties. Irrespective of the type of metal ions, similar uptake capacities are observed for same initial ion concentration. Hence, this study successfully establishes that concentration of metal ions in multi-ion systems is best characterized using the concept of equivalent weights (rather than atomic weight or molar weight) and the external monitoring and control of pH is essential in order to ensure removal by adsorption mechanism alone. With this knowledge, a methodology for optimal adsorption can be designed to ensure sustainability of adsorption systems.

Keywords: adsorption, multi-metal systems, kinetics, equilibria, equivalent weights

1 INTRODUCTION

Removal of heavy metal ions from drinking water and industrial effluents is a mandatory requirement for the protection of environment and human health. Out of all the techniques available for heavy metal removal from water, adsorption is more popular owing to its high removal efficiency and comparatively lower cost. Investigations on the feasibility of adsorption for removal of mono-ions from solution phase have been carried out extensively for different metal ions as well as by using different adsorbents (Uddin, 2017; Burakov et al., 2018). Effect of process parameters such as adsorbent characteristics, solution properties and other abiotic parameters like temperature, rate of agitation and contact time have been investigated to understand their influence on the adsorption process. However, real water and wastewater streams may consist of two or more metal ions with varied chemical properties. Only a handful of studies have been carried out to understand the competitive adsorption process in multi-ion systems. Some of the available studies on multi-ion systems and crucial process parameters have been summarised in Table 1.

Exploration of available literature on multi-ion systems highlighted lacunae in several aspects of experimental as well as data analysis. One such major drawback observed was that the solution pH (most important parameter in the adsorption process) was not monitored during experimentation and completely ignored in analysis. Initial records of pH measurements and during the course of experiment have not been reported in most studies and no attempt to maintain pH at a constant level to ensure the availability of metal ions in soluble form was undertaken (Baig et al., 2009; Debnath and Ghosh, 2011). Maintaining constant initial ion concentration gradient for comparison of the experimental results of mono- and multi-ion system has not received much attention yet. Moreover, initial concentration of all metal ions was expressed either in terms of

Table 1. Process parameters of multi-metal ions system

Target metals	Adsorbent	Initial conc. in	pH	Reference
Co(II), Ni(II), Cr(III)	IRN-77 resin	mg/L	Unmonitored Uncontrolled	Kang et al., 2004
Cd(II), Ni(II)	Bagasse fly ash	mg/L	Monitored, Uncontrolled	Srivastava et al., 2005
Cu(II), Pb(II)	MOCS	mmol/L	Monitored Uncontrolled	Han et al., 2006
Cu(II), Cd(II), Pb(II)	Ca-Alginate beads	mmol/L	Unmonitored Uncontrolled	Papageorgoiu et al., 2008
Ni(II), Zn(II)	Wheat straw	mg/L	Unmonitored Uncontrolled	Baig et al., 2009
Cd(II), Cu(II)	Titanium oxide	mg/L	Monitored, Uncontrolled	Debnath and Ghosh, 2011

gram molecular weight or molar weight basis instead of equivalent weights, which do not account for the difference in electrovalence and atomic weight of different ions during simultaneous adsorption (Srivastava et al., 2005; Papageorgoiu et al., 2008). Thus, the phenomenon of adsorption is rather complicated in a multi-ion scenario and conclusions cannot be exclusively drawn from mono-ion system analysis. Adsorption process in multi-ion systems needs to be further studied with pH monitoring and control and constant ionic concentration gradient in terms of equivalent weights to make inter-comparisons among different systems meaningful and design sustainable adsorption systems, providing maximum uptake while utilising optimum adsorbent.

In the present study, a binary-ion system consisting of Cr(III) and Pb(II) was investigated with same initial ion concentration expressed in meq/L and same initial pH, constant ionic concentration gradient and monitoring and control of pH during the experimentation process.

2 MATERIALS AND METHODS

The heavy metals – Chromium [Cr(III)] and Lead [Pb(II)] were selected as target metal ions for the study, based on their difference in chemical properties, as presented in Table 2. Commercial grade granular activated alumina (GAA) was selected as adsorbent, with particle size range of 0.40 – 1.20 mm and a minimum surface area of 360 m^2/g. Cr(III) and Pb(II) stock solution of 1000 mg/L was prepared as per standard methods (APHA, 2005). Preliminary experiments were carried out to obtain the different parameters for carrying out reaction kinetics and equilibria, as described in Table 3. Each experiment was carried out under two conditions of pH – (i) Controlled: Solution pH was initially adjusted to 5 and controlled during the experiment using suitable buffer solutions, (ii) Uncontrolled: Solution pH was initially adjusted to 5 and left uncontrolled during the experiment.

Table 2. Chemical properties of selected metal ions

Metal ion	Charge	Atomic weight (g)	Ionic radius (A°)
Chromium, Cr	+3	51.996	0.615
Lead, Pb	+2	207.200	1.330

Under each pH condition, at first, mono-ion systems of both Cr(III) and Pb(II) were investigated for reaction kinetics and equilibria, with an initial ion concentration of 0.6 meq/L. Then, binary-ion systems were prepared with both Cr(III) and Pb(II) having individual ion concentrations as mentioned in Table 3, but keeping the total ion concentration of 0.6 meq/L. A separate set of similar experiment was carried out with initial ion concentration double that of the other experiments, in order to make inter-comparisons and emphasize on the importance of constant ionic concentration gradient. In each experiment, one metal ion was considered as 'target metal (T)' and the other as 'non-target metal (NT)'. Therefore, the five different combinations of initial ion concentrations of target and non-target metal ions were selected as: C-1 (0.60 meq/L of T + 0 meq/L of NT), C-2 (0.45 meq/L of T + 0.15 meq/L of NT), C-3 (0.30 meq/L of T + 0.30 meq/L of NT), C-4 (0.15 meq/L of T + 0.45 meq/L of NT), C-5 (0.60 meq/L of T + 0.60 meq/L of NT). The combination C-1 is essentially mono-ion system while combinations C-2 to C-5 are binary-ion systems, wherein C-2 to C-4 have the same initial total ion concentration and C-5 has double the initial ion concentration. Each experiment was carried out at room temperature, in triplicates and average values were considered for analysis to amplify the consistency of results.

Table 3. Experimental conditions adopted for kinetics and equilibria

Parameters	Kinetics	Equilibria
Initial solution pH	5	5
Initial solution volume (mL)	50	50
Contact time (h)	4	3
Adsorbent dose (g/L)	12	4–32
Shaker speed (rpm)	67–68	67–68
Mono ion conc. (meq/L)	Cr=0.60, Pb=0.60	
Binary (Cr+Pb) (meq/L)	Cr=0.45 + Pb=0.15 Cr=0.30 + Pb=0.30 Cr=0.15 + Pb=0.45 Cr=0.60 + Pb=0.60	

3 RESULTS AND DISCUSSION

3.1 Adsorption models for kinetics and equilibria

The simplest and most accepted models developed for explaining reaction kinetics and equilibria were used for experimental analysis in the present study, as described in Table 4. Reaction kinetics and equilibria were carried out for the five combinations of binary-ion systems – C-1 to C-5, as described in section 2. The experimental data for metal uptake at different contact time for mono- and binary-ion systems under controlled and uncontrolled pH was fitted to pseudo-first order model by using the values of q_e and k_1 calculated by method of least squares, while the values of k_2 and q_e for the pseudo-second order model had been estimated through the slope and intercept of experimental plots. Similarly, experimental data for metal uptake at different adsorbent dose was fitted to the linearised forms of Langmuir and Freundlich isotherm models to determine the isotherm constants for target metal uptake for each of the combinations.

Table 4. Adsorption models for kinetics and equilibria

Model	Mathematical Form	Reference

	Model	Mathematical Form	Reference
Kinetics	Pseudo 1st order rate equation	$q_t = q_e(1-e^{-k_1 t})$	Langergren and Svenska, 1898
	Pseudo 2nd order rate equation	$q_t = \frac{k_2 q_e^{\ 2} t}{1+k_2 q_e t}$	Ho and McKay, 2000
Equilibria	Langmuir equation	$q_e = \frac{abC_e}{1+bC_e}$	Langmuir, 1918
	Freundlich equation	$q_e = k_f C_e^{\frac{1}{n}}$	Freundlich, 1926

Here, q_t and q_e are amounts of metal ions adsorbed at time t and at equilibrium respectively; k_1 and k_2 are rate constants of first and second order reaction respectively; *a* is max adsorption capacity; *b* is Langmuir constant; Ce is adsorbed concentration at equilibrium; k_f and *n* are temperature dependent constants

3.2 Adsorption kinetics in binary-ion systems

3.2.1 Effect of contact time on target ion uptake in presence of non-target ion

The effect of variation in contact time on metal-ion uptake and subsequent variation in pH was studied in mono- and binary-ion systems under controlled and uncontrolled pH. Ion uptake was observed to increase rapidly during the first 20 minutes of contact time and appeared to have reached a fixed value after 180 minutes.

Uptake of Cr(III) as target metal with Pb(II) as non-target metal from binary-metal system under conditions of controlled and uncontrolled pH did not overlap at 95% confidence intervals for any of the combinations except for C–2 and C–5. Cr(III) uptake was observed to be highest for combination C–1 and thereafter progressively decreased for combinations C–2 to C–4 with decrease in Cr(III) ion initial concentration in binary combination both under controlled as well as uncontrolled pH (as shown in Figure 1). Further, the observed decrease in Cr(III) uptake of combination C–5 with respect to C–1 clearly indicated the suppressive action of presence of 0.6 meq/L of non-target metal. It was also observed that uptake of target metal Pb(II) was marginally higher than that of target metal Cr(III) for each corresponding binary-ion combination, C–2 to C–5 which indicated lesser impact of presence of non-target metal Cr(III) on target metal Pb(II) uptake compared to impact of presence of non-target metal Pb(II) on target metal Cr(III) uptake (not shown in figure).

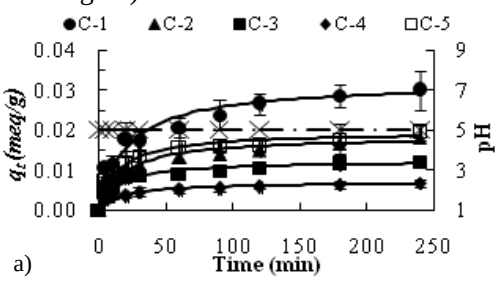

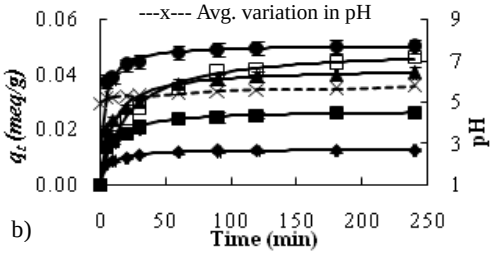

Fig. 1. Effect of contact time on Cr(III) - target metal uptake in presence of Pb(II) - non-target metal for (a) controlled pH and (b) uncontrolled pH

3.2.2 Effect of contact time on total ion uptake

Total uptake for binary-ion systems under controlled and uncontrolled pH was observed to overlap at 95% confidence intervals, the overlap being higher under controlled pH (as shown in Figure 2). This indicated that the total uptake was similar irrespective of the type of metal ion, when compared on the basis of their equivalent weights. Hence, it could be preempted that the difference in atomic weight and electrovalence did not play significant relevance in the uptake property of the adsorbent, if weight was considered in terms of equivalent weight.

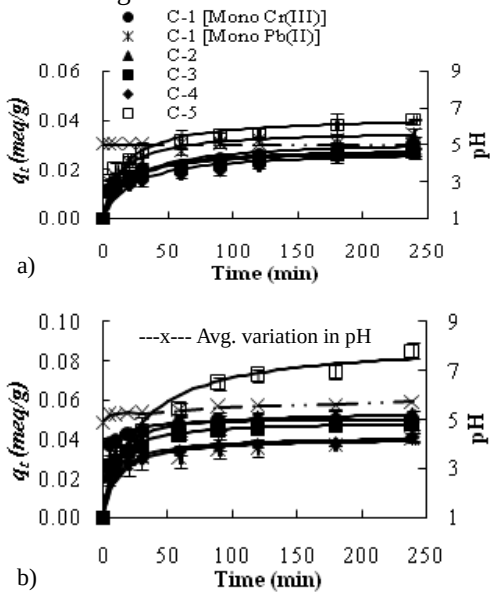

Fig. 2. Effect of contact time on total metal uptake for (a) controlled pH and (b) uncontrolled pH

3.3 Adsorption equilibria

3.3.1 Effect of adsorbent dose on target ion uptake in presence of non-target ion

The experimental data for target metal uptake of Cr(III) at equilibrium, in presence of non-target metal Pb(II) and vice-versa from binary-ion systems under controlled as well as uncontrolled pH conditions was fitted to the linearised forms of Freundlich isotherm models to determine the isotherm constants for target metal uptake for each of the combinations (as shown in Figure 3).

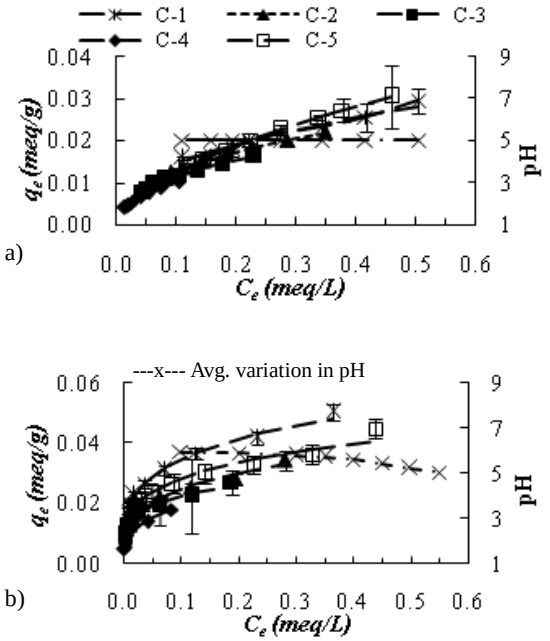

Fig. 3. Adsorption isotherm plots of target metal Pb(II) using experimental data and fitted Freundlich isotherm model for (a) controlled pH and (b) uncontrolled pH

Barring a few exceptions, the R^2 values obtained from the linearised plots of both the models were above 0.900 for all which indicated that both models may be representative of the experimental data. The experimental data was re-plotted along with the best fitted isotherm model (Freundlich model was used here). Uptake of target metal Cr(III) for binary combinations C–2 to C–5 tend to vary within a narrow band for the entire range of selected equilibrium concentration i.e. up to 0.60 meq/l. However, plot obtained for uptake of target metal Cr(III) from mono-metal system (combination C–1) was highest and deviated away from the other binary combinations (as shown in Figure 4). Whereas for uptake of target metal Cr(III) under uncontrolled pH was not similar to that obtained under controlled pH. Combinations C–1, C–2 and C–3 tend to vary within a narrow band for the entire range of equilibrium concentration, while Cr(III) uptake in combination C–4 was observed to be lowest and deviated from other binary combinations. The uptake of target metal Cr(III) from combination C–5 was much less than other binary combinations which is indicative of the suppressive action of presence of non-target metal in the system.

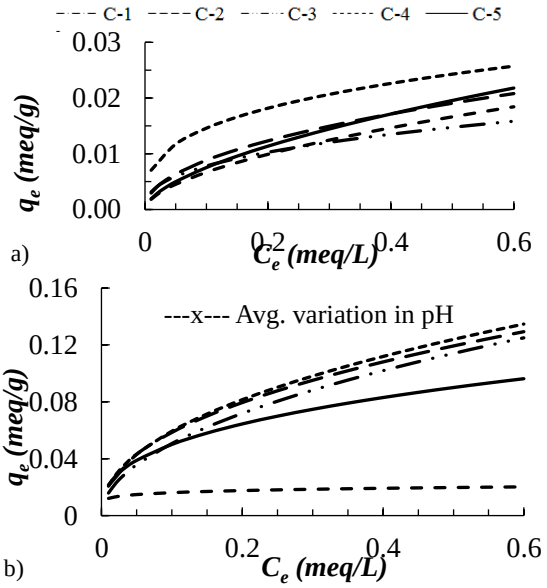

Fig. 4. Adsorption isotherm plots of target metal Cr(III) with fitted Freundlich isotherm model for (a) controlled pH and (b) uncontrolled pH

Similar plots were obtained for target metal Pb(II) for Freundlich isotherm model for controlled and uncontrolled pH indicated that all binary combinations (except C-4 for uncontrolled pH) tend to vary in a narrow band for the entire range of selected equilibrium concentration.

3.3.2 Effect of adsorbent dose on total ion uptake

It was evident that both the ions were being simultaneously adsorbed by the adsorbent from binary-ion systems. The total metal ion uptake was analysed in a similar manner as explained in section 3.3.1. The total metal uptake (target and non-target) under controlled pH was observed to overlap at 95% confidence interval for combinations C-1 to C-4 with total initial concentration of 0.60 meq/L (as shown in Figure 5). Hence, it clearly indicated that the total metal uptake at equilibrium was fairly independent of proportion of initial metal ion concentrations in mono- and binary-metal ion systems as long as total initial concentration was the same, i.e. 0.60 meq/L. On the other hand, when concentration of total initial metal ion was doubled to 1.20 meq/L in combination C–5 of binary-metal ion system, the total metal uptake was observed to be higher than all combinations and it did not overlap at 95% confidence intervals. Similarly, overlap of experimental data points also observed at 95% confidence levels for combinations C-1 to C-4 under uncontrolled pH throughout the entire contact period. However, comparative extent of overlap was observed to be higher under controlled pH than that of uncontrolled pH.

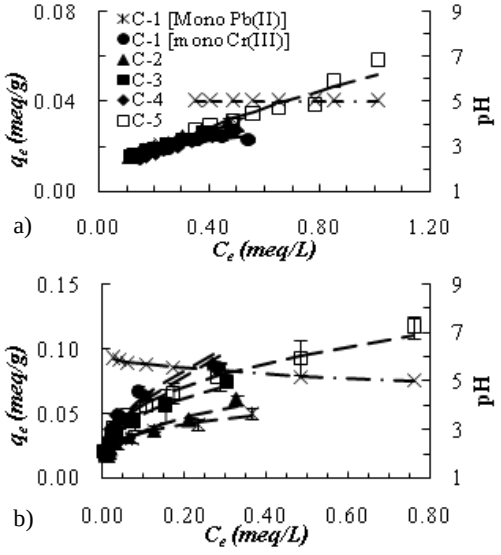

Fig. 5. Adsorption isotherm plots of total metal ion using experimental data and fitted Freundlich isotherm model for (a) controlled pH and (b) uncontrolled pH

With a view to inter-comparing the uptake of different combinations, the experimental data obtained were fitted to Freundlich model up to an equilibrium concentration of 1.20 meq/L which incidentally was the highest equilibrium concentration of binary-ion systems. It was observed from the Freundlich plots of total metal uptake, that combinations C–1 to C–4 vary within a fairly narrow band for the entire equilibrium concentration range, whereas uptake of combination C–5 was highest as expected due to higher concentration gradient (as shown in Figure 6)**.** Combination C–1 [mono Cr(III)] was observed to have the lowest uptake and did not appear in close proximity with any of the combinations. For plots of Freundlich model under uncontrolled pH, deviation was observed among the combinations and narrow band formation was observed only for combinations C–1 [mono Cr(III)] and C–4. Uptake of combination C–5 was observed to decrease in case of uncontrolled pH

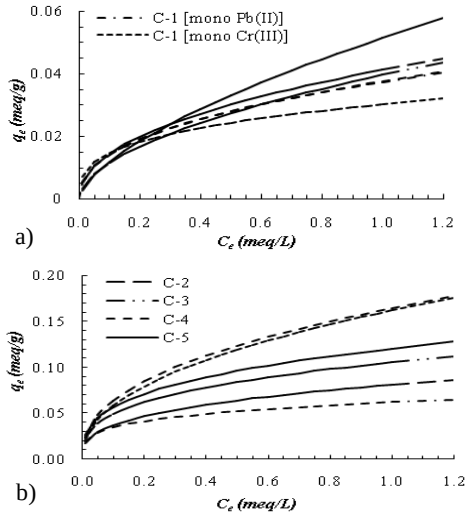

Fig. 6. Adsorption isotherm plots of total metal ion with fitted Freundlich isotherm model for (a) controlled pH and (b) uncontrolled pH

4 CONCLUSIONS

The primary objective of the study is to investigate the kinetics and equilibria of metal uptake from mono- and binary-ion systems with fixed ionic concentration gradient, with initial concentrations expressed in meq/L, under conditions of controlled as well as uncontrolled pH. Some of the major conclusions deduced from the study are summarized below:

1. In general, metal uptake is lower under controlled pH conditions, compared to uncontrolled pH, possibly due to precipitation of a fraction of ions at pH higher than 6.
2. The reaction kinetics of the experimental data is very closely represented by pseudo-second order model. As expected, target ion uptake for binary-ion systems increase with the increase in proportion of target ion in the solution, both under controlled and uncontrolled pH conditions. However, the trends of total metal ion uptake are similar for all combinations of binary ion

systems having same initial concentration.

3. Equilibrium studies reveal that both Langmuir and Freundlich isotherm models best fitted the experimental data for all binary-ion systems. The total metal uptake at equilibrium overlap at 95% confidence intervals for all combinations of mono- and binary-ion systems having same initial concentration of 0.6 meq/L.

Hence, the most important inference from the study is that monitoring and controlling of solution pH is most crucial for assessing the adsorption process. Secondly, the adsorption is observed to be independent of the proportion of individual metal ions in multi-ion systems as long as total concentration is fixed, highlighting the influence of concentration gradient on the adsorption process.

REFERENCES

1) APHA (2005): Standards Methods for the Examination of Water and Wastewater, 20th Ed., published by American Public Health Association, American *Water Works Association and Water Environment Federation*, Washington, USA.
2) Baig, K.S., Doan, H.D. and Wu, J. (2009): Multicomponent isotherm for biosorption of Ni^{2+} and Zn^{2+}, *Desalination*, 249, 429-439.
3) Burakov, A.E., Galunin, E.V., Burakova, I.V., Kucherova, A.E., Agarwal, S., Tkachev, A.G. and Gupta, V.K., (2018): Adsorption of heavy metals on conventional and nanostructured materials for wastewater treatment purposes: A review, *Ecotoxicology and Environmental Safety*, 148, 702-712.
4) Debnath, S. and Ghosh, U.C. (2011): Equilibrium modeling of single and binary adsorption of Cd(II) and Cu(II) onto agglomerated nano structured titanium(IV) oxide, *Desalination*, 273, 330-342.
5) Freundlich, H. (1926). *Colloid and Capillary chemistry*, Methuen, and Co., Ltd., London.
6) Han, R., Lu Z., Zou, W., Daotong, W., Shi, J. and Jiujun, Y. (2006): Removal of copper(II) and lead(II) from aqueous solution by manganese oxide coated sand II. Equilibrium study and competitive adsorption, *Journal of Hazardous Materials*, 137, 480-488.
7) Ho, Y.S., McKay, G. (2000): The kinetics of sorption of divalent metal ions onto sphagnum moss peat, *Water Research*, 34(3), 735-742.
8) Kang, S.Y., Lee, J.U., Moon, S.H. and Kim, K.W. (2004): Competitive adsorption characteristics of Co^{2+}, Ni^{2+}, and Cr^{3+} by IRN-77 cation exchange resin in synthesized wastewater, *Chemosphere*, 56, 141-147.
9) Langergren, S. and Svenska, B.K. (1898): Zurtheorie der sogenannten adsorption geloesterstoffe, *Veternskapsakad Handlingar*, 24(4), 1-39.
10) Langmuir, I. (1918): The adsorption of gases on plane surfaces of glass, mica and platinum, *Journal of American Chemical Society*, 40, 1362-1403.
11) Papageorgiou, S.K., Katsaros, F.K., Kouvelos, E.P. and Kanellopoulos, N.K. (2008): Prediction of binary adsorption isotherms of Cu^{2+}, Cd^{2+} and Pb^{2+} on calcium alginate beads from single adsorption data, *Journals of Hazardous Materials*, 162, 1347-1354.
12) Srivastava, V.C., Mall, I.D. and Mishra, I.M. (2005): Equilibrium modeling of single and binary adsorption of cadmium and nickel into bagasse fly ash, *Chemical Engineering Journal*, 117, 79-91.
13) Uddin, M.K. (2017): A review on the adsorption of heavy metals by clay minerals, with special focus on the past decade, *Chemical Engineering Journal*, 308, 438-462.

Proposal for a waste-water treatment plant in Bharalumukh (Guwahati)

Bora, A.[1] and Baruah, D.[2]

[1] Engineer Trainee (Civil) at Power Grid Corporation of India Limited, NER(India).
[2] UG student, Department of Civil Engineering, Assam Engineering College, Guwahati-781013, India.

ABSTRACT

This paper is based on the problems associated with the unscientific disposal of untreated sewage into the River Brahmaputra through River Bharalu, a tributary of Brahmaputra in Bharalumukh area of Guwahati (Assam) and tries to give some remedies to mitigate the serious environmental issue. Everyone living in the Bharalumukh area or travelling via the Bharalamukh area face immense problems due to the unbearable foul smell which is coming from the polluted River Bharalu. This is due to the fact that the natural water body, the River Bharalu is now a manmade drain, which collects domestic, commercial and industrial wastes across the Guwahati city. Moreover, Guwahati being an unplanned city, the residential, commercial and industrial areas are not properly well defined and due to lack of public utilities such as proper sewerage and drainage system, the waste is sometimes directly discharged into the River Bharalu. The situation becomes worse during the rainy days where the streets of Guwahati remain submerged for days. The flood water is naturally and artificially discharged into the River Bharalu using pumps. The street washing comprising of the flood water containing floating debris, is made to flow into the River Bharalu and ultimately discharges into the mighty river Brahmaputra. This results into excessive sedimentation in the River Brahmaputra; this is one of the main reasons which cause sedimentation in the river Brahmaputra and ultimately decreases the water carrying capacity of the river due to decrease in the depth of flow. A wastewater treatment plant is being advised in the paper and to resolve the problem, the proposed waste-water plant can be constructed partly on land and party on water by constructing marine structures to resolve the problems of scarcity of land in an urban area like the Bharalamukh area in Guwahati. So if waste-water treatment plant is established in the outlet of the River Bharalu in the Bharalumukh area, the scenario will completely change.

The solid matter obtained such as plastics by mechanical screening can be reused and the sludge so generated in the clarifiers can be transported to areas, where the density of inhabitants is less using large dumpers or trucks so that these can be used for filling up the low lying areas, some may be given to those NGOs in Guwahati which primarily use organic and inorganic wastes to obtain fertilizers, papers, bricks and those which are of no economic value should be burn in incinerators with out most care.

Keywords: sewage, sedimentation, screening, sludge, solid wastes, waste water treatment plant

1. INTRODUCTION

The city of Guwahati lies between the banks of the river Brahmaputra and the foothills of Khasi hills, where Bharalumukh is a locality near south bank of river Brahmaputra in Guwahati surrounded by Santipur and Pan Bazaar localities. But the people living in the Bharalumukh area have to face a lot of problems associated with the unscientific disposal of untreated sewage into the River Brahmaputra through River Bharalu. They have to face the the unbearable foul smell which is coming from the polluted River Bharalu. This is due to the fact that the natural water body, the River Bharalu is now a manmade drain, which collects domestic, commercial and industrial wastes across the Guwahati city. Moreover the Guwahati city being an unplanned city lacks in proper public utilities like sewerage and drainage systems and as such the waste is sometimes directly discharged into the River Bharalu. The situation becomes worse during the rainy days where the streets of Guwahati remain submerged for days. The street washing comprising of the flood water containing floating debris, is made to flow into the River Bharalu and ultimately discharges into the mighty river Brahmaputra. This results into excessive sedimentation in the River Brahmaputra; this is one of the main reasons which cause sedimentation in the river Brahmaputra and ultimately decreases the water carrying capacity of the river due to decrease in the depth of flow. So considering all the

problems a waste-water treatment plant is being advised in the paper and to resolve the problem, the proposed waste-water plant can be constructed partly on land and party on water by constructing marine structures to resolve the problems of scarcity of land in an urban area like the Bharalamukh area in Guwahati. So if waste-water treatment plant is established in the outlet of the River Bharalu in the Bharalumukh area, the scenario will completely change. The working principle of the proposed plant will be illustrated later.

The government of India has sponsored a water supply project for the entire city of Guwahati, in which the water will be taken from the river Brahmaputra as its source. The water of the river Brahmaputra is not clean today, as it was few decades ago. For this the proposed water treatment plants are under construction in different parts of Guwahati, along the river. For this the load on the water treatment plants should be minimised and the water should contain minimum pollution to secure the health of the inhabitants of Guwahati. The proposed waste water treatment plant will minimise the load and increase the quality of water.

The solid matter obtained such as plastics by mechanical screening can be reused and the sludge so generated in the clarifiers can be transported to areas, where the density of inhabitants is less using large dumpers or trucks so that these can be used for filling up the low lying areas, some may be given to those NGOs in Guwahati which primarily use organic and inorganic wastes to obtain fertilizers, papers and those which are of no economic value should be burn in incinerators with out most care.

2. OBJECTIVES

The main objectives of the study are -

i) To propose a waste water treatment plant in Bharalumukh to control the pollution.

ii) To study the working efficiency of the proposed treatment plant.

3. STUDYAREA

Guwahati city is located at 26.1445^{o}N latitude and 91.7362^{o}E longitude. Our study is going to confine within the Bharalumukh area of Guwahati. It experiences an average annual temperature of 24.2^{o}C and average rainfall of 1722 lit/m^{2}. The area lies at a height of 55-56 m from the mean sea level.

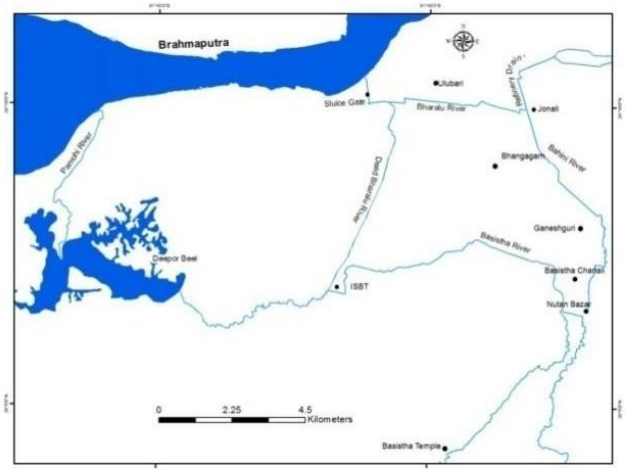

Fig. 1. Study Area Map

4. MATERIALS AND METHODOLOGY

4.1 Material

- GI Screens and racks
- Grit Chamber,
- Skimming Tank,
- sedimentation tanks,
- trickling filter,
- GI Pipes,
- Scrappers,
- Dumper Trucks,
- Pipe Fittings of Different Diameters ranging from 1m to 2m and Valves,
- LED Screen,
- Data updating and monitor system,
- Pressure Pump,
- Flocculent,
- Nuts and Bolts,
- ceramic or plastic filter media,
- M40 Concrete for marine structures,
- solar panels etc.

4.2 Methodology

The methodologies adopted to study the site and the construction of the wastewater treatment plant are as follows-

- **Screen-** The first step in the treatment of sewage is to remove floating debris and suspended matter such as cloth, paper, kitchen refuse, pieces of wood, cork, hair, fiber, faecal solids etc. The objective to achieve in screening is to prevent the formation of unsightly scums in settling tanks. And also to prevent the clogging of sprinkler nozzle, surface of trickling filters etc. For this screens and racks are

which a screen of spacing of about 25mm is first placed and subsequently two or more screens of lesser spacing can be established.

Fig. 2. Mechanical Screening

- **Grit Chamber-** A grit chamber is an RCC structure with enlarged channel or a long basin in which the cross-section is increased gradually to reduce the velocity of sewage flow. This makes the heavier inorganic matter such as grit, sand and gravel of around 0.2 mm or larger to settle. While the organic matter in suspension is made to flow and is not allowed to settle down.
- **Skimming Tank-** A skimming tank is a large chamber so arranged that the floating matter such as oil, grease, fat etc rise and remain in the surface of the sewage until removed, while the liquid flows out continuously under the partition walls or baffles. The rise of floating matter is brought about by blowing air into the sewage from diffusers placed at the bottom. It is necessary to remove the floating matter from sewage otherwise it may appear in the form of unsightly scum on the surface of settling tank or clarifier. The removal of the floating matter can be done by hand or by mechanical scrapping . The chamber consists of a long trough- shaped structure divided up into two or three lateral compartments by vertical baffle walls having slots for a short distance below the sewage surface and permitting oil and grease to escape into stilling compartments. The sewage is made to enter the tank from one end flow through one end having a detention period of about 3 minutes
- **Sedimentation Tank-** The wastewater when flows from the preliminary treatment processes such as screen ,rack, grit chamber and the skimming tank are now allowed to flow into the sedimentation tank, where the fine suspended particles are made to coagulate with the help of chemical substances like the alum, which is economically convenient. The particles are made to settle down on the clarifier bed and later it can be removed mechanically. The size of the sedimentation tank should be sufficiently large enough, so that it can handle maximum discharge during the rainy season; the rectangular shape of the sedimentation tank is proposed, as it matches with the limited available land mass and also the rectangular shape gives the benefit of continuous flow of wastewater into and from the tank. The sludge so produced can be use to make paper and fertilizers based on the present day technologies adopted by a few NGOs based in Guwahati. Those which cannot be use to recycle should be burn in incinerators or can be use to dump in low lying areas.

Fig. 3. Sedimentation Tank

- **Trickling Filter-** The above stated process of preliminary treatment reduces the presence of solid, suspended and colloidal particles to a great extend. The efficiency can be assumed to be approximately 60% -65%. That is a majority of the waste is removed. If sufficient fund is available and if there is minimal inconvenience to set up a large sized trickling filter, the efficiency of the entire wastewater treatment plant can be expected to be about 70%-80%. If a high rate trickling filter is used, with 1-2 re-circulations of the filtered waste;

then the efficiency could be further increased. Today the efficiency of a filter medium can be further increased by using indestructible ceramic and plastic filter media in bed. Moreover as the locality is near the river side, no mechanical aeration is required into the trickling filter, natural ventilation is quite sufficient to minimize the cost of power supply and also to make the plant compact. The power requirement of the trickling filter, sedimentation tank and the entire plant as a whole can be produced by using solar panels to make it self-sufficient. With these steps, when properly executed, can give a maximum approximated efficiency of about 80% and the treated water can be now discharged into the mighty river Brahmaputra. Hence, the amount of sediment deposited by the river Bharalu is minimised and pollution level of the river Brahmaputra is controlled.

Fig. 4. Trickling Filter Technological Advntages-

- Use of LED screen at the downstream of the plant and make it visible to the public, so that the extend of pollution is reduced and the values obtained are within the permissible limits can be analysed.

The values of the pollution level are to be updated and analysed by a monitoring system installed at the downstream of the plant regularly. This is a better and quicker way to check the pollution level instead of conventional board and manual evaluation of the pollution level.

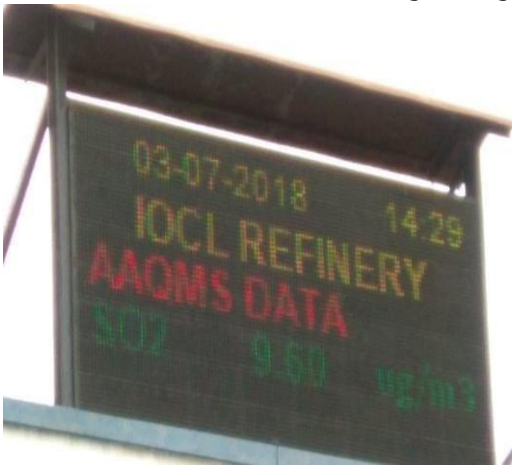

Fig. 5. Display Screen (Courtesy IOCL)

- The use of solar panels is encouraged to make the plant usable independently and for all weather conditions
- The 3 "R's"-Reduce, Reuse and Recycle are encouraged.

RESULTS AND CONCLUSION

The problem of foul smell and water pollution in Bharalumukh area is very severe, affecting the general day to day activities of the people of Guwahati. The research presented in this paper using the methodology which we have discussed viz., the proposal of waste water treatment plant can mitigate this problem to a great extent. It is expected that around 60% to 65% efficiency can be achieved if only primary treatment is done and about 80% can be achieved if we do both primary as well as secondary treatment. Depending upon the fund provided by the government and space available at the site secondary treatment may or may not be done. Even if secondary treatment is done we are supposed to get around 60% improvements. So something is better than nothing. Infact 60% is a good percentage. So we believe if this proposal is accepted we can a get a new scenario of the Bharalumukh area.

ACKNOWLEDGEMENT

The study was carried out by both the authors while studying Bachelor of Engineering (BE) in the department of Civil Engineering at Assam Engineering College, Guwahati for the session 2018. We would like to express our gratitude to Dr. Bipul Talukdar sir, Dr. Jayanta Pathak sir and the

entire faculty members of civil department of Assam Engineering College. We are really overwhelmed by the help of Water Pollution Department (Govt. of Assam). We extend our heartfelt gratitude to GMDA. Special thanks to IOCL. Lastly we would like to express our gratitude to all those who are connected directly or indirectly with our paper and helped in making it a successful one.

REFERENCE

1) Guidelines for Preparation of Project Reports under National River Conservation Plan and National Ganga River Basin Authority. Prepared by Alternate Hydro Energy Centre, Indian Institute of Technology (December 2010).
2) Pollution Control Board, Assam 2010, Detailed Project Report for Conservation of River Bharalu. Prepared by Centre for the Environment, Indian Institute of Technology, Guwahati 2006. City Development Plan (July 2006) by GMDA.
3) Water Supply, Storm Water Drainage, Underground Sewerage & Road Restoration of Guwahati City under JNNURM, Detailed Project Report - Water Supply - South Guwahati Central Tahal Consultant,
4) District Disaster Management Plan, Kamrup Metropolitan district.
5) Eco-restoration strategy for wetlands in Assam: a case study in the southern part of Deepor Beel, Assam, India. Praschaya Kaushik, Department of Urban and Regional planning, CEPT University, Ahmadabad, India
6) Status of Water Quality in India- 2010 by Pollution Control Board
7) Pollution Control Board, Assam Water quality data for Bharalu 2004-2013.
8) Cross-Section of Bharalu, Water Resource Department, Guwahati Mechanical Division.
9) Concession Agreement between GMC and Guwahati Waste Management Company Private Limited with respect to the "Integrated MSW Management System Project", February 2008.
10) Municipal Solid Waste (Management and Handling Rules), 2000 by MoEF, Government of India.
11) Manual on Municipal Solid Waste Management by CPHEEO, MoUD, Government of India.

2nd International Conference of Civil Engineering for Sustainable Development-Opportunities and Challenges
CESDOC-2018, 18th to 19th December, 2018, Assam Engineering College

A study on tolerance and sensitivity of roadside trees to air pollution along a stretch of National Highway 15 at Tezpur, Assam, India

Hazarika, M. [1], Gohain, S. [2], Mahanta, A. [2], Borah, S. [2], Das, C. [2]

[1] Assistant Professor, Department of Civil Engineering, GIMT - Tezpur, Assam, Pin - 784001, India.
[2] UG Student, Department of Civil Engineering, GIMT - Tezpur, Assam, Pin - 784001, India.

ABSTRACT

Today, with the increasing rate of population, massive industrialization there has been a large scale increase of human interaction with environment. Many a times, these interactions have somehow or other disturbed the natural balance of the environment thereby leading to serious threat to human health and loss of its pristine glory, vigor, vitality and utility thus raising the need of studies related to the environment. Different primary pollutants like particulate matter (PM), SO_2, NO_x, emitted from automobile exhausts as well as secondary pollutants like O_3, peroxy acetyl nitrate (PAN) etc. affect the plant tissues on prolonged contact. This study is intended to observe the tolerance and sensitivity of some road side trees to air pollution grown along a particular stretch of National Highway 15 near Tezpur town of Sonitpur district of Assam and compare the characteristics of the same trees grown in a controlled roadside of Borjhargaon area of the same district. For this, nine dominant trees from both the sites were selected and the air pollution tolerance index (APTI) of the leaf samples were determined for a period of 4 months by using four universal bio-chemical parameters, (relative water content, pH ,total chlorophyll content and ascorbic acid content). The monthly APTI values revealed highest in *Ficus bengalensis* (24.36) in controlled site and lowest in *Tectona grandis* (5.30) in the polluted site. The average APTI values of all leaf samples of the trees for 4 months revealed highest in *Ficus bengalensis* (16.86 and 21.32) and lowest in *Ziziphus jujuba* (6.21 and 7.30) both for the polluted site as well as the controlled site. 56% of the trees were found to be moderately tolerant to pollution and 44% were sensitive to pollution at both the sites. A correlation analysis revealed significant positive correlation of average ascorbic acid with APTI ($R^2 = 0.88$; $y = 0.954x – 5.289$) for the polluted site and ($R^2 = 0.84$; $y = 0.959x – 6.265$) for the controlled site which clearly indicates that ascorbic acid has a major impact and is dominant over the other biochemical parameters in abating air pollution of the trees grown across the roadsides. Ascorbic acid plays a key role in cell wall synthesis, cell defense and cell division and is mainly concentrated in the chloroplasts of plants. It is a natural detoxicant and can prevent the effects of air pollutants on plant tissues. So, the tolerant species have higher ascorbic acid content and APTI values as compared to the sensitive ones. Thus, from the present study it can be concluded that *Ficus bengalensis, Cedrus deodara, Neolamarckia cadamba, Mimusops elengi* and *Mangifera indica* were intermediately tolerant to air pollution and can be suggested to be planted along roadsides as a green belt cover for sustainable management of environment in polluted urban areas as well as along national highways so as to make the ambient atmosphere clean and healthy.

Keywords: APTI, biochemical parameters, air pollutants, ascorbic acid content, urban green belt.

1 INTRODUCTION

Living organisms, more specifically human beings are a vital part of the ecosystem that carries the tag of being most intellectual and interacts with the environment in various ways. Humans make use of growing science and technology to exploit the environment for obtaining food, water, fuel, medicines, building materials etc for their benefit. They are so obsessed and possessed of industrial growth for making life easier that the surrounding natural environment has undergone many changes. Air pollution is the buzzword in most of the cities today. Though, various efforts are put into practice to abate air pollution, still the solution seems to be a far cry from reality. Air pollution is caused basically by rapid industrialization, massive plying of vehicular traffic, rapid economic development and high energy consumption. It has a direct impact on the green vegetation due to which the crop yield and the photosynthetic activity decrease. In cities as well as along national highways, different trees can be planted which not only provide fresh air, shade and enhance the aesthetic essence of the city but also act as a sink for air pollutants as well as indicate the presence of any impact of pollution on the public health. In this study, an attempt has been made to study the tolerant and sensitive nature of some roadside plants to air pollution along a stretch of National Highway 15 near Tezpur, Assam by assessing it through a universal parameter, air pollution tolerance index (APTI) and provide suggestive measures to reduce air pollution by planting suitable trees along the outskirts of the city.

2 STUDY AREA

Tezpur, the cultural capital of Assam and the administrative headquarters of the Sonitpur district is

located between 26.6528° N latitude and 92.7926°E longitude at an elevation 48 m (157 ft) from the mean sea level with 40 km^2 area. With a glorious past, clean green surroundings and availability of all amenities for a modern economic city life, Tezpur is a fast growing city on the northern bank of the river Brahmaputra and is the largest of all districts of North Assam with a population of 102,505 as per Census 2011. The average temperature in summer is around 36 °C (97 °F) while the average winter temperature is around 13 °C (55 °F). Tezpur is easily accessible by road, rail and air with rest of the country.

Since the beginning of the work, different sites of Tezpur were surveyed with the primary objective of finding the most polluted site having common road side plant species that is being easily accessible from the work place (GIMT-Tezpur). A total of five polluted sites and a controlled site have been visited and studied to collect the necessary data for the work. After considering the pros and cons, a part of the NH 15 i.e. from Mission-Chariali to Balipara was finally selected as polluted site against the controlled site near from NH 15 to GIMT-Tezpur campus via Borjhargaon. The heavy plying of different vehicles along the NH 15 at different times of the day has made it the most polluted site compared to the other sites surveyed. The site also adds with availability of all the common road side plant species with higher frequency as that of controlled side. Moreover it was highly preferable due to feasibility of sample collection, shortest distance from the college campus where all the tests were carried out.

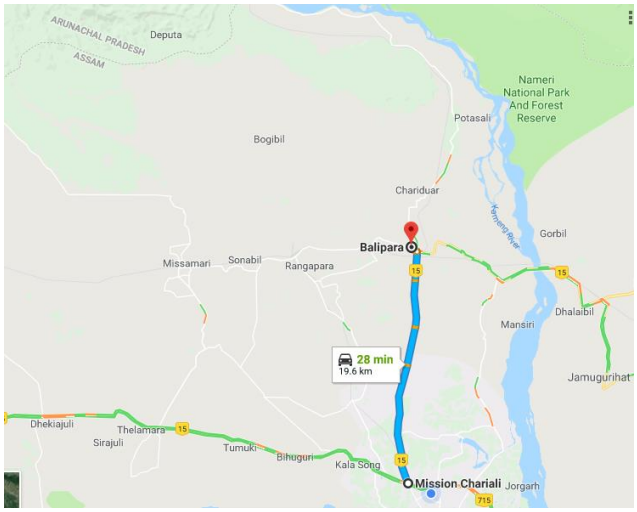

Fig 1: Location of the polluted road site (*Courtesy: Google Maps*)

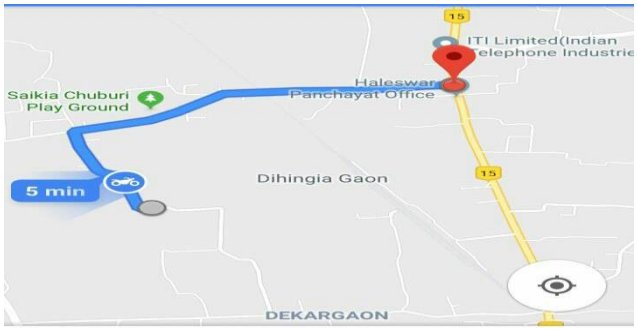

Fig 2: Location of the controlled road site (*Courtesy: Google Maps*)

3 MATERIALS AND METHODS

After proper site selection, it was decided to select the plant species for the study. In view of occurrence of the frequencies of common road side trees, preferring the availability of the ones with greater frequency, nine species namely *Delonix regia, Ziziphus jujuba, Mangifera indica, Ficus bengalensis, Neolamarckia cadamba, Phylanthus emblica, Mimusops elengi, Tectona grandis and Cedrus deodara* were selected based on their common occurrence in both the sites. The leaves of the trees were collected in clean PET bags and transferred to the laboratory. The samples were serially numbered as S1(P) to S9(P) and S1(C) to S9(C), P refer to polluted site sample and C refer to controlled site sample. The samples were preserved in the refrigerator at 4°C for further analysis.

4 RESULTS AND DISCUSSIONS

4.1 Determination of relative water content (RWC)

Relative water content (RWC) is the amount of water present in a leaf relative to its maximum water holding capacity. It is expressed in percentage and determined by taking its fresh weight (FW) first, then immersing in water overnight to get its turgid weight (TW) next day, followed by drying it fully in an oven at 105°C for two hours to get its dry weight (DW). A higher RWC among plants is an indication of high drought resisting capacity during adverse situations. Under stressed conditions when transpiration rates in plants are high, a higher RWC content will help to maintain its physiological balance.

$$\text{RWC} = \frac{\mathbf{FW-DW}}{\mathbf{TW-DW}} \times \mathbf{100} \qquad (1)$$

In the study, it was found that five leaf samples in the polluted and eight leaf samples in the controlled site were found having high water content more than 70% while rest with moderate water content in between 45% to 70%. Similar results were observed by Sisodia A. & Dutta S. (2016).

Table 1: RWC of the polluted site plant species

S/N	Plant species	Sept-17	Oct-17	Nov-17	Dec-17	Avg. RWC	SD (±)
1	*Delonix regia*	69.23	60.37	62.24	57.1	62.24	5.11
2	*Ziziphus jujuba*	58.82	52.72	54.29	52.30	54.53	2.98
3	*Mangifera indica*	73.52	78.78	76.77	68.4	74.37	4.52
4	*Ficus bengalensis*	64.00	82.22	72.65	71.7	72.65	7.47
5	*Neolamarckia cadamba*	85.00	80.43	84.54	77.3	81.81	3.66
6	*Phylanthus emblica*	48.21	75.00	69.14	84.2	69.14	15.27
7	*Mimusops elengi*	80.02	85.71	77.74	67.50	77.74	7.61
8	*Tectona grandis*	65.90	40.00	44.34	48.1	49.59	11.37
9	*Cedrus deodara*	76.90	69.04	74.96	78.9	74.96	4.27

Table 2: RWC of the controlled site plant species

S/N	Plant species	Sept-17	Oct-17	Nov-17	Dec-17	Avg. RWC	SD (±)
1	*Delonix regia*	80.48	76.31	79.1	80.56	79.1	1.98
2	*Ziziphus jujuba*	77.14	54.54	60.3	55.00	61.7	10.59
3	*Mangifera indica*	84.48	77.41	78.3	72.86	78.3	4.78
4	*Ficus bengalensis*	92.73	88.57	86.3	80.55	87	5.08
5	*Neolamarckia cadamba*	81.25	82.86	85	78.92	82	2.57
6	*Phylanthus emblica*	69.23	71.43	72.90	78.04	72.90	3.74
7	*Mimusops elengi*	81.81	83.08	81.7	81.08	81.9	0.84
8	*Tectona grandis*	85.29	75.60	72.7	57.11	72.7	11.69
9	*Cedrus deodara*	80.48	86.11	84.9	88.00	84.9	3.19

4.2 Determination of leaf extracts pH

The leaf extracts pH is a measure of tolerance and sensitivity with regard to air pollution. Stomatal activity of the plants changes due to change in leaf extract pH. It also helps in regulating SO_2 sensitivity in plants. In presence of an acidic pollutant, pH gets reduced and the decline is more in sensitive species. In the laboratory, pH was determined by crushing nearly 1g of the leaf in mortar and pestle, diluting it with distilled water and filtered properly. The filtrate so collected was tested in a digital pH meter at 25°C.

Table 3: pH of the polluted site plant species

S/N	Plant species	Sept-17	Oct-17	Nov-17	Dec-17	Avg. pH	SD (±)
1	*Delonix regia*	7.05	8.07	7.80	8.40	7.83	0.57
2	*Ziziphus jujuba*	6.82	6.46	6.23	5.23	6.18	0.68
3	*Mangifera indica*	6.86	6.41	6.39	5.56	6.31	0.54
4	*Ficus bengalensis*	7.78	9.83	9.89	9.68	9.29	1.01
5	*Neolamarckia cadamba*	5.31	5.77	5.45	5.54	5.52	0.19
6	*Phylanthus emblica*	4.66	4.87	4.37	4.82	4.68	0.23
7	*Mimusops elengi*	7.30	9.15	8.97	9.50	8.73	0.98
8	*Tectona grandis*	8.29	11.32	10.55	9.78	9.98	1.29
9	*Cedrus deodara*	7.59	8.98	8.72	8.36	8.41	0.60

S/N	Plant species	Sept-17	Oct-17	Nov-17	Dec-17	Avg. pH	SD (±)
1	*Delonix regia*	7.70	7.89	7.92	8.00	7.88	0.13
2	*Ziziphus jujuba*	6.30	6.61	6.32	5.72	6.24	0.37
3	*Mangifera indica*	6.18	6.52	6.48	5.74	6.23	0.36
4	*Ficus bengalensis*	8.94	10.26	10.11	9.85	9.79	0.59
5	*Neolamarckia cadamba*	5.73	5.72	5.78	5.67	5.72	0.05
6	*Phylanthus emblica*	4.24	5.50	4.67	5.80	5.05	0.72
7	*Mimusops elengi*	7.74	9.83	9.21	9.80	9.14	0.98
8	*Tectona grandis*	8.86	8.35	8.63	9.26	8.78	0.38
9	*Cedrus deodara*	7.49	7.87	7.78	8.01	7.79	0.22

Table 4: pH of the controlled site plant species

4.3 Determination of total chlorophyll (TChl) content

Chlorophyll, being the green pigment in leaves, its change in colour at different seasons can be used to identify the intensity of stress on being exposed to air pollutants. In the study, 0.5g of the fresh leaves were grounded and diluted to 10ml in distilled water. A sub-sample of 2.5ml was mixed with 10ml acetone and filtered. The filtrate so obtained was transferred to a UV-Spectrophotometer to calculate the optical density (OD) at 645 nm and 663 nm wavelength.

$$\text{Optical density, } C_T = 20.2(D_{645}) + 8.02(D_{663}) \quad (2)$$

$$\text{TChl content} = 0.1\ C_T \times (DW/FW) \quad (3)$$

Table 5: TChl content of the polluted site plant spec

S/N	Plant species	Sept-17	Oct-17	Nov-17	Dec-17	Avg. TChl	SD (±)
1	*Delonix regia*	2.80	2.78	1.42	1.30	2.07	0.83
2	*Ziziphus jujuba*	0.34	0.36	0.17	0.19	0.26	0.10
3	*Mangifera indica*	0.62	0.68	0.31	0.47	0.52	0.17
4	*Ficus bengalensis*	1.28	1.32	0.77	0.83	1.05	0.29
5	*Neolamarckia cadamba*	1.33	1.28	0.62	0.51	0.93	0.43
6	*Phylanthus emblica*	3.67	4.10	3.01	2.46	3.31	0.72
7	*Mimusops elengi*	0.86	0.86	0.73	0.61	0.76	0.12
8	*Tectona grandis*	0.81	0.79	0.47	0.44	0.63	0.20
9	*Cedrus deodara*	3.69	3.53	1.01	1.45	2.42	1.39

The TChl content of the plant species was determined by a procedure recommended by Liu and Ding (2008).TChl content is expressed in mg/g of DW.

Table 6: TChl content of the controlled site plant species

S/N	Plant species	Sept-17	Oct-17	Nov-17	Dec-17	Avg. TChl	SD (±)
1	*Delonix regia*	3.20	3.33	1.22	1.13	2.22	1.21
2	*Ziziphus jujuba*	0.48	0.42	0.20	0.23	0.33	0.14
3	*Mangifera indica*	0.64	0.72	0.39	0.51	0.56	0.15
4	*Ficus bengalensis*	1.52	1.41	0.93	0.90	1.19	0.32
5	*Neolamarckia cadamba*	1.64	1.30	0.60	0.57	1.03	0.53
6	*Phylanthus emblica*	4.24	4.57	2.42	2.31	3.38	1.19
7	*Mimusops elengi*	0.91	0.92	0.65	0.69	0.79	0.14
8	*Tectona grandis*	0.88	0.83	0.48	0.50	0.67	0.21
9	*Cedrus deodara*	3.78	3.72	1.57	1.51	2.64	1.28

4.4 Determination of ascorbic acid (AA) content

Ascorbic acid (or Vitamin C) is a naturally occurring organic compound having antioxidant properties. A higher ascorbic acid content in plants is an indication of tolerance against SO_2 pollution and lower ascorbic acid content indicates the sensitive nature of plants to air pollutants particularly automobile exhausts as observed by Chaudhary and Rao (1977). Ascorbic acid was determined by the titrimetric method formulated by Sadasivam (1997) using 2,6-dichlorophenol-indo phenol dye. 0.5g of the leaf sample was extracted with 4% oxalic acid solution and titrated against the dye until a pink colour appears. A separate 0.5g leaf sample is again extracted in with 4% oxalic acid and the volume is made upto 50ml and filtered to separate the solid particles present in leaf extract. A sub-sample of 5ml is taken and again titrated against the dye until a pale pink colour with bubbles is formed which marks the end point of titration.

Table 7: AA content of the polluted site plant species

S/N	Plant species	Sept-17	Oct-17	Nov-17	Dec-17	Avg. AA	SD (±)
1	*Delonix regia*	1.70	1.20	1.50	1.80	1.55	0.26
2	*Ziziphus jujuba*	1.35	1.39	1.17	0.70	1.15	0.32
3	*Mangifera indica*	9.72	11.82	14.76	13.10	12.35	2.13
4	*Ficus bengalensis*	10.63	9.21	8.92	8.46	9.30	0.94
5	*Neolamarckia cadamba*	13.74	12.44	12.98	14.26	13.35	0.81
6	*Phylanthus emblica*	2.00	0.50	0.97	1.30	1.19	0.63
7	*Mimusops elengi*	11.37	7.80	10.45	6.78	9.10	2.16
8	*Tectona grandis*	2.54	1.08	1.66	1.23	1.68	0.66
9	*Cedrus deodara*	9.12	8.12	9.08	8.16	8.62	0.55

Table 8: AA content of the controlled site plant species

S/N	Plant species	Sept-17	Oct-17	Nov-17	Dec-17	Avg. AA	SD (±)
1	*Delonix regia*	3.50	0.80	1.10	1.00	1.60	1.27
2	*Ziziphus jujuba*	1.85	1.40	1.75	1.91	1.73	0.23
3	*Mangifera indica*	11.82	12.89	14.93	14.07	13.43	1.36
4	*Ficus bengalensis*	14.43	9.89	10.56	11.34	11.55	2.01
5	*Neolamarckia cadamba*	14.55	15.10	13.87	14.80	14.58	0.52
6	*Phylanthus emblica*	1.23	1.00	1.73	2.30	1.56	0.58
7	*Mimusops elengi*	10.96	7.69	10.87	6.44	8.99	2.28
8	*Tectona grandis*	1.57	0.53	0.96	0.48	0.88	0.50
9	*Cedrus deodara*	9.50	7.83	8.72	8.88	8.73	0.69

4.5 Determination of air pollution tolerance index (APTI)

APTI is a parameter to assess the plants resistivity and susceptibility on being exposed to different air pollutants like PM10, O_3, SO_2, CO, NO_2. The air pollution effects are high in sensitive plants and low in tolerance plant species. The air pollution tolerance index of the present study is determined by the method of Singh and Rao (1983). The formula for APTI is given by;

$$APTI = \frac{\{A(T+P)+R\}}{10} \quad (4)$$

where, A is the ascorbic acid content (mg/g); T is the total chlorophyll content (mg/g); P is the leaf extracts pH & R is the relative water content (%).

Table 9: Range of APTI (Chaudhary and Rao, 1977)

Range of APTI	Response
Less than 1	Very sensitive
Between 1 to 16	Sensitive
Between 16 to 30	Intermediately tolerant
Between 30 to 100	Tolerant

Table 10: APTI of the polluted site plant species

S/N	Plant species	Sept-17	Oct-17	Nov-17	Dec-17	Avg. APTI	SD (±)
1	*Delonix regia*	8.59	7.33	7.61	7.46	7.75	0.57
2	*Ziziphus jujuba*	6.85	6.21	6.18	5.61	6.21	0.51
3	*Mangifera indica*	14.60	16.25	17.56	14.74	15.79	1.40
4	*Ficus bengalensis*	16.03	18.49	16.85	16.06	16.86	1.15
5	*Neolamarckia cadamba*	17.63	16.81	16.33	16.35	16.78	0.61
6	*Phylanthus emblica*	6.49	7.94	7.63	9.36	7.85	1.18
7	*Mimusops elengi*	17.27	16.32	17.91	13.60	16.27	1.90
8	*Tectona grandis*	8.90	5.30	6.26	6.07	6.63	1.57
9	*Cedrus deodara*	17.97	17.06	16.33	15.89	16.81	0.91

Table 11: APTI of the controlled site plant species

S/N	Plant species	Sept-17	Oct-17	Nov-17	Dec-17	Avg. APTI	SD (±)
1	*Delonix regia*	11.86	8.52	8.92	8.96	9.56	1.54
2	*Ziziphus jujuba*	8.96	6.43	7.17	6.63	7.30	1.15
3	*Mangifera indica*	16.51	17.07	18.08	16.08	16.93	0.86
4	*Ficus bengalensis*	24.36	20.39	20.28	20.24	21.32	2.03
5	*Neolamarckia cadamba*	18.84	18.88	17.35	17.12	18.05	0.94
6	*Phylanthus emblica*	7.96	8.15	8.53	9.66	8.57	0.76
7	*Mimusops elengi*	17.66	16.78	18.88	14.86	17.04	1.69
8	*Tectona grandis*	10.06	8.04	8.14	6.17	8.10	1.59
9	*Cedrus deodara*	18.75	17.68	16.64	17.25	17.58	0.89

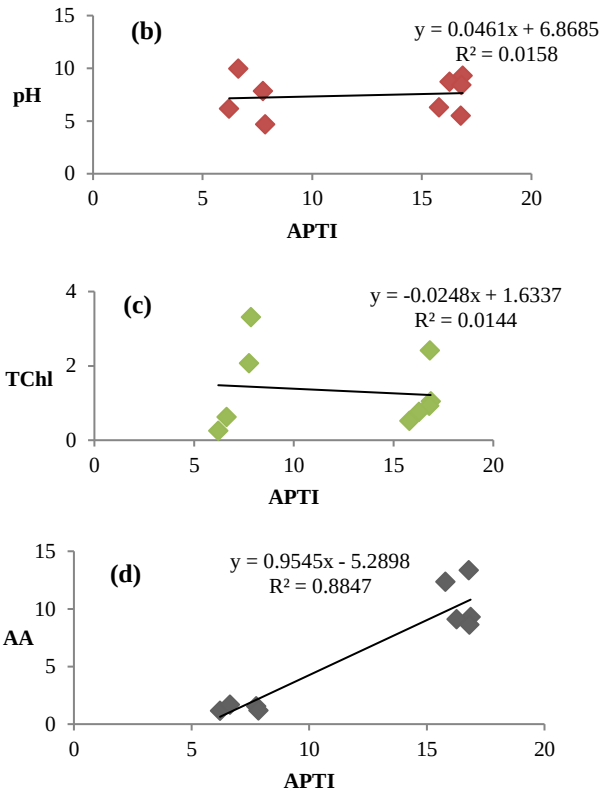

Fig. {3(a-d)} Correlation between APTI and the parameters for the polluted site

4.6 Correlation between avg. APTI & RWC, pH, TChl and AA for the plants at the polluted and controlled site

A linear correlation analysis revealed that ascorbic acid content is the dominating factor in changing the behaviour of different plants on a monthly basis since it is a major metabolite in plants and protects the plants from oxidative damage resulting from aerobic metabolism, photosynthesis and a range of pollutants. Greater the ascorbic acid content in plants, greater is its potential to tolerate pollution. Ascorbic acid (AA) showed significant positive correlation with APTI (R^2 = 0.88, $p \leq 0.01$) for the polluted site and (R^2 = 0.84, $p \leq$ 0.01) for the controlled site compared to correlation between APTI and RWC (R^2 = 0.77, $p \leq 0.01$). The leaf extract pH and TChl content did not showed any significant correlation with APTI.

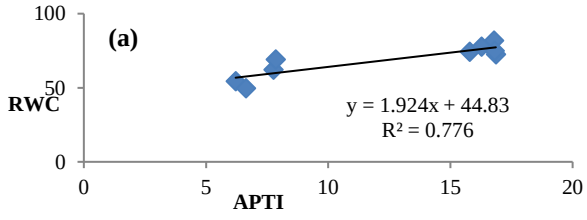

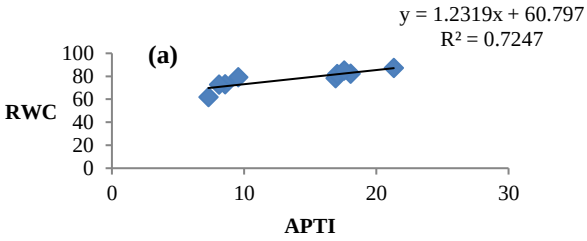

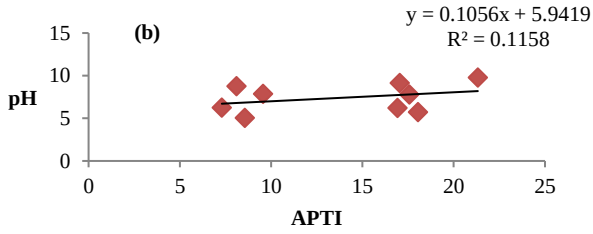

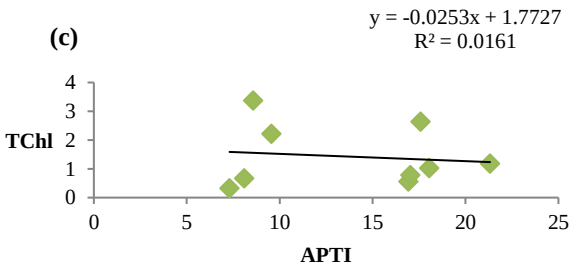

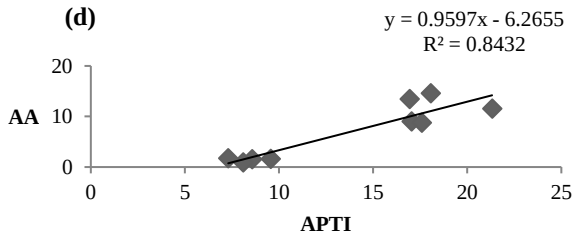

Fig. {4(a-d)} Correlation between APTI and the parameters for the controlled site

5 CONCLUSIONS

From the present study it can be concluded that *Ficus bengalensis, Neolamarckia cadamba, Cedrus deodara, Mimusops elengi* and *Mangifera indica* were found to be intermediately tolerant with highest average APTI in *Ficus bengalensis* of about 21.32 and 16.86 at polluted and controlled site respectively. Rest of the plant species; *Delonix regia, Phylanthus emblica, Tectona grandis, Ziziphus jujuba* were sensitive with APTI ranging from 5 to 16. *Ziziphus jujuba* with average APTI of about 6.21 & 7.30 at the polluted & controlled site respectively was found to be most sensitive among the species studied. It was obvious to have higher APTI value in the controlled site than on polluted site and so these plants can be used as indicators of pollution. Also from the correlation analysis, ascorbic acid is seen as a dominating bio-chemical parameter over others in tolerating pollution and is significantly correlated (R^2 = 0.88, $p \leq 0.01$) for the polluted site and (R^2 = 0.84, $p \leq$ 0.01) for the controlled site respectively. The identification of tolerant plant species reveals it to be planted suitably for green-belt development and social-forestry programs to reduce the growing pollution in today's world.

REFERENCES

1) Chaudhury, C.S., & Rao, D.N. (1977). "Study of some factors in plants controlling their susceptibility to SO2 pollution." In *Proceedings of Indian National Science Academy, 43*: pp: 236-241
2) Das, S., & Prasad, P. (2010). "Seasonal variation in air pollution tolerance indices and selection of plant species for industrial areas of Rourkela". *Indian Journal of Environmental Protection, 30*(12), pp: 978-988.
3) Department of Biology, East China Normal University, Experiment instruction of plant physiology, People's Education Press, 1980.
4) Dehury, S.S., Das, S., Mallick, S.N., Padhi, S.K., Acharya, B.C., & Prasad, P. (2010). "Air Pollution Tolerance Indices (APTI) of Various Plant Species Growing in Industrial Areas of Rourkela". *Indian Journal Environmental Protection, 30*(7), pp: 563-567.
5) Deswal, S., & Kumari J. (2017). "Assessment of Air Pollution Tolerance Index of Selected Plants Unveil To Traffic Roads of Noida, Uttar Pradesh". *International Journal on Emerging Technologies, 8*(1), pp: 179-184.
6) Liu, Y., & Ding H. (2008). "Variation in air pollution tolerance index of plants near a steel factory: Implications for landscape plant species select ion for industrial areas". *Wseas Transactions on Environment and Development, 4*(1), pp: 24-32.
7) Mohan, G.V.K. (2013). "Identification of plant species for bio-monitoring of Air Pollution at Visakhapatnam". *Indian Journal of Applied Research, 3*(8), pp: 69-71.
8) Rai, P.K., & Panda, L.L.S. (2013). "Dust capturing potential and air pollution tolerance index (APTI) of some road side tree vegetation in Aizawl, Mizoram, India: An Indo-Burma hot spot region". *Air Quality Atmosphere and Health, 7*(1), pp: 93-101.
9) Robinson, M.F., Heath, J., & Mansfield, T.A. (1997). "Disturbances in stomatal behavior caused by air pollutants". *Journal of Experimental Botany, 49*(March), pp: 461-469.
10) Sadasivam, S. and Manickam, A. (1997). "Estimation of dehydroascorbic acid". *Biochemical Methods*, pp: 184-186.
11) Singh, S.K., & Rao D.N. (1983). "Evaluation of plants for their tolerance to air pollution". In *proceedings symposium on Air Pollution Control, Indian Association for Air Pollution Control*, 1, pp: 218-224.
12) Singh, V. (2013). "Role of medicinal plant in controlling environmental (air) pollution". *International Ayurvedic Medicinal Journal, 1*(5), pp: 1-7.
13) Sisodia, A., & Dutta, S. (2016). "Air Pollution Tolerance Index of certain plant species: A study of National Highway No-8, India". *Journal of Environmental Research and Development, 10*(4), pp: 723-728.
14) Tiwari, S., & Tiwari, M. (2006). "Air Pollution Tolerance Indices of few plants growing near Raigarh (India)". *Journal of Environmental Research and Development, 1*(2), pp: 129-135.
15) Varshney, S.R.K., & Varshney, C.K. (1984). "Effects of SO_2 on ascorbic acid in crop plants". *Environment Pollution Series A, Ecological and Biological, 35*(4), pp: 285-290.

Reduction of arsenic concentration in water using locally available materials

Nath, P.[1], Lunawat, R.[1], Saleh, R.N.[1], Devi, P[1], Dey, Y.[2]

[1]UG Student, Department of Civil Engineering, Royal School of Engineering & Technology, Guwahati-781035, India.
[2]Assistant Professor, Department of Civil Engineering, Royal School of Engineering & Technology, Guwahati-781035, India.

ABSTRACT

The metalloid arsenic is a natural environmental contaminant to which humans are routinely exposed. In many areas of the world, high levels of arsenic are present in drinking water and is a major concern. Acute effects of arsenic range from gastrointestinal distress to cancer. Depending on the duration of exposure, arsenic may affect several major organ systems. Although arsenic occurs naturally in the environment, their concentration has increased and they have become more widely distributed because of human activities. The World Health Organization has labelled increasing arsenic in the biosphere as the worst mass poisoning in history.

A recent survey showed that 20 districts of Assam are facing arsenic contamination and are at risk of arsenic poisoning due to the presence of excess arsenic in the groundwater. Although the government has already implemented many piped-water projects to supply safe drinking water in the arsenic affected habitations but only a few areas could be covered under these projects. Hence, a simple and easy method of purification which have easy accessibility to every affected locality has been chosen for study in this project work.

This report gives a brief insight into the techniques or phenomenon that can be been used for removal of arsenic from water and also discusses about two of the tests to determine arsenic concentration in water. In this project, the technique used for minimizing arsenic is adsorption. Different proportions of red soil, bentonite and water spinach (Water spinach) are used as adsorbents in trials for preparation of the filter beds. Some of the groundwater samples of the arsenic affected areas (Nalbari District) were analysed and the one having the highest concentration among them was taken up for study. The results obtained before and after the filtration were analysed and thus a co-relation between discharge, arsenic concentration and different filter media was drawn out.

Keywords:, Arsenic, Bentonite, filtration, red soil, skin diseases, water spinach

1. INTRODUCTION

Arsenic contamination of groundwater in different parts of the world is an outcome of natural and anthropogenic sources, leading to adverse effects on human health and ecosystem. Millions of people from different countries are heavily dependent on groundwater containing elevated level of Arsenic for drinking purposes. Arsenic contamination of groundwater possesses a serious risk to human health. Excessive and prolonged exposure of inorganic Arsenic with drinking water is causing arsenicosis, a deteriorating and disabling disease characterized by skin lesions and pigmentation of the skin, patches on palm of the hands and soles of the feet. Arsenic poisoning culminates into potentially fatal diseases like skin and internal cancer. This project includes the problem of arsenic contamination in the North-East region of India, Assam to be specific and also its treatment using soil as a filtering material. The project also critically reviews the Arsenic led human health risks. The project provides an overview of the state-of-the-art knowledge on the alternative Arsenic free drinking water and various technologies (oxidation, coagulation flocculation, adsorption, and microbial) for mitigation of the problem of As contamination of groundwater.

Arsenic contamination of groundwater in 20 of the 33 districts of Assam has been detected, said Public Health Engineering Department (PHED). Arsenic is highly toxic in its inorganic form. Contaminated water used for drinking, food preparation and irrigation of food crops possesses the greatest threat to human health from arsenic. Long-term exposure to arsenic from drinking-water and food can cause cancer and skin lesions. It has also been associated with developmental effects, cardiovascular disease, neurotoxicity and diabetes. The most important action in affected communities is the prevention of further exposure to arsenic by provision of a safe water supply. Government has taken up new water supply schemes in the worst arsenic affected districts taking surface water sources as the base. The contaminated groundwater sources in those districts have been discarded. Search for alternative surface water sources are also on. In many cases, shallow ring wells have also been provided to replace the hand pumps that are installed on the

contaminated groundwater sources.

The schemes taken up by government has a slow reach to areas affected by arsenic. Hence a simple and easy method of purification has to be introduced which has easy accessibility to every affected locality. Some of the materials that can be used to remove arsenic and are easily available are red soil, bentonite powder and water spinach (water spinach). The right soil just needs to be identified and a proportioned mixture of red soil, bentonite and water spinach has to be put into use for purification work.

2. METHODS AND METHODOLOGY

The main objective of this chapter is to discuss about the materials and methods that were to be used for the preparation of filter for removal of arsenic. Hence for the work, the chapter has been divided mainly into several subparts or steps. The first subpart consists of selection of the area affected by arsenic and taking sample for initial arsenic concentration and also collecting extra water for filtration purpose. The next part following the collection of water sample was the collection of the filter media constituents i.e. Red Soil, Bentonite and Water Spinach. The third part aims at the preparation of the constituent materials as per the required specification so as to be used in the filter bed. In this part the complete methodology of the preparation of each ingredient were discussed. The method or the technique on which the filter works was adsorption. Higher was the surface area, higher was the adsorption. The last part comprises of preparation of filter media of different proportions through which the collected arsenic contaminated water was passed through and the water after filtration was collected for test.

2.1. Water Sample Collection

In the first phase, samples of water were collected from source where there was possibility of finding arsenic in the ground water. A survey by Public Health Engineering Department (PHED) Assam indicated that approximately 95% of the groundwater of Nalbari district of Assam was having arsenic contamination above the permissible limit of 0.01 ppm or 10 ppb which was the maximum permissible limit as per World Health Organisation(WHO). The water samples were collected in samplers of plastic bottles and were acidified within 2 minutes with conc. HCl to lower the pH of the sample below 2. The concentration of arsenic in the samples was determined and noted. The sample with higher arsenic concentration was taken for our study. The water for filtration was thus collected from the source having higher arsenic concentration.

Table 1: Survey for arsenic in Nalbari, Assam

Sample Number	Pin Point Location	Village	Type of Source	GPS Co-ordinate
Sample 1	Adarsha Vidya MES	Danguapara	THP	26.480N 91.390E
Sample 2	3 No. Danguapara LPS	Danguapara	THP	26.477N 91.381E
Sample 3	199 No. Burinagar Jr. Basic	Burinagar	HTW	26.488N 91.406E
Sample 4	Dharani Kalita	Sandha Kairara	HTW	26.454N 91.468E
Sample 5	MNC LP School	Bhelamari	THP	26.549N 91.480E

THP= TARA HAND PUMP
HTW=HAND TUBE WELL

2.2. Adsorbent materials

The materials red soil, bentonite and water spinach which were very good adsorbents of arsenic were collected and used in the filtration process.

- Red soil is a type of soil that develops in a warm, temperate, moist climate under deciduous or mixed forest, having thin organic and organic-mineral layers overlying a yellowish-brown leached layer resting on an alluvial red layer.
- Bentonite is actually composed of ash made from volcanos. The largest known source of bentonite clay is found in Fort Benton, Wyoming, where numerous volcanos were present. Bentonite is very fine providing high surface area for adsorption. It is an absorbent aluminium phyllosilicate clay consisting mostly of montmorillonite. Bentonite clay readily available in market is collected.
- Ipomoea aquatic, widely known as water spinach is a semiaquatic, tropical plant grown as a vegetable for its tender shoots and leaves. It is found throughout the tropical and subtropical regions of the world, although it is not known where it originated. Water spinach is most commonly grown in East, South and Southeast Asia. It flourishes naturally in waterways and requires little, if any, care. It is very commonly

found in water bodies like *beel*, pond, lakes, etc. In Assam it is locally called *water spinach*.

2.3. Filter setup

An iron frame with three trays was prepared for the filtration process. The filter bed was allowed to rest on the second tray which was again made porous with holes of diameter of 4mm, distributed uniformly. The other tray was for collecting the water. The trays were made of 1.21 mm thick iron sheets having a dimension of 381mm x 381mm x 76.2mm. Filter cloth of 300 micron was used between the materials of filter media and the tray.

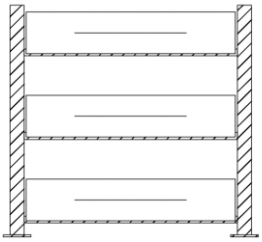

Figure 1: Front View of Stand

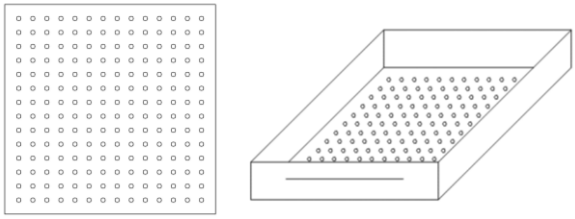

Figure 2: Plan View and Isometric View of Tray

2.4. Materials preparation

Two of the three materials that were used in the filter bed requires separate preparation for use in the filter:

a) Water Spinach:
Water spinach, locally known as *kolmou shak* was procured from the local market and was dried under sunlight for 7 days. The leaves were plucked out of and using a mixer grinder, the leaves and stem were crushed down to small particles until they were of even size.

b) Red Soil:
The red soil was located nearby the Royal School of Engineering & Technology and dug out and collected. The coordinate of the location of the soil was 26.11127N, 91.72609E. The soil was then sieved in the laboratory. The soil lumps were crushed and sieved with IS Sieve 2mm. The IS Sieve 2mm passing soil was taken for the use in preparation of filter media.

2.5. Filter media preparation

The filter media is prepared by using the three materials, red soil, bentonite and *water spinach*. For experimentation, total weight of the material composition was assumed to be 3200 gm. The materials were then taken in different proportions as mentioned in the table below.

Table 2: Experimental Design Composition

Trial Number	Red Soil (in gms)	Bentonite (in gms)	Water Spinach (in gms)
Trial 1	2500	600	100
Trial 2	2000	1000	200
Trial 3	1500	1400	300
Trial 4	1000	1800	400
Trial 5	500	2200	500

2.6. Filtering water sample

Initially the filter media was made saturated by passing distilled water through so as there was no adsorption and since the filter media will be saturated, the discharge will increase. Once the layers were saturated properly, arsenic contaminated water was let to pass through the beds..

2.7. Sampling for tests

The filtered water was sampled in two ways, acidified sample and non-acidified sample. Acidified sample was useful for test using Spectrophotometer and non-acidified sample was useful for Atomic-Absorption Spectroscopy. The test for the determination of concentration was finally carried out with Atomic-Absorption Spectroscopy (AAS) method with the non-acidified sample.

3. RESULTS

The arsenic contaminated samples after filtration were tested with Atomic Adsorption Spectrum(AAS) and the results thus obtained are as mentioned in the table 3.

Table 3: Results of initial arsenic concentration of Survey

Sample Number	Pin Point Location	Initial Arsenic Conc. in ppm
Sample 1	Adarsha Vidya MES	0.070

Sample 2	3 No. Danguapara LPS	0.068
Sample 3	199 No. Burinagar Jr. Basic	0.091
Sample 4	Dharani Kalita	0.072
Sample 5	**MNC LP School**	**0.094**

3.1. Results

The table below shows the result of concentration of arsenic, discharge and proportions of materials used for filtration.

Table 4: Final Results of Arsenic Concentration after filtration

Trial Number	Red Soil in gms	Bentonite (in gms)	Water spinach (in gms)	Arsenic Con. in ppm	Discharge in ml/min
Sample 5	-	-	-	-	-
Trial 1	2500	600	100	0.0150	165
Trial 2	2000	1000	200	0.0188	130
Trial 3	1500	1400	300	0.0193	210
Trial 4	1000	1800	400	0.0195	85
Trial 5	500	2200	500	0.0207	575

3.2. Comparative evaluation

Comparative evaluations may be drawn on the results of final concentration of the arsenic adsorbed obtained for each trial composition beds. The results comparison is shown in table below.

Table 5: Comparison of results

Trial Number	Initial Conc. in ppm	Final Arsenic Conc. in ppm	Percentage Adsorption	Discharge in ml/min
Trial 1	**0.0222**	**0.0120**	**45.95**	**165**
Trial 2	0.0222	0.0188	15.31	130
Trial 3	0.0222	0.0193	13.06	210
Trial 4	0.0222	0.0195	12.16	85
Trial 5	0.0222	0.0207	6.76	575

3.3. Comparison between trials and discharge

From the figure it is seen that discharge decreases with the reduction in the amount of red soil and increment of water spinach and bentonite powder up to trial number 3. After that, with further decrease in red soil till trial number 5, the discharge again increases.

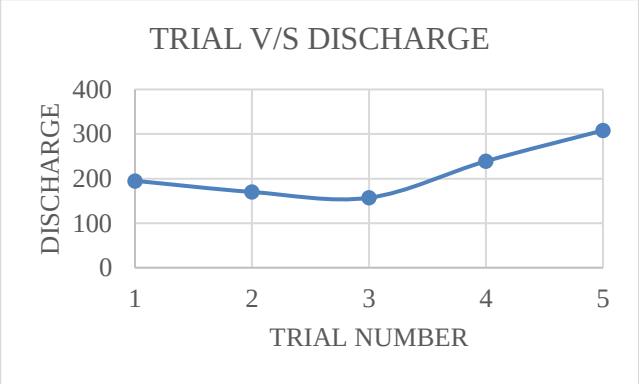

Figure 3: Plot of Trial v/s Discharge

3.4. Comparison between trials and concentration

From Figure 5.2, the trend of concentration of arsenic in water after filtration is that it has highest value for trial number 3 and the lowest value is seen for trial number 1.

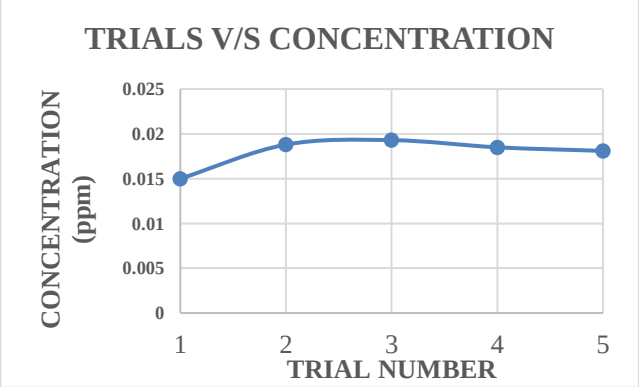

Figure 4: Plot of Trial v/s Concentration

4. CONCLUSION

The main purpose of the project was to prepare a low-cost filter for removal or minimization of arsenic

from ground water sample collected from the arsenic affected areas. It can be observed that there is a vast difference between the initial arsenic concentration of the same sample via two different methods. The more accurate method for finding out the concentration of arsenic is the AAS method, hence the results of the AAS methods were taken to be final and binding.

In the results obtained, it was seen that the concentration of arsenic was reduced from its initial value, which was the purpose of the project. The criteria used to select the best trails out of the five different filter media composition were concentration of arsenic after filtration and discharge, concentration being more important.

Analyzing the data, it can be concluded that the trial number 1, i.e. filter bed with 2500gm of red soil, 600 gm of bentonite powder and 100 gm of water spinach has the least arsenic concentration after filtration or adsorbs maximum amount of arsenic. The discharge from trial 5 is maximum but Arsenic concentration is higher than trial 1, hence it is discarded. The best trial is taken to be trial number 1 since the adsorption is maximum and discharge is also considerable, i.e. 165 ml/minute.

Table 6: Estimated cost of Arsenic filter

Sl. No.	Description	Quantity	Amount (in Rupees)	Remarks
		FIXED COST		
1	Iron Setup for Filter	1	2000.00	Onetime expense
2	Enamel coating Coat	1L	180.00	Onetime expense
	Total Fixed Cost		**2180.00**	
		OPERATION COST		
1	Red Soil	2500 gm	-	Available Locally
2	Bentonite	600 gm	3.00	Rs.250 per 50kg
3	Water Spinach	100 gm	41.00	Rs.410 per kg
4	Filter Cloth of 300micron	1M	80.00	Rs.80 per meter
	Total Operation Cost		**124.00**	**(Approx)**

REFERENCES

1) Sarma, J. and Goswami, A.S. "Arsenic Removal From Water by Adsorption Utilizing Natural Kaolinite Clay of Assam", Research Journal of Chemistry and Environment Vol.15 (2), June 2011(559-563).
2) Sarma, J. and Goswami, A.S. "Study of the Removal of Toxic Anions from Contaminated Water Utilizing Natural Kaolinite Clay of Assam", International Journal of Research in Chemistry and Environment Vol. 1(2), October 2011(92-96)
3) Sarma, J. and Ganguli, M. "Catalytic activity of natural kaolinite clay of Karbi-Anglong District of Assam", Journal of Chemistry and Chemical Engineering.Vol.5(12) 2011 (1116-1121)
4) Rahman, I.M.; Begum, Sawai, Z.A.K.; Maki, T. and Hasega, H. "Decontamination of spent iron-oxide coated sand from filters used in arsenic removal", Chemosphere Vol.92(2), June 2013 (196-200)
5) Mandal, S.; Sahu, M.K.; Patel, R.K. "Adsorption studies of arsenic(III) removal from water by zirconium polyacrylamide hybrid material (ZrPACM-43)", Water Resources and Industry Vol.4, December 2013 (51-67)
6) Singh, R.; Singh, S.; Parul Parihar, Singh, V.P. and Sheo Mohan Prasad, "Arsenic contamination, consequences and remediation techniques", Ecotoxicology and Environmental Safety Vol 112, February 2015 (247-270)
7) Vrajesh S.Mehta, V.S. and Chaudhari, S.K. "Arsenic removal from simulated groundwater using household filter columns containing iron filings and sand", Journal of Water Process Engineerng Vol.6, June 2015 (151-157).
8) Choi, J.; Lee, E.; Choi, S.Q.; Lee, S; Han, Y and Kim, H. "Aesenic removal from contaminated soils for recycling via oil agglomerate flotation", Chemical Engineering Journal Vol.285, February 2016 (207-217)
9) Mishra, T. and Mahato, D.K. "A comparative study on As(V) and As(III) removal by iron oxide and manganese oxide pillared clays from ground water", Jornal of Environmental Chemical Engineering Vol.4(1), March 2016 (1224-1230)
10) Clare, Mahon, J.M. and Gill, L.W. "Development of a continuous flow solar oxidation process for the removal of arsenic for sustainable rural water supply", Journal of Environmental Chemical Engineering Vol.4(1), March 2016 (1181-1190)
11) Aranda, P.R.; Llorens, I.; Perino, E.; Vito, I. and Raba, J. "Removal of arsenic(V) ions from aqueous media by adsorption on multiwall carbon nanotubes thin film using XRF technique", Environmental Nanotechnology, Monitoring & Management Vol.5, May 2016 (21-26)
12) Mandal, P.; Debbarma, S.R.; Saha, A. and Ruj, B. "Disposal Problem of Arsenic Sludge generated during Arsenic removal from drinking water", Procedia Environmental Sciences Vol.35, 2016 (943-949)
13) Mólgora, C.C., Domínguez, A.M., Avila, E.M.; Drogui, P. and Buelna, G. "Removal of arsenic from drinking water: A comparative study between electrocoagulation-microfiltration and chemical coagulation-microfiltration processes", Separation and Purification Technology Vol.118, October 2016 (645-651)
14) Banerji, T., Chaudhari, S. "Arsenic removal from drinking water by electrocoagulation using iron electrodes- an understanding of the process parameters", Journal of Environmental Chemical Engineering Vol.4(4 Pt.A), December 2016 (3990-4000)
15) Nidheesh, P.V. and Singh, T.S.A. "Arsenic removal by electrocoagulation process: Recent trends and removal mechanism", Chemosphere Vol.181, August 2017 (418-432)

Sustainable Ecosystem Management

Sustainable change and adaptation

A new curve for encapsulating the normalized difference vegetation index

Kalita, D. N.

Consultant, L&T Power Development Ltd., Delhi-Mathura Road, Faridabad 121003, India.

ABSTRACT

The normalized difference vegetation index (NDVI) is a simple graphical indicator of plant greenness and is one of the most commonly used vegetation indices. NDVI has been one of the many successful applications of remote sensing data to real world problems in diverse fields - agriculture, forestry, environment etc. The index has been able to attract hydrologists also, due to its potential to account for spatiotemporal land cover changes in model parameterization of rainfall-runoff models. In all these fields, the usual handling of NDVI is in the form of maps and statistics extracted by carrying out GIS operations on remotely sensed data. In this paper, a novel way is proposed to visualize and extract information from NDVI products. Conceptually, in the line of the hypsometric curve, a curve can be drawn using gridded NDVI data to represent the distribution of the index values across any bounded area such as a hydrological catchment, a floodplain zone, or an administrative unit. It is proposed to call this curve the "endiviometric curve". The use and potential of endiviometric curves are demonstrated by drawing such curves from NDVI values derived from Sentinel-2 data for three distinctly different geographical units – a snow-fed Himalayan river catchment, a monsoon-fed floodplain area dotted with wetlands in the Brahmaputra valley, and a perennially drought-prone sub-division in the Deccan plateau. The results show that apart from being a handy way to monitor vegetational changes, the endiviometric curve can provide insights on many aspects of an ecosystem. It can complement the existing methods of monitoring inter-annual and intra-year snow cover changes. A good use of endiviometric curve lies in drought management as found from the exercise carried out in the drought affected area. In all, the endiviometric curve can be a useful tool in the planning and management of sustainable ecosystems.

Keywords: Remote sensing, Sentinel-2, NDVI, endiviometric curve, ecosystem

1 INTRODUCTION

When sunlight strikes the Earth, chlorophyll, the pigment present in the leaves of plants absorbs visible light for use in photosynthesis. On the other hand, near-infrared light is reflected by the leaves. In general, if there is more reflected radiation in near-infrared wavelengths than in visible wavelengths, then the vegetation in that pixel is likely to be dense and forested. If there is very little difference in the intensity of visible and near-infrared wavelengths reflected, then the vegetation is likely to be sparse. Vegetation Indices employ this difference formula to quantify the density of plant growth on the Earth — near-infrared radiation minus visible radiation divided by near-infrared radiation plus visible radiation. The result of this formula is called the Normalized Difference Vegetation Index (NDVI). The normalizing reduces topographic and atmospheric effects and enables the simultaneous examination of a wide area. The NDVI results from the following equation:

$$NDVI=(NearIR - Red)/(NearIR + Red) \quad (1)$$

The values of NDVI range from -1 to 1. Negative values of NDVI (values approaching -1) correspond to water. Values close to zero (-0.1 to 0.1) generally correspond to barren areas of rock, sand, or snow. Low, positive values represent shrub and grassland (approximately 0.2 to 0.4), while high values indicate temperate and tropical rainforests (values approaching 1).

2 HISTORY OF NDVI

With the launch of the first ERTS satellite i.e. Landsat-1 on July 23, 1972, NASA funded a number of investigations to determine the capabilities of the multi-spectral scanner (MSS) carried by the satellite. The sensors of the MSS included bands in the red and near-infrared, which were useful to distinguish vegetation. One of those early studies was directed toward examining the greening up of spring vegetation and subsequent drying down in summer and autumn throughout the expanse of the Great Plains region of the United States. The researchers for this study, PhD student Donald Deering, his advisor Dr. Robert Haas along with mathematician Dr. John Schell developed the difference/sum ratio formulation which they named as the Normalized Difference Vegetation Index (NDVI). The earliest formal reporting of the NDVI was in 1973 by Dr. John Rouse et.al. of the Remote Sensing Center of Texas A&M University where the above mentioned Great Plains study was conducted. Since then, NDVI has been and remains the most successful and well-known vegetation index.

3 NDVI APPLICATIONS

The index gained importance because NDVI values can be averaged over time to establish normal growing conditions in a region for a given time of year. Further analysis can then characterize the health of vegetation in that place relative to the norm. When analyzed through time, NDVI can reveal the spatial extent of where vegetation is thriving and where it is under stress, as well as changes in vegetation due to human activities such as deforestation, natural disturbances such as wild fires, or changes in plants' phenological stage. Due to these characteristics, NDVI immediately found several applications in the agriculture and forestry sectors. Later on, NDVI found applications in diverse fields from mapping land surface emissivity (Valor and Caselles, 1996) to habitat models for predicting breeding birds (McFarland and van Riper, 2013).

3.1 NDVI applications in Hydrology

NDVI has been able to attract hydrologists due to its potential to account for spatiotemporal land cover changes. Classic rainfall-runoff models usually use historical data to estimate model parameters and mean values of parameters are considered for predictions. However, due to climate changes and human effects, model parameters change temporally. To overcome this problem, NDVI derived from remotely sensed data can be used to investigate the effect of land cover variations on hydrological response of watersheds using a conceptual rainfall-runoff model. Studies have shown that model parameters might be determined using temporal NDVI values (Nourani, Fard, Gupta, Goodrich, & Niazi, 2017). NDVI is naturally a good indicator of drought, because when absence of water limits vegetation growth, the affected area has a lower relative NDVI. The index has been found useful for monitoring land surface moisture in semi-arid areas (Zhan, Qin and Wang, 2004). NDVI has also been tested for indicating the effective flood extent in macrophyte dominated floodplain wetlands (Powel, Jakeman and Croke, 2014).

4 NDVI HANDLING

The usual handling of NDVI is in the form of maps containing the NDVI values as gridded data. The maps are produced from remotely sensed data from satellites equipped with optical sensors that include the red and infrared bands. Sentinel-2 is one such satellite launched by the European Space Agency in 2015. The statistics are extracted by carrying out GIS operations on the NDVI maps. A typical NDVI map of Mandakini river basin in Uttarakhand is shown in Fig.1.

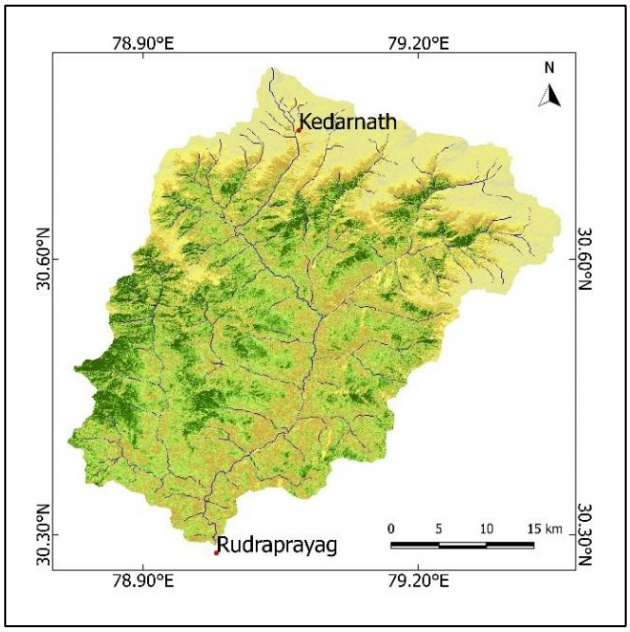

Fig.1. NDVI map of Mandakini basin on 21.02.2018

Fig.1 shows the catchment-scale spatial distribution of vegetation status in Mandakini basin as on 21st February 2018. This map has been processed from data captured by Sentinel-2. We can have a good idea of the state of vegetation throughout the catchment on that particular day. Areas of different classes of vegetation can be computed based on the NDVI values. We can also extract the pertinent statistics from the map.

Fig.2. shows the NDVI map of Mandakini basin on 22nd May 2018. The map clearly shows the improvement of vegetation status between February to May, ostensibly due to rainfall occurring along with the progression of Western Disturbances during the period.

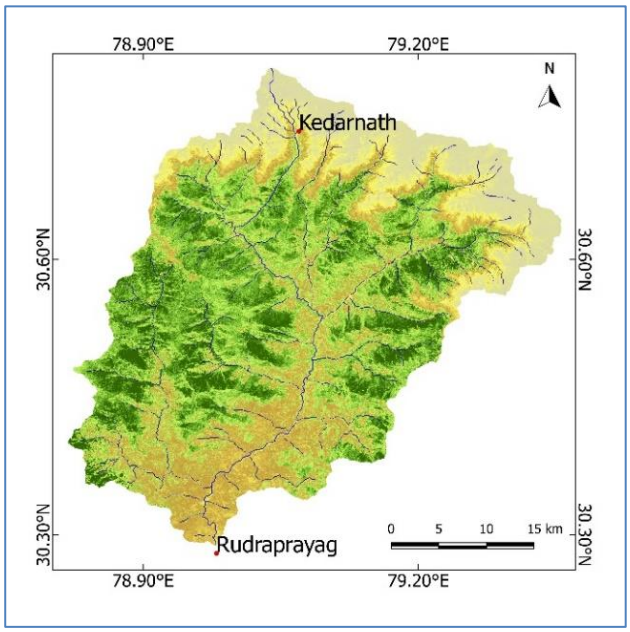

Fig.2. NDVI map of Mandakini basin on 22.05.2018

5 ENDIVIOMETRIC CURVE – A NOVEL WAY OF NDVI APPRECIATION

Conceptually, just as a hypsometric curve can be obtained from a DEM of topographical data which is a gridded raster image containing elevation data, an equivalent curve can be obtained if a gridded raster image contains other data. Thus, if a gridded raster image of NDVI data is used, the equivalent curve that can be obtained is proposed to be called the "endiviometric curve" – a coinage from the synthesis of the two key words "NDVI" and "metric". Fig.3 shows an endiviometric curve for the Mandakini basin as of 21st February 2018.

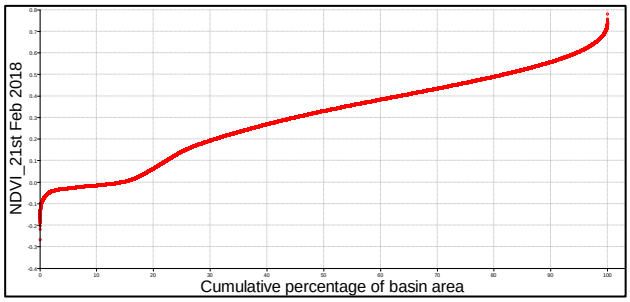

Fig.3. Endiviometric curve of Mandakini basin on 21.02.2018

From the endiviometric curve we get another perspective of the spatial distribution of vegetation state in the basin as compared to the image in Fig.1. We can readily see that 50% of the basin area have NDVI values higher than 0.33. Similarly, 90% of basin area have NDVI values lower than 0.56, or in other words, only 10% of the area have NDVI values higher than 0.56. The initial flat portion of the curve with NDVI values near zero pertains to the snow covered area. In a way, the curve can encapsulate both the visual and quantitative aspect of the vegetation/land cover state in a single graph.

6 USE OF ENDIVIOMETRIC CURVE

Apart from being a graphical aid for visualization and quantitative appreciation of NDVI, the proposed endiviomentric curve can be useful in many other ways. Some of the possible ways are discussed below:

6.1 Monitoring change

It is already stated that the endiviometric curve can encapsulate both the visual and quantitative aspect of the vegetation/land cover state in a single graph. Apart from the spatial aspect, a single graph of multiple endiviometric curves can represent the temporal change with respect to vegetation occurring in the basin, as presented in Fig.4. Here we see that a single graph can represent the information contained in the NDVI images of Fig.1 and Fig.2 in an effective way. The improvement of vegetation of almost all classes throughout the basin can be perceived. Further, the decrease in snow cover area can also be read from the curves from the difference in initial flat portions.

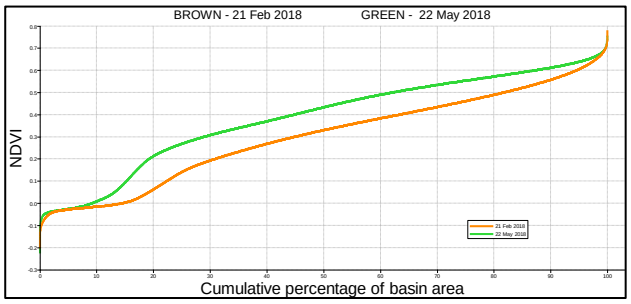

Fig.4. Endiviometric curves of Mandakini basin

6.2 Hydrological similarity

From the above discussion, it becomes apparent that the endiviometric curve may be helpful for establishing hydrological similarity between catchments, which depends on the "catchment form" (physiographic, geomorphologic and precipitation characteristics of the catchment) and "catchment response function" (streamflow, evapotranspiration, etc.). Addressing the spatial variability of catchment form with respect to physiographic and geomorphologic characteristics has received attention due to the development of various morphometric indices and tools during the last century. The spatial variability of vegetation is an important element of the hydro-climatic regime and the endiviometric curve can be useful to capture this. To demonstrate this possibility, the Himalayan sub-basins of Mandakini in Uttarakhand and Malana in Himachal Pradesh are considered. The Mandakini river is a tributary of the Alakananda river flowing in Uttarakhand having a catchment area of 1643 sq km. The northern part of the basin, about 90 sq km is under permanent snow-cover. The Malana is a tributary of the Parvati river flowing through in Himachal Pradesh having a much smaller catchment area of 193 sq km. The snow-fed area is however much more, about 60% of total area. Apparently there is little possibility of hydrological similarity between the two basins. The endiviometric curves of these two basins are compared and presented in Fig.5 which clearly shows that the basins are substantially different from each other.

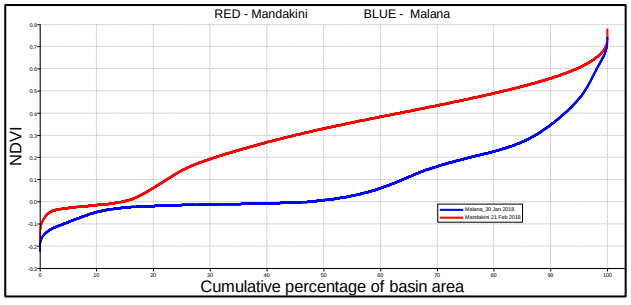

Fig.5. Endiviometric curve of Mandakini & Malana basins during Jan-Feb 2018

The idea of establishing hydrological similarity with the help of endiviometric curves can be extended to state that endiviometric curves can also help in catchment classification schemes.

6.3 NDVI and flood plain dynamics

The endiviometric curve is tested in a different physiographic setting where the monsoon-fed flood plain dynamics play a role like the Kaziranga National Park in the Brahmaputra valley. It is a well known fact that floods play a major role in maintaining the ecological balance of the Park. Its vast grasslands, wetlands and lakes are annually revitalized by the floods. Flood water acts as a natural cleaner as it washes away water hyacinths and other vegetation that is harmful for the animals or hamper the ecology of the Park. However, on 11th August, 2018, in the middle of the monsoon season, forest officials of the Park expressed their worry about the fact that no flood has happened in the Park this year. An inter-annual comparison of this aspect is attempted with the help of endiviometric curves drawn for the same time of the year between 2017 and 2018 and shown in Fig.6.

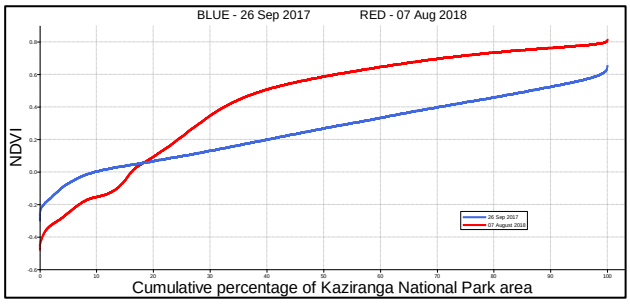

Fig.6. Endiviometric curves of Kaziranga National Park

Satellite remote sensing data from optical sensors is hard to get by during monsoon as areas like the Kaziranga generally remain overcast. However, increasing satellite coverage frequency may increase the chances of obtaining data. It may be mentioned that data from radar sensors as provided by Sentinel-1 can see through clouds and flood maps can be prepared as shown in Fig.7a and Fig.7b. The flood maps, together with the endiviometric curves corroborate the worry of the forest officials. It is felt that valuable ecological insights may be drawn by using Sentinel-2 data in conjunction with Sentinel-1 in such cases.

6.4 Drought studies

NDVI anomalies are commonly used in monitoring drought. NDVI is most widely used for operational assessment of drought owing to the ease in calculation and interpretation and also its ability to partially compensate for the effects of atmosphere, illumination geometry etc. (Manual for Drought Management, GoI, 2016).

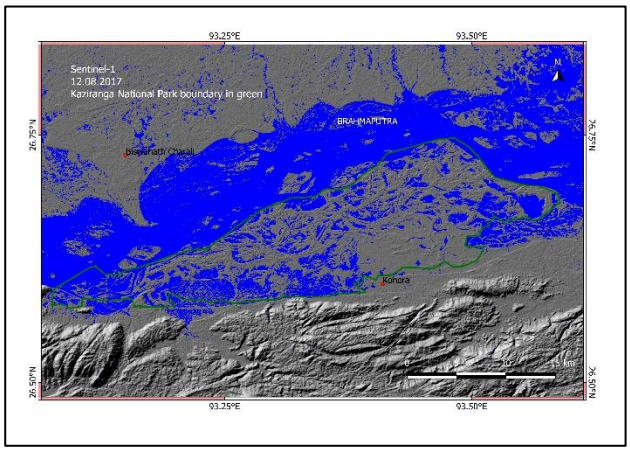

Fig.7a. Flood map of Kaziranga area on 12.08.2017

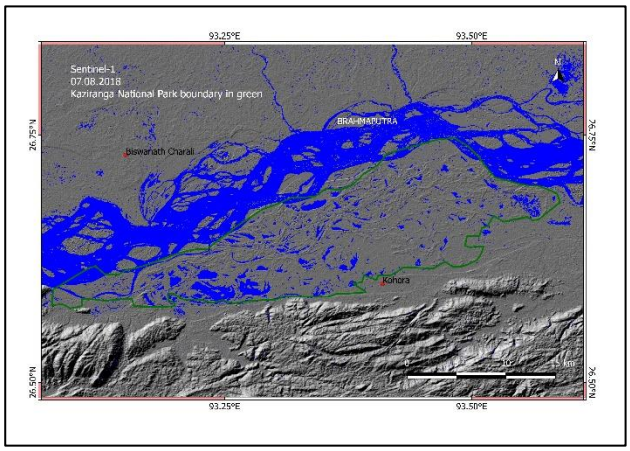

Fig.7b. Flood map of Kaziranga area on 07.08.2018

The possible utility of the endiviometric curve in drought studies is tested for the Anantapur Revenue Division, an administrative division of the Anantapur district of Andhra Pradesh.

The Anantapur district is one of the chronically drought-prone districts of India, located in Andhra Pradesh. The district receives the lowest rainfall in the state and the second lowest in India, after Jaisalmer in Rajasthan, averaging at 522 mm annually. The distribution of rainfall coupled with soil type have made it one of the poorest districts in the country, as it is the only drought-prone district with a meagre 10% of cultivated area under irrigation and the rest 90% under rainfed farming. 2017 saw severe drought conditions prevailing in the district. Fig.8 shows the comparative NDVI curves for 2017 and 2018 during the month of April. We can readily see that 2018 is also no better, and if so, only slightly. It can be inferred that endiviometric curves can be very much helpful in determining the anomalies and region-specific thresholds depending on cropping pattern for drought management.

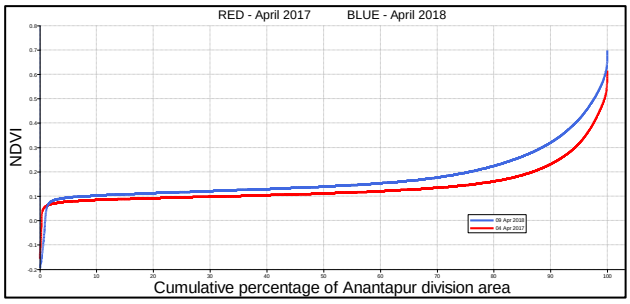

Fig.8. Endiviometric curves of Anantapur Revenue Division

6.5 Effect of forest fires

The summer of 2018 saw deadly heatwaves scorching many parts of the world from Japan to UK and wildfires raging through all the continents, some devastating ones in Greece, British Columbia, California in USA etc. The Carr Fire was one such large wildfire that burned in Shasta and Trinity Counties in California, United States. The fire which started on July 23 burned 92,936 ha causing 36,000 people to be evacuated and 8 fatalities before it was 100% contained late on August 30, 2018. Fig.9 shows affected area as on 01.08.2018 created from Sentinel-2 data. Fig.10 shows the pre-fire and post-containment endiviometric curves on 27th June and 5th September respectively, which bring out the drastic effect on all classes of vegetation due to the devastating fire.

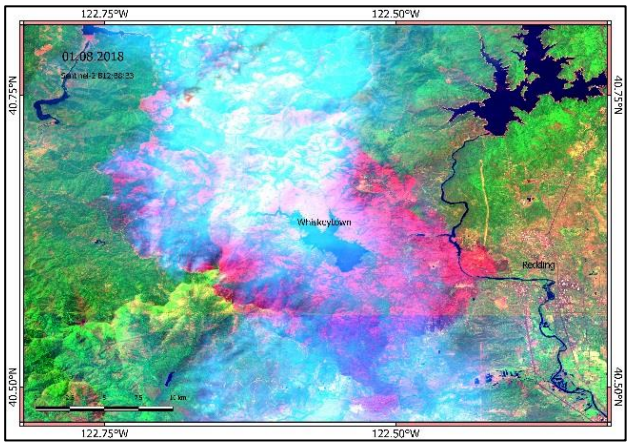

Fig.9. The Carr Fire area as on 01.08.2018

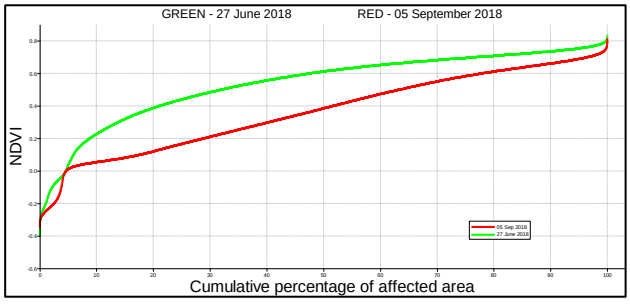

Fig.10. Endiviometric curves of Carr Fire area

7 CONCLUSIONS

Endiviometric curves of different geographical units viz. snow-fed mountainous river basins in the Himalayas, a national park in monsoon-fed flood plain of the Brahmaputra Valley, a chronically drought-prone revenue division in the Deccan and a wildfire ravaged area in Northern California have been studied. In general, it is observed that a convex curve is desirable foe a healthy state. However, in a majorly snow-fed river basin it is not possible to obtain a convex curve, and in certain areas like the Kaziranga it may not be desirable too. The value of the curve lies in the fact that it encapsulates both the visual and quantitative aspect of the vegetation/land cover state of conventional NDVI products within a single graph. Further, a single graph of multiple endiviometric curves can represent the temporal change of NDVI over a period of time to arrive at the normal and derive an anomaly situation. It can complement the existing methods of monitoring inter-annual and intra-year snow cover changes. Endiviometric curves can help confirm hydrological similarities of catchments as well as in catchment classification schemes. The curves offer the potential to draw ecological insights in flood, drought, wildfire or other natural disaster situations and help in creating thresholds for better management and restoration.

ACKNOWLEDGEMENTS

The author would like to express his deep sense of gratitude to the European Space Agency - ESA for the Sentinel-1 and Sentinel-2 data used in this study.

REFERENCES

1) McFarland, T. M. and van Riper, C.III. (2013): Use of Normalized Difference Vegetation Index (NDVI) habitat models to predict breeding birds on the San Pedro River, Arizona: *U.S. Geological Survey Open-File Report 2013–1100.*, 42 p.

2) Ministry of Agriculture & Farmers Welfare, Govt. of India (2016): Manual for Drought Management. *M/s. Royal Offset Printers*., 34-35.

2) Nourani, V., Fard, A. F., Gupta, H. V., Goodrich, D. C. & Niazi, F. (2017): Hydrological model parameterization using NDVI values to account for the effects of land cover change on the rainfall-runoff response. *Hydrology Research*, *48*(6), 1455-1473.

3) Powell, S.J., Jakeman, A., & Croke, B. (2014): Can NDVI response indicate the effective flood extent in macrophytedominated floodplain wetlands? *Ecological Indicators, Vol.45*, 486-493.

4) Valor, E., and Caselles, V. (1996): Mapping land surface emissivity from NDVI: Application to European, African, and South American areas. *Remote Sensing of Environment, Vol.57, Issue 3*, 167-184.

5) Wagener, T., Sivapalan, M., Troch, P. & Woods, R. (2007): Catchment classification and hydrologic similarity. *Geography Compass 1(4)*, 901–931.

6) Zhan, Z., Qin, Q. & Wang, X. (2004): The application of LST/NDVI index for monitoring land surface moisture in semiarid area. *2004 IEEE International Geoscience and Remote Sensing Symposium, Anchorage, AK, Vol.3*., 1551-1554